Investigating the Functional Interaction between RhoGDI Family Proteins and Activated Cdc42 associated-kinase (ACK)

Ana Masara Binti Ahmad Mokhtar

Newnham College

Department of Biochemistry

University of Cambridge

This dissertation is submitted for the degree of Doctor of Philosophy

April 2020

Jika kamu tidak sanggup menahan lelahnya belajar,
Maka kamu harus sanggup menahan perihnya kebodohan
Imam Syafi'i

Declaration

This thesis is the result of my own work and includes nothing which is the outcome of work done in collaboration except as declared in the Preface and specified in the text.

It is not substantially the same as any that I have submitted, or, is being concurrently submitted for a degree or diploma or other qualification at the University of Cambridge or any other University or similar institution except as declared in the Preface and specified in the text. I further state that no substantial part of my thesis has already been submitted, or, is being concurrently submitted for any such degree, diploma or other qualification at the University of Cambridge or any other University or similar institution except as declared in the Preface and specified in the text.

In accordance with the Biology Degree Committee guidelines, this dissertation does not exceed 60,000 words.

Ana Masara Binti Ahmad Mokhtar

April 2020

Abstract

Investigating the Functional Interaction between RhoGDI Family Proteins and Activated Cdc42 associated-kinase (ACK)

Ana Masara Binti Ahmad Mokhtar

ACK is a non-receptor tyrosine kinase and an effector protein for Cdc42. ACK has been implicated in carcinogenesis events especially in promoting cell migration and invasion, indicating a need for a fuller understanding of the cellular roles of ACK both in normal and pathological conditions. A previous yeast-2-hybrid screen in the lab identified RhoGDI-3 as an interacting partner for ACK. RhoGDI-3 is a member of RhoGDI family of proteins, which are negative regulators that maintains Rho-family GTPases in the inactive GDP-bound state and sequesters them in the cytosol. RhoGDIs have also been found to become deregulated in cancer and it is possible therefore that they play role in ACK-driven cancer progression.

In this work, it is shown that ACK binds but does not phosphorylate the RhoGDIs in cells or *in vitro*. ACK was shown to shuttle between the cytoplasm and the nucleus. RhoGDI-1 and -2 have been found only in the cytoplasm, while RhoGDI-3 is localized to both cytoplasm and the nucleus, under the conditions tested. The interaction between RhoGDI-3 and ACK occurs predominantly in the nucleus and RhoGDI-3 levels were shown to decrease following co-expression with ACK, especially in the nucleus. Data generated here shows that ACK-mediates RhoGDI-3 proteasomal degradation potentially by regulating RhoGDI-3 ubiquitination.

In order to determine the cellular effects of the interaction between ACK and the RhoGDIs, all possible Rho-family GTPases that interact with the RhoGDIs were determined in a systematic study. RhoGDI-1 and 2 were found to have relatively restricted activity, mainly binding members of the Rho and Rac subfamilies. RhoGDI-3 displayed wider specificity interacting with several novel interacting partners within the Rho, Rac and Cdc42 subfamilies. Unexpectedly RhoGDI-3 was found to form complexes with the atypical Rho GTPases such as RhoD, Wrch2, Rnd2, Miro2 and RhoH which are not regulated by standard GDP/GTP cycling. The GTP levels of these target proteins were found to decrease following co-expression with RhoGDI-3, confirming its role as a negative regulator of these Rho GTPases. ACK was shown to regulate the activation of these target proteins, including RhoA, RhoB, Rac1 and RhoH, which are known to be involved in cell proliferation and migration. Aberrant activation of these target protein is frequently observed in cancer, suggesting a role for RhoGDI to drive ACK oncogenicity.

Acknowledgements

Alhamdulillah, all praises to God for the strengths and His blessing in completing this thesis. Special appreciation goes to my supervisor, Dr. Darerca Owen for giving me the opportunity to learn, constant support and encouragement. Her invaluable help by providing constructive comments and suggestions throughout my PhD have contributed to the success of this research and also help me to grow as a good researcher. I am grateful to Dr. Helen Mott and all my GTP panels, Dr. Trevor Littlewood, Dr Marc de la Roche and Dr. Jenny Gallop for their continuous support, guidance and assistance. I would also like to thank Dr. Simone Weyand, my PhD advisor, for her encouragement and also Dr. Catherine Lindon and Dr. Anna Git for their advices regarding my work.

I am grateful to have wonderful lab members, without whom the past four years would not be enjoyable. Thanks for the friendship and memories. Special appreciation also given to all staffs in Biochemistry Department, Newnham college and Universiti Sains Malaysia for their help towards my postgraduate affairs.

I would also like to thank Ministry of Higher Education Malaysia, Universiti Sains Malaysia, University of Cambridge, Cambridge Philosophical Society and Newnham College for providing me the financial support over the past 4 years.

Last but not least, my deepest gratitude goes to my beloved family; Mr. Ahmad Mokhtar Bin Abu Bakar, Mrs. Norazizi Binti Hj Ujang, Mrs. Zufarhani Binti Ahmad Mokhtar and Mr. Azam Muzafar Bin Ahmad Mokhtar for their endless love, prayers and encouragement. To those who also indirectly contributed in this research, your kindness means a lot to me. Thank you very much.

Table of contents

List of Tables

List of Figures

List of Abbreviations

AC : Acidic
ACK : Activated Cdc42 associated-kinase
AH : Amphipathic helix
ALK : Anaplastic lymphoma kinase
AR : Androgen receptor
ARE : Androgen-response elements
ATP : Adenosine triphosphate
BACK : BTB and C-terminal Kelch
Baf : Bafilomycin
BiFC : Bimolecular fluorescence complementation
BORGs : Binder of Rho GTPases
BSA : Bovine serum albumin
BTB : Bric-a-brac
CAFs : Cancer-associated fibroblast
cFLIP : Cellular FLICE-like inhibitory protein
CFTR : Cystic fibrosis transmembrane conductance regulator
CHX : Cycloheximide
CL : Clathrin-interacting region
co-IP : Co-immunoprecipitation
COL1A1 : Collagen type 1 alpha 1
CRIB : Cdc42/Rac interacting binding region
CRISPR : Clustered regularly interspaced short palindromic repeats
DGK : Diacylglycerol kinase
DH : Dbl-homology
DISC : Death-inducing signalling complex
DMEM : Dulbecco's Modified Eagle Medium
DMP : Dimethyl pimelimidate
DMSO : Dimethyl Sulfoxide

DPBS : Dulbecco's phosphate buffered saline
EBD : EGFR binding domain
ECL : Enhanced Chemiluminescence solution
EDTA : Ethylenediaminetetraacetic acid
EGF : Epidermal growth factor
EGFR : Epidermal growth factor receptor
EMT : Epithelial-mesenchymal transition
Eph : Ephrin
ER : Oestrogen receptor
ERK3 : Extracellular signal-regulated kinase 3
FBS : Fetal bovine serum
GAP : GTPase-activating protein
GBD : GTPase- binding domain
GDI : Guanine nucleotide-dissociation inhibitor
GDP : Guanosine diphosphate
GEF : Guanine nucleotide-exchange factor
GRAIL : Gene related to anergy in lymphocytes
GSF : GDI-like solubilizing factor
GTP : Guanosine triphosphate
HCC : Hepatocellular carcinoma
HGF : Hepatocyte growth factor
HNSCC : Head and neck squamous cell carcinomas
HPC : Hematopoietic progenitor cell
Hsp56 : Heat shock protein 56
ICMT : Isoprenyl-cysteine carboxyl methyl-transferase
IP : Immunoprecipitation
IPTG : Isopropyl β- d-1-thiogalactopyranoside
LMP1 : Latent membrane protein 1
LTK : Leukocyte tyrosine kinase
LUBAC : Linear ubiquitin chain assembly complex
MLC : Myosin light chain

MVBs : Multivesicular bodies
MW : Molecular weight
NADPH : Nicotinamide adenine dinucleotide phosphate
NES : Nuclear export signal
NFAT : Nuclear factor of activated T-cells
NRTK : Non-receptor tyrosine kinase
NSCLC : Non-small cell carcinoma
PAGE : Polyacrylamide gel electrophoresis
PAK : p21-activated kinases
PBR : Polybasic region
PBS : Phosphate-buffered saline
PBST : Phosphate-buffered saline-Tween 20
PDGFR : Platelet-derived growth factor receptors
PEI : Polyethylenimine
PH : Pleckstrin homology
PIP5K : Phosphatidylinositol-4-phosphate 5-kinase
PKA : Protein kinase A
PKC : Protein kinase C
PMSF : Phenylmethylsulfonyl fluoride
PRK : Protein kinase C-related kinase
PRR : Proline-rich region
PTM : Post-translational modification
RBD : Rho binding domain
RCC1 : Regulator of chromosome condensation
ROCK : Rho-associated protein kinase
RTK : Receptor tyrosine kinase
RT-PCR : Reverse transcription polymerase chain reaction
SAM : Sterile α motif
SDS : Sodium dodecyl sulphate
SGEF : SH3-containing Guanine Nucleotide Exchange Factor
SH2 : SRC-homology 2

SH3 : SRC-homology 3
SNPH : Syntaphilin
SNX9 : Sorting nexin 9
SPEC : Small binding proteins for Cdc42
TAE : Tris-acetate EDTA
TRF1 : Telomeric repeat factor 1
Trx : Thioredoxin
Ub : Ubiquitin
UBA : Ubiquitin-association
UPS : Ubiquitn-proteasome system
VEGF : Vascular endothelial growth factor
WASP : Wiskott–Aldrich Syndrome protein
wt : Wild type
Y2H : Yeast-two-hybrid
ZF : Zinc finger

Chapter 1

Introduction

1.1 Small GTPases

Small GTPases, are monomeric guanine nucleotide binding proteins related to the α subunit of heterotrimeric G proteins. All small GTPases belong to a superfamily, often named as the Ras superfamily because the founding members are encoded by human *ras* genes that were initially discovered as cellular homologs of the viral *ras* oncogene (Harvey, 1964). The Ras superfamily can be further divided into five major families: Ras, Rho, Arf, Ran and Rab. Table 1.1 shows some examples of functions regulated by specific families and subfamilies.

Table 1.1: The Ras superfamily of small GTPases and their functions

Family	Subfamily	Function
Ras	Ras	Cell proliferation, differentiation, survival, apoptosis and gene expression (Barbacid, 1987; Lowy and Willumsen, 1993)
	Ral	Exocytosis, cell motility and actin cytoskeletal rearrangement (Shirakawa and Horiuchi, 2015)
	Rap	Cell adhesion, phagocytosis, cell morphology and cell junction formation (Caron, 2003)
	Rad	Insulin-stimulated glucose uptake (Moyers *et al.,* 1996) and actin cytoskeleton rearrangement (Ward *et al.,* 2002)
	Rheb	mTOR pathway activation (Inoki *et al.,* 2003), cell growth and cell-cycle progression (Patel *et al.,* 2003)
	Rit	Cell proliferation (Rusyn *et al.,* 2000), differentiation and survival (Spencer *et al.,* 2002)
Rho		Actin-cytoskeletal rearrangements, intracellular membrane trafficking (Ridley and Hall, 1992), cell-cycle progression (Olson *et al.,* 1995) and transcriptional activation (Sulciner *et al.,* 1996)
Rab		Intracellular vesicular transport (Zerial and McBride, 2001)
Arf		Vesicular trafficking (Volpicelli *et al.,* 2005)
Ran		DNA replication (Yamaguchi and Newport, 2003)

1.2 The structure of small GTPases

Small G proteins regulate a multitude of signalling pathway by acting as molecular switches. They have the ability to cycle between an inactive guanosine diphosphate (GDP)-bound form and an active guanosine triphosphate (GTP)-bound form to function (Goitre *et al.,* 2014). All Ras superfamily proteins shared a conserved guanine nucleotide binding domain or "G domain", containing five sequence motifs G1-G5 that mediate interaction with nucleotides and effector proteins (Figure 1.1) (Bourne *et al.,* 1991). The G1 motif also known as the Walker A motif or P-loop, is involved in phosphate binding, while the G3 motif binds to the nucleotide-associated Mg^{2+} ion. G4 and G5 are important in recognizing the guanine base of GTP. The G2 motif makes contacts with both the γ-phosphate of GTP and the Mg^{2+} ion (Colicelli, 2004).

The conformations of the "on" and "off" states of these small GTPases are similar but display pronounced differences that are confined primarily to two flexible loop regions called switch 1 and switch 2. In the GTP-bound state, both switch regions adopt conformations that allow downstream effector proteins to recognise and interact with the small GTPases (Milburn *et al.,* 1990). All small G proteins undergo these changes but some of the families undergo additional rearrangement such those seen in the N-terminus of Arf (1-17) and the C-terminus of Ran (173-216) (Antonny *et al.,* 1997; Vetter *et al.,* 1999).

Small G proteins also have a hypervariable region at their C-termini (Figure 1.1) that is essential for facilitating membrane association and subcellular localization. For instance, polybasic region in the hypervariable region of K-Ras4B and Rab35 facilitate their association with the plasma membrane (Hancock *et al.,* 1990; Welman *et al.,* 2000; Li *et al.,* 2014), while similar sequence target R-Ras to focal adhesions (Furuhjelm and Peränen, 2003). Rac1 membrane association and nuclear localisation has also been shown to be regulated by its C-terminal polybasic region (Lanning *et al.,* 2004).

Besides being involved in subcellular targeting, the hypervariable region has been shown to be involved in some protein-protein interactions and can target certain small GTPases to different signalling complexes. For example, phosphatidylinositol-4-phosphate 5-kinase (PIP5K) and diacylglycerol kinase (DGK) were found to interact with Rac1 via its hypervariable region (van Hennik *et al.,* 2003). Phosphorylation of the hypervariable region of K-Ras4B by PKC also results in the interaction between K-Ras4B and Bcl-XL (Bivona *et al.,* 2006).

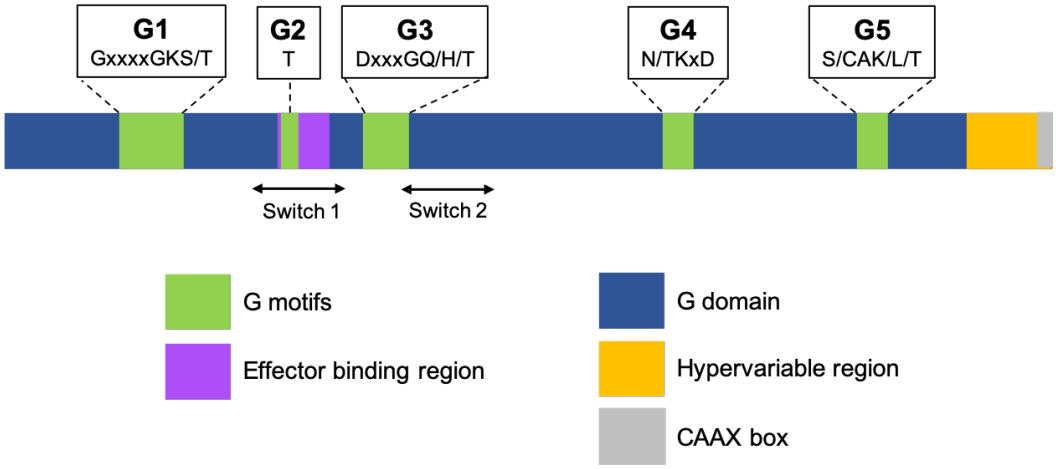

Figure 1.1: The architecture of the Ras superfamily proteins. Most of Ras superfamily proteins, including Rho, Ras and Rab share a conserved G domain, containing five conserved sequence G motifs: G1/P-loop (G10xxxxGKS/T17), G2 (T35), G3 (D57xxGQ/H/T61), G4 (N/T116KxD119) and G5 (S/C145AK/L/T147). The switch 1 and switch 2 regions involved in the conformational changes induced by the GDP/GTP cycle. The effector binding region is critical for direct association with downstream effector proteins. The CAAX box (C: Cys, A: aliphatic residue, X: any residue) is the site of lipid modification.

1.2.1 Lipid modification of small G proteins

Most of the Ras superfamily undergo prenylation at their C-termini, which terminate with a CAAX (C: Cys, A: aliphatic residue, X: any amino acid) tetrapeptide sequence. This process involves 3 main steps which are isoprenylation, proteolysis and carboxyl methylation (Choy *et al.,* 1999). Firstly, an isoprenoid lipid is attached to the CAAX box by a prenyltransferase such as geranylgeranyltransferase (GGTase) or farnesyltransferase (FTase). Both of these enzymes recognise the CAAX sequence before adding a 20-carbon geranylgeranyl or 15-carbon farnesyl to the cysteine residue of the CAAX sequence via a thioether linkage. Prenylation is followed by the proteolysis of the three C-terminal residues (AAX) by a prenyl protein peptidase, for example from the Rce1 family, to release –AAX. The prenylated cysteine is then methylated by isoprenyl-cysteine carboxyl methyl-transferase (ICMT). Unlike Ras and Rho-family members, Rab small GTPases can undergo double geranylgeranylation at the C-terminus, which is important for their correct localization (Pfeffer and Aivazian, 2004). 16-carbon palmitate acids can also be added to

various small G protein which contain further target cysteine residues in their sequence by palmitoyltransferase. This lipid modification is reversible (Smotrys and Linder, 2004). Instead of prenylation, Arf small GTPases undergoes myristoylation at their N-terminus (D'Souza-Schorey and Stahl, 1995), while the Ran small GTPase does not undergo any lipid modification (Wennerberg and Der, 2004).

1.3 Regulation of small GTPases activity

Even though each small G protein has a distinct molecular sequence and cellular function, most of them utilize a shared conformational switch between the GTP and GDP bound forms (Goitre *et al.,* 2014). Generally, in the GTP-bound form, the small GTPases form a hydrogen bond between the NH group of a threonine (Thr) in switch 1 and a glycine (Gly) in switch 2 with an oxygen from the γ-phosphate of GTP (Figure 1.2). These bonds hold the switches in a specific configuration. The release of γ-phosphate following GTP hydrolysis breaks the hydrogen bonds and allows both of the switches to relax (Vetter and Wittinghofer, 2001). The extent of the conformational changes is unique to each small GTPases. For instance, most of the Ras-family members show modest changes restricted only to their switch regions, whereas Arf and Ran experience larger changes especially in their N- and C- terminal extensions, respectively (Goldberg, 1998; Vetter *et al.,* 1999).

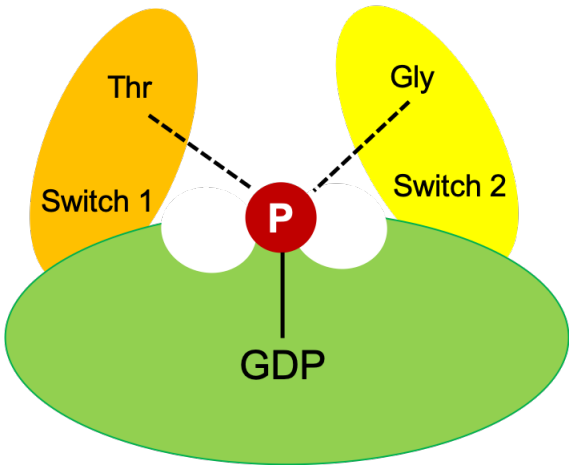

Figure 1.2: Schematic diagram of the universal switching mechanism of small G proteins. The γ-phosphate of the GTP forms a hydrogen bonds with a Thr in switch 1 and a Gly in switch 2 of small G proteins. This configuration is known as the loaded-spring mechanism where the release of the γ-phosphate, allows both of the switches to relax into their GDP-bound conformation. (Adapted from Vetter and Wittinghofer, 2001).

The intrinsic GDP/GTP switching of these small GTPases is relatively slow, thus they require three classes of regulatory proteins to allow them to function. These are known as the guanine nucleotide-exchange factors (GEFs), GTPase-activating proteins (GAPs) and guanine nucleotide-dissociation inhibitors (GDIs). GEFs facilitate GDP dissociation and promote binding of the more abundant GTP in the cytoplasm, thus allowing the small GTPases to become activated and bind to their specific effectors in order to trigger signalling pathways (Cherfils and Zeghouf, 2013). In contrast, GAPs are responsible for terminating small GTPases signalling by stimulating their intrinsic GTPase activity so enhancing the hydrolysis of GTP to GDP (Bos *et al.,* 2007). Unlike Ran and Arf family proteins, Ras, Rho and Rab require a third regulator family known as the GDIs. GDIs are bifunctional negative regulators of small GTPases and act to maintain the small G proteins in their GDP-bound state and also physically sequester small GTPases out of membranes by interacting with their prenyl group. A summary of the regulatory roles of all proteins involved in the activation status of small GTPases is shown in Figure 1.3.

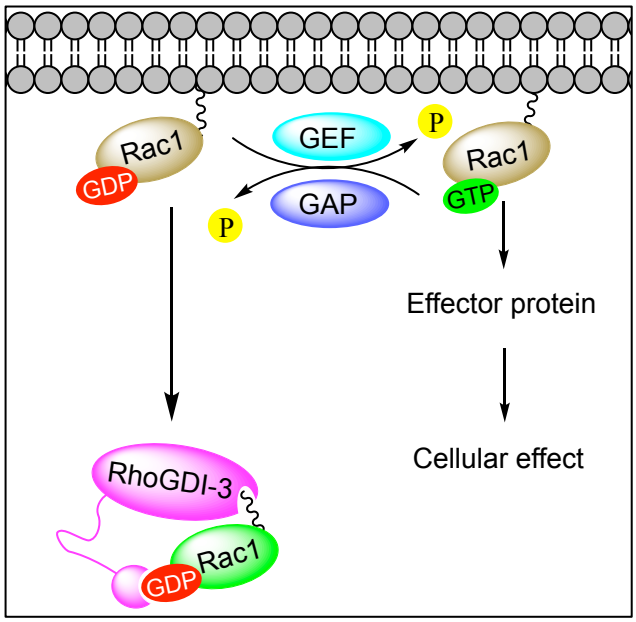

Figure 1.3: The regulatory cycle of Rho-family proteins. Small GTPases, for example the Rho-family small G proteins, cycle between an active GTP-bound and an inactive GDP-bound state. GEFs function to activate these small G proteins, facilitating the exchange of GDP for GTP, which in turn interact with specific effector proteins to mediate diverse biological effects. In contrast, GAPs stimulate the intrinsic GTPase activity of the small G proteins, accelerating their inactivation. GDIs are negative regulators that maintain small GTPases in GDP-bound state in cytoplasm, thus preventing them from localizing to membranes.

1.3.1 Guanine nucleotide exchange factor (GEFs)

The intrinsic nucleotide exchange rate of small G proteins is relatively slow. Thus, the GEFs are required to increase the rate of exchange by several orders of magnitude (Vetter and Wittinghofer, 2001). Different families of GEFs have been shown to regulate different families of small GTPases (Table 1.2). Most of the Ras family are regulated by GEFs containing a CDC25 homology domain (CDC25-HD) (Lai *et al.,* 1993), while GEFs that regulate Rho-family proteins often contain a DH-PH tandem di-domain (Hart *et al.,* 1991). Rho-family proteins can also be regulated by DOCK family proteins containing DOCK-homology regions 1 (DHR1) and 2 (DHR2). GEFs for members of the Arf-family contain a Sec7 domain (Chardin *et al.,* 1996). The regulator of chromosome condensation 1 (RCC1) protein acts as a GEF for Ran (Bischoff and Ponstingl, 1991) and has a ß-propeller structure unique amongst GEFs. There are two main families of GEFs for Rab proteins which contain either a Vps9 domain (Carney *et al.,* 2006) or DENN domain (Allaire *et al.,* 2010).

Despite the large amount of structural diversity amongst the GEFs, in general they all share a similar mechanism to accelerate the dissociation of the nucleotide from the small GTPases. Briefly, the GEFs interact with the switch 1 and/or switch 2 regions and this binding results in conformational changes in both the switch regions and the P-loop of the small GTPases. This disturbs phosphate and Mg^{2+} binding, weakening the interaction between the small G proteins and GDP, resulting in release of GDP and binding of GTP (Vetter and Wittinghofer, 2001).

G proteins are structurally stabilised by their associated nucleotide and a major function of a GEF is to stabilise the nucleotide free form of the small G proteins during exchange. For instance, Sos1 stabilises Ras in its nucleotide-free state by inserting an α-helix from its catalytic domain near to switch 1 and by contacting the side chains of residues in switch 2. This opens up the nucleotide-binding site, blocking the Mg^{2+} and α-phosphate-binding regions (Boriack-Sjodin *et al.,* 1998).

Table 1.2: List of selected examples GEFs

Family	Subfamily	GEFs	Review in/ Reference
Ras	K-Ras, N-Ras	Sos1/ 2, RasGRF1/2, RasGRP1/ 2	Buday and Downward, 2008; Besray *et al.,* 2018
	M-Ras	Sos1, RasGRP1/ 2/ 3, RasGRP3	
	R-Ras	RasGRP2/ 3	
	H-Ras	RasGRP4, PLCε, Sos1, RasGRF1/2, RasGRP1	
	Rap1	RAPGEF1, RasGRP2/3	
Rho	RhoA	ARHGEF11/12/25/18/28, SmgGDS, AKAP13, IpgB2	Toma-Fukai *et al.,* 2019
	Rac1	Tiam, Trio, Vav1, DOCK2, P-Rex1, Kalirin, ARHGEF28	
	Cdc42	Dbs, ITSN1, DOCK7/8/9	
	TCL	ITSN1	Color-Aparicio *et al.,* 2020
Rab	Rab1a/b	TRAPP I	Müller and Goody, 2018
	Rab3a/b/c/d, Rab27a	MADD	
	Rab5a	Rabex-5	
	Rab6a/b	Ric1-Rgp1	
	Rab7a/b	Mon1/Ccz1	
	Rab8a/b	C9Orf72	
	Rab9a/b	DennD2	
	Rab11a/b	SH3BP5	
	Rab12	DennD3	
	Rab13	DennD1C	
	Rab14	DennD6	
Arf	Arf1	GBF1, BIG1/2, Cytohesin-1/2/3/4	Donaldson and Jackson, 2011; Sztul *et al.,* 2019
	Arf3	GBF1, BIG1/2, Cytohesin-2	
	Arf4	BIG1/2	
	Arf5	GBF1, Cytohesin- 4	
	Arf6	BRAG1/2/3, Cytohesin-1/2/3, EFA6A-D	
	Arl1	BIG1/2	
	Arl4A/4D	Cytohesin-1/2/3	
Ran	Ran	RCC1	Bischoff and Ponstingl, 1991

1.3.2 GTPase-activating proteins (GAPs)

The inactivation of small GTPases requires stimulation by GAPs. Similar to GEFs, there are specific GAPs for each family of small GTPases (Table 1.3). The structural details of how the GAPs stimulate intrinsic GTPase activity were initially described for the Ras-p120GAP (Scheffzek *et al.,* 1997) and RhoA-RhoGAP complexes (Rittinger *et al.,* 1997).

p120GAP was shown to neutralise the negative charge building up on the γ- and ß- phosphates of GTP and to stabilise switch 2 of H-Ras by inserting an arginine side chain (Arg789) into the active site of Ras. This arginine residue also known as the arginine finger is conserved among all Ras GAPs and is required to orientate Ras Gln61, which catalyses GTP hydrolysis. Ras Gln61 coordinates a reactive water molecule in the catalytic site which then performs the nucleophilic cleavage of the γ-ß-phosphoanhydride bond of GTP, resulting in the release of the γ-phosphate (Scheffzek *et al.,* 1997). Similarly, p50RhoGAP was shown to enhance the GTP hydrolysis on RhoA through the insertion of Arg85 into the active site of RhoA, resulting in the stabilisation of Gln63 to participate in the GTP-hydrolysis (Rittinger *et al.,* 1997).

The involvement of the arginine finger and the catalytic glutamine and is conserved in the Rab proteins. However, the details of Rab GAPs activity are slightly different. Studies on Gyp1p in yeast showed the involvement of a dual-finger mechanism where both the arginine finger and glutamine are supplied by RabGAP to stimulate GTP hydrolysis of Rab33 (Pan *et al.,* 2006).

Table 1.3: List of selected examples GAPs

Family	Subfamily	GAPs	Review in/ Reference
Ras	H-Ras	p120GAP	Jeong *et al.,* 2007; Besray *et al.,* 2018 Vigil *et al.,* 2010
	N-Ras, H-Ras, Rab48	DAB2IP	
	N-Ras, K-Ras, H-Ras	NF1, RASAL2	
	H-Ras	PLXNB1	
	Rap1A	IQGAP1	
	Rheb2, Rap1A, RalA	TSC2	
	Rap1	RAP1GAP, SIPA1	
	Rap2	SIPA1	
Rho	RhoA	p50RhoGAP, ARAP1, ARAP3, BPGAP1, p73RhoGAP, MgcRacGAP, ArhGAP10, GMIP, p190RhoGAP	Tcherkezian and Lamarche-Vane, 2007; Héraud *et al.,* 2019
	RhoC	p190RhoGAP	
	Rac1	p50RhoGAP, ARAP1, ARAP3, Bcr, Abr, MgcRacGAP, ArhGAP10, srGAP3, p190RhoGAP	
	Cdc42	p50RhoGAP, ARAP1, ARAP3, Bcr, Abr, MgcRacGAP, ArhGAP10, srGAP3	
	Rac2	Bcr, Abr	
	Rnd1/Rnd3	p190RhoGAP	
Rab	Rab1a/b, Rab2a/b	TBC1D20	Müller and Goody, 2018
	Rab3a/b/c/d	Rab3GAP	
	Rab4a/b, Rab6a/b/c, Rab36	TBC1D11	
	Rab5a/b/c	TBC1D3	
	Rab8a/b, Rab10, Rab14	TBC1D1	
	Rab13, Rab33a/b	TBC1D25	
	Rab17, Rab21	TBC1D7	
Arf	Arf1/2/3/4/5	ArfGAP1/ 2/ 3	Donaldson and Jackson, 2011; Sztul *et al.,* 2019
	Arf6	Acap1, Adap1, Agap1, Arap2, Asap1, Git1, Smap1	
	Arl3	RP2, ELMOD2	
Ran	Ran	RanGAP1	Bischoff *et al.,* 1994

1.3.3 Guanine nucleotide-dissociation inhibitors (GDIs)

Within the Ras superfamily, Ras, Rho and Rab small GTPases are known to be regulated by the third class of regulatory protein known as GDIs (Table 1.4). Rho and Rab GDIs contain two domains. The first, a smaller N-terminal domain, interacts with the switches on the G domain of small G proteins to prevent nucleotide exchange. The second, larger, C-terminal domain has a hydrophobic cleft that interacts with the lipid-modified tail of the small GTPases and thus disallows membrane association. The GDIs maintain an inactive cytosolic pool of small G proteins (Wu *et al.,* 1996; Olofsson, 1999) and also act as chaperones targeting the small GTPases to specific subcellular compartments (Brunet *et al.,* 2002; Pfeffer and Aivazian, 2004).

RabGDIα was first identified for Rab3A by Araki *et al.* (1990) and the structure of RabGDIs are conserved across species. Structural studies in yeast demonstrated that the RabGDIs interact only with the GDP-bound form of the Rab GTPases (Alory and Balch, 2000; Rak *et al.,* 2003; Pylypenko *et al.,* 2006).

Unlike the RabGDIs, the RhoGDIs have been shown to interact with both the GDP- and GTP-bound forms of Rho-family GTPases. For instance, RhoGDI-1 can accommodate both the GTP- and GDP-bound forms of Rac1, RhoA and Cdc42 (Hancock and Hall, 1993; Nomanbhoy and Cerione, 1996). In fact, RhoGDI-1 appears to be required to maintain Cdc42 in its active GTP-bound form by preventing both intrinsic and GAP-stimulated GTP hydrolysis, and is crucial for Cdc42-mediated cellular transformation (Hart *et al.,* 1992; Lin *et al.,* 2003).

Besides these two classes of GDIs, there are GDI-like proteins that have been shown to regulate the activation of Ras-family GTPases. The GDI-like solubilizing factor (GSF), PDEδ, interacts with and solubilises farnesylated Ras small GTPases in the cytoplasm through its isoprenoid binding pocket (Alexander *et al.,* 2009; Chandra *et al.,* 2012). Galectin-3 and -8 also contain a hydrophobic pocket with the ability to interact with farnesylated K-Ras4B and this association is important in modulating K-Ras4B oncogenic signalling (Shalom-Feuerstein *et al.,* 2008; Meinohl *et al.,* 2019).

Table 1.4: Complete list of Rho-, Rab- and RasGDIs

Family	Subfamily	GDIs	Review in/ Reference
Rho	RhoA, Cdc42	RhoGDI-1, RhoGDI-2, RhoGDI-3	DerMardirossian and Bokoch, 2005; Adra *et al.,* 1997
	RhoB	RhoGDI-3	Zalcman *et al.,* 1996
	RhoC	RhoGDI-1, RhoGDI-2	DerMardirossian and Bokoch, 2005; Griner *et al.,* 2015
	Rac1, Rac2		DerMardirossian and Bokoch, 2005
	Rac3		DerMardirossian and Bokoch, 2005; Zhang *et al.,* 2009
	RhoG	RhoGDI-1, RhoGDI-3	DerMardirossian and Bokoch, 2005; Adra *et al.,* 1997
	RhoH	RhoGDI-1, RhoGDI-2, RhoGDI-3	Li *et al.,* 2002
Rab	Rab9	RabGDI-1	Shapiro and Pfeffer, 1995
	Rab3B		Sidhu and Bhullar, 2001
	Rab2A, Rab4A, Rab5A, Rab8A, Rab9A, Rab11A	RabGDI-2	Shisheva *et al.,* 1999
Ras	K-Ras4B	Galectin-3 and -8	Shalom-Feuerstein *et al.,* 2008; Meinohl *et al.,* 2019
	K-Ras, N-Ras, H-Ras	PDEδ	Alexander *et al.,* 2009; Chandra *et al.,* 2012

1.4 The Rho-family small GTPases

The Rho (Ras homologous) family of small GTPases is one of the families of the Ras superfamily. The Rho-family GTPases are best studied for their role in promoting actin cytoskeleton reorganization, however they also play roles in cell division, cell adhesion and motility, vesicular

trafficking, phagocytosis and transcriptional regulation (Ridley and Hall, 1992; Olson *et al.,* 1995; Jaffe and Hall, 2005; Sulciner *et al.,* 1996).

In humans, there are 23 Rho-family GTPases members that can be further categorized into six major subfamilies (Figure 1.4). RhoD, RhoF and RhoH do not belong to any subfamily. The subfamilies are categorised based on their similarity in primary amino acid sequence (Appendix 1.1), structural motifs and biological functions (Hodge and Ridley, 2016).

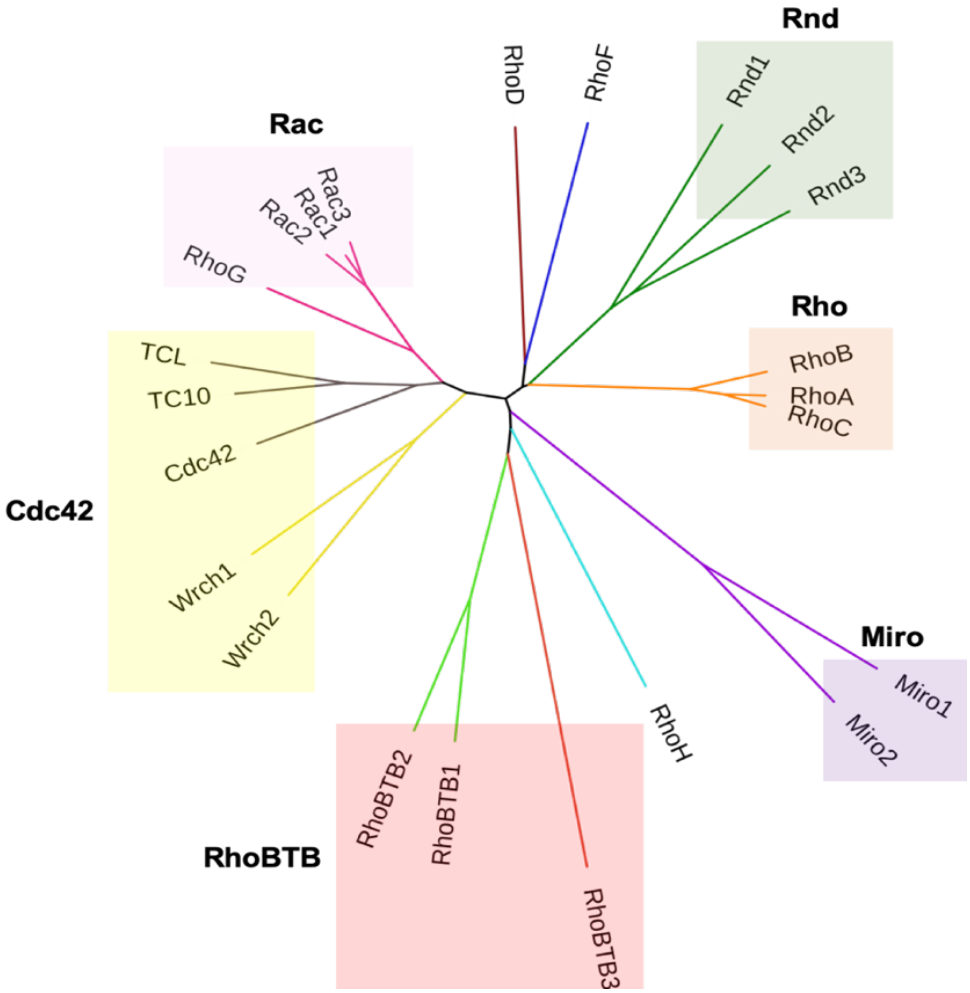

Figure 1.4: Phylogenetic tree of the Rho-family GTPases. A phylogenetic analysis of the amino acid sequences of the 23 Rho-family GTPases members made with Clustal Omega. The Rho-family can be divided into 6 major subfamilies: Rho, Rac, Cdc42, Rnd, Miro and RhoBTB. RhoD, RhoH and RhoF does not belong to any subfamily.

Among these Rho-family GTPases, the most extensively studied members are RhoA, Rac1 and Cdc42. These proteins and their subfamilies are also known as classical Rho-family GTPases. The other Rho-family proteins are known as the non-classical or atypical Rho GTPases and include the RhoBTB, Rnd and Miro subfamilies. This classification is made based on the ability of the Rho-family GTPases to undergo the classical GTPase cycle as described in section 1.2 (Wennerberg and Der, 2004; Aspenström, 2017).

1.4.1 The classical Rho-family GTPases

Compared to other Ras superfamily proteins, the defining feature of Rho-family small G proteins is the Rho insert region, a unique α-helical sequence located between the fifth β strand and the fourth α helix in the G domain (Valencia *et al.,* 1991). The role for this insert region is still not well understood. However, previous studies show that this insert region regulates some RhoA, Rac1 and Cdc42 functions. For instance, the insert region of Rac1 is essential to support NADPH oxidase activity (Freeman *et al.,* 1996). Deletion of the RhoA insert region also prevented the activation of Rho kinase (ROCK) *in vivo* and therefore the ability of RhoA to induce stress fibre formation (Zong *et al.,* 2001).

Most of the classical Rho-family GTPases are found to have only a Rho-type G domain with short N-terminal and C-terminal extensions (Wennerberg and Der, 2004; Citalán-Madrid *et al.,* 2013). Similar to other Ras superfamily members, they also have a hypervariable region encoding a prenylation site at their C-termini (Figure 1.5) and sometimes a polybasic region. These signals allow them to associate with specific membrane compartment (Table 1.5) (Michaelson *et al.,* 2001). Some of the Rho-family GTPases also have cysteine residues upstream of the CAAX motif that can be palmitoylated.

Most of the classical Rho-family GTPases are geranyl-geranylated or farnesylated, with only a few palmitoylated for example RhoB, TC10 and Rac1 (Table 1.5) (Adamson *et al.,* 1992; Michaelson *et al.,* 2001; Navarro-Lérida *et al.,* 2012).

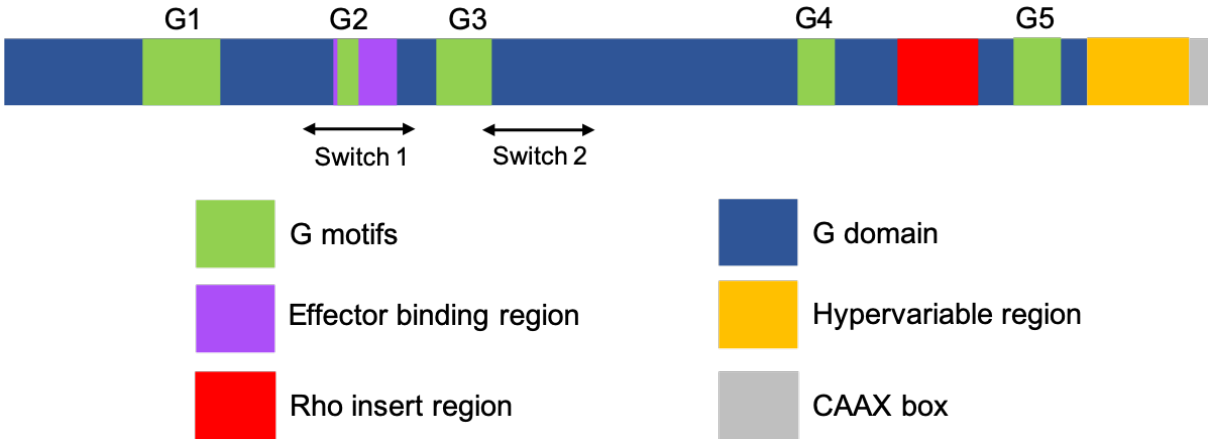

Figure 1.5: The architecture of the classical Rho-family proteins. All classical Rho-family GTPases shared a conserved G domain, effector binding region, hypervariable region and CAAX box. They also have a Rho insert region that is exclusive to Rho-family GTPases.

Palmitoylation is known to affect protein function by regulating membrane interactions and subcellular distribution (Salaun *et al.,* 2010). For example, RhoB undergoes palmitoylation at both Cys189 and Cys192. However, only Cys192 has been shown to inhibit anchorage-independent growth and maintain proper distribution of RhoB to endosomes (Wang and Sebti, 2005). Inhibition of palmitoylation was also found to mis-localise TC10 to the endoplasmic reticulum rather than to the plasma membrane and endosomes (Michaelson *et al.,* 2001; Watson *et al.,* 2003). Rac1 palmitoylation at Cys178 is also important to maintain correct distribution of Rac1 to the plasma membrane, cytosol and nucleus, which are required to regulate actin cytoskeleton remodelling (Navarro-Lérida *et al.,* 2012).

Interestingly, palmitoylation is exclusive to Rac1 in the Rac subfamily, despite all three Rac isoforms sharing a conserved cysteine at residue 178. This may be due to the distinct sequences between Cys178 and the prenylation site in the Rac isoforms (Table 1.5) that favour palmitoylation in Rac1 (Navarro-Lérida *et al.,* 2012). TCL is also predicted to undergo palmitoylation since it is shown to possess two C-terminal putative palmitoylation sites. However, a biotin labelling assay suggest that it is not (Roberts *et al.,* 2008).

Table 1.5: C-terminal sequences of the classical Rho-family GTPases and their subcellular distribution

Rho Protein	C-terminal sequence	Lipid modification	Localisation
RhoA	KDGVREVFEMATRAALQARRGKKKSGCLVL	GG	PM, C, G, N
RhoB	VREVFETATRAALQKRYGSQNG**C**IN**C**CKVL	GG/ F, P	PM, G, E, N
RhoC	KEGVREVFEMATRAGLQVRKNKRRRGCPIL	GG	PM, C, N
Rac1	RGLKTVFDEAIRAVL**C**PPPVKKRKRKCLLL	GG, P	PM, C, N
Rac2	RGLKTVFDEAIRAVLCPQPTRQQKRACSLL	GG	PM, G, ER, NE
Rac3	RGLKTVFDEAIRAVLCPPPVKKPGKKCTVF	GG	PM, EM, N
RhoG	QDGVKEVFAEAVRAVLNPTPIKRGRSCILL	GG	PM, E, MT
Cdc42	QKGLKNVFDEAILAALEPPEPKKSRRCVLL	GG	PM, G, ER, NE
TCL	AVFDEAILTIFHPKKKKKRCSEGHSCCSII	F	PM, E
TC10	DEAIIAILTPKKHTVKKRIGSR**C**IN**C**CLIT	F, P	PM, E

Putative palmitoylated cysteines are in boldface type and coloured red and CAAX prenylation motifs are underlined. (Data taken from: Adini *et al.,* 2003; Ridley, 2006; Wennerberg and Der, 2004; Roberts *et al.,* 2008; Dubash *et al.,* 2011; Kim *et al.,* 2013; Murali and Rajalingam, 2014). GG: geranylgeranyl, F: farnesyl, P: palmitoyl, PM: plasma membrane, C: cytosol, N: nucleus, G: Golgi, E: endosomes, ER: endoplasmic reticulum, NE: nuclear envelope and EM: endomembrane.

1.4.1.1 The Rho subfamily proteins

The Rho subfamily consists of RhoA, RhoB and RhoC. RhoA and RhoC share 92% similarity while RhoA and RhoB share 85% sequence similarity (Appendix 1.1). The most divergent sequences between RhoA, B and C are located towards the C-termini (Wheeler and Ridley, 2004), with some of the differences also concentrated in the Rho insert region (Schaefer *et al.,* 2014).

As described previously, the C-termini of all Ras superfamily proteins are important for lipid modification and therefore the subcellular distribution of the small GTPases. Both RhoA and RhoC are geranylgeranylated, whereas RhoB can be either geranylgeranylated or farnesylated, and palmitoylated. These differences in lipid modifications are reflected in their subcellular distribution, with RhoA and RhoC predominantly found in the cytosol or at the plasma membrane,

while RhoB is found at the plasma membrane, endosomes and Golgi (Adamson *et al.,* 1992; Michaelson *et al.,* 2001). Different forms of RhoB are shown to associate with different membranes. For instance, geranylgeranylated RhoB has been shown to localise to late endosomes, whilst the farnesylated form of RhoB localises to the plasma membrane (Wherlock *et al.,* 2004). Geranylgeranylated and not farnesylated RhoB is crucial for stress fibre and focal adhesion formation (Allal *et al.,* 2002). Palmitoylation is known to support the role of RhoB as a tumour suppressor by inhibiting anchorage-independent growth and stimulating apoptosis of PC3 tumour cells (Wang and Sebti, 2005).

To date, there are a large number of effector proteins identified for Rho subfamily proteins (Table 1.6). For instance, Rhotekin, Rhophilin and the PRKs have a Rho binding region at their N-termini, which share 27-40% sequence similarity (Reid *et al.,* 1996; Watanabe *et al.,* 1996). In contrast, the serine/threonine protein kinases, ROCK1 and ROCK2 have a Rho-binding domain at their C-termini, located in between a coil-coil structure and a pleckstrin homology (PH) domain (Leung *et al.,* 1996). Another family of Rho effector belong to the formin family and are known as mDia1, 2 and 3. However, they are not specific for Rho subfamily members as they have also been found to interact with other Rho-family GTPases such as Cdc42, Rac1 and RhoF (Lammers *et al.,* 2008; Pellegrin and Mellor, 2005).

RhoB was the first member of the Rho subfamily protein to be associated with endosomal trafficking by activating and translocating its downstream targets PRK1 and mDia1 to endosomes (Adamson *et al.,* 1992; Mellor *et al.,* 1998; Fernandez-Borja *et al.,* 2005). RhoB was also found to facilitate the trafficking of several signalling molecules such as Akt (Adini *et al.,* 2003), Src (Sandilands *et al.,* 2004) and PDGFR-β (Minzhou *et al.,* 2007) to the nucleus, plasma membrane and endosomes, respectively.

Table 1.6: The examples of interacting proteins for the classical Rho-family GTPases

Group	Rho GTPases	Interacting proteins
Rho	RhoA	ROCK1/2, Rhotekin, Citron, CRK, Rhophilin, mDia1, mDia2, Daam1, MRK, PRK1
	RhoB	ROCK1/2, Rhotekin, PRK1, mDia1, mDia2, Daam1
	RhoC	ROCK1/2, Rhotekin, mDia1, Daam1, FMNL2, FMNL3, MRK, PRK1
Rac	Rac1	PAK1-6, WAVE, IQGAP3, mDia1, mDia2, Daam1, FMNL1, IRSp53, PLC-β, $p67^{phox}$, PRK1, ROCK1
	Rac2	PAK1-4, mDia1, mDia2
	Rac3	PAK1-4
	RhoG	ELMO, Kinectin
Cdc42	Cdc42	ACK, WASP, N-WASP, PAK1-6, PAR6, IQGAP3, BORG1-5, mDia2, mDia3, Daam1, FMNL1, FMNL2, SPEC1, SPEC2
	TC10/RhoQ	WASP, N-WASP, PAK1-3, BORG1-3,5, Exo70
	TCL/RhoJ	WASP, N-WASP, PAK1-3

(Data taken from: Vignal *et al.,* 2001; Cotteret *et al.,* 2003; Pandey *et al.,* 2002; Schwartz *et al.,* 2004; Ridley, 2006; Wang *et al.,* 2007; Koh *et al.,* 2008; Lam *et al.,* 2013; Korkina *et al.,* 2013; Fujita *et al.,* 2013; Kühn and Geyer, 2014; Prudnikova *et al.,* 2015; Farrugia and Calvo, 2016; Soriano-Castell *et al.,* 2017; Siddique *et al.,* 2019)

All three Rho subfamily proteins are frequently deregulated in a variety of cancers. RhoA and RhoC are known as pro-oncogenic, whilst RhoB is anti-oncogenic. Overexpression of RhoA has been described in colon, breast, lung, ovarian, gastric and liver cancers (Fritz *et al.,* 1999; Horiuchi *et al.,* 2003; Pan *et al.,* 2004; Li *et al.,* 2006) with overexpression found to correlate with cancer progression. For instance, overexpression of RhoA promotes cervical cancer cell proliferation and migration via its effectors, ROCK1 and 2 (Liu *et al.,* 2014). In contrast however, reduced RhoA was shown to increase breast cancer metastasis by promoting a pro-tumour microenvironment by increasing the infiltration of cancer-associated fibroblast (CAFs) and macrophages, and by increasing the CXCR4-CXCL12 and CCR5-CCL5 chemokine axes in primary tumour (Kalpana *et al.,* 2019).

RhoC has also been shown to associate with pancreatic cancer (Suwa *et al.,* 1998), skin cancer (Clark *et al.,* 2000), breast cancer (Kleer *et al.,*2002), gastric cancer (Kondo *et al.,* 2004; Liu *et al.,*

2007) and cervical cancer (He *et al.,* 2004). Despite its high similarity with RhoA, increased activation of RhoC but not RhoA was shown to stimulate the epithelial-mesenchymal transition (EMT) process and metastasis in colon cancer (Bellovin *et al.,* 2006). Silencing RhoC, but not RhoA also decreased the anchorage-independent growth of LNCaP cells (Giang Ho *et al.,* 2011). These opposing roles of RhoA and RhoC in regulating cell migration might be due to them acting on different effector targets. For example, RhoA was shown to be involved in migratory cell polarity by suppressing Rac1 activity in lamellipodia via ROCK2, while RhoC enhanced migration by restricting lamellipodia broadening through FMNL3 (Vega *et al.,* 2011).

In contrast to RhoA and RhoC, RhoB expression levels decrease during cancer progression, indicating a role for RhoB as a tumour suppressor (Huang and Prendergast, 2006). RhoB was shown to promote apoptosis and inhibit cell migration and invasion by antagonizing the Ras/PI3K/Akt pathway *in vivo* (Jiang *et al.,* 2004). Loss of RhoB, induced by miR-21 (microRNA 21), enhanced cell proliferation and invasion in colon cancer (Liu *et al.,* 2011). Different forms of RhoB have also been shown to be involved with cancer progression. Geranylgeranylated RhoB was found to prevent cell proliferation in Ras-transformed NIH3T3 mouse fibroblast (Mazières *et al.,* 2005), while farnesylated RhoB supported cell survival (Milia *et al.,* 2005).

1.4.1.2 The Rac subfamily proteins

All Rac subfamily proteins are known to stimulate the formation of membrane ruffles and lamellipodia (Ridley *et al.,* 1992; Nobes and Hall, 1995) by interacting with the WASP (Wiskott–Aldrich syndrome protein), WAVE (WASP-family verprolin homologue) or PAK (p21-activated kinases) families of effector proteins. These then activate the Arp2/3 complex and subsequently induce actin polymerization (Aspenström *et al.,* 1996; Machesky and Insall, 1998; Eden *et al.,* 2002; Ten Klooster *et al.,* 2006). Rac subfamily proteins are also involved in regulating cytoskeleton reorganization via LIM kinase-1 (LIMK-1), which in turn inactivates cofilin-induced actin depolymerization (Yang *et al.,* 1998).

Within the subfamily, Rac1, Rac2 and Rac3 share ≥89% sequence similarity, with the major differences within the C-terminal region (Haataja *et al.,* 1997). Despite their similarity, Rac1 is the only Rac subfamily member that can be palmitoylated at Cys178 and this has been shown

to regulate cell spreading and migration (Navarro-Lérida *et al.,* 2012). The final subfamily member, RhoG is a bit different as it shares only ~70% sequence similarity with the other members (Vincent *et al.,* 1992).

The role of Rac1 in cell proliferation, apoptosis and migration has been described (Moore *et al.,* 1997; Lassus *et al.,* 2000; Nikolova *et al.,* 2007; Nishiya *et al.,* 2005). For instance, Rac1 is involved in regulating cell cycle progression by activating the c-Jun kinase (JNK/SAPK) pathway (Olson *et al.,* 1995). Active Rac1 was targeted to membrane ruffles and focal adhesions in the leading edge of migrating cells by its interaction with a GEF, β-Pix (Ten Klooster *et al.,* 2006). Thus, deregulation of Rac1 activity is highly correlated with cancer progression, with overexpression of Rac1 found to increase cell growth and invasion in gastric cancer cells (Ji *et al.,* 2015). Rac1 was also required for K-Ras-induced proliferation and tumorigenicity of lung cancer *in vivo* (Kissil *et al.,* 2007).

Several *in vivo* studies show that depletion of Rac2 results in hematopoietic defects such as a lack of integrin-directed migration (Pradip *et al.,* 2003), adhesion (Yang *et al.,* 2001) and angiogenic response (De *et al.,* 2009). Overexpression of Rac2 induces the proliferation of quiescent cells in non-small cell carcinoma (NSCLC) by enhancing the expression of the transcription factor Jun-B (Pei *et al.,* 2018). It was also found to associate with poor prognosis of renal cancer by increasing the proliferation, migration and invasion of renal carcinoma cells (Liu *et al.,* 2019).

Despite having 93% sequence similarity with Rac1, Rac3 has been shown to oppose Rac1 function in regulating cell adhesion and differentiation, with Rac1 promoting and Rac3 inhibiting cell adhesion in neuronal cells (Hajdo-Milašinović *et al.,* 2007). Rac3 gene was mapped to 17q25.3, near the tumour suppressor gene BROV, that is frequently deleted in breast and ovarian cancer (Morris *et al.,* 2000). This indicates possible transcriptional deregulation of Rac3 in these cancers, consistent with previous findings that showed Rac3 was hyperactive in a highly proliferative breast cancer cell line and was important in promoting tumour growth via the Rac3-PAK pathway (Mira *et al.,* 2000).

The last member of the Rac subfamily proteins, RhoG is known to promote actin polymerization by regulating nuclear factor of activated T cells (NFAT) gene transcription in lymphocytes (Vigorito *et al.,* 2003) and stimulating macropinocytosis in fibroblasts in response to SH3-

containing Guanine Nucleotide Exchange Factor (SGEF) activation (Ellerbroek *et al.,* 2004). Several studies have shown an upstream role for RhoG in regulating Cdc42 and Rac1, with the activation of Cdc42 and Rac1 by RhoG necessary for the formation of membrane ruffles and filopodia (Gauthier-Rouvière *et al.,* 1998). For example, the role of RhoG in regulating cell migration was shown to involve the activation of Rac1 via the RhoG effector, ELMO and the ELMO-binding protein Dock180, which functions as a Rac1-specific GEF (Katoh *et al.,* 2006). In contrast, RhoG and Rac1 were found to have opposite roles in regulating the dynamics of invadopodia in breast cancer cells and this involved the activation of SGEF and adaptor protein, paxillin (Goicoechea *et al.,* 2017).

1.4.1.3 The Cdc42 subfamily proteins

Among the Cdc42 subfamily proteins, Cdc42, TCL and TC10 are classified as classical small GTPases, whereas Wrch1 and Wrch2 belong to the non-classical or atypical class, due to their unique N- and C-terminal extensions and being constitutively active because of their high intrinsic GDP dissociation rate. All the classical Rho, Rac1 and Cdc42 subfamily proteins share a series of effector proteins including the PAKs and formins (Manser *et al.,* 1994; Yasuda *et al.,* 2004) except for ACK, the BORGs and the SPECs that are exclusive for Cdc42 subfamily members (Manser *et al.,* 1993; Joberty *et al.,* 1999; Pirone *et al.,* 2000).

Cdc42 is known to mediate the formation of filopodia and cell polarity (Kozma *et al.,* 1995; Nobes and Hall, 1999). It is also shown to regulate cell cycle progression, growth, transformation and migration (Olson *et al.,* 1995; Qiu *et al.,* 1997; Raftopoulou and Hall, 2004). Cdc42 is also a negative regulator for Cbl-induced EGFR degradation (Wu *et al.,* 2003) and disrupting this mechanism leads to cell proliferation and migration in breast cancer (Hirsch *et al.,* 2006). Overexpression of Cdc42 has been found to promote cell migration and invasion in melanoma by regulating the E-cadherin and β-catenin expression (Tucci *et al.,* 2007). Similarly, upregulation of Cdc42 was found to promote cervical cancer cell migration by promoting pseudopodia formation (Ye *et al.,* 2014).

TC10 and TCL share 76% sequence similarity. They have 14 and 18 amino acids N-terminal extensions, respectively, that have been shown to influence their membrane association (Chunqiu

Hou and Pessin, 2003; Ackermann *et al.,* 2016). The N-terminus of TCL is also crucial in regulating the nucleotide binding pocket to allow effective GTP loading, however this was not observed for TC10 (Ackermann *et al.,* 2016; Florke *et al.,* 2017). TCL has been shown to be implicated in clathrin-mediated endocytosis and recycling of receptor-dependent internalized transferrin (De Toledo *et al.,* 2003). It has also been shown to modulate vessel formation and cell migration (Sukhbir, *et al.,* 2011), with overexpression of TCL found to promote angiogenesis and cancer cell migration through regulation of PAK1 (Kim *et al.,* 2014; Ho *et al.,* 2013).

TC10 is the only classical member of the Cdc42 subfamily that is palmitoylated and this palmitoylation event is important for the correct distribution of TC10 to the plasma membrane and endosomes (Michaelson *et al.,* 2001; Watson *et al.,* 2003). Active TC10 has been shown to be involved in transmembrane trafficking of the cystic fibrosis transmembrane conductance regulator (CFTR) (Cheng *et al.,* 2005) and exocytosis of GLUT4 (Chiang *et al.,* 2001). In cancer, mutated TC10 (N136S) was also found to promote actin cytoskeletal reorganization and cell invasion in colorectal cancer (Han *et al.,* 2014).

1.4.2 The non-classical Rho-family GTPases

The second group of Rho-family GTPases are known as atypical Rho GTPases and includes Wrch1, Wrch2, RhoD, RhoF, RhoH and the RhoBTB, Rnd and Miro subfamilies. Several comparative studies do not include Miro subfamily proteins and RhoBTB3 as genuine Rho-family members due to the lack of similarity between these proteins and the other members of the Rho-family. For instance, Miro subfamily proteins lack the Rho insert region and are assumed to be non-catalytic as the sequence in the highly conserved G2-G5 loops responsible for nucleotide binding and hydrolysis is very different in comparison to canonical GTPase domains (Fransson *et al.,* 2003; Boureux *et al.,* 2006). RhoBTB3 shares 25% sequence similarity with, and contains the same BTB domains as RhoBTB1 and RhoBTB2. However, this protein is not considered to be a Rho GTPase by some studies due to its lack of similarity with Rho and Ras (Boureux *et al.,* 2006; Aspenström *et al.,* 2007).

The atypical Rho GTPases often contain extra domains and are therefore longer than classical Rho GTPases (Figure 1.5) and importantly, they are not regulated by the standard GDP/GTP cycling

of small G proteins. These atypical small GTPases are further divided into fast-cycling and GTPase defective G proteins (Table 1.7).

Table 1.7: Selected amino acid sequences of the atypical and classical Rho GTPases

Amino acids 12, 59 and 61			
Group	**Subfamily**	**Member**	**Sequence**
Classic	Cdc42	Cdc42	**12** **59** **61** GD**G**AV---**A**G**Q**ED
Fast-cycling	Cdc42	Wrch1	GD**G**AV---**A**G**Q**ED
		Wrch2	GD**G**AV---**A**G**Q**DE
	RhoD		GD**G**GC---**A**G**Q**DD
	RhoF		GD**G**GC---**A**G**Q**ED
GTPase defective	RhoBTB	RhoBTB-1	GD**N**AV---**F**G**D**HH
		RhoBTB-2	GD**N**AV---**F**G**D**HH
	Rnd	Rnd1	GD**V**QC---**S**G**S**PY
		Rnd2	GD**A**EC---**S**G**S**SY
		Rnd3	GD**V**QC---**S**G**S**PY
	RhoH		GD**S**AV---**A**G**N**DA
Amino acids 28			
Classic	Rac	Rac1	**28** SYTTNA**F**PGEYIP
Fast-cycling	Cdc42	Wrch1	SYTTNGYPTEYIP
		Wrch2	SYTCNGYPARYRP
	RhoD		VFADGA**F**PESYTP
	RhoF		VYSQGS**F**PEHYAP

Amino acid residues 12, 28, 59 and 61 are in boldface type and underlined (Aspenström, 2017).

In resting cells, classical Rho-family GTPases are assumed to be in their inactive GDP-bound form either alone or in complex with RhoGDIs (Dovas and Couchman, 2005). Unlike the typical Rho-family GTPases, RhoD, RhoF, Wrch1 and Wrch2 have been shown to have a rapid nucleotide exchange compared to standard GTP hydrolysis which classifies them as "fast-cycling" small G proteins (Jaiswal *et al.,* 2012; Shutes *et al.,* 2004; Shutes *et al.,* 2006). Several studies identified Phe28 mutations of Ras, Rac1, Cdc42 and RhoA have rapid nucleotide exchange and can induce

oncogenic transformation (Lin *et al.,* 1997; Aspenström, 2018). Wrch1 and Wrch2 also have a mutated phenylalanine at position 28 (Table 1.7) and this might be one of the reasons to include both of these proteins as fast-cycling small G proteins.

Moreover, the fast-cycling Rho GTPases do have GTPase activity and have been shown to be identical to Cdc42 at amino acids Gly12, Ala59 and Gln61 (Ras numbering) (Table 1.7) (Aspenström, 2017). Gly12 and Ala59 are important for GTP hydrolysis, while Gln61 is necessary to stabilise the transition state of hydrolysis (Prive *et al.,* 1992). These amino acid residues have been reported to be mutated in GTPase-deficient Ras (Muñoz-Maldonado *et al.,* 2019). In contrast, the GTPase defective atypical Rho-family members, including Rnd1, Rnd2, Rnd3, RhoBTB1, RhoBTB2 and RhoH do not possess the conserved Gly12, Ala59 and Gln61, compared to Cdc42 (Table 1.7) (Aspenström *et al.,* 2007; Aspenström, 2017).

Many of the atypical small GTPases have been shown to have a functional CAAX box that allow them to undergo prenylation, the exceptions being Wrch1 and Wrch2, which have been shown to only undergo palmitoylation. Miro and RhoBTB subfamily proteins do not possess a canonical CAAX motif, except for RhoBTB3, which suggests this protein could undergo lipid modification, potentially farnesylation, however this is currently unproven (Table 1.8).

Table 1.8: C-terminal sequences of the atypical Rho-family GTPases and their subcellular distribution

Rho-family	C-terminal sequence	Lipid modification	Localisation
Wrch1/ RhoU	QQQPKKSKSRTPDKMKNLSKSWWKKYC**C**FV	P	PM, E
Wrch2/ RhoV/ Chp	EHKARLEKKLNAKGVRTLSRCRWKKFF**C**FV	P	PM, E
RhoD	AVFQEAAEVALSSRGRNFWRRITQGFCVVT	F, GG	PM and E
RhoF	EDVFREAAKVALSALKKAQRQKKRRLCLLL	F, GG	PM
Rnd1/ RhoS	LSKRLLHLPSRSELISSTFKKEKAKSCSIM	F	PM
Rnd2/ RhoN	MQRSAQLSGRPDRGNEGEIHKDRAKSCNLM	F	E, C
Rnd3/ RhoE	KRISHMPSRPELSAVATDLRKDKAKSCTVM	F	PM, G, C
RhoH/ TTF	VFECAVRTAVNQARRRNRRRLFSINECKIF	GG, F	EM
RhoBTB1	KREREKEDIALNKHRSRRKWCFWNSSPAVA	Unknown	V, G
RhoBTB2	KRRWLFWNSPSSPSSSAASSSSPSSSSAVV	Unknown	V
RhoBTB3	KHRWPSNMYLKQLAEYRKYIHSRKCRCLVM	Unknown	G
Miro1	KSSTFWLRASFGATVFAVLGFAMYKALLKQR	Unknown	MT
Miro2	SFWLRGLLGVVGAAVAAVLSFSLYRVLVKSQ	Unknown	MT

Putative palmitoylated cysteines are in boldface type and coloured red and CAAX prenylation motifs are underlined. (Data taken from: Ridley, 2006; Fransson *et al.,* 2006; Roberts *et al.,* 2008; Espinosa *et al.,* 2009; Murali and Rajalingam, 2014). GG: geranylgeranyl, F: farnesyl, P: palmitoyl, PM: plasma membrane, C: cytosol, N: nucleus, G: Golgi, E: endosomes, ER: endoplasmic reticulum, NE: nuclear envelope and EM: endomembrane.

1.4.2.1 Wrch1 and Wrch2

Wrch1 (RhoU) and Wrch2 (RhoV) belong to the Cdc42 subfamily due to sequence similarity. However, both have extended N-terminal and C-terminal regions (Figure 1.6). The N-terminus of Wrch1 contains 3 proline-rich motifs that are not crucial for nucleotide exchange activity (Shutes *et al.,* 2004) but facilitate the interaction with SH3 domain-containing adaptor proteins such as

Grb2 and Nck1 (Risse *et al.,* 2013). The interaction with Grb2 has been shown to promote Wrch1 activation and Wrch1-PAK1 association (Shutes *et al.,* 2004). Similarly, an N-terminally truncated mutant of Wrch2 has been found to promote transformation and increase anchorage-independent growth in NIH3T3 fibroblasts (Chenette *et al.,* 2005).

At their C-termini, Wrch proteins are modified by palmitoylation, which is essential for their localisation to plasma membrane and endosomes (Berzat *et al.,* 2005; Chenette *et al.,* 2006).

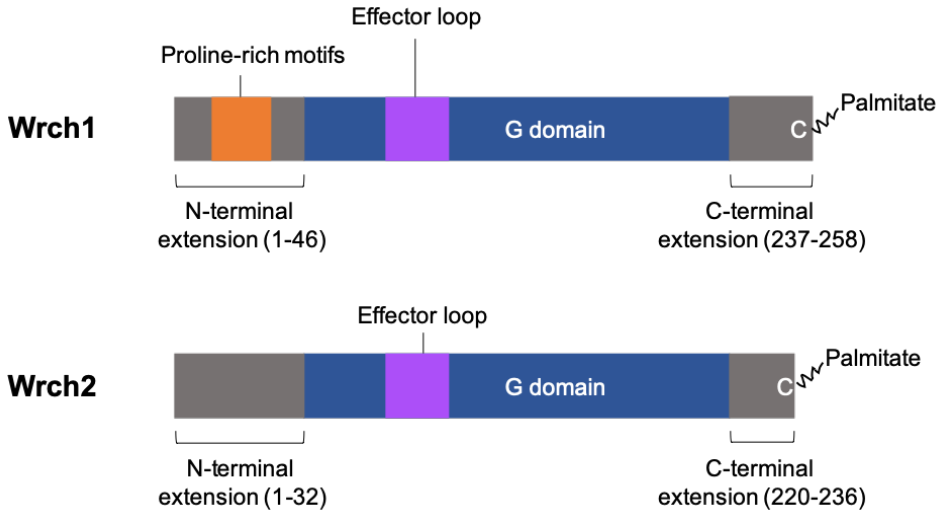

Figure 1.6: The architecture of Wrch1 and Wrch2. Both Wrch1 and Wrch2 contain a conserved G domain with N- and C-terminal extensions. The N-terminal extension of Wrch1 contains proline-rich motifs. There is a CFV motif at their C-termini, the cysteine of which is modified by palmitoylation.

Wrch1 has been found to regulate focal adhesion formation, potentially by modulating Myosin light chain (MLC) phosphorylation (Chuang *et al.,* 2007). Interestingly, Saras *et al.* (2004) also show that Wrch1 is more efficient than Cdc42 in stimulating filopodia formation. In cancer, PAK4 has been shown to interact with and protect Wrch1 from ubiquitination and degradation to drive breast cancer cell migration (Dart *et al.,* 2015). In contrast, low levels of Wrch1 has been shown to promote cell migration in colorectal cancer by increasing RhoA signalling (Slaymi *et al.,* 2019)

Wrch2 was initially discovered as an interacting partner for WASP and PAK2 in a yeast-two-hybrid (Y2H) screen (Aronheim *et al.,* 1998). Wrch2 was found to induce lamellipodia formation and apoptosis of PC12 cells by activating the JNK pathway (Aronheim *et al.,* 1998; Shepelev *et al.,* 2011) but the relevance of this to cancer progression is not known. Wrch2 mRNA levels have been shown to be upregulated in several cancer cell lines, including gastric, cervical, pancreatic, blood and lung (Katoh, 2002; Bhavsar *et al.,*2013; Shepelev and Korobko, 2013).

1.4.2.2 RhoD and RhoF

RhoD and RhoF were first classified as classical Rho-family GTPases due to their sequence similarity and overall architecture. However, a recent study by Jaiswal *et al.* (2012) proposes that both of these small G proteins should be classified as atypical Rho-family proteins due to their fast nucleotide exchange. They both also contain extra N-terminal sequences which are important for their correct subcellular distribution. For instance, the N-terminal extension of RhoD is important for regulating vesicle dynamics and plasma membrane localisation (Blom *et al.,* 2018). Both of these proteins have been found to be involved in the reorganisation of the actin cytoskeleton (Ellis and Mellor, 2000).

RhoD was initially shown to play a role in endosomal trafficking and dynamics through the activation of hDia2C and c-Src (Murphy *et al.,* 1996; Murphy *et al.,* 2001; Gasman *et al.,* 2003). This is consistent with data from Nehru *et al.* (2013) that found RhoD interacted with Rab5 effector, Rabankyrin-5, and colocalize to Rab5-positive endosomes. In addition, RhoD was also shown to promote actin filament formation through the FGF/RhoD/mDia3C pathway (Koizumi *et al.,* 2012) and therefore be involved in cell migration (Blom *et al.,* 2017). RhoD has been identified as a Golgi localized protein that is important in regulating Golgi homeostasis and is involved in vesicle trafficking from the endoplasmic reticulum to the plasma membrane (Blom *et al.,* 2015). An *in vivo* study revealed that overexpression of RhoD promotes cell proliferation and overduplication of centrosomes, suggesting a role in promoting cancer progression, which is still not well studied (Kyrkou *et al.,* 2013).

Compared to the ubiquitously expressed RhoD, RhoF is more tissue specific with highest expression in colon, stomach and spleen (Ellis and Mellor, 2000). RhoF was shown to promote

filopodia formation by targeting its effector mDia2 to the plasma membrane, independent of Cdc42 signalling (Pellegrin and Mellor, 2005; Gorelik *et al.,* 2010). Hence, overexpression of RhoF has been found to promote cell migration and enhance chemoresistance of pancreatic cancer by increasing the activation of the EMT process (Yang *et al.,* 2017).

1.4.2.3 The Rnd subfamily

Rnd subfamily proteins are most similar to the Rho subfamily compared to other Rho-family proteins, sharing ~40% sequence similarity. However, they possess a C-terminal extension and both Rnd1 and Rnd3 also have an additional 8 and 18 amino acids, respectively at their N-termini, which is important for plasma membrane targeting, These N-terminal extensions are also required for plasma membrane targeting of p190RhoGAP and correlated with its activity to mediate RhoA inhibition (Oinuma *et al.,* 2012). They are modified by farnesylation, not geranylgeranylation, at their C-termini and this is important for plasma membrane association (Roberts *et al.,* 2008). Within the subfamily, although they share more than 50% sequence similarity, the subcellular localization of the Rnd subfamily proteins is different, with Rnd1 and Rnd3 are plasma membrane associated and Rnd2 can be found in the cytosol or endomembranes (Roberts *et al.,* 2008). Rnd1 also shows mainly brain and liver expression, Rnd2 in testis, while Rnd3 is ubiquitously expressed but at low levels (Nobes *et al.,* 1998). The difference in their subcellular localisation is due to distinct sequences upstream of the CAAX motif (Pacary *et al.,* 2011).

Since Rnd subfamily proteins lack intrinsic GTPase activity and constitutively active, they are assumed not to be regulated by standard GTP/GDP cycling but by expression and post-translational modification (PTM). Several studies show that the expression of Rnd subfamily proteins is highly influenced by growth factors, for instance, Rnd1 transcript expression can be induced by VEGF (Suehiro *et al.,* 2014). Rnd3 is also induced by multiple DNA damage-inducing stimuli such as UV irradiation (Boswell *et al.,* 2007) and chemotherapeutic agents (Shurin *et al.,* 2008). The steroid hormone, oestradiol, upregulates both Rnd2 and Rnd3 expressions (Shimomura *et al.,* 2009). Phosphorylation of Rnd3 at Ser240 by PKCα was shown to prevent Rnd3 membrane localisation and promote stress fibre disruption by competing binding to ROCK1 and therefore inhibiting the RhoA-ROCK1 pathway (Riento *et al.,* 2005; Madigan *et al.,* 2009).

Rnd1 and Rnd3 have been shown to prevent actin stress fibres, membrane ruffles and focal adhesions formation, leading to cell rounding (Nobes *et al.,* 1998). This inhibitory effect was shown to involve Rnd1 interacting partners, including p190RhoGAPs and Syx (Table 1.9), which result in the inhibition of RhoA activity (Wennerberg *et al.,* 2003; Goh and Manser, 2010).

Table 1.9: List of examples interacting proteins for atypical Rho-family GTPases

Group	Rho GTPases	Interacting proteins
Cdc42	Wrch1	PAK1/4, ARHGAP30, Pyk2, PAR6, NCKβ
	Wrch2	PAK1/2/6, N-WASP, MLK
RhoBTB	RhoBTB1	Cullin 3, MUF1
	RhoBTB2	Cullin 3, Cullin 5, Hsp90, MUF1
	RhoBTB2	Cullin 3, Cullin 5, Cyclin B1, Cyclin E1, Hrs, 5-HT7a, LIMD1, Hsp90, MUF1, PHD2, Rab9A, Rab9B, TIP47
Rnd	Rnd1	p190RhoGAP, Socius, Plexin A1, Plexin B1, FLRT1, SCG10, FRS2α/β, Syx, Grb7
	Rnd2	p190RhoGAP, Socius, Pragmin, Plexin D1, Rapostlin, Vps4-A, MgcRacGAP
	Rnd3	p190RhoGAP, Socius, ROCK1, MgcRacGAP, Syx, Plexin B2
Miro	Miro1	TRAK1, TRAK2, KIF5, Dynein, DISC1, Parkin, Pink1, Mfn1/2, Cenp-F, HUMMR, Myo19
	Miro2	TRAK1, TRAK2, Parkin, Pink1, Mfn1/2, DISC1, Cenp-F
RhoH		PAK1-6, Lck, Csk, Zap70, Syk, Kaiso
RhoD		hDia2, c-src
RhoF		mDia1/2

(Data taken from: Murphy *et al.,* 1996; Murphy *et al.,* 2001; Gasman *et al.,* 2003; Saras *et al.,* 2004; Pellegrin and Mellor, 2005; Gorelik *et al.,* 2010; Azzarelli *et al.,* 2015; Tang *et al.,* 2015; Ji and Rivero, 2016; Hodge and Ridley, 2017; Mino *et al.,* 2018; Mouly *et al.,* 2019)

Rnd1 gene expression levels are frequently decreased or the genes deleted in cancer such as in breast cancer and hepatocellular carcinoma (HCC), in which low expression of Rnd1 has been shown to promote cell migration and invasion by increasing EMT via the MAPK pathway (Okada *et al.,* 2015; Qin *et al.,* 2018). Low levels of Rnd1 have also been shown to correlate with a decreased in overall survival of glioblastoma patients potentially by increasing cancer metastasis (Boyrie *et al.,* 2018).

In contrast to Rnd1, active Rnd2 was shown to bind and activate p190RhoGAP but this does not result in stress fibre disassembly and cell rounding (Wennerberg *et al.,* 2003). This suggests that Rnd2 acts differently to Rnd1 in regulating RhoA signalling especially in cancer. For instance, overexpression of Rnd2 has been found to stimulate RhoA-induced cell contraction in HeLa cells (Tanaka *et al.,* 2006) and result in aberrant neuronal differentiation and migration (Avansini *et al.,* 2018).

Similarly to Rnd1, Rnd3 has been shown to inhibit Ras- and Raf-induced fibroblast transformation (Villalonga *et al.,* 2004). Reduced expression of Rnd3 was also found to be inversely associated with tumour progression in glioblastoma (Liu *et al.,* 2015), suggesting a role as a tumour suppressor. This could be achieved by antagonizing RhoA signalling either by interacting with RhoA regulators and/or effector proteins. For instance, the interaction between Rnd3 and p190RhoGAP has been shown to stimulate GTP hydrolysis of RhoA (Wennerberg *et al.,* 2003) and Rnd3 interaction with ROCK1 was found to prevent stress fibre formation and cell migration (Riento *et al.,* 2003; Hidalgo-Carcedo *et al.,* 2011). Rnd3 also has a role as a cell-cycle regulator that does not involve RhoA signalling but is due to a decrease in the expression of cell cycle regulators, cyclin D1 and $p21^{cip1}$ (Villalonga *et al.,* 2004).

1.4.2.4 The RhoBTB subfamily

Similar to the Rnd subfamily, RhoBTB subfamily proteins are constitutively active due to defective hydrolysis activity. There are 3 members of ubiquitously expressed RhoBTBs, however only RhoBTB1 and RhoBTB2 are widely accepted as members of the Rho-family GTPases; RhoBTB3 has a considerably divergent G domain and found to bind and hydrolyse ATP instead of GTP (Aspenström *et al.,* 2007; Berthold *et al.,* 2008; Espinosa *et al.,* 2009).

Among the Rho-family GTPases, the RhoBTBs are the only subfamily that contains broad complex, tramtrack, and bric-a-brac (BTB) domains (Figure 1.7). BTB domains have been shown to be involved in protein dimerization and stabilisation. These domains interact with Cullin 3, a scaffold protein of ubiquitin ligase complexes involved in protein ubiquitination (Berthold *et al.,* 2008). Missense mutations in this domain of RhoBTB2 have been found to cause a developmental and epileptic encephalopathy (Straub *et al.,* 2018; Belal *et al.,* 2018). RhoBTB proteins also

contain a proline-rich region which is a potential SH3 domain-binding site and a C-terminal BACK (BTB and C-terminal Kelch) domain that is probably involved with substrate-recognition and orientation of Cullin 3-based ubiquitin ligase complexes (Stogios and Privé, 2004; Pintard *et al.,* 2004; Ji and Rivero, 2016).

RhoBTB3 also differs from RhoBTB1 and RhoBTB2 due to a short insert in the first BTB domain and a CAAX motif at its C-terminus, conferring the ability to undergo isoprenylation (Berthold *et al.,* 2008) but is not necessary for Golgi targeting (Espinosa *et al.,* 2009; Lu *et al.,* 2013).

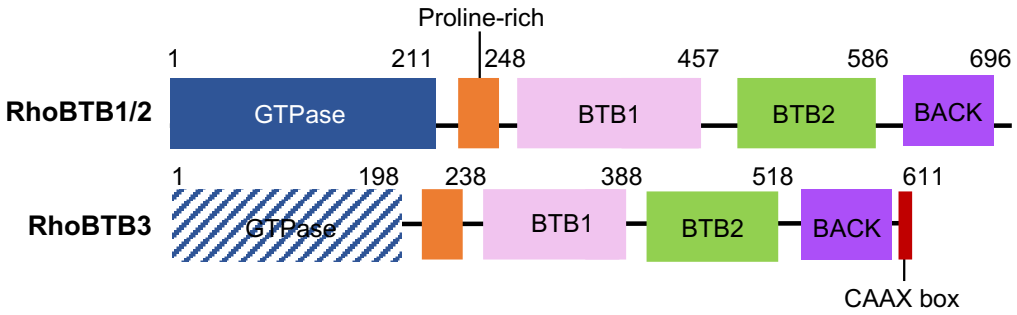

Figure 1.7: The domain architecture of RhoBTB proteins. The GTPase domain is followed by a proline-rich region, BTB domains and a carboxyl terminal BACK domain. The GTPase domain of RhoBTB3 is extremely divergent from other G domains. RhoBTB3 also has a shorter insert in the first BTB domain (BTB1) and contains a CAAX motif at the end.

Little is known about the normal cellular functions of RhoBTB1. However, it has been shown to localise to vesicular structures and is not thought to be involved in the regulation of the actin cytoskeleton organization (Aspenström *et al.,* 2004). RhoBTB1 is required to control Golgi integrity and inhibit breast cancer cell invasion by increasing METTL7B expression, a Golgi-associated methyltransferase (McKinnon and Mellor, 2017). The role of RhoBTB1 as a tumour suppressor was also observed in head and neck squamous cell carcinomas (HNSCC) (Beder *et al.,* 2006) and colon cancer, where it inhibits cell proliferation and invasion (Xu *et al.,* 2013).

The second member, RhoBTB2 acts as a transcriptional regulator by regulating CXCL14 expression, a chemokine that is involved in leukocyte migration and angiogenesis (McKinnon *et al.,* 2008). It has also been shown to be involved in cell cycle progression and apoptosis (Freeman, *et al.,* 2008), in which loss of RhoBTB2 was found to induce cell proliferation, colony formation and prevent apoptosis of breast cancer cells (Hamaguchi *et al.,* 2002; Mao *et al.,* 2011; Choi *et al.,* 2017). Loss of RhoBTB2 has also been found in several other cancers such as gastric (Gu Cho *et al.,* 2008) and osteosarcoma (Jin *et al.,* 2013).

Golgi-associated RhoBTB3 has been shown to maintain Golgi structure and be associated with Rab9 to mediate protein trafficking from endosomes to the Golgi (Lu and Pfeffer, 2013; Espinosa *et al.,* 2009). Similar to the other two RhoBTB proteins, loss of RhoBTB3 has been reported in several cancers such as breast and kidney (Berthold *et al.,* 2008).

1.4.2.5 The Miro subfamily

Miro subfamily members are mitochondria- and peroxisome-associated small G proteins (Fransson *et al.,* 2003; Covill-Cooke *et al.,* 2020). They have been shown to control mitochondrial dynamics, motility and apoptosis (Frederick *et al.,* 2004; MacAskill *et al.,* 2009; Fransson *et al.,* 2003) and have been found to regulate peroxisomal size and morphology (Covill-Cooke *et al.,* 2020). Both Miro proteins have two GTPase domains, one each at the N- and C-termini (Figure 1.8). The N-terminal GTPase domain has been shown to be involved in GTP hydrolysis and is required for regulating mitochondria morphology (Peters *et al.,* 2018; Babic *et al.,* 2015).

They also contain a pair of calcium binding EF-hand motifs, that are important for the binding to Ca^{2+} to regulate mitochondrial motility, and a C-terminal transmembrane domain that is needed for association with the mitochondrial outer membrane and the cytosolic chaperone, Pex19 (Fransson *et al.,* 2003; Frederick *et al.,* 2004; MacAskill *et al.,* 2009; Covill-Cooke *et al.,* 2020). Furthermore, Miro proteins also contain two non-canonical “hidden” EF (hEF) hand motifs, followed by LM helices that are important for stabilisation of the adjacent EF hands (Yamaoka and Hara-Nishimura, 2014; Klosowiak *et al.,* 2013). Less is known about the C-terminal G domain of the Miro proteins but recent studies show that this domain is structurally similar to the Ras

homologue, Rheb and catalytically active as an NTPase with binding propensities towards both GTP and ATP (Klosowiak *et al.,* 2013; Peters *et al.,* 2018).

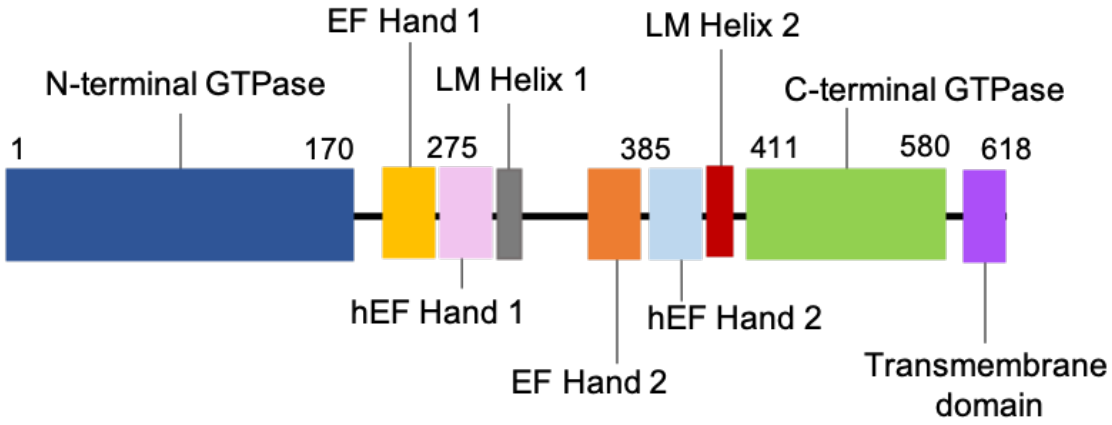

Figure 1.8: The architecture of Miro proteins. Miro subfamily proteins contain an N-terminal and a C-terminal GTPase domain, two EF hand motifs, two hidden EF hand (hEF) motifs, two ligand mimic (LM) helices and a C-terminal transmembrane domain.

Within the subfamily, Miro1 shares 60% sequence similarity with Miro2. Miro1 was found to mediate mitochondrial trafficking through its interacting partners, the KIF5 motor proteins (Table 1.9) (MacAskill *et al.,* 2009; Schuler *et al.,* 2017) and by stabilising a myosin, Myo19 (Oeding *et al.,* 2018). Miro1 is also required to maintain correct mitochondrial morphology and intracellular distribution during embryogenesis (Yamaoka *et al.,* 2011). Miro2 has been shown to promote mitochondrial motility and prevent mitochondria fragmentation by forming a multiprotein complex with PINK1 kinase and a motor adaptor protein, Milton/TRAK (Weihofen *et al.,* 2009). Both Miro1 and Miro2 are subjected to PINK1- and Parkin E3 ligase-mediated degradation in mitophagy with Miro2 degradation occurring at a much slower rate compared to Miro1 (Liu *et al.,* 2012). This is necessary because Miro2 is required to facilitate Parkin translocation to depolarised mitochondria to induce ubiquitination and start the mitophagy process (Wang *et al.,* 2019).

Defects in mitochondrial motility and distribution due to aberrant regulation of Miro proteins have been reported in several neurological disease such as Parkinson disease and Alzheimer's (Kay *et*

al., 2018). Miro proteins also have a role in cancer with high levels of Miro1 found to promote cell proliferation and migration by suppressing the expression of SMAD4 (Desai *et al.,* 2013; Li *et al.,* 2015). Reduced expression of Miro1 but not Miro2 was shown to suppress tumour cell invasion in response to low levels of its interacting partner, the mitochondrial motility regulator, Syntaphilin (SNPH) (Caino and Altieri, 2017).

1.4.2.6 RhoH

RhoH contains a shorter Rho insert region that is more similar to classical Rho-family proteins but is GTPase defective due to the absence of conserved residues corresponding to Gly12, Ala59 and Gln61 (Ras numbering) (Table 1.7). RhoH does have a CAAX box at its C-terminus which allows isoprenylation and membrane targeting. RhoH also has a unique C-terminal region located in between its polybasic region and CAAX box that is important in regulating RhoH stability via chaperone-mediated autophagy (Troeger *et al.,* 2013).

Unlike other Rho-family proteins, RhoH does not regulate actin reorganisation in NIH3T3 or MDCK cells (Li *et al.,* 2002). However, a study from Mino *et al.* (2018) showed that RhoH is involved in modulating the structure of the actin-cytoskeleton and transcriptional activity during T cell migration and adhesion by forming a multi-protein complex with p120 catenin and the transcriptional regulator, Kaiso, to attenuate Rac1 signalling. RhoH has also been shown to negatively regulate cell proliferation, survival and chemokine-induced migration of hematopoietic progenitor cells (HPCs) (Gu *et al.,* 2005). However, RhoH has also been shown to promote cell migratory polarity in prostate cancer by directing Rac1 and PAK2 to membrane protrusions (Tajadura-Ortega *et al.,* 2018).

1.4.3 Regulation of Rho-family GTPases

The classical or typical Rho-family GTPases are regulated by switching between an inactive GDP-bound form and an active GTP-bound form in a similar fashion to other members of the Ras superfamily. This cycle is regulated by RhoGEF, RhoGAP and RhoGDI proteins, as described in Section 1.3. However, there are other ways in which their activation is modulated such as regulation by gene expression and post-translational modification.

1.4.3.1 RhoGEF proteins

As described previously, most of classical Rho-family GTPases are regulated by GEFs from the Dbl-homology family, which containing a DH-PH tandem domain (Hart *et al.,* 1991; Abdrabou and Wang, 2018). Examples of this family are the Vav-family members: Vav1, Vav2 and Vav3. Vavs behave as phosphorylation-dependent molecular switches and are controlled by several tyrosine kinases, including Syk, Src and Janus kinases (Bustelo, 2014). The Vav proteins are phosphorylated at tyrosine residues in their AC domain (Figure 1.9) and this activates their exchange activity towards target small GTPases. The link between phosphorylation and Vav1 activation was initially found by Crespo *et al.* (1997), by comparing the ability of non-phosphorylated Vav1 and phosphorylated Vav1 to catalyse GDP/GTP exchange on Rac1.

The catalytic activity of Vav proteins towards Rho-family GTPases requires the cooperation of the DH and PH domains with the zinc finger (ZF) region. The DH domain functions to catalyse guanine nucleotide exchange and the PH domain is responsible for stabilising the DH domain for efficient GEF activity (Turner and Billadeau, 2002; Rapley *et al.,* 2008). The ZF domain coordinates with the catalytic DH region to promote both the binding to Rho-family GTPases and the exchange of GDP for GTP (Movilla and Bustelo, 1999).

All the Vav-family proteins share a similar domain architecture (Figure 1.9) and have been found to regulate Rac1, RhoA, RhoG and Cdc42 (Kaminuma *et al.,* 2001; Rapley *et al.,* 2008; Schuebel, 1998; Movilla and Bustelo, 1999; Abe *et al.,* 2000).

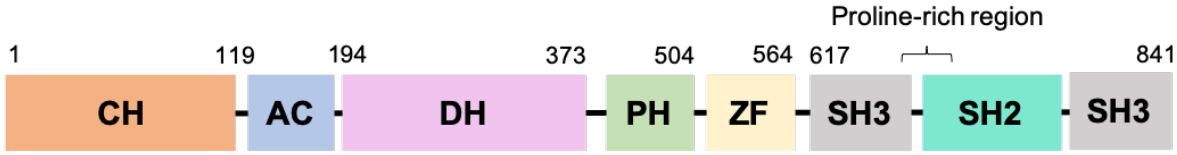

Figure 1.9: Schematic representation of Vav protein domain architecture. CH: Calponin-homology domain, AC: Acidic domain, DH: Dbl-homology domain, PH: Pleckstrin homology domain, ZF: Zinc finger domain, SH3: SRC-homology 3 domain and SH2: SRC-homology 2 domain.

Vav1 was initially discovered as an oncogene due to its ability to induce tumorigenic growth in NIH3T3 mouse fibroblasts (Katzav *et al.,* 1989). Later research also showed overexpression of Vav1 to be associated with several cancers, including pancreatic (Fernandez-Zapico *et al.,* 2005) and lung (Lazer, *et al.,* 2009). Vav2 has been found to be hyperactivated in HNSCC (Patel *et al.,* 2007), whilst overexpression of Vav3 has been identified in prostate cancer (Dong *et al.,* 2006), breast cancer (Lee *et al.,* 2008) and colorectal cancer (Uen *et al.,* 2015). Aberrant expression of Vav family proteins has also been reported to inversely correlate with cancer patient survival rate by promoting carcinogenesis events such as increased tumour cell survival, proliferation, neoangiogenesis and invasion (Razidlo *et al.,* 2015).

1.4.3.2 RhoGAP proteins

RhoGAPs function to terminate the signal transduction of most of Rho-family GTPases by stimulating their intrinsic GTP hydrolysis activity, which is relatively slow. ~70 RhoGAPs have been identified to date and this obviously outweigh the number of Rho-family GTPases considerably. A few of the RhoGAPs display a broad specificity but most are specific for a single Rho GTPases (Table 1.3). p50RhoGAP, ARAP1 and ARAP3 are examples of RhoGAPs that have broad specificity and have been found to interact with and inactivate RhoA, Rac1 and Cdc42, whereas GMIP only shows activity towards RhoA (Tcherkezian and Lamarche-Vane, 2007; Aresta *et al.,* 2002).

One of the best studied RhoGAPs is p190RhoGAP, which has been reported to bind and inactivate RhoA, RhoC, Rac1 and Rnd3. RhoA inactivation by p190RhoGAP is needed to stimulate cell spreading and migration (Arthur and Burridge, 2001). Rnd1 and Rnd3 have been shown to bind and activate p190RhoGAP to inhibit RhoA activity, indicating a role for p190RhoGAP in mediating Rho-family GTPases co-ordinated signalling (Oinuma *et al.,* 2012).

There are two isoforms of p190RhoGAP, known as p190A and p190B. Both of these are multidomain proteins, containing an N-terminal GTPase domain (N-GTPase) which has been recently classified as a pseudo-GTPase domain that binds to GTP/Mg^{2+} but have lacks intrinsic catalytic activity (Stiegler and Boggon, 2018). They also have four FF domains, which are important for binding interacting partners such as the transcriptional factor TFII-I (Jiang *et al.,*

2005) and Rac1•GTP (Bustos *et al.,* 2008), and two pseudo-GTPase domain (pG1/pG2), which have no nucleotide-binding activity (Stiegler and Boggon, 2018). The pG1/G2 domains and the FF domains are necessary for regulating GAP activity and lamellipodia targeting of p190RhoGAP (Bidaud-Meynard *et al.,* 2019). The polybasic region interacts with acidic phospholipids and is required to regulate the GAP catalytic function of p190RhoGAP (Lévay *et al.,* 2013; Héraud *et al.,* 2019).

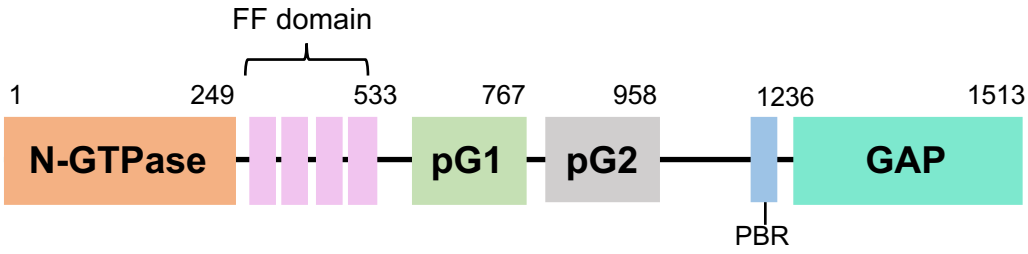

Figure 1.10: Schematic representation of p190RhoGAP protein structure. N-GTPase: N-terminal GTPase domain, four FF domains, pG1/pG2: pseudo GTPase domain 1 and 2, PBR: polybasic region and a GAP domain: GTPase activating proteins domain.

p190RhoGAP was initially identified as a tumour suppressor by Wang *et al.* (1997) as its overexpression was shown to inhibit Ras-induced malignant transformation in fibroblasts. Furthermore, inactivation of Rho signalling by p190RhoGAP has been shown to induce apoptosis in breast cancer (Ludwig and Parsons, 2011). However, several studies have also reported the involvement of p190RhoGAP in promoting cancer progression as it was found to be upregulated in several cancers, including osteosarcoma, colorectal cancer, lung adenocarcinoma and breast cancer, where increased levels correlate with increased cell migration, invasion and poor survival of patients (Shen *et al.,* 2008; Héraud *et al.,* 2019).

1.4.3.3 RhoGDI proteins

While approximately 150 RhoGEFS and RhoGAPs are currently known, only three RhoGDIs have been identified in mammals and their roles are not yet fully understood (Rocks *et al.,* 2018). Thus, it is interesting to know how the three RhoGDIs control the complexity of Rho GTPase signalling. As discussed in section 1.3.3, there is growing evidence showing the involvement of RhoGDIs not only as the negative regulators of Rho-family GTPases but also act as chaperones which target these small GTPases to their correct subcellular compartments. For instance, the interaction between RhoGDI-1 and Rac1 is needed to ensure the correct plasma membrane localisation of Rac1 in response to hepatocyte growth factor (HGF) stimulation (Chianale *et al.,* 2010). Similarly, a Cdc42 mutant that failed to interact with RhoGDI-1 was found to accumulate in the perinuclear membrane region as opposed to the cytoplasm and therefore affect Cdc42-stimulated cellular transformation (Lin *et al.,* 2003).

RhoGDIs also function to protect the Rho-family GTPases from proteasome-mediated degradation. For example, RhoGDI-1 has been shown to stabilise RhoA, RhoB, Rac1 and Cdc42 protein levels (Boulter *et al.,* 2010; Ho *et al.,* 2008). RhoGDIs also help to maintain both the inactive cytosolic pool and active membrane pool of Rho-family GTPases by forming a high affinity complex with the C-terminal isoprene of the small GTPases in the cytoplasm and mediating the correct delivery and extraction of Rho-family GTPases to and from membranes (Cho *et al.,* 2019).

The interaction between the RhoGDIs and the target Rho GTPases involves both major domains of the RhoGDIs; the N-terminal regulatory arm domain and the C-terminal immunoglobulin-like domain (Figure 1.11). Both domains contribute significantly to the binding and inhibitory actions of the RhoGDI proteins. The C-terminal IgG domain of the RhoGDIs forms a hydrophobic cleft that binds to the isoprenylated group at the C-termini of the Rho-family proteins (Figure 1.11B) thus disallowing membrane association. The N-terminal domain binds to the switch regions of the target small GTPases, preventing nucleotide exchange (Dransart, *et al.,* 2005; Cho *et al.,* 2019). The N-terminal domain was also found to target the RhoGDI-1-Rac1 complex to the phagosome (Ueyama *et al.,* 2013). While all three RhoGDIs share the same domain architecture, RhoGDI-3 has an N-terminal extension predicted to contain an additional amphipathic helix (AH) from

residues 5-28, crucial for Golgi targeting and stabilizing the cytoplasmic RhoG-RhoGDI-3 complex (Brunet *et al.,* 2002) (Figure 1.12).

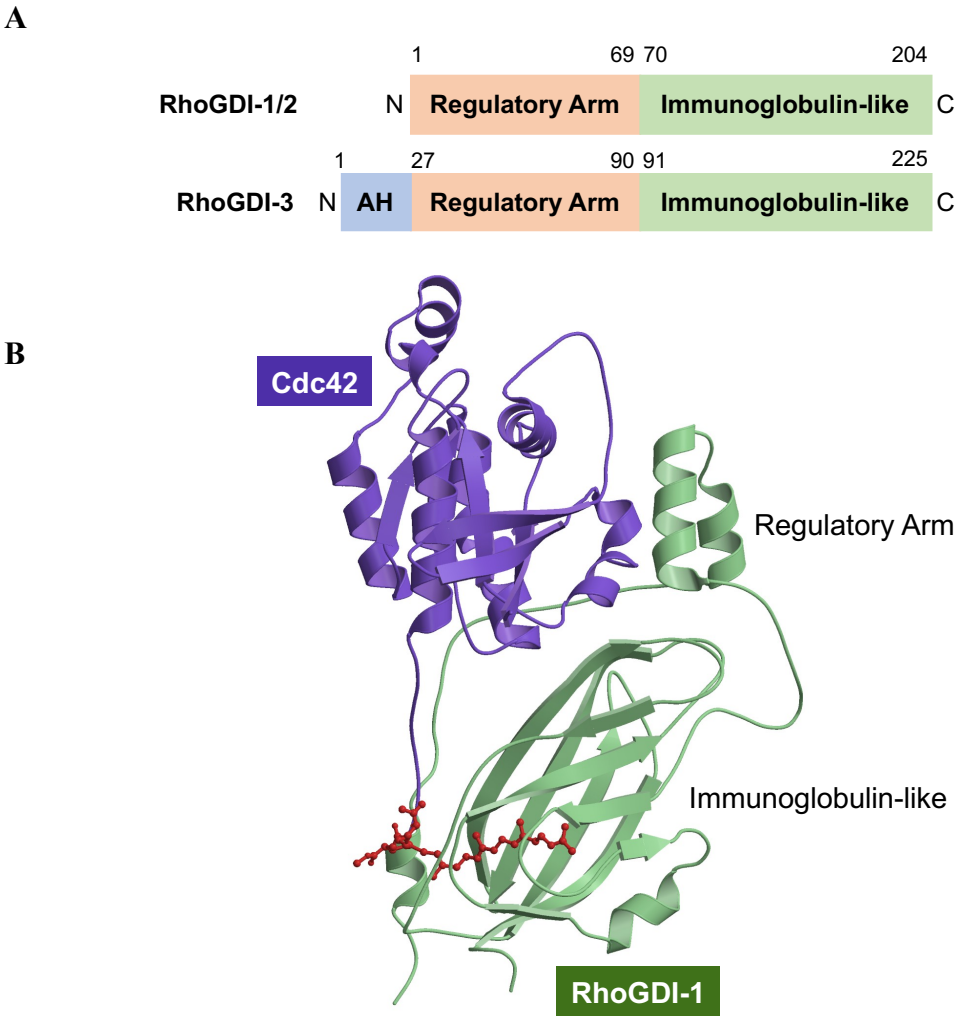

Figure 1.11: Structure and architecture of the RhoGDIs protein. (A) Each of the RhoGDIs shares an N-terminal regulatory arm domain (residues 1–69, RhoGDI-1 numbering) and a C-terminal immunoglobulin-like domain (residues 70–204, RhoGDI-1 numbering). RhoGDI-3 has a small additional amphipathic helix (AH) (residues 1-26, RhoGDI-3 numbering) towards its N-terminus. **(B)** Ribbon structure of RhoGDI-1-Cdc42 complex is adapted from Owen and Mott, (2005), with Cdc42 in purple and RhoGDI-1 in green. Cdc42 prenyl group is shown as sticks in red.

RhoGDI-1 and 2 share 70% sequence similarity, whereas RhoGDI-3 shows 60% identity with either RhoGDI-1 and RhoGDI-2. The most divergent amino acids between these three RhoGDIs are concentrated at their N-termini (Figure 1.12). Despite their sequence similarities, all three differ in terms of protein expression and selectivity towards Rho-family GTPases.

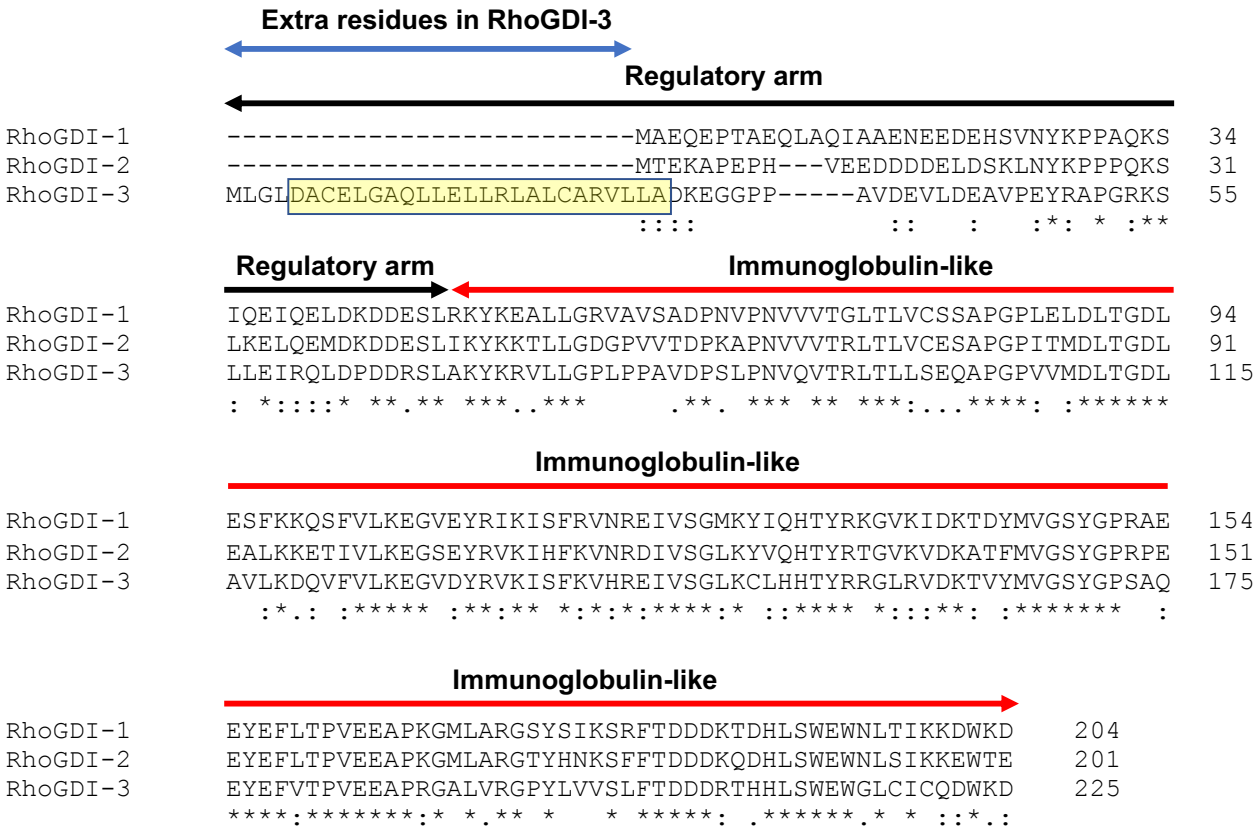

Figure 1.12: Sequence alignment of all three RhoGDIs. The sequence of all three RhoGDIs was aligned using the multiple sequence alignment programme, Clustal Omega. The regulatory arm and immunoglobulin-like domains are shared by all three RhoGDIs, and are shown by black and red lines, respectively. The additional N-terminal amino acids of RhoGDI-3 (1-26) are shown by the blue line. The amphipathic helix (AH) predicted to extends from residues 5-28 in RhoGDI-3 is highlighted in yellow. Asterisk (*) single, fully conserved residue, colon (:) conservation between groups of strongly similar properties and period (.) conservation between groups of weakly similar properties.

RhoGDI-1 is ubiquitously expressed and was found to form complexes with RhoA, RhoC, Rac1, Rac2, Cdc42 and RhoG (Olofsson, 1999; Elfenbein *et al.,* 2009). In contrast, RhoGDI-2 was

discovered to express primarily in hematopoietic and endothelial cells (Lelias *et al.,* 1993). RhoGDI-2 has been shown to interact with several Rho-family GTPases, including RhoA, Rac1, Cdc42, Rac2 and RhoC (Scherle *et al.,* 1993; Adra *et al.,* 1993; Golovanov *et al.,* 2001; Griner *et al.,* 2015). However, RhoGDI-2 appears to be less potent than RhoGDI-1 (Adra *et al.,* 1993) and this may be due to differences at the amino acid levels (Platko *et al.,* 1995; Nomanbhoy and Cerione, 1996). The third member of the RhoGDI family is RhoGDI-3, which is widely expressed especially in brain, lung, kidney and testis. By Y2H screening, Zalcman *et al.* (1996) found that RhoGDI-3 bound to RhoB and RhoG, but not to RhoA, RhoC or Rac1 proteins.

1.4.3.3.1 Regulation of the RhoGDI proteins

The target binding specificities of the RhoGDIs suggest that different RhoGDIs might influence different signalling pathway but the molecular reason behind their selectivity is still not well understood. However, their interactions could be regulated by several mechanisms such as by phospholipids, interactions and post-translational modifications (Cho *et al.,* 2019).

Regulation involving several biological lipids has been shown to modulate the interaction between RhoGDIs and target Rho-family GTPases (Chuang *et al.,* 1993). For example, binding between RhoA and RhoGDI-1 was shown to be affected by the presence of the phosphoinositides, $PtdIns_4P$ and $PtdIns_{4,5}P_2$, allowing the activation of RhoA (Fauré *et al.,* 1999). The stability of the Rac1- or 2-RhoGDI-1 complexes were also found to be regulated by phagocyte membranes enriched in anionic phospholipids (Ugolev *et al.,* 2006). Furthermore, phosphatidic acid generated by DGKζ, (diacylglycerol kinase) has been shown to activate PAK1 which then leads to RhoGDI-1 phosphorylation and subsequently promotes dissociation of Rac1 from RhoGDI-1 (Abramovici *et al.,* 2009).

The association between Rho-family GTPases and RhoGDIs can also be modulated by specific proteins, including the tyrosine kinase Etk, the Eph receptor ligand EphrinB1 and the adaptor protein 14-3-3τ. Etk was shown to interact with and phosphorylate RhoA at Ser88 and Thr100, resulting in RhoA dissociation from RhoGDI-1 and therefore stimulate membrane translocation and activation of RhoA and its activation (Kim *et al.,* 2002; Tong *et al.,* 2016). A recent study from Cho *et al.* (2018) also discovered that the interaction between EphrinB1 and RhoGDI-1

enhances RhoA-induced cell migration in lymph node and breast cancer cell lines by displacing RhoA from RhoA-RhoGDI-1 complex. The adaptor protein, 14-3-3τ has also been shown to interact with RhoGDI-1 and this disturbs its association with Rho-family GTPases. This then promotes breast cancer cell invasion and metastasis through EGF-induced RhoA, Rac1, and Cdc42 activation (Xiao *et al.,* 2014).

Regulation involving post-translational modification of RhoGDIs either through phosphorylation, ubiquitination and sumoylation has also been observed (Table 1.10). For instance, DerMardirossian *et al.* (2006) found that Src binds and phosphorylates RhoGDI-1 at Tyr156. This phosphorylation event caused a dramatic decrease in the ability of RhoGDI-1 to form a complex with RhoA, Rac1 or Cdc42. Dephosphorylation of RhoGDI-1 by integrin-bound PTP-PEST stimulated the release of RhoGDI-1 from the membrane and promoted its interaction with GDP-bound Rac1 or Cdc42 in the cytoplasm (Lee *et al.,* 2015). Fei *et al.* (2010) have also shown that phosphorylation of RhoGDI-1 by Fer tyrosine kinase prevents the binding of Rac1 to RhoGDI-1 and, as a result, promotes localization of Rac1 to the membrane where it can exert its function. Besides promoting the release of Rho-family GTPases from RhoGDIs, phosphorylation has also been shown to stabilise some complexes and this subsequently inhibits signalling. For instance, phosphorylation of RhoGDI-1 by PKA at Ser174 increased the binding between RhoA and RhoGDI-1, resulting in the inhibition of RhoA signalling and morphological changes in cardiac fibroblasts (Oishi *et al.,* 2012).

Ubiquitination and sumoylation of RhoGDIs can also regulate their interaction with Rho-family GTPases. Sumoylation of RhoGDI-1 at Lys138 is important for RhoGDI-1 to inhibit RhoA, Rac1 and Cdc42 activation and this then prevents cancer cell motility (Yu *et al.,* 2012; Cao *et al.,* 2014). An E3 ligase, gene related to anergy in lymphocytes (GRAIL) has been shown to interact with and stimulate RhoGDI-1 poly-ubiquitination via Lys63 linkage. However, RhoGDI-1 ubiquitination did not lead to its degradation but rather increased RhoGDI-1 stability and therefore prevented RhoA activation by promoting association of RhoA-RhoGDI-1 (Su *et al.,* 2006).

Table 1.10: Post-translational modifications of RhoGDIs

PTMs	Regulator	Target site	RhoGDI	Effect
Phosphorylation	Src	Tyr27, Tyr156	RhoGDI-1	Dissociation of RhoA, Rac1 and Cdc42
	PKA	Ser174		Association of RhoA
	PKCα	Ser96, Ser34		Dissociation of RhoA and Rac1
	Src	Tyr24, Tyr153	RhoGDI-2	Dissociation of Rac1
	PKCα	Ser34		Dissociation of Rac1
	Syk	Tyr24, Tyr153		Increase RhoGDI-2 association with the membrane
	c-Abl	Tyr130, Tyr153		Regulate PSGL-1-induced β1 integrin-mediated lymphocyte adhesion to VCAM-1.
Dephosphorylation	PTP-PEST	Tyr156	RhoGDI-1	Inactivation of Rac1 and Cdc42
	PPM1B	Ser174	RhoGDI-1	Inactivation of RhoA, Rac1 and Cdc42
Sumoylation	ND	Lys138		
Ubiquitination	GRAIL	ND	RhoGDI-1 RhoGDI-2	Inhibit RhoA activation
Acetylation	p300, pCAF	Lys127, Lys141	RhoGDI-1	Dissociation of RhoA
Oxidation	ND	ND		Activation of RhoA

(Data taken from: DerMardirossian *et al.,* 2006; Wu *et al.,* 2009; Griner *et al.,* 2013; Luo *et al.,* 2013; Cho *et al.,* 2019; Liu *et al.,* 2019). ND: not determine

1.4.3.3.2 Regulation of the RhoGDI-Rho-family target interactions

RhoGDI-Rho complexes can also be regulated by the phosphorylation of Rho-family proteins. Phosphorylation of RhoA at Ser188 by PKA increases its association with RhoGDI-1 and this then terminates RhoA activity at the leading edge of migratory cells (Tkachenko *et al.,* 2011). Rac1 phosphorylation at Tyr64 by FAK and Src has also been shown to promote its association with RhoGDI-1 and prevent Rac1 association with focal adhesion complex and therefore prevent Rac1-induced cell spreading (Chang *et al.,* 2011).

Correct RhoGDI-Rho protein interactions are also important to ensure proper signalling activation. For instance, the dynamic balance between RhoA and RhoC mediated by RhoGDI-1 has been shown to be important in regulating cancer cell growth and migration (Giang Ho *et al.,* 2011). Furthermore, Golding *et al.* (2019) have shown that RhoGDI-1 differentially regulates Cdc42 and RhoA extraction from plasma membrane to ensure correct spatiotemporal patterning around cell wounds. Phosphorylation of RhoA by PKG was also shown to increase RhoA association with RhoGDI-1, leading to displacement of bound Rac1. Free Rac1 can then translocate to the membrane and be activated by, for example, the GEF, Vav3 (Rolli-Derkinderen *et al.,* 2010).

1.4.3.3.3 RhoGDI proteins in cancer

The levels of RhoGDIs proteins appear to be approximately equal to the total levels of RhoA, Rac1 and Cdc42 in the cell, suggesting that any condition that contributes to an imbalance in this system would affect the activation of Rho-family proteins, a situation frequently observed in cancer (Michaelson *et al.,* 2001; Gildea *et al.,* 2002). For instance, overexpression of RhoGDI-1 was found to increase RhoA protein levels and therefore promotes RhoA-induced PI3K-Akt signalling pathway in hepatocellular carcinoma (Wang *et al.,* 2014). In contrast, downregulation of RhoGDI-1 was found to promote the EMT process by stimulating the expression of the transcription factor, Snail (Song *et al.,* 2014), suggesting its role as a tumour suppressor.

RhoGDI-2 is also differentially expressed in cancer. Increased expression of RhoGDI-2 has been found in ovarian, gastric and pancreatic cancers (Tapper *et al.,* 2001; Cho *et al.,* 2009; Yi *et al.,* 2015). In gastric cancer, upregulation of RhoGDI-2 was shown to stimulate gastric cancer cell metastasis and chemoresistance by enhancing VEGF-C (vascular endothelial growth factor C) expression (Jun Cho *et al.,* 2014). In addition, the regulation of multi-drug resistance in gastric cancer was reported to involve RhoGDI-2-mediated P-glycoprotein expression via Rac1 activation (Zheng *et al.,* 2015). Decreased expression of RhoGDI-2 was found to be highly associated with invasive and metastatic phenotypes in bladder cancer, breast cancer and leukemia (Theodorescu, 2004; Hu *et al.,* 2007; Nakata *et al.,* 2008). RhoGDI-2 has also been shown to suppress cell invasion in lung cancer by regulating the expression of genes involved in EMT, including E-cadherin, Slug, Snail and α-SMA (Niu *et al.,* 2014).

Compared to the other RhoGDIs, the role of RhoGDI-3 has been poorly studied. However, decreased expression of RhoGDI-3 expression has been found in breast cancer and in the late stage of pancreatic cancer, which correlate with metastasis (Jiang *et al.,* 2003; de León-Bautista *et al.,* 2016).

1.5 Cdc42 signalling

As discussed previously, Cdc42 is a known regulator of the actin cytoskeleton, controlling basic physiological processes such as cell proliferation and migration (Gómez Del Pulgar *et al.,* 2008). In response to various upstream signals which either come from cell surface receptors or cell adhesion molecules, Cdc42 activates a series of distinct effector proteins (Table 1.6), thus promoting diverse signalling cascades.

1.5.1 Activated Cdc42-associated kinase (ACK)

1.5.1.1 The domain architecture of ACK

ACK was the first effector protein to be identified for Cdc42 and is a non-receptor kinase (NRTK) (Manser *et al.,* 1993). There are 10 families of mammalian NRTKs: Src, Abl, Jak, ACK, Csk, Fak, Fes, Frk, Tec and Syk (Blume-Jensen and Hunter, 2001). Among the NRTKs, ACK is the only kinase with an SH3 domain located C-terminal to the kinase domain. Thus, it is likely that the regulation of ACK is different from other NRTKs.

The *TNK2* (ACK) gene encodes for 1038 amino acids (~120 kDa) and is located on human chromosome 3q29. Figure 1.13 shows the domain architecture of human ACK which includes an N-terminal SAM (sterile alpha motif) domain. SAM domains are generally known to be involved in self-association and facilitated protein-protein interaction (Kim and Bowie, 2003). In ACK, the SAM domain has been shown to mediate ACK dimerization and promote its autophosphorylation (Prieto-Echagüe *et al.,* 2010). Lin *et al.* (2010) also found the SAM domain regulates ACK ubiquitination by NEDD4-1, which suggests the involvement of this domain in modulating ACK stability.

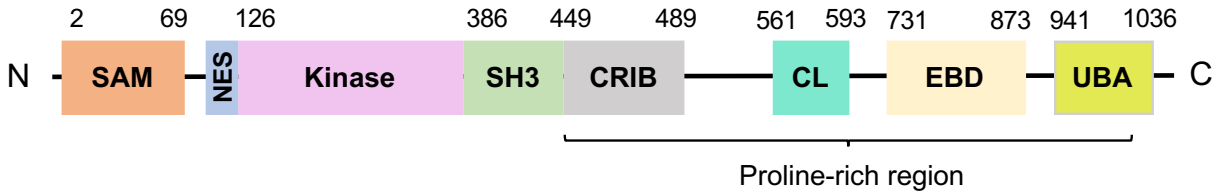

Figure 1.13: Domain architecture of ACK. SAM: sterile α motif, NES: nuclear export signal, Kinase: tyrosine kinase domain, SH3: Src Homology 3 domain, CRIB: Cdc42/Rac interacting binding region, CL: Clathrin-interacting region, EBD: EGFR binding domain and UBA: ubiquitin-association domain.

ACK also contains an NES (nuclear export signal), suggesting a role for ACK in the nucleus (Ahmed *et al.,* 2004) but how ACK enters the nucleus is still undefined. However, the interaction of ACK with Cdc42 has been shown to promote nuclear localisation of ACK (Ahmed *et al.,* 2004). ACK has an SH3 domain that appears to be involved in the autoinhibition of ACK by forming an intramolecular interaction with proline-rich sequences, present within the C-terminus of the EBD region (Galisteo *et al.,* 2006) (Figure 1.14), as discussed in section 1.5.1.2. A CRIB (Cdc42/Rac interacting binding) region is also found in ACK which is necessary for Cdc42 binding (Manser *et al.,* 1993).

The C-terminus of ACK consist of a clathrin binding region (CL), an EGFR binding domain (EBD) and a ubiquitin-association (UBA) domain. The clathrin binding region was shown to interact with clathrin and is involved in clathrin-mediated endocytosis especially during receptor internalization (Teo *et al.,* 2001). The EGFR binding domain of ACK was shown to interact with the EGFR and this interaction is dependent on the phosphorylation or the kinase activity of the EGFR. Binding of ACK leads to EGFR ubiquitination and degradation, which required the UBA domain of ACK (Shen *et al.,* 2007; Grøvdal *et al.,* 2008). Collectively, these C-terminal regions/domains have been shown to be involved in ACK-mediated EGFR ubiquitination, endocytosis and degradation which will be described in section 1.5.1.3.

1.5.1.2 The regulation and activation of ACK

ACK is ubiquitously expressed and is activated by numerous extracellular stimuli such as integrin-mediated cell adhesion, the M3 muscarinic receptor, the Mer receptor tyrosine kinase, the EGFR and the PDGFR, leading to activation of its kinase activity (Yang *et al.,* 1999; Linseman *et al.,* 2001; Mahajan *et al.,* 2005; Galisteo *et al.,* 2006). The interaction between ACK and RTKs is usually direct but it also has been found to involve several adaptor proteins, including Grb2, H2S2 and Nck (Satoh *et al.,* 1996; Oda *et al.,* 2001; Galisteo *et al.,* 2006).

ACK is thought to be constitutively active due to a lack of conformation changes in its kinase domain between the phosphorylated and non-phosphorylated forms (Lougheed *et al.,* 2004). However, the kinase activity of ACK can be regulated by a series of intramolecular interactions. The SH3 domain of ACK, containing a non-canonical ligand-binding site (Gajiwala *et al.,* 2013), has been shown to bind a proline-rich region (PRR) situated within the C-terminus of the EBD domain (Galisteo *et al.,* 2006; Gajiwala *et al.,* 2013) (Figure 1.14). The SH3-PPR interaction is postulated to orientate the EBD domain, allowing it to form an inhibitory interaction with the kinase domain. This blocks the kinase domain from dimerization-induced activation (Galisteo *et al.,* 2006). The binding of the EBD domain to RTKs such as the EGFR alleviates this inhibition and releases the kinase domain, leading to ACK activation (Lin *et al.,* 2012; Gajiwala *et al.,* 2013).

ACK has also been found to interact with and be phosphorylated at Tyr284 by Src and Hck (Yokoyama and Miller, 2003; Chan *et al.,* 2011). This suggests that the activation of ACK can also be regulated by other kinases and is not solely induced by ACK dimerization.

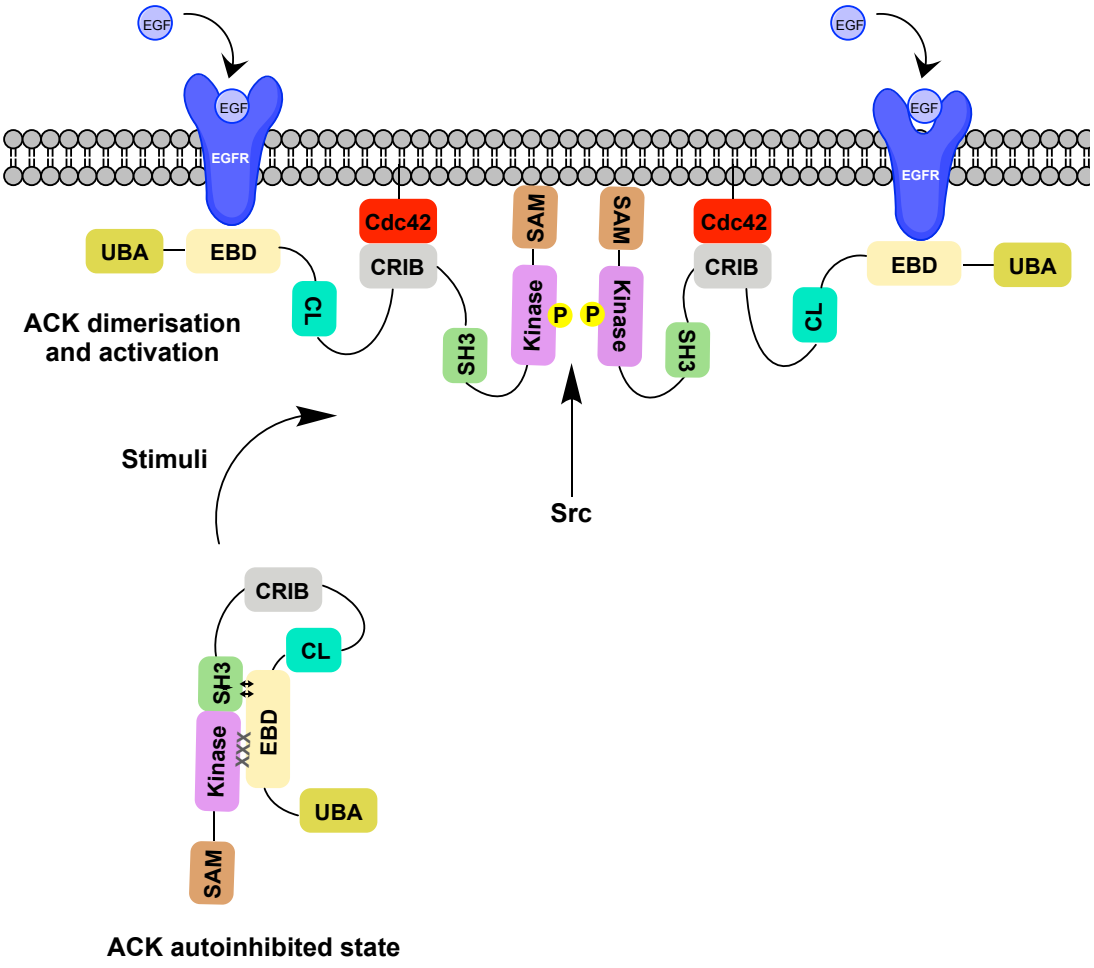

Figure 1.14: Regulation of ACK activation. ACK activation is inhibited by intramolecular interactions. The interaction between the SH3 domain and PRR within the C-terminus of the EBD domain of ACK orientate the EBD, allowing it to form an inhibitory interaction with the kinase domain. Activation of ACK by dimerization is thought to be mediated by the SAM domain. Full activation of ACK might also involve Src-mediated phosphorylation at Tyr284 within the kinase domain of ACK. Membrane localisation of ACK could be provided by the interaction between the EBD and RTKs, for example the EGFR, the CRIB region and Cdc42 or the SAM domain with the membrane directly. Phosphorylation sites are shown as yellow circles (Adapted from Fox *et al.,* 2019).

1.5.1.3 Roles of ACK in cytoskeletal remodeling, apoptosis and trafficking

Cdc42-induced activation of ACK has been shown to be involved in cell migration by phosphorylating the adaptor protein, $p130^{cas}$ (Modzelewska *et al.,* 2006). This promotes $p130^{cas}$ interaction with another adaptor protein, Crk, which in turn interact with a Rac1 GEF, Dock180 to activate Rac1 and stimulate filopodia formation (Bourdoulous *et al.,* 1998; Albert *et al.,* 2000; Gustavsson *et al.,* 2004; Modzelewska *et al.,* 2006). ACK has also been found to mediate the activation of other Rho-family proteins by phosphorylating a GEF, Dbl, which is important for EGF-stimulated reorganization of actin cytoskeleton (Kato *et al.,* 2000; Kato-Stankiewicz *et al.,* 2001). Furthermore, ACK was shown to regulate TRAIL-induced apoptosis by promoting translocation of the TRAIL receptor into lipid rafts and therefore its clustering and DISC (death-inducing signaling complex) formation (Linderoth *et al.,* 2013). A role for ACK in regulating apoptosis was also shown to involve phosphorylation of Akt at Tyr176, which results in the translocation of the ACK-Akt complex into the nucleus to repress FoxO-responsive apoptotic gene expression, including p21, GADD45 and Bim-1 (Mahajan *et al.,* 2010).

ACK-induced actin polymerization has been shown to involve the phosphorylation of WASP at both Ser242 and Tyr256, which then stimulates the activation of Arp2/3 (Yokoyama *et al.,* 2005). Additional regulation of Arp2/3 dynamics by ACK requires the interaction and phosphorylation of cortactin, an Arp2/3 regulatory protein at Tyr421, Tyr466 and Tyr482. These phosphorylation events are required to maintain EGFR signalling as knockdown of ACK or cortactin has been shown to decrease EGFR degradation (Kelley *et al.,* 2012).

The involvement of ACK in mediating EGFR endocytosis and trafficking was recognized due to several pieces of evidence showing the association between ACK, EGFR and several proteins involved in vesicle dynamics. ACK has been shown to interact with clathrin, adaptor protein AP-2 and sorting nexin 9 (SNX9). ACK colocalised with clathrin in large vesicular structures and has been found to be involved in clathrin-coated assembly and clathrin-mediated endocytosis (Teo *et al.,* 200; Shen *et al.,* 2007; Shen *et al.,* 2011). Following EGF stimulation, ACK was found to phosphorylate SNX9 at Tyr287 (Lin *et al.,* 2002) and to promote EGFR degradation (Shen *et al.,*

2007). Overall, it is postulated that ACK-mediates EGFR degradation probably by stimulating its endocytosis and this event requires ACK association with several vesicle-associated proteins, as described previously. This suggests a role for ACK in modulating EGF-mediated cell survival, proliferation and differentiation (Lin *et al.,* 2002; Fox *et al.,* 2019).

Following activation, EGFR is endocytosed and targeted to early endosomes for either membrane recycling or to the endosomal pathway for lysosomal degradation (Goh *et al.,* 2010) (Figure 1.15). In response to EGF stimulation, ACK interacts with the EGFR via the EBD and promotes its degradation (Shen *et al.,* 2007). The interaction between ACK and EGFR was assumed to be indirect and to require an adaptor protein, specifically Grb2, as this has been identified in several studies of EGF-induced EGFR internalization (Yamazaki *et al.,* 2002; Fox *et al.,* 2020). Grb2 is a binding partner of ACK and is required for the interaction with and ACK-mediated degradation of several RTKs such as leukocyte tyrosine kinase (LTK), Axl family kinase and anaplastic lymphoma kinase (ALK) (Pao-Chun *et al.,* 2009).

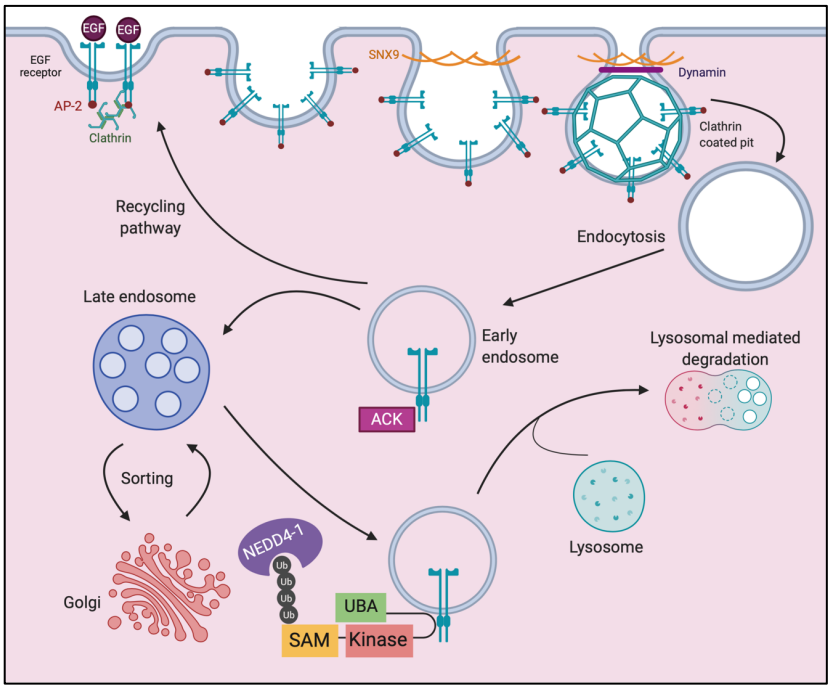

Figure 1.15: The role of ACK in regulating receptor endocytosis. The diagram shows the stages of receptor-mediated endocytosis and EGFR internalization following EGFR stimulation. ACK: activated Cdc42-associated kinase, AP-2: adaptor protein 2, EGF: epidermal growth factor, EGFR: epidermal growth factor receptor, NEDD4-1: neural precursor cell expressed developmentally down-regulated protein 4, SNX9: sorting nexin 9, Ub: ubiquitin (Adapted from Fox *et al.,* 2019).

ACK has also been shown to undergo ubiquitination by NEDD4-1 and is degraded together with the EGFR upon EGF stimulation, suggesting co-transportation of the ACK-EGFR complex during EGFR endocytosis (Chan *et al.,* 2009; Lin *et al.,* 2010). This is consistent with data from Shen *et al.* (2007) who showed co-localisation of ACK and the EGFR on EEA-1 positive vesicles in response to EGF stimulation and subsequently showed their co-transportation to the lysosome for degradation (Lin *et al.,* 2010). ACK ubiquitination by NEDD4-1 is mediated by its SAM domain as lack of this domain has been shown to decrease ACK ubiquitination (Lin *et al.,* 2010). Although ACK contains an UBA domain, deletion of this domain results in an increase of ACK ubiquitination suggesting that the UBA domain of ACK is responsible for regulating the interaction with NEDD4-1 and therefore is necessary to prevent excessive ubiquitination (Fox *et al.,* 2019). The ACK UBA domain has also been found to regulate EGFR degradation and lack of this domain was shown to promote ACK and EGFR stability even after EGF stimulation (Tin *et al.,* 2010). Taken together, all these studies indicated that ubiquitination of ACK serves as a sorting signal for trafficking the EGFR-ACK complex to the lysosome. This is consistent with a study by Grøvdal *et al.* (2008), which showed that overexpression of ACK resulted in the retention of the EGFR on early endosomes and prevented its translocation to multivesicular bodies (MVBs). Overall, the role of ACK in mediating EGFR endocytosis and degradation is important to prevent excessive EGF signalling and deregulation of this mechanism will promote the uncontrolled signal transduction that frequently occur in cancer.

1.5.1.4 Roles of ACK in mediating cancer progression

Several studies have shown a role for ACK as an oncogenic kinase. For instance, overexpression of pTyr284-ACK was found to regulate PI3-Kinase signalling in breast and prostate cancer by increasing the levels of pTyr176-Akt (Mahajan *et al.,* 2010). ACK has also been shown to regulate the PI3-Kinase regulatory subunits by interacting and phosphorylating the p85 regulatory subunits at Tyr607, leading to their stabilisation. This promotes cell proliferation through an, as yet undiscovered, mechanism (Clayton *et al.,* 2019). The phosphorylated p85 isoforms can form either homo- or heterodimers via the C-terminal regions of p85 and this was shown to occur predominantly in the nucleus. These nuclear dimers are predicted to drive the pro-proliferative functions of ACK via their free SH3 or RhoGAP domains (Clayton *et al.,* 2019; Fox *et al.,* 2019).

ACK has been found to be involved in prostate cancer progression and this was by phosphorylating the tumour suppressor Wwox, which results in rapid dissociation of the ACK-Wwox complex and subsequent Wwox poly-ubiquitination and degradation (Mahajan *et al.,* 2005). Phosphorylation of the androgen receptor (AR) at Tyr267 by ACK was also shown to promote AR recruitment to androgen-response elements (ARE), resulting in the transcription of AR target genes in the absence of androgen to drive prostate cancer progression (Mahajan *et al.,* 2007). Besides regulating the transcriptional activity of the AR, ACK has also been found to phosphorylate Histone H4 on Tyr88, upstream of the AR transcriptional start site to promote AR transcription and subsequently its protein levels in androgen-starved prostate cancer cell lines (Mahajan *et al.,* 2017). This suggests a role for ACK as an epigenetic regulator, which has also been seen in breast cancer cell lines. ACK was found to phosphorylate KDM3A, a histone demethylase, on Tyr1114, which mediates the transactivation of the oestrogen receptor (ER) target gene, HOXA-1, an oncogene involved in mammary tumour progression (Mahajan *et al.,* 2014).

Abnormal activation or expression of ACK either through amplification or mutation has been shown to have a significant correlation with poor prognosis in various cancer types such as breast, prostate, pancreatic, hepatocellular, stomach and lung carcinoma (Van der Horst *et al.,* 2005; Mahajan *et al.,* 2010; Mahajan *et al.,* 2012; Mahajan and Mahajan, 2013; Fox *et al.,* 2019). Overexpression of ACK has been shown to stimulate EMT and therefore promote cell migration and invasion in gastric cancer and HCC (Xu *et al.,* 2015; Lei *et al.,* 2015). A study to find somatic mutations in genes encoding 518 protein kinases in 210 diverse human cancer identified four somatic mutations in ACK. These four missense mutations include R34L in SAM domain, R99Q in between the SAM and the kinase domains, E346K in the kinase domain and M409I in SH3 domain. Each of these mutations was identified in a different type of cancer: R34L in lung adenocarcinoma, R99Q and E346K in ovarian cancer and M409I in gastric adenocarcinoma (Greenman *et al.,* 2007).

This growing evidence showing the involvement of ACK and its interacting proteins in cancer progression indicate that they may be good therapeutic targets and/or prognostic markers for certain cancer. Thus, to understand as much as possible about the role of ACK both in normal and in pathological conditions will be an important prelude to the development of truly effective and safe ACK inhibitors.

1.6 Aim of the study

A Y2H screen previously undertaken by a PhD student in the lab, Dr. J. Vicenté-García, identified an interaction with RhoGDI-3 (Dr. J. Vicenté-García, PhD thesis, University of Cambridge, 2009). As described previously, RhoGDIs are one of the important regulatory proteins involved in controlling the activation state and accessibility of Rho-family GTPases. Furthermore, RhoGDI-3 has also been implicated in cancer progression in its own right. Thus, it was hypothesized that regulation of RhoGDI-3 might underpin some aspects of ACK-driven cancer progression.

The RhoGDI-3 interaction with ACK was validated in this study and the interactions with the other RhoGDIs were also identified using co-immunoprecipitation. Since ACK is a kinase, the effect of ACK on the phosphorylation status of the RhoGDIs was also assayed in cells and *in vitro*. ACK is also known as a nuclear-cytoplasmic shuttling kinase, therefore the site of interaction with RhoGDIs was also investigated through subcellular fractionation. The role of ACK in regulating the stability of each RhoGDIs was identified using cycloheximide chase and ubiquitination assays. The effect of ACK on RhoGDI target proteins was also determined in this work. To date, relatively few targets have been identified for the RhoGDIs and these in a sporadic manner. Thus, a systematic study was performed to determine all possible Rho-family GTPases that interact with the RhoGDIs. The effect of ACK on the binding and activation status of these targets was identified using co-immunoprecipitation and effector pull-down assays. In summary, all the data obtained in this study should help to elucidate the functional differences between the three RhoGDIs and also provide insight into the role of the RhoGDIs in ACK signalling.

Chapter 2

Materials and Methods

2.1 Molecular biology

2.1.1 Media and reagents

Table 2.1 Bacterial media and plates

Media/plates	Ingredients
Luria Bertani (LB) Broth	10 g/L Tryptone 5 g/L Yeast Extract 10 g/l NaCl
2TY Media	16 g/L Tryptone 10 g/L Yeast Extract 5 g/l NaCl
2TY Media Plates	16 g/L Tryptone 10 g/L Yeast Extract 5 g/L NaCl 16 g/L Agar

Table 2.1 List of reference cDNA

Template	Accession No.
Homo sapiens Rho GDP dissociation inhibitor (GDI) alpha (RhoGDI-1)	BC106044.1
Homo sapiens Rho GDP dissociation inhibitor (GDI) beta (RhoGDI-2)	BC009200.2
Homo sapiens Rho GDP dissociation inhibitor (GDI) gamma (RhoGDI-3)	NM_001176.4
Homo sapiens tyrosine kinase non receptor 2 (TNK2), transcript variant 1	NM_005781.4
Synthetic yeast ubiquitin gene	M15704.1

Table 2.3: Bacterial strains

***E. coli* strains**	**Antibiotic resistance**	**Genotype**
TOP 10 (Invitrogen)	None	F- *mcrA* Δ(*mrr-hsd*RMS-*mcr*BC) Φ80*lac*ZΔM15 Δ *lac*X74 *rec*A1 *ara*D139 Δ(*ara-leu*)7697 *gal*U *gal*K *rps*L (StrR) *end*A1 *nup*G
TOP 10F′ (Invitrogen)	Tet	F′{*lac*Iᑫ Tn*10* (Tet^R)} *mcr*A Δ(*mrr-hsd*RMS-*mcr*BC) Φ80*lac*ZΔM15 Δ*lac*X74 *rec*A1 *ara*D139 Δ(*ara-leu*)7697 *gal*U *gal*K *rps*L *end*A1 *nup*G
XLI MRF′ Blue	Tet	endA1 gyrA96(nal^R) thi-1 recA1 relA1 lac glnV44 F'[::Tn10 $proAB^+$ $lacI^q$ Δ(lacZ)M15] hsdR17(r_K^- m_K^+)
XL10-Gold® (Agilent)	Tet	TetrD(*mcrA*)*183* D(*mcrCB-hsdSMR-mrr*)*173 endA1 supE44 thi-1 recA1 gyrA96 relA1 lac* Hte [F′ *proAB lacI*qZD*M15* Tn*10* (Tetr) Amy Camr]
BL21	None	F^- *ompT gal dcm lon* $hsdS_B(r_B^-m_B^-)$ [$malB^+$]$_{K-12}(\lambda^S)$
BL21 DE3	Amp	F^- *ompT gal dcm lon* $hsdS_B(r_B^-m_B^-)$ λ(DE3 [*lacI lacUV5-T7p07 ind1 sam7 nin5*]) [$malB^+$]$_{K-12}(\lambda^S)$
BL21 DE3 PlysS	Cam	F^- *ompT gal dcm lon* $hsdS_B(r_B^-m_B^-)$ λ(DE3 [*lacI lacUV5-T7p07 ind1 sam7 nin5*]) [$malB^+$]$_{K-12}(\lambda^S)$ pLysS[*T7p20* ori_{p15A}](Cm^R)

Table 2.4: List of DNA constructs and sources

Construct	Expression tag	Source
pXJ-HA-GFP	HA	Gift from Prof. Ed Manser, ICMB Singapore
pXJ-HA-ACK	HA	
pXJ-HA-dACK	HA	
pGEX-2TK-PAK1 PBD (56-272)	GST	Gift from Dr. Heidi Welch, Babraham Institute, Cambridge
pDEST™ 26-His-RhoGDI 1	His	Previously made in the lab
pCMV-Myc-Ub	Myc	Gifts from Dr. Catherine Lindon, Department of Pharmacology, University of Cambridge
pCMV-Myc-Ub K48R	Myc	
pDEST™ 12.2-FLAG-RhoGDI 3	FLAG	Previously made in the lab
pGEX-2T-Rhotekin (1-89)	GST	Previously made in the lab
pcDNA™ 3.1/nV5-DEST-RhoA	V5	Previously made in the lab
pcDNA™ 3.1/nV5-DEST-RhoB	V5	Previously made in the lab
pcDNA™ 3.1/nV5-DEST-RhoC	V5	Previously made in the lab
pcDNA™ 3.1/nV5-DEST-Rac1	V5	Previously made in the lab
pcDNA™ 3.1/nV5-DEST-Rac2	V5	Previously made in the lab
pcDNA™ 3.1/nV5-DEST-Rac3	V5	Previously made in the lab
pcDNA™ 3.1/nV5-DEST-RhoG	V5	Previously made in the lab
pcDNA™ 3.1/nV5-DEST-Cdc42	V5	Previously made in the lab
pcDNA™ 3.1/nV5-DEST-TC10	V5	Previously made in the lab
pcDNA™ 3.1/nV5-DEST-TCL	V5	Previously made in the lab
pcDNA™ 3.1/nV5-DEST-Wrch1	V5	Previously made in the lab
pcDNA™ 3.1/nV5-DEST-Wrch2	V5	Previously made in the lab
pcDNA™ 3.1/nV5-DEST-RhoD	V5	Previously made in the lab
pcDNA™ 3.1/nV5-DEST-RhoH	V5	Previously made in the lab
pcDNA™ 3.1/nV5-DEST-RhoF	V5	Previously made in the lab
pcDNA™ 3.1/nV5-DEST-Rnd1	V5	Previously made in the lab
pcDNA™ 3.1/nV5-DEST-Rnd2	V5	Previously made in the lab
pcDNA™ 3.1/nV5-DEST-Rnd3	V5	Previously made in the lab
pcDNA™ 3.1/nV5-DEST-Miro1	V5	Previously made in the lab
pcDNA™ 3.1/nV5-DEST-Miro2	V5	Previously made in the lab
pcDNA™ 3.1/nV5-DEST-RhoBTB1	V5	Previously made in the lab
pcDNA™ 3.1/nV5-DEST-RhoBTB2	V5	Previously made in the lab
pcDNA™ 3.1/nV5-DEST-RhoBTB3	V5	Previously made in the lab

2.1.2 Preparation of chemically competent *E. coli*

1 mL of an fresh overnight culture of the desired *E. coli* strain was diluted into 50 mL 2TY media and grown at 37 °C for ~ 1 to 2 h with continuous shaking (180 rpm) until the OD_{600} reached 0.4 to 0.6. Cells were then pelleted at 2000 x g for 5 min and resuspended in 25 mL ice cold 100 mM $MgCl_2$. Cells were pelleted again and resuspended in 5 mL ice cold 100 mM $CaCl_2$ before being left on ice for 1 h 30 min. Cells were then pelleted and resuspend in 1 mL ice cold $CaCl_2$ (85 mM) containing 17% glycerol. The competent *E. coli* cells were stored at -80 °C for further used.

2.1.3 Transformation of chemically competent *E. coli*

Transformation of chemically competent *E. coli* cells was performed by mixing 50 to 100 µL of competent cells with 100-200 ng of DNA before incubation on ice for 5 min. Cells were then heat shocked at 42 °C for 45 sec, cooled on ice for another 2 min and finally resuspended in 350 µL 2TY media. Cells were incubated at 37 °C with shaking for 1 h before being spread on selective agar and grown at 37 °C overnight.

2.1.4 Small-scale purification of plasmid DNA

Plasmid DNA was purified from 5 mL overnight bacterial culture using the GenElute™ Plasmid Miniprep Kit (Sigma-Aldrich, Cat. No. PLN350-1KT), according to manufacturer's instructions. DNA was eluted with sterile Analytical Reagent Grade Water (Fisher Scientific, Cat. No. W/0100/21) and quantified using the A_{260} reading before storage at -20 °C.

2.1.5 Digestion of plasmid DNA and TAE-agarose gel electrophoresis

1 µg of plasmid DNA were digested with the relevant restriction enzymes in a total reaction volume of 20 µL for ~1 h at 37 °C. Following incubation, the reactions were stopped by addition of 5X DNA loading buffer (Table 2.5). Gels were prepared by dissolving 0.5-1 % Molecular

biology grade agarose (Bioline, Cat. No. BIO-41025) in 1X TAE buffer (Table 2.6). The fragments of interest were identified by visualizing using a UV transilluminator in comparison with a DNA ladder (Bioline, Cat. No. BIO-33025). The plasmid DNA was then sent for sequencing (DNA sequencing facility, Department of Biochemistry, University of Cambridge) if necessary.

Table 2.5: Buffers in TAE-agarose gel electrophoresis

Buffer	Ingredients
5X DNA Loading Buffer	50 % Sucrose 50 mM 0.2 M EDTA 0.1 % Bromophenol Blue
1X TAE Buffer pH 8.3	40 mM Tris-base 20 mM Acetic acid 1 mM EDTA 0.2 µM Ethidium Bromide

2.1.6 Gateway® cloning

Gateway entry clones for all constructs were available in the lab. Gateway entry clones were then purified (section 2.1.4) and recombined into Gateway expression vector using the site-specific LR recombination reaction. 8 µL recombination reactions were prepared containing ~150 ng of entry clone, ~150 ng destination vector and 2 µL of Gateway® LR Clonase® II enzyme before incubating at room temperature for 1 h. Next, 1 µL of the Proteinase K solution was added to the reaction which was incubated for another 10 min at 37 °C, before 1 µL of the reaction was transformed into One Shot™ TOP 10 chemically competent *E. coli* cells following manufacturer's instructions.

Colonies of transformed cells were patched on selective plates and their plasmid DNA analysed using restriction enzyme digestion (section 2.1.5). The correct size of the insert was determined using TAE-agarose gel electrophoresis (section 2.1.5) and validated by DNA sequencing. Table 2.6 lists all the Gateway® destination vectors used in this study.

Table 2.6: Gateway® destination vectors

Gateway® destination vectors	Expression	Features
pDEST26	Mammalian	Encodes an N-terminus His tag
pDEST12.2-FLAG	Mammalian	Encodes an N-terminus FLAG® tag
pcDNA3.1/nV5-DEST	Mammalian	Encodes an N-terminus V5 tag
pDEST15T	Bacterial	Encodes an N-terminus GST tag

2.1.7 Site- and multi site-directed mutagenesis

Mutagenesis was performed either using a QuikChange Site-Directed Mutagenesis Kit (Cat. No. 210518-5) or a QuikChange Multi site-Directed Mutagenesis Kit (Cat. No. 210513-5) from Agilent Technologies following manufacturer's instructions. Briefly, plasmid DNA was denatured, mutagenic primers annealed, and extended using a Pfu-Phusion-based enzyme blend. This resulted in a double-stranded DNA molecule composed of a parental (wild type) strand and a mutagenic strand. The DNA was then treated with the restriction endonuclease *Dpn*I, which cleaves the methylated, parental strand. The remaining single-stranded mutagenic DNA was then transformed into XL10-Gold® ultracompetent *E. coli* cells.

The primers used in this study are detailed in Table 2.7. The cycling parameters for each single and multi site-directed mutagenesis reactions are described in Table 2.8 and 2.9. Transformed colonies were patched, purified and sent for sequencing (sections 2.14 and 2.15)

Table 2.7: List of primers used for site-directed mutagenesis

Mutation	Primer
RhoGDI-2 (Y24F)	5′ GGACAGCAAGCTCAATTTTAAGCCTCCACCACAG 3′
RhoGDI-2 (Y48F)	5′ GAGAGTCTAATTAAGTTCAAGAAAACGCTGCTGGG 3′
RhoGDI-2 (Y107F)	5′ GTTAAAGGAAGGTTCTGAATTTAGAGTCAAAATTCACTTC 3′
RhoGDI-2 (Y125F)	5′ GTGTCAGGCCTGAAATTCGTTCAGCACACC 3′
RhoGDI-2 (Y130F)	5′ GTTCAGCACACCTTCAGGACTGGGG 3′
RhoGDI-2 (Y146F)	5′ GGTTGGCAGCTTTGGACCTCGGCCTG 3′
RhoGDI-2 (Y172F)	5′ GCCCGAGGCACGTTCCACAACAAGTCC 3′
*att*B1 (RhoGDI-1, RhoGDI-2 and RhoGDI-3)	5′ CTAGATCAACAAGTTTGTTCAAAAAAGCAGGCTCCGC 3′
RhoGDI-3 (K73R)	5′ CTGGCCAAGTACCGGCGGGTGCTGCTGGGG 3′
RhoGDI-3 (K126R)	5′ GACCAGGTGTTTGTCCTGCGGAAGGTGTTGATTACAG 3′
RhoGDI-3 (K134R)	5′ GGTGTTGATTACAGAGTGCGGATCTCCTTCAAGGTCCAC 3′
RhoGDI-3 (K162R)	5′ GCCTGCGCGTGGACCGGACCGTCTACATGGTG 3′
Ubiquitin (K63R)	5′ CTGATTACAACATTCAGAGGGAGTCGACCTTACATC 3′
ACK (S985N)	5′ GTGCCACGGCTGGAACGTGCAGAGGGCTG 3′
ΔNRhoGDI-3 (Forward)	5′ GCCGCCCCCTTCACCCTGGCTGACAAGGAG 3′
ΔNRhoGDI-3 (Reverse)	5′ CTCCTTGTCAGCCAGGGTGAAGGGGGCGGC 3′

Mutagenesis site

Table 2.8: Cycling parameters used for site-directed mutagenesis

Site-directed mutagenesis of pDEST12.2-FLAG-RhoGDI-3 (ΔNRhoGDI-3)			
Step	**Temperature**	**Time**	**Cycle**
Initial Denaturation	95 °C	2 min	1
Denaturation	95 °C	20 sec	30
Primer annealing	55 °C	30 sec	
Extension	65 °C	3 min 12 sec	
Final extension	65 °C	5 min	1

Table 2.9: Cycling parameters used for multi site-directed mutagenesis

Multi site-directed mutagenesis of **A. pDEST26-RhoGDI-1** **B. pDEST26-RhoGDI-2** **C. pDEST26-RhoGDI-3** **D. pCMV-Myc-Ubiquitin** **E. pXJ-HA-ACK**			
Step	**Temperature**	**Time**	**Cycle**
Initial Denaturation	95 °C	2 min	1
Denaturation	95 °C	20 sec	30
Primer annealing	55 °C	30 sec	
Extension	65 °C	30 sec/ kb: A. 3 min 12 sec B. 3 min 12 sec C. 3 min 15 sec D. 1 min 59 sec E. 3 min 42 sec	
Final extension	65 °C	5 min	1

2.2 Expression and purification of recombinant proteins

2.2.1 Small-scale expression trials in *E. coli*

A single bacterial colony was inoculated into 10 mL sterile 2TY media supplemented with selective antibiotic and grown for ~ 16 h at 37 °C while shaking at 180 rpm. 1 mL of overnight culture was diluted into each of two 10 mL 2TY that were grown at 37 °C with continuous shaking until reaching OD_{600} 0.8. One of the cultures was then induced with the optimised amount of IPTG, as described in Table 2.10. Both the induced and non-induced cultures were then incubated at either 37 °C for 5 h or 20 °C for ~ 16 h with continuous shaking at 180 rpm.

After incubation, a 1 mL aliquot of non-induced and 3X 1 mL aliquots of induced culture were pelleted at 6000 x g for 10 min after their A_{600} readings were measured. The protein concentration of the non-induced and one induced cultures were then normalized by adding a calculated volume of sterile MilliQ water, before mixing with 2X SDS sample buffer (Table 2.23). The remaining 2 mL aliquot of induced culture was also resuspended in a calculated volume of sterile MilliQ before being sonicated three times on ice using a 1.9 mm probe at 70% amplitude using Fisherbrand™ Q125 sonicator. The lysed cells were then pelleted at 6000 x g for 10 min and the supernatant was transferred to a new tube before being mixed with 2X SDS sample buffer at a 1:1 ratio. The remaining pellets representing the insoluble fraction of protein, were resuspended in MilliQ water and an equal volume of 2X SDS sample buffer added.

All protein samples were then separated by SDS-PAGE (section 2.4.3) in order to determine the optimum conditions for production of soluble fusion protein. The optimum induction conditions and strain of *E. coli* used to express each protein is described in Table 2.10. These conditions were then used for large-scale expression of all proteins.

Table 2.10: Optimum induction conditions for soluble fusion-protein expression

Fusion protein construct	*E. coli* strain	Antibiotic resistance	IPTG	Temperature	Duration
pDEST15T-RhoGDI-1	BL21 (DE3) (+Trx)[a]	Amp + Cam	1 mM	37 °C	~5 h
pDEST15T-RhoGDI-2	BL21 (DE3) (+GroEL/ES)[b]	Amp + Cam	1 mM	37 °C	~5 h
pDEST15T-RhoGDI-3	BL21 (DE3) (+Trx)[a]	Amp + Cam	1mM	20 °C	~16 h
pGEX-2TK-PAK1 GBD (56-272)	BL21	Amp	0.1 mM	37 °C	~5 h
pGEX-2T-Rhotekin RBD (1-89)	BL21 (DE3) pLysS	Amp + Cam	1 mM	20 °C	~16 h

[a] Thioredoxin (Trx), an oxidoreductase
[b] GroEL and GroeES (GroEL/ES), a bacterial chaperone

2.2.2 Large-scale protein expression in *E. coli*

2.2.2.1 Purification of GST-RhoGDIs

A 50 mL overnight culture was transferred into 500 mL sterile 2TY media and allowed to grow at 37 °C with continuous shaking at 180 rpm until the cells had reached late-log phase (OD_{600} ~0.8). The cells were then induced with 1mM IPTG and grown under optimum conditions that maximised the production of each soluble GST-RhoGDIs (Table 2.10).

Following induction by IPTG, cells were harvested and pelleted at 8000 x g for 15 min at 4 °C. The cell pellets were resuspended in lysis buffer (Table 2.11) and lysed using an Emulsiflex cell disruptor (Avestin). 1 mM PMSF and 0.1% Triton X-100 were then added to the cell lysates which were cleared by centrifugation at 45000 x g for 30 min at 4 °C. The supernatant was applied to an MTPBS-equilibrated glutathione sepharose column. The lysates were loaded onto the column at a flow rate of 1 mL/min. The column was then washed with MTPBS (Table 2.11) until the A_{280} returned to baseline. GST-RhoGDIs were then eluted from the column with elution buffer (Table

2.11). Eluted proteins were collected in 2 mL fractions and monitored at A_{280}. Appropriate fractions were analysed by SDS-PAGE and Coomassie staining (section 2.4.3).

Column fractions containing GST-RhoGDIs were collected after glutathione sepharose purification and concentrated to ~2 mL using an Amicon® Ultra 15 10K, centrifugation filter (Merck, Cat. No. UFC901024). The concentrated fused proteins were then applied to a HiLoad™ 16/600 Superdex™ 200 (S200) gel filtration column (pre-equilibrated with MTPBS) at a flow rate of 1 mL/min. The eluate in 2 mL fractions was monitored by A_{280} and collected in 2 mL fractions. Appropriate fractions were analysed by SDS-PAGE and Coomassie staining (section 2.4.3). The relevant fractions were pooled, concentrated and quantified using A_{280} (section 2.2.3) before storage at -80 °C.

Table 2.11: Buffers used for GST-RhoGDIs purification

Buffer	Ingredient
Lysis buffer	50 mM Tris-HCl pH 7.5 50 mM NaCl 1 mM PMSF (Melford Laboratories, Cat. No. P20270) 1X Protease Inhibitor Cocktail (Sigma-Aldrich, Cat. No. S8830)
MTPBS pH 7.4	16 mM Na_2HPO_4 4 mM NaH_2PO_4 150 mM NaCl 0.05% Sodium Azide
Elution buffer	50 mM Tris-HCl pH 8.0 150 mM NaCl 10 mM Glutathione (Sigma-Aldrich, Cat. No. G4251)

2.2.2.2 Purification of GST-PAK1-GBD (56-272)

A single colony of *E. coli* BL21 expressing GST-PAK1-GBD (56-272) (a kind gift from Dr. Heidi Welch, Babraham Institute, Cambridge) was inoculated into 4X 50 mL 2TY and grown for ~16 h at 37 °C. These cultures were used to inoculate 4X 500 mL 2TY and grown at 37 °C with continuous shaking at 180 rpm until reaching A_{600} ~0.8. The cultures were then induced with 0.1 mM IPTG and grown for another 5 h at 37 °C. Cells were pelleted by centrifugation at 8000 x g

for 15 min at 4 °C, resuspended in ice cold lysis buffer (Table 2.12) and lysed using an Emulsiflex. 1 mM PMSF and 0.1% Triton X-100 were added to the lysates before pelleted at 45000 x g for 30 min at 4 °C.

The cleared supernatant was then applied to glutathione-agarose beads equilibrated in MTPBS and rotated at 4 °C for ~30 min. The beads were then washed three times with MTPBS containing 0.1% Triton X-100 to remove any unbound proteins. Samples were collected at all stages for further analysis by SDS-PAGE and Coomassie staining (Section 2.4.3). The bound protein was then eluted from the beads by incubating the beads with elution buffer for ~30 min at 4 °C (Table 2.12) followed by centrifugation at 1000 x g at 4 °C for 10 min. The elution process was repeated four times to maximize the amount of eluted protein from the beads. All the elutes samples were then pooled and concentrated to ~2 mL using an Amicon stirred cell centrifugation filter. The amount of protein was quantified using A_{280} (section 2.2.3) and stored at -80 °C.

Table 2.12: Buffers used for GST-PAK1-GBD (56-272) purification

Buffer	Ingredient
Lysis buffer pH 7.4	16 mM Na_2HPO_4 4 mM NaH_2PO_4 150 mM NaCl 1 mM PMSF 1X Protease Inhibitor Cocktail (Sigma-Aldrich, Cat. No. S8830)
Elution buffer pH	50 mM Tris-HCl pH 8.0 10 mM Glutathione

2.2.2.3 Purification of GST-Rhotekin-RBD (1-89)

GST-Rhotekin-RBD was purified according to the protocol adapted from Professor Harry Mellor, University of Bristol. A single colony of *E. coli* BL21 (DE3) pLysS expressing GST-Rhotekin-RBD (1-89) was inoculated into 4X 50 mL 2TY and grown for ~16 h at 37 °C. The cultures were used to inoculate 4X 500 mL 2TY and grown at 37 °C with continuous shaking at 180 rpm. The cultures were then induced with 1 mM IPTG when the cells reached the late-log phase (OD_{600}

~0.8) after which they were grown for another ~16 h at 20 °C. Cells were harvested and pelleted at 4000 x g for 30 min at 4 °C.

Pelleted cells were resuspended in ice-cold lysis buffer (Table 2.13) and lysed using an Emusiflex. 0.1 mM PMSF and 1 mM DTT were added to the lysates before centrifugation at 45000 x g for 30 min at 4 °C. The cleared lysate was then applied to 400 uL glutathione-sepharose 4B beads (GE Healthcare, Cat. No. 17-0756-01), pre-equilibrated in lysis buffer and rotated for 5 min at 4 °C. After incubation, the beads were washed six times with 12 mL wash buffer (Table 2.13) and once with 12 mL wash buffer containing 10% glycerol by centrifuging at 1000 x g for 2 min at 4 °C. The beads were finally resuspended in 8 mL wash buffer containing 10% glycerol and stored at -80 °C as 1 mL aliquots.

Table 2.13: Buffers used for GST-Rhotekin-RBD (1-89) purification

Buffer	Ingredient
Lysis buffer	50 mM Tris-HCl pH 7.5 150 mM NaCl 5 mM $MgCl_2$ 1 mM DTT (Melford Laboratories, Cat. No. D11000) 0.1 mM PMSF 1X Protease Inhibitor Cocktail (Sigma-Aldrich, Cat. No. S8830)
Wash buffer	50 mM Tris-HCl pH 7.5 150 mM NaCl 5 mM $MgCl_2$ 1 mM DTT 0.5% Triton X-100

2.2.3 Quantification and storage of purified protein

Protein was quantified using a A_{280} reading, measured within the linear range of 0.1 to 1, using a spectrophotometer (Shimadzu, Cat. No. UV-1800 UV-VIS). The concentration was then calculated using to the equation below,

$$A = \varepsilon c l$$

where A is the absorbance at 280 nm, ε is the extinction coefficient (M^{-1} cm^{-1}), c is the concentration (M) and l is the pathlength (cm). The extinction coefficient was predicted from the number of tryptophan and tyrosine residues in the sequence.

2.3 Mammalian cell culture

2.3.1 Cell lines and reagents

The cell line primarily used in this study was Human Embryonic Kidney, HEK293T cells. Other cell lines used include human pancreatic cancer (PANC-1) and prostate cancer (LNCaP) cell lines. All the plasticwares and reagents used in the maintenance of mammalian cell line are described in Tables 2.14 and 2.15.

Table 2.14: Culture vessel and plasticware

Culture vessel or plasticware	Manufacturer	Catalogue number
10 cm Falcon 100 x 20mm Dish	BD Falcon	353003
60 mm TC easy-grip dish	BD Falcon	353004
Corning 6 well TC plate	Corning	3516
12 Well Flat-Bottomed Tissue Culture Plate	BD Falcon	353043
CELLSTAR 25cm cell scraper	Greiner	541070
Cryovials, 1mL	Greiner	123263

Table 2.15: Reagents for cell maintenance

Culture vessel or plasticware	Manufacturer	Catalogue number
Dulbecco's Modified Eagle Medium (DMEM), High Glucose (4.5 g/L)	Life Technologies	41965-062
Antibiotic, Antimycotic (100X)	Life Technologies	15240-096
L-Glutamine (200 mM)	Life Technologies	25030-081
Fetal Bovine Serum (FBS)	Life Technologies	10108-165
Trypsin-EDTA (0.05%)	Life Technologies	25300-054
Dulbecco's Phosphate Buffered Saline (DPBS)	Sigma-Aldrich	D8537
Dimethyl Sulphoxide (DMSO) sterile filtered	Sigma-Aldrich	D2650

2.3.2 Cell maintenance

Cells were maintained in DMEM (High Glucose) media supplemented with 10% Fetal Bovine Serum (FBS), 2 mM L- Glutamine and 1% Antibiotic-Antimycotic in a 37 °C humidified incubator with 5% CO_2. Cells were split when 80 to 90% confluence was reached. Old media was discarded, and the cells washed with 2 mL of Dulbecco's phosphate buffer saline (DPBS). After DPBS was removed, 1 mL of 0.05% trypsin solution was added, and the cells were incubated at 37 °C for ~5 min. The cells were then resuspended in supplemented DMEM and replated at 1:2 to 1:20 depending on the requirement of each cell line.

2.3.3 Cell freezing and revival

Cells at ~80% confluency were trypsinised, resuspended in DMEM and counted using a hemocytometer. Cell were then pelleted at 1000 x g for 10 min and resuspended at the correct density in 1 mL DMEM containing 10% FBS and 10% DMSO before being transferred to cryovial. The vials were frozen slowly at -20 °C for 24 h, subsequently transferred to -80 °C for another 24 h and finally transferred to liquid nitrogen for long-term storage. Frozen cells were revived by rapid defrosting in a 37 °C water bath. The defrosted cells aliquot was added to 10 mL supplemented DMEM and pelleted at 1000 x g for ~10 min. Cell pellets were then resuspended in 10 mL supplemented DMEM and transferred to a 10 cm dish for growth at 37 °C in an humidified incubator with 5% CO_2.

2.3.4 Transfection of mammalian cells

Plasmid DNA used for transfection were purified from *E. coli* using an Endofree Plasmid Maxi Kit (Qiagen, Cat. No. 12362) following manufacturer's instructions. The DNA concentration was measured at A_{260} and calculated using the formula below,

$$C = (A \times 50) \times df$$

where C is the DNA concentration (μg/mL), A is the absorbance at 260 nm and df is the dilution factor.

2.3.4.1 Transfection using Lipofectamine®

Cells were transfected at ~50-60% confluency using Lipofectamine® 2000 Transfection reagent (Life Technologies, Cat. No. 11668-019) and Opti-Mem. A minimum of 1 µg pXJ-HA-GFP construct DNA was always included as a transfection control. All the volumes of transfection reagents described here represent the volume used for a 10 cm dishes and were adjusted as appropriate for other dishes according to surface area.

Briefly, prior to transfection, 20 µL Lipofectamine® was diluted in 1 mL Opti-Mem and left at room temperature for 5 min. The appropriate amount of plasmid DNA was diluted in 1 mL Opti-Mem reagent in a separate tube. 1 mL of Lipofectamine-Opti-Mem mix was then added to the diluted plasmid DNA and incubated at room temperature for 20 min. The transfection solution was then added dropwise to the cells. The transfected cells were grown at 37 °C in an humidified incubator with 5% CO_2 for ~40 h, before harvesting.

2.3.4.2 Transfection using Polyethylenimine (PEI)

Plasmid DNA was mixed with 30 µL 1 mg/mL PEI and 1 mL DMEM, and left at room temperature for ~10 min. The transfection solution was then added dropwise to the cells. Transfected cells were grown for ~40 h at 37 °C in an humidified incubator with 5% CO_2, before harvesting for future analysis.

2.3.5 Cell lysis and sample preparation

Unless otherwise stated, cells were harvested and lysed at 80-90% confluency using 1 mL ice cold lysis buffer (Table 2.16) for each 10 cm dish. The whole cell lysates were then pelleted at 13000 x g for 20 min. Supernatant was collected and mixed with 2X LDS sample buffer for further analysis (Table 2.16).

Table 2.16: Buffers used for cell lysis

Buffer	Ingredient
Lysis buffer (Protein G Dynabeads)	50 mM Tris-HCl pH 7.4 150 mM NaCl 1 mM EDTA 1 mM Sodium orthovanadate (Na_3VO_4) (Sigma-Aldrich, Cat. No. S6508) 1 mM β-glycerophosphate Disodium Salt Hydrate (Merck, Cat. No. 35675) 1X Mammalian Protease Inhibitor Cocktail (Sigma-Aldrich, Cat. No. P8340) 1% Triton X-100
Lysis buffer (His-tag Dynabeads)	50 mM Tris-HCl pH 7.4 150 mM NaCl 1 mM Sodium orthovanadate (Na_3VO_4) 1 mM β-glycerophosphate Disodium Salt Hydrate 1X Mammalian Protease Inhibitor Cocktail 1% Triton X-100
Lysis buffer (ubiquitination assay)	50 mM Tris-HCl pH 7.5 225 mM KCl 10 mM NaF 1% NP-40 Alternative (Calbiochem, Cat. No. 492016) 1 mM Na_3VO_4 1X Mammalian Protease Inhibitor Cocktail
2X LDS sample buffer	250 µL 4X NuPAGE® LDS Sample buffer (ThermoFisher, Cat. No. NP0007) 170 µL sterile MilliQ 80 µL β-mercaptoethanol (Merck, Cat. No. 805740)

2.3.6 Cell fractionation

Mammalian cell fractionation was performed according to a protocol adapted from Life Technologies. Cells were transfected with plasmid DNA before harvesting and separation into cytoplasmic and nuclear-enriched fractions, ~40 h post-transfection. Culture media was aspirated from the cells, which were then washed with 2 mL DPBS. Cells were then resuspended in 5 mL fresh DPBS and pelleted at 1000 x g for 15 min at 4 °C. The supernatant was discarded and the cell pellet was resuspended in 500 µL hypotonic buffer (Table 2.17) and incubated on ice for 15 min. 0.5% NP40 Alternative was then added to the cells which were lysed by vortexing for 10 sec. Lysates were centrifuged at 1000 x g for 15 min at 4 °C and the supernatant containing the

cytoplasmic contents was collected and mixed with 2X LDS sample buffer (Table 2.16) or kept on ice for further analysis.

The remaining pellet was washed with 500 µL hypotonic buffer (Table 2.17) by centrifugation at 1000 x g for 15 min at 4 °C. The cell pellet was then resuspended in 500 µL cells extraction buffer (Table 2.17). The nuclear-enriched pellet was incubated on ice for 30 min with brief vortexing for every 10 min. Following incubation, the samples were pelleted at 13000 x g and the supernatant containing nuclear-enriched content was collected and mixed with 2X LDS sample buffer or kept on ice for further analysis.

Both the cytoplasmic and nuclear-enriched fractions were analysed by western blotting (section 2.4.4) or used for further analysis such as co-immunoprecipitation studies (section 2.3.9). Histone H3 and Heat shock protein 56 (Hsp56) or GAPDH were used as nuclear and cytoplasmic markers, respectively.

Table 2.17: Buffers used for cell extraction

Buffer	Ingredient
Hypotonic buffer	20 mM Tris-HCl pH 7.4 10 mM NaCl 3 mM $MgCl_2$
Cells extraction buffer	100 mM Tris-HCl pH 7.4 100 mM NaCl 1 mM EDTA 1 mM EGTA 0.1% SDS 1 mM NaF 2 mM Na_3VO_4 1% Triton X-100 10% Glycerol 0.5% Sodium deoxycholate 20 mM $Na_4P_2O_7$ 1 mM PMSF 1X Mammalian Protease Inhibitor Cocktail

2.3.7 Inhibition of mammalian protein synthesis

~24 h post-transfection, cells were serum-starved overnight with DMEM containing 0.5% FBS. ~40 h post-transfection, cells were treated with 25 μg/mL cycloheximide (CHX) (Sigma-Aldrich, Cat. No. C4859) or DMSO for 2 to 8 h. At various time points, cells were harvested and lysed with lysis buffer (Table 2.16). The cell lysate was centrifuged at 13000 x g for 20 min at 4 °C. The supernatant was collected and mixed in a 1:1 ratio with 2X LDS sample buffer (Table 2.16).

2.3.8 Inhibition of mammalian protein degradation

Protein degradation was inhibited either using MG132 (Sigma-Aldrich, Cat. No. M7449) or Bafilomycin A1 (Baf) (Sigma-Aldrich, Cat. No. B1793). 10 μM MG132, 1 μM Baf or DMSO were added to transfected cells, ~40 h post-transfection. Treated cells were then incubated for ~6 h at 37 °C before being harvested and lysed in lysis buffer (Table 2.16). The cell lysate was centrifuged at 13000 x g for 20 min at 4 °C. The supernatant was collected and mixed with 2X LDS sample buffer (Table 2.16).

2.3.9 Co-immunoprecipitation

2.3.9.1 Co-immunoprecipitation using Protein G Dynabeads

Transfected cells were harvested and lysed in lysis buffer (Table 2.16), ~40 h post-transfection. Cell lysates were centrifuged at 13000 x g for 20 min at 4 °C. Supernatants were then transferred to tube containing 30 μL Protein G Dynabeads™ (ThermoFisher, Cat. No. 10004D) that were pre-washed once with 1X PBS-tween 20 (1X PBST) (Table 2.18). Tubes were rotated for ~1 h at 4 °C to remove any non-specific binding proteins.

Whilst the samples were pre-clearing, another 30 μL of Protein G Dynabeads™ were aliquoted into tubes and washed with 1X PBST. 1 mg/mL of the selected antibody (Table 2.19) were diluted in 200 μL 1X PBST and added to each tube before rotation for 30 min at room temperature to allow for antibody-Protein G binding. All excessive antibody was removed by washing the beads

three times with 500 µL 1X PBST. The beads were either incubated directly with lysates or were cross-linked with DMP (dimethyl pimelimidate) (ThermoFisher, 21666) before incubation with lysates. For cross-linking, the beads were washed twice with 500 µL 0.2 M Triethanolamine pH 8.2, resuspended in 500 µL 200 mM DMP in 0.2 M Triethanolamine pH 8.2 and rotated at room temperature for another 20 min. Following the 20 min incubation, the cross-linked antibody-bead complex was rotated with 50 mM Tris-HCl pH 7.4 for another 15 min and subsequently washed three times with 500 µL 1X PBST.

1 mL of pre-cleared cell lysate was then added to the beads and incubated for at least 1 h at 4 °C. All unbound proteins were removed, and the beads were washed three times with 500 µL cold lysis buffer (Table 2.16). Lastly, the beads were resuspended in 20 µL 1X PBS (Table 2.18) and mixed with 2X LDS sample buffer (Table 2.16) at a 1:1 ratio for future analysis by western blotting (section 2.4.4).

Table 2.18: Buffers used for co-immunoprecipitation

Buffer	Ingredient
1X PBS	150 mM NaCl 16 mM Na_2HPO_4 4 mM NaH_2PO_4 pH 7.4
1X PBST	150 mM NaCl 16 mM Na_2HPO_4 4 mM NaH_2PO_4 pH 7.4 0.1% Tween-20 (Sigma-Aldrich, Cat. No. P1379)

Table 2.19: Antibodies used for co-immunoprecipitation

Antibody	Manufacturer	Catalogue number
Anti-FLAG	Sigma-Aldrich	F3165
Anti-ACK	Santa Cruz Biotechnology	sc-28336
Anti-HA	Santa Cruz Biotechnology	Sc-7392
Anti-RhoGDI-1	Santa Cruz Biotechnology	sc-373724
Anti-Myc	Santa Cruz Biotechnology	sc-40

2.3.9.2 Co-immunoprecipitation with His-tag Dynabeads

His-tagged proteins were co-immunoprecipitated using His-tag Dynabeads™ (ThermoFisher, Cat. No. 10103D), a cobalt-coated magnetic bead. ~40 h post-transfection, transfected cells were harvested and lysed with ice cold lysis buffer (Table 2.16). Cell lysates were centrifuged at 13000 x g for 20 min at 4 °C and supernatants were transferred to tubes containing 30 µL pre-washed His-tag Dynabeads™ (pre-washed with 1X PBST). Tubes were rotated at 4 °C for ~1 h and subsequently washed three times with 500 µL cold lysis buffer. Lastly, the beads were resuspended in 30 µL 1X PBS (Table 2.18) and mixed with 2X LDS sample buffer (Table 2.16) at 1:1 ratio for future analysis by western blotting (section 2.4.4).

2.3.10 Effector pull-down

2.3.10.1 GST-Rhotekin-RBD pull-down

Transfected cells were grown for ~24 h before being serum-starved with DMEM supplemented with 0.5% FBS overnight. ~40 h post-transfection, cells were washed once with 2 mL DPBS before resuspended in 5 mL DPBS. The cells were pelleted at 1000 x g for 5 min at 4 °C. 100 µL (~10 µg) GST-Rhotekin-bead suspension were equilibrated with ice cold lysis buffer (Table 2.20). The cell pellets were resuspended in 600 µL lysis buffer and incubated on ice for 2 min before centrifugation at 13000 x g for 5 min at 4 °C. The cleared supernatant was transferred to the pre-equilibrated GST-Rhotekin-RBD-bead suspension and rotated at 4 °C for 45 min. Following incubation, the beads were washed 2X with lysis buffer before centrifugation at 1000 x g at 4 °C. The GTP-bound Rho-family proteins were eluted from the beads with 2X LDS sample buffer (Table 2.16) and analysed by western blotting (section 2.4.4).

Table 2.20: Buffer used for effector pull-down

Buffer	Ingredient
Lysis buffer pH 7.5	20 mM Tris pH 7.5 150 mM NaCl 5 mM $MgCl_2$ 0.5% NP40 Alternative 5 mM β-glycerophosphate 1 mM DTT 1X Mammalian Protease Inhibitor Cocktail

2.3.10.2 GST-PAK1-GBD pull-down

~24 h post-transfection, transfected cells were serum-starved overnight. Cells were then washed once with 2 mL DPBS and resuspended in 5 mL DPBS. The cells were then centrifuged at 1000 x g for 5 min at 4 °C. Pelleted cells were then lysed with 600 µL ice cold lysis buffer (Table 2.20) containing 10 µg GST-PAK1-GBD. The lysates were incubated on ice for 2 min before being pelleted at 13000 x g for 5 min at 4 °C. 10 µL glutathione sepharose 4B beads (GE Healthcare, Cat. No. 17-0756-01) were equilibrated with lysis buffer before incubation with the cleared supernatant for 45 min at 4 °C. Following incubation, the beads were washed twice with ice cold lysis buffer by centrifugation at 1000 x g for 2 min at 4 °C. The presence of GTP-bound Rho-family proteins were identified by western blotting (section 2.4.4).

2.3.11 Cell fractionation and effector pull-down

Transfected cells were serum-starved overnight in 0.5% FBS before harvesting, ~40 h post-transfection. Cells were resuspended in 5 mL DPBS and pelleted at 1000 x g for 5 min at 4 °C. The supernatant was discarded, and the cell pellets were resuspended in 300 µL ice cold hypotonic buffer (Table 2.17) alone for GST-Rhotekin-RBD pull-down assays or with buffer containing 10 µg GST-PAK1-GBD for GST-PAK1-GBD pull-down assays. Cells were then incubated on ice for 10 min. 0.5% NP40 Alternative was added to the cells, which were lysed by vortexing for 10 sec. The lysates were centrifuged at 1000 x g for 5 min at 4 °C. The pellets were kept on ice for nuclear-

enriched extraction, whereas the supernatants were transferred to tubes containing pre-equilibrated GST-Rhotekin-RBD-bead suspension or glutathione sepharose 4B beads (pre-equilibrated with lysis buffer) The tubes were rotated at 4 °C for 45 min. Following incubation, the beads were washed twice with lysis buffer and mixed with 2X LDS sample buffer (Table 2.16).

The remaining pellets retained for nuclear extraction were washed with 300 µL hypotonic buffer and resuspended in 300 µL ice cold lysis buffer (Table 2.20) alone for GST-Rhotekin-RBD pull-down or with buffer containing 10 µg GST-PAK1-GBD for GST-PAK1-GBD pull-down. The nuclear-enriched pellets were incubated on ice for 30 min with brief vortexing every 10 min. Following incubation, the samples were pelleted at 13000 x g and the supernatants, containing nuclear-enriched contents, were collected and transferred to tubes containing pre-equilibrated GST-Rhotekin-RBD-bead suspension or glutathione sepharose 4B beads. The tubes were rotated at 4 °C for 45 min before being washed twice with lysis buffer (Table 2.20) and mixed with 2X LDS sample buffer. Gel samples from the whole cell lysate and both the cytoplasmic and nuclear-enriched were also collected and analysed by western blotting (section 2.4.4)

2.4 Protein techniques

2.4.1 Reagents used for protein techniques

Table 2.21: Reagents for western blotting

Reagent	Manufacturer	Catalogue number
NuPAGE Novex 4-12% Bis-Tris Gel	ThermoFisher	NP0323
PageRuler Prestain Protein ladder	ThermoFisher	26616
Immobilon-P Transfer PVDF membranes	Millipore	IPVH00010
BF2 Chromatography paper	Sartorius	FT-2-519-460507N
Skimmed milk powder	Marvel	7888067
Luminol Sodium salt	Sigma-Aldrich	A4685
Para-hydroxy coumaric acid	Sigma-Aldrich	C9008
Acrylamide: Bis-Acrylamide solution	Biorad	20260005
Fuji X-ray film	Fuji	XRY001
Restore™ Western Blot Stripping Buffer	ThermoFisher	21059
Ammonium Persulphate	Melford Laboratories	A1512
TEMED	Sigma-Aldrich	T22500
Instant*Blue*™ stain	Expedeon	ISB1L
Ponceau- S	Sigma-Aldrich	P7170

2.4.2 Determination of protein concentration

Protein concentration was estimated using a Bradford assays, a colorimetric protein assay. 1 µL sample was added to 1 mL mixture solution containing 800 µL MilliQ water and 200 µL protein assay dye reagent concentrate (Bio-Rad, Cat. No. 500-0006) in a 1 mL cuvette. The solution was left at room temperature for ~5 min before measuring the A_{595}. Protein concentrations were estimated using a standard straight-line equation derived from Bovine serum albumin (BSA) standards.

2.4.3 SDS-PAGE and Coomassie staining

All purified proteins were resolved using Tris-glycine gels. Gels were prepared using the recipes in Table 2.22 into Novex® Mini 1.0 mm gel cassettes (Life Technologies, Cat. No. NC2010). 10 µL of protein samples were mixed with 2X SDS sample buffer (Table 2.23) at a 1:1 ratio. Gels were run in 1X SDS-PAGE running buffer (Table 2.23) in an XCell SureLock™ Mini-Cell Electrophoresis System (Life Technologies) at 200 volts for 55 min and stained using the Instant*Blue*™ stain (Table 2.21) for 1 h.

Table 2.22: Recipe for Tris-glycine gels

Ingredient	Resolving gel (12%)	Stacking gel (5%)
1.5 M Tris-HCL pH 8.8	1500 µL	-
0.5 M Tris-HCL pH 6.8	-	500 µL
30% Acrylamide[a]	2400 µL	250 µL
Sterile MilliQ	2000 µL	1200 µL
10% SDS	60 µL	20 µL
10% Ammonium Persulphate	48 µL	40 µL
TEMED	6 µL	2 µL

[a] 29:1 Acrylamide:Bis-Acrylamide solution

Table 2.23: Buffers used for SDS-PAGE

Buffer	Ingredient
2X SDS sample buffer	33.3 mM Tris-HCl pH 7.4 6 M Urea 3.3% SDS 66.7 mM 2-Mercaptethanol 0.1% (w/v) Bromophenol Blue
SDS-PAGE running buffer pH 8.3	25 mM Tris Base 192 mM Glycine 0.1% SDS

2.4.4 Western blotting

Proteins were resolved using SDS-PAGE either using precast NuPAGE® Novex® 4-12% gels at 200 volts for 35 min according to manufacturer's protocol or Tris-glycine gels (Table 2.22) run at 200 volts for 55 min. The PageRuler Prestained Protein ladder (ThermoFisher, Cat. No. 26616) was used as a marker. The proteins were then transferred to Immobilon®-P PVDF membrane either using an XCell II™ Blot Module (Invitrogen, Cat No. EI9051) or Semi-Phor™ Blotter (Hoefer Scientific Instrument, Cat. No. TE70), according to manufacturer's instruction.

After transfer, membranes were stained with Ponceau-S (Table 2.21) for 1 min to check the efficiency of protein transfer before blocking with 10% skimmed milk (Table 2.24) at 4 °C for a minimum of 1 h. Next, the membrane was incubated with specific antibodies towards the protein of interest for a specific period of time (Table 2.25) before being washed three times with 1X PBST (Table 2.18) for 20 min each. Proteins were visualized by treating with enhanced chemiluminescence solution (ECL) (Table 2.24) for 2 min and exposing the membrane to medical X-ray film.

Table 2.24: Buffers used for western blotting

Buffer	Ingredient
NuPAGE® running Buffer	50 mM Tris-HCl pH 7.3 50 mM MES 0.1% SDS 1 mM EDTA
1X Transfer buffer	26 mM Tris-HCl pH 7.2 149 mM Glycine 20% Methanol
Blocking solution	50 mL 1X PBS-Tween 5 g skimmed milk powder
Luminol solution	100 mM Tris-HCl pH 8.6 1.25 mM Sodium Luminol Salt
Enhancer solution	11 mg para-hydroxy coumaric acid 10 mL DMSO
Enhanced Chemiluminescence solution	5 mL Luminol Solution 50 µL Enhancer Solution 1.5 µL 30% H_2O_2 (Fisher Scientific, Cat. No. H/1800/15)

Table 2.25: Antibodies used in western blotting

Antibody	Manufacturer	Catalogue number	Dilution
Anti-FLAG-HRP	Sigma-Aldrich	A8592	1:5000
Anti-His-HRP	Santa Cruz Biotechnology	sc-8036 HRP	1:2500
Anti-V5-HRP	ThermoFisher	R961-25	1:5000
Anti-HA-HRP	Santa Cruz Biotechnology	sc-7392 HRP	1:500
Anti-pTyr-HRP	Santa Cruz Biotechnology	sc-7020 HRP	1:500
Donkey anti-Goat-HRP	Abcam	Ab6885	1:5000
Goat anti-Rabbit-HRP	Newmarket Scientific	GTXRB-DHRPX	1:5000
Goat anti-Mouse-HRP	Newmarket Scientific	GTXMU-DHRPX	1:5000
Anti-HA	Santa Cruz Biotechnology	Sc-7392	1:500
Anti-ACK	Santa Cruz Biotechnology	sc-28336	1:2500
Anti-RhoGDI-1	Sigma-Aldrich	06730	1:5000
Anti-RhoGDI-1	Santa Cruz Biotechnology	sc-373724	1:5000
Anti-RhoGDI-2	Proteintech	16122-1-AP	1:5000
Anti-RhoGDI-3	Santa Cruz Biotechnology	sc-393690	1 :100
Anti-RhoGDI-3	Aviva System Biology	ARP33854	1:1000
Anti-GAPDH	Santa Cruz Biotechnology	sc-47724	1:2500
Anti-GST	GE Healthcare	27-4577-01	1:50000
Anti-pTyr 284	Merck	09-142	1:2500
Anti-pTyr 607	Abnova	PAB24722	1:1000
Anti-Histone H3	Abcam	Ab1791	1:10000
Anti-Hsp56	Santa Cruz Biotechnology	sc-100758	1:1250
Anti-p53	Cell Signalling Technology	2524	1:1250
Anti-RhoA	Santa Cruz Biotechnology	Sc-418	1:500
Anti-RhoB	Proteintech	14326-1-AP	1:3000
Anti-RhoC	Cell Signalling Technology	3430	1:1000
Anti-Rac1	Merck	05-389	1:1250
Anti-Myc	Santa Cruz Biotechnology	sc-40	1:500
Anti-pSTAT3	Cell Signalling Technology	9145	1:5000

2.4.5 *In vitro* kinase assays

0.3 μM GST-ACK (1-489) was allowed to auto-phosphorylate by incubating with 0.5 mM ATP in 1X Kinase Buffer (Table 2.26) for 10 min at 30 °C. Following incubation, auto-phosphorylated ACK was added to 1X Kinase buffer containing 10 μM GST-RhoGDI-1 or GST-RhoGDI-2 and

0.5 mM ATP, in a total reaction volume of 50 µL. Reactions were incubated at 30 °C for 1 h before mixing with 2X LDS sample buffer (Table 2.16) at a 1:1 ratio. Gel samples from each reaction were collected and analysed by western blotting (section 2.4.4).

Table 2.26: Buffer used for *in vitro* kinase assays

Buffer	Ingredient
1X Kinase Buffer	20 mM Tris-HCl pH 7.5 10 mM $MgCl_2$ 0.5 mM DTT 0.1 mM Na_3VO_4

Chapter 3

The interaction of ACK with the RhoGDIs

A previous PhD student in the lab, Dr. J. Vicenté-García, performed a Y2H screen to identify novel ACK-interacting proteins (Clayton *et al.,* 2019). Using a construct spanning the N-terminal half of ACK as shown in Figure 3.1A, 14 novel interacting partners including RhoGDI-3 were identified. A construct spanning amino acids 73-225 of RhoGDI-3 (Figure 3.1B) was found to interact with the N-terminal half of ACK. This chapter describes the subsequent validation of the ACK-RhoGDI-3 interaction and the interactions found between ACK and all three RhoGDI family members through co-expression in mammalian cells and co-immunoprecipitation.

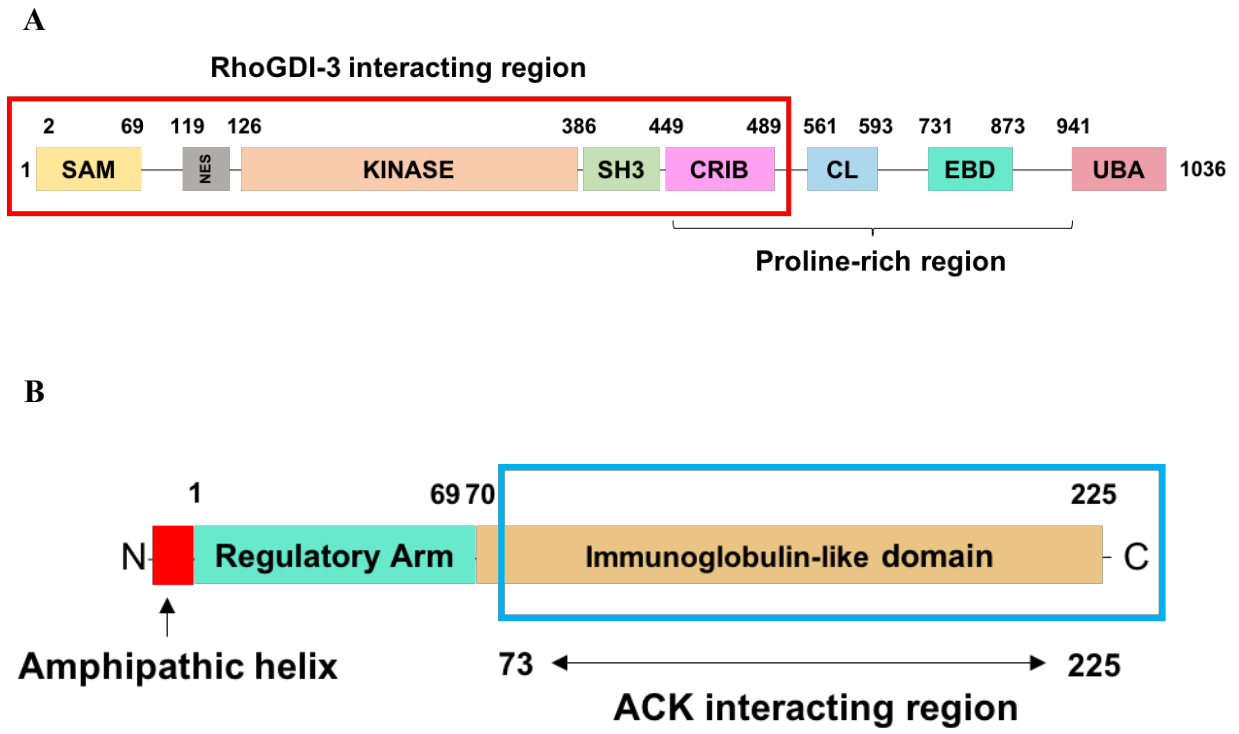

Figure 3.1: Regions of ACK and RhoGDI-3 involved in the interaction as identified by Y2H screening. (A) The N-terminal half of ACK (red box) (A) was found to interact with **(B)** the C-terminal of RhoGDI-3 (72-225 amino acids) as indicated by the blue box. SAM: sterile α motif, NES: nuclear export signal, Kinase: tyrosine kinase domain, SH3: Src Homology 3 domain, CRIB: Cdc42/Rac interacting binding region, CL: Clathrin-interacting region, EBD: EGFR binding domain and UBA: ubiquitin-association domain.

Generally, even though Y2H screening is known for its rapid identification of interacting proteins in a eukaryotic system, it also has some drawbacks such as high rates of false negative or positive result. These can be due to a potential decrease in the stability of proteins of interest in a non-native environment and the possibility that a lack of native post-translational modifications will affect binding between proteins (Brückner *et al.,* 2009). Thus, it is important for any interaction identified by Y2H to be validated by an orthogonal method, for example co-immunoprecipitation, which is a widely accepted method used to detect physiological interactions between proteins. However, low affinity and transient protein-protein interaction can also be difficult to detect through co-immunoprecipitation.

Co-immunoprecipitation utilizes immunoaffinity between the primary protein (bait) and the support reagent to detect secondary protein(s) (targets) bound to the primary. For instance, in this work, for immuno-based detection of an interaction, Protein G coated Dynabeads™ were used as a support to immobilise antibodies specific for the bait. Protein G is a bacterial cell wall protein that has the ability to recognize and bind to the Fc region of mammalian immunoglobulin G (IgG) antibodies. It also possible to utilize innate affinity where the highly selective affinity between, for example, poly-histidine (6X His) and beads coated with cobalt can be used to separate His-tagged proteins. The latter method is especially good for removing non-specific background caused, for example, by antibody heavy and light chains, which is especially important when analysing proteins that run at ~55 and ~25 kDa. Since all three RhoGDI family members are ~25 kDa, their detection can be masked by the presence of these chains, thus the latter method was more suitable in some cases. His-tagged proteins and cobalt-coated Dynabeads were therefore used to analyse the interactions between ACK and Rho-GDI-1 or -2. Attempts were made to identify the interaction between His-tagged RhoGDI-3 and ACK using the same method, however His-RhoGDI-3 expression could not be detected using anti-His antibody. Therefore, the interaction between ACK and RhoGDI-3 was validated using FLAG-RhoGDI-3 and Protein G coated Dynabeads™.

3.1 Validation of the ACK-RhoGDI-3 interaction

The interactions between exogenously transfected full-length *Homo sapiens* RhoGDI-3 and ACK together with a kinase dead form of ACK (K158R), dACK, were analysed in HEK293T cell by co-immunoprecipitation. An expression construct for HA-tagged ACK was a kind gift from Prof. Ed Manser (Institute of Molecular and Cell Biology, Singapore). Both of the mammalian constructs encoding FLAG-tagged RhoGDI-3 and HA-tagged dACK were already available in the lab.

3.1.1 Expression trials of FLAG-RhoGDI-3, HA-ACK and HA-dACK

Prior to co-immunoprecipitation, expression trials of all constructs were performed. 5 µg each of HA-ACK, HA-dACK and FLAG-RhoGDI-3 were transfected, either alone or together, into HEK293T cells and allowed to express for ~40 h as described in section (section 2.3.4). Protein levels were analysed by western blotting using anti-HA antibody for ACK and dACK and anti-FLAG antibody for RhoGDI-3.

Figure 3.2 shows that expression levels of HA-dACK were generally lower than HA-ACK and this has been observed previously in the lab. FLAG-RhoGDI-3 was detected under all three condition but decreased in the presence of dACK and decreased even more substantially in the presence of ACK. These transfections conditions were therefore used for co-immunoprecipitation and other future analyses.

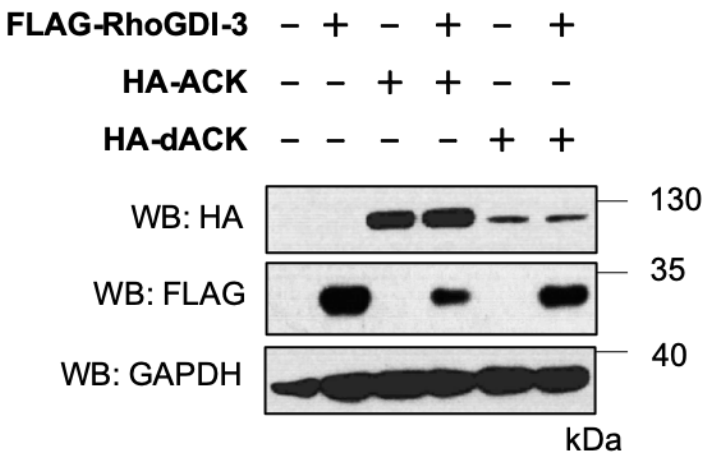

Figure 3.2: Expression of FLAG-RhoGDI-3, HA-ACK and HA-dACK in HEK293T cell. 5 µg each of FLAG-RhoGDI-3, HA-ACK and HA-dACK were transfected either alone or in combination into HEK293T cells and harvested after ~40 h. The expression of the recombinant proteins was assessed using western blot analysis. GAPDH was used as a marker to indicate even loading of samples.

3.1.2 The interaction of RhoGDI-3 with ACK and dACK

Following expression trials, the interactions between RhoGDI-3 and ACK or dACK were analysed by co-immunoprecipitation using anti-FLAG antibody to pull-down FLAG-RhoGDI-3 or anti-ACK antibody to precipitate HA-ACK or HA-dACK. Briefly, FLAG-RhoGDI-3, HA-ACK and HA-dACK were transfected into HEK293T cells alone or in combinations and allowed to express for ~40 h before harvesting and lysis. Pre-cleared supernatant samples were immunoprecipitated with anti-FLAG or anti-ACK antibodies that was cross-linked to a set of pre-washed Protein G Dynabeads. Bound proteins were then detected using anti-ACK antibody for ACK and dACK or anti-FLAG antibody for RhoGDI-3.

As shown in Figure 3.3, RhoGDI-3 was seen to interact with both ACK or dACK when lysates were immunoprecipitated with either FLAG (RhoGDI-3) or ACK. These data also suggest that the interaction is independent of ACK kinase activity. These data therefore validated the interaction found through Y2H and hence suggested a possible new role for ACK in regulating Rho-family GTPases via one of their main regulators, RhoGDI-3.

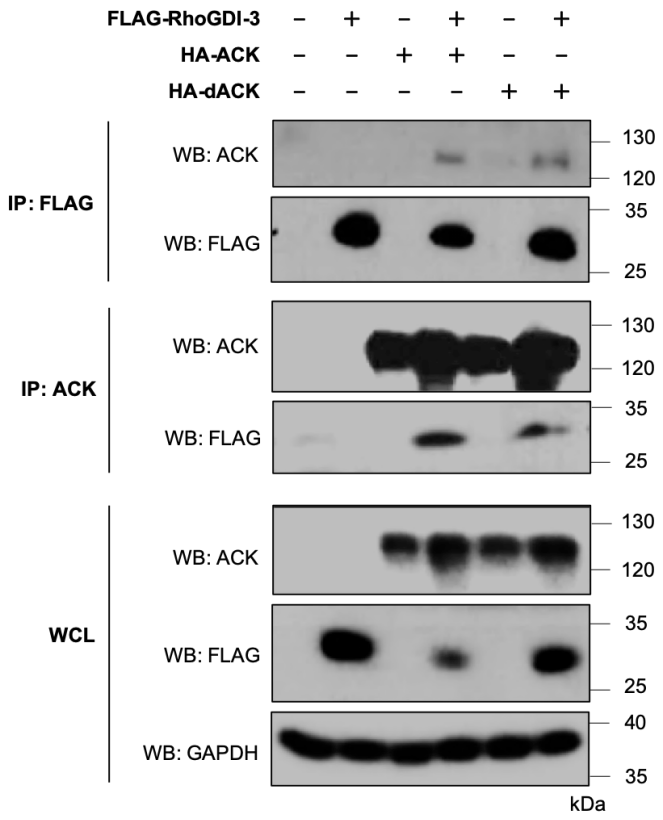

Figure 3.3: Co-immunoprecipitation of RhoGDI-3 with ACK and dACK. FLAG-RhoGDI-3, HA-ACK and HA-dACK were transfected either alone or in combination into HEK293T cells and harvested after ~40 h. Cells were then lysed and immunoprecipitated with anti-FLAG or anti-ACK antibodies. Co-immunoprecipitated protein were assessed using anti-FLAG antibody for FLAG-RhoGDI-3 or anti-ACK antibody for HA-ACK and HA-dACK. The expression of the recombinant protein in the whole cell lysate (WCL) is shown in the bottom 3 panels, while the co-immunoprecipitated (IP) samples are shown in the top 4 panels. In whole cell lysates, analysis of GAPDH was used to assess equal loading of samples across the wells. The western blot shown is representative of at least three independent experiments. **WCL:** whole cell lysate; **IP:** immunoprecipitation.

3.2 The interaction of ACK with other RhoGDI family members

The Y2H data indicated that residues 73-225 of RhoGDI-3 mediates the interaction with ACK (Figure 3.1). As all three human RhoGDI proteins share more than 50% similarity at their C-termini (Figure 1.12) (Olofsson, 1999), it was postulated that RhoGDI-1 and 2 could also interact with ACK. His-tagged RhoGDI-1 and His-tagged RhoGDI-2 constructs were therefore used to analyse any possible interactions with HA-ACK and HA-dACK.

3.2.1 Cloning of full-length RhoGDI-2 into the mammalian expression vector, pDEST26

A His-tagged full length RhoGDI-1 mammalian expression vector, a Gateway entry clone for His-RhoGDI-2 and a Gateway mammalian expression vector, pDEST26, were already available in the lab. Full length *Homo sapiens* RhoGDI-2 was transferred from the Gateway entry clone into the Gateway expression vector, pDEST26 by LR recombination. The LR reaction utilises the Lambda recombination system to facilitate the transfer of DNA surrounded by *att* sites, a site-specific attachment sequences, from entry clones into appropriate destination vectors. RhoGDI-2 was recombined into pDEST26 and the resultant DNA was transformed into chemically competent *E. coli* TOP10 cells. DNA from individual colonies was analysed using *Bsr*G1 restriction analysis. The correct size of the insert was determined by gel electrophoresis and confirmed by DNA sequencing.

As shown in Figure 3.4, clone 1 showed the correct size of insert at ~605 bp. This expression clone was then used for mammalian trial expressions and co-immunoprecipitation.

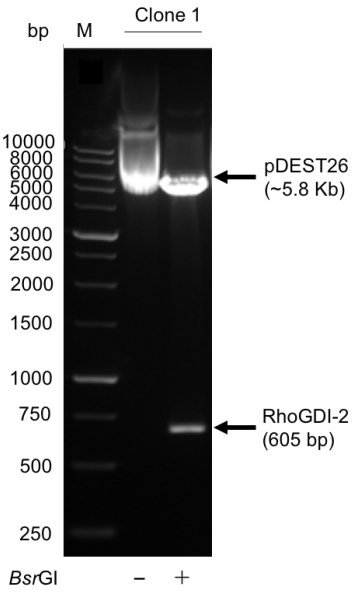

Figure 3.4: *Bsr*GI digestion of a full length RhoGDI-2 mammalian expression clone. A selected colony from Gateway cloning of pDEST26-RhoGDI-2 was digested with *Bsr*GI and the digested products were separated by agarose gel electrophoresis. **M:** Marker

3.2.2 Expression of RhoGDI-1 and -2 in mammalian cell lines

The expression of His-RhoGDI-1 and His-RhoGDI-2 constructs was analysed in HEK293T cells. A range of DNA concentrations from 1 μg to 5 μg was transfected into HEK293T cells. A minimum of 0.5 μg of GFP expression construct was used as a transfection control. The expression level for each protein, under each condition was determined by western blotting with an anti-His antibody.

Figure 3.5A shows the expression level of His-RhoGDI-1 and His-RhoGDI-2 increased with the increasing amount of DNA in each transfection. Conditions were chosen where the band intensity for RhoGDI-1 and -2 expression were similar to each other and to that of RhoGDI-3 to allow all the interactions to be easily viewed in the same experiments. 2 μg of RhoGDI-1 and 4.5 μg of RhoGDI-2 showed similar expression levels as 5 μg of FLAG-RhoGDI-3 (Figure 3.5B).

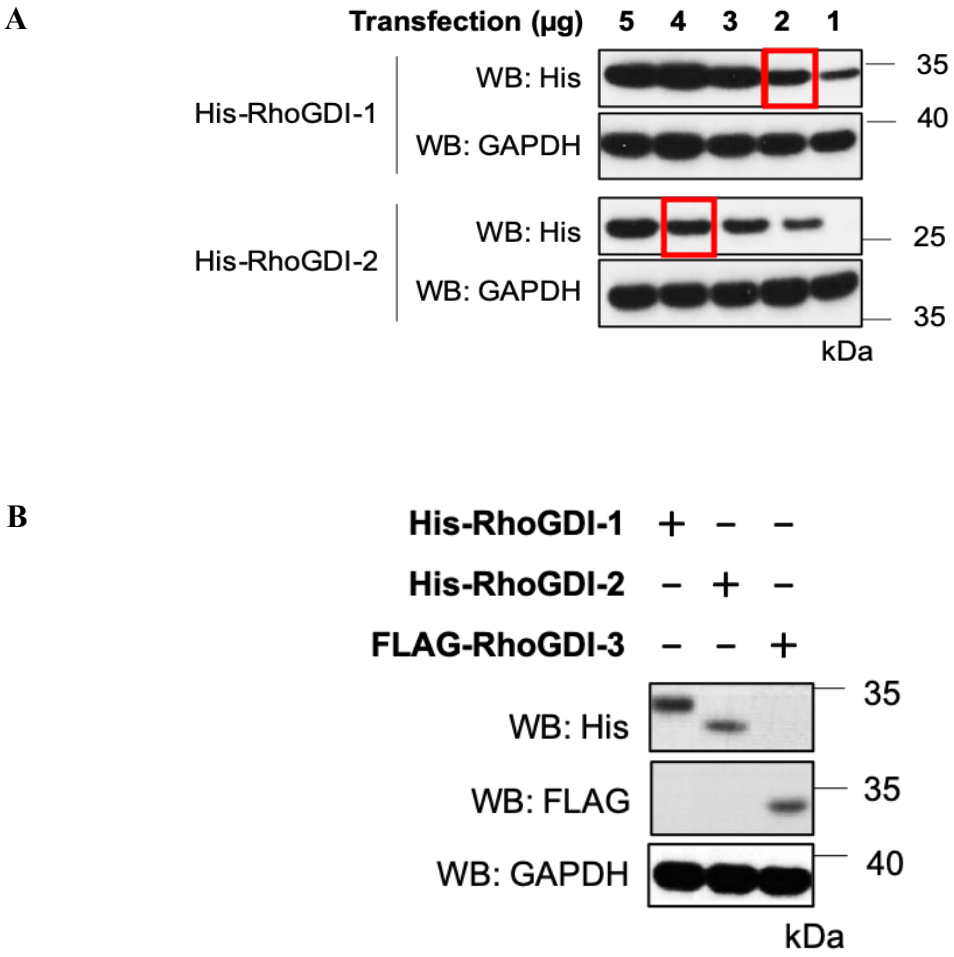

Figure 3.5: Expression of full length His-RhoGDI-1 and His-RhoGDI-2 in HEK293T cells. **(A)** Transfection trials of His-RhoGDI-1 and His-RhoGDI-2 using DNA between 1 µg to 5 µg. Cells were harvested after ~40 h transfection and subjected to western blotting analysis. Red boxes indicate similar levels of RhoGDI-1 and -2. **(B)** Transfection trials of 2 µg of His-RhoGDI-1, 4.5 µg of His-RhoGDI-2 and 5 µg of FLAG-RhoGDI-3. Analysis of GAPDH was used to asses equal loading of samples across the wells.

These optimised conditions were then used to analyse expression levels with ACK and dACK (Figure 3.6). Both His-RhoGDI-1 and His-RhoGDI-2 showed similar pattern of expression to FLAG-RhoGDI-3, with a noticeable decrease in expression when co-expressed with HA-ACK and a smaller decrease with HA-dACK. The levels of ACK increased in cells co-expressing RhoGDI-

1 but not RhoGDI-2, whereas dACK increased in both cells co-expressing RhoGDI-1 and RhoGDI-2.

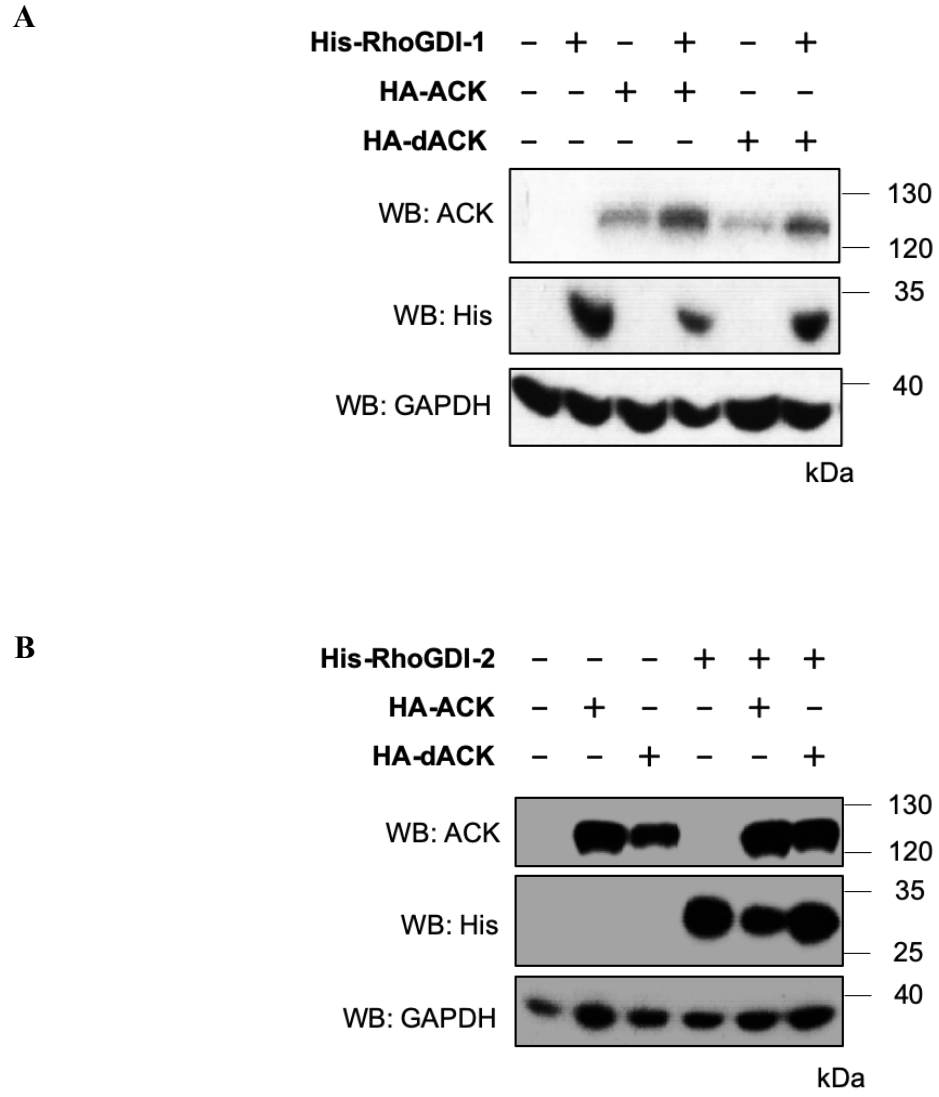

Figure 3.6: Co-expression of full length RhoGDI-1, RhoGDI-2, ACK and dACK in HEK293T cells. (A) Co-expression of His-RhoGDI-1, HA-ACK and HA-dACK. **(B)** Co-expression of His-RhoGDI-2, HA-ACK and HA-dACK. Cells were harvested after ~40 h transfection and subjected to western blotting analysis. Analysis of GAPDH was used to asses equal loading of samples across the wells.

3.2.3 The interactions of RhoGDI-1 and -2 with ACK and dACK

The interactions of RhoGDI-1 or -2 with ACK or dACK were analysed using cobalt-coated magnetic beads. Briefly, His-RhoGDI-1 and -2 were co-expressed with HA-ACK or HA-dACK for ~40 h. The lysates were then incubated with cobalt-coated magnetic beads at 4 °C and the precipitated proteins were analysed by western blotting with anti-His and anti-ACK antibodies.

RhoGDI-1 (Figure 3.7) and RhoGDI-2 (Figure 3.8) were shown to interact with ACK. This work therefore identified a further two new binding targets of ACK in addition to RhoGDI-3 and indicated that ACK may regulate the whole mammalian Rho-GDI family.

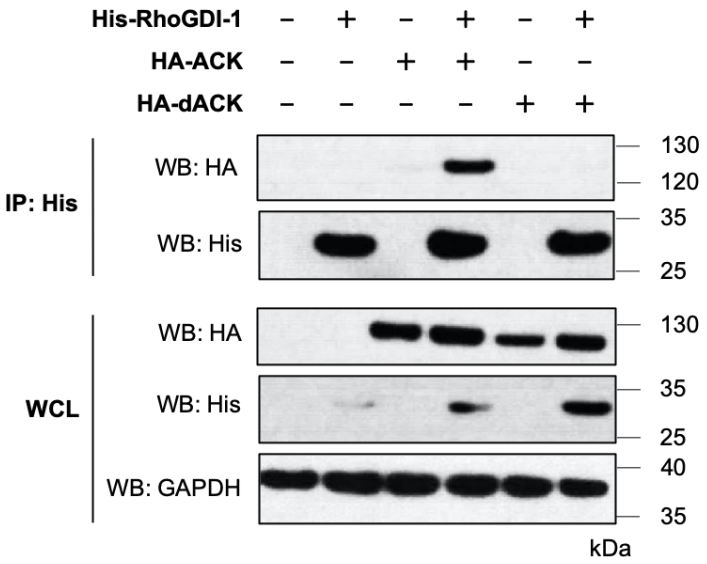

Figure 3.7: Co-immunoprecipitation of RhoGDI-1 with ACK and dACK. His-RhoGDI-1 was transfected alone or together with HA-ACK or HA-dACK into HEK293T cells. Constructs were allowed to express for ~40 h before harvested and lysed. The lysates were then precipitated with cobalt-coated magnetic beads for ~1 h. The precipitated proteins were assessed using anti-His or anti-ACK antibodies. The expression of the recombinant protein in the whole cell lysate (WCL) is shown in the bottom 3 panels, while the co-immunoprecipitated (IP) samples are shown in the top two panels. In whole cell lysate, GAPDH was used to assess equal loading of samples across the wells. The western blot shown is representative of at least two independent experiments. **WCL:** whole cell lysate; **IP:** immunoprecipitation.

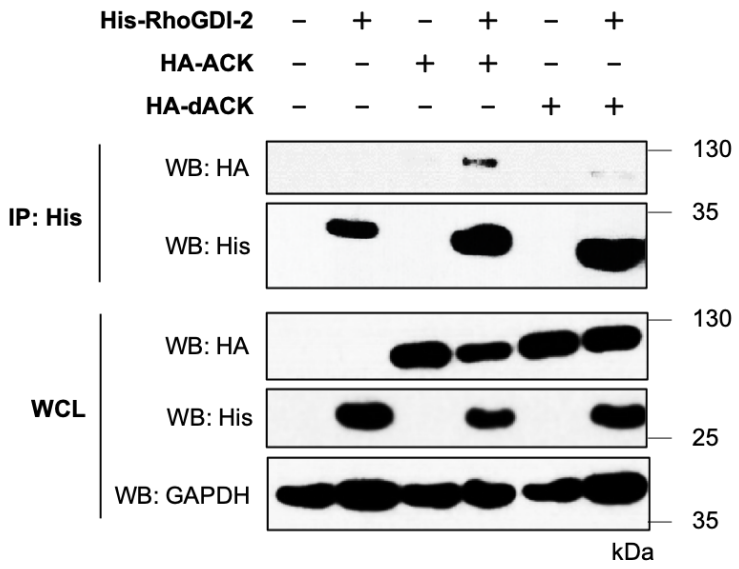

Figure 3.8: Co-immunoprecipitation of RhoGDI-2 with ACK and dACK. His-RhoGDI-2 was transfected alone or together with HA-ACK or HA-dACK into HEK293T cells. Constructs were allowed to express for ~40 h before harvested and lysed. The lysates were then precipitated with cobalt-coated magnetic beads for ~1 h. The precipitated proteins were assessed using anti-His or anti-ACK antibodies. The expression of the recombinant protein in the whole cell lysate (WCL) is shown in the bottom 3 panels, while the co-immunoprecipitated (IP) samples are shown in the top two panels. In whole cell lysate, GAPDH was used to assess equal loading of samples across the wells. The western blot shown is representative of at least three independent experiments. **WCL:** whole cell lysate; **IP:** immunoprecipitation.

3.3 The interaction between endogenous ACK and RhoGDI-1

3.3.1 Antibody selection for RhoGDI

All the interactions shown so far relied on exogenous expression of all proteins. Thus, attempts were made to show the interaction between endogenous ACK and RhoGDIs. A selection of commercially available RhoGDI antibodies were tested for specificity. Five antibodies were

available which were suggested to be specific for certain RhoGDI family members (Table 3.1). These antibodies were tested with exogenously expressed RhoGDIs in HEK293T cells.

Table 3.1 Commercial antibodies for RhoGDI proteins

RhoGDI	Manufacturer	Catalogue number
RhoGDI-1	Sigma-Aldrich	06730
	Santa Cruz Biotechnology	sc-373724
RhoGDI-2	Proteintech	16122-1-AP
RhoGDI-3	Santa Cruz Biotechnology	sc393690
	Aviva System Biology	ARP33854

His-RhoGDI-1 was predicted to have a MW of ~27 kDa, while His-RhoGDI-2 was ~26 kDa. Endogenous RhoGDI-1 and -2 were expected to be 24 and 23 kDa, respectively. Figure 3.9A shows that the commercially available antibody for RhoGDI-1, 06730, cross-reacts with RhoGDI-2. However, the second antibody for RhoGDI-1, sc-373724, is specific for RhoGDI-1. The RhoGDI-2 antibody, 16122-1-AP, recognises both RhoGDI-1 and RhoGDI-2 but not RhoGDI-3 (Figure 3.9B).

FLAG-RhoGDI-3 was anticipated to be at ~28 kDa and the endogenous RhoGDI-3 would be at ~25 kDa. Unfortunately, neither of the antibodies for RhoGDI-3 were specific, as they also detected RhoGDI-1 (Figure 3.10). The epitope used to raise the antibody sc393690 is confined within amino acids 1-95 of mouse RhoGDI-3, however human RhoGDI-3 is ~80% similarity in this region. Since the other RhoGDIs also share ~40% sequence similarity in this particular region, this may contribute to the non-specificity of the antibody. The second RhoGDI-3 antibody, ARP33854, is raised against a synthetic peptide from N-terminal region of human RhoGDI-3, nevertheless, this antibody also detects RhoGDI-1.

As only one specific antibody was identified and this recognized endogenous RhoGDI-1, this work was taken forward to investigate the interaction between endogenous RhoGDI-1 and ACK.

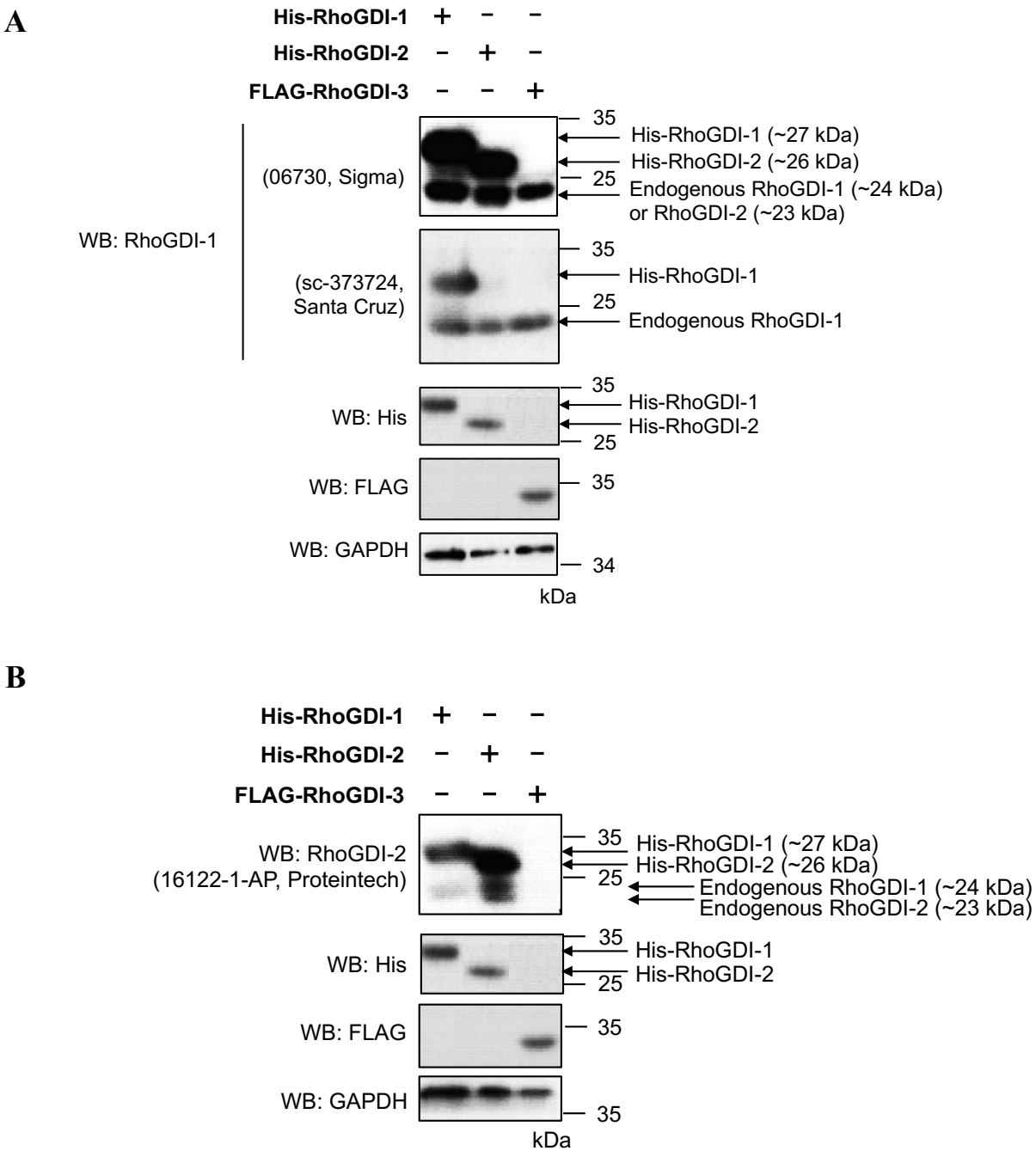

Figure 3.9: The specificity profiles of commercially available antibodies for RhoGDI-1 and -2. Commercially available antibodies for both RhoGDI-1 and -2 were tested using exogenously expressed RhoGDIs by western blot analysis. HEK293T cells were transfected with His-RhoGDI-1, -2 and FLAG-RhoGDI-3. Constructs were allowed to express for ~ 40 h before being harvested and lysed. The specificity of the antibodies was assessed by western blotting with **(A)** RhoGDI-1 and **(B)** RhoGDI-2 antibodies.

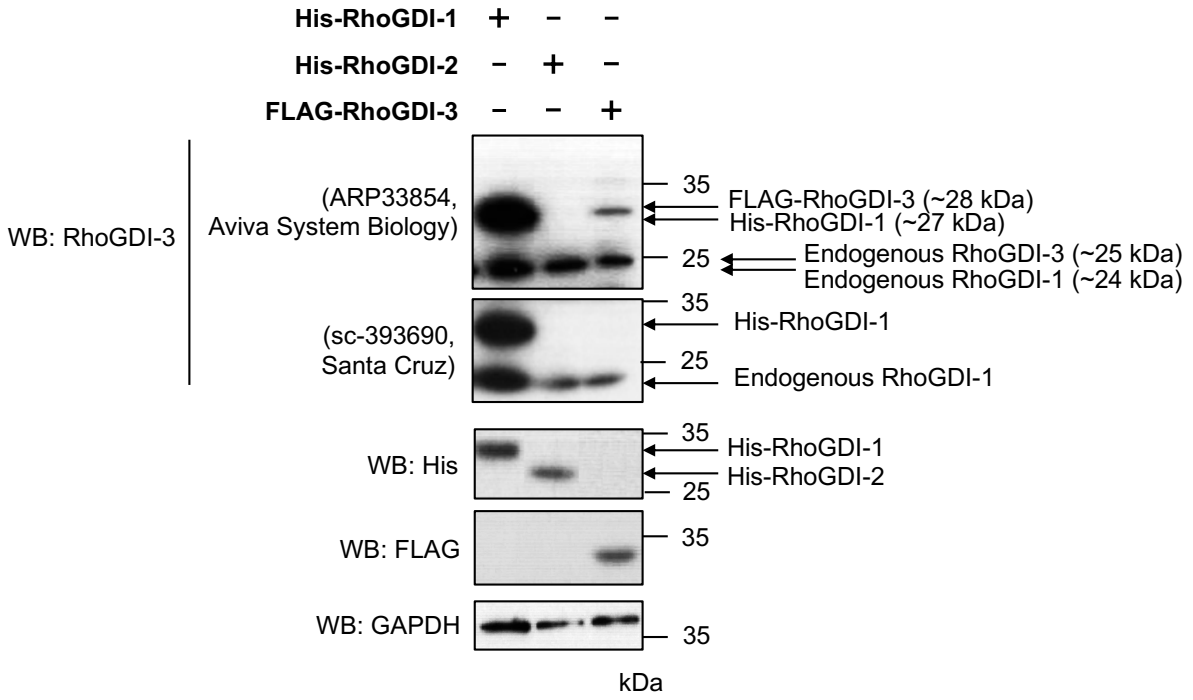

Figure 3.10: The specificity profiles of commercially available antibodies for RhoGDI-3. Commercially available antibodies for RhoGDI-3 were tested using exogenously expressed RhoGDIs by western blot analysis. HEK293T cells were transfected with His-RhoGDI-1, -2 and FLAG-RhoGDI-3. Constructs were allowed to express for ~ 40 h before being harvested and lysed. The specificity of the antibodies was assessed by western blotting.

3.3.2 Visualization of endogenous ACK and RhoGDI-1

Amongst the three RhoGDIs, RhoGDI-1 is ubiquitously expressed (Olofsson, 1999). Endogenous levels of ACK have also been visualized in several cancer cell lines such as pancreatic cancer (PANC-1, CD18), prostate cancer (LAPC-4 and LNCaP), breast cancer (MCF7), lung cancer (H292) and ovarian cancer (A2780-CP) (Mahajan *et al.,* 2012). Since PANC-1 and LNCaP cells were available in the lab, they were tested for detection of endogenous ACK and RhoGDI-1 by western blotting with specific antibodies for ACK and RhoGDI-1.

As shown in Figure 3.11, endogenous levels of both ACK and RhoGDI-1 were identified in both PANC-1 and LNCaP cells. These cell lines were therefore used to determine if there was an endogenous interaction between ACK and RhoGDI-1.

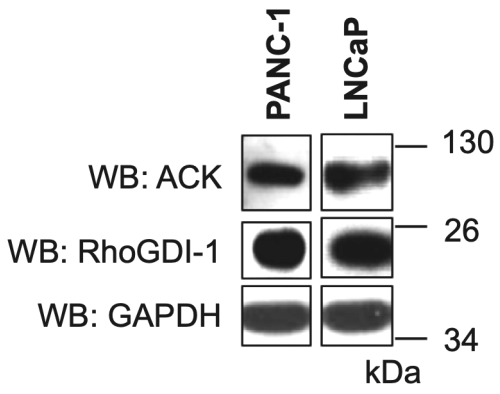

Figure 3.11: Endogenous levels of ACK and RhoGDI-1 in PANC-1 and LNCaP cells. PANC-1 and LNCaP cells were allowed to grow to 80% confluency before being harvested and lysed. The endogenous protein levels of ACK and RhoGDI-1 were identified by western blotting. GAPDH was used to assess equal loading of samples across the wells.

3.3.3 The interaction between endogenous ACK and RhoGDI-1

The interaction between endogenous ACK and RhoGDI-1 was investigated by co-immunoprecipitation. Briefly, the cells were allowed to grow to 80% confluency before being harvested and lysed. The lysates were then immunoprecipitated with either anti-IgG (mouse or rabbit) as a control, anti-ACK or anti-RhoGDI-1 antibodies for ~1 h at 4°C. The precipitated proteins were assessed by western blotting.

Endogenous RhoGDI-1 was seen to interact with ACK in LNCaP cells (Figure 3.12A). RhoGDI-1 appears to be in all precipitated PANC-1 samples (Figure 3.12B) making the interaction between ACK and RhoGDI-1 in PANC-1 cells inconclusive.

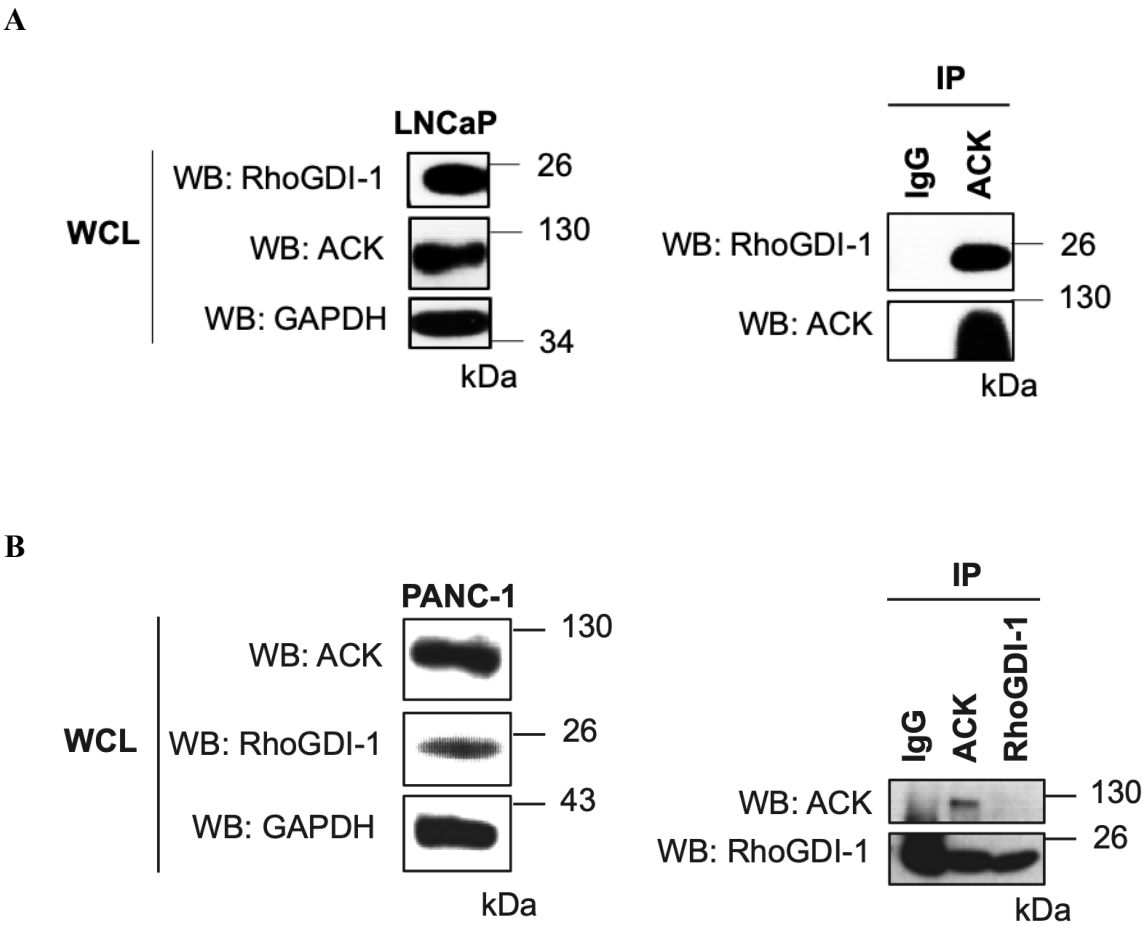

Figure 3.12: The interaction between endogenous ACK and RhoGDI-1 in LNCaP and PANC-1 cells. LnCaP and PANC-1 cells were allowed to grow to 80% confluency before being harvested and lysed. The lysates were then immunoprecipitated with anti-IgG, anti-ACK or anti-RhoGDI-1 antibodies. The precipitated proteins were determined by western blotting. The endogenous expression of each protein in the whole cell lysate (WCL) is shown on the left, while the co-immunoprecipitated (IP) samples are shown on the right. In whole cell lysates, GAPDH was used to assess equal loading of samples across the wells. **WCL:** whole cell lysate; **IP:** immunoprecipitation. **(A)** LNCaP cells and **(B)** PANC-1 cells.

3.4 Summary

The data presented in this chapter show that all three RhoGDIs are binding partners of ACK.

Attempts were made to validate the interaction between ACK and all three RhoGDIs with endogenous proteins. However, since commercially available antibodies were only specific for RhoGDI-1 and not for RhoGDI-2 and RhoGDI-3, the interaction with endogenous ACK was only validated for RhoGDI-1. ACK was also shown to interact with RhoGDI-1 only in the prostate cancer cell line, LNCaP.

Chapter 4

The effect of ACK on the phosphorylation status of RhoGDI proteins

This chapter will discuss all the efforts undertaken to determine whether the RhoGDIs are substrates for ACK. The initial findings showed ACK might phosphorylate the RhoGDIs. Unfortunately, as the work continue to identify the phosphorylation sites on RhoGDI-2, it become apparent that the observed phosphorylation was on a tyrosine present within the *att*B1 site on the Gateway expression vector used to express the protein.

4.1 Initial analysis of the phosphorylation status of the RhoGDI proteins

ACK was shown to interact with all three RhoGDIs in the previous chapter. Thus, it was hypothesized that these proteins could be substrates for ACK, so their phosphorylation status was

analysed using co-immunoprecipitation and western blotting with a pan anti-pTyr antibody. The phosphorylation status of RhoGDIs was only determined for RhoGDI-1 and -2 but not RhoGDI-3 as the His-tagged version of RhoGDI-3 did not express in HEK293T cells. Attempts were made to use different expression constructs of RhoGDI-3 but these gave a high background that made the analysis difficult.

Briefly, full-length His-RhoGDI-1 and -2 expression constructs were transfected into HEK293T cells alone or co-transfected with HA-ACK or dACK. ~40 h post-transfection, cells were harvested and lysed. The lysates were then precipitated with cobalt-coated magnetic beads for ~1 h at 4°C. Following incubation, the beads were washed and eluted with sample buffer and analysed by western blotting with a pan anti-pTyr antibody.

As shown in Figure 4.1A, phospho-ACK, (pACK, ~120 kDa) was detected in the cells transfected with ACK alone, while no pACK was detected in cells transfected with dACK. These expression patterns for ACK and dACK were expected and useful as an antibody control as ACK undergoes autophosphorylation at Tyr284 and dACK, the kinase-dead form of ACK does not autophosphorylate. The data in Figure 4.1B show that both RhoGDI-1 and -2 were phosphorylated with the phospho-RhoGDI (pRhoGDI) bands only appearing in cells expressing ACK, and not in the controls. These data suggested that both RhoGDI-1 and -2 were substrates of ACK.

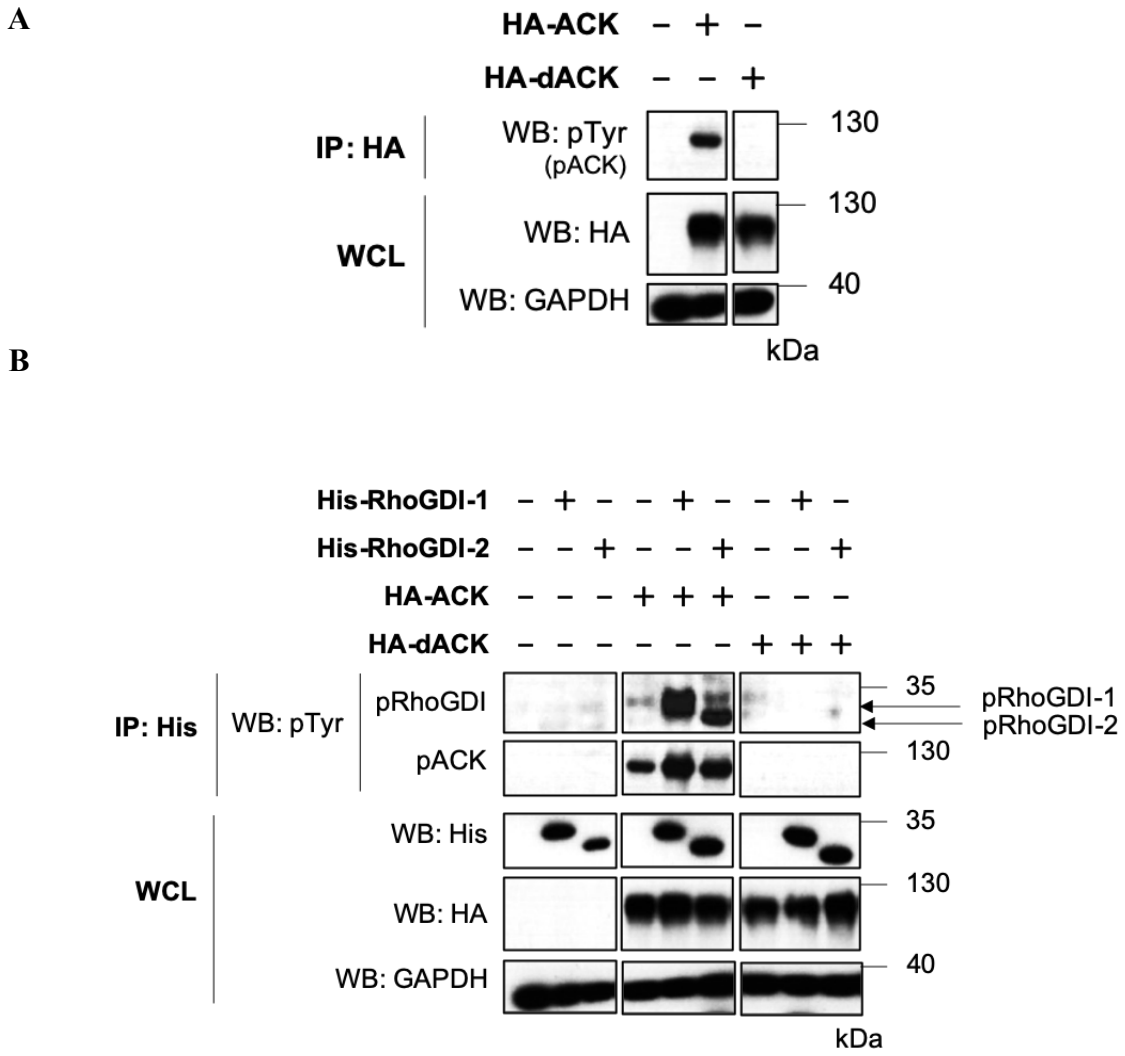

Figure 4.1: The phosphorylation status of RhoGDI-1 and -2 in the presence of ACK. His-tagged RhoGDIs, HA-ACK and HA-dACK were transfected alone or in combination into HEK293T cells. Constructs were allowed to express for ~40 h before being harvested and lysed. The lysates were then precipitated with anti-HA antibody or cobalt-coated magnetic beads before elution with sample buffer. The presence of pACK and pRhoGDIs were identified by western blotting with a pan anti-pTyr antibody. The expression of the recombinant protein in the whole cell lysate (WCL) is shown in the bottom two or 3 panels, while the co-immunoprecipitated (IP) samples are shown in the top one or two panels. GAPDH was used to assess the equal loading of samples. **WCL:** whole cell lysate; **IP:** immunoprecipitation. **(A)** pACK and **(B)** pRhoGDI-1 and -2.

4.2 Identification of the primary ACK phosphorylation sites on RhoGDI-2

ACK has been shown to phosphorylate multiple substrates on tyrosine and in one case on serine residues (Yokoyama *et al.,* 2005). For instance, ACK was found to phosphorylate cortactin, an Arp2/3 regulatory protein on Tyr421, Tyr466 and Tyr482 (Kelley *et al.,* 2012). Since ACK has been shown to interact with all three RhoGDIs, it was assumed that ACK would phosphorylate both RhoGDI-1 and -2 at conserved tyrosine residues shared by the RhoGDIs (Figure 4.2).

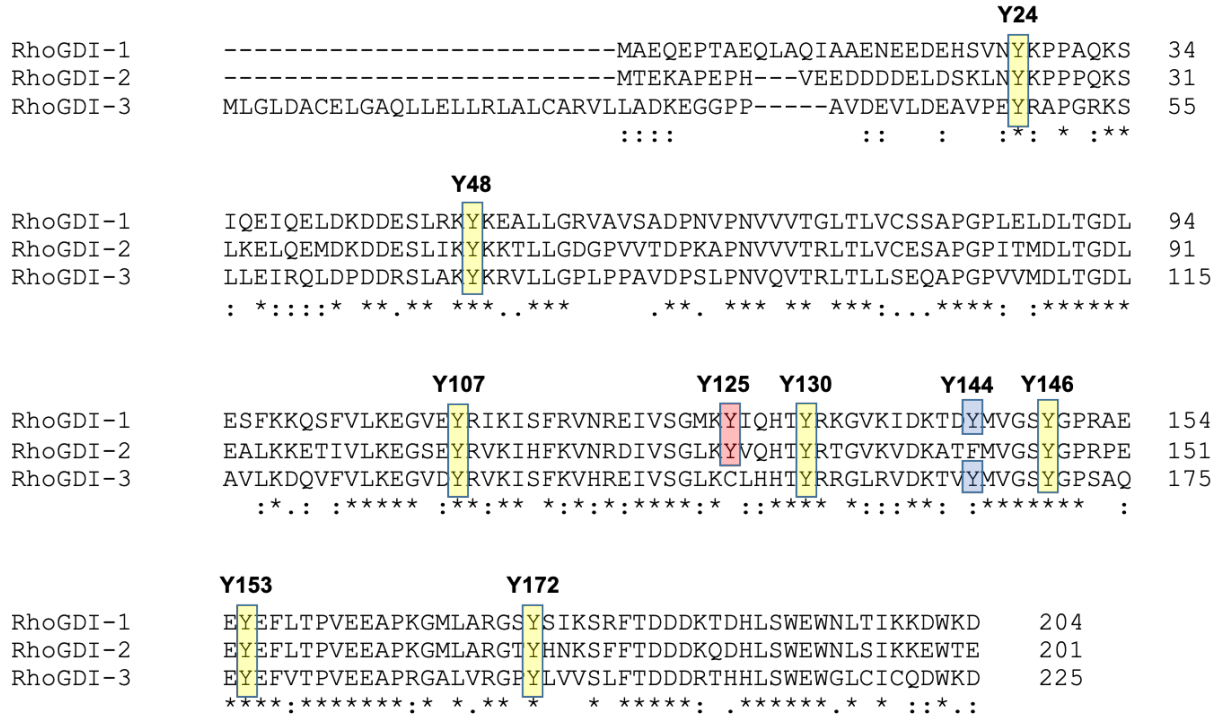

Figure 4.2: Conserved tyrosine sites between the three RhoGDIs. The sequence of all three RhoGDIs was aligned using multiple sequence alignment programme, Clustal Omega. Conserved tyrosine sites between all three RhoGDIs are highlighted in yellow, with RhoGDI-2 numbering. A tyrosine sites not fully conserved but shared between RhoGDI-1 and -2 (RhoGDI-2 numbering) is highlighted in red, while one shared between RhoGDI-1 and -3 is blue (RhoGDI-1 numbering). Asterisk (*) single, fully conserved residue, colon (:) conservation between groups of strongly similar properties and period (.) conservation between groups of weakly similar properties.

RhoGDI-1 and -2 have been shown to be phosphorylated at a conserved Tyr156 and Tyr153, respectively, by several kinases such as Src, Syk, c-Abl (DerMardirossian *et al.,* 2006; Wu *et al.,* 2009; Liu *et al.,* 2019; Luo *et al.,* 2013). This tyrosine is also conserved in RhoGDI-3, suggesting that ACK might also phosphorylate the RhoGDIs at this residue. To test this, Tyr153 of RhoGDI-2 was mutated to phenylalanine (His-Y153F-RhoGDI-2) and its phosphorylation by ACK was re-examined.

Figure 4.3 shows that the Y153F-RhoGDI-2 mutant retained its ability both to interact with and be phosphorylated by ACK, indicating that Tyr153 was not the target phosphorylation site for ACK on RhoGDI-2.

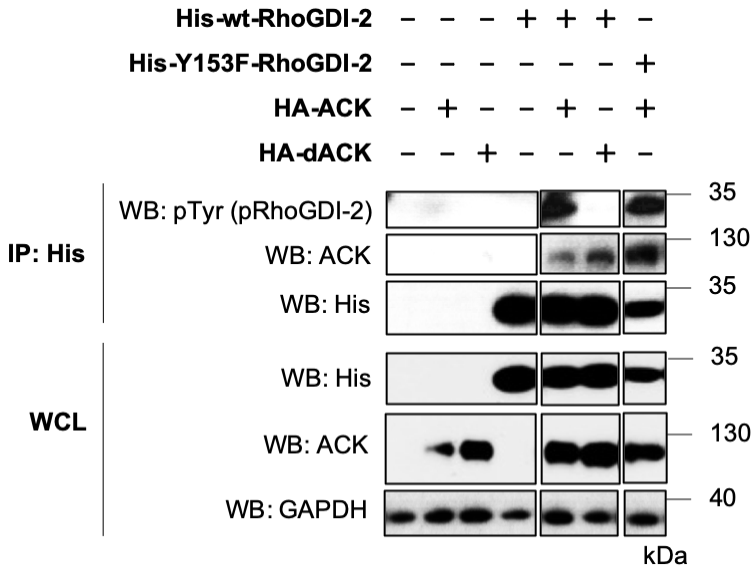

Figure 4.3: Phosphorylation at Y153F-RhoGDI-2 by ACK. His-Y153F-RhoGDI-2 and His-wt-RhoGDI-2 was transfected into HEK293T cells either alone or together with HA-ACK. Constructs were allowed to express for ~40 h before harvested and lysed. The lysates were then precipitated with cobalt-coated magnetic beads before eluted with sample buffer. The interaction and phosphorylation levels of Y153F-RhoGDI-2 mutant were determined by western blotting with an anti-ACK and a pan anti-pTyr antibody, respectively. The expression of the recombinant protein in the whole cell lysate is shown in the bottom 3 panels, while the co-immunoprecipitated (IP) samples are shown in the top 3 panels. GAPDH was used to assess the equal loading of samples. **WCL:** whole cell lysate; **IP:** immunoprecipitation.

As Tyr153 was not the target phosphorylation site for ACK on RhoGDI-2, all 6 remaining conserved tyrosine residues (Figure 4.2) were mutated individually to phenylalanine and then assessed for their binding and phosphorylation status when expressed with ACK in HEK293T cells. RhoGDI-2 wt was used as a control.

Firstly, the ability for each of the mutant to bind to ACK was assessed. The data in Figure 4.4 shows all the RhoGDI-2 mutants retain the ability to interact with ACK.

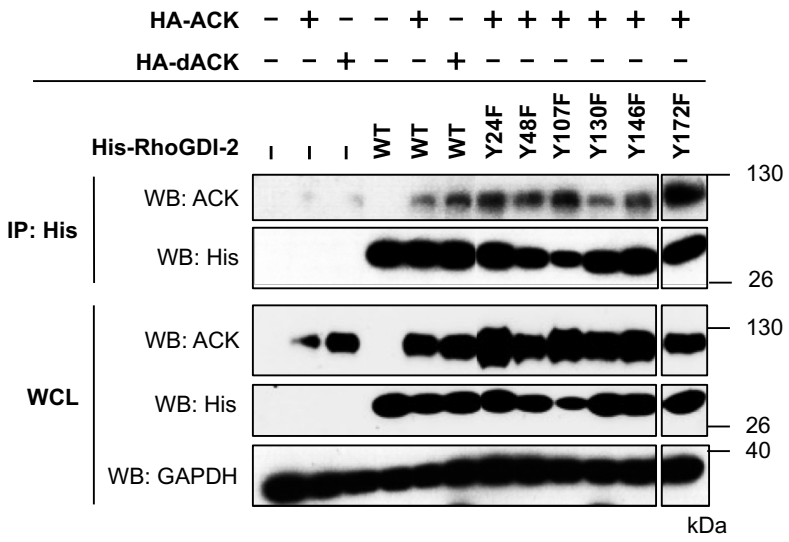

Figure 4.4: Co-immunoprecipitation of RhoGDI-2 mutants with ACK. His-tagged RhoGDI-2 mutants and wt were co-transfected with ACK into HEK293T cells. Constructs were allowed to express for ~40 h before harvested and lysed. The lysates were then precipitated with cobalt-coated magnetic beads for ~1 h. The precipitated proteins were assessed using anti-His or anti-ACK antibodies. The expression of the recombinant protein in the whole cell lysate (WCL) is shown in the bottom 3 panels, while the co-immunoprecipitated (IP) samples are shown in the top two panels. In whole cell lysate, GAPDH was used to assess equal loading of samples. **WCL:** whole cell lysate; **IP:** immunoprecipitation.

Next, the phosphorylation status of each mutant was identified in cells expressing ACK and compared to wt. As shown in Figure 4.5, all the mutants were phosphorylated by ACK. These data suggested that indicating that ACK might phosphorylate the final tyrosine present in RhoGDI-2, which is not shared by RhoGDI-3 (Figure 4.2).

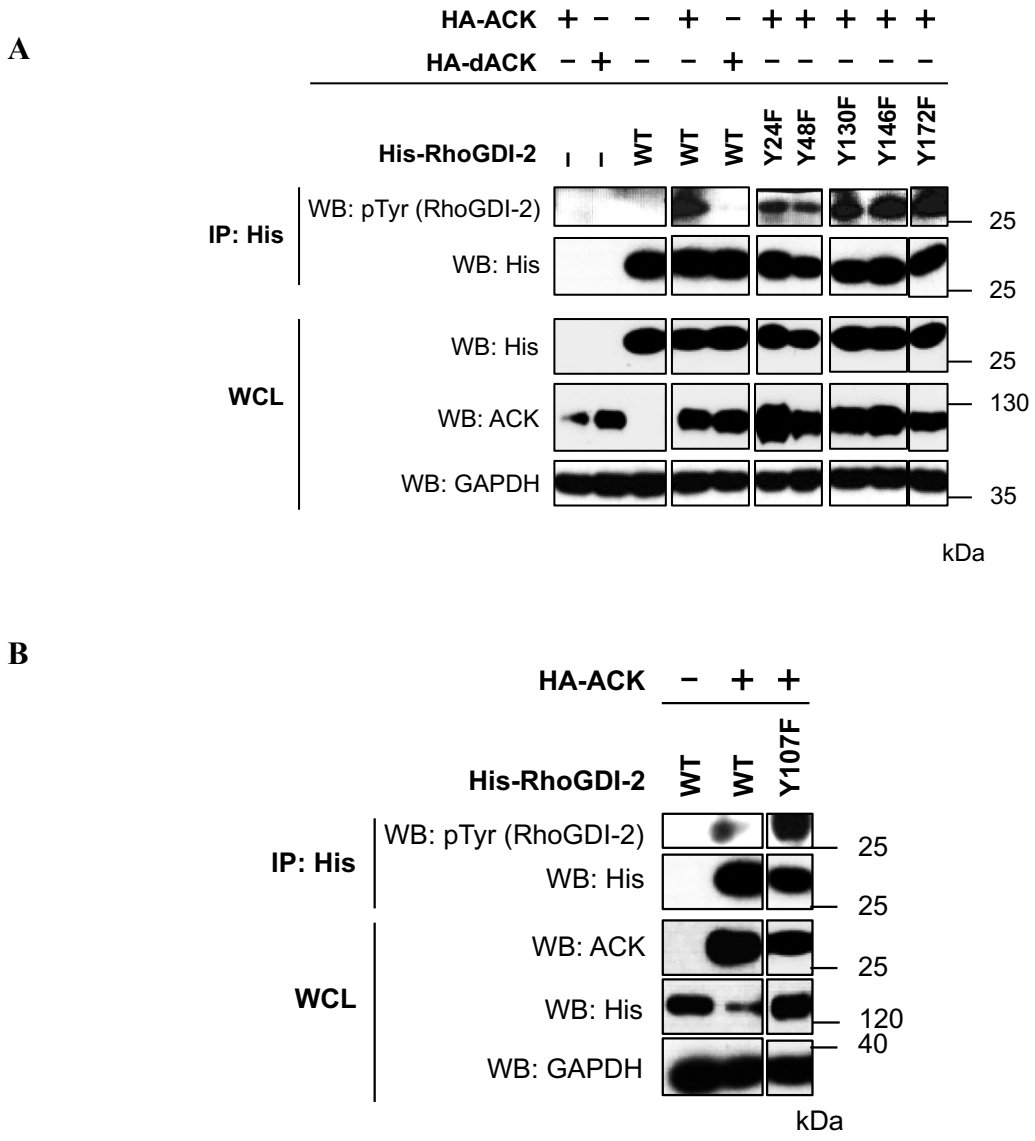

Figure 4.5: Identification of ACK phosphorylation sites on RhoGDI-2. His-tagged RhoGDI-2 mutants and wt were co-transfected with ACK into HEK293T cells. Constructs were allowed to express for ~40 h before harvested and lysed. The lysates were then precipitated with cobalt-coated magnetic beads for ~1 h at 4°C. The phosphorylated RhoGDI-2 proteins were determined using a pan anti-pTyr antibody. The expression of the recombinant protein in the whole cell lysate (WCL) is shown in the bottom 3 panels, while the co-immunoprecipitated (IP) samples are shown in the top two panels. In whole cell lysate, GAPDH was used to assess equal loading of samples. **WCL:** whole cell lysate; **IP:** immunoprecipitation. **(A)** Y24F, Y48F, Y130F, Y146F, Y172F and **(B)** Y107F.

Since mutation of all the conserved tyrosine residues in RhoGDI-2 did not prevent the phosphorylation by ACK, the remaining tyrosine residue in RhoGDI-2, Tyr125, which is not conserved between the three RhoGDIs was postulated to be the target phosphorylation site for ACK. To test this, all the tyrosine residues present in RhoGDI-2, including Tyr125 were mutated to phenylalanine (His-ΔYRhoGDI-2) and its phosphorylation levels were compared to wt RhoGDI-2 in the presence of ACK (Figure 4.6).

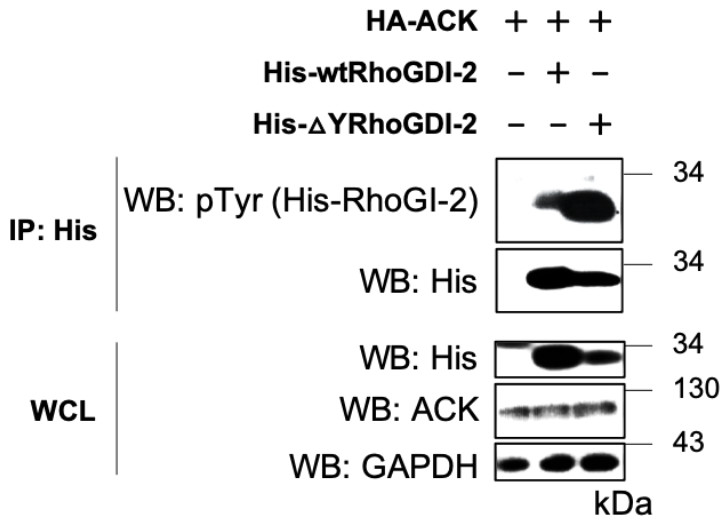

Figure 4.6: Identification of ACK phosphorylation sites on Tyr125 of RhoGDI-2. His-wt RhoGDI-2 and His-ΔYRhoGDI-2 were co-transfected with ACK into HEK293T cells. Constructs were allowed to express for ~40 h before harvested and lysed. The lysates were then precipitated with cobalt-coated magnetic beads for ~1 h at 4°C. Following incubation**,** the phosphorylation status of His-ΔYRhoGDI-2 was determined by western blotting with a pan anti-pTyr antibody. The expression of the recombinant protein in the whole cell lysate (WCL) is shown in the bottom 3 panels, while the co-immunoprecipitated (IP) samples are shown in the top two panels. In whole cell lysate, GAPDH was used to assess equal loading of samples. **WCL:** whole cell lysate; **IP:** immunoprecipitation.

Surprisingly, (His-ΔYRhoGDI-2) was still phosphorylated by ACK, suggesting that ACK might phosphorylate tyrosine which is not on RhoGDI-2 but potentially in the construct.

4.2.1 ACK phosphorylates the tyrosine present within the *att*B1 site of pDEST26

ACK was still able to phosphorylate His-ΔYRhoGDI-2, which indicated that ACK might phosphorylate the last tyrosine left in the construct, which resides within the *att*B1 site of pDEST26 (Figure 4.7). To evaluate this, the tyrosine within the *att*B1 site was mutated to phenylalanine together with every tyrosine present on RhoGDI-2 (His-Δ*att*B1-RhoGDI-2).

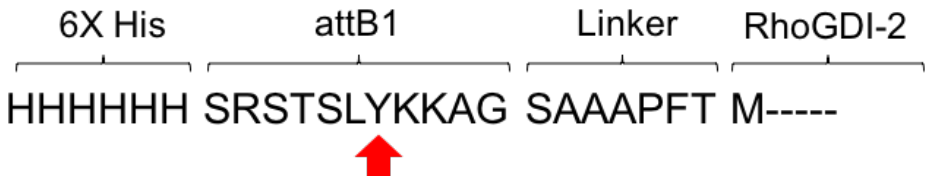

Figure 4.7: The position of a tyrosine within the *att*B1 in pDEST26-RhoGDI-2. Tyrosine present within the *att*B1 site in pDEST26-RhoGDI-2 was indicated by red arrow.

Firstly, the ability for the mutant to interact with ACK was identified. Figure 4.8 shows that the His-Δ*att*B1-RhoGDI-2 mutant retained its ability to interact with ACK.

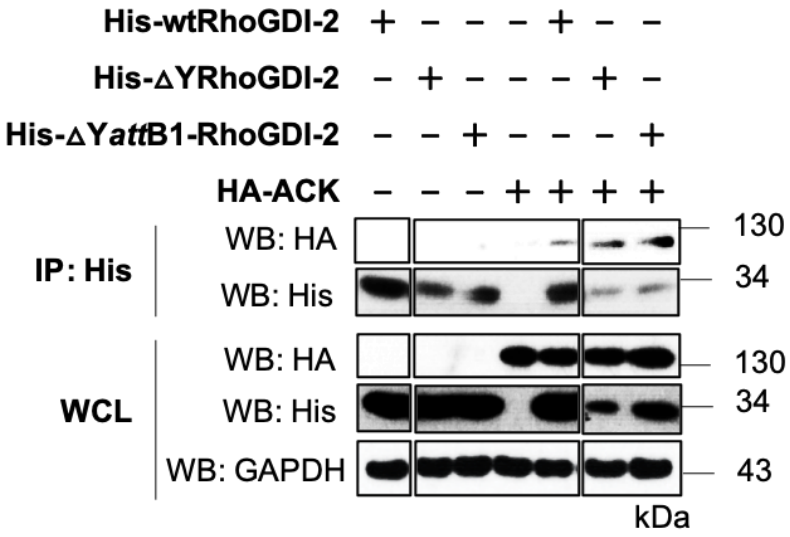

Figure 4.8: The interaction between the a*tt*B1 mutant and ACK. His-ΔY*att*B1-RhoGDI-2, His-ΔYRhoGDI-2 and His-wtRhoGDI-2 were transfected into HEK293T cells alone or together with ACK. Constructs were allowed to express for ~40 h before precipitated with cobalt-coated magnetic beads for ~1 h at 4 °C. The presence of ACK in immunoprecipitated sample was identified by western blotting with anti-HA antibody. The expression of the recombinant protein in the whole cell lysate (WCL) is shown in the bottom 3 panels, while the co-immunoprecipitated (IP) samples are shown in the top two panels. In whole cell lysate, GAPDH was used to assess equal loading of samples across the wells. **WCL:** whole cell lysate; **IP:** immunoprecipitation.

Next, the phosphorylation levels of ΔY*att*B1-RhoGDI-2 were compared to wt RhoGDI-2 and ΔYRhoGDI-2 in the presence of ACK. The data in Figure 4.9 shows that the wt and ΔYRhoGDI-2 mutants were both phosphorylated by ACK but not the ΔY*att*B1-RhoGDI-2 mutant.

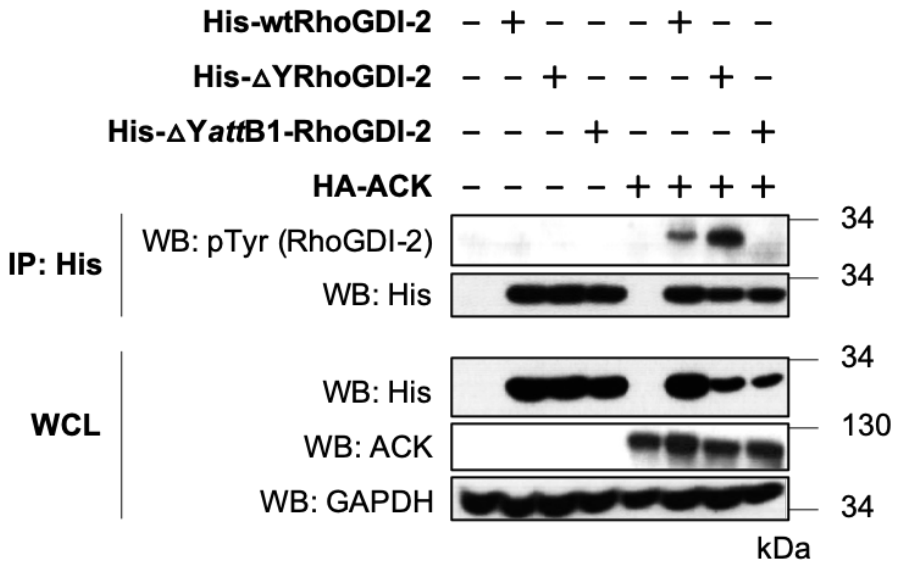

Figure 4.9: The phosphorylation levels of the a*tt*B1 mutants by ACK. HEK293T cells were transfected with His-ΔY*att*B1-RhoGDI-2, His-ΔYRhoGDI-2 and His-wtRhoGDI-2 either alone or together with ACK. Constructs were allowed to express for ~40 h before harvested, pelleted and lysed. The lysates were precipitated with cobalt-coated magnetic beads for ~1 h at 4 °C. The phosphorylation levels were identified by western blotting with a pan anti-pTyr antibody. The expression of the recombinant protein in the whole cell lysate (WCL) is shown in the bottom 3 panels, while the co-immunoprecipitated (IP) samples are shown in the top two panels. In whole cell lysate, GAPDH was used to assess equal loading of samples. **WCL:** whole cell lysate; **IP:** immunoprecipitation.

To confirm that the tyrosine within the *att*B1 site was the phosphorylation site by ACK, a final mutant was made where the tyrosine within the *att*B1 site was mutated to phenylalanine in wt RhoGDI-2 (His-*att*B1wt-RhoGDI-2). The ability of the mutant to interact with and phosphorylated by ACK was analysed and compared to wt RhoGDI-2.

As shown in Figure 4.10, the His-*att*B1wt-RhoGDI-2 mutant still bound to ACK but its phosphorylation levels decreased significantly compared to the wt. This suggests that Tyr^{attB1} is a major and probably the only phosphorylation site for ACK in RhoGDI-2 construct.

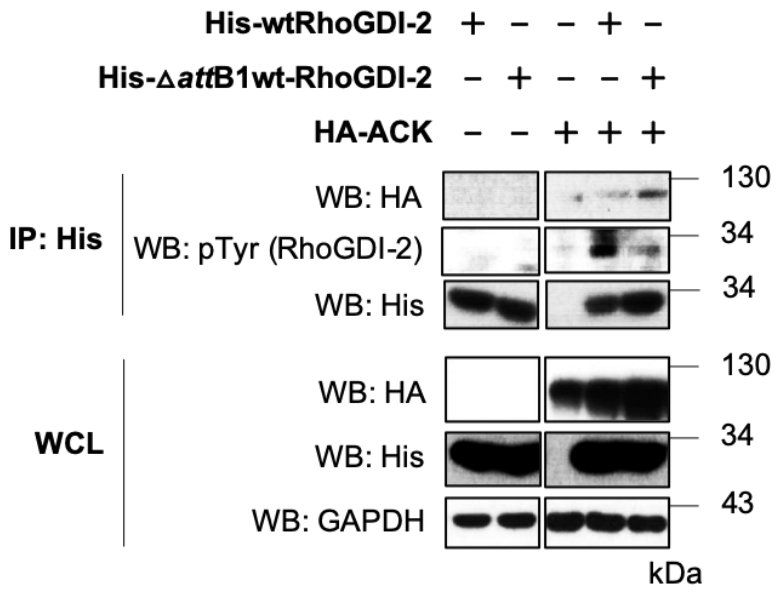

Figure 4.10: The interaction and phosphorylation levels of RhoGDI-2 wt and the a*tt*B1 mutants by ACK. HEK293T cells were transfected with His-ΔY*att*B1wt-RhoGDI-2 and His-wtRhoGDI-2 either alone or together with ACK. Constructs were allowed to express for ~40 h before harvested, pelleted and lysed. The lysates were precipitated with cobalt-coated magnetic beads for ~1 h at 4 °C. Following incubation, their ability to interact and their phosphorylation levels were analysed by western blotting with anti-HA and a pan anti-pTyr antibodies, respectively. The expression of the recombinant protein in the whole cell lysate (WCL) is shown in the bottom 3 panels, while the co-immunoprecipitated (IP) samples are shown in the top 3 panels. In whole cell lysate, GAPDH was used to assess equal loading of samples. **WCL:** whole cell lysate; **IP:** immunoprecipitation.

4.3 The effect of ACK interaction on the phosphorylation of RhoGDI-1 and -2 *in vitro*

Whilst the analysis in cells utilising mutants, presented in the previous section was underway, an *in vitro* kinase assay was performed in parallel to investigate the ability of ACK to phosphorylate RhoGDI-1 and -2. The *in vitro* kinase assay was performed using purified ACK, RhoGDI-1 and -

2. Attempts were also made to purify RhoGDI-3 in *E. coli* but these were unsuccessful, possibly because of the N-terminal extension that is highly hydrophobic.

Figure 4.11 shows the fragment of ACK (1-489) used in this assay. The purified protein was a kind gift from Ms. Millie Fox.

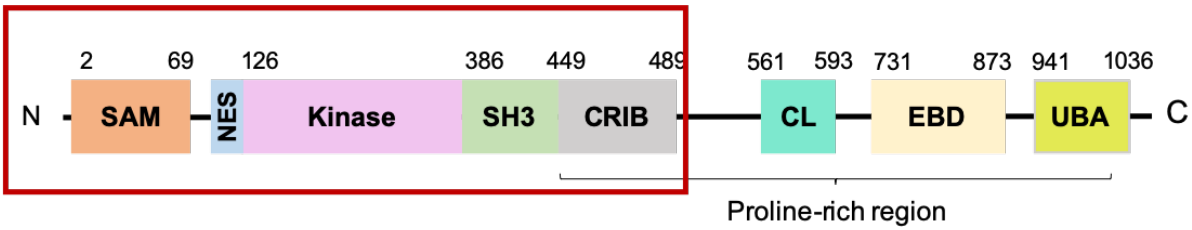

Figure 4.11: Schematic of the GST-tagged ACK construct purified from *E. coli*. An ACK construct spanning amino acids 1-489 (red box) was used to assess the effect of ACK on RhoGDI phosphorylation *in vitro*. SAM: sterile α motif, NES: nuclear export signal, Kinase: tyrosine kinase domain, SH3: Src Homology 3 domain, CRIB: Cdc42/Rac interacting binding motif, CL: Clathrin-interacting region, EBD: EGFR binding domain and UBA: ubiquitin-association domain.

4.3.1 Purification of full-length RhoGDI proteins from *E. coli*

4.3.1.1 Generation of RhoGDI bacterial expression constructs

In order to express full-length GST-tagged RhoGDI proteins in *E. coli,* the Gateway entry clone containing each RhoGDIs were recombined with a bacterial expression vector, pDEST15T using the LR recombination reaction, according to the manufacturer's protocol (section 2.1.6). This vector is a modified version of pDEST15T available in the lab, where a thrombin protease site has been inserted between the GST tag and the fusion protein. The resultant DNA was transformed into chemically competent *E. coli* TOP10 cells. Individual colonies were analysed using *Bsr*G1 restriction analysis. The correct size of the inserts was determined by gel electrophoresis and confirmed by DNA sequencing.

As shown in Figure 4.12, all three RhoGDIs were successfully transferred into pDEST15T with recombinant plasmids identified that carried the correctly sized inserts of 614, 605, and 675 bp respectively.

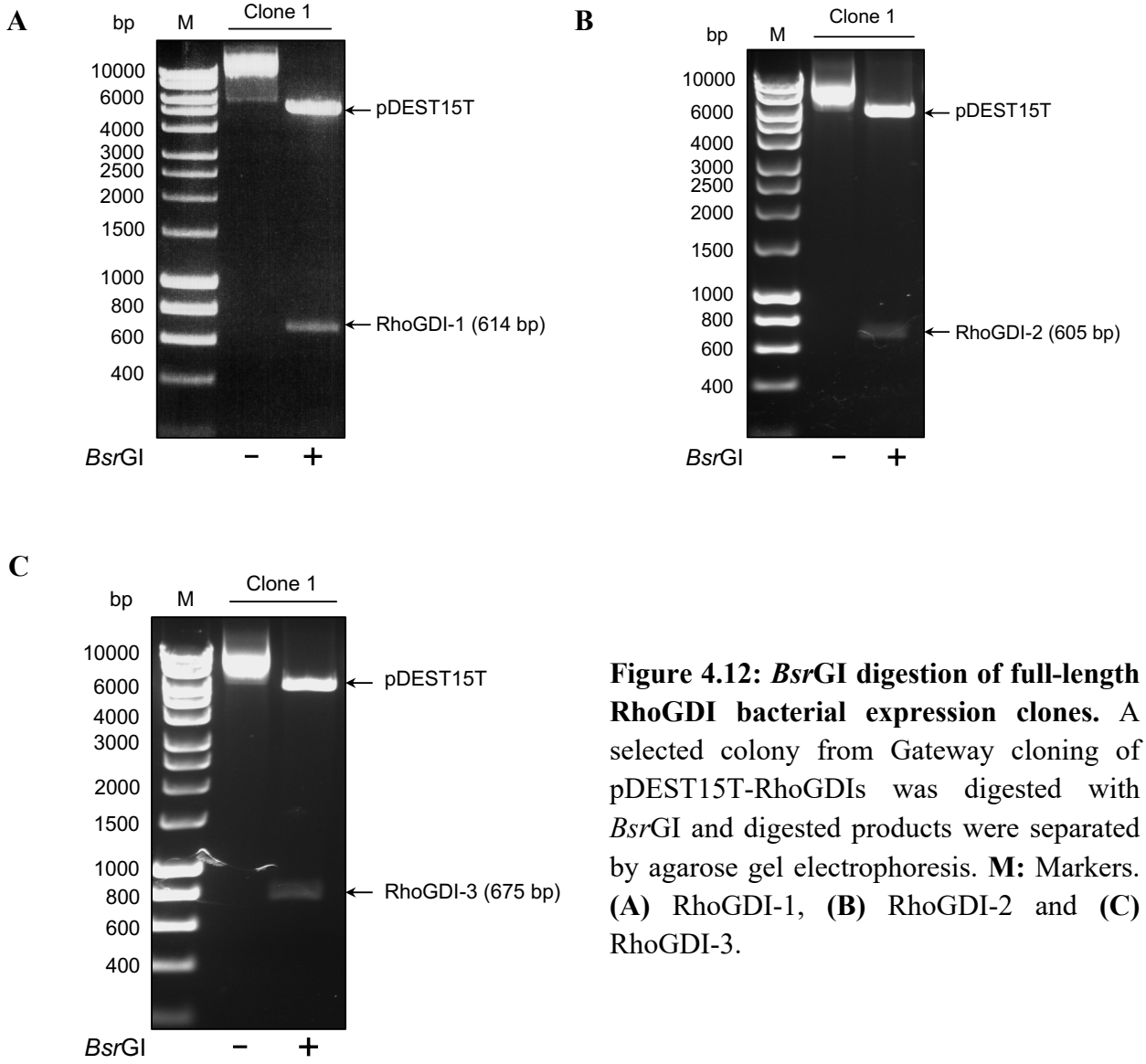

Figure 4.12: *Bsr*GI digestion of full-length RhoGDI bacterial expression clones. A selected colony from Gateway cloning of pDEST15T-RhoGDIs was digested with *Bsr*GI and digested products were separated by agarose gel electrophoresis. **M:** Markers. **(A)** RhoGDI-1, **(B)** RhoGDI-2 and **(C)** RhoGDI-3.

4.3.1.2 Small-scale expression trials of GST-RhoGDI in *E. coli*

The expression of all three RhoGDIs was initially trialled in *E. coli* BL21 (DE3). The DE3 lysogen encodes T7 polymerase and allows expression of the full-length RhoGDIs, which are under the

control of the T7 promoter in pDEST15T. The cells were induced with IPTG and grown for either 5 h at 37 °C or overnight at 20 °C. The soluble and insoluble fractions were collected and analysed by SDS-PAGE and Coomassie staining (section 2.4.3).

Although all three RhoGDIs were found to express well in both the conditions following IPTG induction, they were not soluble (Figure 4.13). Thus, additional efforts were trialled to improve the solubility of these RhoGDIs by transforming them in *E. coli* BL21 (DE3) strains that expressed either the bacterial chaperone proteins, GroEL and GroeES (GroEL/ES) or thioredoxin (Trx). Both of these proteins are known to prevent the aggregation and precipitation of fused proteins by aiding their correct folding and hence can improve their solubility (Laminet *et al.,* 1990; LaVallie *et al.,* 1993).

RhoGDI-1 (Figure 4.14A) and -3 (Figure 4.15) are shown to be most soluble when co-expressed with Trx at 37 °C or 20 °C, while the best soluble expression of RhoGDI-2 (Figure 4.14B) was achieved with GroEL/ES at 37 °C. These *E. coli* strains and induction condition were then used for large-scale expression of all three RhoGDIs.

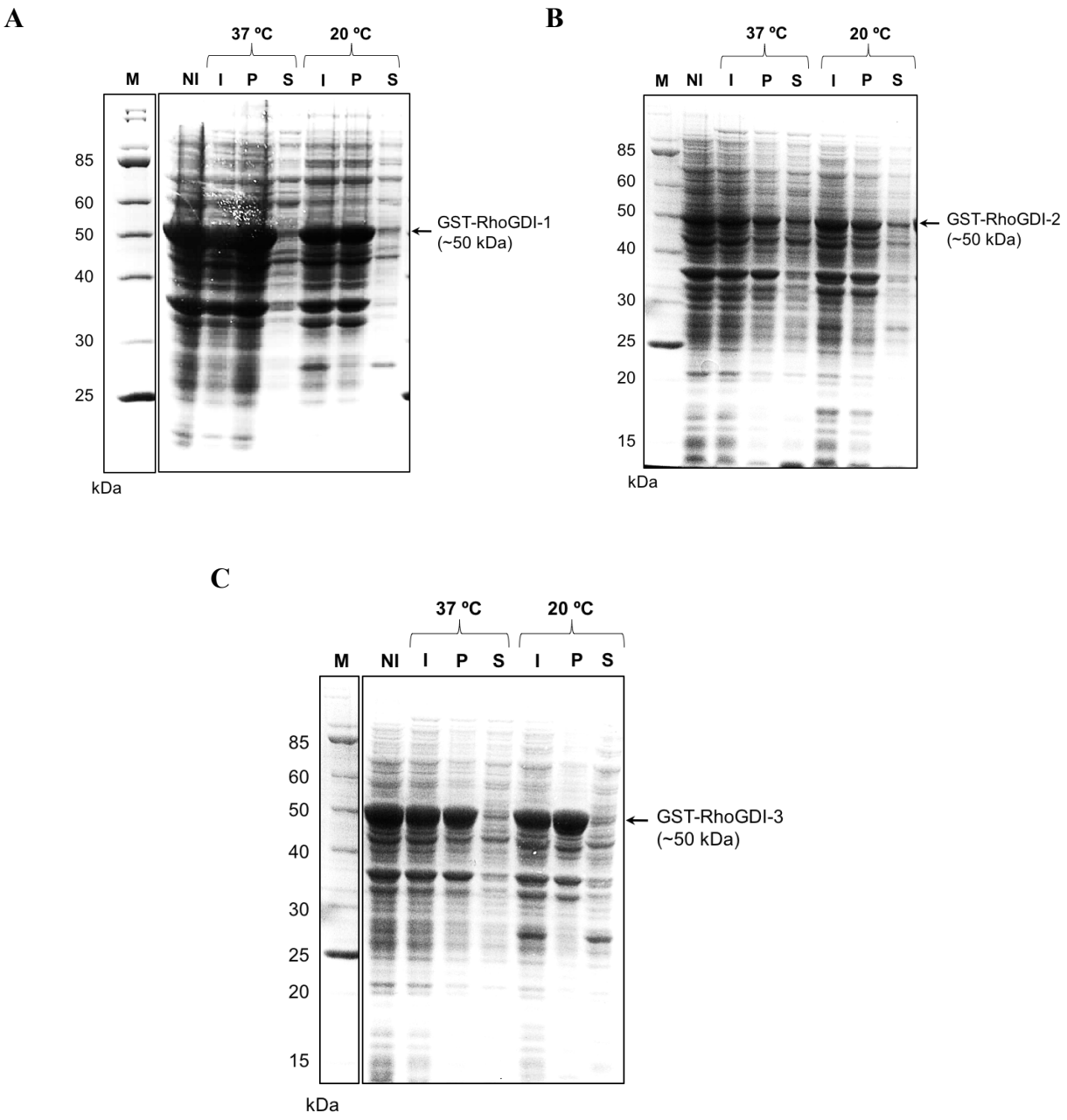

Figure 4.13: Small-scale expression trial of GST-RhoGDI proteins in *E. coli* BL21 (DE3). *E. coli* BL21 (DE3) cells transformed with GST-RhoGDIs and induced with IPTG for either ~5 h at 37 °C or ~16 h at 20 °C. Cells were then harvested, pelleted and lysed using a sonicator. Gel samples were collected from non-induced (NI), induced (I), insoluble (P) and soluble (S) fractions of induced cells. The level of expression of the GST-RhoGDIs and their solubility under each condition was assessed by SDS-PAGE and Coomassie staining. **M:** MW markers. **(A)** RhoGDI-1, **(B)** RhoGDI-2 and **(C)** RhoGDI-3.

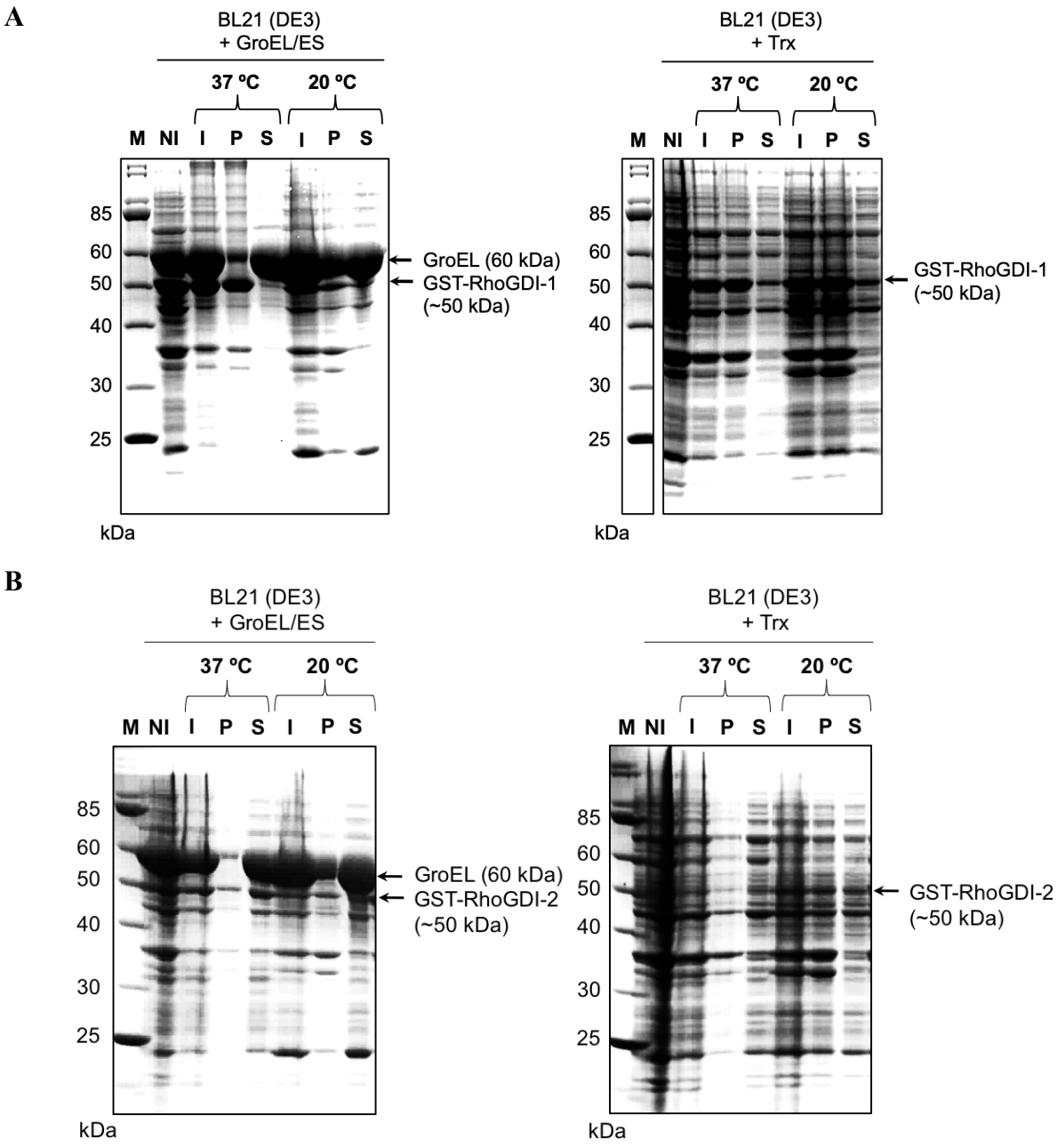

Figure 4.14: Small-scale expression trials of GST-RhoGDI-1 and -2 proteins in *E. coli* BL21 (DE3) expressing bacterial chaperone proteins, GroEL/ES or Trx. *E. coli* BL21 (DE3) expressing either GroEL and GroeES (GroEL/ES) or thioredoxin (Trx) were transformed with GST-RhoGDIs and induced with IPTG for either ~5 h at 37 °C or ~16 h at 20 °C. Cells were then harvested, pelleted and lysed using a sonicator. Gel samples were collected from non-induced (NI), induced (I), insoluble (P) and soluble (S) fractions of induced cells. The level of GST-RhoGDIs and their solubility under each condition was assessed by SDS-PAGE and Coomassie staining. **M:** MW markers. **(A)** RhoGDI-1 and **(B)** RhoGDI-2

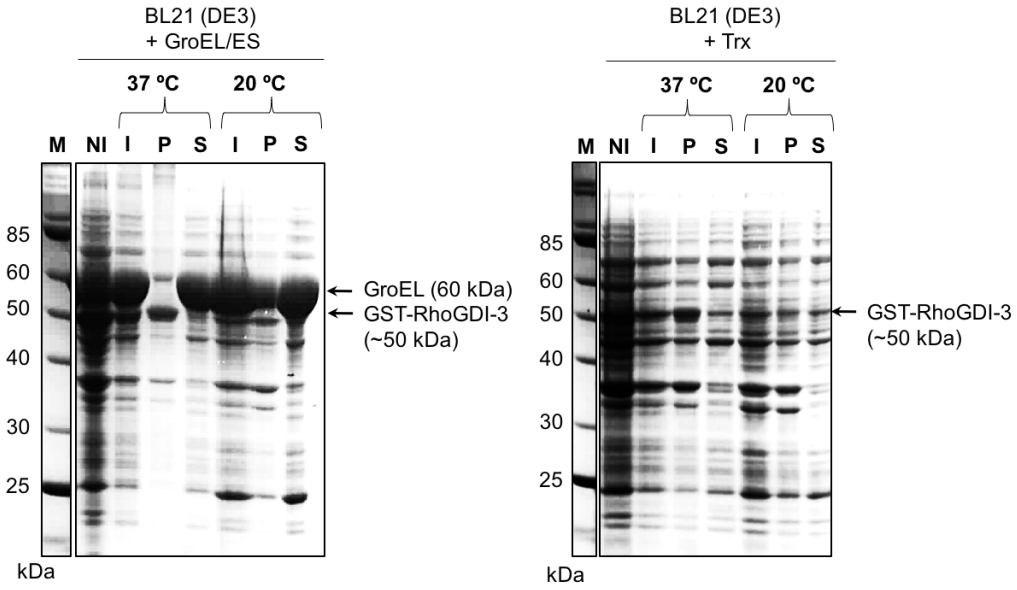

Figure 4.15: Small-scale expression trials of GST-RhoGDI-3 protein in *E. coli* BL21 (DE3) expressing bacterial chaperone proteins, GroEL/ES or Trx. *E. coli* BL21 (DE3) expressing either GroEL and GroeES (GroEL/ES) or thioredoxin (Trx) were transformed with GST-RhoGDI-3, and induced with IPTG for either ~5 h at 37 °C or ~16 h at 20 °C. Cells were then harvested, pelleted and lysed using a sonicator. Gel samples were collected from non-induced (NI), induced (I), insoluble (P) and soluble (S) fractions of induced cells. The level of GST-RhoGDI-3 and its solubility under each condition was assessed by SDS-PAGE and Coomassie staining. **M:** MW markers.

4.3.1.3 Large-scale expression and purification of GST-RhoGDI proteins in *E. coli*

All three GST-fusion RhoGDIs were expressed in 3 L *E. coli* cultures under optimised conditions and purified as described in section 2.2.21. Briefly, following induction by IPTG, cells were harvested, pelleted and lysed using an Emulsiflex in lysis buffer (Table 2.11). The lysates were cleared by centrifugation and the supernatant applied to a glutathione sepharose column at a flow rate of 1 mL/min. The glutathione sepharose column was then washed with MTPBS (Table 2.11) to remove unbound proteins. GST-tagged RhoGDIs were then eluted from the glutathione sepharose column with 10 mM reduced glutathione. Eluate was collected in 2 mL fractions and

the absorbance monitored at 280 nm. Appropriate fractions were analysed by SDS-PAGE and Coomassie staining, together with samples from the column flow-through and the MTPBS wash. Purifications using the glutathione sepharose column was not sufficient to remove all contaminating proteins. Hence, an additional size exclusion column was used to further purify the proteins.

4.3.1.3.1 Purification of GST-tagged RhoGDI-1

Figure 4.16A shows the present of 4 major peaks following glutathione sepharose purification of RhoGDI-1. Fractions 2 to 11 from peaks 1 to 3 and fractions 18 and 19 from peak 4 were collected and analysed by SDS-PAGE and Coomassie staining.

As shown in Figure 4.16B, GST-RhoGDI-1 with a MW ~50 kDa can be observed in all the collected fractions. However, the GST-RhoGDI-1 present in peaks 1 to 3 bound less tightly to glutathione sepharose, being eluted at ~1.5 mM glutathione, compared to peak 4 that was eluted at ~3 mM glutathione. This could potentially be because the GST-RhoGDI-1 in peaks 1 to 3 has an altered conformation of GST, thereby reducing the affinity of GST-RhoGDI-1 for glutathione sepharose column. Thus, it was decided to proceed with the tighter bound GST-RhoGDI-1 species in peak 4. Fractions 13 to 25 were pooled and concentrated to ~2 mL in an Amicon stirred cell and then applied to a HiLoad™ 16/600 Superdex™ 200 pg gel filtration column.

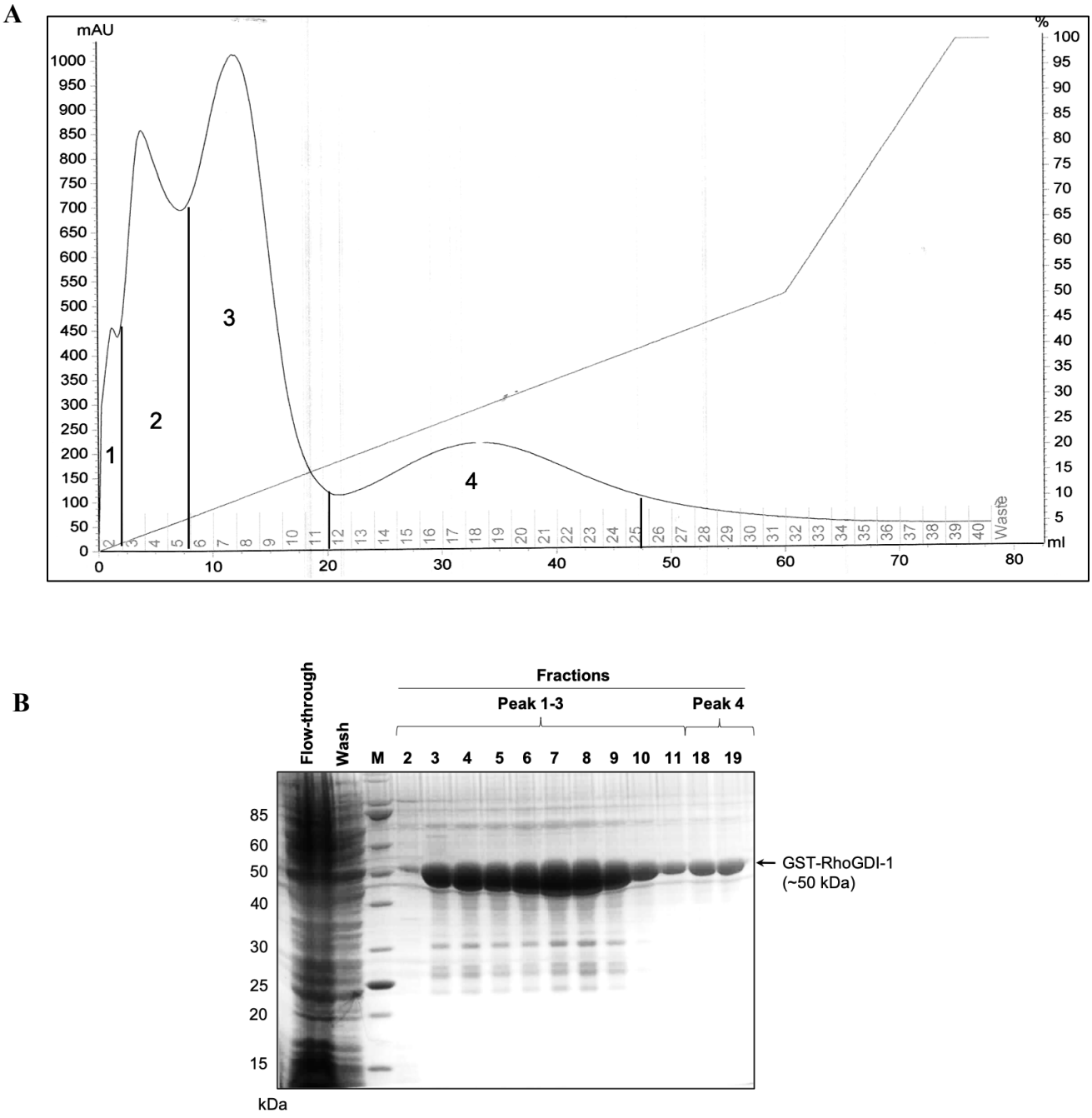

Figure 4.16: Purification of full-length GST-RhoGDI-1 protein from *E. coli* using affinity chromatography. *E. coli* BL21 (DE3) cells expressing Trx were transformed with an expression construct for GST-RhoGDI-1 and induced with IPTG for ~5 h at 37 °C before being harvested, pelleted and lysed using an Emulsiflex. The cleared lysates were then **(A)** applied to glutathione sepharose column. **(B)** Fractions 2 to 11 from peak 1 to 3 and fractions 18 and 19 from peak 4 were collected together with samples from each stages and analysed by SDS-PAGE and Coomassie staining. **M:** MW markers.

Purified GST-RhoGDI-1 from the glutathione sepharose purification was applied to a HiLoad™ 16/600 Superdex™ 200 pg gel filtration column. As shown in the elution chromatogram (Figure 4.17), two peaks were obtained and gel samples from both of the peaks together with samples from each stages were collected and analysed by SDS-PAGE and Coomassie staining. The first peak covering fractions 23 to 30, represented the void volume of the column and so contains proteins too large to enter the column. These fractions were also seen to contain GST-RhoGDI-1 (Figure 4.17-gel on the right) but this protein was likely large, insoluble or aggregated material. Fractions 31 to 37 (peak 2) also contained GST-RhoGDI-1 and this was likely to be well-folded protein of the correct MW and was largely free from contaminants. These fractions were pooled and concentrated to ~0.5 mL. The protein was quantified using A_{280} and store at -80 °C.

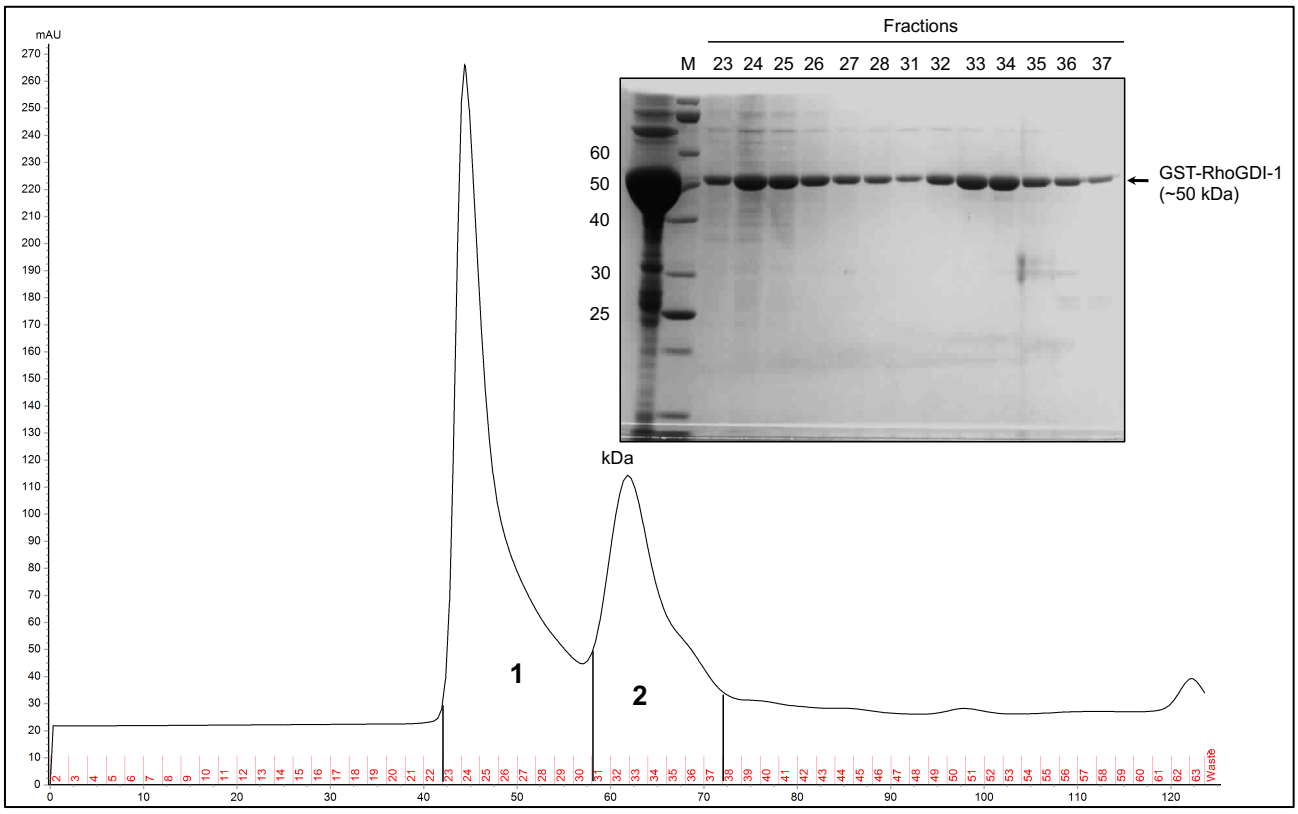

Figure 4.17: Additional purification of full-length GST-RhoGDI-1 from *E. coli* by size exclusion chromatography. The eluted fractions 13 to 25 obtained from affinity chromatography were pooled, concentrated and passed over a HiLoad™ 16/600 Superdex™ 200 pg gel filtration column. Gel samples collected from fractions 23 to 28 from peak 1 and 31 to 37 from peak 2 were analysed by SDS-PAGE and Coomassie staining. Load sample obtained from affinity purification was also included in the analysis. **M:** MW markers.

4.3.1.3.2 Purification of GST-tagged RhoGDI-2

The purification of GST-RhoGDI-2 by affinity chromatography is shown in Figure 4.18. In this case GST-RhoGDI-2 was eluted with a 10 mM glutathione step. In the elution chromatogram, there were two peaks observed following glutathione sepharose purification of RhoGDI-2. Fractions 3 to 6 from peak 1 and fractions 7 to 13 from peak 2 were pooled and concentrated separately before being applied to size exclusion column to further purified the protein.

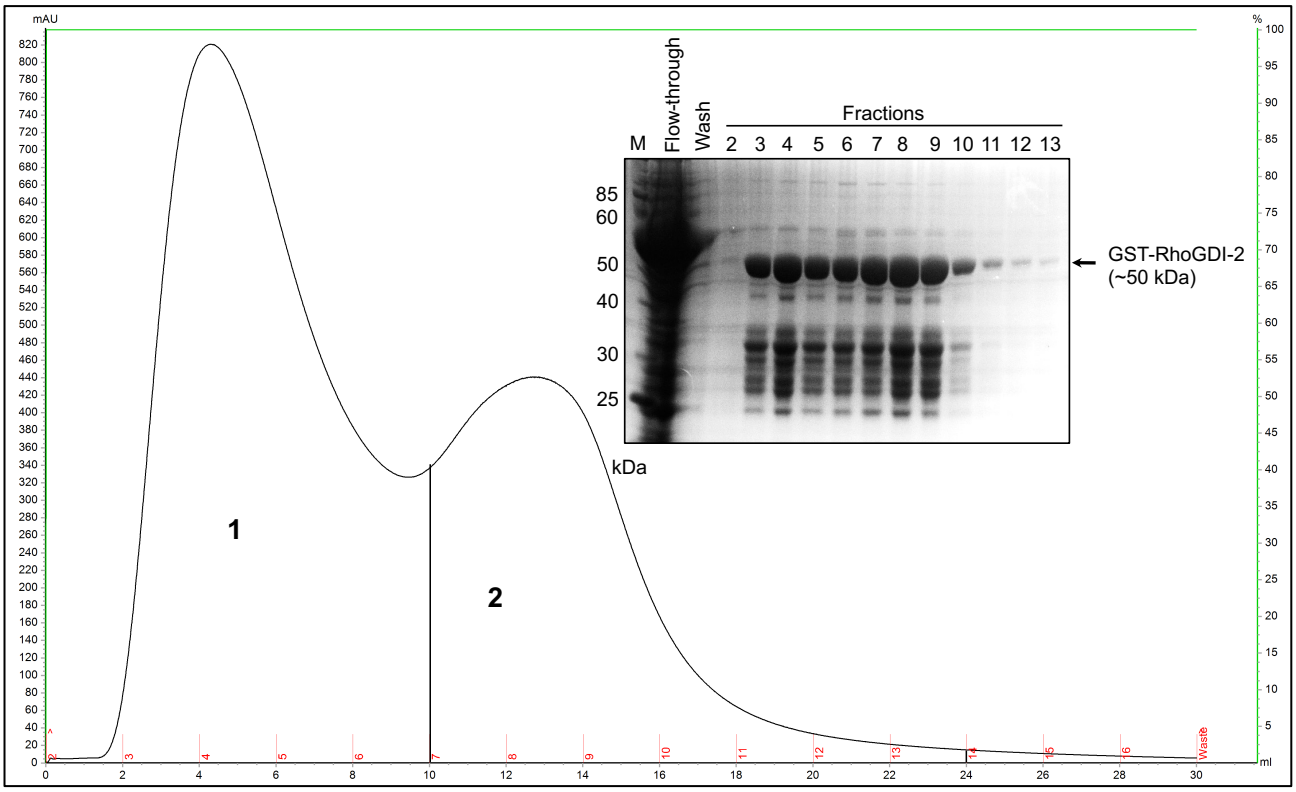

Figure 4.18: Purification of full-length GST-RhoGDI-2 protein from *E. coli* using affinity chromatography. *E. coli* BL21 (DE3) cells expressing GroEL/ES were transformed with GST-RhoGDI-2 and induced with IPTG for ~5 h at 37 °C before harvested, pelleted and lysed using an Emulsiflex. The cleared lysates were then applied to glutathione sepharose column and bound GST-RhoGDI-2 was eluted from the column with steep gradient of elution buffer, up to 10 mM reduced glutathione. Gel samples were collected from each stage of purification and analysed by SDS-PAGE and Coomassie staining. **M:** MW markers.

Figure 4.19 shows the separation by gel filtration for both peaks obtained from the previous affinity purification; peak 1 containing fractions 3 to 6 (Figure 4.19A) and peak 2 comprising fractions 7 to 13 (Figure 4.19B). Following gel filtration, there were five peaks observed and gel samples from peaks 1 to 4 were collected and analysed by SDS-PAGE and Coomassie staining.

The first peak from both gel filtrations column which covered fraction 23 to 27 (Figure 4.19A) and fractions 23 to 29 (Figure 4.19B) represented the void volume of the column. These fractions were shown to contain GST-RhoGDI-2 but as for RhoGDI-1, these fractions were not considered useful. The later peaks from both gel filtration column, containing fractions 33 to 41 (Figure 4.19A) and fractions 33 to 42 (Figure 4.19B) were also seen to contain GST-RhoGDI-2 together with several low MW proteins. This suggests that separation by gel filtration did not fully separate the low MW contaminants from GST-RhoGDI-2 or that degradation was continuing to occur during the purification. However, fractions 31 to 33 (Figure 4.19A) and 30 to 33 (Figure 4.19B) that showed the fewest contaminants were pooled together and concentrated to ~0.5 mL. The amount of GST-RhoGDI-2 was quantified at A_{280} and store at -80 °C.

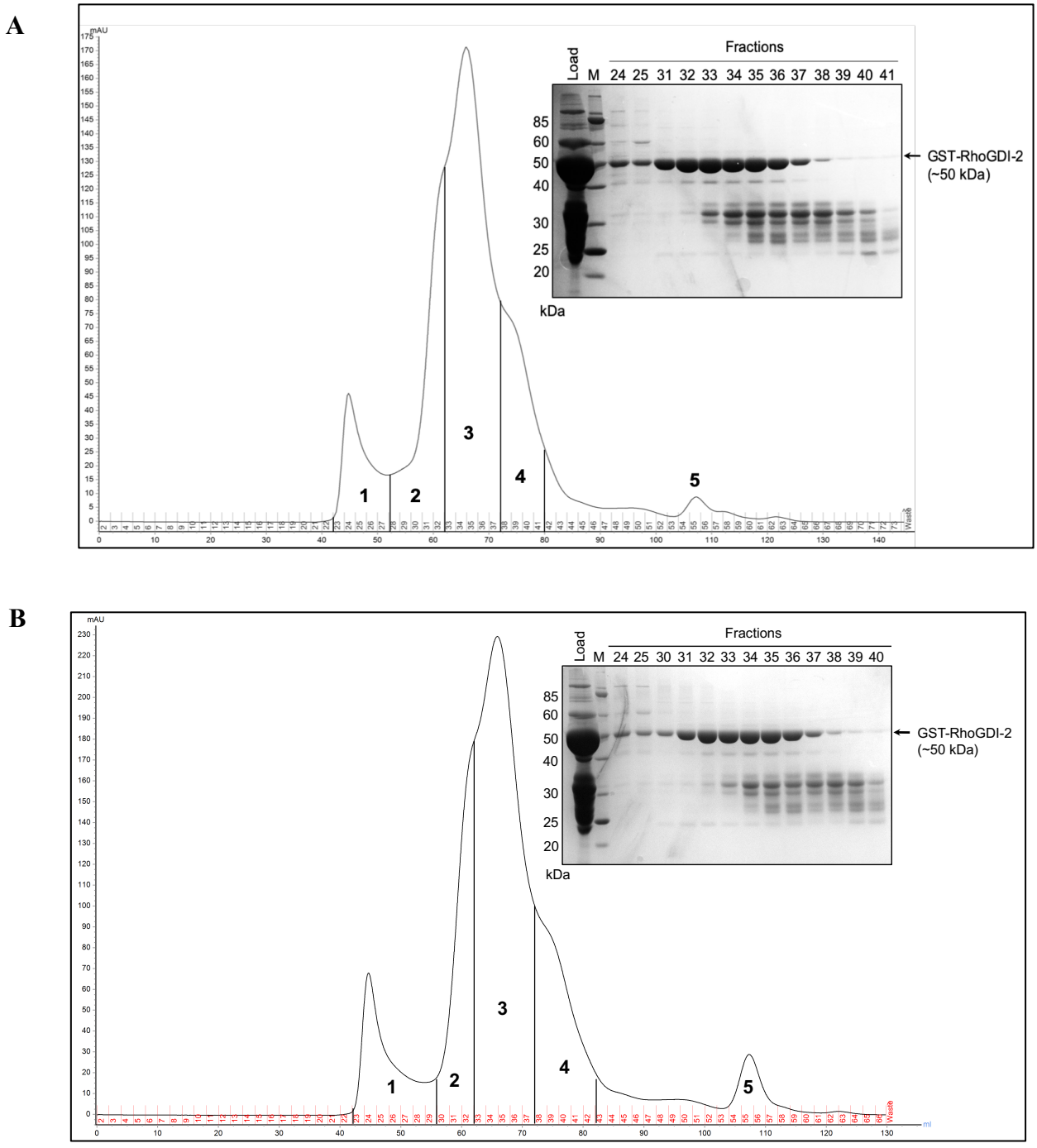

Figure 4.19: Additional purification of full-length GST-RhoGDI-2 protein from *E. coli* by size exclusion chromatography. (A) The eluted fractions 3 to 6 and **(B)** 7 to 13 obtained from the previous affinity purification were pooled, concentrated and passed over a HiLoad™ 16/600 Superdex™ 200 pg gel filtration column. Gel samples collected from respective fractions, as shown in elution chromatogram were analysed by SDS-PAGE and Coomassie staining. The load sample obtained from affinity purification was also included. **M:** MW markers.

4.3.1.3.3 Purification of GST-tagged RhoGDI-3

RhoGDI-3 was purified in the same way as RhoGDI-1 and -2 with a combination of affinity and size exclusion chromatography.

There were two peaks observed from glutathione sepharose chromatography that included fraction 2 to 5 (peak 1) and 6 to 13 (peak 2) (Figure 4.20A). Gel samples from both the peaks were collected and analysed by SDS-PAGE and Coomassie staining. As shown in Figure 4.20B, GST-RhoGDI-3 were present in all the fractions and its was seen to be relatively pure. However, these fractions were pooled and applied to a HiLoad™ 16/600 Superdex™ 200 pg gel filtration column for further purification.

As shown in Figure 4.21A, following separation by gel filtration, although 5 peaks were obtained, all the GST-RhoGDI-3 was eluted in peak 1 (fractions 23 to 26), the void volume of the column, suggesting it was in a higher molecular weight complex containing aggregated proteins. This may be due to the N-terminal extension of RhoGDI-3 that contains two cysteines, which could drive protein aggregation. Thus, 5 mM DTT was included in a second attempt of purification.

However, the additional DTT did not reduce the aggregation of GST-tagged RhoGDI-3 (Figure 4.21B) and all the protein remained in fractions 23 to 28, corresponding to the void volume of the column. There was also potential that GST-tagged RhoGDI-3 was aggregating with other contaminants such as DNA. However, the lysis buffer used in these purifications contained 500 mM NaCl, which should eliminate interactions with DNA. Similar problems were encountered previously by Adra *et al.* (1997) who showed full-length RhoGDI-3 was in inclusion bodies in *E. coli*, making purification difficult. No additional attempts were made to overcome these issues and *in vitro* kinase assay were only taken forward for RhoGDI-1 and -2.

A

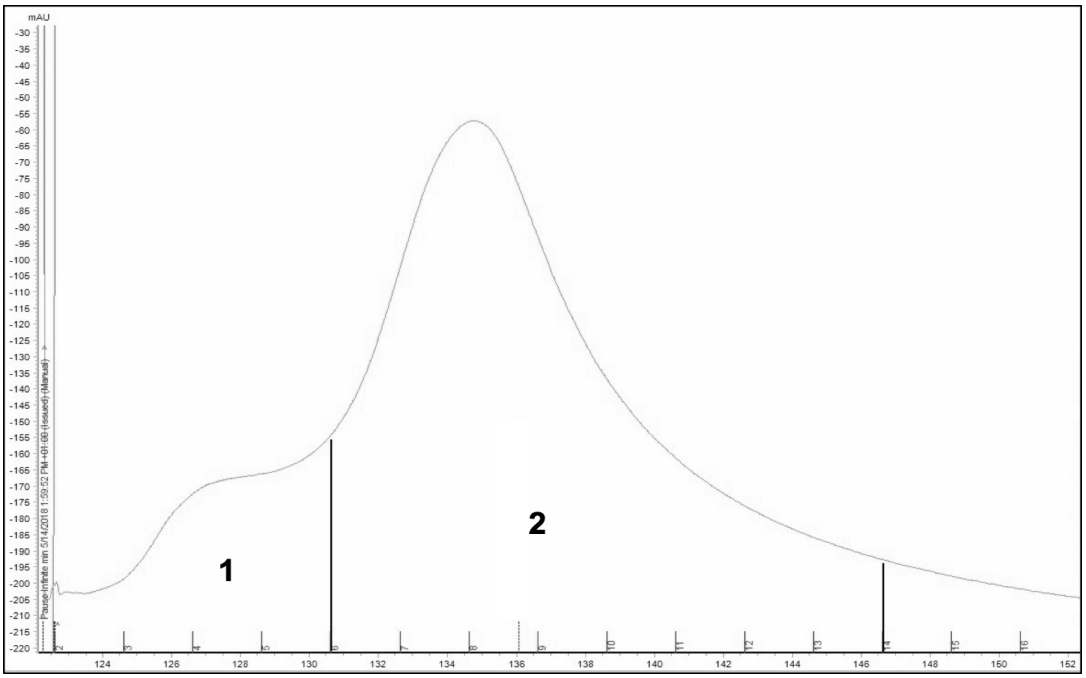

B

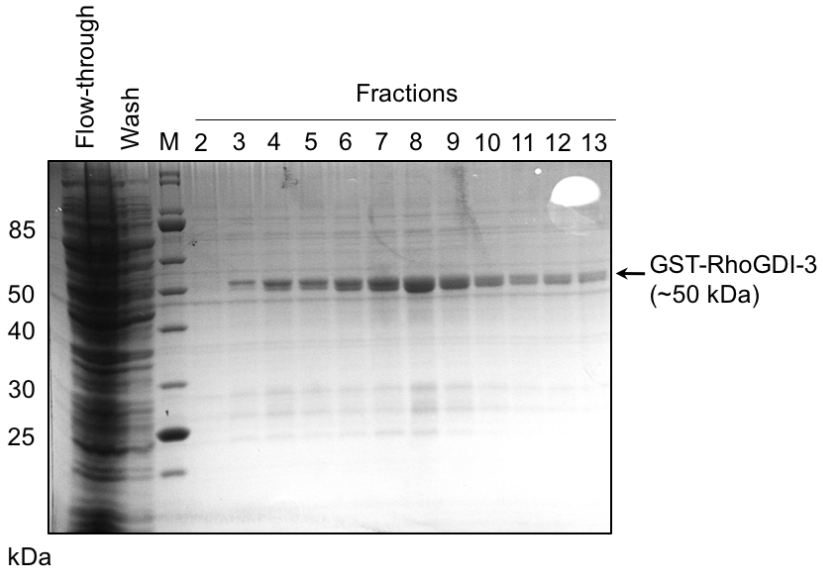

Figure 4.20: Purification of full-length GST-RhoGDI-3 protein from *E. coli* using affinity chromatography. *E. coli* BL21 (DE3) expressing Trx was transformed with GST-RhoGDI-3 and induced with IPTG overnight at 20 °C. Cells were harvested, pelleted and lysed using an Emulsiflex. The cleared lysates were then applied to glutathione sepharose column and bound GST-RhoGDI-3 was eluted from the column with a gradient of elution buffer, up to 10 mM reduced glutathione. **(A)** The absorbance at 280 nm. **(B)** Gel samples were collected from each stage of glutathione sepharose purification and analysed by SDS-PAGE and Coomassie staining. **M:** MW markers.

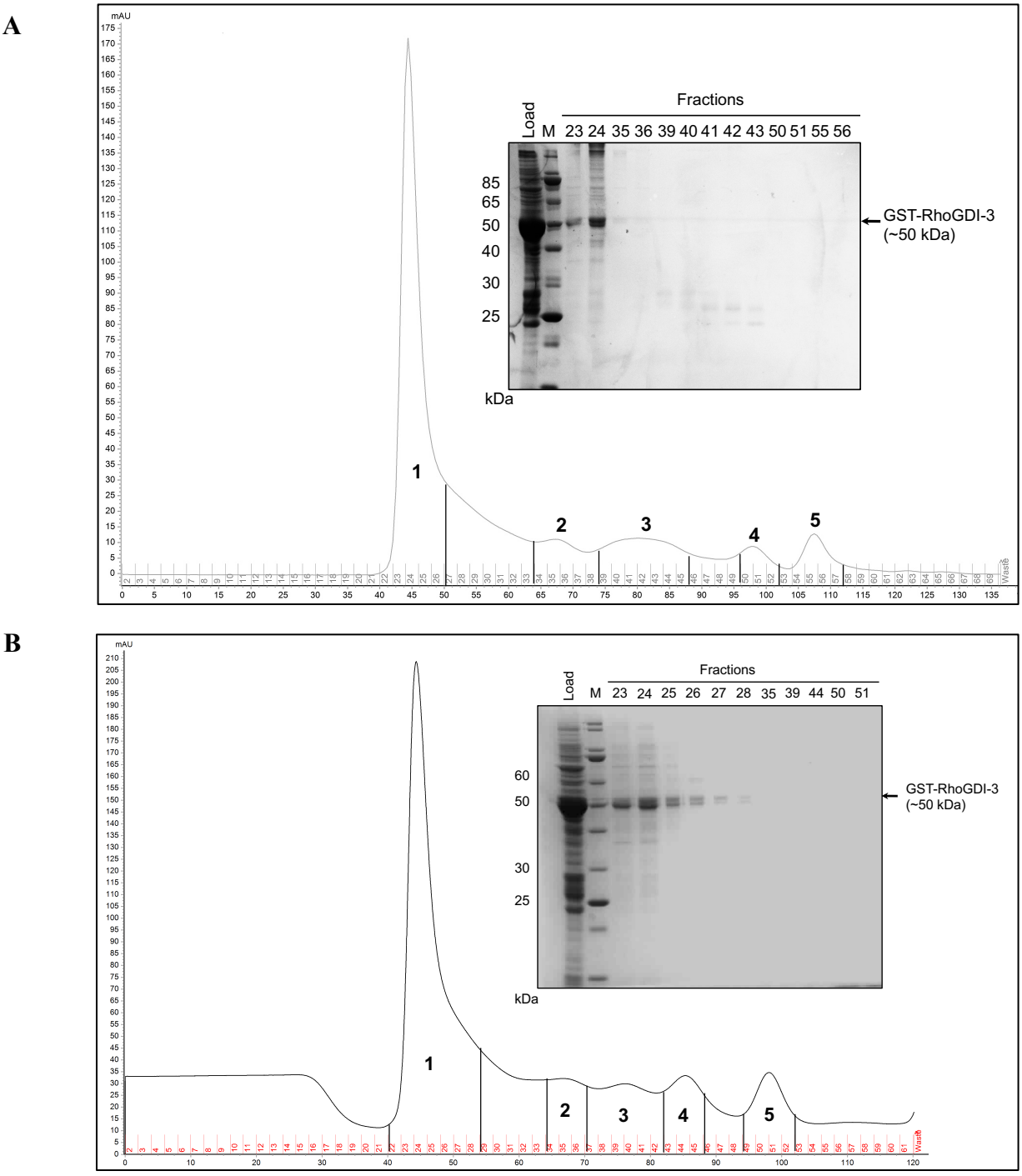

Figure 4.21: Additional purification of full-length GST-RhoGDI-3 from *E. coli* by size exclusion chromatography. The eluted fractions 2 to 13 from affinity were pooled, concentrated and passed over a HiLoad™ 16/600 Superdex™ 200 pg gel filtration column. Gel samples collected from respective fractions, as shown in the chromatogram were analysed by SDS-PAGE and Coomassie staining. Load sample obtained from affinity purification was also included in the analysis. **M:** MW markers. **(A)** without adding DTT and **(B)** with DTT.

4.3.2 ACK does not phosphorylate RhoGDI-1 and -2 *in vitro*

The effect of ACK on RhoGDI-1 and -2 phosphorylation *in vitro* was assessed using an *in vitro* kinase assay. Briefly, 0.3 μM ACK was allowed to undergo autophosphorylation to ensure full activity before incubating with 10 μM GST-RhoGDI-1 or RhoGDI-2 for ~1 h at 30 °C. Samples from each reaction were collected and analysed by SDS-PAGE and western blotting with a pan anti-pTyr antibody.

Figure 4.22 shows the presence of GST control proteins, GST-RhoGDI-1 and -2. GST-ACK was not detected when blotting with the anti-GST antibody as the levels of enzyme were very low in the reactions. However, the presence of GST-ACK was identified by western blotting with anti-pY284. No phosphorylated RhoGDI-1 and -2 were detected when blotting with a pan anti-pTyr antibody, indicating that RhoGDI-1 and -2 are not substrates for ACK kinase activity.

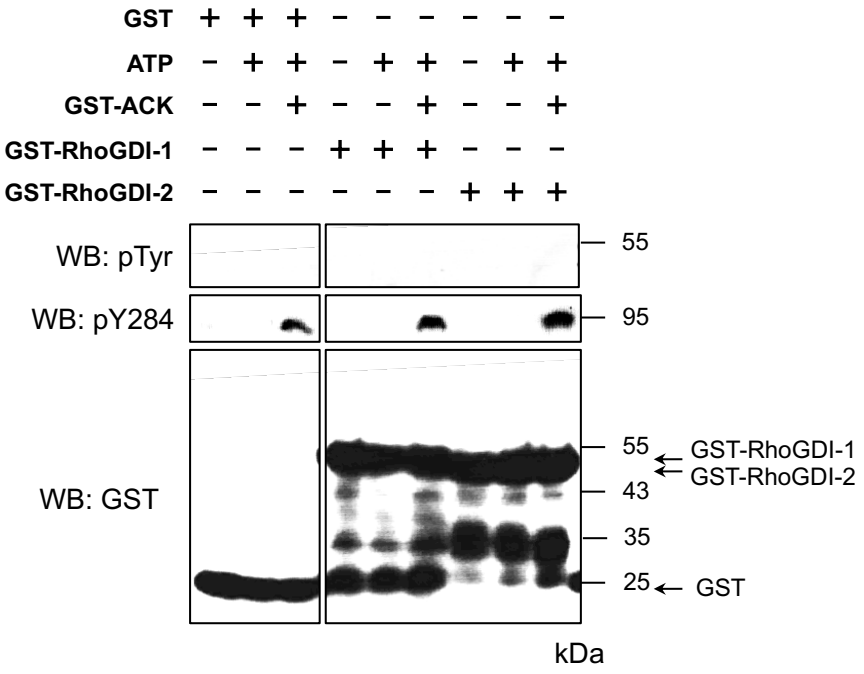

Figure 4.22: Phosphorylation status of RhoGDI-1 and -2 by ACK *in vitro*. 10 μM GST control proteins, GST- RhoGDI-1 and -2 were incubated with 0.5 mM ATP only or together with 0.3 μM autophosphorylated GST-ACK at 30 °C for ~1 h. Samples from each reaction were collected and analysed by SDS-PAGE and western blotting with anti-GST, anti-pY284 and a pan anti-pTyr antibodies.

4.4 Summary

Initial findings indicated that ACK potentially phosphorylated both RhoGDI-1 and -2 in cells, however, as work continued to identify the specific ACK phosphorylation site on RhoGDI-2, ACK was found to phosphorylate the tyrosine present within the *att*B1 site of the expression construct rather than any residue within RhoGDI-2 itself. In parallel with the cellular analysis, an *in vitro kinase* assay was performed using GST-tagged RhoGDI-1 and -2. Again, no phosphorylation by ACK was observed. All the data described in this chapter indicate that ACK binds to but does not phosphorylate the RhoGDI proteins, at least RhoGDI-1 and -2. It remains to be formally demonstrated whether RhoGDI-3 is a substrate for ACK, however this appears to be unlikely.

Chapter 5

Subcellular localization of the RhoGDIs, ACK and the ACK-RhoGDI complexes

5.1 Subcellular localization of the RhoGDIs

All three RhoGDIs have been previously documented to localize in both the nucleus and cytoplasm (Marzouk *et al.,* 2007; Krieser and Eastman, 1999). However, their functional roles are more defined in the cytoplasm. For instance, cytoplasmic RhoGDIs are known to form complexes with small GTPases and maintain them in their inactive state (Dovas and Couchman, 2005). As for their nuclear functions, RhoGDI-1 has been found to bind and regulate oestrogen receptor α (ERα) in MCF-7 cells (Marzouk *et al.,* 2007). N-terminally truncated RhoGDI-2 has also been found to accumulate in the nucleus following Caspase 3-induced cleavage during apoptosis (Krieser and Eastman, 1999). Interestingly, RhoGDI-3 has been found to cluster around the nucleus (Adra *et al.,* 1997) and to localize in both the cytoplasm and the nucleus of normal pancreatic cells but only

in the cytoplasm of cancerous cells (de León-Bautista *et al.,* 2016). This suggests nuclear roles for all three RhoGDI proteins and a potential role for RhoGDI-3 in cancer.

In this work, RhoGDI localization was analysed using subcellular fractionation as described in section 2.3.6. Briefly, His-RhoGDI-1, His-RhoGDI-2 and FLAG-RhoGDI-3 were transfected into 50% confluent HEK293T cells. Constructs were allowed to express for ~24 h before incubation in 0.5% serum, overnight. Cells were fractionated into cytoplasmic and nuclear-enriched fractions ~40 h post-transfection. To isolate the cytoplasmic compartment, the cells were incubated with hypotonic buffer (Table 2.17) to induce cell swelling and then lysed with the addition of 0.5% NP40 Alternative. Cells were then centrifuged at low speed and the supernatant containing the cytoplasmic contents were collected. The remaining pellets were washed with hypotonic buffer before lysed with cell extraction buffer (Table 2.17) to rupture the nuclear membrane. The samples were pelleted at high speed and supernatants containing nuclear-enriched contents were collected. The presence of proteins in each compartment was identified by western blotting. Histone H3 and Heat shock protein 56 (Hsp56) or GAPDH were used as nuclear and cytoplasmic markers, respectively.

Figure 5.1 shows the nuclear and cytoplasmic distribution of the RhoGDIs. RhoGDI-1 and -2 were only found in the cytoplasm (Figure 5.1A). This data contradicts previous findings that show nuclear localization for both RhoGDIs (Marzouk *et al.,* 2007; Krieser and Eastman, 1999). This could be due to the difference in the types of cells used in the different studies. Also, for RhoGDI-2, only the N-terminally truncated version of RhoGDI-2 has been found in the nucleus previously (Krieser and Eastman, 1999), whereas in this study, full-length RhoGDI-2 was analysed and detected only in the cytoplasm. Interestingly, RhoGDI-3 was observed in both the cytoplasmic and nuclear-enriched fractions as previously reported (Figure 5.1B).

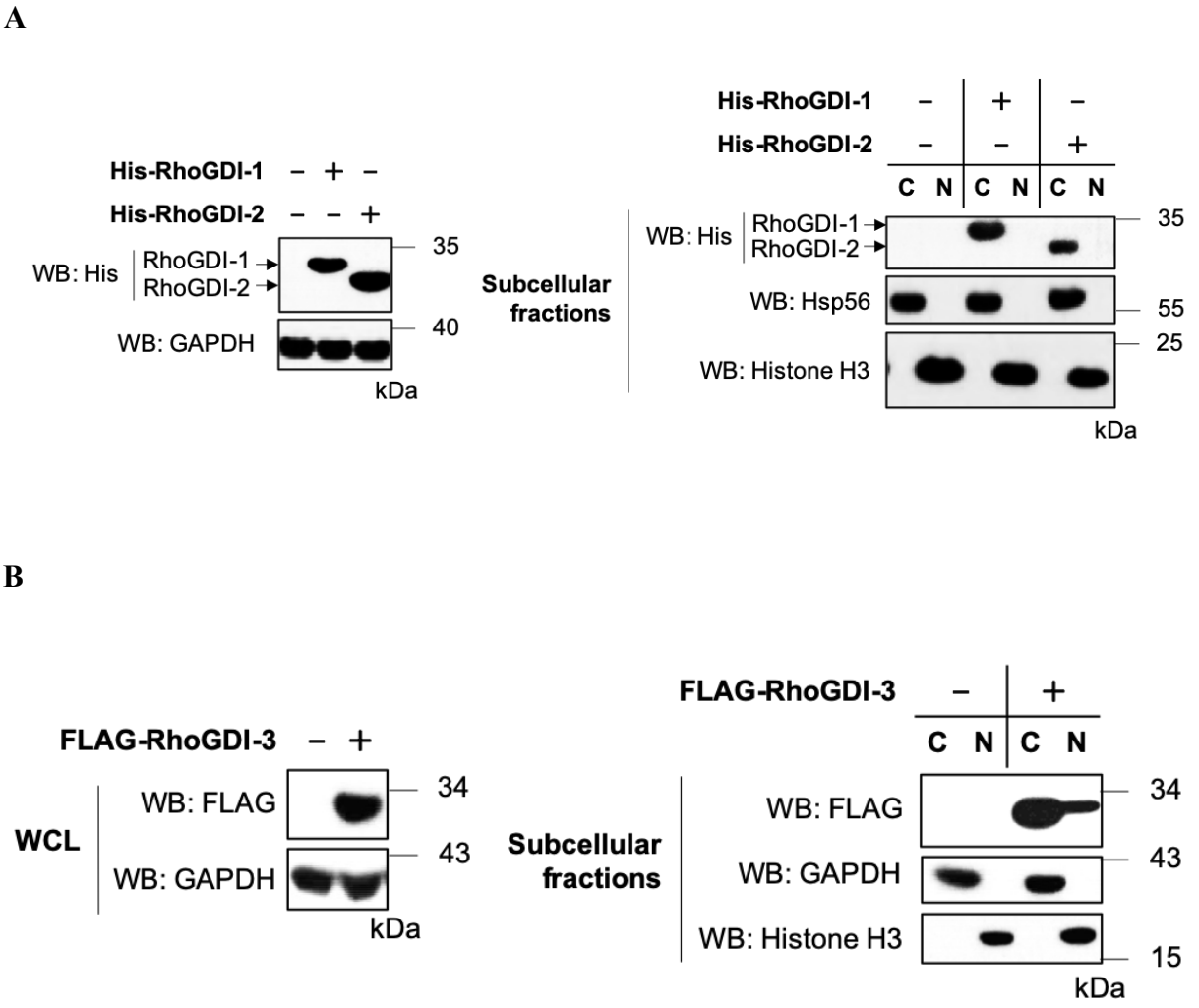

Figure 5.1: Subcellular localization of the RhoGDIs. HEK293T cells were transfected with His-RhoGDI-1, His-RhoGDI-2 or FLAG-RhoGDI-3. Constructs were allowed to express for ~24 h before serum starvation overnight. Cells were then harvested and fractionated into cytoplasmic and nuclear-enriched compartments. **(A)** The levels of RhoGDI-1, RhoGDI-2 and **(B)** RhoGDI-3 in the whole cell lysates (WCL) is shown on the left, while their levels in each subcellular compartment is shown on the right. Hsp56 or GAPDH and Histone H3 were used as cytoplasmic and nuclear markers, respectively. GAPDH was used to assess equal loading of samples across the wells in the whole cell lysates. The western blot shown is representative of at least three independent experiments. **WCL:** whole cell lysate; **C:** cytoplasmic fraction; **N:** nuclear-enriched fraction.

5.2 The N-terminus of RhoGDI-3 is essential in regulating RhoGDI-3 subcellular localization

All three RhoGDIs share two homologous structural domains: An N-terminal regulatory arm domain (residues 1–69) and a C-terminal immunoglobulin-like domain (residues 70-225) (Figures 1.11 and 1.12). Both domains contribute significantly to the binding and inhibitory actions of the RhoGDI proteins towards Rho-family proteins. However, RhoGDI-3 has an additional 26 amino acids at its N-terminus. This unique extension is predicted to contain a small additional amphipathic helix, which extends from residue 5 to 28 and has been shown to play an important role in Golgi targeting and stabilizing the cytoplasmic RhoG-RhoGDI-3 complex (Brunet *et al.,* 2002). RhoGDI-3 has been found to associate with membranous and cytoskeletal fractions (Zalcman *et al.,* 1996). This unique subcellular localization among the RhoGDIs has been assumed to involve the unique hydrophobic N-terminus of RhoGDI-3. Thus, to investigate the function of the N-terminal 26 amino acids of RhoGDI-3, a deletion mutant was created.

An N-terminal deletion mutant of RhoGDI-3 (FLAG-ΔNRhoGDI-3) was generated using QuikChange Site-Directed Mutagenesis Kit (section 2.1.7) according to the manufacturer's protocol. A selected clone was sent for DNA sequencing for validation before further used.

In order to assess the contribution of RhoGDI-3 residues, 1 to 26, to the nuclear localization of RhoGDI-3, FLAG-ΔNRhoGDI-3 was transfected into HEK293T cells and the cells were fractionated into the cytoplasmic and nuclear-enriched fraction ~40 h post-transfection. The levels of FLAG-ΔNRhoGDI-3 in each fraction were determined by western blotting and quantified by ImageJ. The nuclear-cytoplasmic ratio of the FLAG-ΔNRhoGDI-3 mutant was then compared to wt RhoGDI-3.

As shown in Figure 5.2, the N-terminally truncated mutant of RhoGDI-3 was expressed at higher levels than wt RhoGDI-3, indicating it might be more stable. The mutant was still able to localize to both the cytoplasm and the nucleus of HEK293T cells. Interestingly, however, the nuclear-cytoplasmic ratio of FLAG-ΔNRhoGDI-3 mutant was significantly higher compared to wt,

indicating a potential involvement of the N-terminus of RhoGDI-3 in mediating RhoGDI-3 nuclear export.

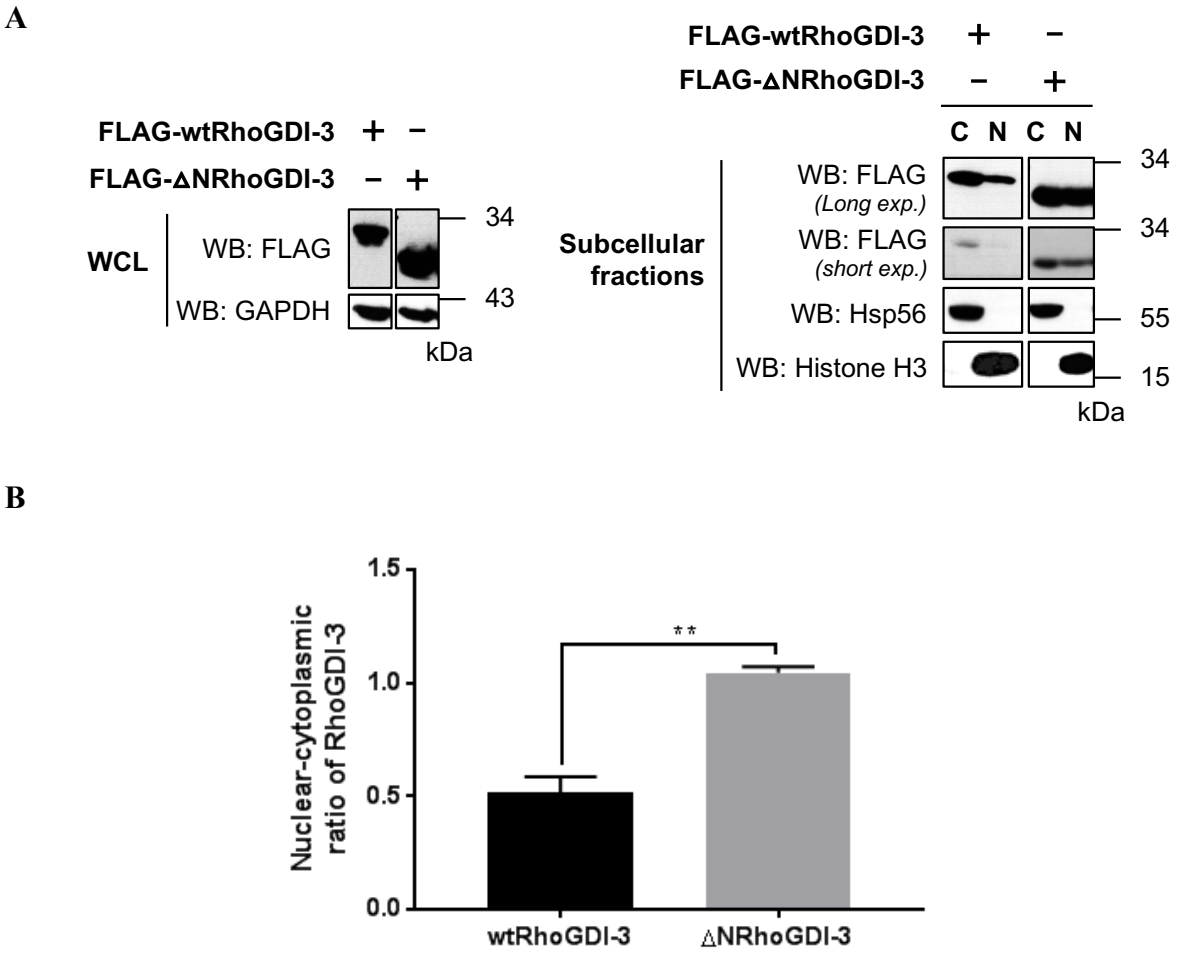

Figure 5.2: The role of the N-terminus of RhoGDI-3 in regulating RhoGDI-3 subcellular localization. FLAG-ΔNRhoGDI-3 and FLAG-wtRhoGDI-3 were transfected into HEK293T cells. Constructs were allowed to express for ~24 h before serum starvation overnight. Cells were then harvested and fractionated into cytoplasmic and nuclear-enriched ~40 h post-transfection. **(A)** The levels of FLAG-ΔNRhoGDI-3 and FLAG-wtRhoGDI-3 in each fraction were determined by western blotting and quantified by ImageJ. The expression of recombinant proteins in the whole cell lysate (WCL) is shown in the left, while their expression in each fraction is shown in the right hand panels. Hsp56 and Histone H3 were used as cytoplasmic and nuclear markers, respectively. GAPDH was used to assess equal loading of samples across the wells in the total whole cell lysate. **(B)** The nuclear-cytoplasmic ratio of each protein was then plotted. The relative amounts are shown as average values ± SEM of three experiments **p≤ 0.005. **WCL:** whole cell lysate; **C:** cytoplasmic fraction; **N:** nuclear-enriched fraction.

This is consistent with data obtained from the nuclear prediction tool, NetNES1.1 (La Cour *et al.,* 2004) that suggest the N-terminus of RhoGDI-3 could contain an NES. The NES motif is predicted to be the leucine-rich sequence spanning amino acids 14 to 21 (LELLRLAL) because the calculated NES scores for these amino acids exceed the threshold (0.5) value (Figure 5.3).

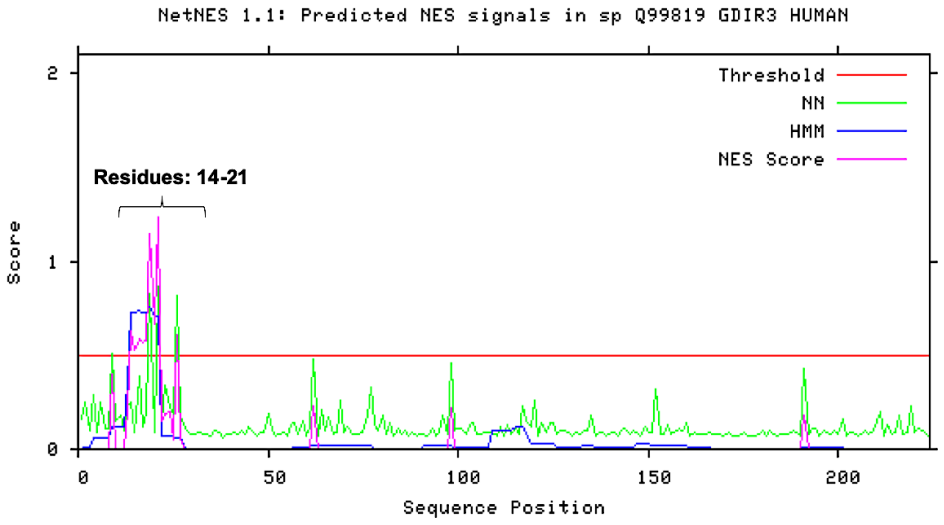

Residues	NES score
Leu14	0.625
Glu15	0.531
Leu16	0.588
Leu17	0.564
Arg18	0.580
Leu19	1.144
Ala20	0.667
Leu21	1.238

Figure 5.3: Nuclear export signal (NES) prediction for RhoGDI-3. The likelihood of an NES sequence occurring in RhoGDI-3 was predicted using NetNES1.1 prediction tool. An NES motif is predicted to be the leucine-rich sequence spanning amino acids Leu14 to Leu21. **HMM**: Hidden Markov Model and **NN**: Neural Network. The table on the right describes the calculated NES score for each residue predicted to be involved in the NES signal.

5.3 Subcellular localization of ACK

ACK can shuttle between the cytosol and the nucleus to rapidly transduce extracellular signals from the RTKs to intracellular effectors in both the cytosol and nucleus (Mahajan and Mahajan, 2015). ACK localization can also be affected by the confluency state the cells. ACK mainly resides in the nucleus of semi-confluent glioblastoma cells but is found in the cytoplasm of confluent cells. Furthermore, the interaction with Cdc42 was found to drive the nuclear localization of ACK

(Ahmed *et al.,* 2004). Hence, the localization of ACK was analysed in this study using subcellular fractionation.

HA-ACK and HA-dACK were transfected into 50% confluent HEK293T cells. Constructs were allowed to express for ~24 h before serum starvation overnight. Cells were then harvested ~40 h post-transfection (80-90% confluency) and fractionated into cytoplasmic and nuclear-enriched fractions as described previously.

Figure 5.4 shows that both ACK and dACK localize to both the cytoplasm and nuclear-enriched fractions, suggesting that ACK localization is not dependent on the kinase activity of ACK. Slightly more ACK and dACK were observed in the cytoplasm compared to the nuclear-enriched compartments.

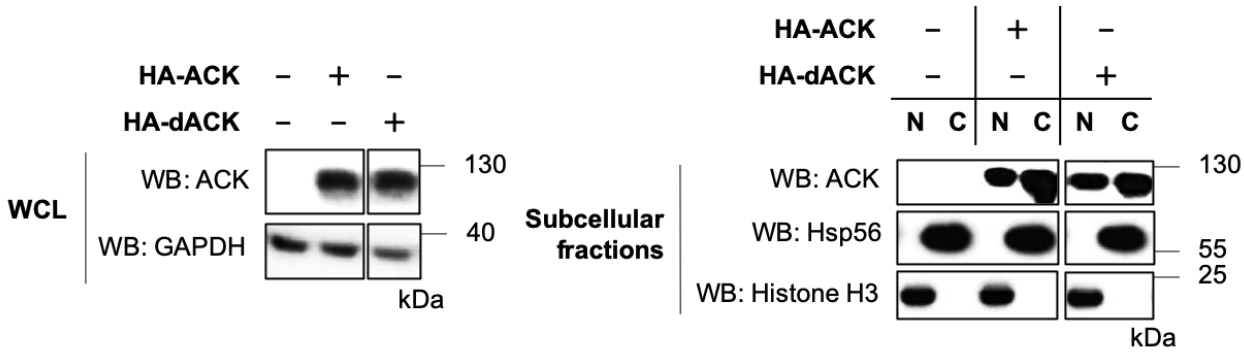

Figure 5.4: Subcellular localization of ACK and dACK in HEK293T cells. HA-ACK and HA-dACK were transfected into HEK293T cells. Constructs were allowed to express for ~24 h before serum starvation overnight. Cells were then harvested and fractionated into cytoplasmic and nuclear-enriched compartments before being subjected to western blotting. The expression of ACK and dACK in the whole cell lysate (WCL) is shown on the left, while their levels in each subcellular compartment is shown on the right. Histone H3 and Hsp56 were used as nuclear and cytoplasmic markers, respectively. GAPDH was used to assess equal loading of samples across the wells in the total whole cell lysate. The western blot shown is representative of at least three independent experiments. **WCL:** whole cell lysate; **C:** cytoplasmic fraction; **N:** nuclear-enriched fraction.

5.4 The effect of co-expression on ACK or RhoGDI subcellular localization

5.4.1 The effect of RhoGDI on ACK subcellular localization

Since ACK has been shown to shuttle between the nucleus and cytoplasm, it was important to investigate whether co-expression with the RhoGDIs would affect its localization.

To investigate this, HA-ACK was transfected alone or together with either His-RhoGDI-1, His-RhoGDI-2 or FLAG-RhoGDI-3 into HEK293T cells. Constructs were allowed to express for ~24 h before serum starvation overnight. ~40 h post-transfection, cells were harvested and separated into cytoplasmic and nuclear-enriched compartments. The proteins levels in each fraction were determined by western blotting.

The subcellular localization of ACK was not affected by co-expression with any of the RhoGDIs, suggesting that ACK shuttles between different compartments independently of the RhoGDIs.

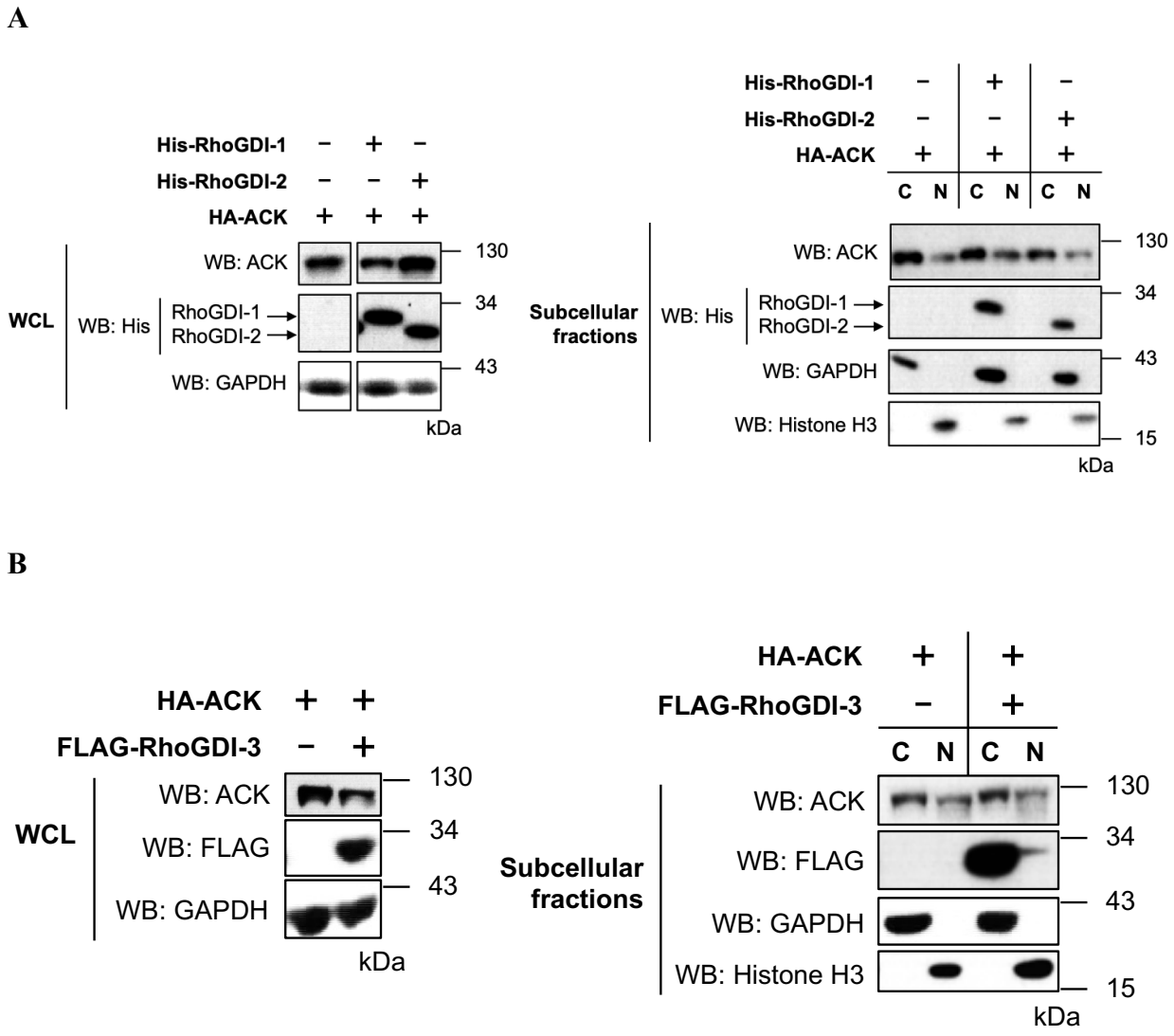

Figure 5.5: Subcellular localization of ACK following co-expression with the RhoGDIs. HEK293T cells were transfected with HA-ACK alone or together with His-RhoGDI-1, His-RhoGDI-2 or FLAG-RhoGDI-3. Constructs were allowed to express for ~24 h before serum starvation overnight. Cells were then harvested and fractionated into cytoplasmic and nuclear-enriched compartments ~40 h post-transfection. The levels of ACK in each fraction were determined by western blotting. The expression of recombinant proteins in whole cell lysate (WCL) is shown in the left, while their expression in each subcellular compartment is shown in the right hand panels. Histone H3 and GAPDH were used as nuclear and cytoplasmic markers, respectively. GAPDH was used to assess equal loading of samples across the wells in the total whole cell lysates. The western blot shown is representative of at least three independent experiments. **WCL:** whole cell lysate; **C:** cytoplasmic fraction; **N:** nuclear-enriched fraction.

5.4.2 The effect of ACK on RhoGDI subcellular localization

Both RhoGDI-1 and -2 were only found in the cytoplasm in this study and it was possible that the cytoplasmic localization of both RhoGDI-1 and -2 could be altered when co-expressed with ACK. Furthermore, it was postulated that ACK might also altered the subcellular localization of RhoGDI-3 as it was found to reside in both the cytoplasmic and nucleoplasmic compartments, in a similar manner to ACK.

To test this, all three RhoGDIs were transfected alone or in combination with ACK into HEK293T cells. Following subcellular fractionation, the presence of each RhoGDI in both the cytoplasmic and nuclear-enriched fractions was identified by western blotting.

Figure 5.6 shows that both RhoGDI-1 and -2 maintained their cytoplasmic localization, even when co-expressed with ACK.

The same experiment was performed for RhoGDI-3. Interestingly, RhoGDI-3 was still able to maintain its cytoplasmic and nuclear localization but the overall levels and the nuclear levels of RhoGDI-3 decreased when co-expressed with ACK (Figure 5.7A), suggesting ACK plays a role in controlling the levels of RhoGDI-3 in the cell. The nuclear-cytoplasmic ratio of RhoGDI-3 (Figure 5.7B) also decreased significantly in the presence of ACK, suggesting that ACK could mediate degradation of RhoGDI-3 in the nucleus or play role in its nuclear targeting.

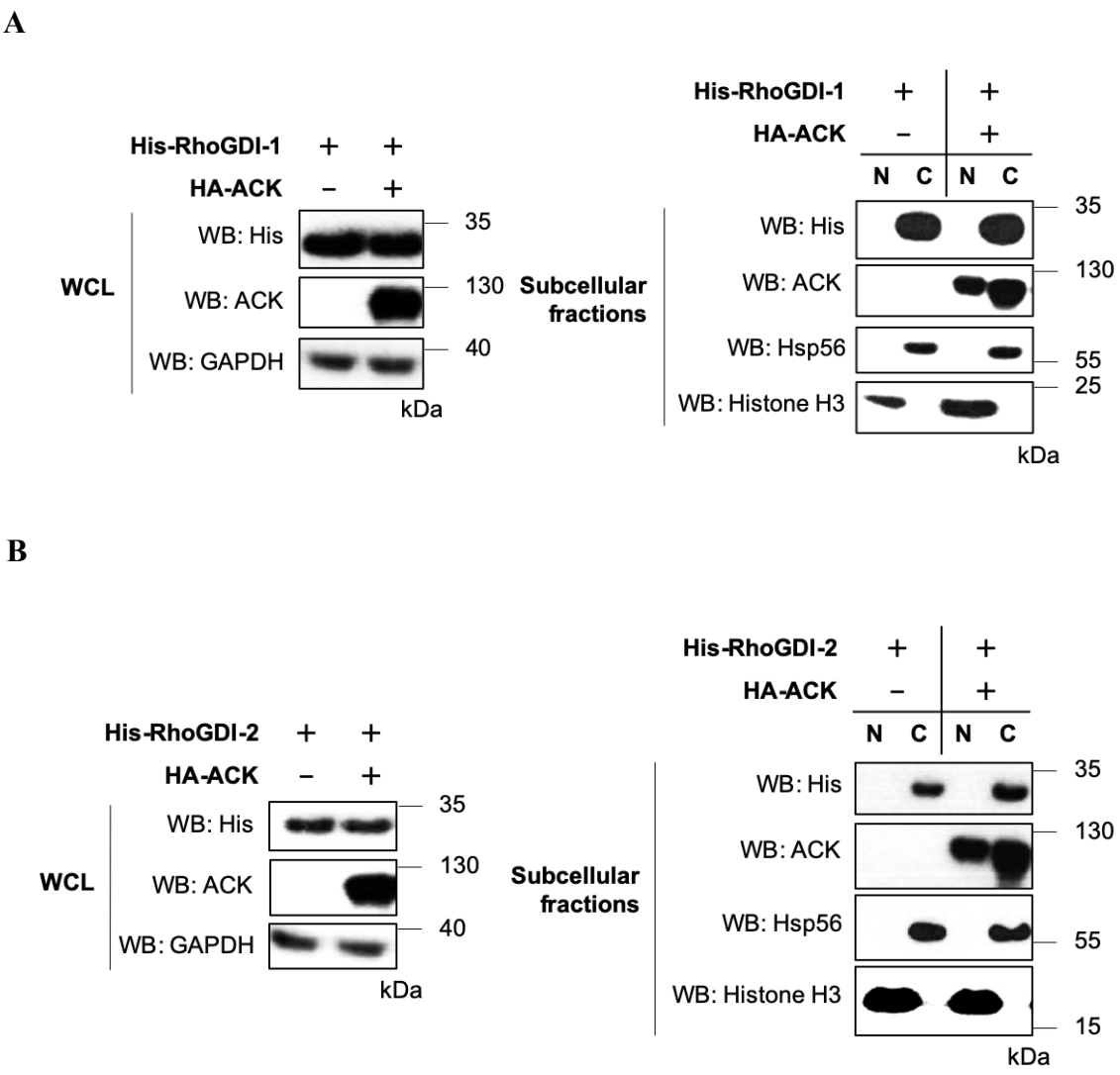

Figure 5.6: Subcellular localization of RhoGDI-1 and -2 in HEK293T cells following co-expression with ACK. HEK293T cells were transfected with His-RhoGDI-1 and His-RhoGDI-2 either alone or together HA-ACK. Constructs were allowed to express for ~24 h before serum starvation overnight. Cells were then harvested and fractionated into cytoplasmic and nuclear-enriched compartments ~40 h post-transfection. The levels of both RhoGDIs in each fraction were determined by western blotting. The expression of recombinant proteins in whole cell lysates (WCL) is shown in the left, while their expression in each subcellular compartment is shown in the right hand panels. Histone H3 and Hsp56 were used as nuclear and cytoplasmic markers, respectively. GAPDH was used to assess equal loading of samples across the wells in the total whole cell lysate. The western blot shown is representative of at least three independent experiments. **WCL:** whole cell lysate; **C:** cytoplasmic fraction; **N:** nuclear-enriched fraction.

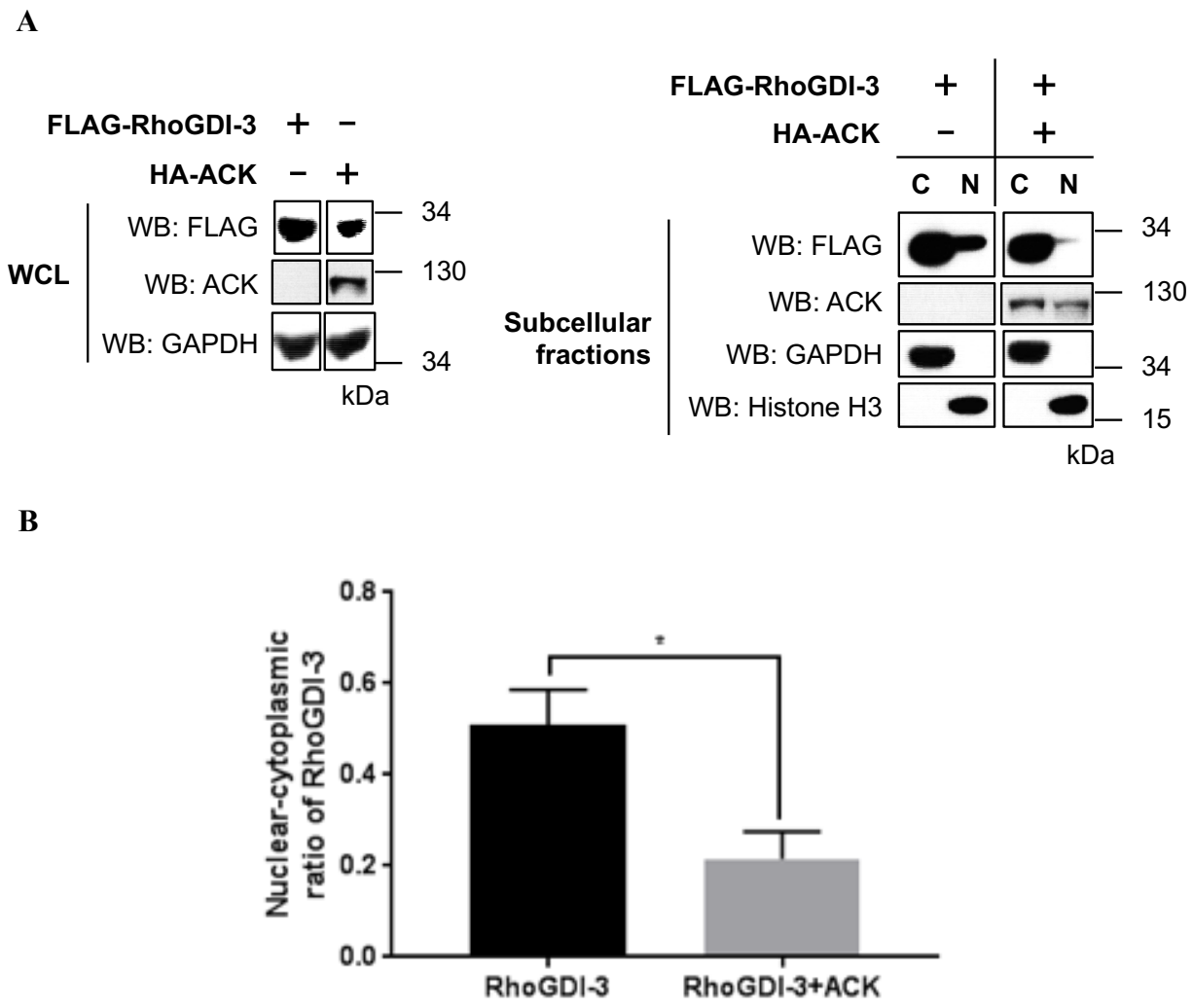

Figure 5.7: Subcellular localization of FLAG-RhoGDI-3 in HEK293T cells following co-expression with ACK. FLAG-RhoGDI-3 was transfected alone or in combination with HA-ACK into HEK293T cells. Constructs were allowed to express for ~24 h before serum starvation overnight. Cells were then harvested ~40 h post-transfection and fractionated into cytoplasmic and nuclear-enriched extracts. **(A)** The levels of RhoGDI-3 in each fraction were determined by western blotting and quantified by ImageJ. The expression of recombinant proteins in whole cell lysate (WCL) is shown in the left, while their expression in each subcellular compartment is shown in the right hand panels. Histone H3 and GAPDH were used as nuclear and cytoplasmic markers, respectively. GAPDH was also used to assess equal loading of samples across the wells in the total whole cell lysate. **(B)** The nuclear-cytoplasmic ratio of RhoGDI-3 was then plotted. The relative amounts are shown as average values ± SEM of three experiments *p≤ 0.05. **WCL:** whole cell lysate; **C:** cytoplasmic fraction; **N:** nuclear-enriched fraction.

5.5 Subcellular localization of the ACK-RhoGDI-3 complex

Subcellular localisation of the ACK-RhoGDI-1 or -2 complexes were not tested due to time constraint but it is likely that they form in the cytoplasm. This is mainly because both RhoGDIs were found to localise exclusively in the cytoplasm and co-expression with ACK does not alters their localisation. However, both RhoGDI-3 and ACK were demonstrated to be present in both the cytoplasm and in nuclear-enriched fractions. Co-expression with ACK did not alter RhoGDI-3 localization but decreased RhoGDI-3 protein levels, predominantly in the nuclear-enriched fraction. These data suggest that ACK might interact with and mediate RhoGDI-3 degradation in the nucleus. ACK could also promote the export of RhoGDI-3 out of the nucleus and its subsequent degradation in the cytoplasm. Both possibilities are consistent with decreased total levels of RhoGDI-3 in cells expressing ACK. To investigate this, the subcellular localization of the ACK-RhoGDI-3 complex was determined through fractionation and co-immunoprecipitation using an anti-FLAG antibody to pull-down FLAG-RhoGDI-3-HA-ACK complex.

Briefly, FLAG-RhoGDI-3 and HA-ACK were transfected into HEK293T cells alone or in combination and allowed to express for ~24 h before serum starvation overnight. ~40 h post-transfection, cells were harvested and fractionated into cytoplasmic and nuclear-enriched fractions. An anti-FLAG antibody was then added to both the pre-cleared fractions and incubated at 4 °C for 45 min. FLAG-RhoGDI-3 was immunoprecipitated using pre-washed Protein G Dynabeads for 30 min and eluted with sample buffer. The presence of bound ACK in each fraction was determined by western blotting with an anti-ACK antibody.

Interestingly, data shown in Figure 5.8 shows that RhoGDI-3 binds to ACK almost exclusively in the nucleus. This suggests that ACK potentially mediates RhoGDI-3 degradation in the nucleus or export RhoGDI-3 out of the nucleus and promotes its degradation in the cytoplasm. These data also imply that ACK has a role in regulating RhoGDI-3 nuclear function, which is presently unknown.

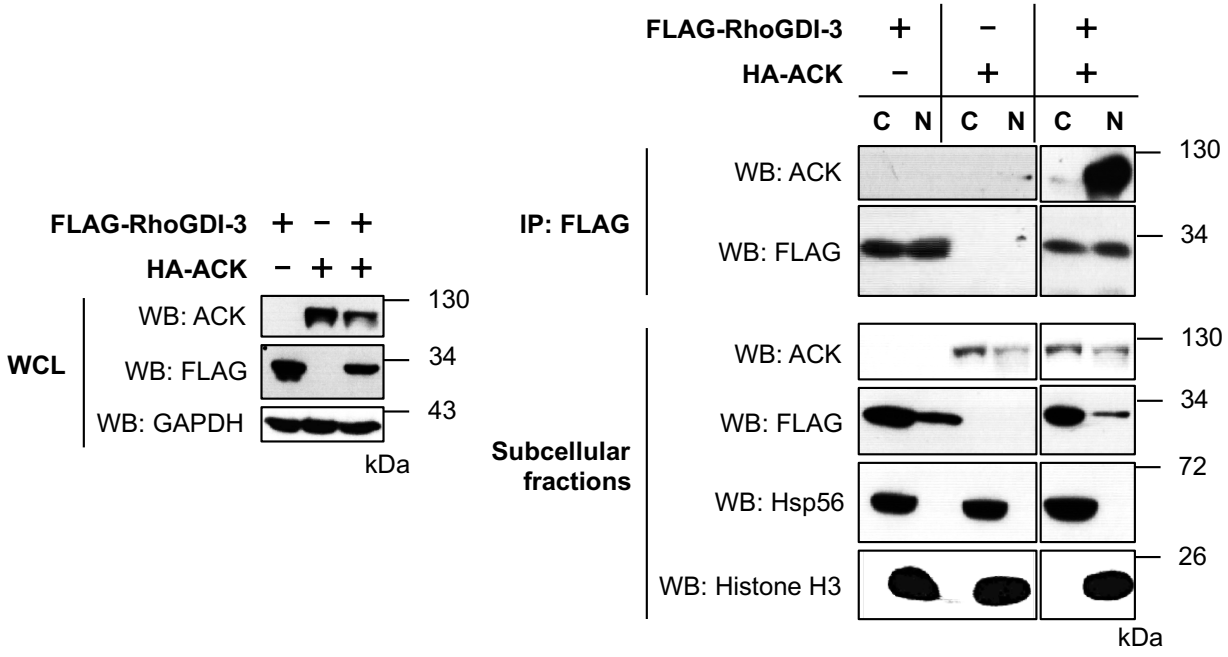

Figure 5.8: The subcellular localization of the FLAG-RhoGDI-3-HA-ACK complex in HEK293T cells. FLAG-RhoGDI-3 was transfected alone or in combination with HA-ACK into HEK293T cells. ~24 h post-transfection, cells were serum-starved overnight. Cells were then harvested and fractionated into cytoplasmic and nuclear-enriched compartments. Each of the fractions was incubated with anti-FLAG antibody before immunoprecipitation with Protein G Dynabeads. Co-immunoprecipitated ACK in each fraction was assessed by blotting with anti-ACK antibody, as shown in the top 2 panels on the right. The expression of recombinant proteins in the whole cell lysate (WCL) is shown in the left hand panel, while their expression in each fraction is shown in the bottom 4 panels, in the right hand panel. Histone H3 and Hsp56 were used as nuclear and cytoplasmic markers, respectively. GAPDH was used to assess equal loading of samples across the wells in the total whole cell lysate**. WCL:** whole cell lysate; **C:** cytoplasmic fraction; **N:** nuclear-enriched fraction.

5.6 Summary

Data presented in this chapter demonstrated that both RhoGDI-1 and -2 are located in the cytoplasm, whereas RhoGDI-3 can be in both cytoplasmic and nuclear-enriched fractions. Interestingly, the nuclear targeting of RhoGDI-3 was not regulated by its first 26 amino acids, contrary to previous finding (Brunet *et al.,* 2002). Conversely, we found that these extra 26 amino acids are predicted to contain an NES motif and are therefore potentially involved in mediating nuclear export of RhoGDI-3.

ACK was found to be in both the cytoplasm and nuclear-enriched fractions and this localization was shown to be kinase-independent. RhoGDI-1 and -2 localization was not affected by ACK under the conditions tested. Since both of the RhoGDIs can interact with ACK and localize exclusively in the cytoplasm, it is assumed that the ACK-RhoGDI-1 and -2 complexes must form in the cytoplasm.

In a similar manner to other RhoGDIs, RhoGDI-3 localization was not affected by the presence of ACK. However, its nuclear levels and nuclear-cytoplasmic ratio were seen to decrease significantly when co-expressed with ACK. Interestingly, ACK was also found to interact with RhoGDI-3 exclusively in the nuclear-enriched fraction. Collectively, these data suggest that binding of ACK and RhoGDI-3 in the nucleus might either mediate RhoGDI-3 degradation in the nucleus or promote the export of RhoGDI-3 out of the nucleus and its subsequent degradation in the cytoplasm.

Chapter 6

The effect of ACK on RhoGDI protein stability

It was observed that co-expression with ACK resulted in decreased protein levels of RhoGDI-3. Since the activation of Rho-family GTPases activation is tightly regulated by the RhoGDIs, aberrant levels of these regulators have been found to associate with the deregulation of Rho-family GTPases activity, which can contribute to cancer progression (Cho *et al.,* 2019). For instance, low levels of RhoGDI-1 have been found to promote breast cancer development (Bozza *et al.,* 2015), while high levels of RhoGDI-1 are shown to be associated with hepatocellular carcinoma (Wang *et al.,* 2014). Loss of RhoGDI-2 protein levels have been shown to be highly associated with invasive and metastatic phenotypes in both bladder cancer and leukaemia (Theodorescu, 2004; Nakata *et al.,* 2008), while increased RhoGDI-2 protein levels are found in breast and gastric cancer (Moon *et al.,* 2010; Cho *et al.,* 2014). Low levels of RhoGDI-3 have been observed in late stages of pancreatic cancer (de León-Bautista *et al.,* 2016).

6.1 The effect of ACK on RhoGDI-1 and -2 stability

To investigate the effect of ACK on RhoGDIs protein levels, a stability assay was performed. This assay utilises cycloheximide (CHX), a protein synthesis inhibitor. Briefly, His-RhoGDI-1 and His-RhoGDI-2 were transfected into HEK293T cells alone or in combination with ACK. Constructs were allowed to express for ~24 h before serum starvation overnight. Cells were then treated with 25 μg/mL CHX, or DMSO as a control, for 2, 5 and 8 h. At various time points, cells were harvested and lysed. The levels of both RhoGDIs were analysed by western blotting, quantified with ImageJ and the relative amounts were plotted.

As shown in Figure 6.1 and 6.2, RhoGDI-1 and -2 were relatively stable alone for up to 8 h. RhoGDI-1 protein levels was not affected by the presence of ACK (Figure 6.1B), while RhoGDI-2 stability increased marginally (Figure 6.2B).

A

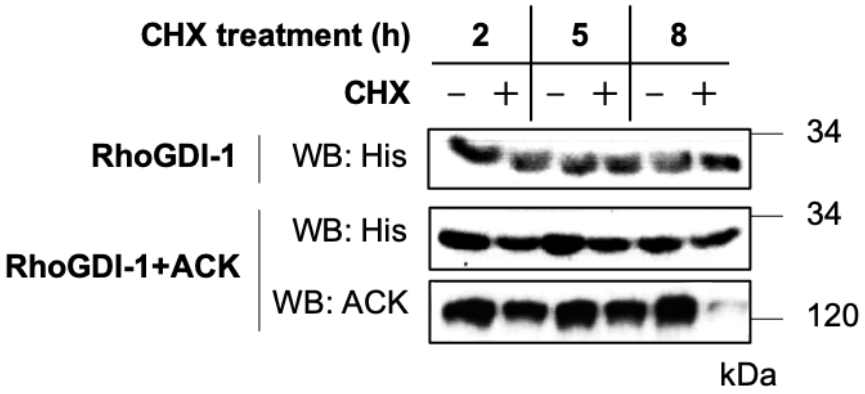

B

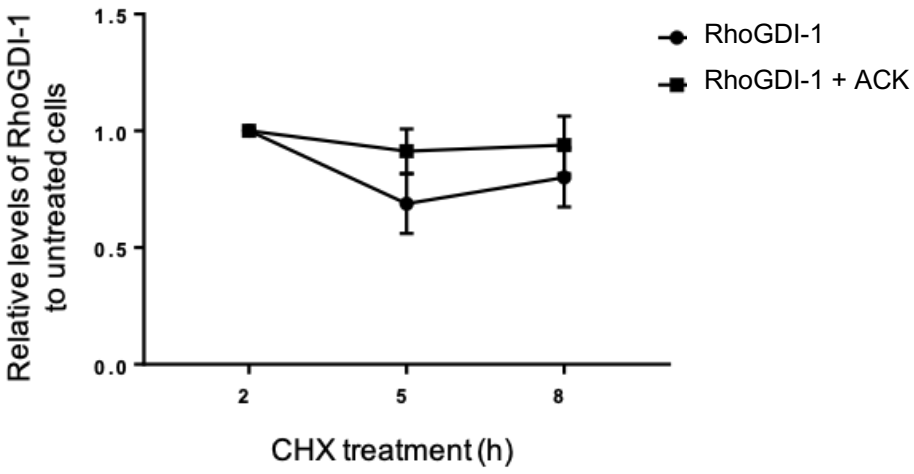

Figure 6.1: RhoGDI-1 protein stability assay. HEK293T cells were transfected with His-RhoGDI-1 alone or in combination with HA-ACK. Constructs were allowed to express for ~24 h before serum starvation overnight. Cell were then treated with DMSO or 25 μg/mL CHX for 2, 5 and 8 h. At each time point, cells were harvested and lysed. **(A)** The level of RhoGDI-1 at each time point was identified by western blotting. **(B)** RhoGDI-1 protein levels in CHX-treated cells were quantified with ImageJ and normalised to levels in DMSO-treated cells. The protein levels, relative to levels at 2 h are plotted. Results are shown as average values ± SEM of three independent experiments.

A

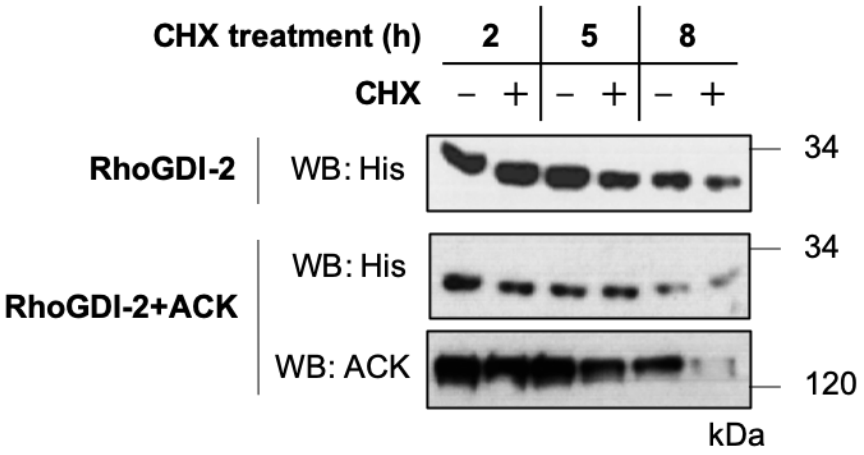

B

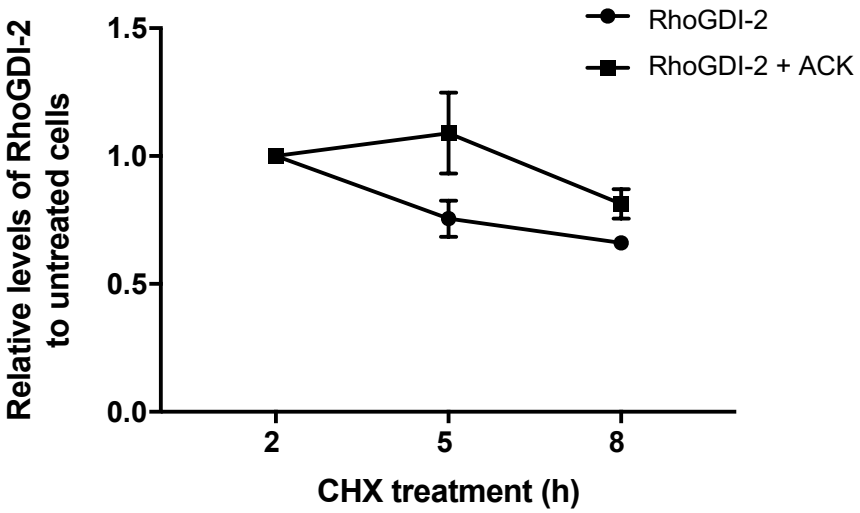

Figure 6.2: RhoGDI-2 protein stability assay. HEK293T cells were transfected with His-RhoGDI-2 alone or in combination with HA-ACK. Constructs were allowed to express for ~24 h before serum starvation overnight. Cells were then treated with DMSO or 25 μg/mL CHX for 2, 5 and 8 h. At each time point, cells were harvested and lysed. **(A)** The level of RhoGDI-2 at each time point was identified by western blotting. **(B)** RhoGDI-2 protein levels in CHX-treated cells were quantified with ImageJ and normalised to the levels in DMSO-treated cells. The protein levels, relative to levels at 2 h are plotted. Results are shown as average values ± SEM of three independent experiments.

6.2 The effect of ACK on RhoGDI-3 stability

Data presented in previous chapters demonstrate that RhoGDI-3 protein levels decrease in cells expressing ACK. Thus, the effect of ACK on RhoGDI-3 stability was analysed. As shown in Figure 6.3, RhoGDI-3 protein levels were relatively stable over time but co-expression with ACK decreased the levels of RhoGDI-3 significantly, suggesting a role for ACK in mediating RhoGDI-3 degradation.

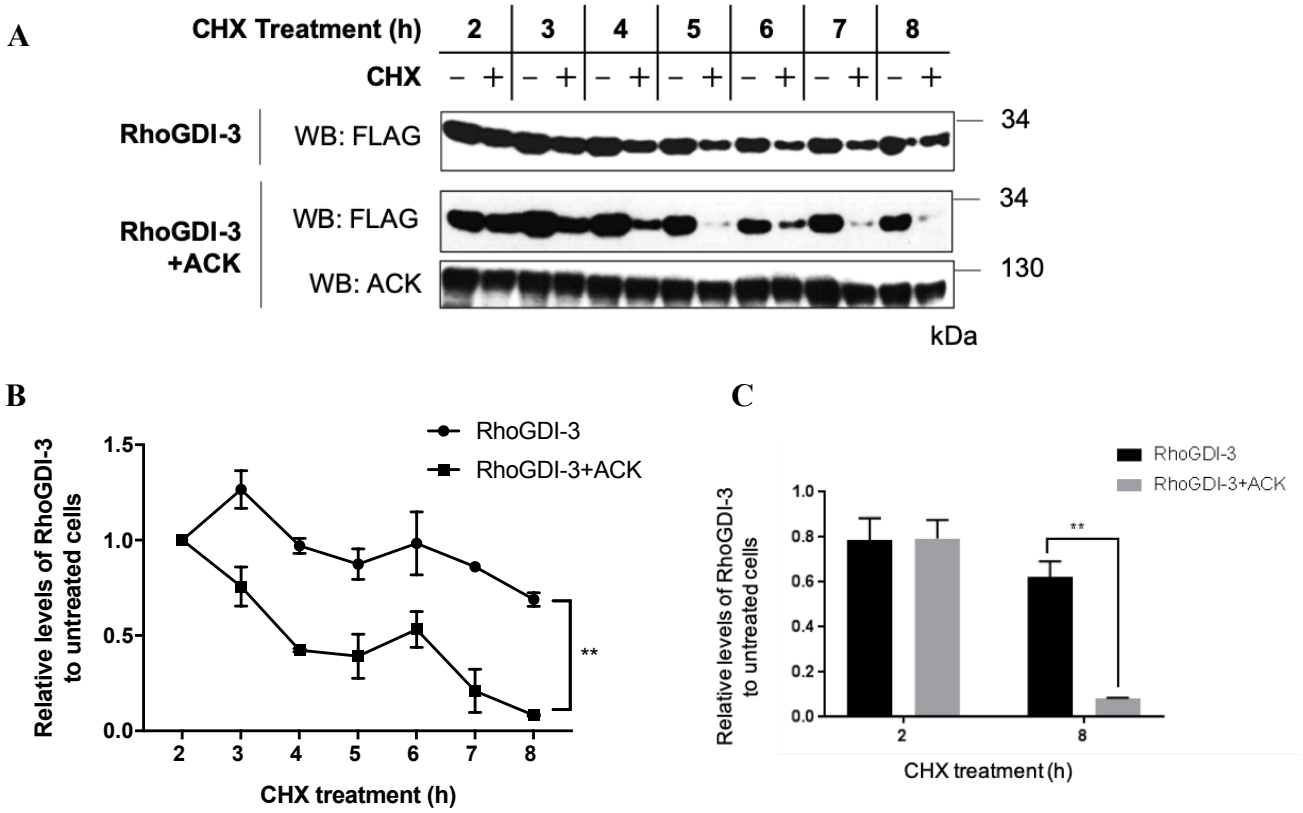

Figure 6.3: RhoGDI-3 protein stability assay. HEK293T cells were transfected with FLAG-RhoGDI-3 alone or in combination with HA-ACK. Constructs were allowed to express for ~24 h before serum starvation overnight. Cells were treated with DMSO or 25 µg/mL CHX for up to 8 h. At each time point, cells were harvested and lysed. **(A)** The level of RhoGDI-3 at each time point was identified by western blotting. **(B)** RhoGDI-3 protein levels in CHX-treated cells were quantified with ImageJ and normalised to levels in DMSO-treated cells. The protein levels, relative to levels at 2 h are plotted. **(C)** The relative levels of RhoGDI-3 at 2 and 8 h. Results are shown as average values ± SEM of three independent experiments, ****p<0.0001.

6.3 ACK mediates RhoGDI-3 degradation through the proteasome

Among RhoGDI family members, ACK exclusively acts to lower the levels of RhoGDI-3. This could be achieved by increasing the degradation of RhoGDI-3, which could be mediated by either the proteasome or the lysosome. Proteasomal degradation, usually referred to as the ubiquitin-proteasome system (UPS) involves the covalent attachment of four or more Ubiquitin (Ub) molecules to lysine residues on targeted proteins. These poly-ubiquitinated proteins are then recognised and cleaved by the 26S proteasome into small peptides, which are later digested into single amino acids by cytosolic proteases.

The UPS also exists in the nucleus (nUPS) and targets misfolded nuclear proteins in order to maintain nuclear quality control (Mikecz, 2006). Some substrates of nUPS have been identified, for examples Jun, Myc, Fos, p53, STAT1, Far1 and MyoD (Ciechanover *et al.,* 1991; Kim and Maniatis, 1996; Blondel *et al.,* 2000; Floyd *et al.,* 2001). Protein degradation through the lysosome, also known as autophagy, involves the sequestration of proteins directly by the lysosome, a membrane-bound intracellular compartment with a concentration of proteases (Mizushima *et al.,* 2008).

In order to distinguish between proteasomal and lysosomal degradation, an inhibitor specific for each pathway was used. MG132 blocks the proteolytic activity of 26S proteasome complex, while Bafilomycin A1 (Baf), blocks autophagic flux by inhibiting autolysosome acidification.

Briefly, HEK293T cells were transfected with FLAG-RhoGDI-3 alone or together with HA-ACK. Constructs were allowed to express for ~40 h before being treated with DMSO, 10 μM MG132 or 1 μM Baf, individually for 6 h. Cells were then harvested, lysed and RhoGDI-3 protein levels were identified by western blotting. Cyclin B1 and RhoB were used as positive control for MG132 and Baf, respectively. The levels of RhoGDI-3 in MG132 or Baf-treated cells were quantified with ImageJ and normalised to levels in DMSO-treated cells.

As shown in Figure 6.4A, Cyclin B1 levels increase following treatment with MG132, consistent with previous reports that show it is degraded by the UPS (Potapova *et al.,* 2009). The levels of RhoB in non-transfected cells also increased after treatment with Baf (Figure 6.4B), consistent with Pérez-Sala *et al.* (2009). RhoGDI-3 levels were seen to increased marginally in both MG132- and Baf-treated cell, suggesting that RhoGDI-3 can be regulated by the proteasome as well as the lysosome. Interestingly, however, ACK-mediated degradation of RhoGDI-3 was inhibited prominently by MG132 (Figure 6.4A) and not by Baf (Figure 6.4B), indicating that ACK stimulated the degradation of RhoGDI-3 is through the proteasome and not the lysosome. RhoB protein levels also increased in cells expressing RhoGDI-3 alone or when co-expressed with ACK, indicating a role for either or both these proteins in increasing RhoB stability.

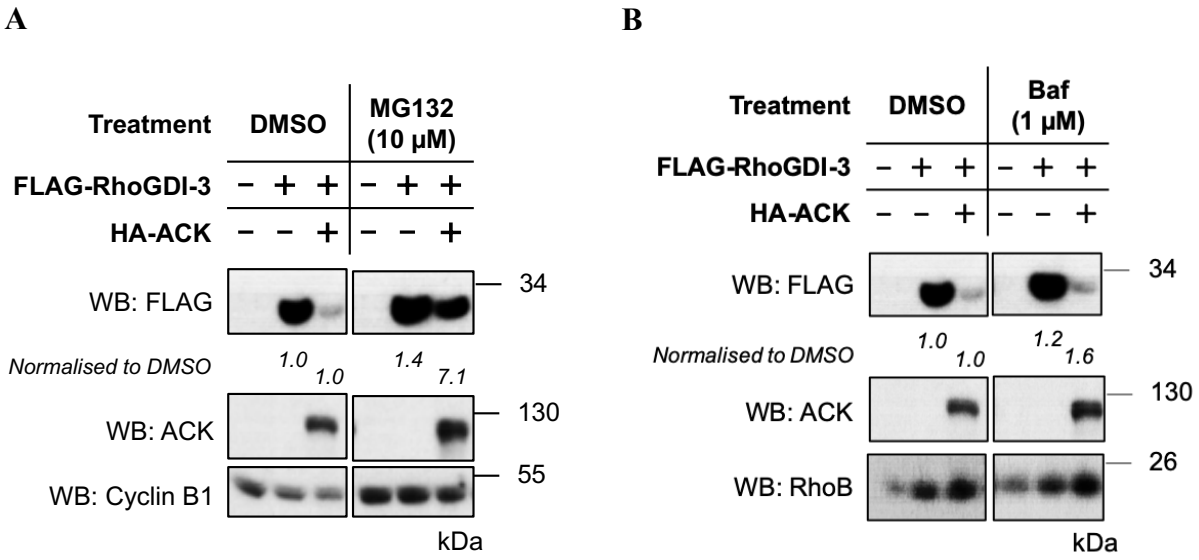

Figure 6.4: Proteasome inhibition blocks RhoGDI-3 degradation following co-expression with ACK. FLAG-RhoGDI-3 was transfected into HEK293T cells alone or together with HA-ACK. Constructs were allowed to express for ~40 h. DMSO, 10 μM MG132 or 1 μM Baf were then added for the last 6 h before cells were harvested and lysed. The levels of RhoGDI-3 were identified by western blotting. Cyclin B1 and RhoB were used as positive controls for MG132 and Baf treatments, respectively. RhoGDI-3 protein levels in treated cells were quantified with ImageJ and normalised to levels in DMSO-treated cells. Relative values are shown below the blot.

6.4 ACK mediates degradation of RhoGDI-3 in the nucleus

Data presented in section 5.5 showed that ACK interacts with RhoGDI-3 in the nuclear-enriched fraction and this interaction was linked to a decrease in RhoGDI-3 protein levels, especially in the nuclear-enriched fraction. Thus, it was hypothesized that ACK might either mediate RhoGDI-3 degradation in the nucleus or regulate export of RhoGDI-3 out from the nucleus and stimulate its degradation in the cytoplasm.

To investigate this, HEK293T cells were transfected with RhoGDI-3 either alone or in combination with ACK. Constructs were allowed to express for ~24 h before serum starvation overnight. Cells were then treated with DMSO or 25 μg/mL CHX for a further 2 and 5 h. At each time point, cells were fractionated into cytoplasmic and nuclear-enriched extracts. RhoGDI-3 protein levels in each fraction were identified by western blotting, quantified with ImageJ and the relative amounts were plotted.

Figure 6.5 show RhoGDI-3 protein levels are relatively stable when expressed alone, in both the cytoplasmic and nuclear-enriched fractions. However, the levels of RhoGDI-3 in each fraction decrease in cells expressing ACK, but this loss was more significant in the nuclear-enriched fraction. These findings show that ACK likely stimulates RhoGDI-3 degradation in the nucleus.

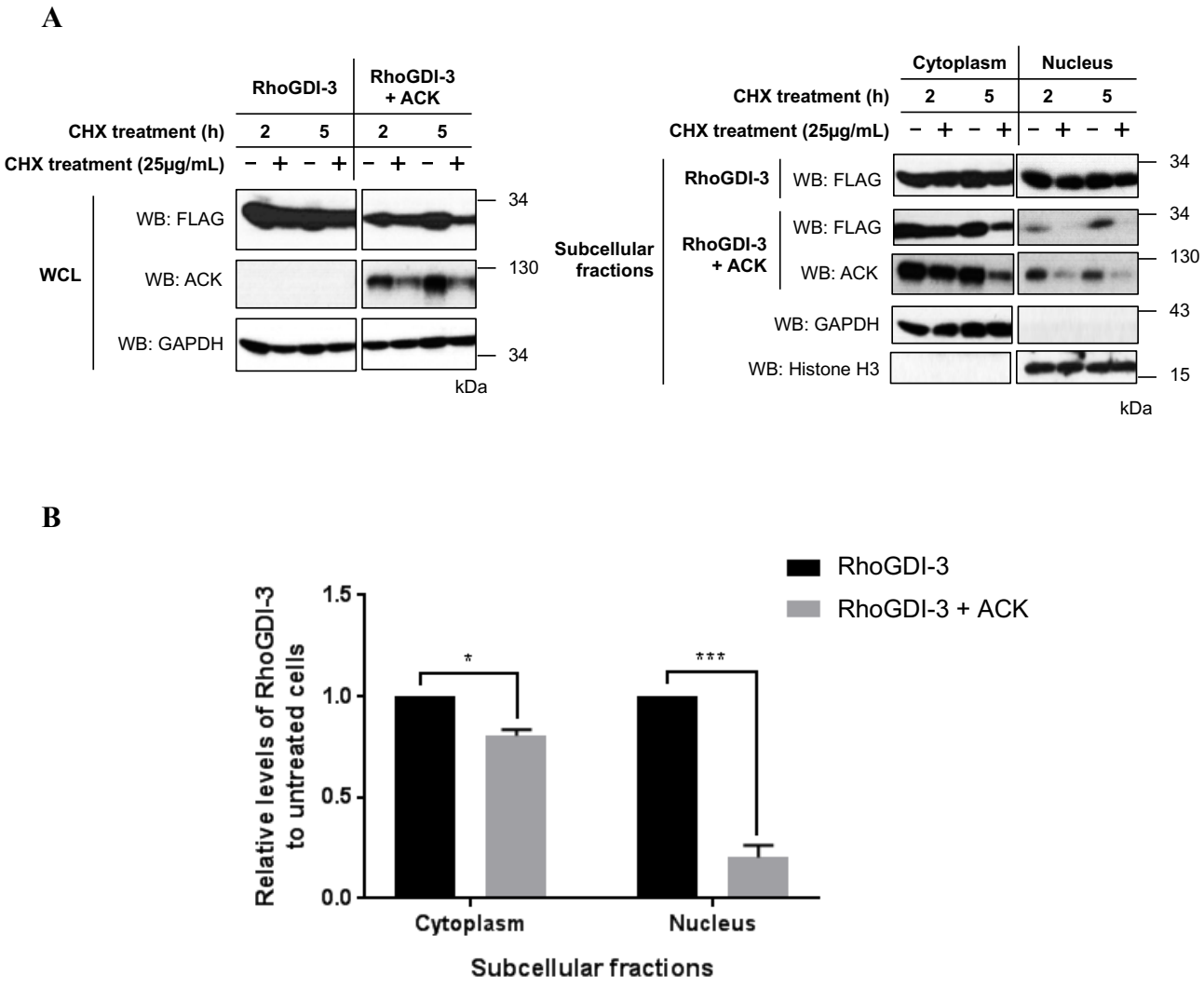

Figure 6.5: RhoGDI-3 protein stability upon ACK co-expression in cytoplasmic and nuclear-enriched fractions. HEK293T cells were transfected with FLAG-RhoGDI-3 alone or together with HA-ACK. Constructs were allowed to express for ~24 h before serum starvation overnight. DMSO and 25 µg/mL CHX were then added to control and treated cells, respectively. Cells were fractionated into cytoplasmic and nuclear-enriched compartments, 2 and 5 h post-treatments. **(A)** The levels of RhoGDI-3 in each fraction, at each time point were identified by western blotting. Histone H3 and GAPDH were used as nuclear and cytoplasmic markers, respectively. GAPDH was also used to assess equal loading of samples across the wells in the total whole cell lysate. **(B)** RhoGDI-3 protein levels in CHX-treated cells were quantified with ImageJ and normalised to levels in DMSO-treated cells. The protein levels at 5 h, relative to levels at 2 h are plotted. Results are shown as average values ± SEM of three independent experiments, ***p≤ 0.001. **WCL:** whole cell lysate.

6.5 The role of the N-terminus of RhoGDI-3 in regulating RhoGDI-3 stability

6.5.1 The N-terminus of RhoGDI-3 is not necessary for the interaction with ACK

Previous data presented in this work (section 6.2) show that RhoGDI-3 stability is affected when co-expressed with ACK and that this is not the case for both RhoGDI-1 and -2. An N-terminally truncated mutant of RhoGDI-3 was also shown to be more stable than the wt RhoGDI-3 (section 5.2). Thus, it was postulated that the N-terminal extension of RhoGDI-3 is important for ACK to regulate RhoGDI-3 degradation.

First, the role of the N-terminus of RhoGDI-3 in regulating the interaction between ACK and RhoGDI-3 was investigated by co-immunoprecipitation. Interestingly, the original construct of RhoGDI-3 identified by the Y2H screen contained only residues 73 to 225 of RhoGDI-3, thus it was likely that an N-terminal deleted mutant of RhoGDI-3 would still be able to bind to ACK.

Data in Figure 6.6 shows that the N-terminally truncated mutant of RhoGDI-3 does indeed retain the ability to bind to ACK.

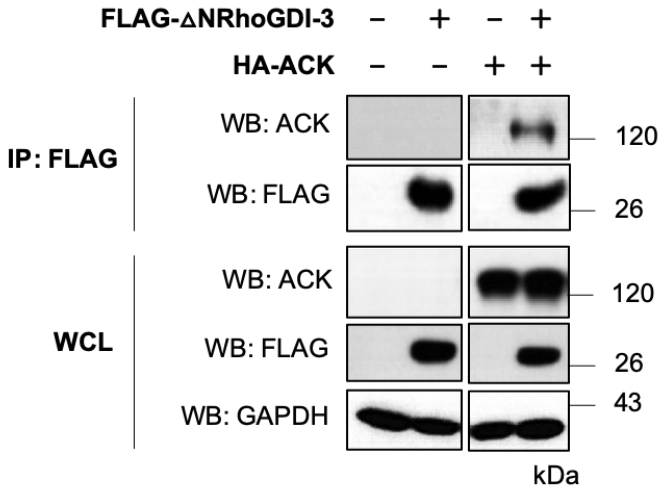

Figure 6.6: The role of the N-terminus of RhoGDI-3 in regulating the interaction between RhoGDI-3 and ACK. HEK293T cells were transfected with FLAG-ΔNRhoGDI-3 alone or in combination with HA-ACK. Constructs were allowed to express for ~40 h before being harvested and lysed. Anti-FLAG antibody was then added to pre-cleared cell lysates and incubated for 45 min. FLAG-ΔNRhoGDI-3 was immunoprecipitated with pre-washed Protein G Dynabeads and bound ACK was identified by western blot analysis. The expression of the recombinant protein in the whole cell lysate (WCL) is shown in the bottom 3 panels, while the co-immunoprecipitated (IP) samples are shown in the top two panels. In the whole cell lysate, GAPDH was used to assess equal loading of samples across the wells. **WCL:** whole cell lysate; **IP:** immunoprecipitation.

6.5.2 ACK regulates RhoGDI-3 stability through the N-terminus

To further investigate the function of the N-terminus in regulating RhoGDI-3 stability especially in cells expressing ACK, a CHX stability assay was performed by transfecting HEK293T cells with either ΔNRhoGDI-3 or wt RhoGDI-3 alone or together with ACK.

As shown in Figure 6.7, the ΔNRhoGDI-3 mutant is relatively stable alone, similar to wt RhoGDI-3. Co-expression with ACK did not decrease ΔNRhoGDI-3 protein levels compared to its effect on wt RhoGDI-3. These data suggest that the N-terminus of RhoGDI-3 is important in regulating RhoGDI-3 stability in the presence of ACK.

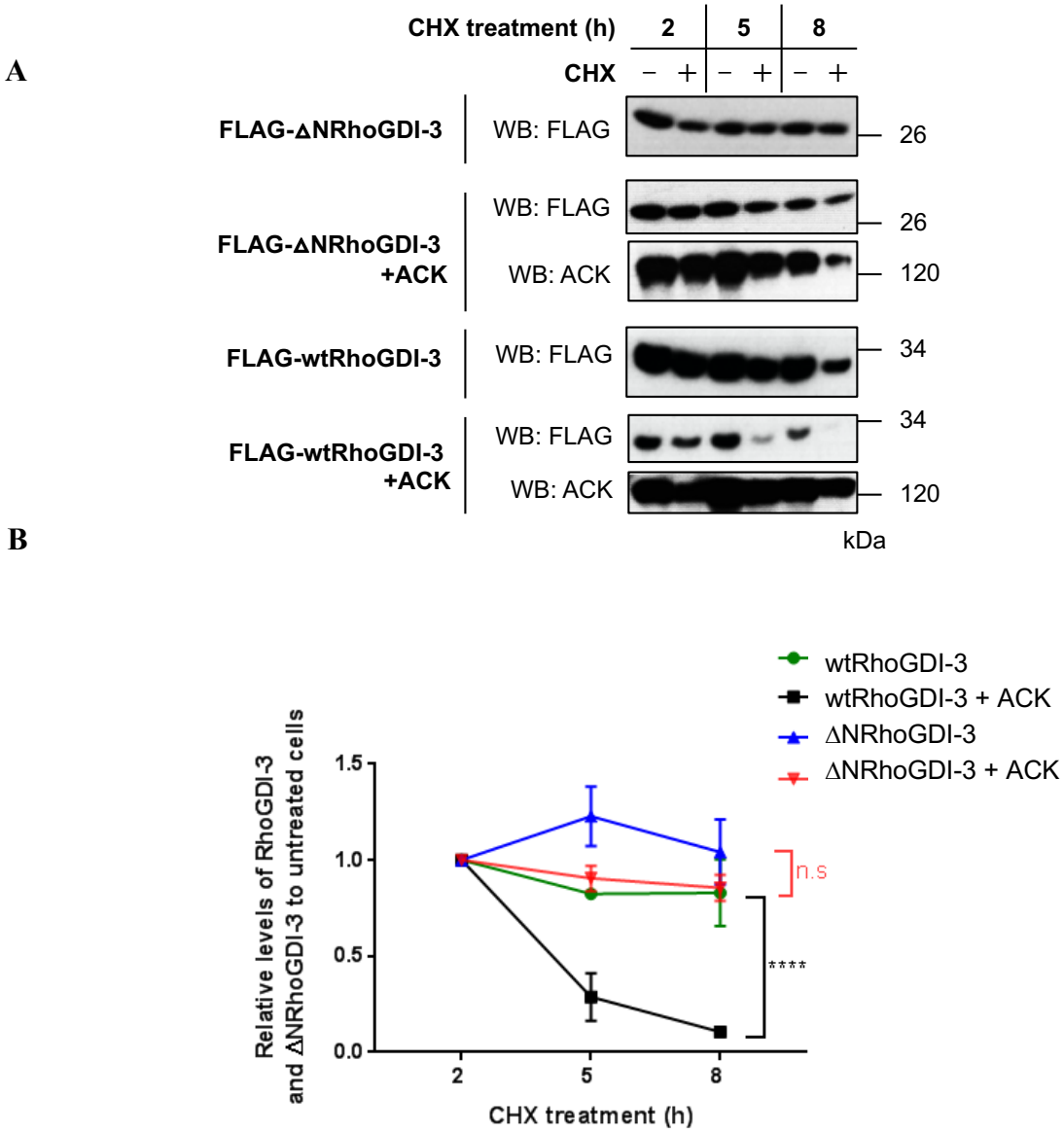

Figure 6.7: The role of the N-terminus of RhoGDI-3 in regulating RhoGDI-3 stability in the presence of ACK. FLAG-RhoGDI-3 and FLAG-ΔNRhoGDI-3 were transfected into HEK293T cells alone or together with ACK. Constructs were allowed to express for ~24 h before serum starvation overnight. Cells were then treated with DMSO or 25 µg/mL CHX for 2, 5 and 8 h. At each time point, cells were harvested and lysed. **(A)** The levels of wtRhoGDI-3 and ΔNRhoGDI-3 were identified by western blotting. **(B)** RhoGDIs protein levels in CHX-treated cells were quantified with ImageJ and normalised to levels in DMSO-treated cells. The protein levels, relative to levels at 2 h are plotted. Results are shown as average values ± SEM from three independence experiments, *p≤ 0.05, ****p<0.0001.

6.6 The effect of RhoGDI interaction on ACK stability

Previous data presented in this work demonstrate that ACK decreases RhoGDI-3 stability but not RhoGDI-1 or -2. The effect of all three RhoGDI on ACK stability was also investigated in similar stability assays.

As shown in Figure 6.8, ACK is stable in the absence of exogenous RhoGDIs for over 8 h. However, ACK levels decreased when co-expressed with all three RhoGDIs, suggesting a role for RhoGDIs in regulating ACK stability.

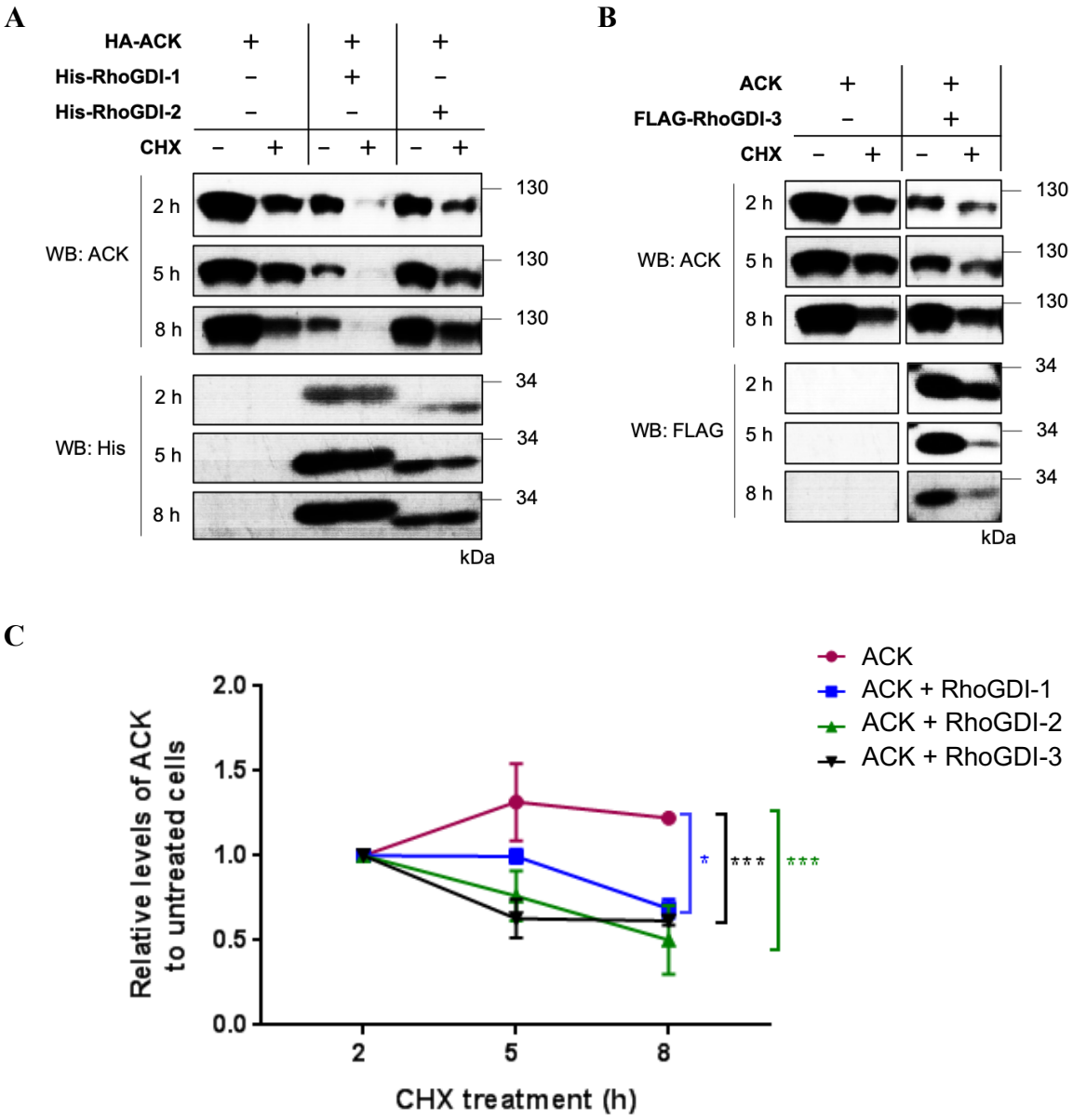

Figure 6.8: ACK protein stability assay. HEK293T cells were transfected with ACK alone or in combination with His-RhoGDI-1, His-RhoGDI-2 or FLAG-RhoGDI-3. Constructs were allowed to express for ~24 h before serum starvation overnight. Cells were then treated with DMSO or 25 µg/mL CHX for 2, 5 and 8 h. At each time point, cells were harvested and lysed. The levels of ACK at each time point either alone or when co-expressed with **(A)** RhoGDI-1 or -2 and **(B)** RhoGDI-3 were identified by western blotting and quantified with ImageJ. **(C)** ACK protein levels in CHX-treated cells were quantified with ImageJ and normalised to levels in DMSO-treated cells. The protein levels, relative to levels at 2 h are plotted. Results are shown as average values ± SEM for three independent experiments, *p≤ 0.05, ***p≤ 0.001.

6.7 Summary

The data presented in this chapter show that RhoGDI-1 stability was not affected by ACK, while levels of RhoGDI-2 slightly increased in the presence of exogenous ACK. Cellular levels of RhoGDI-3, however substantially decreased in the presence of exogenous ACK. ACK was shown to mediate RhoGDI-3 degradation via the proteasome and this degradation occurred mainly in the nucleus. Furthermore, the N-terminus of RhoGDI-3 seems to be necessary for ACK-mediated degradation of RhoGDI-3 as an N-terminally truncated mutant of RhoGDI-3 was more stable when co-expressed with ACK, compared to wt RhoGDI-3.

Interestingly, ACK was also shown to be less stable when co-expressed with any of the RhoGDIs, suggesting that RhoGDIs may also regulate ACK stability.

Chapter 7

The effect of ACK on RhoGDI-3 ubiquitination

Previous data described in Chapter 6 shows lower levels of RhoGDI-3 in the presence of ACK and indicated that regulation of ubiquitin-proteasome degradation could be the mechanism behind this. Thus, further studies to investigate the effect of ubiquitination on RhoGDI-3 stability and localization were undertaken and especially the role of ACK in this process.

Ubiquitination is known to affect protein function by regulating activity, stability, localization and the ability to bind to partners (Jaffrey and Xu, 2011). This PTM involves the covalent attachment of the last amino acid of a Ub, Gly76, to one or more lysines of a target protein, through a cascade of three classes of enzymes: E1 ubiquitin-activating enzyme, E2 ubiquitin-conjugating enzyme and E3 ubiquitin ligase (Figure 7.1). An E1 activates Ub by forming a thioester-linked E1-Ub intermediate through the catalytic cysteine of the E1. The activated Ub is then transferred to the catalytic residues of an E2. The E3 is important in catalysing the transfer of Ub either directly from

the E2-Ub intermediate or after thioester linkage of Ub with the E3 itself, to specific protein substrates (Sardowski and Sarcevic, 2010).

Unconventional substrate recognition and targeting can involve the conjugation of Ub at the free N-terminus of a substrate. For instance, a transcriptional activator, MyoD, has been shown to be ubiquitinated at its N-terminus, which then leads to its degradation (Breitschopf *et al.,* 1998). Other examples of proteins modulated in this way include cell-cycle-dependent kinase inhibitor p21 (Bloom *et al.,* 2003), human papillomavirus 16 oncoprotein E7 (Reinstein *et al.,* 2000), extracellular signal-regulated kinase 3 (ERK3) (Coulombe *et al.,* 2004) and latent membrane protein 1 (LMP1) of Epstein Barr virus (Aviel *et al.,* 2000). Interestingly, the substitution of internal lysine residues in some of these proteins was also shown to decrease ubiquitination and degradation events, suggesting that both the N-terminus and internal lysine residues might serve as ubiquitin anchors (Ciechanover and Ben-saadon, 2004).

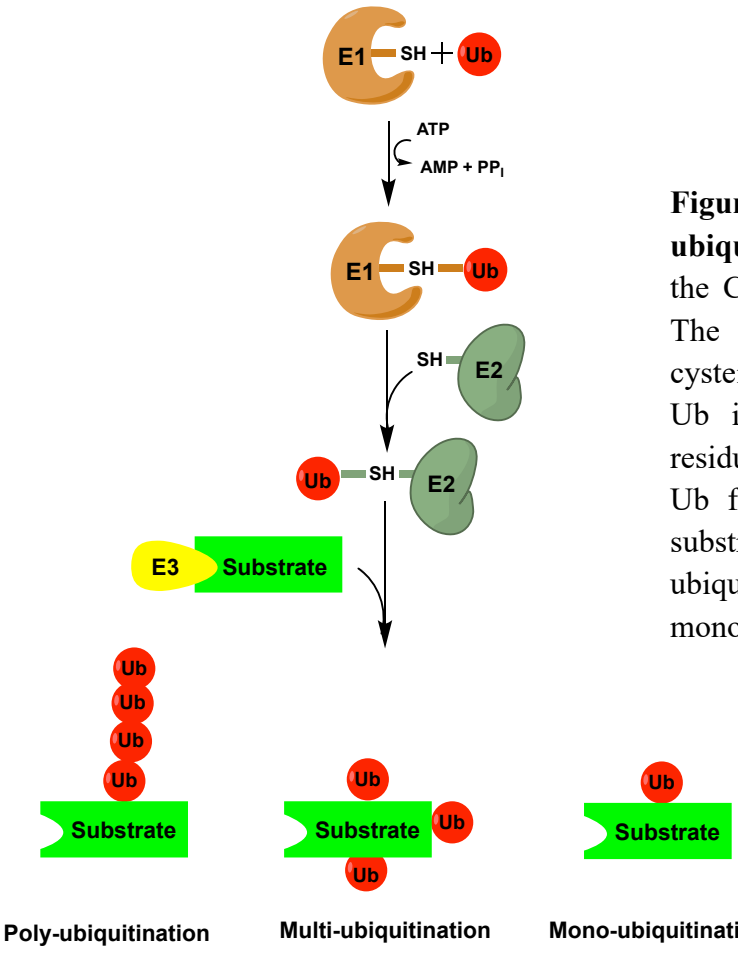

Figure 7.1: A schematic diagram of the ubiquitination system. The E1 activates the C-terminal residue of a Ub molecule. The activated Ub is then attached to a cysteine residue in the E1 active site. The Ub is then transferred to the catalytic residue of E2. E3 facilitates the transfer of Ub from the E2-Ub intermediate to the substrate protein, resulting in poly-ubiquitination, multi-ubiquitination or mono-ubiquitination.

Ubiquitin modifications can occur in many formats: as a single Ub attached to a single lysine (mono-ubiquitination, Mono-Ub), a single Ub unit on multiple lysines in the same protein (multi-ubiquitination, Multi-Ub) or multiple Ub on the same lysine, forming ubiquitin chains (poly-ubiquitination, poly-Ub) (Figure 7.1). This structural diversity is highly dependent on the lysine residues of the target proteins and the Ub itself.

The simplest form of ubiquitination, mono-ubiquitination, is known to regulate both proteasome-dependent (Isasa *et al.,* 2010) and independent functions (Trotman *et al.,* 2008). In a poly-Ub chain, ubiquitin chains that consist of only a single linkage, are called homotypic (Figure 7.2) and the most prevalent linkages are found through Lys48 or Lys63 of Ub. Different types of linkages confer different fates on the substrates (Sadowski and Sarcevic*,* 2010). For instance, a poly-Ub linkage through Lys48 is known to induce proteasomal degradation, whereas linkage via Lys63 may lead to proteasome-independent fates, such as altering the subcellular localization of target proteins (Glickman and Ciechanover, 2002; Wang *et al.,* 2018) or kinase activation (Deng *et al.,* 2000). Recently, different types of poly-Ub linkage known as heterotypic poly-Ub have also been found to promote both proteasome-depended and independent functions of the modified substrate (Meyer and Rape, 2014; Ohtake and Tsuchiya, 2016; Ohtake *et al.,* 2018; Stolz and Dikic, 2018). This poly-Ub linkage can occurred through mixed linkages occurring within the same polymer (non-branched), or one ubiquitin molecule is modified by two or more subsequent ubiquitin molecule (branched).

There is also another atypical poly-Ub linkage, which occurs through the ubiquitination of the N-terminal methionine, commonly known as Met1-Ub or linear ubiquitination (Kirisako *et al.,* 2006). The addition of Met1-Ub is catalysed by linear ubiquitin chain assembly complex (LUBAC) E3 ligase, which is composed of three subunits; HOIL-1L, HOIP, and SHARPIN (Kirisako *et al.,* 2006; Gerlach *et al.,* 2011; Tokunaga *et al.,* 2011) to promote proteasomal degradation of the modified substrate. For instance, LUBAC-mediated ubiquitination of cellular FLICE-like inhibitory protein (cFLIP), an anti-apoptotic molecule, has been shown to stimulate TNF-induced cell death and inflammation (Tang *et al.,* 2018).

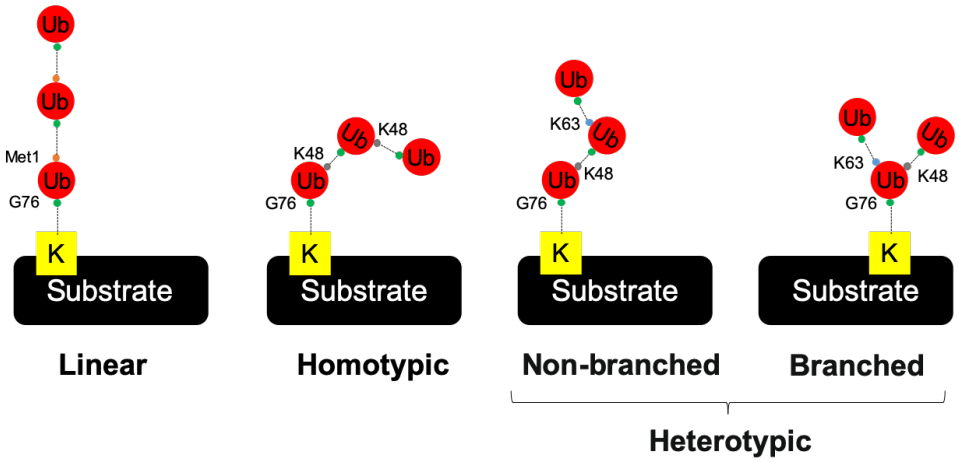

Figure 7.2: Different types of poly-Ub linkage. Poly-Ub chains linkage can occur through the linear ubiquitination, a single lysine residue (homotypic) or a multiple lysine residue on a single Ub unit (heterotypic).

RhoGDI-1 has been shown to undergo ubiquitination upon interaction with an E3 ligase known as GRAIL. GRAIL-mediated polyubiquitination of RhoGDI-1 has been shown to occur through a Lys63 linkage and this does not lead to RhoGDI-1 degradation. The potential ubiquitination site on RhoGDI-1 is still unknown but RhoGDI-1 ubiquitination was found to inhibit RhoA activation (Su *et al.,* 2006). To date, no study has investigated RhoGDI-3 ubiquitination but there are several potential ubiquitination sites on RhoGDI-3, as predicted by UbiSite (Table 7.1).

Table 7.1: Prediction of lysine ubiquitination sites in RhoGDI-3 by UbiSite

Amino acid	Putative ubiquitination sites	Score
73	RSLAKY K RVLLGP	0.533472
126	DQVFVL K EGVDYR	0.530605
134	GVDYRV K ISFKVH	0.572311
162	RGLRVD K TVYMVG	0.580189

This prediction software relies on a pool of known substrate motifs for ubiquitin conjugation. The reliability prediction is based on the score calculated, which are categorised into $0.5 \leq s \geq 1.0$ (high), $0.25 \leq s \geq 0.5$ (medium) and $0.125 \leq s \geq 0.25$ (low).

7.1 RhoGDI-3 undergoes ubiquitination

As described in Table 7.1, there are several predicted ubiquitination sites on RhoGDI-3, suggesting a possibility that RhoGDI-3 undergoes ubiquitination. To test this, FLAG-RhoGDI-3 was transfected alone or in combination with Myc-Ub (a kind gift from Dr. Catherine Lindon, Department of Pharmacology, University of Cambridge) into HEK293T cells. Constructs were allowed to express for ~24 h before serum starvation. ~40 h post-transfection, cells were treated with 10 μM of MG132 or DMSO for ~6 h and then harvested. The pre-cleared lysates were immunoprecipitated with anti-FLAG antibody that was cross-linked to pre-washed protein G Dynabeads. The ubiquitination level of RhoGDI-3 was then analysed by western blotting with an anti-Myc antibody.

In both the WCL and IP samples, there were "laddering" pattern of RhoGDI-3 in lanes showing RhoGDI-3 with Myc-Ub (lanes 2, 4, 6 and 8) compared to RhoGDI-3 alone (lanes 1, 3, 5 and 7) and these ubiquitin "smears" increased with MG132 treatment (lanes 4 and 8) (Figure 7.3). These data suggest RhoGDI-3 undergoes ubiquitination which is affected by MG132 treatment.

There was a ~55 kDa band observed in all lanes. However, this band was thought not to be a ubiquitinated form of RhoGDI-3 but potentially a non-specific protein detected by the anti-Myc antibody. An ~43 kDa protein was also detected in the WCL samples, only when treated with MG132 (lanes 3 and 4) but this band was also assumed not to be a ubiquitinated form of RhoGDI-3 as it also appears in lane without Myc-Ub (lane 3).

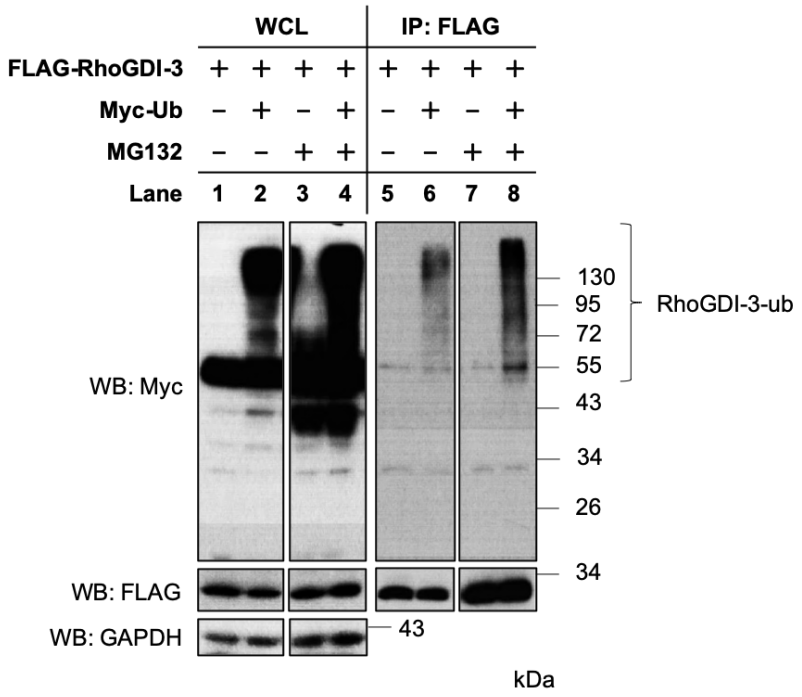

Figure 7.3: Ubiquitination of RhoGDI-3. FLAG-RhoGDI-3 and Myc-Ub were transfected alone or together, into HEK293T cells and allowed to express for ~24 h. Cells were serum-starved overnight before being treated with MG132 or DMSO for ~6 h. Cells were then harvested, lysed and immunoprecipitated using anti-FLAG antibody, ~40 h post-transfection. The ubiquitination level of RhoGDI-3 was assessed by western blotting using anti-Myc and anti-FLAG antibodies. The expression of the recombinant protein in the whole cell lysates (WCL) is shown on the left, while the co-immunoprecipitated (IP) samples are shown in the right hand panels. In whole cell lysates, GAPDH was used to assess equal loading of samples across the wells. The western blot shown is representative of at least three independent experiments. **WCL:** whole cell lysate; **IP:** immunoprecipitation.

7.2 Types of RhoGDI-3 ubiquitination

Previous data showed that RhoGDI-3 undergoes ubiquitination. The presence of high MW ubiquitinated species suggests that multiple ubiquitin molecules have been added to RhoGDI-3 and this is potentially due to progressive poly-ubiquitination. Poly-Ub can occur through several linkages but the most prevalent linkages are found through Lys48 or Lys63. To investigate the type of poly-Ub linkages on RhoGDI-3, Myc-K48R and Myc-K63R Ub mutants were utilized. These Ub mutants prevent poly-Ub linkage via Lys48 or Lys63, respectively. The Myc-K48R-Ub construct was a kind gift from Dr. Catherine Lindon (Department of Pharmacology, University of Cambridge), while Myc-K63R-Ub was generated in this work.

Each of the mutants was transfected alone or together with RhoGDI-3 into HEK293T cells and allowed to express for ~24 h before serum-starved overnight. ~40 h post-transfection, cells were harvested, lysed and immunoprecipitated with an anti-FLAG antibody. The ubiquitinated RhoGDI-3 was analysed by western blotting and the pattern observed with both K48R and K63R Ub mutants were compared to wt Ub.

As shown in Figure 7.4, wt and both the Ub mutants expressed at similar levels. When co-expressed with RhoGDI-3, the ubiquitin smears in the WCL decreased with wt Ub and K63R Ub but not with K48R Ub, suggesting that both wt Ub and K63R Ub molecules were incorporated into RhoGDI-3 but K48R Ub was not. In the IP samples, cells expressing RhoGDI-3 and wt Ub (lane 4) show a smear starting from ~55 and reaching to >130 kDa, suggesting that RhoGDI-3 undergoes poly-Ub. However, the smear slightly decreased with K63R Ub (lane 6), while it increased substantially with K48R Ub (lane 5). Correspondingly, in the WCL, the levels of Ub monomer increase in cells co-expressing RhoGDI-3 and K48R Ub but not with wt Ub and K63R Ub. These data suggest that addition of the K48R Ub mutant to RhoGDI-3 may terminate different stages of poly-Ub chain formation, resulting in multiple bands that appears as a smear. Hence, these data suggest that RhoGDI-3 undergoes poly-ubiquitination which contain K48 linkages. However, the multiple bands observed in cells co-expressing RhoGDI-3 and K48R Ub could also suggest that RhoGDI-3 undergoes poly-Ub following multi-Ub at different lysine residues, linear ubiquitination, linear-Lys48 mixed poly-Ub or other heterotypic poly-Ub linkage that are highly dependent on Lys48.

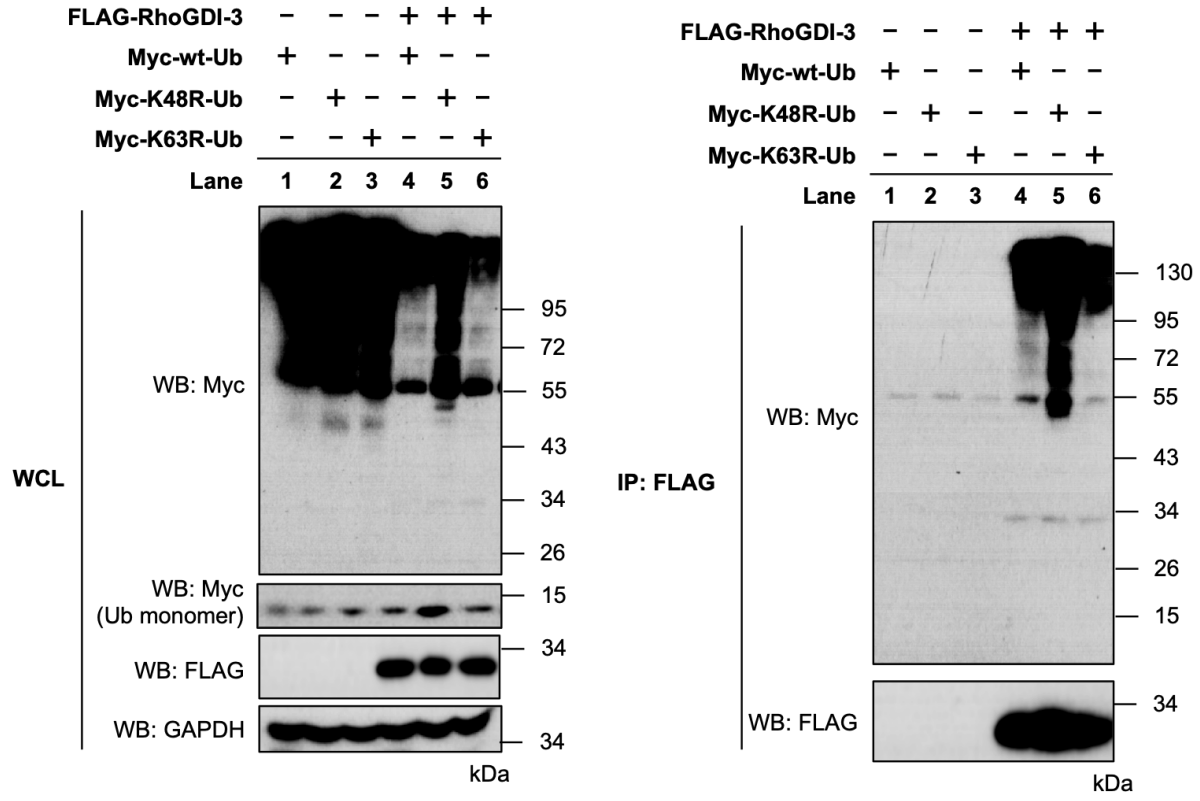

Figure 7.4: Potential poly-ubiquitin-linkage of RhoGDI-3. FLAG-RhoGDI-3 was transfected alone or together with Myc-wt-Ub, Myc-K48R-Ub or Myc-K63R-Ub into HEK293T cells. Constructs were allowed to express for ~24 h before serum-starved overnight. Cells were then harvested, lysed and immunoprecipitated using anti-FLAG antibody, ~40 h post-transfection. The ubiquitination level of RhoGDI-3 was assessed by western blotting using anti-Myc antibody. The expression of the recombinant protein in the whole cell lysate (WCL) is shown in the left hand panel, while the co-immunoprecipitated (IP) samples are shown in the right hand panel. In whole cell lysate, GAPDH was used to assess equal loading of samples across the wells. The western blot shown is representative of at least three independent experiments. **WCL:** whole cell lysate; **IP:** immunoprecipitation.

To investigate the possibility that RhoGDI-3 undergoes multi-Ub prior to Lys48 poly-Ub, a KO Ub mutant (Addgene plasmid # 17603, a gift from Prof. Ted Dawson) was used in which all 7 lysine residues have been mutated to arginines. This KO Ub mutant retains the ability to bind to a substrate through Gly76 and can be incorporated as a single or multiple-mono-Ub molecules onto

a targeted protein. However, unlike wt Ub, it cannot form the homotypic and heterotypic poly-Ub chain (Figure 7.2). This KO mutant would not prevent the possibility of RhoGDI-3 undergoing atypical linear poly-ubiquitination (Figure 7.2).

Briefly, HEK293T cells were transfected with FLAG-RhoGDI-3, HA-wt-Ub and HA-KO-Ub either alone or in combination. ~24 h post-transfection, cells were serum-starved overnight. Cells were then harvested, lysed and immunoprecipitated with anti-FLAG antibody. Any differences in RhoGDI-3 ubiquitination with wt and the KO Ub mutant were identified by western blotting with an anti-Myc antibody.

As shown in Figure 7.5, cells expressing KO Ub alone seem to have slightly less KO Ub incorporated into the ubiquitin smear in the WCL (lane 3) compared to the wt Ub (lane 2). Consistent with this, free KO Ub was also visible, suggesting that this mutant was linked to substrate less often as expected. The same pattern is seen in the WCL samples when RhoGDI-3 is present. In the IP samples, the same pattern of ubiquitin smears can be observed either with wt (lane 5) or KO Ub (lane 6), implying that both wt and KO Ub can still be added to RhoGDI-3. These data suggest that RhoGDI-3 might undergo linear ubiquitination instead of multi-Ub.

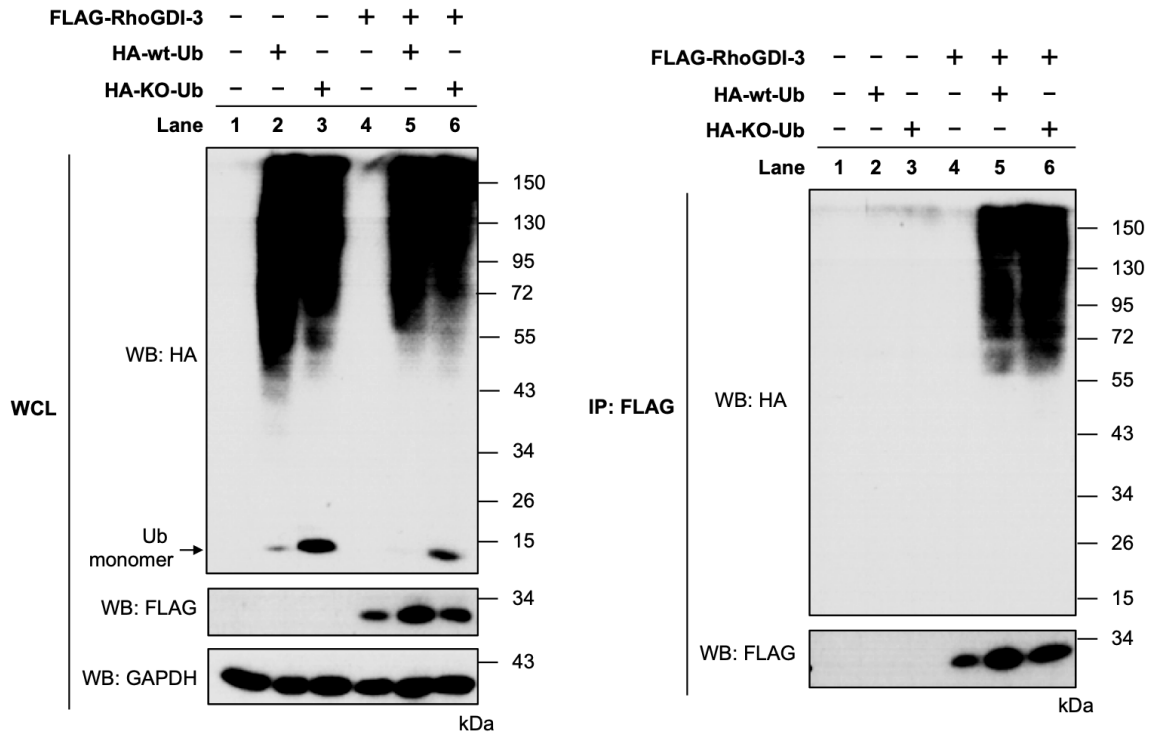

Figure 7.5: The ubiquitination structures on RhoGDI-3. FLAG-RhoGDI-3 was transfected alone or together with HA-wt-Ub or HA-KO-Ub into HEK293T cells. Constructs were allowed to express for ~24 h before serum-starved overnight. Cells were then harvested, lysed and immunoprecipitated using anti-FLAG antibody, ~40 h post-transfection. The ubiquitination level of RhoGDI-3 was assessed by western blotting using anti-HA antibody. The expression of the recombinant protein in the whole cell lysate (WCL) is shown on the left panel, while the co-immunoprecipitated (IP) samples are shown on the right. In whole cell lysate, GAPDH was used to assess equal loading of samples across the wells. The western blot shown is representative of at least three independent experiments. **WCL:** whole cell lysate; **IP:** immunoprecipitation

7.3 Ubiquitination promote RhoGDI-3 degradation

The previous data shows that RhoGDI-3 potentially undergoes poly-Ub via Lys48 linkages or linear ubiquitination. A poly-Ub linkage through Lys48 has been shown to induce proteasomal degradation of target proteins (Glickman and Ciechanover, 2002). Thus, to further characterize any role for ubiquitination in RhoGDI-3 stability, HEK293T cells were transfected with FLAG-RhoGDI-3 alone or in combination with either Myc-wt-Ub or Myc-K48R-Ub before being subjected to a CHX stability assay. Constructs were allowed to express for ~24 h prior to serum starvation overnight. ~40 h post-transfection, cells were treated with 25 μg/mL CHX or DMSO for 2, 5 and 8 h. At various time points, cells were harvested, lysed and analysed by western blotting. The levels of RhoGDI-3 in CHX-treated cells were quantified with ImageJ and normalised to levels in DMSO-treated cells. Relative values for RhoGDI-3 protein levels were then plotted in a graph.

Figure 7.6 shows that RhoGDI-3 undergoes K48-poly-Ub-mediated degradation as RhoGDI-3 protein levels significantly decreased in cells expressing wt Ub but not in the presence of K48R Ub when compared to cells expressing RhoGDI-3 alone.

A

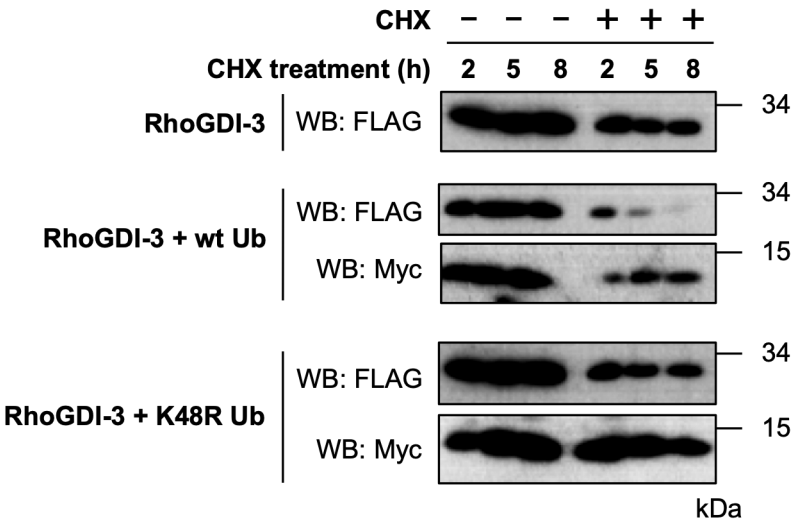

B

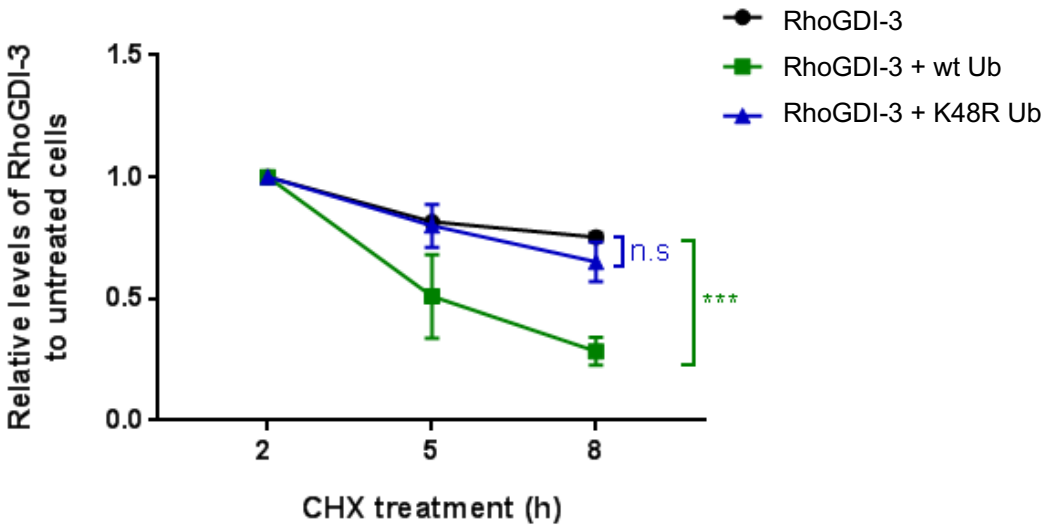

Figure 7.6: The role of ubiquitination in promoting RhoGDI-3 degradation. FLAG-RhoGDI-3 was transfected alone or together with Myc-wt-Ub or Myc-K48R-Ub in HEK293T cells. ~24 h post-transfection, cells were serum-starved overnight. ~40 h post-transfection, cells were treated with DMSO or 25 µg/mL CHX for 2, 5 and 8 h. At each time point, cells were harvested and lysed. **(A)** The level of RhoGDI-3 at each time point was identified by western blotting. **(B)** RhoGDI-3 protein levels in CHX-treated cells were quantified with ImageJ and normalised to levels in DMSO-treated cells. The protein levels, relative to levels at 2 h are plotted. Results are shown as average values ± SEM of three independent experiments, ***p≤ 0.001.

7.4 The effect of ACK on RhoGDI-3 ubiquitination

7.4.1 ACK decreases the levels of RhoGDI-3 ubiquitination

Phosphorylation of the tumour suppressor Wwox by ACK results in rapid dissociation of the ACK-Wwox complex and the subsequent induction of Wwox poly-ubiquitination and degradation (Mahajan *et al.,* 2005). ACK has also been shown to promote EGFR ubiquitination and degradation and this is mediated by its UBA domain (Shen *et al.,* 2006). Although in this case, ACK does not phosphorylate RhoGDI proteins, it was speculated that ACK could play a role in changing the ubiquitination modification of RhoGDI-3 and therefore regulate RhoGDI-3 degradation.

To identify the effect of ACK on RhoGDI-3 ubiquitination, HEK293T cells were transfected with FLAG-RhoGDI-3, Myc-Ub and HA-ACK alone or in combination. Constructs were allowed to express for ~24 h before serum starvation overnight. Cells were harvested and lysed, ~40 h post-transfection. The pre-cleared lysates were then immunoprecipitated with anti-FLAG antibody. The ubiquitination level of RhoGDI-3 was identified by western blotting with an anti-Myc antibody.

Figure 7.7 shows that co-expression of RhoGDI-3 with ACK ablates RhoGDI-3 ubiquitination. Levels of ubiquitination are undetectable, although there are significantly lower levels of RhoGDI-3 as well. This suggests that ACK promotes RhoGDI-3 degradation either by interfering with ubiquitin attachment to RhoGDI-3 or by binding to the Ub-RhoGDI-3 complex and promoting its recognition by the UPS.

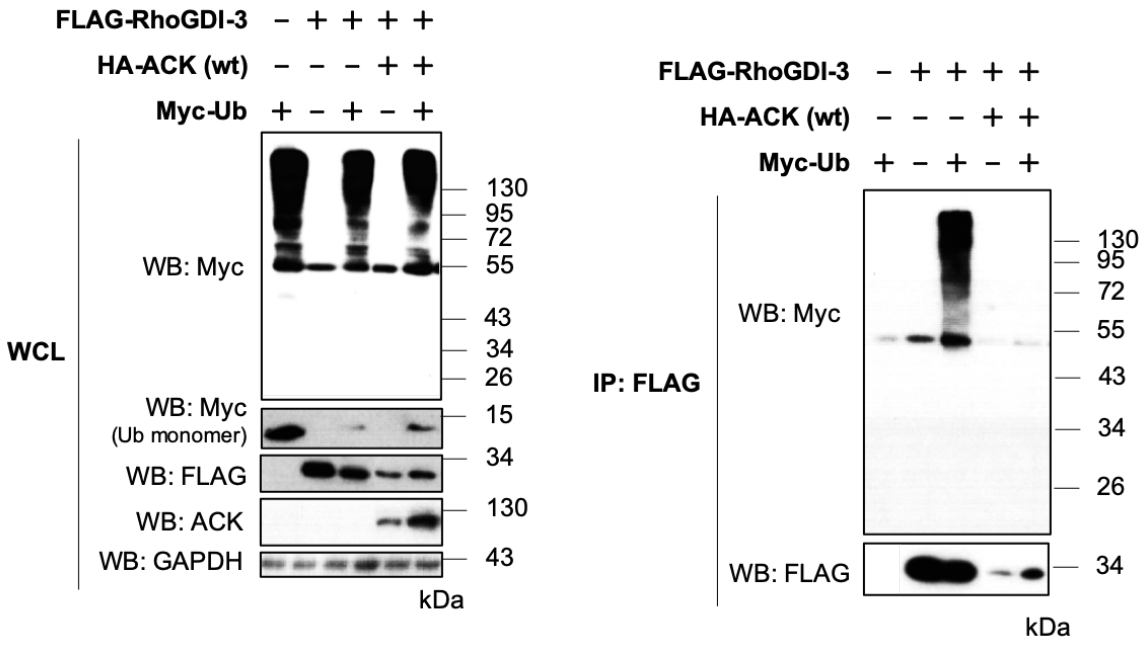

Figure 7.7: The effect of ACK on RhoGDI-3 ubiquitination. HEK293T cells were transfected with FLAG-RhoGDI-3, Myc-Ub and HA-ACK either alone or in combination. Constructs were allowed to express for ~24 h before serum starvation overnight. Cells were then harvested and lysed, ~40 h post-transfection. The pre-cleared supernatant was immunoprecipitated with anti-FLAG antibody. The ubiquitination level of RhoGDI-3 was identified by western blotting with an anti-Myc antibody. The expression of the recombinant protein in the whole cell lysate (WCL) is shown on the left panel, while the co-immunoprecipitated (IP) samples are shown on the right. In whole cell lysate, GAPDH was used to assess equal loading of samples. The western blot shown is representative of at least three independent experiments. **WCL:** whole cell lysate; **IP:** immunoprecipitation.

7.4.2 The effect of ACK on the subcellular distribution of ubiquitinated RhoGDI-3

Previous data described in sections 5.5 and 6.4 show ACK interacts with and mediates RhoGDI-3 degradation predominantly in the nucleus. Since ACK has been shown to decrease the ubiquitination of RhoGDI-3, it is possible that this event occurs in the nucleus.

To test this, HEK293T cells were transfected with FLAG-RhoGDI-3, Myc-Ub and HA-ACK alone or together. Constructs were allowed to express for ~24 h before serum starvation overnight. Cells were then harvested and fractionated into cytoplasmic and nuclear-enriched fractions. Each of the pre-cleared fractions were immunoprecipitated with an anti-FLAG antibody. The presence of ubiquitinated RhoGDI-3 in each fraction was identified by western blotting with anti-Myc and anti-FLAG antibodies.

Figure 7.8 shows the ubiquitinated forms of RhoGDI-3 were found in both the fractions, but predominantly in the cytoplasm. The levels of ubiquitinated proteins in general (Figure 7.8A) significantly decreased in cells co-expressing RhoGDI-3, Ub and ACK compared to previous data and this was probably because the proportion of exogenous Ub relative to endogenous Ub varied between experiments. The levels of ubiquitinated proteins were shown to decrease most significantly in the nucleus (Figure 7.8B) compared to the cytoplasm. Interestingly, the level of ubiquitinated RhoGDI-3 in the immunoprecipitated samples was almost completely absent in both the fractions when co-expressed with ACK, suggesting that ACK may affects the ubiquitination of RhoGDI-3 in both the compartments.

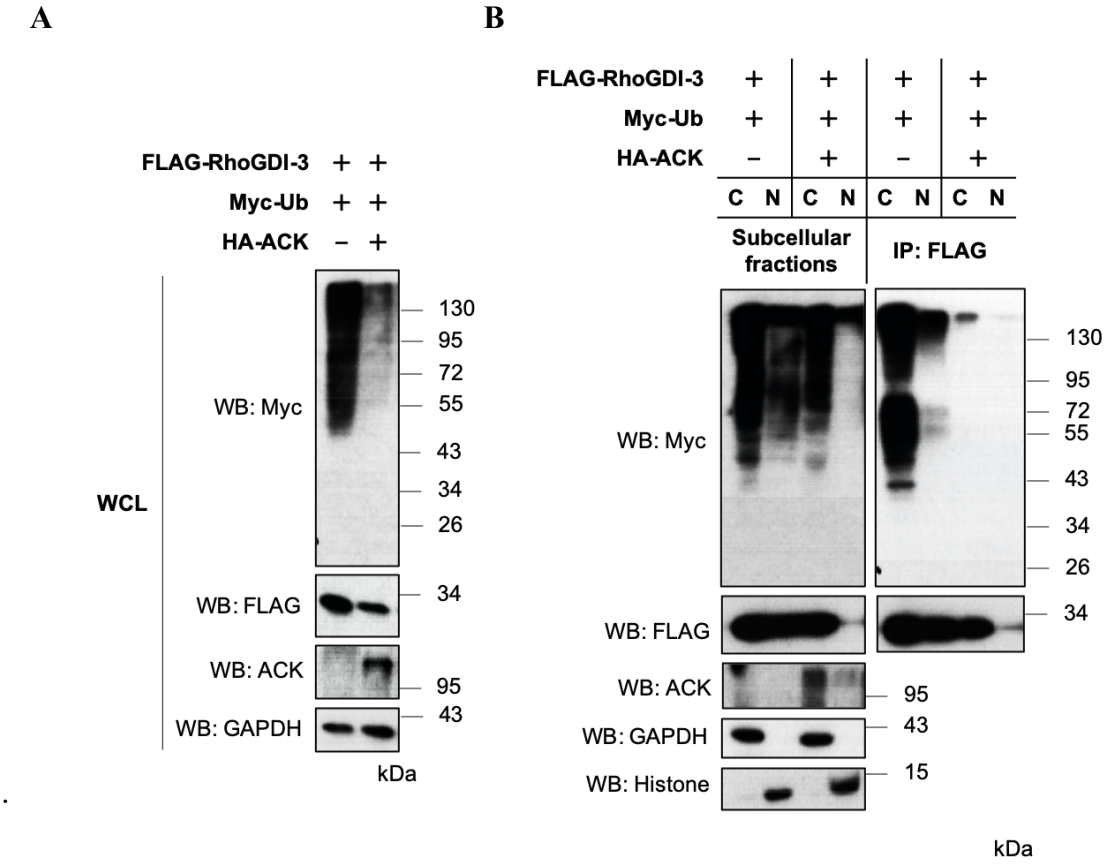

Figure 7.8: The effect of ACK on RhoGDI-3 ubiquitination in the cytoplasmic and nuclear-enriched fractions. FLAG-RhoGDI-3 and Myc-Ub were transfected alone or in combination with HA-ACK into HEK293T. Constructs were allowed to express for ~24 h before serum starvation overnight. ~40 h post-transfection, cells were harvested and fractionated into cytoplasmic and nuclear-enriched fractions. Each of the extracts were immunoprecipitated with anti-FLAG antibody. The presence of ubiquitinated RhoGDI-3 in each of the fraction was identified by western blotting. **(A)** Protein levels in the whole cell lysate (WCL). GAPDH was used to assess the equal loading of samples. **(B)** Protein levels in each fraction are shown on the left panel with GAPDH and Histone H3 were used as cytoplasmic and nuclear markers, respectively. The ubiquitination levels of RhoGDI-3 in immunoprecipitated samples are shown on the right panel. The western blot shown is representative of at least three independent experiments. **WCL:** whole cell lysate; **IP:** immunoprecipitation.

7.4.3 The role of the UBA domain of ACK in regulating RhoGDI-3 ubiquitination

ACK has been shown to decrease the overall levels of RhoGDI-3 protein and its ubiquitination. This could be achieved potentially by ACK binding to Ub-RhoGDI-3 via is UBA domain and enhancing RhoGDI-3 proteasomal degradation. The UBA domain of ACK has been found to facilitate the interaction with ubiquitinated proteins and regulates EGFR ubiquitination and degradation (Shen *et al.,* 2007). Hence, ACK may regulate RhoGDI-3 degradation through modulation of its ubiquitination via the UBA domain. To determine the function of the UBA domain of ACK in regulating RhoGDI-3 degradation, a point mutation, S985N, was introduced into the UBA domain of ACK (HA-S985N-ACK), which has been shown previously to prevent ACK binding to ubiquitin-conjugated proteins (Tin *et al.,* 2010).

Firstly, the efficacy of the ACK S985N mutation was assessed by investigating Ub binding ability compared to wt ACK. Briefly, Myc-Ub was transfected alone or in combination with HA-wt-ACK or HA-S985N-ACK. Constructs were allowed to express for ~40 h before being harvested and lysed. The pre-cleared lysates were then immunoprecipitated with anti-Myc antibody and co-immunoprecipitated ACK detected by western blotting with anti-HA antibody.

Data shown in Figure 7.9 shows that the ACK S985N mutant was unable to interact with ubiquitinated proteins, compared to wt ACK.

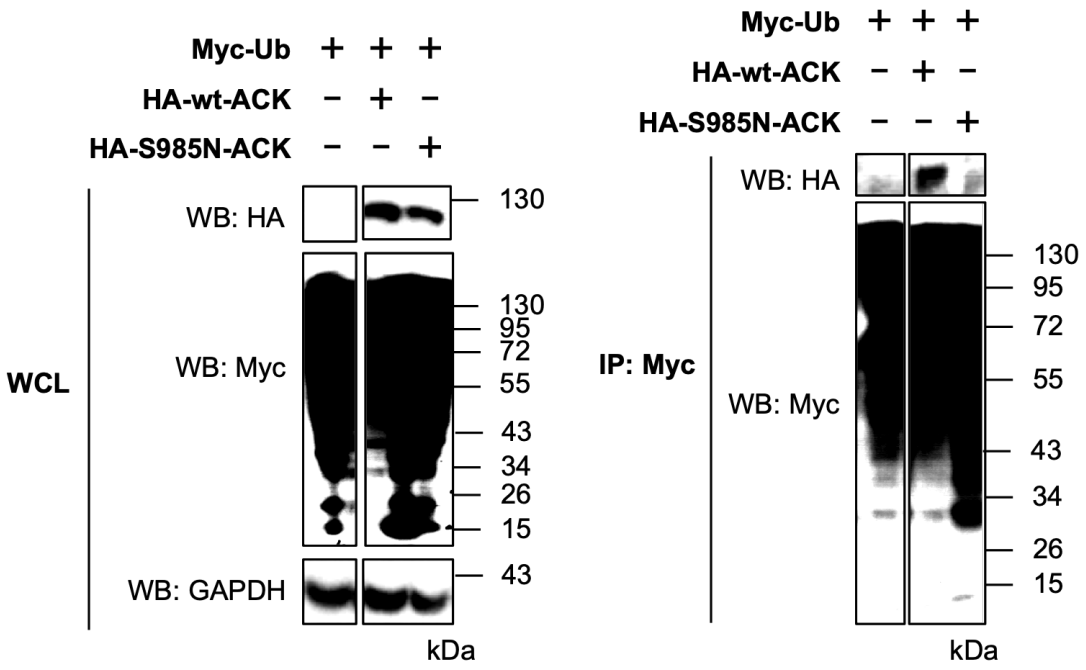

Figure 7.9: Co-immunoprecipitation of Ub with ACK wt and ACK S985N. Myc-Ub was transfected alone or together with HA-wt-ACK or HA-S985N-ACK into HEK293T cells. Constructs were allowed to express for ~40 h before being harvested and lysed. The pre-cleared lysates were then immunoprecipitated with anti-Myc antibody. Bound ACK was detected by western blotting with an anti-HA antibody. The expression of the recombinant protein in the whole cell lysate (WCL) is shown on the left panel, while the co-immunoprecipitated (IP) samples are shown on the right. In whole cell lysate, GAPDH was used to assess equal loading of samples across the wells. **WCL:** whole cell lysate; **IP:** immunoprecipitation.

The ability of ACK S985N to interact with RhoGDI-3 was investigated by co-expressing FLAG-RhoGDI-3 alone or together with the HA-wt-ACK or HA- S985N-ACK in HEK293T cells. Cells were harvested and lysed ~40 h post-transfection. FLAG-RhoGDI-3 was then immunoprecipitated with an anti-FLAG antibody and bound ACK was identified by western blotting with an anti-HA antibody.

Data shown in Figure 7.10 demonstrates that ACK S985N was still able to interact with RhoGDI-3. However, the levels of RhoGDI-3 also increased when co-transfected with ACK S985N

compared to wt ACK, suggesting that the UBA domain of ACK might be involved in regulating RhoGDI-3 stability.

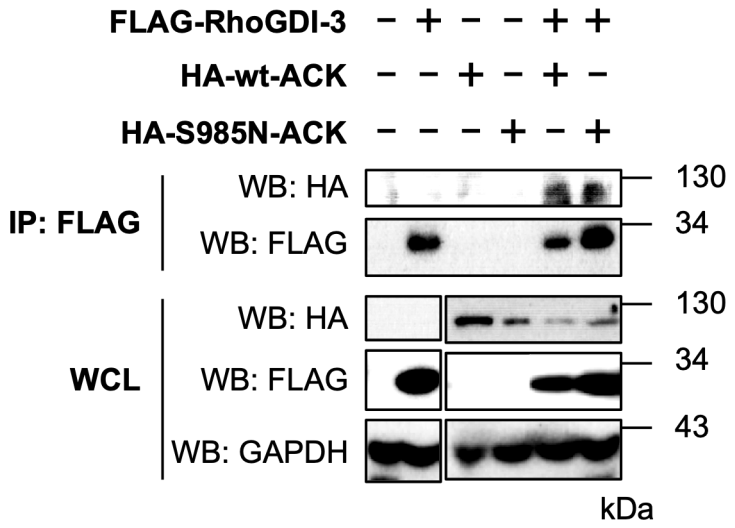

Figure 7.10: Co-immunoprecipitation ACK S985N with RhoGDI-3. FLAG-RhoGDI-3, HA-wt-ACK or HA-S985N-ACK were transfected alone or together into HEK293T cells. Constructs were allowed to express for ~40 h before being harvested and lysed. Anti-FLAG antibody was then added to the pre-cleared supernatant and FLAG-RhoGDI-3 was immunoprecipitated with a set of pre-washed Protein G Dynabeads. Bound ACK S985N was detected by western blotting with an anti-HA antibody. The expression of the recombinant protein in the whole cell lysate (WCL) is shown in the bottom 3 panels, while the co-immunoprecipitated (IP) samples are shown in the top 2 panels. In the whole cell lysate, GAPDH was used to assess the equal loading of samples. **WCL:** whole cell lysate; **IP:** immunoprecipitation.

Next, the effect of the S985N mutation on RhoGDI-3 ubiquitination was investigated by co-expressing FLAG-RhoGDI-3, Myc-Ub and HA-S985N-ACK in HEK293T cells. ~40 h post-transfection, FLAG-RhoGDI-3 was immunoprecipitated with anti-FLAG antibody and the levels of ubiquitinated RhoGDI-3 was identified by western blotting with an anti-Myc antibody.

Co-expression with ACK S985N did not rescue RhoGDI-3 ubiquitination, on the contrary Ub-RhoGDI-3 levels were very similar to co-expression with wt ACK (Figure 7.11), suggesting that although ACK S895N can sustain RhoGDI-3 protein levels, this is not through regulating levels of RhoGDI-3 ubiquitination.

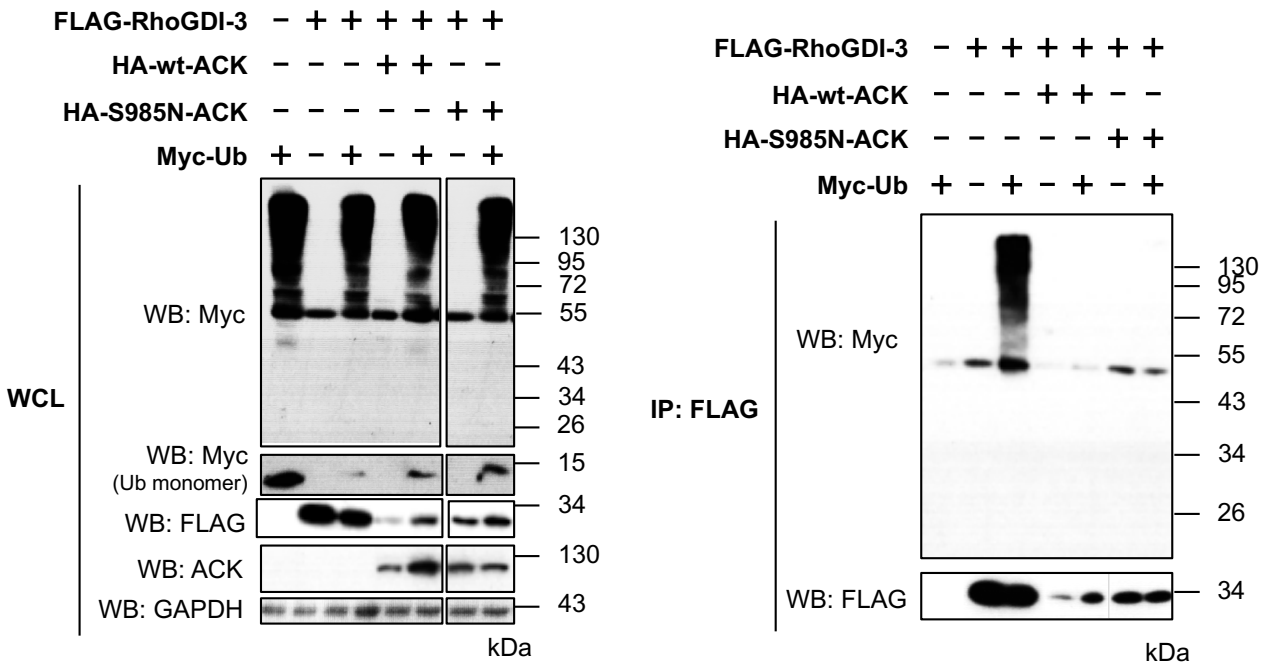

Figure 7.11: The effect of ACK S985N on RhoGDI-3 ubiquitination. HEK293T cells were transfected with FLAG-RhoGDI-3, Myc-Ub, HA-wt-ACK and HA-S985N-ACK. Constructs were allowed to express for ~24 h before serum starvation overnight. Cells were harvested and lysed, ~40 h post-transfection. The pre-cleared supernatant was immunoprecipitated with anti-FLAG antibody. The ubiquitination level of RhoGDI-3 was identified by western blotting with an anti-Myc antibody. The expression of the recombinant protein in the whole cell lysate (WCL) is shown on the left panel, while the co-immunoprecipitated (IP) samples are shown on the right. In whole cell lysate, GAPDH was used to assess equal loading of samples. The western blot shown is representative of at least three independent experiments. **WCL:** whole cell lysate; **IP:** immunoprecipitation.

7.5 Summary

RhoGDI-3 has been shown to undergo ubiquitination but the type of Ub conjugation is still undefined due to inconsistency of the data obtained. Analysis in cells utilising several Ub mutants suggest that RhoGDI-3 undergoes Lys48 poly-Ub, linear ubiquitination or linear-Lys48 mixed poly-Ub. A poly-Ub linkage through Lys48 has been shown to promote RhoGDI-3 degradation.

Co-expression with ACK completely abolished RhoGDI-3 ubiquitination. This was very clear even though there were lower levels of RhoGDI-3. Co-expression with ACK S985N, a UBA domain mutant, did not rescue RhoGDI-3 ubiquitination but the UBA domain of ACK is still potentially involved in regulating RhoGDI-3 stability.

Chapter 8

The effect of RhoGDIs on their target

8.1 Identification of RhoGDIs target

There is a total of ~145 RhoGEFS and RhoGAPs in mammalian cells but only three RhoGDIs and their role is still not fully understood (Rocks *et al.,* 2018). There is growing evidence showing the functions of the RhoGDIs not only as negative regulators of Rho GTPases but also as chaperones to target the Rho GTPases to specific subcellular compartments such as the Golgi (Brunet *et al.,* 2002). The RhoGDI-Rho protein complex also helps to stabilize the Rho proteins and prevents them from being targeted for proteasomal degradation (Ho *et al.,* 2008). RhoGDI-1 depletion has been found to increase the accumulation of newly synthesized Rho-family proteins in the endoplasmic reticulum, where post-translational modification occurs, again indicating a role for RhoGDI-1 as a chaperone (Boulter *et al.,* 2010). Besides functioning to stabilize the inactive GDP-bound form of the small GTPases, RhoGDIs have also been shown to be necessary for maintaining the GTP-bound state of certain small GTPases. For instance, RhoGDI-1 needs to bind to active Cdc42 to allow for Cdc42-induced cell proliferation and transformation (Lin *et al.,* 2003). The

RhoGDI-1-Rac1 interaction is also crucial for stimulating NADPH oxidase system in neutrophils (Abo *et al.,* 1991). In contrast, the RhoGDI-1-Rac2 complex was found to abrogate the activation of NADPH oxidase (Abo *et al.,* 1994), suggesting that RhoGDI-1 target specific Rho-family proteins for specific functions.

Studies to date with RhoGDIs usually focus on the interaction between the 'typical' or 'classical' small GTPases such as RhoA, Rac1 and Cdc42 with RhoGDI-1 or RhoGDI-2. Less is known about the third member of the family, RhoGDI-3, and its interacting partners, although RhoGDI-3 has been shown to target RhoB and RhoG to endomembranes (Zalcman *et al.,* 1996). To allow a more thorough understanding of RhoGDI function, a systematic study has been undertaken here to determine all possible Rho-family GTPases that interact with the RhoGDIs. These data should help to elucidate any functional differences between the three RhoGDIs.

A panel of expression constructs encoding all V5-tagged Rho-family GTPases (Table 8.1) was already available in the lab. Through co-immunoprecipitation, the interaction between each of the RhoGDIs and Rho-family GTPases were determined.

Co-immunoprecipitations were performed to verify known interactions and also determine any new targets of the RhoGDIs. Analysis of most of the interactions between RhoGDI-1 or -2 and the Rho-family GTPases were performed using His-tagged RhoGDI-1 or -2 and cobalt-coated magnetic beads while RhoGDI-3 interactions were analysed with FLAG-tagged RhoGDI-3 and Protein G-coated magnetic beads. However, FLAG-tagged RhoGDI-1 and -2 were used to identify any interactions with RhoD, RhoF, Wrch2, Miro1, Miro2, RhoH and Rnd2 due to non-specific interaction between these Rho-family GTPases and the cobalt-coated magnetic beads.

Briefly, His-tagged or FLAG-tagged RhoGDIs were co-expressed with V5-tagged versions of all Rho-family GTPases in HEK293T cells. Constructs were allowed to express for ~40 h before being harvested and lysed with mammalian lysis buffer (Table 2.16). The lysates were then incubated with cobalt-coated magnetic beads or anti-FLAG-coated Protein G Dynabeads for ~1 h. The precipitated proteins were eluted from the beads with sample buffer (Table 2.16) and analysed by western blotting. RalB was included as a negative control.

Table 8.1: List of Rho-family small GTPases used in the screening

Type	Group	Rho GTPase	Accession no. (UniProt)
Classical	Rho	RhoA	P61586
		RhoB	P62745
		RhoC	P08134
	Rac	Rac1	P63000
		Rac2	P15153
		Rac3	P60763
		RhoG	P84095
	Cdc42	Cdc42	P60953
		TC10/RhoQ	P17081
		TCL/RhoJ	Q9H4E5
Non-classical	RhoD		O00212
	RhoF/Rif		Q9HBH0
	Cdc42	Wrch1/RhoU	Q7L0Q8
		Wrch2/RhoV/Chp	Q96L33
	Rnd	Rnd1/RhoS	Q92730
		Rnd2/RhoN	P52198
		Rnd3/RhoE	P61587
	Miro	Miro1/RhoT1	Q8IXI2
		Miro2/RhoT2	Q8IXI1
	RhoBTB	RhoBTB1	O94844
		RhoBTB2	Q9BYZ6
		RhoBTB3	O94955
	RhoH/TTF		Q15669

8.1.1 Expression trials of Rho-family GTPases

Expression and co-expression trials were carried out to determine the appropriate conditions to co-express all combination of proteins. This was achieved for all combinations (data not shown) except for the RhoBTB subfamily (Figure 8.1A) and Rnd3 (Figure 8.2) where expression could not be achieved in the presence of any of the RhoGDIs. Additionally, RhoGDI-2 could not be co-expressed with Miro2 (Figure 8.1B), while Rnd1 are not expressed when co-transfected with RhoGDI-3 (Figure 8.2). RhoBTB3 expression was not achieved even alone (Figure 8.1A)

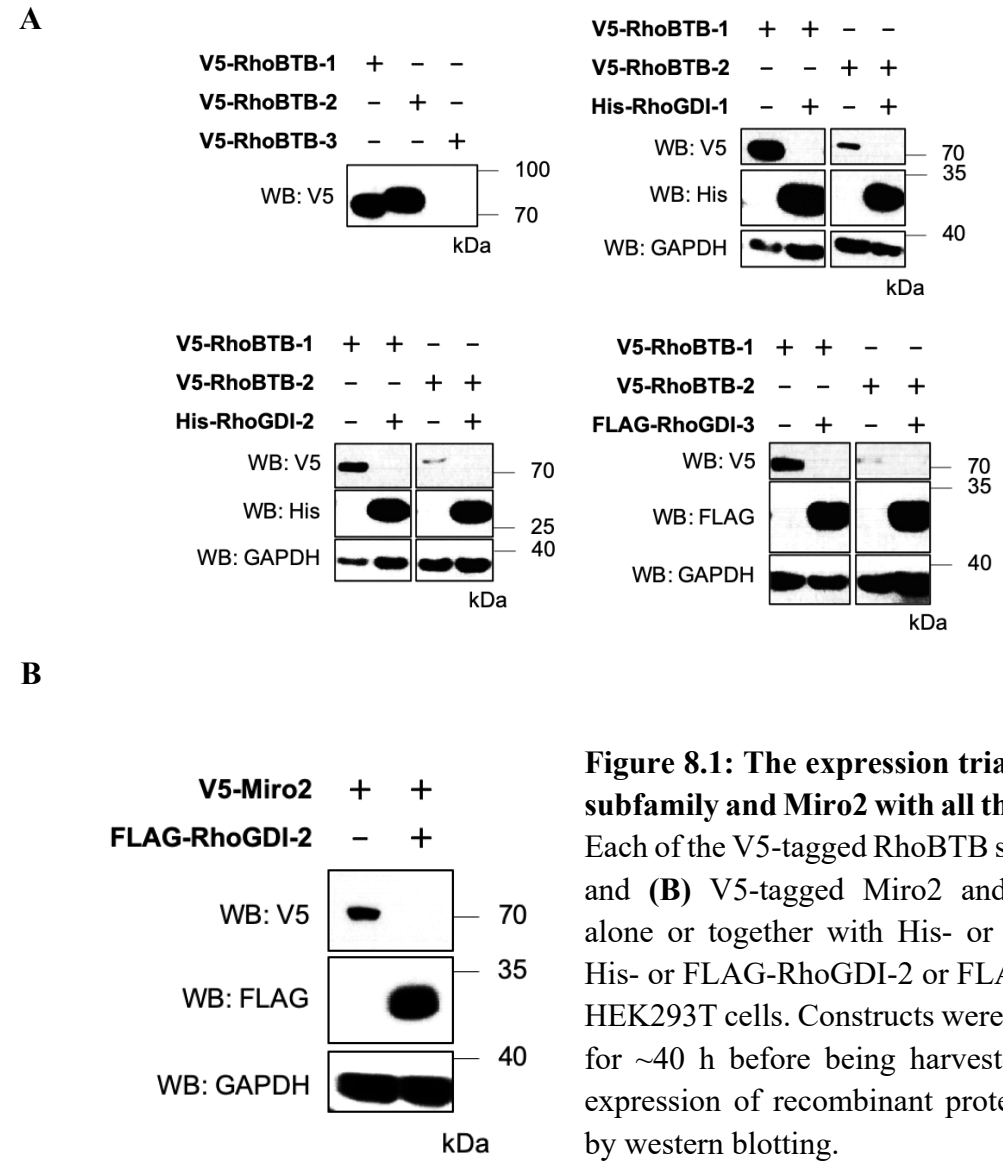

Figure 8.1: The expression trials of the RhoBTB subfamily and Miro2 with all three RhoGDIs. (A) Each of the V5-tagged RhoBTB subfamily members and **(B)** V5-tagged Miro2 and were transfected alone or together with His- or FLAG-RhoGDI-1, His- or FLAG-RhoGDI-2 or FLAG-RhoGDI-3 into HEK293T cells. Constructs were allowed to express for ~40 h before being harvested and lysed. The expression of recombinant proteins was identified by western blotting.

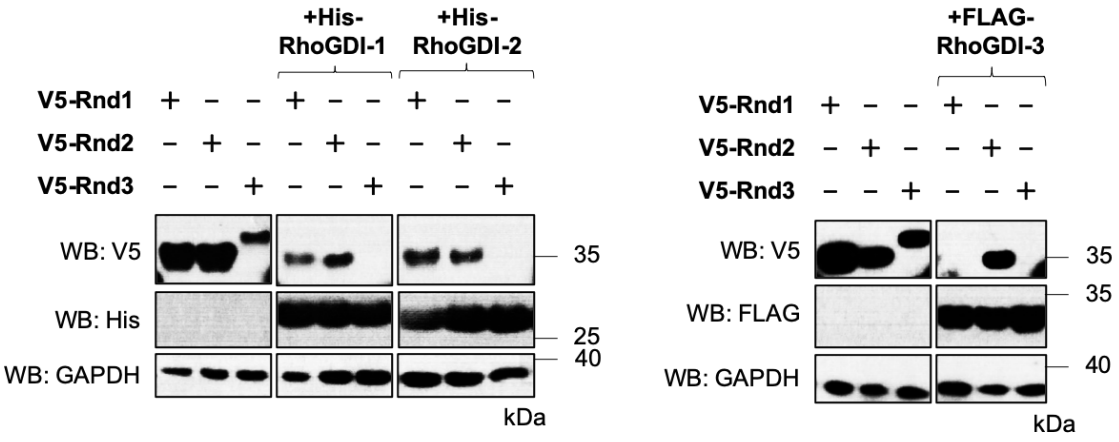

Figure 8.2: The expression trials of the Rnd subfamily with all three RhoGDIs. Each of the V5-tagged Rnd subfamily members were transfected alone or together with His-RhoGDI-1, His-RhoGDI-2 or FLAG-RhoGDI-3 into HEK293T cells. Constructs were allowed to express for ~40 h before being harvested and lysed. The expression of recombinant proteins was identified by western blotting.

8.1.2 RhoGDI-1 targets

8.1.2.1 RhoGDI-1 binding to classical Rho-family members

RhoGDI-1 is ubiquitously expressed and has been shown previously to form complexes with RhoA, RhoC, Rac1, Rac2, Cdc42 and RhoG (Olofsson, 1999; Elfenbein *et al.,* 2009). All of the Rho-family GTPases identified as RhoGDI-1 targets to date are known regulators of actin cytoskeletal reorganization and play crucial roles in controlling cell proliferation and migration (Gómez Del Pulgar *et al.,* 2008).

Co-immunoprecipitations were performed to verify the known interactions and also identify any new targets for RhoGDI-1. Briefly, His-RhoGDI-1 were co-expressed with V5-tagged versions of all 10 classical members of the Rho-family GTPases. Constructs were allowed to express for ~40 h before being harvested and incubated with cobalt-coated magnetic beads. The precipitated proteins were analysed by western blotting.

As shown in Figure 8.3, RhoGDI-1 can be seen to interact with every member of the Rac and Rho subfamilies except for RhoB. These data confirmed the interaction profile for RhoGDI-1 that was already known and validated Rac3 as a RhoGDI-1 partner for the first time. Despite binding to Cdc42, RhoGDI-1 failed to interact with the other classical members of the Cdc42 subfamily; TC10 and TCL (Figures 8.3C and D).

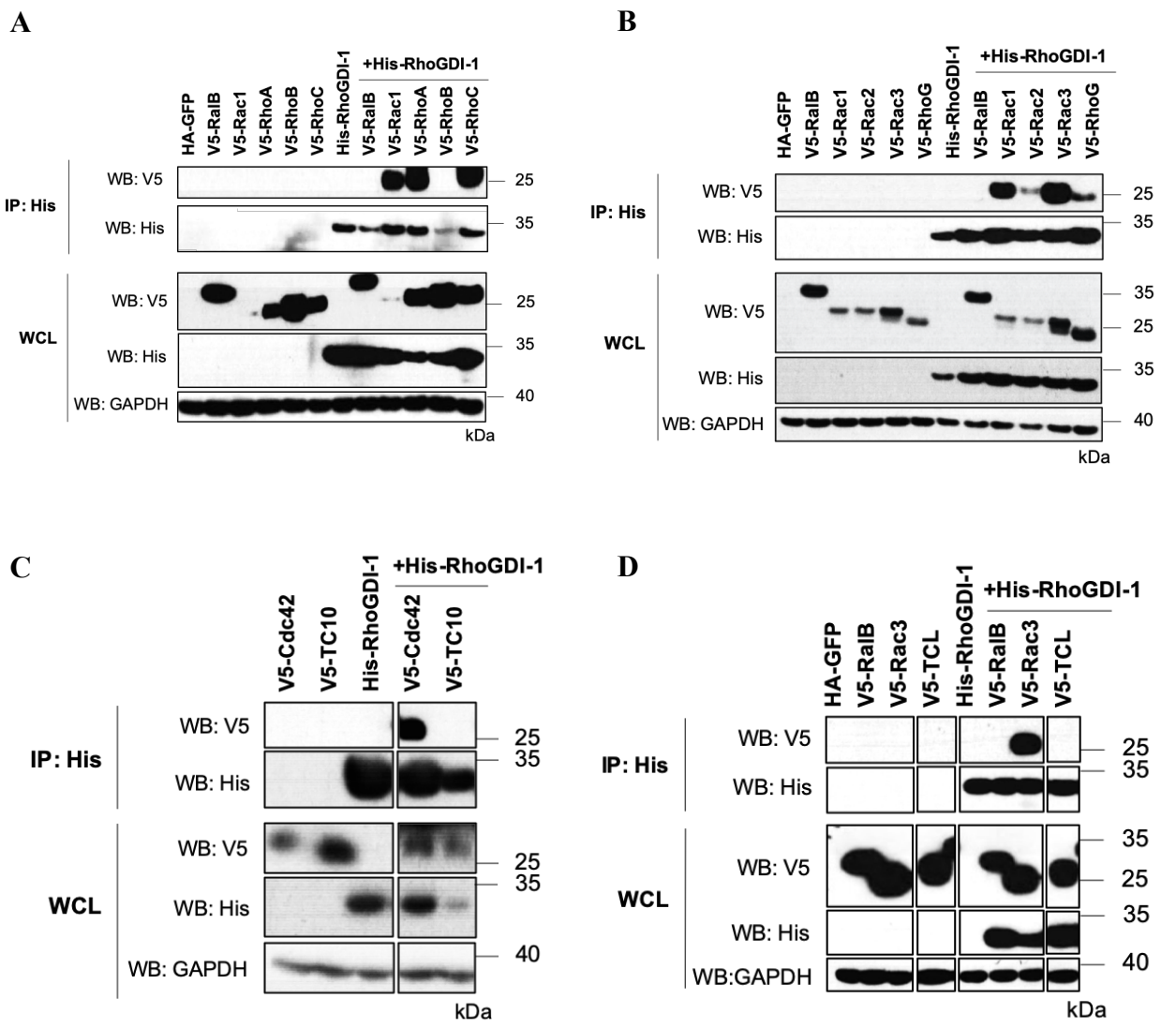

Figure 8.3: The interaction of RhoGDI-1 with the typical Rho-family GTPases. HEK293T cells were transfected with His-RhoGDI-1 alone or together with V5-tagged **(A)** RhoA, RhoB, RhoC, **(B)** Rac1, Rac2, Rac3, RhoG, **(C)** Cdc42, TC10 and **(D)** TCL. Constructs were allowed to express for ~40 h. Cells were then harvested, lysed and precipitated with cobalt-coated magnetic beads. The precipitated proteins were eluted from the beads and identified by western blotting. RalB and Rac3 (only for TCL interaction) were used as negative and positive controls, respectively. The expression of the recombinant protein in the whole cell lysate (WCL) is shown in the bottom 3 panels, while the co-immunoprecipitated (IP) samples are shown in the top two panels. GAPDH was used to assess the equal loading of samples across the wells. Results are representative of at least two independent experiments. **WCL:** whole cell lysate; **IP:** immunoprecipitation. **(A)** the Rho subfamily, **(B)** the Rac subfamily, **(C and D)** the Cdc42 subfamily (Cdc42, TC10 and TCL).

8.1.2.2 RhoGDI-1 binding to non-classical Rho-family members

Very few studies have been undertaken to identify any interactions between RhoGDI-1 and the atypical Rho-family GTPases. Here, co-immunoprecipitation was performed by transfecting HEK293T cells with the 9 non-classical Rho-family GTPases for which co-expression was achieved alone or together with His- or FLAG-RhoGDI-1. The lysates were precipitated with cobalt-coated magnetic beads or anti-FLAG antibody coupled to Protein G Dynabeads. Bound Rho-family GTPases were determined by western blotting with anti-V5 antibody.

The remaining members of the Cdc42 subfamily, Wrch1 (Figure 8.4A) and Wrch2 (Figure 8.4B) failed to interact with RhoGDI-1. This result shows that Cdc42 is the sole target for RhoGDI-1 within Cdc42 subfamily.

RhoGDI-1 also did not bind to RhoD (Figure 8.4C). RhoGDI-1 potentially bound to RhoF although a low level of precipitated RhoF was seen in the absence of RhoGDI-1 (Figure 8.4D).

There was no interaction detected between RhoGDI-1 and RhoH (Figure 8.4G), despite being observed in a previous study (Li *et al.,* 2002). No interactions were identified for Rnd1 and 2 (Figures 8.4E and G) and the Miro subfamilies (Figures 8.4F and G), suggesting that other RhoGDIs or alternative mechanisms are involved in mediating the activity of these non-classical Rho-family GTPases.

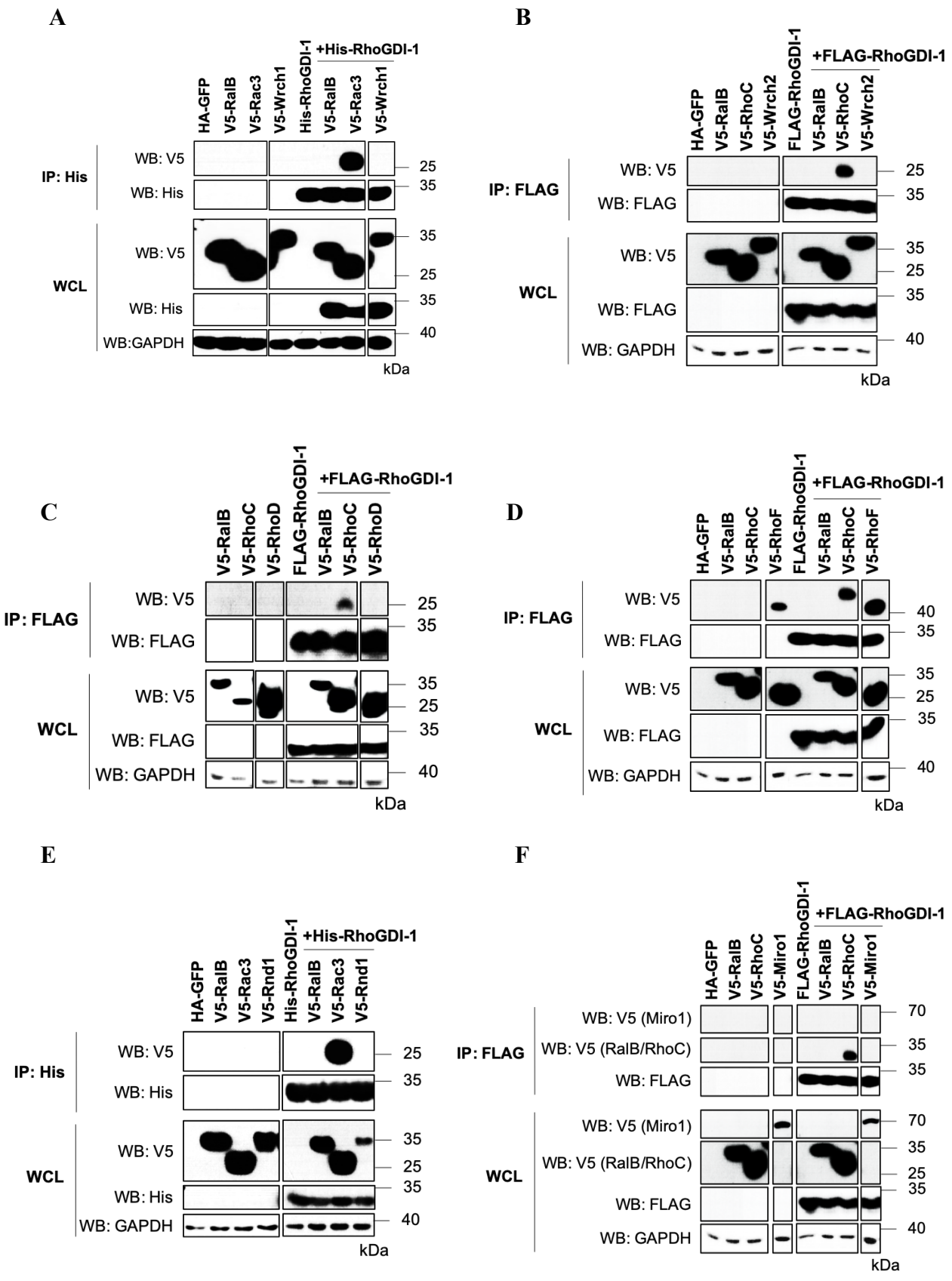
A
HA-GFP
V5-RalB
V5-Rac3
V5-Wrch1
His-RhoGDI-1
+His-RhoGDI-1
V5-RalB
V5-Rac3
V5-Wrch1
IP: His
WB: V5
WB: His
WCL
WB: V5
WB: His
WB:GAPDH
25
35
35
25
35
40
kDa
B
HA-GFP
V5-RalB
V5-RhoC
V5-Wrch2
FLAG-RhoGDI-1
+FLAG-RhoGDI-1
V5-RalB
V5-RhoC
V5-Wrch2
IP: FLAG
WB: V5
WB: FLAG
WCL
WB: V5
WB: FLAG
WB: GAPDH
25
35
35
25
35
40
kDa
C
V5-RalB
V5-RhoC
V5-RhoD
FLAG-RhoGDI-1
+FLAG-RhoGDI-1
V5-RalB
V5-RhoC
V5-RhoD
IP: FLAG
WB: V5
WB: FLAG
WCL
WB: V5
WB: FLAG
WB: GAPDH
25
35
35
25
35
40
kDa
D
HA-GFP
V5-RalB
V5-RhoC
V5-RhoF
FLAG-RhoGDI-1
+FLAG-RhoGDI-1
V5-RalB
V5-RhoC
V5-RhoF
IP: FLAG
WB: V5
WB: FLAG
WCL
WB: V5
WB: FLAG
WB: GAPDH
40
35
35
25
35
40
kDa
E
HA-GFP
V5-RalB
V5-Rac3
V5-Rnd1
His-RhoGDI-1
+His-RhoGDI-1
V5-RalB
V5-Rac3
V5-Rnd1
IP: His
WB: V5
WB: His
WCL
WB: V5
WB: His
WB: GAPDH
25
35
35
25
35
40
kDa
F
HA-GFP
V5-RalB
V5-RhoC
V5-Miro1
FLAG-RhoGDI-1
+FLAG-RhoGDI-1
V5-RalB
V5-RhoC
V5-Miro1
IP: FLAG
WB: V5 (Miro1)
WB: V5 (RalB/RhoC)
WB: FLAG
WCL
WB: V5 (Miro1)
WB: V5 (RalB/RhoC)
WB: FLAG
WB: GAPDH
70
35
35
70
35
25
35
40
kDa

G

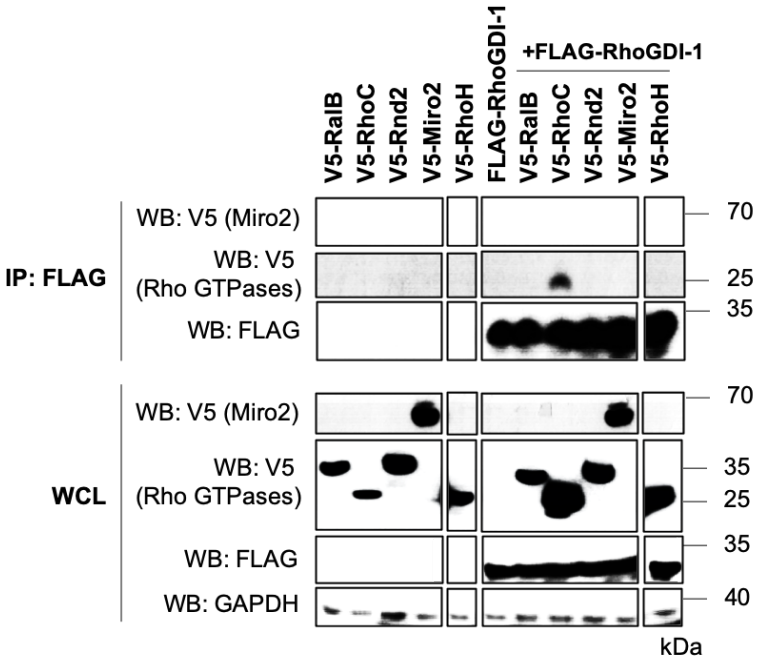

Figure 8.4: The interaction of RhoGDI-1 with the atypical Rho-family GTPases. HEK293T cells were transfected with His- or FLAG-RhoGDI-1 alone or together with V5-tagged **(A)** Wrch1, **(B)** Wrch2, **(C)** RhoD, **(D)** RhoF, **(E)** Rnd1, **(F)** Miro1, **(G)** Rnd2, Miro2 and RhoH. Constructs were allowed to express for ~40 h before being harvested, lysed and precipitated with cobalt-coated beads or anti-FLAG antibody coupled to Protein G Dynabeads. The precipitated proteins were identified by western blotting. RalB and Rac3 or RhoC were used as negative and positive controls, respectively. The expression of the recombinant protein in the whole cell lysate (WCL) is shown in the bottom 3 or 4 panels, while the co-immunoprecipitated (IP) samples are shown in the top two or 3 panels. GAPDH was used to assess the equal loading of samples across the wells. Results are representative of at least two independent experiments. **WCL:** whole cell lysate; **IP:** immunoprecipitation.

8.1.3 RhoGDI-2 targets

8.1.3.1 RhoGDI-2 binding to classical Rho-family GTPases

The second member of the RhoGDI family is RhoGDI-2 (also known as D4/Ly-GDI). RhoGDI-2 is selectively expressed in hematopoietic cells such as B and T lymphocytes (Scherle *et al.,* 1993). Although the full target profile for RhoGDI-2 still remains unclear, it has been shown to bind to Rac2, RhoA, RhoC and, to a lesser extent, Rac1, Rac3, Cdc42 and RhoG (Scheffzek *et al.,* 2000; Moissoglu *et al.,* 2009; Griner *et al.,* 2015).

All potential interactions for RhoGDI-2 were analysed by co-immunoprecipitation and the precipitated proteins were analysed by western blotting. RalB was included as negative control.

Figure 8.5 shows Rac1, Rac3 and RhoC are targets of RhoGDI-2. No binding was seen with RhoB, Rac2, TC10 and TCL. No binding was also observed with RhoA, Cdc42 or RhoG in this system, despite being reported in previous studies (Scherle *et al.,* 1993; Platko *et al.,* 1995; Adra *et al.,* 1993). This maybe because RhoGDI-2 is reported to have a lower affinity than RhoGDI-1 for Rho-family GTPases (Platko *et al.,* 1995), potentially making interactions are more difficult to identify.

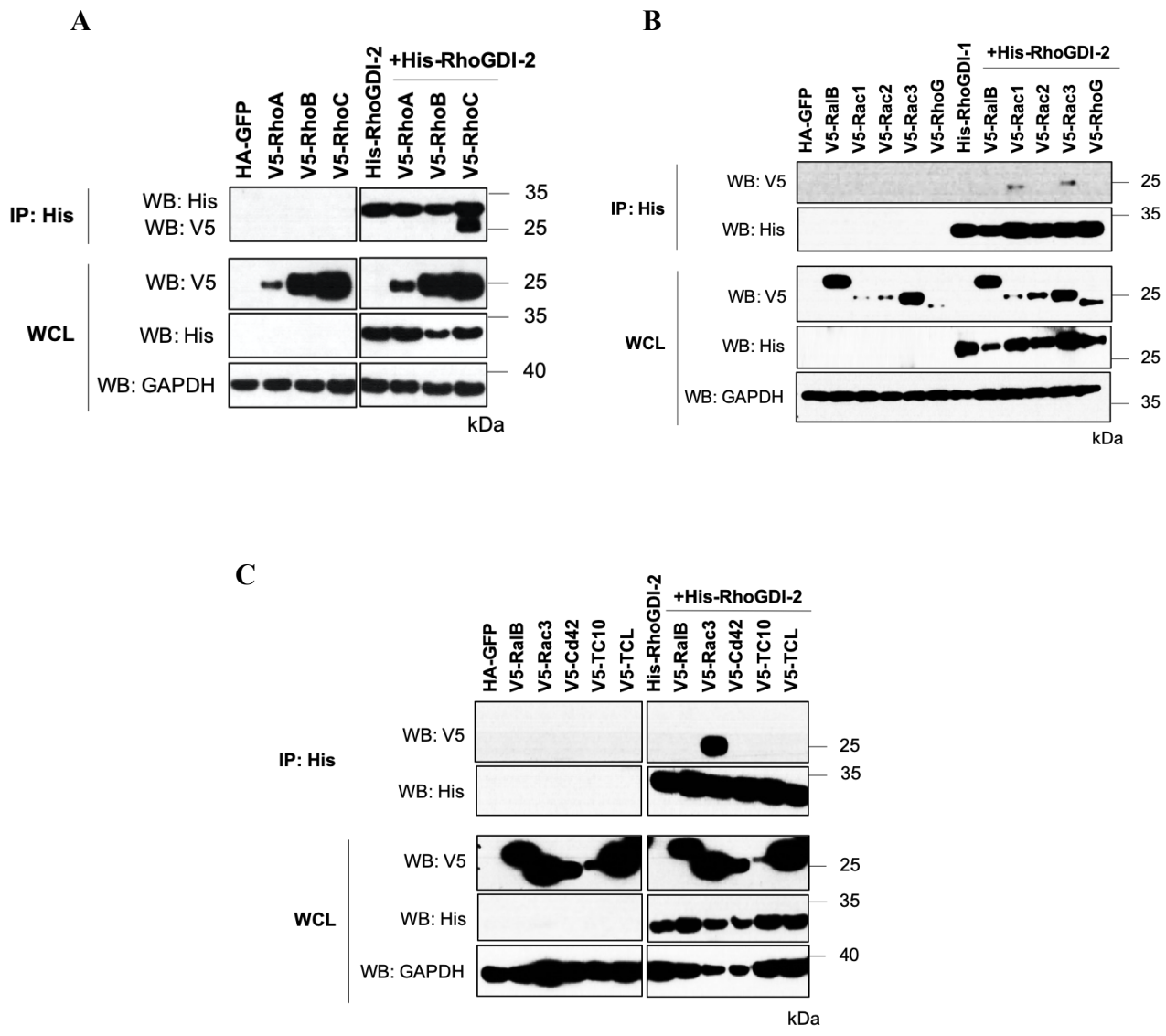

Figure 8.5: The interaction of RhoGDI-2 with the typical Rho-family GTPases. His-RhoGDI-2 was transfected alone into HEK293T cells or together with V5-tagged **(A)** RhoA, RhoB, RhoC, **(B)** Rac1, Rac2, Rac3, RhoG, **(C)** Cdc42, TC10 and TCL. Constructs were allowed to express for ~40 h before being harvested and lysed. The pre-cleared cell lysates were then precipitated with cobalt-coated magnetic beads. The precipitated Rho proteins were then eluted from the beads and identified by western blotting. RalB and Rac3 were used as negative and positive controls, respectively. The expression of the recombinant protein in the whole cell lysate (WCL) is shown in the bottom 3 panels, while the co-immunoprecipitated (IP) samples are shown in the top two panels. GAPDH was used to assess the equal loading of samples across the wells. Results are representative of at least two independent experiments. **WCL:** whole cell lysate; **IP:** immunoprecipitation.

8.1.3.2 RhoGDI-2 binding to non-classical Rho-family GTPases

Similarly to RhoGDI-1, fewer studies have been reported which analyse the interaction between RhoGDI-2 and the atypical Rho-family GTPases.

Thus, all possible interactions were analysed by co-immunoprecipitation with either cobalt-coated magnetic beads or anti-FLAG antibody coupled to Protein G Dynabeads. Any co-precipitated Rho-family GTPases were identified by western blotting.

Figure 8.6 shows that RhoGDI-2 failed to interact with any of the atypical Rho-family GTPases, even with RhoH, despite this interaction being observed in a previous study (Li *et al.,* 2002).

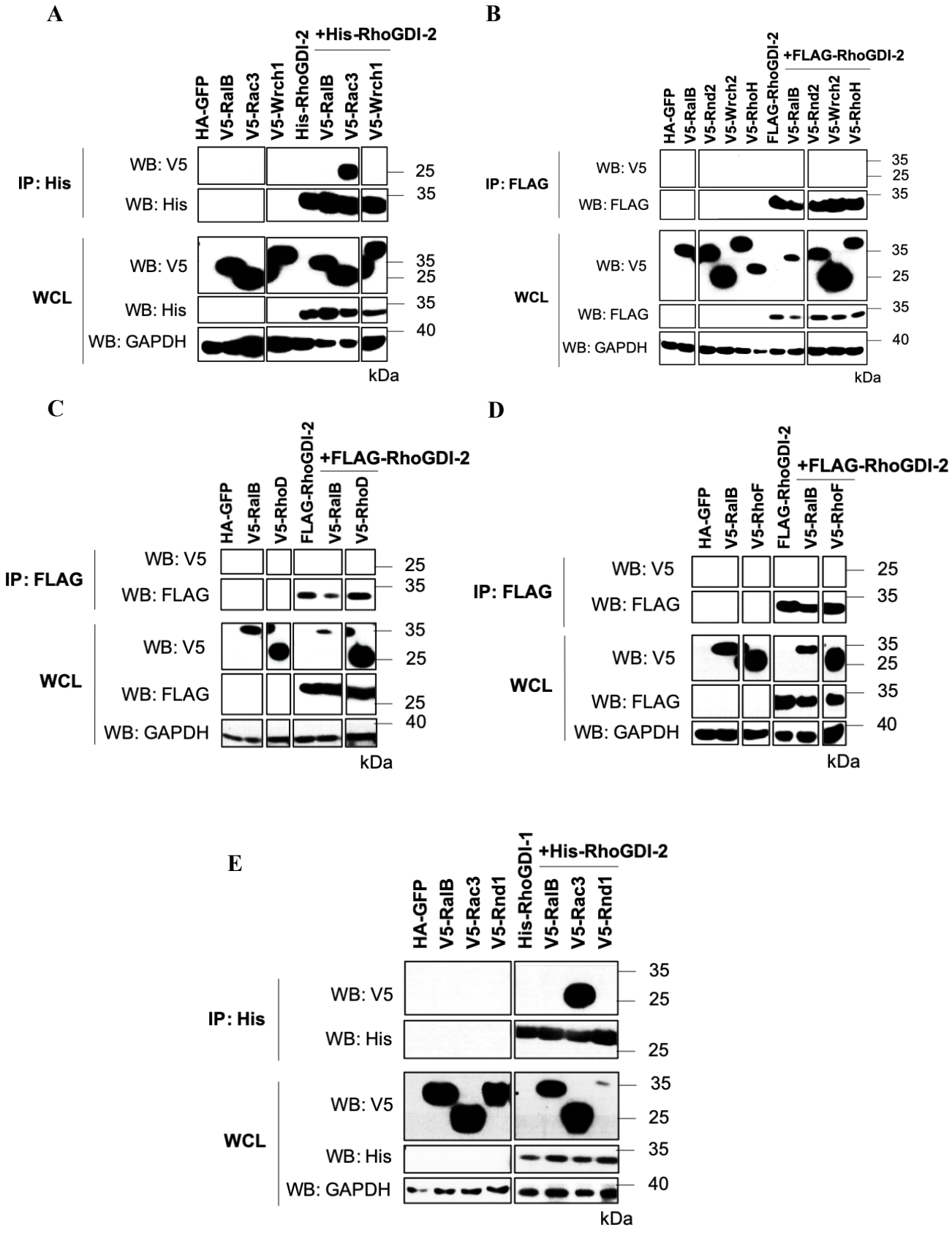
A
HA-GFP
V5-RalB
V5-Rac3
V5-Wrch1
His-RhoGDI-2
+His-RhoGDI-2
V5-RalB
V5-Rac3
V5-Wrch1
IP: His
WB: V5
WB: His
WCL
WB: V5
WB: His
WB: GAPDH
25
35
35
25
35
40
kDa
B
HA-GFP
V5-RalB
V5-Rnd2
V5-Wrch2
V5-RhoH
FLAG-RhoGDI-2
+FLAG-RhoGDI-2
V5-RalB
V5-Rnd2
V5-Wrch2
V5-RhoH
IP: FLAG
WB: V5
WB: FLAG
WCL
WB: V5
WB: FLAG
WB: GAPDH
35
25
35
35
25
35
40
kDa
C
HA-GFP
V5-RalB
V5-RhoD
FLAG-RhoGDI-2
+FLAG-RhoGDI-2
V5-RalB
V5-RhoD
IP: FLAG
WB: V5
WB: FLAG
WCL
WB: V5
WB: FLAG
WB: GAPDH
25
35
35
25
25
40
kDa
D
HA-GFP
V5-RalB
V5-RhoF
FLAG-RhoGDI-2
+FLAG-RhoGDI-2
V5-RalB
V5-RhoF
IP: FLAG
WB: V5
WB: FLAG
WCL
WB: V5
WB: FLAG
WB: GAPDH
25
35
35
25
35
40
kDa
E
HA-GFP
V5-RalB
V5-Rac3
V5-Rnd1
His-RhoGDI-1
+His-RhoGDI-2
V5-RalB
V5-Rac3
V5-Rnd1
IP: His
WB: V5
WB: His
WCL
WB: V5
WB: His
WB: GAPDH
35
25
25
35
25
35
40
kDa

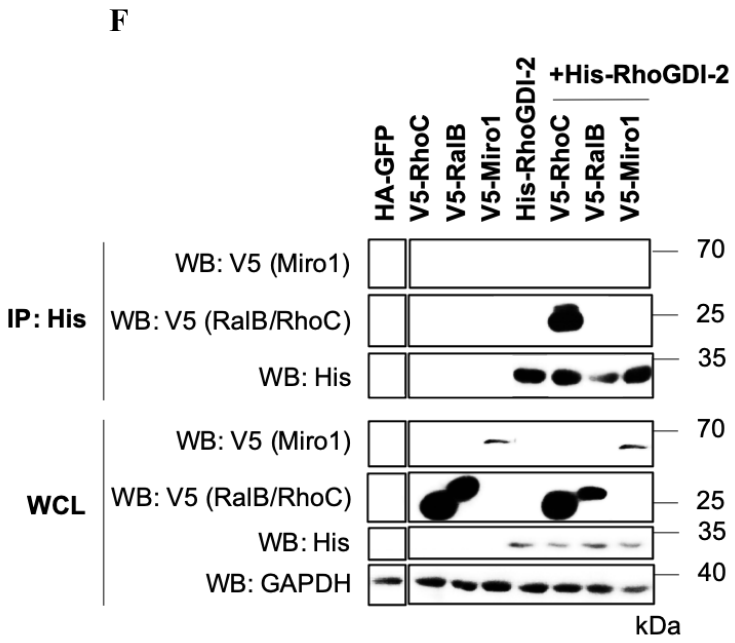

Figure 8.6: The interaction of RhoGDI-2 with the atypical Rho-family GTPases. HEK293T cells were transfected with His- or FLAG-RhoGDI-2 alone or in combination with V5- tagged **(A)** Wrch1 **(B)** Wrch2, Rnd2, RhoH, **(C)** RhoD **(D)** RhoF, **(E)** Rnd1 and **(F)** Miro1. Constructs were allowed to express for ~40 h before harvested and lysed. The cell lysates were then precipitated with cobalt-coated magnetic beads or anti-FLAG antibody cross-linked to pre-washed protein G Dynabeads. The precipitated proteins were then identified by western blotting. RalB and Rac3 or RhoC were used as negative or positive controls. The expression of the recombinant protein in the whole cell lysate (WCL) is shown in the bottom 3 or 4 panels, while the co-immunoprecipitated (IP) samples are shown in the top two or 3 panels. GAPDH was used to assess the equal loading of samples across the wells. Results are representative of at least two independent experiments. **WCL:** whole cell lysate; **IP:** immunoprecipitation.

8.1.4 RhoGDI-3 targets

8.1.4.1 RhoGDI-3 binding to classical Rho-family GTPases

The final member of the RhoGDI family proteins is RhoGDI-3, which is widely expressed but is found at particularly high levels in brain, lung, kidney and testis (Zalcman *et al.,* 1996). Although less well studied than the other two members of the family, some RhoGDI-3 interacting Rho-family proteins have been identified. In a previous Y2H screen, mouse RhoGDI-3 was shown to interact with RhoB and RhoG but not with RhoA, RhoC, or Rac1 proteins (Zalcman *et al.,* 1996). An alternative study using purified proteins identified interactions between human RhoGDI-3 and both RhoA and Cdc42 but not with Rac1 or Rac2 (Adra *et al.,* 1997).

To verify the interaction seen in previous studies and also identify all the possible targets of RhoGDI-3, co-immunoprecipitation was undertaken by co-expressing FLAG-RhoGDI-3 with V5-tagged versions of all 10 classical Rho-family GTPases into HEK293T cells. The pre-cleared cell lysates were incubated with beads cross-linked to an anti-FLAG antibody for ~1 h at 4°C and the precipitated proteins were then analysed by western blotting.

RhoGDI-3 was found to interact with 7 out of 10 classical Rho-family GTPases. The interactions with RhoA, RhoB (Figure 8.7A) and RhoG (Figure 8.7B) (data obtained from Ms. Tiffany Fung, under supervision of the candidate) that had been observed previously were confirmed, along with 4 novel interactions: RhoC (Figure 8.7C), Rac1, Rac2 and Rac3 (Figure 8.7D). As shown in Figure 8.7E, no interaction has been observed between RhoGDI-3 and Cdc42, in contrast to earlier studies (Adra *et al.,* 1997). TC10 and TCL also failed to interact with RhoGDI-3 in this system (Figure 8.7E)

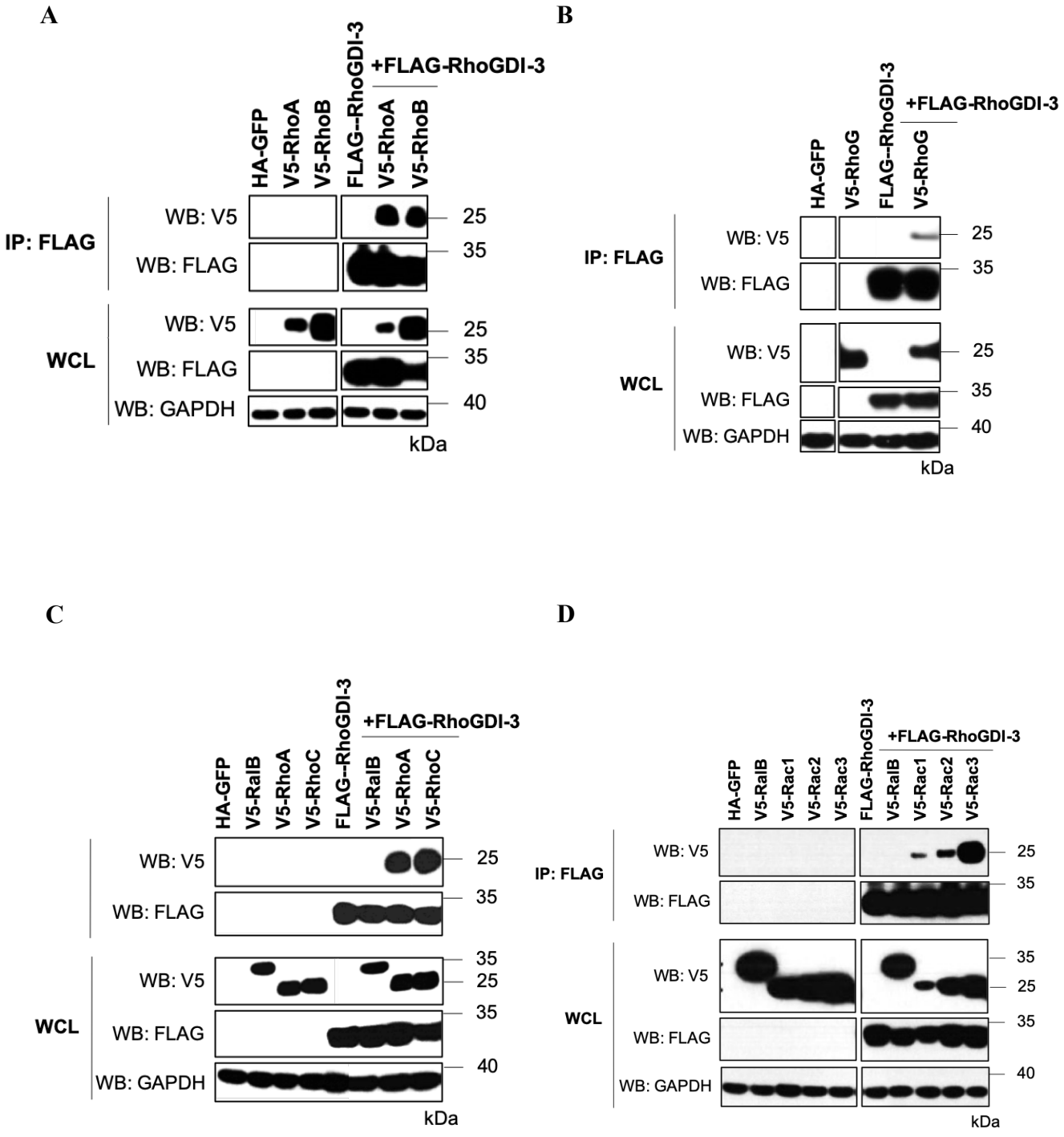
A
HA-GFP
V5-RhoA
V5-RhoB
FLAG--RhoGDI-3
+FLAG-RhoGDI-3
V5-RhoA
V5-RhoB
IP: FLAG
WB: V5
WB: FLAG
WCL
WB: V5
WB: FLAG
WB: GAPDH
25
35
25
35
40
kDa
B
HA-GFP
V5-RhoG
FLAG--RhoGDI-3
+FLAG-RhoGDI-3
V5-RhoG
IP: FLAG
WB: V5
WB: FLAG
WCL
WB: V5
WB: FLAG
WB: GAPDH
25
35
25
35
40
kDa
C
HA-GFP
V5-RalB
V5-RhoA
V5-RhoC
FLAG--RhoGDI-3
+FLAG-RhoGDI-3
V5-RalB
V5-RhoA
V5-RhoC
WB: V5
WB: FLAG
WCL
WB: V5
WB: FLAG
WB: GAPDH
25
35
35
25
35
40
kDa
D
HA-GFP
V5-RalB
V5-Rac1
V5-Rac2
V5-Rac3
FLAG-RhoGDI-3
+FLAG-RhoGDI-3
V5-RalB
V5-Rac1
V5-Rac2
V5-Rac3
IP: FLAG
WB: V5
WB: FLAG
WCL
WB: V5
WB: FLAG
WB: GAPDH
25
35
35
25
35
40
kDa

E

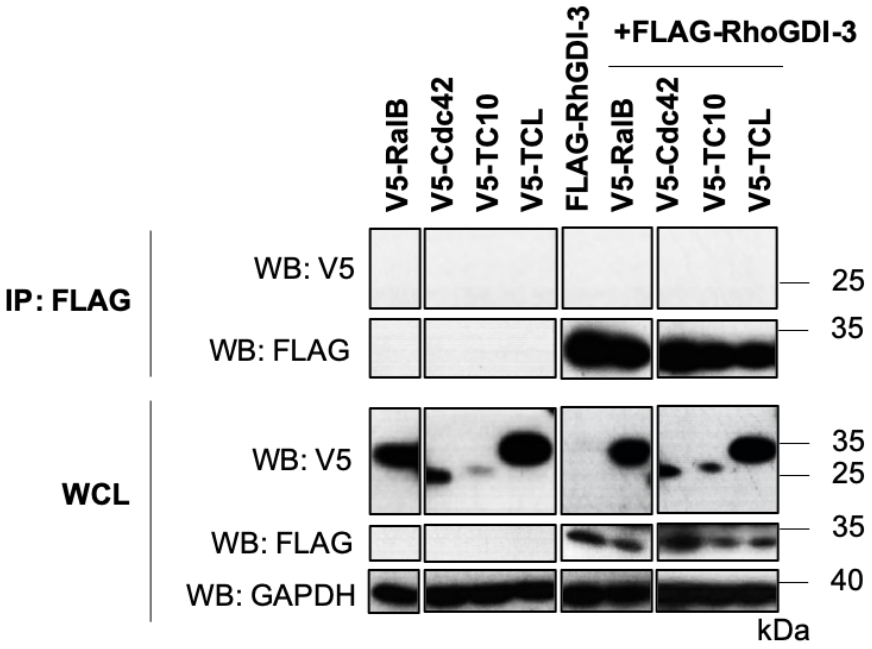

Figure 8.7: The interaction of RhoGDI-3 with the typical Rho-family GTPases. FLAG-RhoGDI-3 was transfected alone or together with V5-tagged **(A)** RhoA, RhoB, **(B)** RhoG, **(C)** RhoC, **(D)** Rac1, Rac2, Rac3, **(E)** Cdc42, TC10 and TCL into HEK293T cells. Constructs were allowed to express for ~40 h before being harvested, lysed and immunoprecipitated with anti-FLAG antibody cross-linked to pre-washed Protein G Dynabeads. The precipitated proteins were identified by western blotting. RalB was used as a negative control. The expression of the recombinant protein in the whole cell lysate (WCL) is shown in the bottom 3 panels, while the co-immunoprecipitated (IP) samples are shown in the top two panels. GAPDH was used to assess the equal loading of samples across the wells. Results are representative of at least two independent experiments. **WCL:** whole cell lysate; **IP:** immunoprecipitation.

8.1.4.2 RhoGDI-3 binding to non-classical Rho-family GTPases

Similarly to the other two GDIs, the interactions between RhoGDI-3 and the atypical Rho-family GTPases have not been studied, with the exception for RhoH (Li *et al.,* 2002). Thus, co-immunoprecipitation was performed by co-expressing FLAG-RhoGDI-3 with 9 the atypical members of Rho-family GTPases in HEK293T cells. The pre-cleared cell lysates were then immunoprecipitated with anti-FLAG antibody cross-linked to pre-washed Protein G Dynabeads. Bound Rho-family GTPases were analysed by western blotting.

The interaction with RhoH (Figures 8.8A and B) that had been observed previously was confirmed (Li *et al.,* 2002). Interestingly, RhoGDI-3 was found to interact for the first time with Wrch2 (Figure 8.8A), RhoD (Figure 8.8B), RhoF (Figure 8.8C), Rnd2 (Figure 8.8D) and Miro2 (Figure 8.8F). These novel interactions found in this screen are exclusive for RhoGDI-3 and are not seen with the other GDIs, suggesting a novel role for RhoGDI-3 in regulating atypical Rho-family GTPases.

Wrch1 (Figure 8.8A) and Miro1 (Figure 8.8E) were not seen to interact with RhoGDI-3.

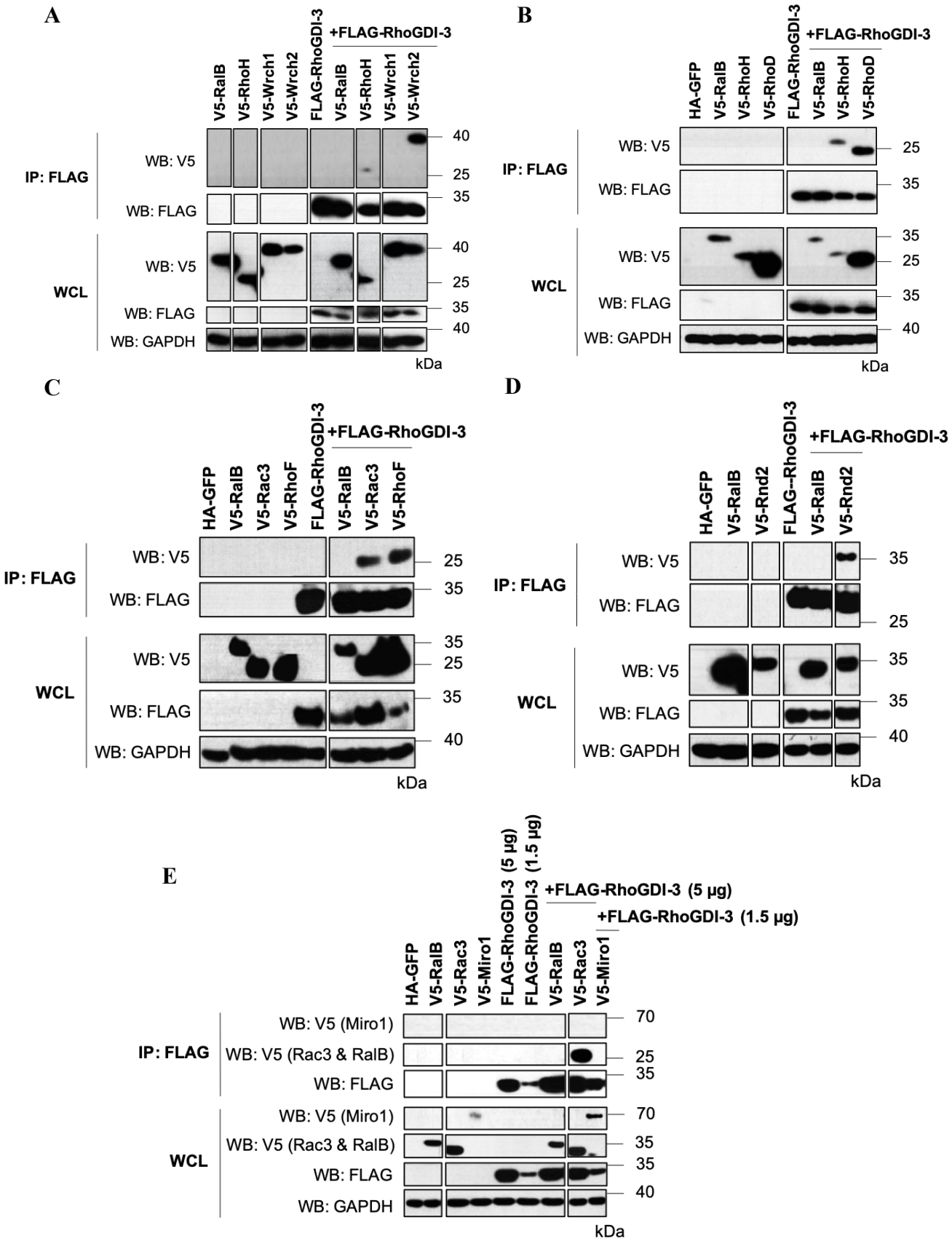
A
+FLAG-RhoGDI-3
V5-RalB
V5-RhoH
V5-Wrch1
V5-Wrch2
FLAG-RhoGDI-3
V5-RalB
V5-RhoH
V5-Wrch1
V5-Wrch2
IP: FLAG
WB: V5
WB: FLAG
WCL
WB: V5
WB: FLAG
WB: GAPDH
40
25
35
40
25
35
40
kDa
B
+FLAG-RhoGDI-3
HA-GFP
V5-RalB
V5-RhoH
V5-RhoD
FLAG-RhoGDI-3
V5-RalB
V5-RhoH
V5-RhoD
IP: FLAG
WB: V5
WB: FLAG
WCL
WB: V5
WB: FLAG
WB: GAPDH
25
35
35
25
35
40
kDa
C
+FLAG-RhoGDI-3
HA-GFP
V5-RalB
V5-Rac3
V5-RhoF
FLAG-RhoGDI-3
V5-RalB
V5-Rac3
V5-RhoF
IP: FLAG
WB: V5
WB: FLAG
WCL
WB: V5
WB: FLAG
WB: GAPDH
25
35
35
25
35
40
kDa
D
+FLAG-RhoGDI-3
HA-GFP
V5-RalB
V5-Rnd2
FLAG--RhoGDI-3
V5-RalB
V5-Rnd2
IP: FLAG
WB: V5
WB: FLAG
WCL
WB: V5
WB: FLAG
WB: GAPDH
35
25
35
35
40
kDa
E
+FLAG-RhoGDI-3 (5 µg)
+FLAG-RhoGDI-3 (1.5 µg)
HA-GFP
V5-RalB
V5-Rac3
V5-Miro1
FLAG-RhoGDI-3 (5 µg)
FLAG-RhoGDI-3 (1.5 µg)
V5-RalB
V5-Rac3
V5-Miro1
IP: FLAG
WB: V5 (Miro1)
WB: V5 (Rac3 & RalB)
WB: FLAG
WCL
WB: V5 (Miro1)
WB: V5 (Rac3 & RalB)
WB: FLAG
WB: GAPDH
70
25
35
70
35
35
40
kDa

F

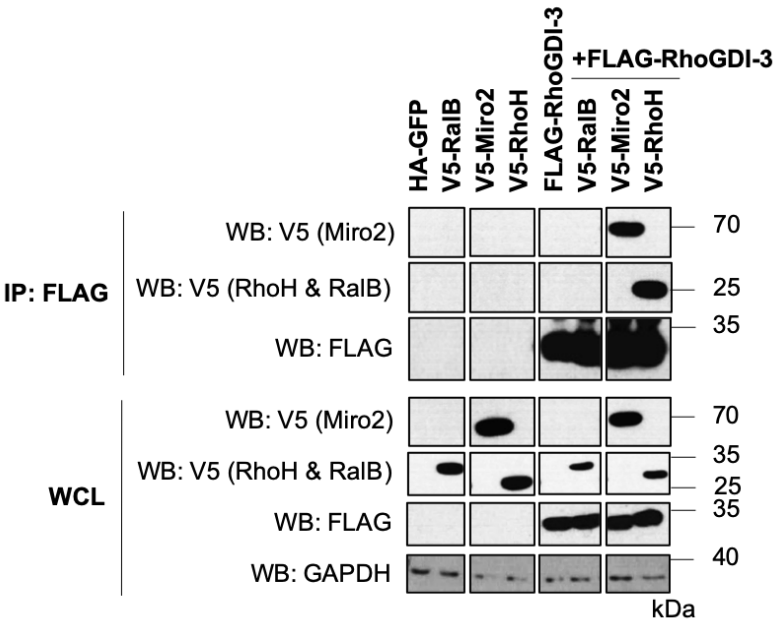

Figure 8.8: The interaction of RhoGDI-3 with the atypical Rho-family GTPases. HEK293T cells were transfected with FLAG-RhoGDI-3 alone or in combination with V5-tagged **(A)** Wrch1, Wrch2, RhoH, **(B)** RhoD, **(C)** RhoF, **(D)** Rnd2 **(E)** Miro1 and **(F)** Miro2. ~40 h post-transfection, cells were harvested and lysed. The pre-cleared cell lysates were then immunoprecipitated with anti-FLAG antibody cross-linked to pre-washed Protein G Dynabeads, for ~1 h. The precipitated proteins were then analysed by western blotting. RalB was used as a negative control. The expression of the recombinant protein in the whole cell lysate (WCL) is shown in the bottom 3 or 4 panels, while the co-immunoprecipitated (IP) samples are shown in the top two or 3 panels. GAPDH was used to assess the equal loading of samples across the wells. Results are representative of at least two independent experiments. **WCL:** whole cell lysate; **IP:** immunoprecipitation.

8.1.5 The interaction of the RhoGDIs with endogenous Rho-family GTPases

All the data presented so far utilised exogenous expression of Rho-family GTPases. Thus, some of the interactions observed in this screen, especially between RhoGDI-3 with its novel targets; RhoC and Rac1 were verified in parallel using endogenous Rho-family GTPases. Despite being reported in previous studies, the interactions between RhoGDI-1 or -2 and RhoA, RhoC or Rac1 were also validated using endogenous GTPases. It was still necessary to use the exogenously expressed RhoGDI proteins in these experiments due to lack of available specific antibodies (section 3.3.1).

Briefly, His-RhoGDI-1, His-RhoGDI-2 and FLAG-RhoGDI-3 were transfected into HEK293T cells and allowed to express for ~40 h. Cells were then harvested and lysed. The pre-cleared cell lysates were precipitated with either cobalt-coated magnetic beads or anti-FLAG antibody coupled to Protein G Dynabeads. The presence of endogenous Rac1, RhoA or RhoC in co-immunoprecipitated (co-IP) samples were identified using antibodies specific for each Rho-family GTPases by western blotting.

All three exogenously expressed RhoGDI proteins interacted with endogenous Rac1 (Figure 8.9) and RhoC (Figure 8.10). Whereas, only RhoGDI-1 and RhoGDI-3 interacted with endogenous RhoA (Figure 8.11) as shown previously in Figures 8.3A and 8.7A. Confirmation of these interactions with endogenous Rho-family GTPases also goes some way to validating the exogenous system used in the full screen. These data also validate the novel targets of RhoGDI-3, Rac1 and RhoC.

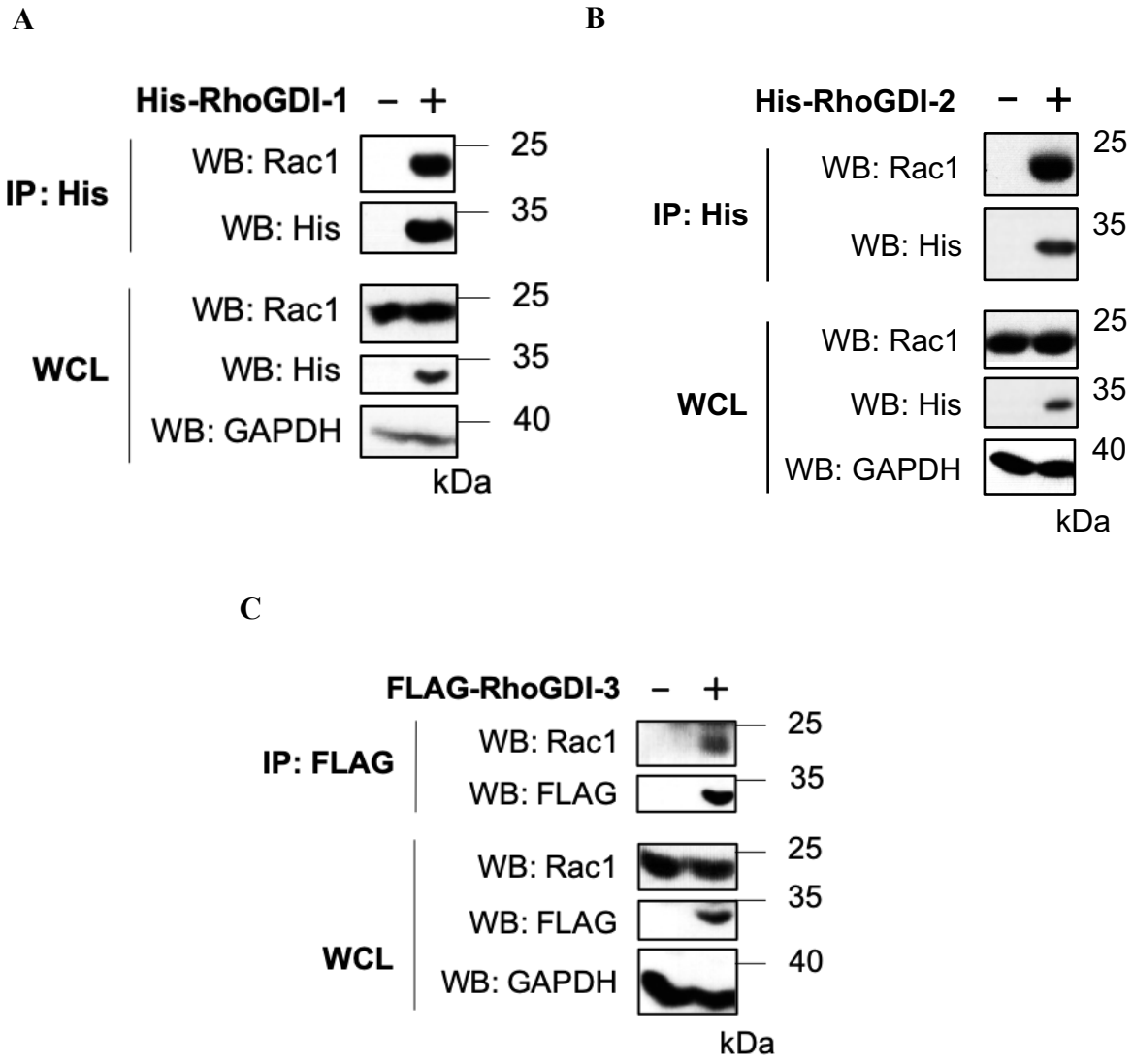

Figure 8.9: The interaction of exogenous RhoGDIs with endogenous Rac1. HEK293T cells were transfected with FLAG or His-tagged RhoGDIs and allowed to express for ~40 h before being harvested and lysed. The cell lysates were then precipitated with either cobalt-coated magnetic beads or anti-FLAG antibody that was cross-linked to a set of pre-washed Protein G Dynabeads. The co-immunoprecipitation of endogenous Rac1 was determined using an anti-Rac1 antibody (top panels). The expression of the recombinant proteins in the whole cell lysate (WCL) is shown in the bottom panels along with the level of endogenous Rac1. **WCL:** whole cell lysate; **IP:** immunoprecipitation**. (A)** RhoGDI-1, **(B)** RhoGDI-2 and **(C)** RhoGDI-3.

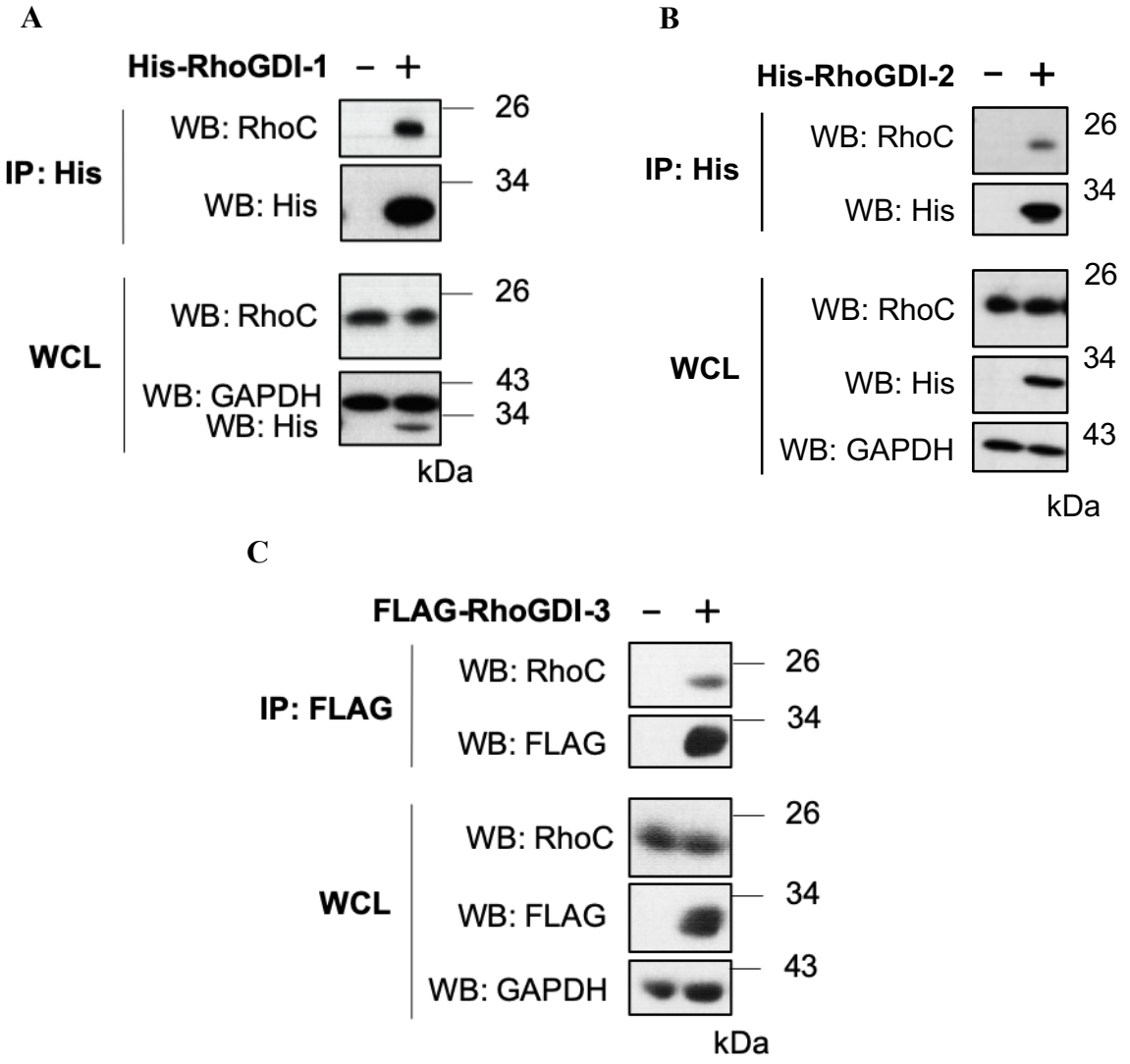

Figure 8.10: The interaction of exogenous RhoGDIs with endogenous RhoC. All three FLAG or His-tagged RhoGDIs were exogenously transfected into HEK293T cells. Constructs were allowed to express for ~40 h before being harvested and lysed. The cell lysates were then precipitated with either cobalt-coated magnetic beads or anti-FLAG antibody that was cross-linked to a set of pre-washed Protein G Dynabeads. The co-immunoprecipitation of endogenous RhoC was determined using an anti-RhoC antibody (top panels). The expression of the recombinant proteins in the whole cell lysate (WCL) is shown in the bottom panels along with the level of endogenous RhoC. **WCL:** whole cell lysate; **IP:** immunoprecipitation. **(A)** RhoGDI-1, **(B)** RhoGDI-2 and **(C)** RhoGDI-3.

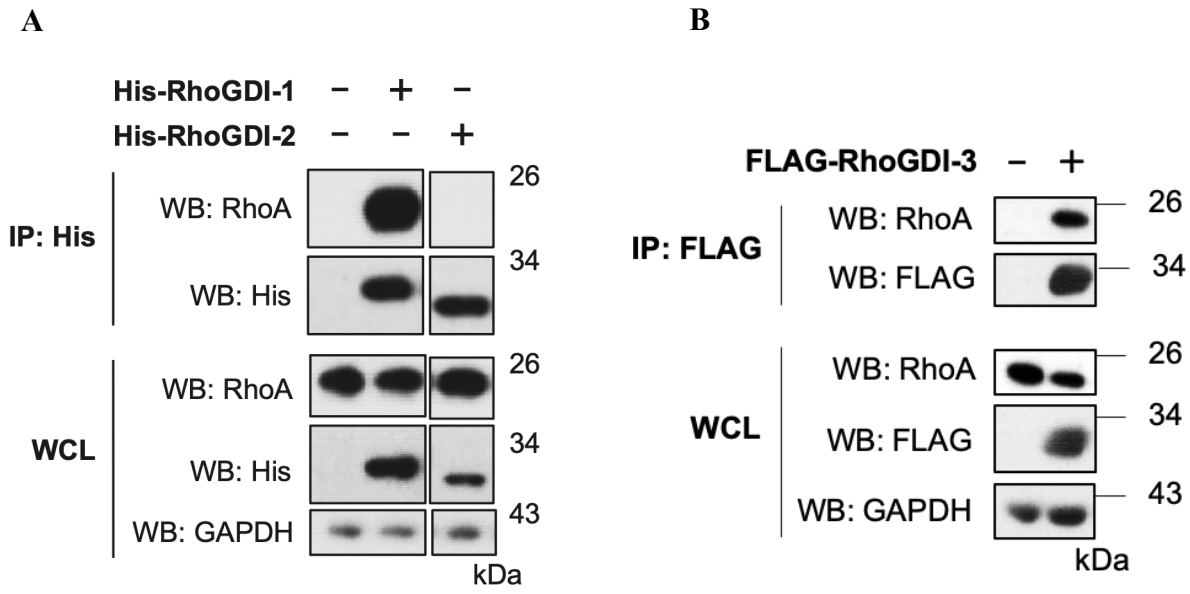

Figure 8.11: The interaction of exogenous RhoGDIs with endogenous RhoA. FLAG or His-tagged RhoGDI-1 were exogenously transfected into HEK293T cells. Constructs were allowed to express for ~40 h before being harvested and lysed. The cell lysates were then precipitated with either cobalt-coated magnetic beads or anti-FLAG antibody that was cross-linked to a set of pre-washed Protein G Dynabeads. The co-immunoprecipitation of endogenous RhoA was determined using an anti-RhoA antibody (top panels). The expression of the recombinant proteins in the whole cell lysate (WCL) is shown in the bottom panels along with the level of endogenous RhoA. **WCL:** whole cell lysate; **IP:** immunoprecipitation. **(A)** RhoGDI-1 and RhoGDI-2 **(B)** RhoGDI-3.

8.1.6 Summary of RhoGDI targets

The interactions identified in this screen are summarised in Table 8.2; green boxes indicate interactions observed in previous studies and confirmed in this work, while yellow boxes highlighted the novel interactions identified in this screen.

Although more effort has to be taken in assessing negative results, this screen also suggests which Rho-family GTPases that are not targets for the RhoGDI proteins, including TC10, TCL, Wrch1 and Miro1 which appear not to interact with any of the RhoGDI proteins.

All interactions previously reported between RhoGDI-1 and Rho-family GTPases were verified in this screen, except for RhoH (Olofsson, 1999). RhoF was shown for the first time to interact with RhoGDI-1. There were no interactions identified with any of the atypical Rho-family GTPases.

RhoGDI-2 appears to be the most selective RhoGDI as it has been shown to interact only with RhoC, Rac1 and Rac3. All of these interactions have already been observed in previous studies (Scheffzek *et al.,* 2000; Moissoglu *et al.,* 2009; Griner *et al.,* 2015). Similarly to RhoGDI-1, no interactions were observed with the atypical Rho-family GTPases.

The interaction of RhoGDI-3 with RhoA, RhoB and RhoG were also verified in this screen (Zalcman *et al.,* 1996; Adra *et al.,* 1997), together with novel interactions with Rac1, Rac2, Rac3, RhoD, RhoF, Wrch2, Rnd2 and Miro2. The interactions seen between RhoGDI-3 and atypical members of Rho-family GTPases suggest a role for RhoGDI-3 in regulating the activity of these small GTPases, in contrast to the other RhoGDIs.

Table 8.2: RhoGDIs targets

Type	Group	Rho GTPase	RhoGDI-1	RhoGDI-2	RhoGDI-3
Classical	Rho	RhoA	Yes	No	Yes
		RhoB	No	No	Yes
		RhoC	Yes	Yes	Yes
	Rac	Rac1	Yes	Yes	Yes
		Rac2	Yes	No	Yes
		Rac3	Yes	Yes	Yes
		RhoG	Yes	No	Yes
	Cdc42	Cdc42	Yes	No	No
		TC10/RhoQ	No	No	No
		TCL/RhoJ	No	No	No
Non-classical	RhoD		No	No	Yes
	RhoF/Rif		Yes	No	Yes
	Cdc42	Wrch1/RhoU	No	No	No
		Wrch2/RhoV/ Chp	No	No	Yes
	Rnd	Rnd1/RhoS	No	No	N/A
		Rnd2/RhoN	No	No	Yes
	Miro	Miro1/RhoT1	No	No	No
		Miro2/RhoT2	No	N/A	Yes
	RhoH/TTF		No	No	Yes

Green boxes: interaction identified in previous studies and confirmed in this work. Yellow boxes: novel interactions identified in this screen. N/A: Not applicable.

8.2 The subcellular localization of RhoGDI-Rho GTPases complexes

8.2.1 The site of interaction of RhoGDI-1 or -2 with Rac1

RhoGDI-1 has been found to form complexes with RhoA, Rac1, Rac2 and Cdc42 in the cytoplasm (Gorvel *et al.,* 1998; Olofsson, 1999). However, the site of interaction for RhoGDI-2 and its targets has not been reported. It is likely however that RhoGDI-2 complexes form in the cytoplasm due to the exclusive cytoplasmic localization of RhoGDI-2 (section 5.1).

The site of complex formation of the GDIs and their targets was investigated in this work and Rac1 was chosen for investigation to allow the study of an endogenous target. To confirm the site of interaction for RhoGDI-1 or -2 with Rac1, HEK293T cells were transfected with His-RhoGDI-1 or -2 and allowed to express for ~24 h before serum starvation overnight. Cells were harvested and fractionated into cytoplasmic and nuclear-enriched fractions. Each of the cell fractions were then precipitated with cobalt-coated magnetic beads for ~1 h. The presence of endogenous Rac1 in co-immunoprecipitated fractionated samples was identified by western blotting.

Rac1 was seen to interact with both RhoGDI-1 (Figure 8.12A) and RhoGDI-2 (Figure 8.12B) only in the cytoplasm as expected. Interestingly, although Rac1 was seen in both the cytoplasmic and nuclear-enriched fractions in the absence of both RhoGDIs, it was present only in the cytoplasm when co-expressed with the RhoGDIs, suggesting a potential role for both of these RhoGDIs in sequestering Rac1 in the cytoplasm, as has been reported previously for RhoGDI-1 (Michaelson *et al.,* 2001).

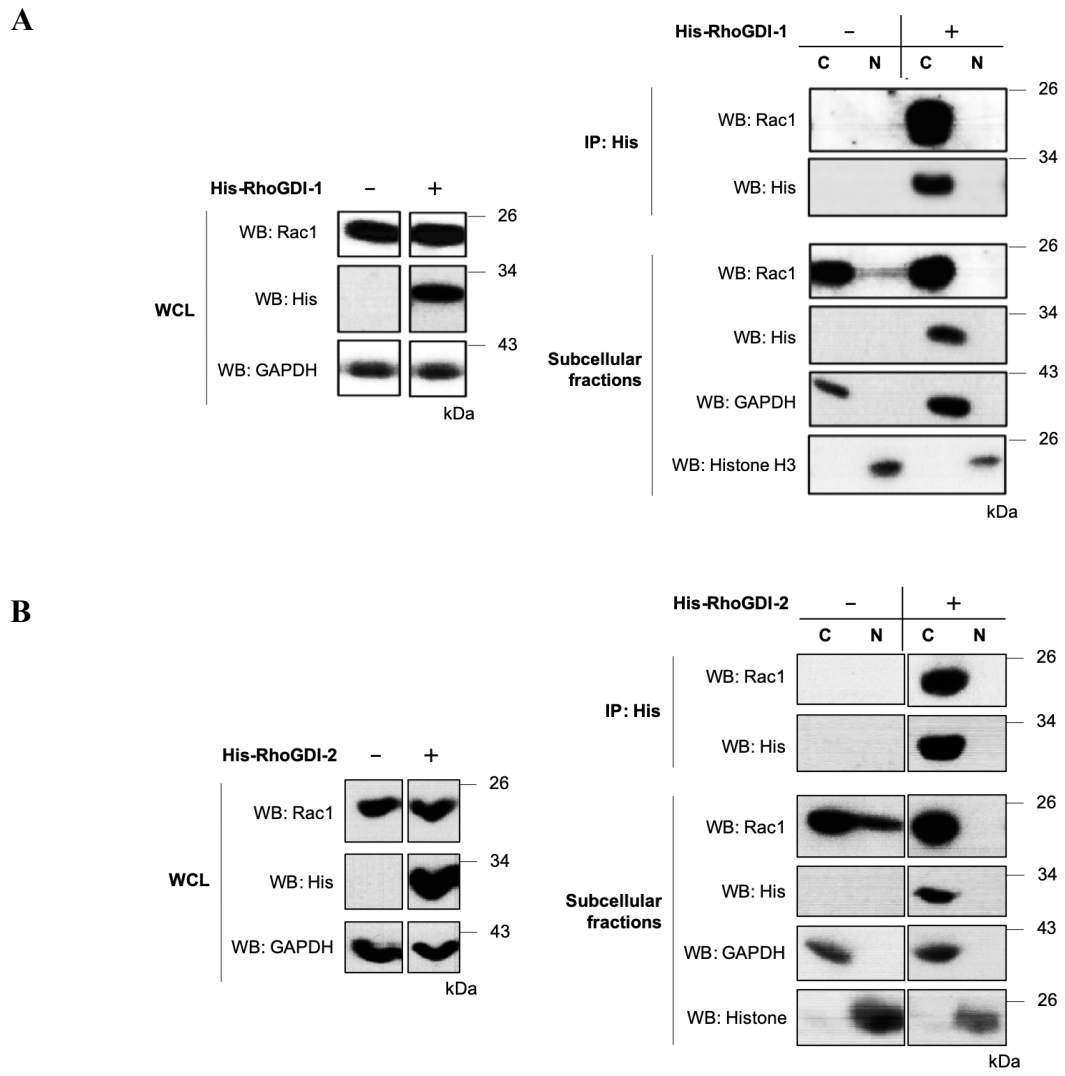

Figure 8.12: The subcellular localization of RhoGDI-1 or -2 -Rac1 complexes in HEK293T cells. His-RhoGDI-1 or -2 were transfected into HEK293T cells and allowed to express for ~24 h before serum starvation overnight. Cells were then harvested and fractionated into cytoplasmic and nuclear-enriched compartments. Each of the fractions were incubated with cobalt-coated magnetic beads for ~1 h. The co-immunoprecipitation of endogenous Rac1 in each fraction were determined using an anti-Rac1 antibody (top right panels). The expression of the recombinant proteins in the whole cell lysate (WCL) is shown on the left, while their expression in each fraction is shown on the bottom 4 panels on the right along with the level of endogenous Rac1. GAPDH and Histone H3 were used as cytoplasmic and nuclear markers, respectively. GAPDH was also used to assess equal loading of samples across the wells in the total lysate**.** The western blot shown is representative of three independent experiments. **WCL:** whole cell lysate; **IP:** immunoprecipitation**; C:** cytoplasmic compartment; **N:** nuclear-enriched compartment. **(A)** RhoGDI-1 and **(B)** RhoGDI-2.

8.2.2 The site of interaction of RhoGDI-3 with its Rho-family targets

8.2.2.1 RhoGDI-3 forms complexes with RhoA, RhoC and Rac1 in the cytoplasm

A previous study undertaken by Morin *et al.* (2010) showed that RhoGDI-3 and its target, RhoG could form a complex on the Golgi and vesicular structures of mammalian cells. Since RhoGDI-3 was found more in the cytoplasm compared to nuclear-enriched fractions in this work (section 5.1), it seemed likely that the Rho-RhoGDI-3 complexes would form in the cytoplasm. However, as a few of the RhoGDI-3 targets such as RhoA, RhoC and Rac1 have also been shown to be present in the nucleus (Dubash *et al.,* 2011; Unsal-Kacmaz *et al.,* 2011; Lanning *et al.,* 2004; Pellinen *et al.,* 2015), this posed the question that RhoGDI-3 could also interact with these Rho-family GTPases in the nucleus and regulate their activities there.

To test this, subcellular fractionation and co-immunoprecipitation were performed by transfecting FLAG-RhoGDI-3 into HEK293T cells. The construct was allowed to express for ~24 h before serum starvation overnight. ~40 h post-transfection, cells were harvested and fractionated into the cytoplasmic and nuclear-enriched fractions. The lysates were then immunoprecipitated with anti-FLAG antibody cross-linked to pre-washed Protein G Dynabeads, for ~1 h. The presence of endogenous RhoA, RhoC and Rac1 in each fraction and in the immunoprecipitated samples were determined by western blotting.

As shown in Figure 8.13, RhoA and RhoC were found only in the cytoplasm, despite being reported previously to be in the nucleus. Rac1 was seen predominantly in the cytoplasm but a small amount was detected in the nuclear-enriched fractions. RhoGDI-3-RhoA and -RhoC complexes were only identified in the cytoplasm as expected. RhoGDI-3-Rac1 complexes were also only observed in the cytoplasm despite the presence of both proteins in both compartments. Furthermore, similar to what was seen with RhoGDI-1 and -2, Rac1 nuclear levels decreased when

co-expressed with RhoGDI-3, indicating a role for RhoGDI-3 in sequestering Rac1 in the cytoplasm.

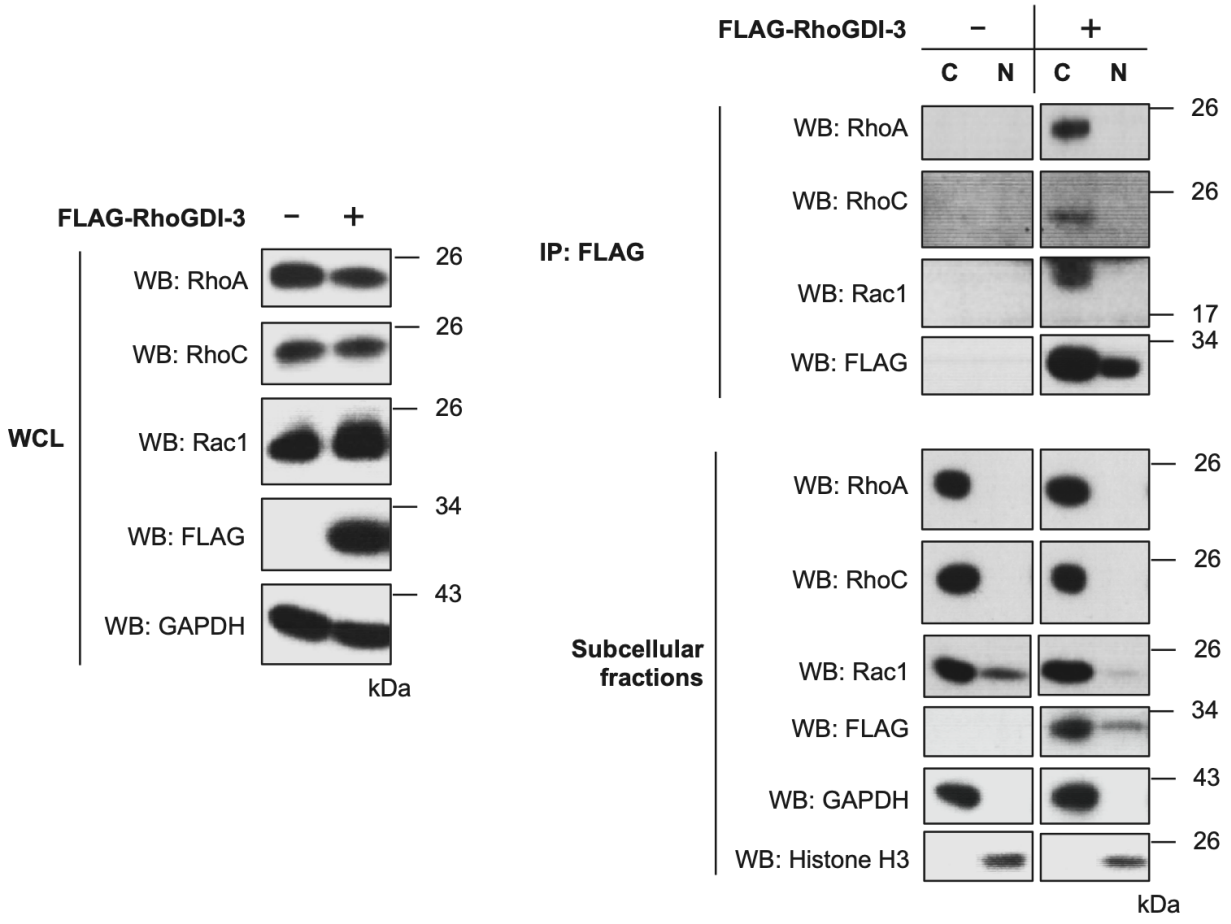

Figure 8.13: The subcellular localization of RhoGDI-3-RhoA, -RhoC and -Rac1 complexes in HEK293T cells. FLAG-RhoGDI-3 was transfected into HEK293T cells and allowed to express for ~24 h before serum-starved overnight. ~40 h post-transfection, cells were harvested and fractionated into cytoplasmic and nuclear-enriched compartments. Each of the fractions were then immunoprecipitated with anti-FLAG antibody cross-linked to pre-washed Protein G Dynabeads, for ~1 h. The co-immunoprecipitation of endogenous RhoA, RhoC and Rac1 was determined using anti-RhoA, anti-RhoC or anti-Rac1 antibodies, respectively (top right panels). The expression of the recombinant proteins in the whole cell lysate (WCL) is shown on the left, while their expression in each fraction is shown on the bottom 6 panels on the right along with the levels of endogenous RhoA, RhoC and Rac1. Histone H3 and GAPDH were used as nuclear and cytoplasmic markers, respectively. GAPDH was used to assess equal loading of samples across the wells in the total whole cell lysate**.** The western blot shown is representative of three independent experiments. **WCL:** whole cell lysate; **IP:** immunoprecipitation**; C:** cytoplasmic compartment; **N:** nuclear-enriched compartment.

8.2.2.2 RhoGDI-3 forms a complex with RhoH in both the cytoplasmic and nuclear-enriched cellular fractions

The site of interaction between RhoGDI-3 and the atypical Rho-family GTPases was also determined. RhoH is known to be in the nucleus of Jurkat cells and to co-localize with a transcriptional regulator, Kaiso, upon chemokine stimulation or after T cell receptor activation to regulate actin-cytoskeleton structure and transcriptional activity during T cell migration (Mino *et al.,* 2018).

To identify the subcellular location of complexes formed between RhoGDI-3 and RhoH, FLAG-RhoGDI-3 and V5-RhoH were transfected into HEK293T cells. ~24 h after serum starvation, cells were harvested and fractionated into cytoplasmic and nuclear-enriched fractions. The lysates were then immunoprecipitated with anti-FLAG antibody and the site of interaction was determined by western blotting.

As expected, RhoH was observed in both the cytoplasmic and nuclear-enriched fractions (Figure 8.14). RhoH total protein also decreased when co-expressed with RhoGDI-3 and this was most marked in the nuclear-enriched fraction. Interestingly, RhoGDI-3 was seen to interact with RhoH in both the fractions, suggesting a role for RhoGDI-3 in regulating RhoH activity in both compartments.

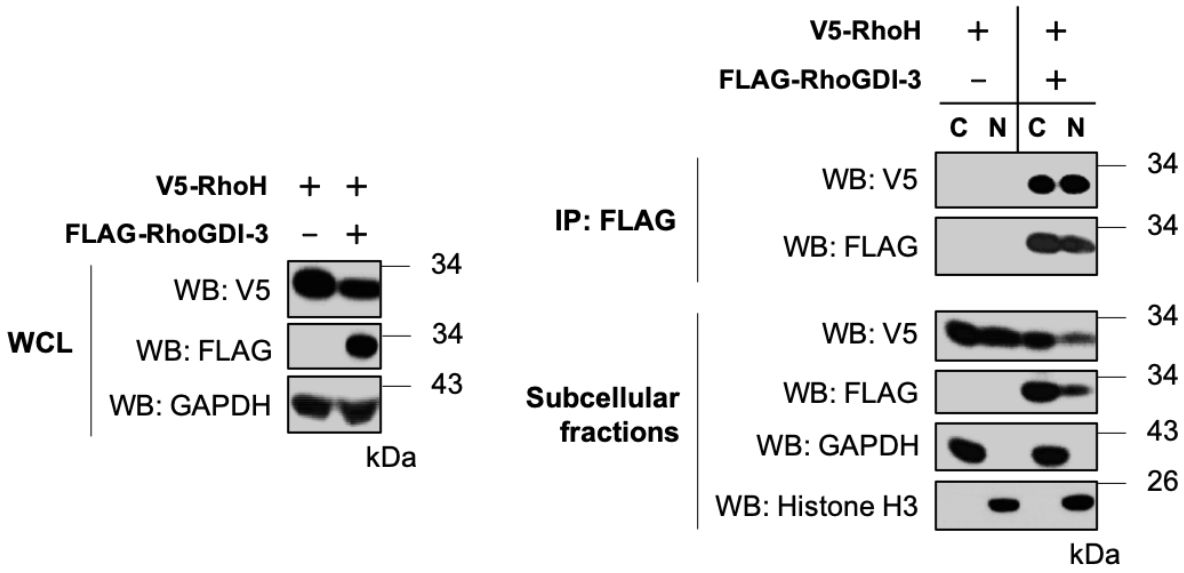

Figure 8.14: The subcellular localization of RhoGDI-3-RhoH complexes in HEK293T cells. FLAG-RhoGDI-3 was transfected together with V5-RhoH into HEK293T cells and allowed to express for ~24 h before serum-starvation overnight. ~40 h post-transfection, cells were harvested and fractionated into cytoplasmic and nuclear-enriched compartments. Each of the fractions were then immunoprecipitated with anti-FLAG antibody for ~1 h. The co-immunoprecipitation of V5-RhoH in each fraction was determined by using anti-V5 antibody (top right panels). The expression of the recombinant proteins in the whole cell lysate (WCL) is shown on the left, while their expression in each fraction is shown on the bottom 4 panels on the right hand side. Histone H3 and GAPDH were used as nuclear and cytoplasmic markers, respectively. GAPDH was used to assess equal loading of samples across the wells in the total whole cell lysate**. WCL:** whole cell lysate; **IP:** immunoprecipitation**; C:** cytoplasmic compartment; **N:** nuclear-enriched compartment.

8.3 The effect of the RhoGDIs on the activation status of their targets

Rho-family GTPases function as molecular switches by alternating between active GTP-bound and inactive GDP-bound forms. In their active GTP-bound state, Rho-family GTPases transduce the signals by interacting with multiple effector proteins. In contrast, Rho-family GTPases are maintained in their inactive GDP-bound state by interacting with RhoGDI proteins (Boulter *et al.,* 2010). Thus, to investigate the inhibitory activity of the RhoGDI proteins towards their Rho GTPase targets, pull-down assays using specific effector proteins for each Rho GTPase were performed. The activation status of Rac1 was assessed in the presence of exogenous RhoGDI-1 and -2. For RhoGDI-3, representative targets: Rac1, RhoA, RhoB and RhoC were tested as examples of classical Rho GTPases, while RhoH was selected as examples of atypical Rho GTPase targets. Rhotekin was used as an effector for all the Rho subfamily proteins, while PAK1 was used for Rac1 and RhoH.

8.3.1 Purification of GST-Rhotekin-RBD from *E. coli*

pGEX-2T-Rhotekin-RBD (1-89) was purified as described in section 2.2.2.3. Briefly, *E. coli* BL21 (DE3) pLysS cells were induced with 1 mM IPTG for ~16 h at 20 °C. Cells were then harvested and lysed. The cleared lysates were collected by centrifugation and incubated with glutathione sepharose 4B beads for 5 min with rotation at 4 °C. Unbound proteins were then washed from the beads with wash buffer containing 0.5% Triton X-100. The GST-Rhotekin-RBD-bead suspension was then stored at -80 °C for future used.

Figure 8.15 shows the final product of GST- Rhotekin (~1 μg) after separation by SDS-PAGE and western blotting with an anti-GST antibody.

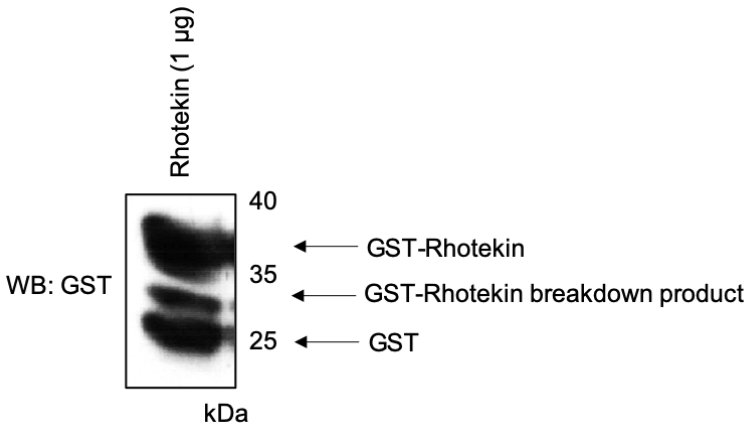

Figure 8.15: Final product of GST-Rhotekin-RBD (1-89). ~1 µg of the GST-Rhotekin-RBD were analysed by 12% SDS-PAGE and western blotting with anti-GST antibody.

8.3.2 Purification of GST-human PAK1-GBD from *E. coli*

8.3.2.1 Small-scale expression trials of GST-PAK1-GBD in *E. coli*

pGEX-2TK-PAK1-GBD (56-272) (a kind gift from Dr. Heidi Welch, Babraham Institute, Cambridge) was transformed into the *E. coli* BL21. Expression trials were performed as described in section 2.2.1. Briefly, 10 mL cultures were induced with 0.1 mM IPTG for either ~5 h at 37 °C or ~16 h at 20 °C. Cells were then harvested, pelleted and lysed. The soluble and insoluble fractions were collected and the level of GST-PAK1-PBD was analysed by SDS-PAGE and Coomassie staining (Figure 8.16).

GST-PAK1-GBD was soluble at 37 °C after ~5 h induction with IPTG (red box). These induction conditions were used for further large-scale protein production.

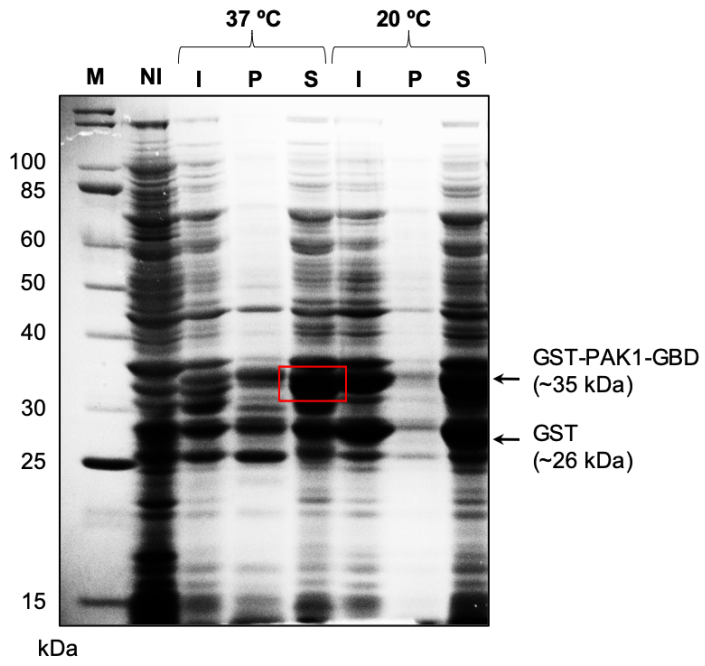

Figure 8.16: Small-scale expression trial of GST- PAK1-GBD (56-272) in *E. coli* BL21. *E. coli* BL21 cells transformed with pGEX-2TK-PAK1-GBD (56-272) and then cultures induced with IPTG for either ~5 h at 37 °C or ~16 h at 20 °C. Cells were then harvested, pelleted and lysed. Gel samples were collected from non-induced (NI), induced (I), insoluble (P) and soluble (S) fractions of induced cells. The level of GST-PAK1-GBD and its solubility under each condition was assessed by SDS-PAGE and Coomassie staining. **M:** MW markers.

8.3.2.2 Large-scale expression and purification of GST-PAK1-GBD (56-272) protein

GST-PAK1-PBD was expressed in 3 L *E. coli* BL21 using the optimised conditions and purified as described in section 2.2.2.2. Briefly, ~5 h post-induction by IPTG, cells were harvested, lysed and the lysate was cleared by centrifugation. The supernatant was incubated with glutathione agarose beads for ~30 min. Unbound proteins were washed from the beads with MTPBS containing 0.1% Triton X-100. The bound protein was then eluted using 10 mM reduced glutathione. Samples from each purification were analysed by SDS-PAGE and Coomassie

staining. All the eluted samples were then pooled and concentrated to ~2 mL using an Amicon stirred cell. The amount of protein was quantified (section 2.2.3) and stored at -80 °C.

As shown in Figure 8.17A, most of the GST-PAK1-GBD (~35 kDa) bound to the beads, with a small amount of GST-PAK1-GBD appearing in the wash samples. Gel samples of the beads showed low levels of contaminating proteins. These non-specific proteins maybe *E. coli* proteins but may also be GST-PAK1-GBD that has been cleaved by *E. coli* proteases and retained the GST-affinity tag.

Following elution with 10 mM glutathione (Figure 8.17B), GST-PAK1-GBD had undergone some degradation by proteases and this could also be seen in the final purified product (Figure 8.17C) that shows 3 major bands (~27 to 35 kDa). Previous purifications performed in the Welch lab show the same pattern of GST-PAK1-GBD degradation (Figure 8.17D), indicating that the construct is not fully stable. Attempts were made to reduce the degradation of GST-PAK1-GBD by adding protease inhibitors into the buffer used during the purification and also reducing the incubation time with the beads, however, there was little improvement in the final product. Nevertheless, the quality of the GST-PAK1-GBD produced was deemed reasonable to use in effector pull-down assays.

A

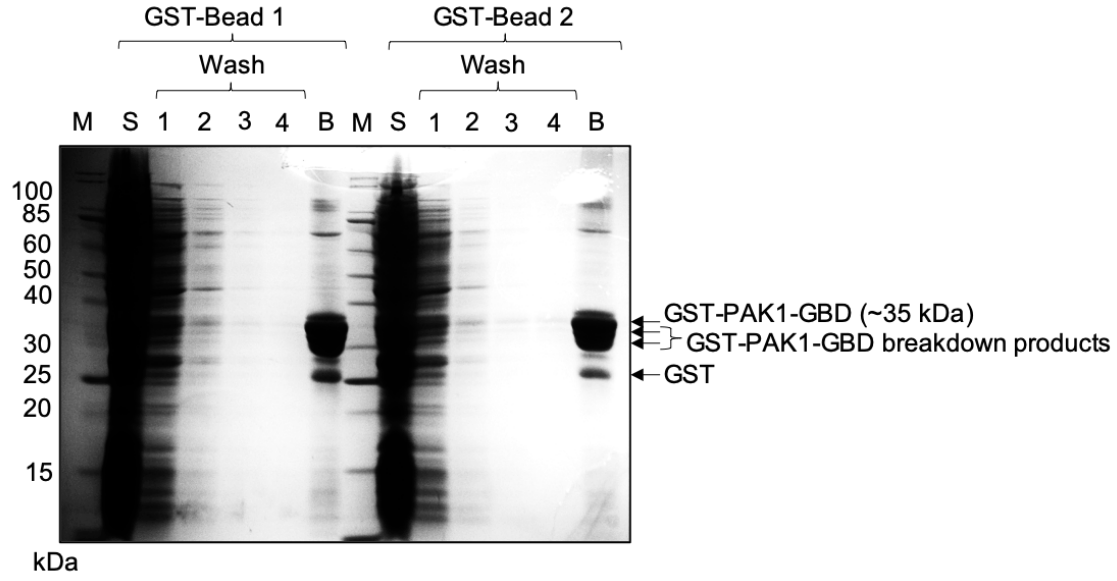

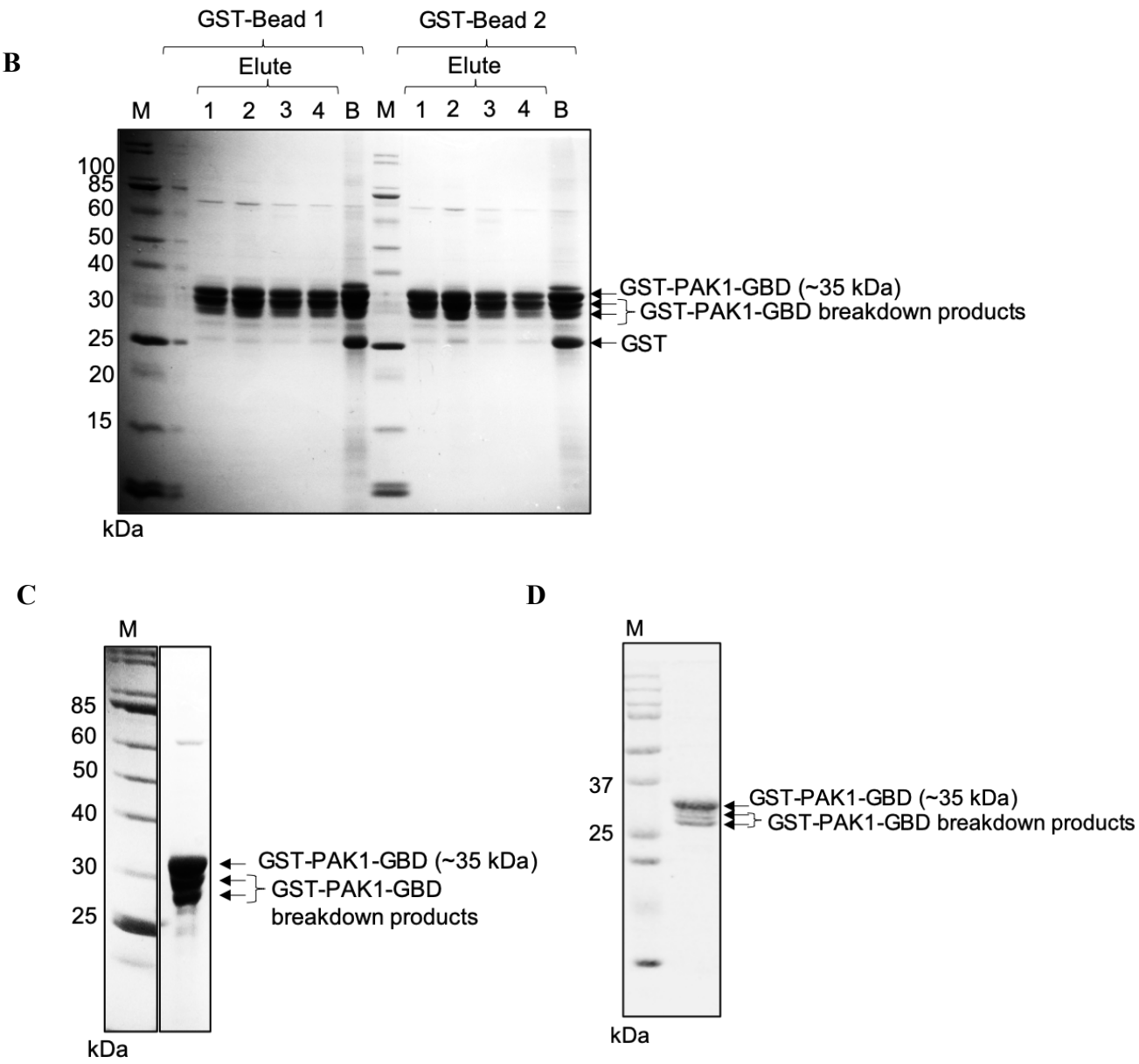

Figure 8.17: Purification of GST-PAK1-GBD from *E. coli* BL21. *E. coli* BL21 cells transformed with GST-PAK1-GBD (56-272) were induced with IPTG for ~5 h at 37 °C. Cells were harvested, pelleted and lysed. The cleared lysates were then added to two sets of glutathione agarose beads and incubated for ~30 min at 4 °C with rotation. **(A)** Beads were washed four times to remove unbound proteins and samples run on SDS-PAGE together with samples from the beads (B) and supernatant (S) before washes. **(B)** The bound protein was then eluted with 10 mM reduced glutathione and analysed by SDS-PAGE and Coomassie staining. **(C)** The GST-PAK1-PBD undergoes partial degradation as seen by SDS-PAGE analysis but **(D)** to similar levels seen previously in the Welch lab (image kindly shared by Dr. Martin Barker)**. M:** MW markers.

8.3.3 RhoGDIs negatively regulate the GTP levels of their targets

8.3.3.1 RhoGDI-1 and -2 negatively regulate the GTP level of Rac1

RhoGDI-1 has been shown to decrease the GTP loading of Rac1 (Chuang *et al.,* 1993) Depletion of RhoGDI-2 has also been seen to promote Rac1 activation in breast cancer cell lines (Zhang *et al.,* 2009). To confirm the consequences of RhoGDI-1 and -2 on the GTP levels of their targets, Rac1, an effector pull-down assay using GST-PAK1-GBD was performed in HEK293T cells.

His-RhoGDI-1 or -2 were transfected into cells and allowed to express for ~24 h before serum starvation overnight. Cells were harvested and lysed in buffer containing GST-PAK1-GBD (10 μg/sample), ~40 h post-transfection. The cleared lysates were then precipitated with GST-PAK1-GBD bound to glutathione sepharose 4B beads for 45 min at 4 °C. Following incubation, the beads were washed to remove any unbound proteins and the levels of GTP-bound endogenous Rac1 were identified by western blotting with anti-Rac1 antibody.

RhoGDI-1 and -2 were seen to exhibit classical GDI function by decreasing the GTP levels of Rac1 (Figure 8.18).

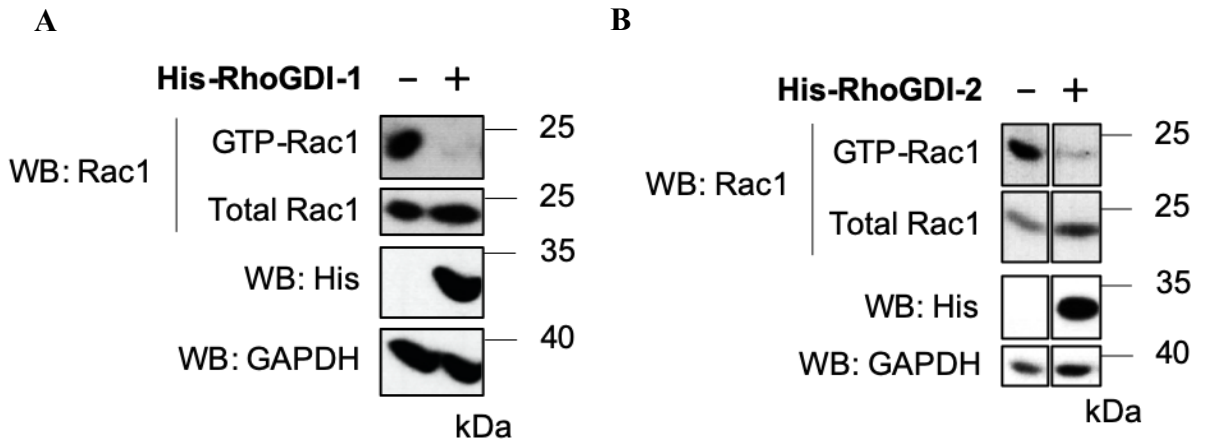

Figure 8.18: RhoGDI-1 and -2 decrease the GTP-bound levels of endogenous Rac1. HEK293T cells were transfected with His-RhoGDI-1 or -2 and allowed to express for ~24 h before serum starvation overnight. ~40 h post-transfection, cells were harvested, pelleted and lysed with buffer containing GST-PAK1-GBD. The lysates were then incubated with glutathione sepharose 4B beads. The levels of GTP-bound Rac1 were determined by western blotting with anti-Rac1 antibody, as shown in top panel. The expression of recombinant proteins in the whole cell lysates is shown in the bottom 3 panels along with the total level of endogenous Rac1. GAPDH was used to assess equal loading of samples across the wells in the total cell lysate**.** The western blot shown is representative of three independent experiments. **(A)** RhoGDI-1 and **(B)** RhoGDI-2.

8.3.3.2 RhoGDI-3 negatively regulates the GTP levels of Rho subfamily members

RhoGDI-3 is known to act as a GDI by negatively regulating the activation status of its binding partners. For instance, RhoGDI-3 was shown to inhibit the activation of RhoB by extracting GDP-bound RhoB from the membrane (Zalcman *et al.,* 1996). Besides RhoB, no studies have been performed to verify the GDI activity of RhoGDI-3 towards its other known target, RhoA. Thus, a GST-Rhotekin pull-down assay was performed to investigate the inhibitory activity of RhoGDI-3 on RhoA and the newly identified target, RhoC. The effect of RhoGDI-3 on RhoB activation was also included in this assay as a control.

Briefly, HEK293T cells were transfected with FLAG-RhoGDI-3 and allowed to express for ~24 h before serum-starvation overnight. ~40 h post-transfection, cells were harvested, pelleted and lysed. The lysates were then incubated with a total of 100 ng/µL of GST-Rhotekin-RBD-bead suspension for 45 min at 4 °C. Following incubation, the beads were washed and eluted with sample buffer. The GTP levels of endogenous RhoA, RhoB and RhoC were identified by western blotting with antibodies specific for each Rho subfamily GTPases.

RhoGDI-3 behaves as a conventional GDI by decreasing the GTP-levels of RhoB (Figure 8.19B), similar to previous study (Zalcman *et al.,* 1996). RhoGDI-3 also seen to inhibit the activation of RhoA (Figure 8.19A) and RhoC (Figure 8.19C). Interestingly, the total levels of RhoB increased considerably in cells expressing RhoGDI-3, suggesting that RhoGDI-3 might stabilises RhoB.

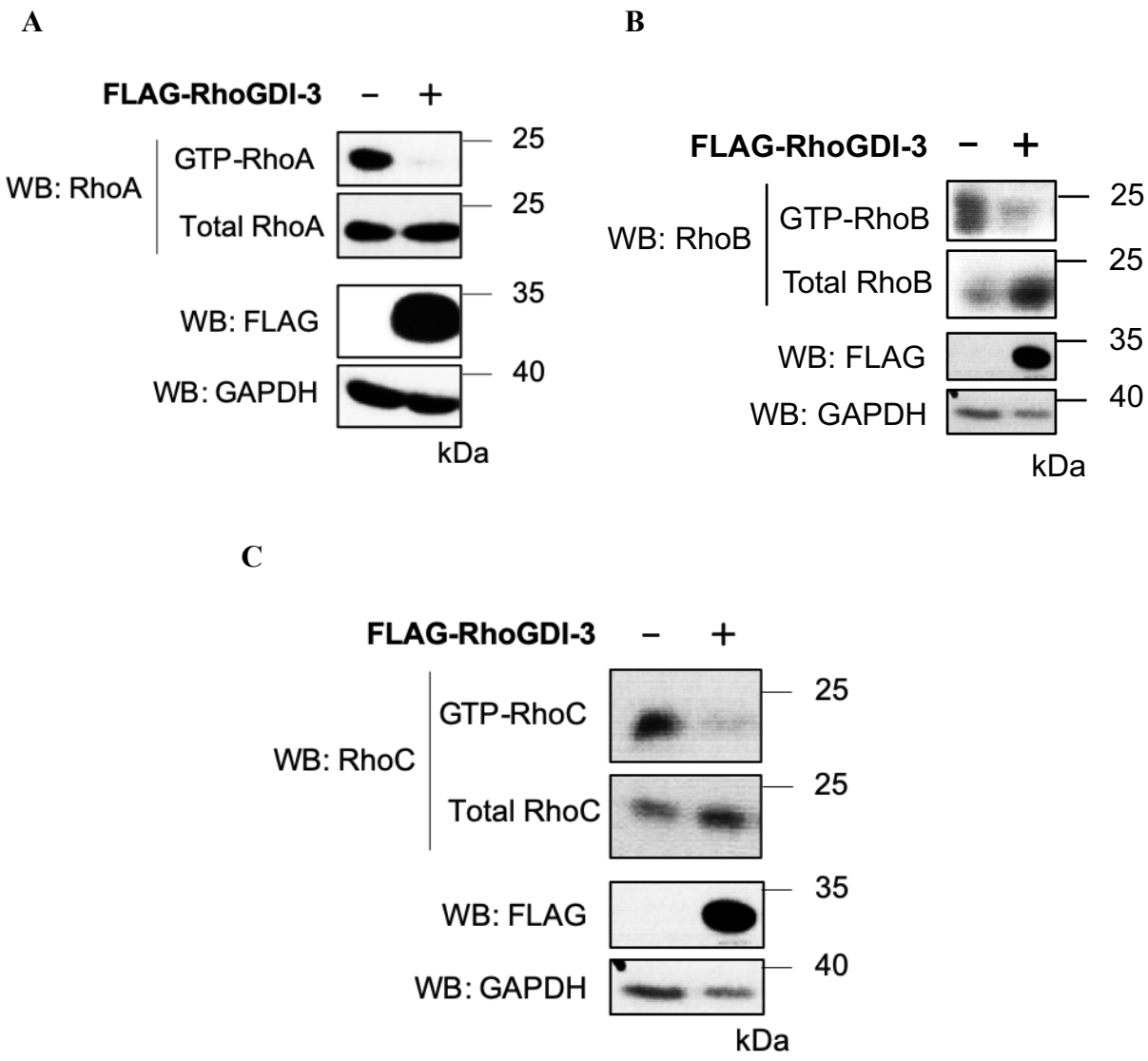

Figure 8.19: RhoGDI-3 decreases the GTP-bound levels of endogenous Rho subfamily members. FLAG-RhoGDI-3 was transfected into HEK293T cells and allowed to express for ~24 h before serum starvation overnight. Cells were harvested, pelleted and lysed, ~40 h post-transfection. The lysates were then incubated with GST-Rhotekin-RBD-bead suspension for 45 min at 4 °C. The levels of GTP-bound Rho subfamily members were determined by western blotting with antibodies specific for each Rho-family GTPases, as shown in top panels. The expression of recombinant proteins in the whole cell lysates is shown in the bottom 3 panels along with the total level of endogenous Rho subfamily proteins. GAPDH was used to assess equal loading of samples across the wells in the total cell lysate. The western blot shown is representative of two independent experiments. **(A)** RhoA, **(B)** RhoB and **(C)** RhoC.

8.3.3.3 RhoGDI-3 negatively regulates Rac1 and RhoH GTP levels

Data described in section 8.1.4 shows Rac1 is a new interacting partner for RhoGDI-3. Interestingly, the data here also shows that RhoH interacts with RhoGDI-3, even though it is thought to exist only as a GTP-bound form due to lacks GTPase activity (Li *et al.,* 2002). Thus, it would be assumed that RhoGDI-3 only binds and extracts RhoH from membranes but does not negatively regulate the GTP-bound levels of RhoH.

To analyse the effect of RhoGDI-3 on the activation status of Rac1 and RhoH, effector pull-down assays were performed using GST-PAK1-GBD. HEK293T cells were either transfected with FLAG-RhoGDI-3 alone or with V5-RhoH. Constructs were allowed to express for ~24 h before serum starvation overnight. ~40 h post-transfection, cells were harvested, and lysed in buffer containing GST-PAK1-GBD. The lysates were then incubated with glutathione sepharose beads for 45 min at 4 °C. The beads were washed and the levels of GTP-bound Rac1 and RhoH were analysed by western blotting using anti-Rac1 or anti-V5 antibodies.

The levels of GTP-bound Rac1 (Figure 8.20A) and RhoH (Figure 8.20B) were shown to decrease in cells expressing RhoGDI-3. These data were expected for Rac1, however contrary to predictions, RhoGDI-3 is still able to negatively regulate the activation of RhoH, even though it is assumed to be GTPase defective.

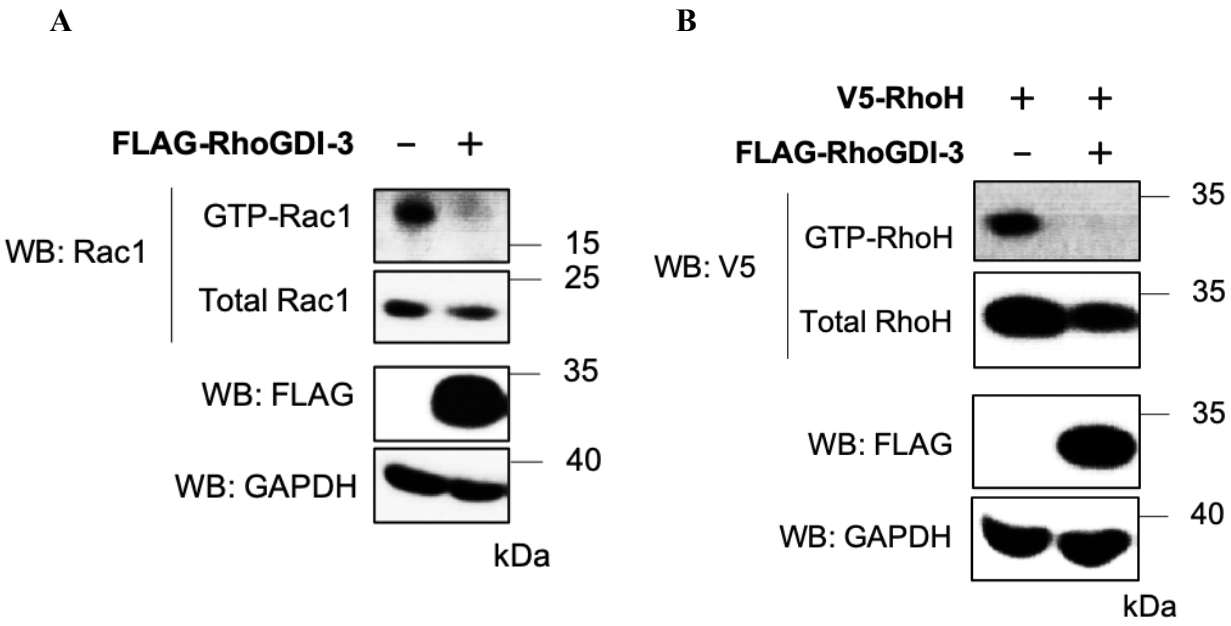

Figure 8.20: RhoGDI-3 decreases the GTP-bound levels of endogenous Rac1 and V5-RhoH. HEK293T cells were transfected with FLAG-RhoGDI-3 alone or with V5-RhoH. Constructs were allowed to express for ~24 h before serum-starvation overnight. ~40 h post-transfection, cells were harvested and lysed in buffer containing GST-PAK1-GBD. The lysates were then incubated with glutathione sepharose beads for 45 min at 4 °C. The levels of GTP-bound Rac1 and RhoH were determined by western blotting with anti-Rac1 or anti-V5 antibodies, as shown on top panels. The expression of recombinant proteins in the whole cell lysates is shown in the bottom 3 panels along with the total level of endogenous Rac1. GAPDH was used to assess equal loading of samples across the wells in the total cell lysate. The western blot shown is representative of three independent experiments. **(A)** Rac1 and **(B)** RhoH.

8.3.4 Subcellular localization of RhoGDI-3's inhibitory activity

8.3.4.1 Subcellular localization of RhoGDI-3's inhibitory activity on RhoA

Both RhoGDI-1 and -2 were found only in the cytoplasm and shown to interact with Rac1 in the same compartment. Thus, it is likely that both of these RhoGDIs negatively inhibiting the GTP levels of Rac1 in the cytoplasm, at least in the system used here, in a similar manner observed for RhoGDI-1 (Chuang *et al.,* 1993).

Data in this study shows RhoGDI-3 bind to RhoA exclusively in the cytoplasm and decrease its GTP levels. Thus, it is predicted that RhoGDI-3 will exert its GDI function towards RhoA in the cytoplasm. To confirm this, a subcellular fractionation and GST-Rhotekin-RBD pull-down assay was performed (section 2.3.11).

Briefly, FLAG-RhoGDI-3 was transfected into HEK293T cells and allowed to express for ~24 h before serum starvation overnight. ~40 h post-transfection, cells were harvested and fractionated into cytoplasmic and nuclear-enriched fractions. The lysates were then incubated with GST-Rhotekin-RBD-bead suspension for 45 min at 4 °C. The level of GTP-bound RhoA in each fraction was determined by western blotting with an anti-RhoA antibody.

As expected, RhoGDI-3 inhibited RhoA activation solely in the cytoplasm (Figure 8.21).

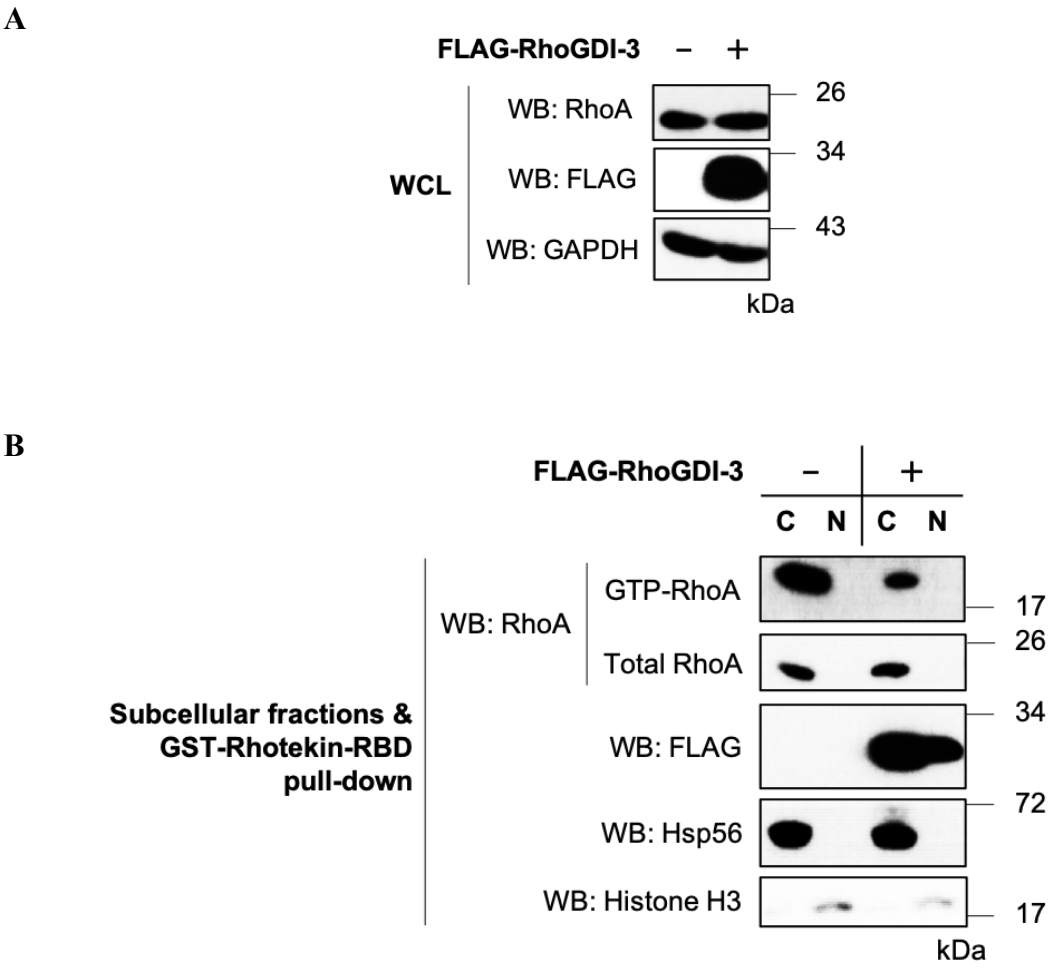

Figure 8.21: The site of action of RhoGDI-3 towards RhoA. HEK293T cells were transfected with FLAG-RhoGDI-3 and allowed to express for ~24 h before serum-starved overnight. Cells were harvested and fractionated into cytoplasmic and nuclear-enriched fractions, ~40 h post-transfection. Each of the fractions was incubated with GST-Rhotekin-RBD-bead suspension for 45 min at 4 °C. The level of GTP-bound RhoA in each fraction was identified by western blotting with an anti-RhoA antibody. **(A)** The expression of recombinant proteins in the whole cell lysates (WCL). GAPDH was used to assess equal loading of samples across the wells in the total whole cell lysate. **(B)** Total proteins levels in each fraction are shown in the bottom 4 panels along with the level of endogenous RhoA. The GTP-bound RhoA in each fraction are shown in the top panel. Hsp56 and Histone H3 were used as cytoplasmic and nuclear-enriched markers, respectively. The western blot shown is representative of three independent experiments. **WCL:** whole cell lysate; **C:** cytoplasmic compartment; **N:** nuclear-enriched compartment.

8.3.4.2 Subcellular localization of RhoGDI-3's inhibitory activity on Rac1 and RhoH

RhoGDI-3 was shown to bind to Rac1 only in the cytoplasm, (section 8.2.2.1) while it forms complexes with RhoH in both the cytoplasmic and nuclear-enriched compartment (section 8.2.2.2). The data for RhoA suggest that RhoGDI-3 might negatively regulate the activity of both Rac1 and RhoH at the site of interaction. This hypothesis was investigated using effector pull-down assays utilizing GST-PAK1-GBD to identify the GTP-bound fractions of Rac1 and RhoH.

~40 h post-transfection, cells were harvested and fractionated into cytoplasmic and nuclear-enriched fractions with buffer containing GST-PAK1-PBD. The lysates were then incubated with glutathione sepharose beads for 45 min. The levels of GTP-bound Rac1 and RhoH in each fraction were determined by western blotting with anti-Rac1 or anti-V5 antibodies.

The data in Figure 8.22 shows that Rac1 was active in both the cytoplasmic and nuclear-enriched fractions. Co-expression with RhoGDI-3 decreased the GTP-bound Rac1 in the cytoplasm. The level of Rac1 in the nuclear-enriched fraction is substantially decreased in cells expressing RhoGDI-3 but this pool of nuclear Rac1 appears to be relatively active.

RhoH alone was active in both the cytoplasmic and nuclear-enriched compartments (Figure 8.23). However, co-expression with RhoGDI-3 decreased RhoH total proteins and GTP-bound levels in both compartments. These data suggest a dual nuclear and cytoplasmic role for RhoGDI-3 in maintaining RhoH in the inactive GDP-bound form in both compartments.

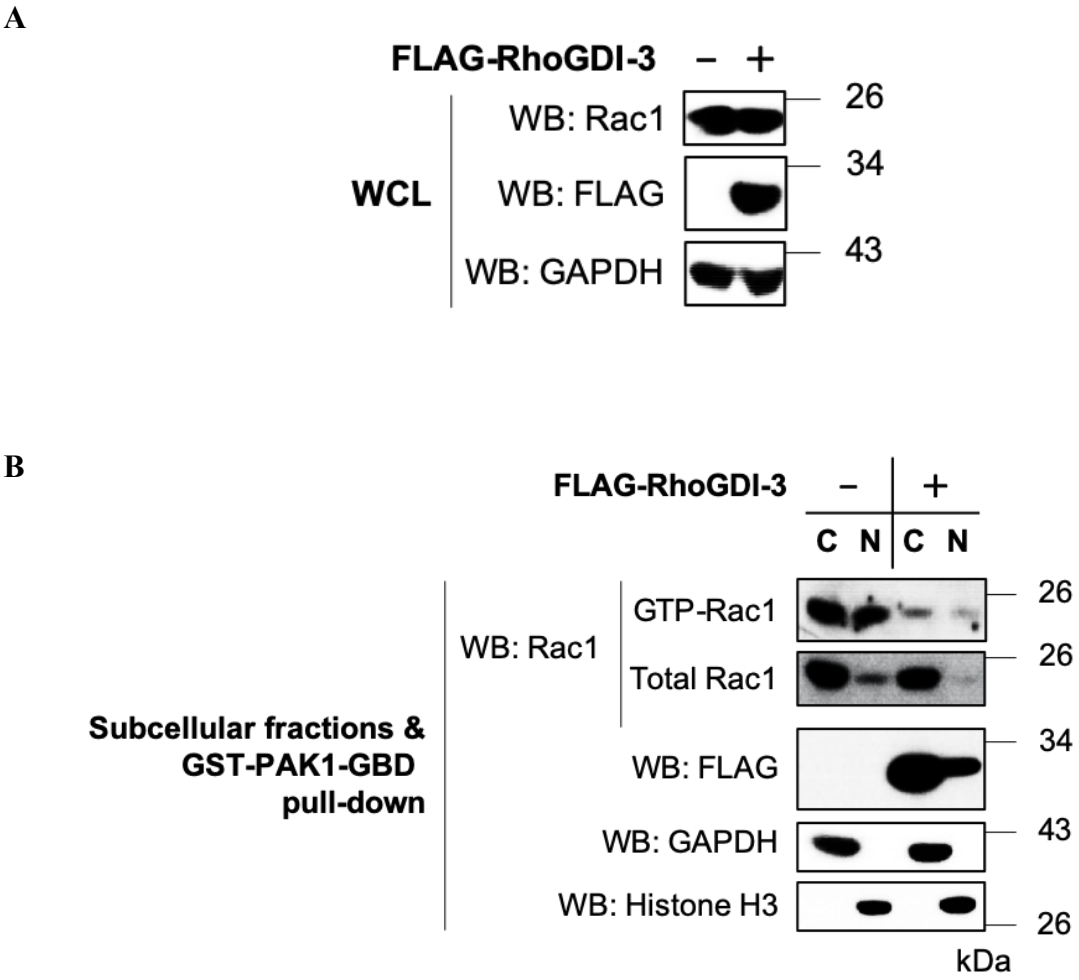

Figure 8.22: The site of action of RhoGDI-3 towards Rac1. HEK293T cells were transfected with FLAG-RhoGDI-3 and allowed to express for ~24 h before serum starvation overnight. ~40 h post-transfection, cells were fractionated into cytoplasmic and nuclear-enriched fractions in buffer containing GST-PAK1-GBD. Each of the fractions was incubated with glutathione sepharose beads. The levels of GTP-bound Rac1 in both the fractions were determined by western blotting with anti-Rac1 antibody. **(A)** The expression of recombinant proteins in the whole cell lysates (WCL). GAPDH was used to assess equal loading of samples across the wells in the total whole cell lysate. **(B)** Total proteins in each fraction are shown in the bottom 4 panels along with the level of endogenous Rac1. The GTP-bound Rac1 in each fraction are shown in the top panel. GAPDH and Histone H3 were used as cytoplasmic and nuclear-enriched markers, respectively. The western blot shown is representative of three independent experiments. **WCL:** whole cell lysate; **C:** cytoplasmic compartment; **N:** nuclear-enriched compartment.

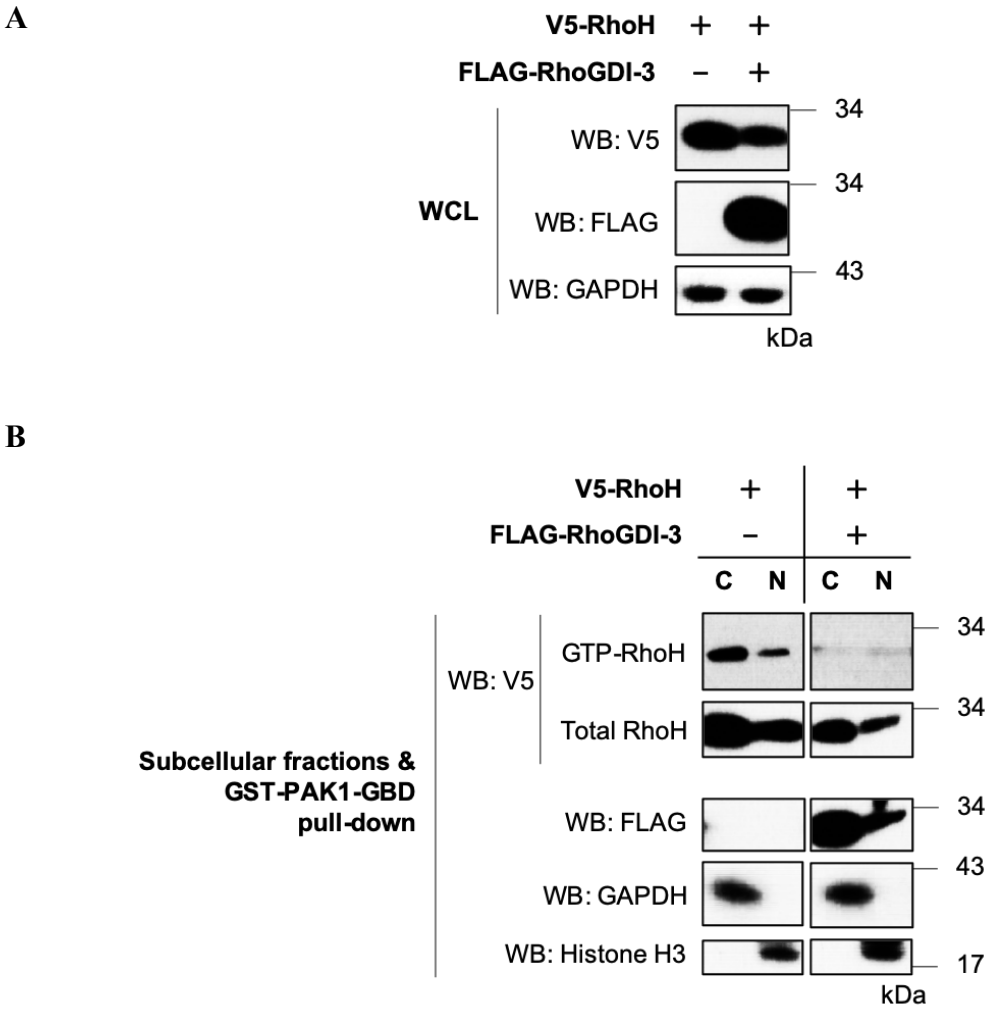

Figure 8.23: The site of action of RhoGDI-3 towards RhoH. FLAG-RhoGDI-3 was transfected alone or with V5-RhoH. Constructs were allowed to express for ~24 h before serum starvation overnight. ~40 h post-transfection, cells were fractionated into cytoplasmic and nuclear-enriched fractions in buffer containing GST-PAK1-GBD. Each of the fractions was incubated with glutathione sepharose beads. The levels of GTP-bound RhoH in both the fractions were determined by western blotting with anti-V5 antibody. **(A)** The expression of recombinant proteins in the whole cell lysates (WCL). GAPDH was used to assess equal loading of samples across the wells in the total whole cell lysate. **(B)** Total proteins in each fraction are shown in the bottom 4 panels, while the GTP-bound RhoH in each fraction are shown in the top panel. GAPDH and Histone H3 were used as cytoplasmic and nuclear-enriched markers, respectively. The western blot shown is representative of two independent experiments. **WCL:** whole cell lysate; **C:** cytoplasmic compartment; **N:** nuclear-enriched compartment.

8.4 The role of the N-terminus of RhoGDI-3 in regulating its functions

The first 22 amino acids of RhoGDI-1 were shown to regulate the binding with its targets, while deletions of the first 45 or 60 residues completely abolished both binding to target proteins and its GDI activity (Nomanbhoy and Cerione, 1996). These data hence indicate a role for the N-terminus regulatory arm of the RhoGDI in regulating binding to their targets. RhoGDI-3 has an additional 26 amino acids at its N-terminus that has been shown to stabilise the RhoG-RhoGDI-3 complex (Brunet *et al.,* 2002). However, no study has been undertaken to identify the role for this amino-terminal extension in regulating RhoGDI-3 inhibitory function. Therefore, to further investigate the involvement of the N-terminus of RhoGDI-3 in mediating the interaction and activation status of its binding partner, Rac1, co-immunoprecipitation and effector pull-down assay were performed by utilizing the ΔNRhoGDI-3 construct (section 5.2).

Briefly, cells were transfected with FLAG-ΔNRhoGDI-3 or FLAG-wtRhoGDI-3 and allowed to express for ~24 h before serum starvation overnight. Cells were harvested and either immunoprecipitated with anti-FLAG antibody cross-linked to Protein G Dynabeads or precipitated with GST-PAK1-GBD and glutathione sepharose beads, ~40 h post-transfection. Co-immunoprecipitated Rac1 and GTP-bound Rac1 were identified by western blotting with anti-Rac1 antibody. The Rac1-ΔNRhoGDI-3 binding ratio was quantified with ImageJ and compared to the wt.

Analysis of the data by densitometry indicate that the ΔNRhoGDI-3 potentially binds Rac1 less effectively than the wt (Figure 8.24A). There is no difference in the GTP levels of Rac1 (Figure 8.24B) when co-expressed with either wt or N-terminally truncated RhoGDI-3, suggesting that the N-terminus of RhoGDI-3 is not involve with the inhibitory function of RhoGDI-3.

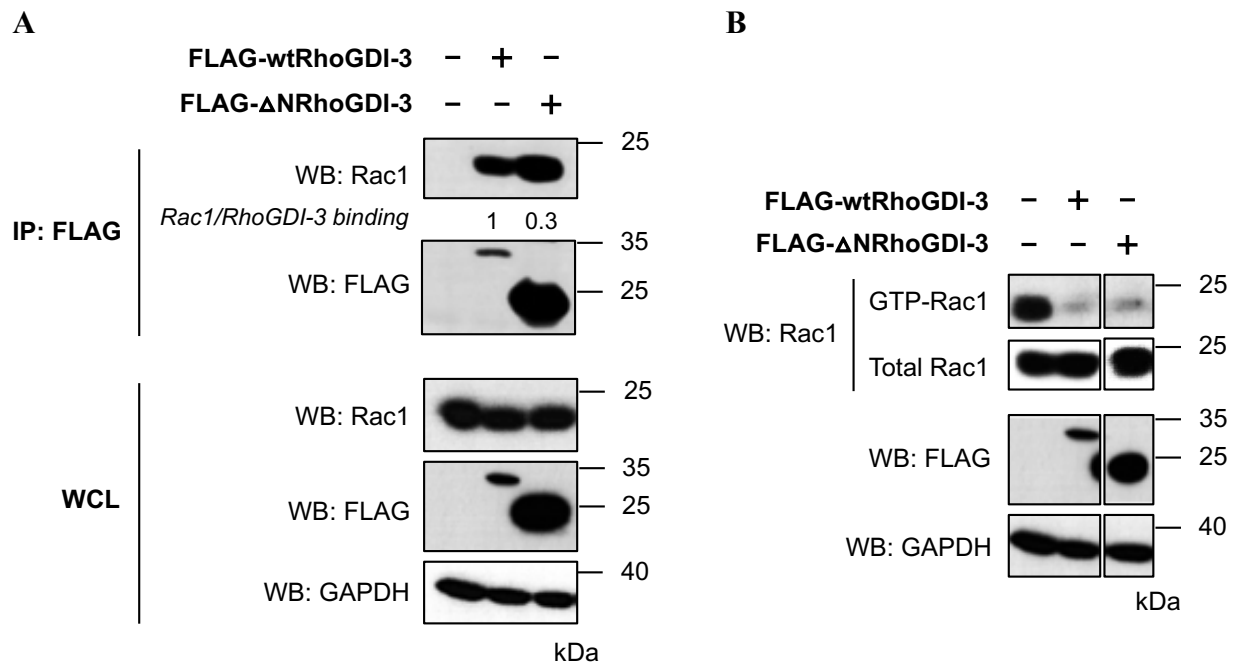

Figure 8.24: The role of N-terminus of RhoGDI-3 in regulating the binding and activation status of Rac1. HEK293T cells were transfected with FLAG-ΔNRhoGDI-3 or with FLAG-wtRhoGDI-3 and allowed to express for ~24 h before serum starvation overnight. ~40 h post-transfection, cells were harvested and proceed to **(A)** immunoprecipitation with anti-FLAG antibody cross-linked to Protein G Dynabeads or **(B)** precipitated with GST-PAK1-GBD and glutathione sepharose beads for ~45 min at 4 °C. Co-immunoprecipitated Rac1 and the levels of GTP-bound Rac1 were identified by western blotting with anti-Rac1 antibody. The expression of recombinant proteins in the whole cell lysate (WCL) is shown in the bottom 3 panels (left and right), along with the total levels of endogenous Rac1. The co-immunoprecipitated (IP) samples are shown in the top two panels in (A), while the GTP-bound Rac1 is shown in the top panel in (B). The Rac1-ΔNRhoGDI-3 binding ratio was quantified by ImageJ and compared to the wt. GAPDH was used to assess equal loading of samples across the wells in the total whole cell lysate**.** The western blot shown is representative of at least two independent experiments. **WCL:** Whole cell lysate. **(A)** Co-immunoprecipitation and **(B)** GST-PAK1-GBD pull-down.

8.5 Summary

Subcellular fractionation data in this study shows that RhoA and RhoC are only localized in the cytoplasm, while Rac1 and RhoH were found to be in both the cytoplasm and nuclear-enriched extracts. Co-expression with any of the RhoGDIs decreases the nuclear-enriched levels of Rac1, suggesting the ability for the RhoGDIs to sequester Rac1 in the cytoplasm and prevent its nuclear targeting.

Both RhoGDI-1 and -2 bind to and negatively regulate their target, Rac1 exclusively in the cytoplasm despite Rac1 being present in both the cytoplasmic and nuclear-enriched compartments. This is the first observation on the subcellular location of the RhoGDI-2-Rac1 complex.

RhoGDI-3 was found to interact with RhoA and RhoC only in the cytoplasm although RhoGDI-3 was found in both the cytoplasmic and nuclear-enriched compartments, and this was due to exclusive cytoplasmic distribution of both RhoA and RhoC. Rac1 was found to interact with RhoGDI-3 in the cytoplasm despite both Rac1 and RhoGDI-3 being located in both the cytoplasmic and nuclear-enriched fractions. Furthermore, RhoGDI-3 has been shown here to exert its inhibitory activity towards RhoA and Rac1 in the cytoplasm and this does not involve the extra 26 residues at the N-terminus of RhoGDI-3.

Interestingly, RhoGDI-3 has been shown to interact and negatively regulate the activity of RhoH in both the cytoplasmic and nuclear-enriched fractions. RhoH was assumed to be a GTPase defective Rho-family protein due to lack of Gly12, Ala59 and Gln61 (Ras numbering) (Table 1.7), shared by the typical Rho-family GTPases. These data hence suggest a novel role for RhoGDI-3 protein to interact with its target protein, RhoH in the nucleus and maintaining it in the inactive GDP-bound form.

Chapter 9

The effect of ACK on RhoGDI functions

As ACK has been demonstrated to be involved in cancer progression (Mahajan and Mahajan, 2014), it was hypothesized that the interaction between the RhoGDIs and ACK could modulate RhoGDI function as regulator of Rho-family GTPases, which are implicated in many oncogenic processes.

Since ACK has been shown to facilitate the degradation of RhoGDI-3 (section 6.2), this would result in less RhoGDI-3 available to bind to its target proteins and subsequently alter their activation status. For RhoGDI-1 and -2, any effect of ACK on their activity towards their target proteins must be through an alternative mechanism.

9.1 The effect of ACK on the binding of RhoGDI-1 and -2 to Rac1

To investigate the functional consequences of ACK on the ability of RhoGDI-1 and -2 to form complexes with their targets, co-immunoprecipitation assays were performed. Briefly, cells were transfected with His-RhoGDI-1 and His-RhoGDI-2 either alone or together with increasing amounts of HA-ACK (0.5 to 5 μg). Cells were then harvested and lysed, ~40 h post-transfection. The lysates were precipitated with cobalt-coated magnetic beads for ~1 h at 4°C. The presence of endogenous Rac1 in co-immunoprecipitated samples was determined by western blotting using an anti-Rac1 antibody. The ability of both RhoGDI-1 and -2 to bind to Rac1 in the presence or absence of ACK was quantified with ImageJ.

Figure 9.1A shows the levels of Rac1 bound to RhoGDI-1 significantly decreased with increasing amounts of ACK. However, this could be due to low levels of RhoGDI-1, which is contrast to the data presented in section 6.1.

ACK seemed not to significantly affect the binding between Rac1 and RhoGDI-2 (Figure 9.1B). Similarly to RhoGDI-1, RhoGDI-2 proteins levels also shown to decrease in the presence of ACK.

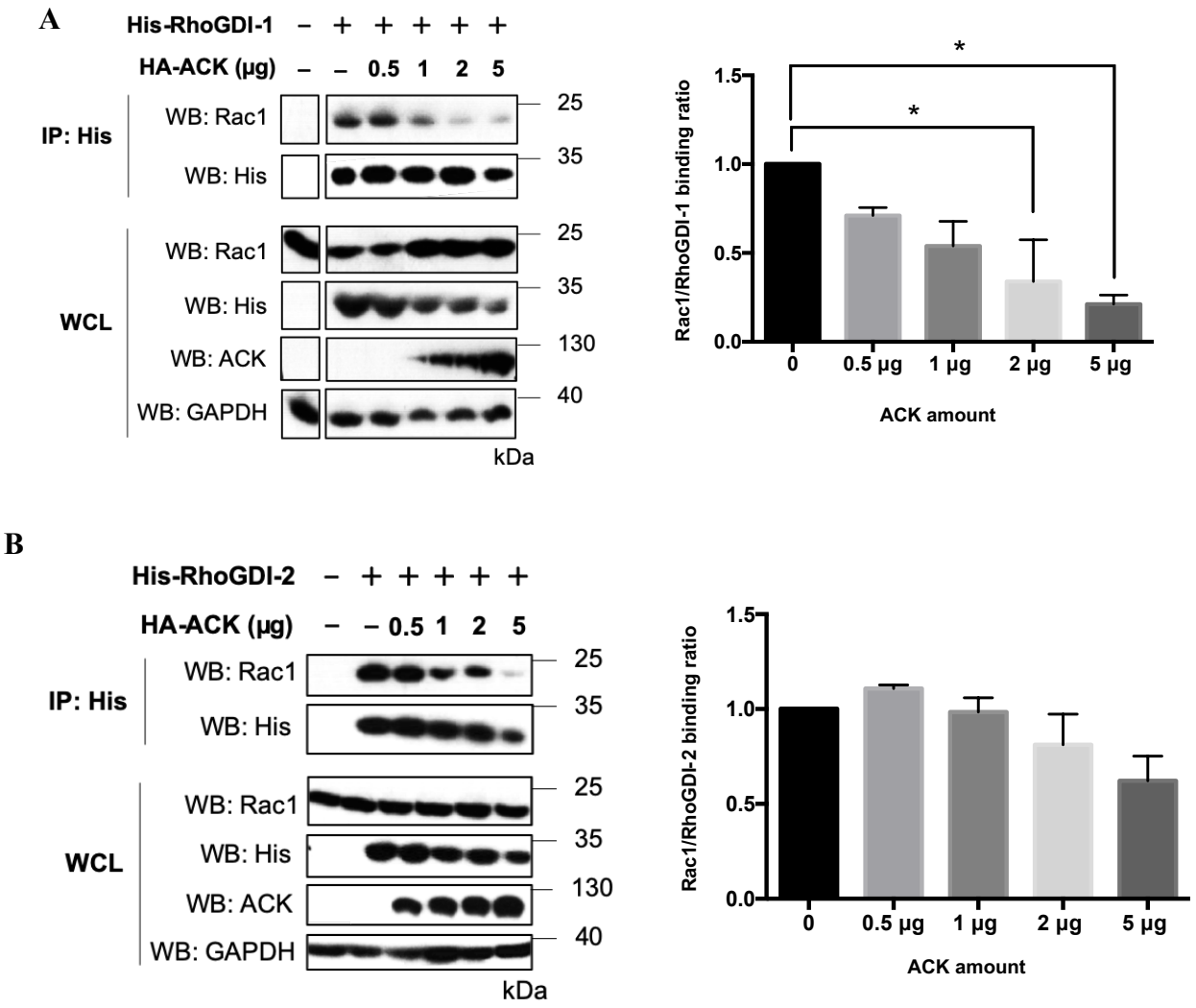

Figure 9.1: The effect of ACK on the binding of RhoGDI-1 and -2 to Rac1. HEK293T cells were transfected with His-RhoGDI-1 or His-RhoGDI-2 alone, or with 0.5 to 5 μg HA-ACK and allowed to express for ~40 h. Cells were then harvested and lysed before precipitated with cobalt coated magnetic beads for ~1 h at 4 °C. Co-immunoprecipitated Rac1 was identified by western blotting with an anti-Rac1 antibody. The co-immunoprecipitated (IP) samples are shown in the top two panels, while the expression of recombinant proteins in the whole cell lysate (WCL) is shown in the bottom 4 panels, along with the total levels of endogenous Rac1. The binding of Rac1 to each RhoGDIs in the presence of ACK was quantified with ImageJ and normalised to cells expressing RhoGDI alone. GAPDH was used to assess equal loading of samples across the wells in the total whole cell lysate**.** The relative amounts are shown as average values ± SEM of three independent experiments, *p≤ 0.05. **WCL:** whole cell lysate; **IP:** immunoprecipitation. **(A)** RhoGDI-1 and **(B)** RhoGDI-2.

9.2 The effect of ACK on the binding of RhoGDI-3 to its targets

Previously, RhoGDI-3 protein levels were shown to reduce when co-expressed with ACK, which would result in less RhoGDI-3 available for binding with its target proteins. This would potentially alter the activation of any unbound Rho-family GTPases targets of RhoGDI-3.

To formally investigate this hypothesis, co-immunoprecipitation was performed by expressing FLAG-RhoGDI-3 alone or with V5-RhoH or HA-ACK in HEK293T cells. Constructs were allowed to express for ~40 h before being harvested and lysed. The lysates were then immunoprecipitated with beads cross-linked to an anti-FLAG antibody for ~1 h at 4 °C. The presence of V5-RhoH, endogenous Rac1 and RhoA in co-immunoprecipitated samples were identified by western blotting.

The levels of RhoGDI-3 decrease when co-expressed with ACK as seen in previous results (section 6.2). Interestingly, the levels of RhoH also decreased in the presence of RhoGDI-3 alone and decreased even more when ACK and RhoGDI-3 were co-expressed (Figure 9.2C). The amount of RhoA (Figure 9.2A), Rac1 (Figure 9.2B) and RhoH (Figure 9.2C) co-immunoprecipitated were also reduced, presumably due to the reduced levels of RhoGDI-3 in the presence of ACK.

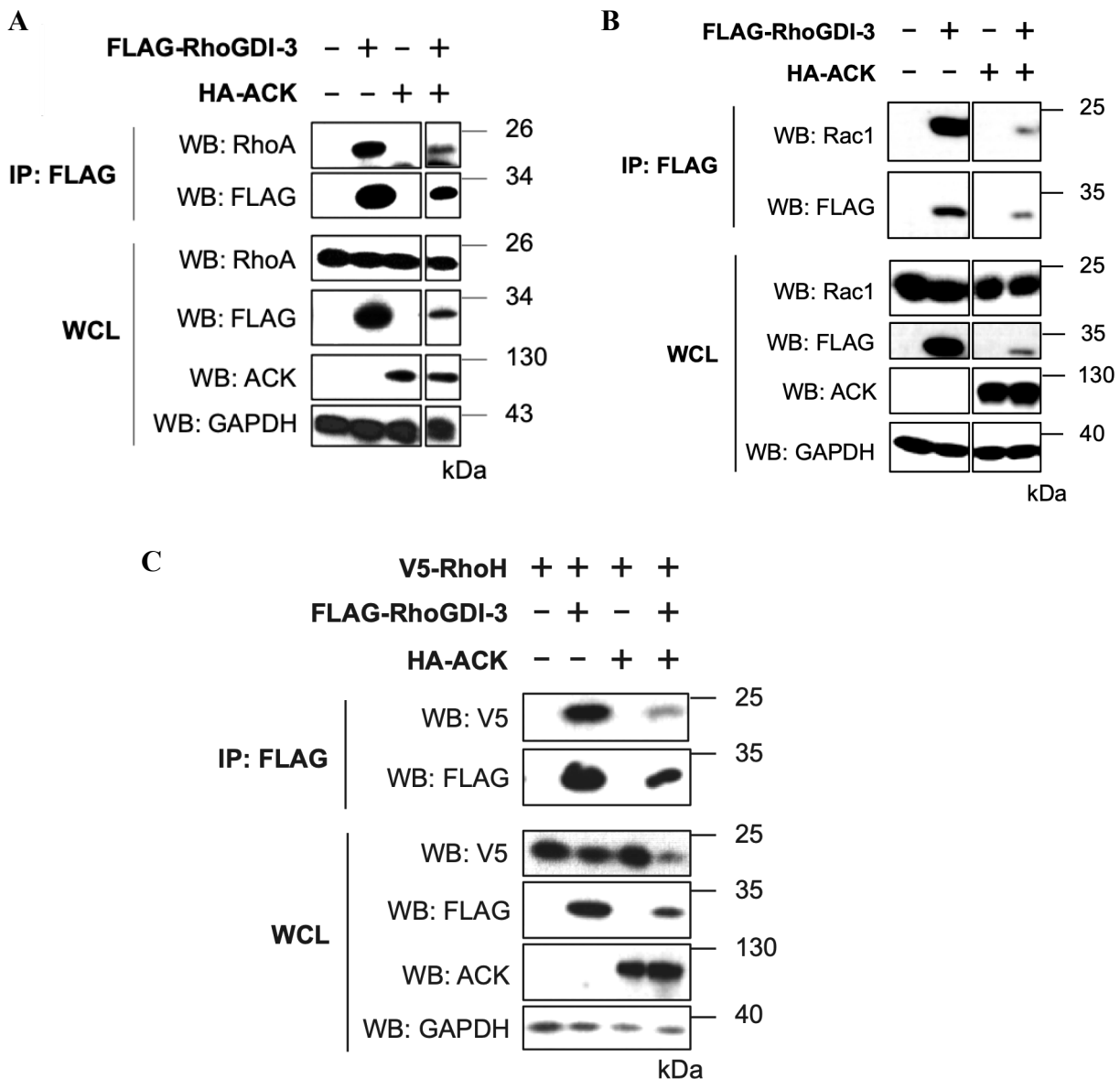

Figure 9.2: The effect of ACK on the binding of RhoGDI-3 to its targets. HEK293T cells were transfected with FLAG-RhoGDI-3 alone or with V5-RhoH and/or HA-ACK. ~40 h post-transfection, cells were harvested, lysed and immunoprecipitated with beads cross-linked to an anti-FLAG antibody for ~1 h at 4 °C. Co-immunoprecipitated RhoA, Rac1 and RhoH were identified by western blotting with anti-RhoA, anti-Rac1 or anti-V5 antibodies, respectively. The co-immunoprecipitated (IP) samples are shown in the top two panels, while the expression of recombinant proteins in the whole cell lysate (WCL) is shown in the bottom 4 panels, along with the total levels of endogenous RhoA and Rac1. GAPDH was used to assess equal loading of samples across the wells in the total whole cell lysate**.** The western blot shown is a representative of at least two independent experiments. **WCL:** whole cell lysate; **IP:** immunoprecipitation. **(A)** RhoA, **(B)** Rac1 and **(C)** RhoH.

9.3 The effect of ACK on the GTP levels of RhoGDI target proteins

9.3.1 The effect of ACK on the GTP levels of RhoGDI-1 and -2 targets

To identify the consequences of exogenous expression of ACK on the activation status of RhoGDI-1 and -2 binding partner, Rac1, a PAK1-GBD pull-down assay was conducted. The results are shown in Figure 9.3.

Cells transfected with either RhoGDI-1 (Figure 9.3A) or RhoGDI-2 (Figure 9.3B) show low levels of GTP-bound Rac1, whereas cells expressing ACK alone have similar levels of Rac1•GTP to control cells. There was no difference in the GTP levels of Rac1 when RhoGDI-1 and ACK were co-expressed compared to RhoGDI-1 alone (Figure 9.3A), suggesting that ACK does not regulate the activation of Rac1 through RhoGDI-1. Co-expression of RhoGDI-2 and ACK increased Rac1•GTP levels marginally, however, this effect probably due to low levels of RhoGDI-2 in the presence of ACK.

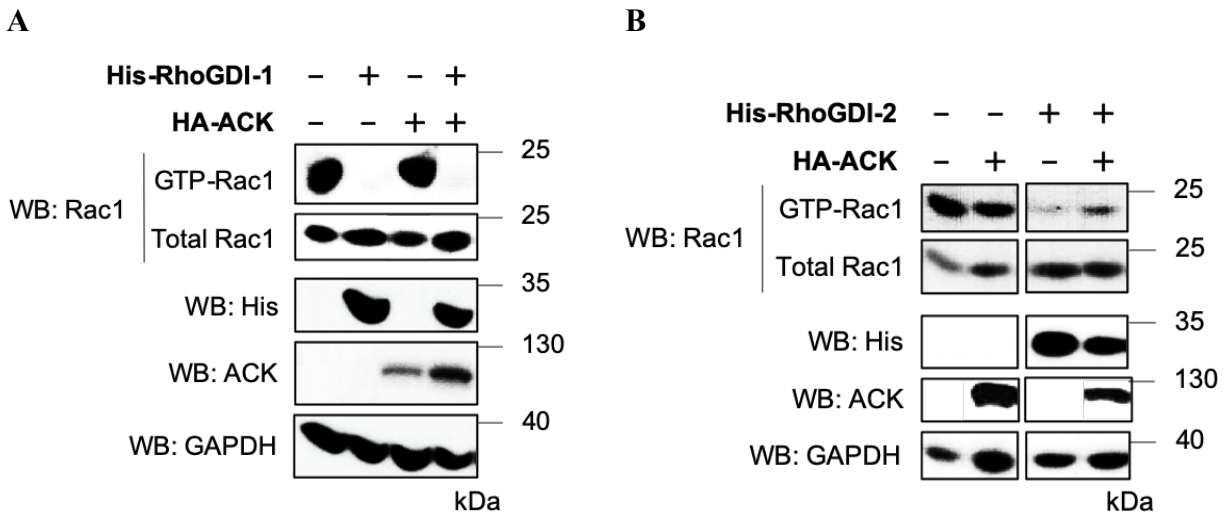

Figure 9.3: The effect of ACK on the GTP levels of RhoGDI-1 and -2 target, Rac1. HEK293T cells were transfected with His-RhoGDI-1 or -2 alone or with HA-ACK and allowed to express for ~24 h before serum starvation overnight. ~40 h post-transfection, cells were harvested, lysed in buffer containing GST-PAK1-GBD and precipitated with glutathione sepharose beads. The levels of GTP-bound Rac1 were determined by western blotting with anti-Rac1 antibody. The expression of recombinant proteins in the whole cell lysates (WCL) is shown in the bottom 4 panels along with the total level of endogenous Rac1, while the levels of GTP-bound Rac1 are shown in the top panels. GAPDH was used to assess equal loading of samples across the wells in the total whole cell lysate**.** The western blot shown is a representative of three independent experiments. **WCL:** whole cell lysate. **(A)** RhoGDI-1 and **(B)** RhoGDI-2

9.3.2 The effect of ACK on the GTP levels of RhoGDI-3 targets

Previous data in section 9.2 demonstrated that ACK expression results in decreased binding of RhoGDI-3 to its target proteins. Thus, it was hypothesized that any unbound small GTPase targets of RhoGDI-3 will be free to be membrane-bound and activated. To investigate this, the effect of ACK on the activation of RhoGDI-3 target proteins: RhoA, RhoB, Rac1 and RhoH was assessed.

9.3.2.1 The effect of ACK on the GTP levels of RhoGDI-3 targets, RhoA and RhoB

To investigate the effect of ACK on the activation of RhoGDI-3 binding targets, HEK293T cells were transfected with RhoGDI-3 alone or with HA-ACK. GTP-bound RhoA and RhoB were identified by effector pull-down assays utilizing GST-Rhotekin-RBD and western blotting.

The overall level of RhoA was unaffected following co-expression with RhoGDI-3 or ACK (Figure 9.4A). GTP-bound RhoA was slightly lower in cells expressing ACK and decreased prominently with RhoGDI-3, compared to the control. However, RhoA GTP levels were seen to increase in cells co-expressing ACK and RhoGDI-3 compared to RhoGDI-3 alone, suggesting that ACK can counteract at least some of the inhibitory effect of RhoGDI-3 towards RhoA.

In contrast, total levels of RhoB increased in the presence of exogenous RhoGDI-3 or ACK, either alone or in combination (Figure 9.4B). In contrast, GTP-bound RhoB was shown to decrease in the presence of either RhoGDI-3 or ACK alone or when co-expressed together.

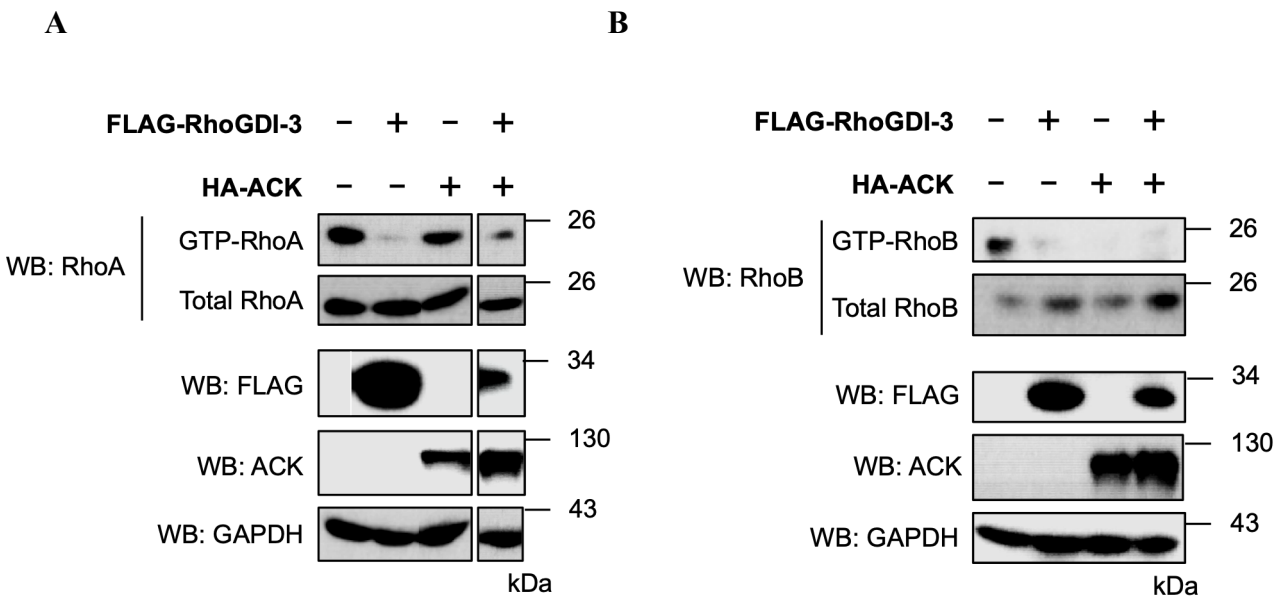

Figure 9.4: The effect of ACK on the GTP levels of the RhoGDI-3 targets, RhoA and RhoB. HEK293T cells were transfected with FLAG-RhoGDI-3 alone or with HA-ACK and allowed to express for ~24 h before serum starvation, overnight. Cells were harvested and lysed, ~40 h post-transfection. The lysates were precipitated with GST-Rhotekin-RBD-bead suspension. The levels of GTP-bound RhoA and RhoB were determined by western blotting with anti-RhoA and anti-RhoB, respectively. The expression of recombinant proteins in the whole cell lysates (WCL) is shown in the bottom 4 panels along with the total levels of endogenous RhoA and RhoB, while the GTP-bound proteins in pull-down samples are shown in the top panels. GAPDH was used to assess the equal loading of samples across the wells in the total cell lysates. The western blot shown is representative of at least two independent experiments. **(A)** RhoA and **(B)** RhoB.

These data suggest that ACK differentially regulates the activation of RhoGDI-3 target proteins, which are known to act synergistically in promoting cancer progression. RhoA is predominantly pro-proliferative (Zohn *et al.,* 1998; Orgaz *et al.,* 2014), while RhoB action is generally anti-proliferative (Chen *et al.,* 2000). Thus, difference regulation of ACK on these Rho subfamily proteins might therefore promote ACK oncogenic properties.

9.3.2.2 The effect of ACK on the GTP levels of RhoGDI-3 targets, Rac1 and RhoH

The effect of ACK and RhoGDI-3 co-expression on the activation status of Rac1 and RhoH were also determined by GST-PAK1-GBD pull-down assays.

The total levels of Rac1 protein was unaffected in the presence of either RhoGDI-3 or ACK alone or when both proteins together (Figure 9.5A). Rac1 was active in control cells but levels decreased with ACK alone and decreased substantially more with RhoGDI-3 alone. Co-expression of ACK and RhoGDI-3 showed Rac1•GTP levels similar to ACK alone, suggesting that ACK counteract the inhibitory effect of RhoGDI-3.

Data in Figure 9.5B shows the total levels of RhoH decreased in the presence of RhoGDI-3 but decreased even more when co-expressed with ACK, as seen previously. Compared to the control, RhoH•GTP levels decreased in the presence of RhoGDI-3 but increased with ACK. Cells expressing both ACK and RhoGDI-3 show high amount of GTP-bound RhoH compared to RhoGDI-3 alone, suggesting that ACK can counteract the inhibitory activity of RhoGDI-3 towards RhoH.

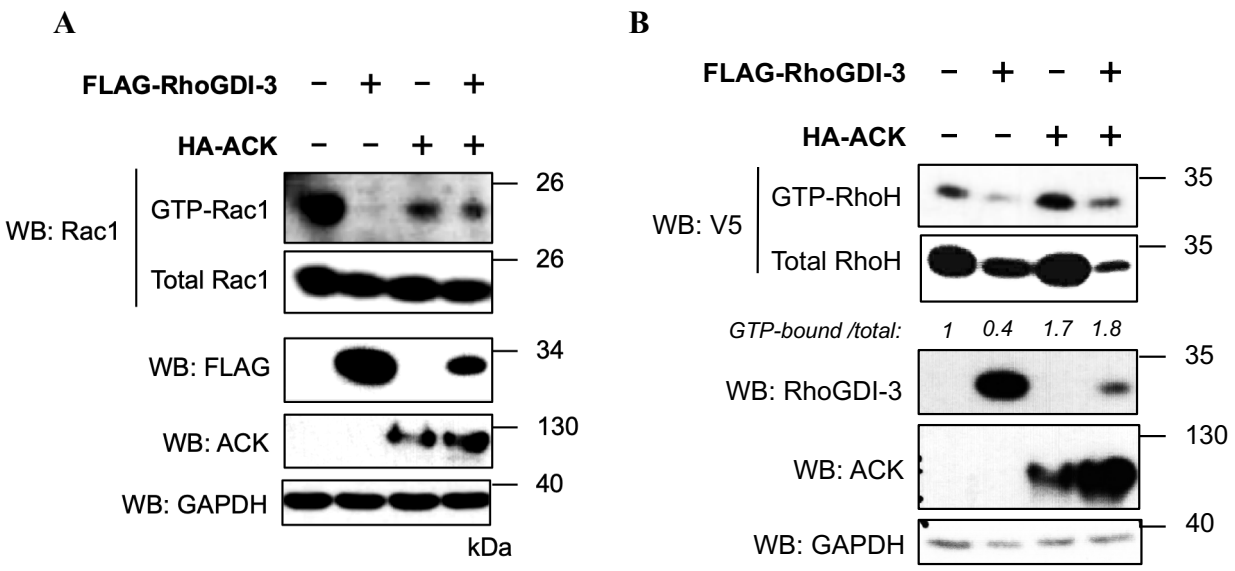

Figure 9.5: The effect of ACK on the GTP levels of RhoGDI-3 targets, Rac1 and RhoH. HEK293T cells were transfected with FLAG-RhoGDI-3 alone or with V5-RhoH and/or HA-ACK. Constructs were allowed to express for ~24 h before serum starvation overnight. Cells were then harvested and lysed in buffer containing GST-PAK1-GBD, ~40 h post-transfection. The lysates were incubated with glutathione sepharose beads, washed and eluted. The levels of GTP-bound Rac1 and RhoH were determined by western blotting with anti-Rac1 or anti-V5 antibodies. The expression of recombinant proteins in the whole cell lysates (WCL) is shown in the bottom 4 panels along with the total level of endogenous Rac1, while the GTP-bound proteins in pull-down samples are shown in the top panels. The amounts of total and GTP-bound Rho-family GTPases were analysed by densitometry using Image J and compared to the control. The western blot shown is representative of three independent experiments. **WCL:** whole cell lysate. **(A)** Rac1 and **(B)** RhoH.

9.4 The effects of ACK and RhoGDI-3 on the subcellular pools of GTP-bound Rac1 and RhoH

Rho-family GTPases have been found to localize to and regulate various functions in the nucleus. For instance, nuclear accumulation of Rac1 is shown to maintain the balance between Rac1-RhoA cellular activity and control cell morphology and invasiveness (Ohta *et al.,* 2006; Chauhan *et al.,* 2011). A pool of active Rac1 in the nucleus is needed to regulate actin polymerization in the nucleus (Navarro- Lérida *et al.,* 2015).

Previous data described in section 8.2.2.1 and 8.3.4.2 show the ability of RhoGDI-3 to interact with, sequestered and negatively regulate Rac1 activation in the cytoplasm. Since ACK was shown to increase Rac1•GTP levels, it is possible that ACK inhibits the sequestering ability of RhoGDI-3 towards Rac1 and therefore promotes its activation in the nucleus. RhoGDI-3 was also shown to interact and decreased the GTP levels of RhoH in both cytoplasmic and nuclear-enriched fractions (sections 8.2.2.2 and 8.3.4.2). When co-expressed with ACK, RhoH•GTP levels were found to increase compared to RhoGDI-3 alone, suggesting that ACK could promote the activation of RhoH in both cytoplasmic and nuclear-enriched compartments. To test these hypotheses, subcellular fractionations and effector pull-down assays were conducted.

As shown in Figure 9.6, the nuclear-cytoplasmic ratio of Rac1 was decreased in cells expressing RhoGDI-3 alone, compared to the control. GTP-bound Rac1 was also seen to decrease considerably in the cytoplasm of RhoGDI-3-transfected cells, indicating that RhoGDI-3 exerts its inhibitory activity towards Rac1 mainly in the cytoplasm. In contrast, Rac1 was able to retain its nuclear localization in the presence of ACK alone but the nuclear-cytoplasmic ratio was still slightly lower compared to the control. The GTP-levels of Rac1 were also seen to decrease in both compartments of cell expressing ACK alone but more prominently in the nucleus. Co-expression of ACK and RhoGDI-3 increased Rac1 nuclear levels partially, suggesting that ACK has the ability to counteract the sequestering ability of RhoGDI-3 towards Rac1, at least partially. However, Rac1•GTP levels were found to increase primarily in the cytoplasm compared to the nucleus-enriched fractions. These data suggest that ACK inhibit the GDI function of RhoGDI-3 towards Rac1 activation mainly in the cytoplasm.

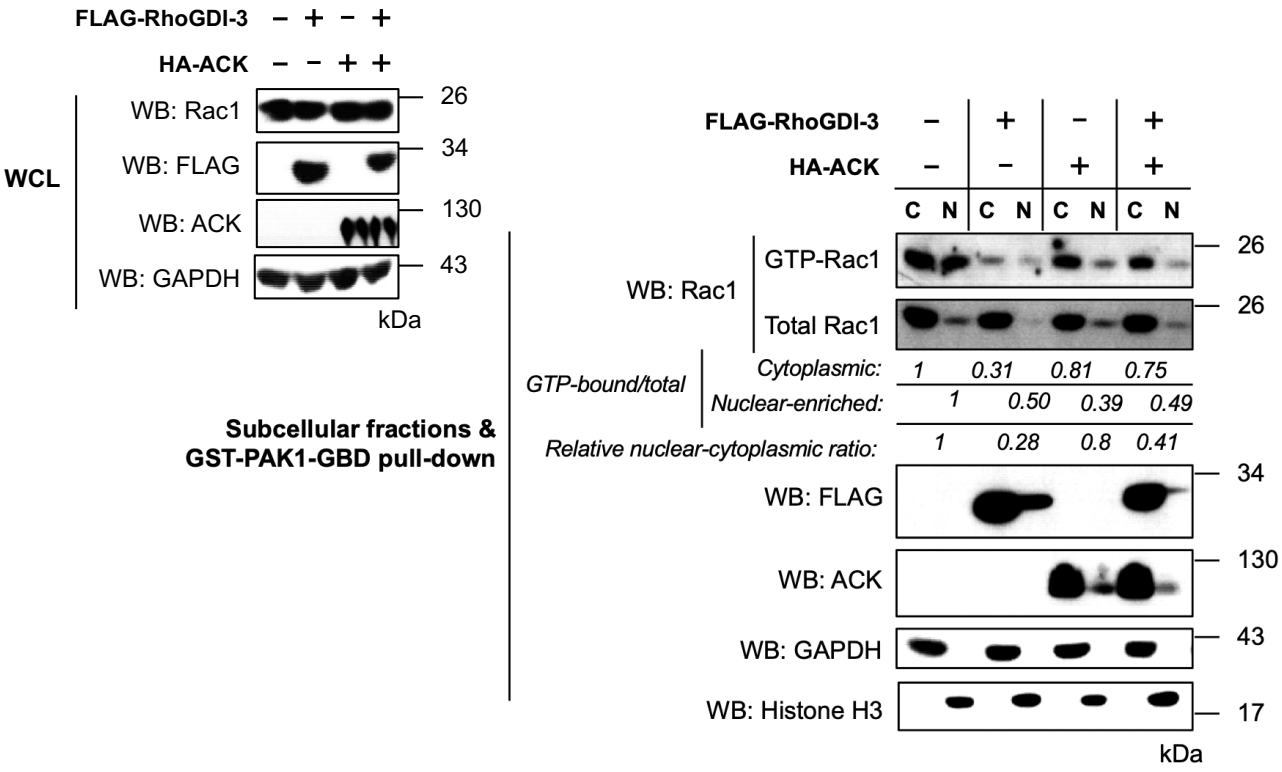

Figure 9.6: The effects of ACK on the subcellular pools of GTP-bound Rac1. HEK293T cells were transfected with FLAG-RhoGDI-3 or HA-ACK alone, or with both proteins. Constructs were allowed to express for ~24 h before serum starvation overnight. Cells were harvested and fractionated into cytoplasmic and nuclear-enriched fractions in buffer containing GST-PAK1-GBD, ~40 h post-transfection. Cells were then incubated with glutathione sepharose beads for 45 min. The levels of GTP-bound Rac1 in both the fractions were determined by western blotting with an anti-Rac1 antibody. The expression of recombinant proteins in the whole cell lysates (WCL) is shown in top left**,** while total proteins in each fraction are shown in the bottom 5 panels along with the level of endogenous Rac1. The level of GTP-bound Rac1 in each fraction is shown in the top right panel. GAPDH was used to assess equal loading of samples across the wells in the total whole cell lysate and used as a cytoplasmic marker**.** Histone H3 was used as a nuclear-enriched marker. The western blot shown is representative of three independent experiments. **WCL:** whole cell lysate; **C:** cytoplasmic compartment; **N:** nuclear-enriched compartment.

Figure 9.7 shows total levels of RhoH decreased with RhoGDI-3 alone but decreased even more when co-expressed with ACK, as seen previously. Less GTP-bound RhoH was also observed in both the cytoplasmic and nuclear-enriched fractions when expressing RhoGDI-3 alone compared to the control. Meanwhile, RhoH total protein and GTP levels were shown to increase in both

compartments in the presence of ACK alone. Although co-expression of ACK and RhoGDI-3 decreased RhoH total protein, the ratio of RhoH•GTP levels in both compartments increased substantially.

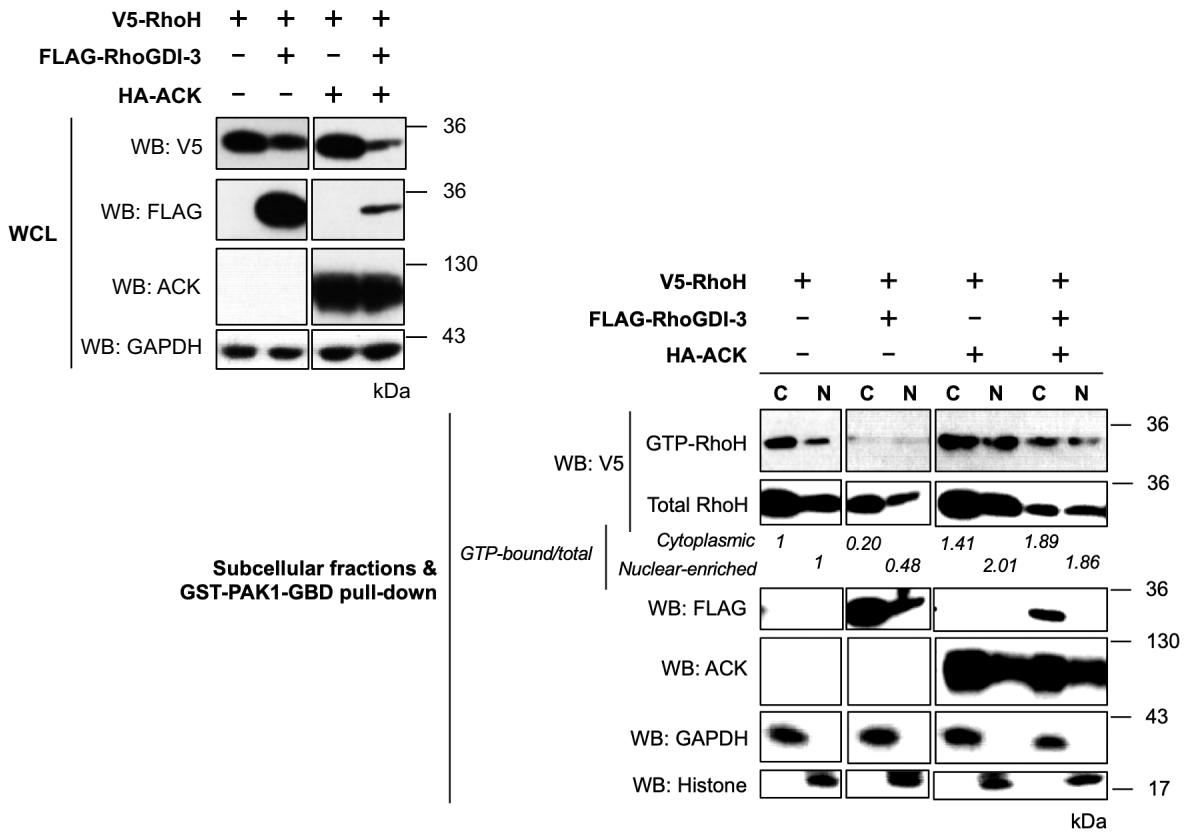

Figure 9.7: The effects of ACK on the subcellular pools of GTP-bound RhoH. HEK293T cells were transfected with V5-RhoH alone or together with FLAG-RhoGDI-3 and/or HA-ACK Constructs were allowed to express for ~24 h before serum starvation overnight. Cells were harvested and fractionated into cytoplasmic and nuclear-enriched fractions in buffer containing GST-PAK1-GBD, ~40 h post-transfection. Cells were then incubated with glutathione sepharose beads. The levels of GTP-bound RhoH in both the fractions were determined by western blotting with an anti-V5 antibody. The expression of recombinant proteins in the whole cell lysates (WCL) is shown in top left**,** while total proteins in each fraction are shown in the bottom 5 panels. The GTP-bound RhoH in each fraction are shown in the top right panel. GAPDH was used to assess equal loading of samples across the wells in the total whole cell lysate and used as a cytoplasmic marker**.** Histone H3 was used as a nuclear-enriched marker. The western blot shown is representative of two independent experiments. **WCL:** whole cell lysate; **C:** cytoplasmic compartment; **N:** nuclear-enriched compartment.

9.5 Summary

Data presented here shows that low levels of RhoGDIs in the presence of ACK resulted in a decreased binding between RhoGDIs and their targets. The levels of the RhoGDI-1-Rac1 complex decreased significantly with increasing amounts of transfected ACK. Conversely, ACK was shown to affect the formation of RhoGDI-2-Rac1 complex marginally. Both of these effects could be due to low levels of RhoGDI-1 and -2 seen in the presence of ACK. Furthermore, co-expression of RhoGDI-1, -2 and ACK did not increased Rac1 activation, suggesting that ACK might not regulate Rac1 activity through these two RhoGDIs.

ACK-mediated RhoGDI-3 degradation was found to decrease the RhoGDI-3 complexes with RhoA, Rac1 and RhoH, consistent with this was an increased in the GTP-bound levels of these Rho-family GTPases. In contrast, RhoB•GTP levels were shown to decrease in cells expressing RhoGDI-3 or ACK alone and also when both were co-expressed. These data suggest ACK differentially regulates the activation of these small G proteins. Furthermore, RhoB protein level was also found to increase in the presence of RhoGDI-3 or ACK alone and increased even more upon combination, suggesting a synergistic role for these proteins in stabilising RhoB.

Co-expression with ACK has been shown to reverse the sequestering ability of RhoGDI-3 towards Rac1 and promotes its activation predominantly in the cytoplasm. RhoH•GTP levels were also found to increase in both cytoplasmic and nuclear-enriched compartments when co-expressed RhoGDI-3 and ACK.

All the data described in this chapter suggest a role for ACK in cancer progression is potentially underpinned by its interaction with the RhoGDI protein and its effect on RhoGDI ability to regulate Rho-family proteins activity in various cellular compartments.

Chapter 10

Discussion and future directions

Through this study, all three RhoGDIs have been found to interact with ACK. Although the RhoGDI-ACK interactions were first investigated using exogenous proteins, the interaction between RhoGDI-1 and ACK was also confirmed using endogenous proteins. It was not possible to work with endogenous RhoGDI-2 and -3 due to the non-specificity of the available commercial antibodies. The interaction between endogenous ACK and RhoGDI-1 was detected in LNCaP cells. There is substantial evidence in the literature suggesting roles for ACK and the RhoGDIs in prostate cancer. ACK has been found to phosphorylate the AR at Tyr267 and promote AR recruitment to the ARE, resulting in the transcription of AR target genes in the absence of androgen, to drive prostate cancer progression (Mahajan *et al.,* 2007). Meanwhile, RhoGDI-1 has been shown to negatively regulate the AR signalling pathway by preventing AR nuclear translocation and inhibiting transactivation of AR target genes (Zhu *et al.,* 2013). These opposing functions of both proteins in regulating AR signalling would result in antagonistic effects especially on the transcription of AR target genes to drive prostate cancer progression. Thus, ACK may interact with RhoGDI-1 to prevent its association with the AR and hence promote the transactivation of AR target genes.

The cellular site of interaction of ACK with the RhoGDI was also determined in this study. Similarly to a previous study from Ahmed *et al.* (2004), ACK was found in both the cytoplasmic and nuclear-enriched fractions and this localisation was shown to be kinase-independent. ACK is known to have an NES towards its N-terminus, which facilitates nuclear export but how ACK enters the nucleus is still unknown. However, the interaction of ACK with Cdc42 may contribute to ACK's nuclear translocation (Ahmed *et al.,* 2004).

All three RhoGDIs have been found previously to localize in both the nucleus and cytoplasm (Marzouk *et al.,* 2007; Krieser and Eastman, 1999). However, their functional roles are more defined in the cytoplasm (Dovas and Couchman, 2005). RhoGDI-1 has been shown to bind and regulate ERα in MCF-7 cells, while N-terminally truncated RhoGDI-2 was shown to accumulate in the nucleus during apoptosis (Marzouk *et al.,* 2007; Krieser and Eastman, 1999). Despite these previous observations, in this study, both RhoGDI-1 and -2 were shown to be exclusively in the cytoplasm, under the conditions tested. This disparity is probably due to differences in the types of cells and growth conditions used in different studies. Furthermore, only the N-terminally truncated version of RhoGDI-2 has been found in the nucleus previously (Krieser and Eastman, 1999), whereas in this study, full-length RhoGDI-2 was analysed and was only identified in the cytoplasm.

In contrast, RhoGDI-3 was found in both the cytoplasmic and nuclear-enriched fractions in this work, which is consistent with previous findings that show RhoGDI-3 to associate with the nucleus, Golgi, plasma membrane and cytoskeleton (Adra *et al.,* 1997; de León-Bautista *et al.,* 2016; Brunet *et al.,* 2002; Zalcman *et al.,* 1996). This unique subcellular localization of RhoGDI-3 among the RhoGDIs has been assumed to involve the unique hydrophobic N-terminus of RhoGDI-3, which is predicted to contain a small additional amphipathic helix extending from residue 5 to 28. Brunet *et al.* (2002) demonstrated that the first 41 amino acids of RhoGDI-3 were involved in Golgi targeting. However, in results presented here, the first 26 amino acids of RhoGDI-3 were shown to be involved in the nuclear export of RhoGDI-3, consistent with prediction data that found a potential NES, spanning amino acids 14 to 21 (LELLRLAL) in RhoGDI-3. The nuclear targeting of RhoGDI-3 was initially reported by Adra *et al.* (1997), who found RhoGDI-3 to cluster around the nucleus, suggesting that this protein might be targeted to the nucleus (de León-Bautista *et al.,* 2016).

The role of RhoGDI-3 in the nucleus is still unknown. However, it has been hypothesised that RhoGDI-3 might regulate the activation of several Rho-family GTPases also found to reside in the nucleus, including RhoA, RhoB, RhoC, Rac1 and Rac3 (Adini *et al.,* 2003; Sandrock *et al.,* 2010; Dubash *et al.,* 2011; Kim *et al.,* 2013). Rac1 accumulation in the nucleus is important to control nuclear membrane morphology and is involved in promoting cell division and migration (Michaelson *et al.,* 2008; Navarro-Lérida *et al.,* 2015). Nuclear RhoA has also been found to be involved in the DNA damage response (Dubash *et al.,* 2011). One of the atypical Rho-family GTPases, RhoH has also been found in the nucleus of Jurkat cells (Mino *et al.,* 2018).

In this study, RhoA and RhoC were exclusively found in the cytoplasm, while Rac1 and RhoH were found to localise in both the cytoplasm and nuclear-enriched compartments. However, RhoGDI-3 was found to interact with Rac1 only in the cytoplasm. Both RhoGDI-1 and -2 were also shown to interact with Rac1 exclusively in the cytoplasm. In cells expressing each of the RhoGDIs, Rac1 nuclear levels decreased, suggesting a role for the RhoGDI proteins to sequester Rac1 in the cytoplasm and prevent its nuclear targeting. Similar data has been published previously for RhoGDI-1 towards Rac1 and RhoA (Michaelson *et al.,* 2001; Dubash *et al.,* 2011).

RhoGDI-3 was found to form a complex with ACK predominantly in the nuclear-enriched fraction, indicating a role for ACK in regulating RhoGDI-3 nuclear function. However, presently, the possibility that ACK might also interact with RhoGDI-3 in early endosomes cannot be excluded as previous studies have shown the localisation of both proteins in that particular compartment (Schröter *et al.,* 1999; Brunet *et al.,* 2002; Shen *et al.,* 2007). The subcellular fractionation assay used in this study only separates the cytoplasm of the cells from other subcellular structures. The nuclear-enriched fractions will therefore contain other subcellular structures such as the mitochondria, endosomes, Golgi network and endoplasmic reticulum. Thus, to identify a more precise location of ACK-RhoGDI-3 complex, further work could possibly include a bimolecular fluorescence complementation (BiFC) assay, a fluorescence imaging technique. In BiFC, the interacting proteins are fused to nonfluorescent halves of a fluorescent protein. If they interact, the nonfluorescent fragments are brought into close proximity, the fluorophore is reconstituted and a fluorescent signal can be detected using confocal microscopy (Pratt *et al.,* 2016). The site of interaction between ACK and both RhoGDI-1 and -2 was not tested in this study due to time constraints, however it is likely that they interact in the cytoplasm due to

the cytoplasmic localisation of both RhoGDIs found here. Furthermore, co-expression with ACK did not alter the cytoplasmic localization of RhoGDI-1 and -2.

Despite ACK being a kinase, all mutagenesis data analysing mutant variants in cells suggest that RhoGDI-2, at least, is not a substrate for ACK. ACK has been shown to phosphorylate a single tyrosine within the *att*B1 site of pDEST26-RhoGDI-2 construct, which was detected by a pan anti-pTyr antibody. Tyrosine^{attB1} is crucial for LR recombination between Gateway entry clones and Gateway expression vectors, therefore it will be in all expression constructs following recombination. Since Tyr^{attB1} has been shown to be a major phosphorylation site for ACK in this study, it is important for all future work analysing the effect of ACK on the phosphorylation status of its binding targets to use an expression construct with a mutated Tyr^{attB1}. In parallel with the cell assays, an *in vitro* kinase assay was also performed using GST-tagged RhoGDI-1 and -2. This assay confirmed that neither RhoGDIs were substrates for ACK kinase activity. The phosphorylation status of RhoGDI-3 by ACK is currently unknown as time constraints disallowed further analysis in cells and the protein was not soluble in *E. coli* preventing its purification. However, it seems likely that ACK will not phosphorylate RhoGDI-3 due to the high sequence similarity between all three RhoGDIs. Furthermore, all the tyrosine residues present within RhoGDI-3 are conserved between the RhoGDIs. ACK has been shown to have a dual kinase activity as it was found to phosphorylate WASP at both Tyr256 and Ser242 (Yokoyama *et al.,* 2005). Thus, it is possible that ACK phosphorylates the RhoGDIs at serine or threonine residues. However, it will be difficult to test this hypothesis due to lack of reliable antibodies. Future work with mass spectrometry could help to generate a definitive answer.

The interaction with ACK has been shown in this work to promote RhoGDI-3 degradation; this does not appear to be the case with RhoGDI-1 or -2. RhoGDI-3 degradation facilitated by ACK potentially involves the N-terminus of RhoGDI-3, as an N-terminally truncated version of RhoGDI-3 was shown to be more stable with ACK compared to wt RhoGDI-3. RhoGDI-3 and a ΔNRhoGDI-3 mutant were found to be relatively stable proteins with half-lives >8 h. However, co-expression with ACK significantly decreased the half-life of wt RhoGDI-3 to ~3.5 h, while having no effect on the ΔNRhoGDI-3 mutant. These data suggest that the interaction between ACK and RhoGDI-3 might stimulate RhoGDI-3 conformational changes that allow the first 26 amino acids of RhGDI-3 to act as a degradation signal. ACK-mediated RhoGDI-3 degradation has

been shown to occur predominantly in the nucleus, which might affect the nuclear function of RhoGDI-3. Interestingly, loss of RhoGDI-3 in the nucleus was found to be associated with pancreatic cancer progression (de León-Bautista *et al.,* 2016), suggesting that ACK-mediated RhoGDI-3 degradation in the nucleus might contribute to ACK-driven oncogenicity.

ACK-mediated RhoGDI-3 degradation has been shown to be proteasomal-dependent and this could be achieved by regulating RhoGDI-3 ubiquitination. Data presented here suggest that RhoGDI-3 can be modified by either linear ubiquitination, Lys48 poly-Ub or linear-Lys48 mixed poly-Ub, which occur in both the cytoplasm and nuclear-enriched fractions. Currently, there is no definitive answer for the type of RhoGDI-3 ubiquitination due to the discrepancy in the data obtained but further work with mass spectrometry would be helpful to properly identify the type of RhoGDI-3 ubiquitination. A poly-Ub via a Lys48 linkage has been shown to promote its degradation. It was initially assumed that ACK would promote RhoGDI-3 degradation by enhancing RhoGDI-3 ubiquitination, consistent with a previous study that showed ACK to phosphorylate and induced Wwox poly-ubiquitination and degradation (Mahajan *et al.,* 2005). However, in this study, the presence of ACK resulted in noticeably decreased RhoGDI-3 ubiquitination, visible even though there were lower levels of RhoGDI-3 present in the cells. The association between the loss of RhoGDI-3 ubiquitination and a decrease in its protein levels was unexpected but ACK may regulate RhoGDI-3 ubiquitination and promote its degradation by binding to the Ub-RhoGDI-3 complex, potentially via its UBA domain.

The UBA domain of ACK has been shown to interact with Ub-conjugated proteins (Shen *et al.,* 2007). Consistent with this, a somatic mutation, S985N, in the UBA domain of ACK has been shown to prevent its interaction with ubiquitinated proteins (Tin *et al.,* 2010). However, a study by Shen *et al.* (2007) found that, while the UBA domain of ACK did not determine the interaction with ubiquitinated EGFR, it was involved in regulating the EGFR degradation in response to EGF stimulation. This would be important to prevent excessive EGF signalling that is frequently observed in cancer (Fox *et al.,* 2019). EGFR degradation has been shown to occur together with ACK degradation and this is mediated by ACK ubiquitination (Tin *et al.,* 2010; Chan *et al.,* 2009; Lin *et al.,* 2010). Conversely, a lack of the UBA domain was shown to promote ACK and EGFR stability even after EGF stimulation (Tin *et al.,* 2010). These data suggest that ACK ubiquitination might serve as a degradation signal for RhoGDI-3 and its UBA domain might therefore be involved

in the regulation of RhoGDI-3 ubiquitination and stability. Nonetheless, in this study, a UBA mutant of ACK was unable to restore RhoGDI-3 poly-ubiquitination status but instead was found to partially increase RhoGDI-3 stability. These data indicate that the UBA domain of ACK does not regulate RhoGDI-3 ubiquitination by binding to the Ub-RhoGDI-3 complex but potentially involved in modulating RhoGDI-3 stability.

In this study, ACK protein levels were also shown to decrease when co-expressed with any of the RhoGDIs, suggesting that the RhoGDIs also promote ACK degradation. ACK can be ubiquitinated by several E3 ligases including NEDD4-1 (Lin *et al.,* 2010), NEDD4-2 (Chan *et al.,* 2009), SIAH1 and SIAH2 (Buchwald *et al.,* 2013), which then leads to its ubiquitination and degradation. A study by Lin *et al.* (2010) showed the potential involvement of the SAM domain of ACK in regulating ACK ubiquitination, as well as the necessity of the UBA domain for the interaction with NEDD4-1. Since the interaction with ACK has been found to enhance RhoGDI-3 proteasomal degradation, it is possible that ACK blocks some ubiquitination sites on RhoGDI-3 and that degradation of the ACK-RhoGDI-3 complex is facilitated by the ubiquitination of ACK at sites in its SAM domain (Figure 10.1). Future work involving the SAM domain of ACK will be needed to identify any potential role in regulating RhoGDI-3 ubiquitination.

RhoGDI-1 protein levels do not appear to be affected by ACK. However, in contrast to RhoGDI-3, the levels of RhoGDI-2 slightly increased when co-expressed with ACK. This is consistent with previous findings that show overexpression of RhoGDI-2 promotes ovarian cancer, gastric cancer and pancreatic cancer (Tapper *et al.,* 2001; Cho *et al.,* 2009; Yi *et al.,* 2015).

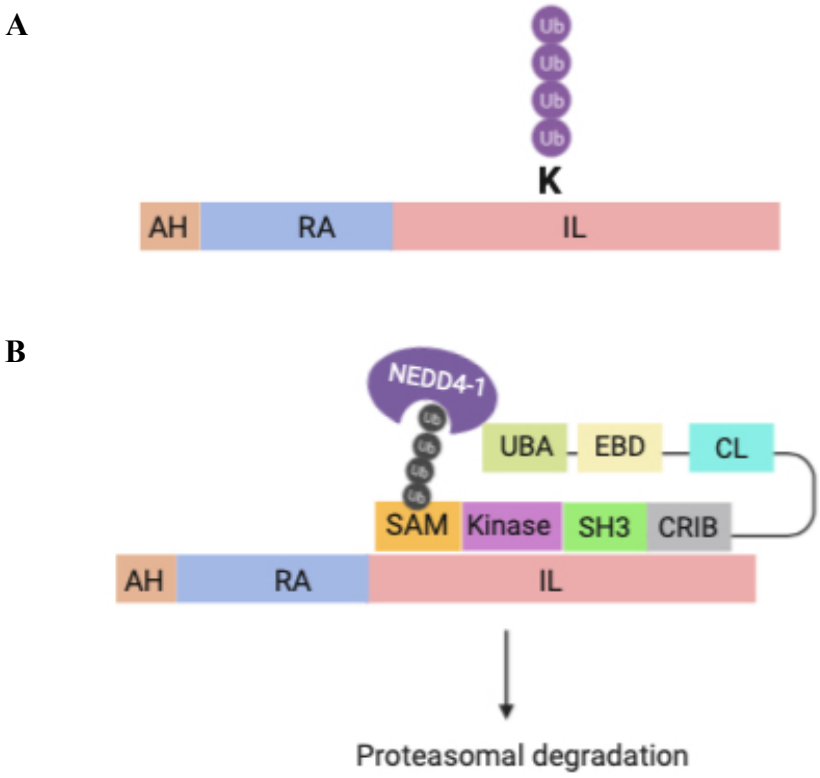

Figure 10.1: Regulation of RhoGDI-3 ubiquitination by ACK. (A) RhoGDI-3 undergoes ubiquitination. **(B)** The interaction with ACK block RhoGDI-3 ubiquitination sites but the degradation of the ACK-RhoGDI-3 complex can be regulated by the interaction with an E3 ligase (example here NEDD4-1) through the ACK UBA domain, which results in ACK ubiquitination at the SAM domain. This will then enhance the degradation of ACK-RhoGDI-3 complex. Ub: Ubiquitin, AH: Amphiphatic helix, RA: Regulatory arm domain, IL: Immunoglobulin-like domain, SAM: sterile α motif domain, NES: nuclear export signal, Kinase: tyrosine kinase domain, SH3: Src Homology 3 domain, CRIB: Cdc42/Rac interacting binding region, CL: Clathrin-interacting region, EBD: EGFR binding domain and UBA: ubiquitin-association domain.

The effect of ACK on RhoGDI target proteins was also determined in this study. Several targets have been identified for the RhoGDIs which mainly come from the typical or classical Rho GTPase subfamilies such as Rho, Rac and Cdc42. Less is known about any RhoGDI interactions with the atypical Rho GTPases, except for RhoH, which has been reported to interact with all three RhoGDIs (Li *et al.,* 2002). Thus, it was reasoned that knowledge of the full spectrum of the

interacting partners for each RhoGDIs would be crucial to determining the cellular effect that may results from the regulation of the RhoGDIs by ACK.

Aberrant activity of RhoGDIs, either through changes in expression levels or modification of their binding to target proteins has been found to be associated with cancer. For instance, the interaction of RhoGDI-1 with EphrinB1 has been shown to stimulate RhoA displacement from the RhoA-RhoGDI-1 complex leading to RhoA activation, which promotes breast cancer cell migration (Cho *et al.,* 2018). Furthermore, the RhoGDI-1 interaction with 14-3-3τ was also shown to support cell migration and invasion in breast cancer by disturbing RhoGDI-1 association with its targets, RhoA, Rac1 and Cdc42 (Xiao *et al.,* 2014). These data suggest that more detailed knowledge of RhoGDI target proteins could help in the search for new therapeutic targets especially for ACK-driven cancer progression (Cho *et al.,* 2019).

Here RhoGDI-1 was shown to form complexes with RhoA, RhoC, Rac1, Rac2, Rac3, RhoG, Cdc42 and RhoF. RhoF is a newly identified target for RhoGDI-1 and this is consistent with its similarity to Rac and Rho subfamilies members (~50%).

Data presented here indicate that RhoGDI-2 has a more limited target profile, which includes RhoC, Rac1 and Rac3. Early studies suggested that RhoGDI-2 had a restricted expression profile and was confined to haematopoietic cells, however more recent data show expression in a wider range of tissues and cancer cell types (Cho *et al.,* 2010). A previous study also identified Cdc42 (Scheffzek *et al.,* 2000) and RhoA (Griner *et al.,* 2015) as RhoGDI-2 targets. However, these were not observed in the system used in this study. RhoGDI-2 has been reported to make weaker affinity complexes with its Rho GTPase targets. For instance, RhoGDI-2 was shown to bind to Cdc42 with 10- to 20-fold weaker affinity than RhoGDI-1 (Platko *et al.,* 1995) potentially due to non-conservation of amino acids between these RhoGDIs (Platko *et al.,* 1995; Nomanbhoy *et al.,* 1996). Due to the potential weak affinity between RhoGDI-2 and its binding targets, it cannot be ruled out that some RhoGDI-2 targets may have been missed in this study.

Here, RhoGDI-1 and RhoGDI-2 were found not to interact with the other Rho-family GTPases: TC10, TCL, Wrch1, Wrch2, the Rnd subfamily, the Miro subfamily, RhoD and RhoH. Initially, RhoD was postulated to be a target for RhoGDI in this study due to its high similarity with the Rac and Rho subfamilies (~50%), however no interaction was identified. An interaction between

RhoGDI-2 and Rac2 was also predicted prior to this screen as a crystal structure of the RhoGDI-2-Rac2 complex has been solved. However, there was no interaction observed between these two proteins in this study, potentially indicating that they do not interacting in a cellular environment.

The least studied RhoGDI, RhoGDI-3 was shown to engage with all the typical members of the Rho-family GTPases, excluding Cdc42, TC10 and TCL. It was also found to associate with several atypical Rho-family GTPases such as RhoD, RhoH, Wrch2, Rnd2 and Miro2. Interestingly, one of the targets, Wrch2, has been shown to be modified solely by palmitoylation. Previously, palmitoylation had been reported to completely abrogate the interaction between RhoGDI-1 and RhoA (Michaelson *et al.,* 2001). Conversely, a study by Navarro-Lérida *et al.* (2012) showed that RhoGDI-1 was also able to bind to palmitoylated Rac1. Since Wrch2 was only found to interact with RhoGDI-3 and not with the other RhoGDIs, it is possible that RhoGDI-3 favours palmitoylated Rho GTPases and is potentially involved in targeting them to specific subcellular compartments.

The interaction between RhoGDI-3 and the GTPase defective Rho-family GTPases such as RhoH and Rnd2 was not expected as these Rho GTPases have been shown to be constitutively active due to their high intrinsic GDP dissociation rate (Fueller and Kubatzky, 2008; Aspenström, 2017). Additionally, Chenette *et al.* (2006) also showed that all three RhoGDIs failed to prevent Wrch2 membrane association, suggesting that Wrch2 is not regulated by the RhoGDI. However, RhoGDI-1 has been observed to accommodate both the GTP- and GDP-bound forms of Rac1, RhoA (Hancock and Hall, 1993) and Cdc42 (Nomanbhoy and Cerione, 1996). This was supported by structural studies that show the main interface between RhoGDI-1 and Cdc42 is not affected by the nucleotide state of Cdc42 (Phillips *et al.,* 2008). There is also a possibility that RhoGDI-3 regulates the activity of these unusual Rho-family GTPases via an adaptor protein, 14-3-3, consistent with previous studies that showed 14-3-3ß negatively regulates Rnd activation (Riou *et al.,* 2013) and also binds to RhoGDI-1 (Xiao *et al.,* 2014).

Miro2, a mitochondria-associated small GTPase, was shown to be a target for RhoGDI-3 in this study but not Miro1, although both are structurally similar and localize to the same cell compartment. Nevertheless, these proteins have been shown to be functionally different with the degradation of Miro2 and not Miro1 found to inhibit mitochondrial retrograde trafficking

(O'Mealey *et al.,* 2017). Furthermore, Nguyen *et al.* (2014) also found that Miro2 did not rescue neural respiratory defects due to the loss of Miro1 function in Miro1 KO mice. The molecular details of the RhoGDI-3-Miro2 interaction are however unclear as Miro2 does not undergo any lipid modification due to the lack of a CAAX motif and palmitoylated cysteines. Nevertheless, these data indicate a potential new role for RhoGDI-3 in regulating mitochondrial processes through its target, Miro2.

As mentioned previously, RhoGDI-3 has been found on endomembranes and early endosomes (Brunet *et al.,* 2002). Several Rho-family GTPases have also been found to localize at these same sites, for example, RhoB (Adamson *et al.,* 1992), Rac3 (Chan *et al.,* 2005), RhoG (Morin *et al.,* 2010), Wrch2 (Hodge and Ridley, 2017), Rnd2 (Tanaka *et al.,* 2002) and RhoD (Gasman *et al.,* 2003). This suggests that RhoGDI-3 might interact with its partners in these compartments and possibly play a new role in regulating their intracellular trafficking.

The differences in the binding capabilities of the RhoGDIs are still not well understood. However, despite sharing 70% sequence similarities, the divergent amino acids between the three RhoGDIs are found to concentrate within their N-termini (Figure 1.12) and this might contribute to their binding preferences. The first 25 amino acids of RhoGDI-1 have been shown to play a pivotal role in retaining RhoGDI-1 in the cytoplasm, suggesting that the N-termini of the RhoGDIs are important in regulating their subcellular localization and therefore facilitate the binding with Rho GTPases that reside within the same compartments (Ueyama *et al.,* 2013). In the same study it was found that RhoGDI-1 also localised to phagosomes and this required an interaction with Rac1, indicating that the RhoGDIs and Rho GTPases were mutually involved in the signal directing them to specific cell compartments.

The effect of the RhoGDIs on the activation status of their binding targets was also investigated here. In this study, co-expression with any of the RhoGDIs was found to decrease the GTP levels of their binding partners, even for small G proteins considered constitutively active such as RhoH. Both RhoGDI-1 and -2 were able to inhibit the activation of Rac1 in the cytoplasm, consistent with a previous study (Quinn *et al.,* 1993). RhoGDI-3 was also found to interact and inhibit the activation of its target proteins, Rac1 and RhoA in the cytoplasm. Conversely, the RhoH-RhoGDI-3 complex was found in both the cytoplasm and nuclear-enriched compartments and resulted in

RhoH deactivation in both locations. The nuclear function of RhoH is still not well understood but it is required to regulate the nuclear translocation of Kaiso, a transcriptional regulator, in response to chemokine stimulation and T cell receptor activation during T cell migration (Mino *et al.,* 2018). This suggests a role for RhoH in modulating the localization of its binding partners, which might also apply to RhoGDI-3.

With increased knowledge of the targets of the RhoGDIs and the outcome of the interactions, this work now focused on the effect of ACK as a new player that might influence the binding and inhibitory capabilities of RhoGDIs. The presence of ACK does not promote Rac1 dissociation from Rac1-RhoGDI-1 or -2 complexes which is consistent with the low levels of active Rac1 observed in cells where ACK and the RhoGDIs are co-expressed, similar to levels in cells expressing the RhoGDIs alone.

ACK has been shown to mediate RhoGDI-3 degradation and thereby reduce the levels of RhoGDI-3 available for binding with its target proteins. Subsequently, this should promote the activation of the unbound small GTPases. As hypothesized, the amount of RhoGDI-3 in complex with RhoA, Rac1 and RhoH was seen to decrease when co-expressed with ACK, and this resulted in the increased activation of these small GTPases. In contrast, the activation of tumour suppressor RhoB decreased in the presence of ACK. These Rho subfamily proteins have been shown to act in opposition in cancer, with RhoA being mainly pro-oncogenic and RhoB commonly anti-oncogenic (Zohn *et al.,* 1998; Orgaz *et al.,* 2014; Chen *et al.,* 2000). Thus, it is likely that the opposing effects of ACK on these proteins would lead to a harmonised outcome and promote ACK-driven cancer progression.

Usually, RhoA and Rac1 activity to control cytoskeleton dynamics is regulated in a co-ordinated manner with suppression of RhoA and upregulation of Rac1 activity or vice versa. For instance, RhoA is commonly active towards the rear of the cell and involved in cell retraction, whereas Rac1 is active towards the front of the cell during migration (Machacek *et al.,* 2009; Nguyen *et al.,* 2018). This spatial activation is commonly regulated through GEF, GAP, GDI or effector proteins shared by both Rho GTPases (Guilluy *et al.,* 2011). Their activation has also been found to be dependent on each other, for example active Rac1 interacts with the RhoA GEF, Dbs, resulted in the activation of RhoA (Horii *et al.,* 1994; Cheng *et al.,* 2004). Furthermore, the RhoA effector

proteins, mDia1 and ROCK have also been shown to act in opposition to promote Rac1 activation and hence membrane ruffle formation in fibroblasts (Tsuji *et al.,* 2002). Although RhoA is predominantly active at the rear of the cell, a pool of active RhoA has also been found at the leading edge of cells during migration to initiate cell protrusion, preceding the activation of Rac1, which supports the newly expanded protrusion (Machacek *et al.,* 2009). Therefore, it is possible that ACK spatially regulates the activity of both RhoA and Rac1 through RhoGDI-3 especially during cell invasion and metastasis.

The presence of ACK has been shown to promote RhoGDI-3 degradation, predominantly in the nucleus. Thus, it is expected that the activation of Rho GTPase localized in the nucleus would be elevated. High levels of active Rac1 in the nucleus have been found to promote cell division and invasion (Michaelson *et al.,* 2008; Navarro-Lerida *et al.,* 2015). Thus, it was hypothesized that ACK would increase Rac1•GTP levels in the nucleus and this could contribute to its association with cancer cell proliferation (Clayton *et al.,* 2019), migration and invasion (Xu *et al.,* 2015; Lei *et al.,* 2015). Furthermore, in this study, co-expression with ACK has been shown to partially inhibit the ability of RhoGDI-3 to sequester Rac1 in the cytoplasm, promoting its nuclear localisation. However, co-expression with ACK did not increase Rac1•GTP in the nucleus but surprisingly, GTP-bound Rac1 was shown to increase in the cytoplasm. These data suggest that ACK might modulate the activation of other Rho GTPases that are known to be in the nucleus.

As described previously, RhoA showed a restricted cytoplasmic distribution in the system used here, while RhoH can be found in both cytoplasmic and nuclear-enriched fractions. RhoH has been shown to promote prostate cancer cell migration by forming a ternary complex with Rac1 and its effector, PAK2, to direct GTP-bound Rac1 to membrane protrusion (Tajadura-Ortega *et al.,* 2018). Effector proteins shared by these two Rho GTPases (Wang *et al.,* 2010; Kuželová *et al.,* 2014) suggest a signalling crosstalk which could be regulated by ACK. Furthermore, since ACK has been shown to increase RhoH activity in both the cytoplasmic and nuclear-enriched by regulating RhoGDI-3 stability, it is possible that ACK mediates PAK1 activation in the nucleus through RhoH and in the cytoplasm via Rac1. The activation of both of these Rho GTPases occurs due to low levels of RhoGDI-3 present in and shuttled out from the nucleus. This would then result in the increased activation of PAK1 in both compartments, a situation which is frequently observed in cancer (Kumar *et al.,* 2006). For instance, an over activated Rac1/PAK1 cascade has been shown

to promote ß-catenin phosphorylation at Ser675 in the cytoplasm, leading to increase colon cancer cell proliferation (Zhu *et al.,* 2012). Nuclear PAK1 has been shown to promote transcription repressor activity of Snail from E-cadherin, occludin and aromatase promoters, leading to increased EMT process and cell invasion (Yang *et al.,* 2005).

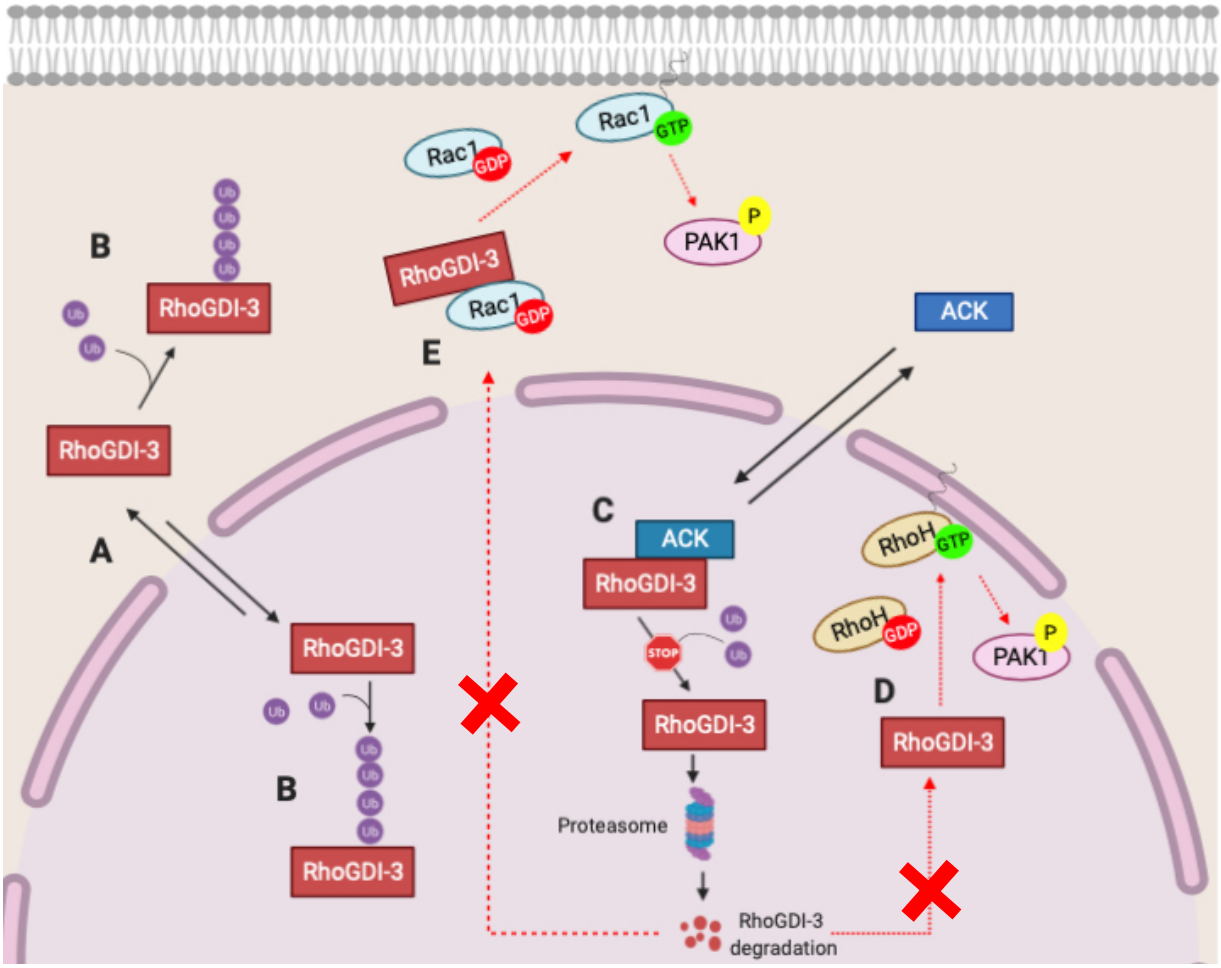

Figure 10.2: A proposed mechanism for the effect of ACK on RhoGDI-3 functions. (A) RhoGDI-3 is found in both the cytoplasm and the nucleus, indicating it undergoes nuclear-cytoplasmic shuttling. **(B)** RhoGDI-3 undergoes ubiquitination in both the cytoplasm and the nucleus. **(C)** ACK interacts with RhoGDI-3 exclusively in the nucleus and regulates its ubiquitination. This results in degradation of RhoGDI-3 by the proteasome. **(D)** Subsequently, the levels of free RhoGDI-3 will decrease, disallowing complex with RhoH in the nucleus and promoting RhoH activation in the nucleus. **(E)** Furthermore, less RhoGDI-3 will be export out from the nucleus, making free RhoGDI-3 less available for binding with Rac1 and therefore promotes Rac1 activation.

Collectively, all the data presented in this study show a new kinase-independent function for ACK in regulating RhoGDI proteins. In particular ACK plays a role in controlling levels of RhoGDI-3 and thereby modulates its function as a regulator for Rho GTPases (Figure 10.2). Since RhoGDI-3 has been shown to interact with Miro2, a mitochondria-associated Rho GTPase, it is possible that ACK might deregulate the function of Miro2 in maintaining mitochondria homeostasis through RhoGDI-3, which has been commonly observed in cancer (Caino and Altieri, 2017).

Further investigation is also needed to fully identify the biological consequences of the action of ACK towards the RhoGDIs' target proteins especially in regard to cell proliferation and migration. Attempts were made to study the effect of knockdown of each RhoGDIs on ACK-induced cell proliferation and migration. However, since there was only a specific antibody available for RhoGDI-1, successful knockdown was monitored using mRNA levels for each RhoGDIs in the breast cancer cell lines, MCF-7 and MDA-MB-436. Both of these cell lines were shown to have high mRNA levels of ACK and all three RhoGDIs in a screen by Dr. Anna Git (Department of Biochemistry, University of Cambridge, personal communication). However, due to time constraints, the RT-PCR for each RhoGDIs was not optimised. Thus, future studies including siRNA or CRISPR cell lines of RhoGDIs would be useful to identify a role for the RhoGDIs in underpinning the oncogenic properties of ACK especially in cell proliferation and migration. Furthermore, it would be especially useful to raise a specific antibody for both RhoGDI-2 and -3 especially RhoGDI-3, which would facilitate endogenous studies with ACK.

This work set out to investigate a potential role of the RhoGDI proteins in underpinning the oncogenic potential of ACK. Although ACK has been shown to interact with all three RhoGDIs, the outcome of the interaction is more pronounced for RhoGDI-3. Future work looking at different targets of both RhoGDI-1 and -2 would be useful to understand a role for these RhoGDIs in supporting ACK oncogenic properties. Overall, all the data presented here show the involvement of ACK in disturbing the balance between the levels of RhoGDIs, especially RhoGDI-3, and the Rho-family proteins, allowing free Rho-family GTPases to become membrane-bound and activated. This happens because RhoGDIs protein levels have been shown to be approximately equal to the levels of RhoA, Rac1 and Cdc42 in the cells and any disturbance in this equilibrium alters the activation of Rho-family proteins, which have been observed frequently in cancer. Although the role of RhoGDI-3 in mediating the effects of ACK on cell proliferation and migration

has not yet been studied, it can now be postulated that ACK mediates the degradation of RhoGDI-3, resulting in an increased pool of its active target Rho GTPases. This leads to the activation of the Rho-family effector proteins such as Rhotekin and PAK1, which could underpin ACK oncogenicity in regard to these processes.

References

Abdrabou, A., and Wang, Z. (2018). Post-translational modification and subcellular distribution of Rac1: An Update. *Cells*, *7*(12), 263. https://doi.org/10.3390/cells7120263

Abe, K., Rossman, K. L., Liu, B., Ritola, K. D., Chiang, D., Campbell, S. L., Burridge, K., and Der, C. J. (2000). Vav2 is an activator of Cdc42, Rac1, and RhoA. *The Journal of Biological Chemistry*, *275*(14), 10141–10149. http://www.ncbi.nlm.nih.gov/pubmed/10744696

Abo, A., Pick, E., Hall, A., Totty, N., Teahan, C. G., and Segal, A. W. (1991). Activation of the NADPH oxidase involves the small GTP-binding protein p21rac1. *Nature*, *353*(6345), 668–670. https://doi.org/10.1038/353668a0

Abo, A., Webb, M. R., Grogan, A., and Segal, A. W. (1994). Activation of NADPH oxidase involves the dissociation of p21rac from its inhibitory GDP/GTP exchange protein (rhoGDI) followed by its translocation to the plasma membrane. *Biochem J*, *298 Pt 3*, 585–591. https://doi.org/10.1042/bj2980585

Abramovici, H., Mojtabaie, P., Parks, R. J., Zhong, X.-P., Koretzky, G. A., Topham, M. K., and Gee, S. H. (2009). Diacylglycerol Kinase ζ regulates actin cytoskeleton reorganization through dissociation of Rac1 from RhoGDI. *Molecular Biology of the Cell*, *20*(7), 2049–2059. https://doi.org/10.1091/mbc.e07-12-1248

Ackermann, K. L., Florke, R. R., Reyes, S. S., Tader, B. R., and Hamann, M. J. (2016). TCL/RhoJ plasma membrane localization and nucleotide exchange is coordinately regulated by amino acids within the N terminus and a distal loop region. *The Journal of Biological Chemistry*, *291*(45), 23604—23617. https://doi.org/10.1074/jbc.M116.750026

Adamson, P., Paterson, H. F., and Hall, A. (1992). Intracellular localization of the P21rho proteins. *The Journal of Cell Biology*, *119*(3), 617–627. https://doi.org/10.1083/jcb.119.3.617

Adini, I., Rabinovitz, I., Sun, J. F., Prendergast, G. C., and Benjamin, L. E. (2003). RhoB controls Akt trafficking and stage-specific survival of endothelial cells during vascular development. *Genes and Development* , *17*(21), 2721–2732. https://doi.org/10.1101/gad.1134603

Adra, C. N., Ko, J., Leonard, D., Wirth, L. J., Cerione, R. A., and Lim, B. (1993). Identification of a novel protein with GDP dissociation inhibitor activity for the ras-like proteins

CDC42Hs and Rac 1. *Genes, Chromosomes and Cancer*, *8*(4), 253–261. https://doi.org/10.1002/gcc.2870080408

Adra, C. N., Manor, D., Ko, J. L., Zhu, S., Horiuchi, T., Van Aelst, L., Cerione, R. A., and Lim, B. (1997). RhoGDIγ: A GDP-dissociation inhibitor for Rho proteins with preferential expression in brain and pancreas. *Proceedings of the National Academy of Sciences*, *94*(9), 4279 LP-4284. https://doi.org/10.1073/pnas.94.9.4279

Ahmed, I., Calle, Y., Sayed, M. A., Kamal, J. M., Rengaswamy, P., Manser, E., Meiners, S., Nur-E-Kamal, A., Ijaz Ahmed, a, 1 Yolanda Calle, a, 1 Mohammed A. Sayed, b Jabeen M. Kamal, a Padmanabhan Rengaswamy, c Ed Manser, d Sally Meiners, and A. N.-E.-K., Ahmed, I., Calle, Y., Sayed, M. A., Kamal, J. M., Rengaswamy, P., Manser, E., Meiners, S., and Nur-E-Kamal, A. (2004). Cdc42-dependent nuclear translocation of non-receptor tyrosine kinase, ACK. *Biochemical and Biophysical Research Communications*, *314*(2), 571–579. https://doi.org/https://doi.org/10.1016/j.bbrc.2003.12.137

Albert, M. L., Kim, J.-I., & Birge, R. B. (2000). αvβ5 integrin recruits the CrkII–Dock180–Rac1 complex for phagocytosis of apoptotic cells. *Nature Cell Biology*, *2*(12), 899–905. https://doi.org/10.1038/35046549

Alexander, M., Gerauer, M., Pechlivanis, M., Popkirova, B., Dvorsky, R., Brunsveld, L., Waldmann, H., and Kuhlmann, J. (2009). Mapping the isoprenoid binding pocket of PDEδ by a semisynthetic, photoactivatable N-Ras lipoprotein. *ChemBioChem*, *10*(1), 98–108. https://doi.org/10.1002/cbic.200800275

Allaire, P. D., Marat, A. L., Dall'Armi, C., Di Paolo, G., McPherson, P. S., and Ritter, B. (2010). The connecdenn DENN domain: A GEF for Rab35 nediating cargo-specific exit from early endosomes. *Molecular Cell*, *37*(3), 370–382. https://doi.org/https://doi.org/10.1016/j.molcel.2009.12.037

Allal, C., Pradines, A., Hamilton, A. D., Sebti, S. M., and Favre, G. (2002). Farnesylated RhoB prevents cell cycle arrest and actin cytoskeleton disruption caused by the Geranylgeranyltransferase I Inhibitor GGTI-298. *Cell Cycle*, *1*(6), 430–437. https://doi.org/10.4161/cc.1.6.272

Alory, C., and Balch, W. E. (2000). Molecular basis for Rab prenylation. *The Journal of Cell Biology*, *150*(1), 89–104. https://doi.org/10.1083/jcb.150.1.89

Antonny, B., Beraud-Dufour, S., Chardin, P., and Chabre, M. (1997). N-terminal hydrophobic residues of the G-protein ADP-ribosylation factor-1 insert into membrane phospholipids upon GDP to GTP exchange. *Biochemistry*, *36*(15), 4675–4684. https://doi.org/10.1021/bi962252b

Aoki, H., Yokoyama, T., Fujiwara, K., Tari, A. M., Sawaya, R., Suki, D., Hess, K. R., Aldape, K. D., Kondo, S., Kumar, R., and Kondo, Y. (2007). Phosphorylated Pak1 level in the cytoplasm correlates with shorter survival time in patients with glioblastoma. *Clinical Cancer Research*, *13*(22), 6603 LP-6609. https://doi.org/10.1158/1078-0432.CCR-07-0145

Araki, S., Kikuchi, A., Hata, Y., Isomura, M., Takai, Y., Journal, T. H. E., and Biological, O. F. (1990). Regulation of reversible binding of smg p25A, a ras p21-like GTP-binding protein, to synaptic plasma membranes and vesicles by its specific regulatory protein, GDP dissociation inhibitor. *Journal of Biological Chemistry* , *265*(22), 13007–13015. http://www.jbc.org/content/265/22/13007.abstract

Aresta, S., de Tand-Heim, M.-F., Béranger, F., and de Gunzburg, J. (2002). A novel Rho GTPase-activating-protein interacts with Gem, a member of the Ras superfamily of GTPases. *The Biochemical Journal*, *367*(Pt 1), 57–65. https://doi.org/10.1042/BJ20020829

Aronheim, A., Broder, Y. C., Cohen, A., Fritsch, A., Belisle, B., and Abo, A. (1998). Chp, a homologue of the GTPase Cdc42Hs, activates the JNK pathway and is implicated in reorganizing the actin cytoskeleton. *Current Biology*, *8*(20), 1125–1129. https://doi.org/https://doi.org/10.1016/S0960-9822(98)70468-3

Arthur, W. T., and Burridge, K. (2001). RhoA inactivation by p190RhoGAP regulates cell spreading and migration by promoting membrane protrusion and polarity. *Molecular Biology of the Cell*, *12*(9), 2711–2720. https://doi.org/10.1091/mbc.12.9.2711

Aspenström, P. (2017). Fast-cycling Rho GTPases. *Small GTPases*, 1–8. https://doi.org/10.1080/21541248.2017.1391365

Aspenström, P. (2018). Activated Rho GTPases in cancer-The beginning of a new paradigm. *International journal of molecular sciences* (Vol. 19, Issue 12). https://doi.org/10.3390/ijms19123949

Aspenström, P., Fransson, Å., and Saras, J. (2004). Rho GTPases have diverse effects on the organization of the actin filament system. *Biochemical Journal*, *377*(2), 327–337. https://doi.org/10.1042/bj20031041

Aspenström, P., Lindberg, U., and Hall, A. (1996). Two GTPases, Cdc42 and Rac, bind directly to a protein implicated in the immunodeficiency disorder Wiskott–Aldrich syndrome. *Current Biology*, *6*(1), 70–75. https://doi.org/https://doi.org/10.1016/S0960-9822(02)00423-2

Aspenström, P., Ruusala, A., and Pacholsky, D. (2007). Taking Rho GTPases to the next level: The cellular functions of atypical Rho GTPases. *Experimental Cell Research*, *313*(17), 3673–3679. https://doi.org/https://doi.org/10.1016/j.yexcr.2007.07.022

Avansini, S. H., Torres, F. R., Vieira, A. S., Dogini, D. B., Rogerio, F., Coan, A. C., Morita, M. E., Guerreiro, M. M., Yasuda, C. L., Secolin, R., Carvalho, B. S., Borges, M. G., Almeida, V. S., Araújo, P. A. O. R., Queiroz, L., Cendes, F., and Lopes-Cendes, I. (2018). Dysregulation of NEUROG2 plays a key role in focal cortical dysplasia. *Annals of Neurology*, *83*(3), 623–635. https://doi.org/10.1002/ana.25187

Aviel, S., Winberg, G., Massucci, M., and Ciechanover, A. (2000). Degradation of the epstein-barr virus latent membrane protein 1 (LMP1) by the ubiquitin-proteasome pathway. Targeting via ubiquitination of the N-terminal residue. The Journal of Biological Chemistry, 275(31), 23491–23499. https://doi.org/10.1074/jbc.M002052200

Azzarelli, R., Guillemot, F., and Pacary, E. (2015). Function and regulation of Rnd proteins in cortical projection neuron migration. In *Frontiers in Neuroscience* (Vol. 9, p. 19). https://www.frontiersin.org/article/10.3389/fnins.2015.00019

Babic, M., Russo, G. J., Wellington, A. J., Sangston, R. M., Gonzalez, M., and Zinsmaier, K. E. (2015). Miro's N-terminal GTPase domain is required for transport of mitochondria into axons and dendrites. *Journal of Neuroscience*, *35*(14), 5754–5771. https://doi.org/10.1523/JNEUROSCI.1035-14.2015

Barbacid, M. (1987). ras genes. *Annual Review of Biochemistry*, *56*, 779–827. https://doi.org/10.1146/annurev.bi.56.070187.004023

Beder, L. B., Gunduz, M., Ouchida, M., Gunduz, E., Sakai, A., Fukushima, K., Nagatsuka, H., Ito, S., Honjo, N., Nishizaki, K., and Shimizu, K. (2006). Identification of a candidate tumor suppressor gene RHOBTB1 located at a novel allelic loss region 10q21 in head and neck cancer. *Journal of Cancer Research and Clinical Oncology*, *132*(1), 19–27. https://doi.org/10.1007/s00432-005-0033-0

Belal, H., Nakashima, M., Matsumoto, H., Yokochi, K., Taniguchi-Ikeda, M., Aoto, K., Amin, M. B., Maruyama, A., Nagase, H., Mizuguchi, T., Miyatake, S., Miyake, N., Iijima, K., Nonoyama, S., Matsumoto, N., and Saitsu, H. (2018). De novo variants in RHOBTB2, an atypical Rho GTPase gene, cause epileptic encephalopathy. *Human Mutation*, *39*(8), 1070–1075. https://doi.org/10.1002/humu.23550

Bellovin, D. I., Simpson, K. J., Danilov, T., Maynard, E., Rimm, D. L., Oettgen, P., and Mercurio, A. M. (2006). Reciprocal regulation of RhoA and RhoC characterizes the EMT and identifies RhoC as a prognostic marker of colon carcinoma. *Oncogene*, *25*(52), 6959–6967. https://doi.org/10.1038/sj.onc.1209682

Berthold, J., Schenková, K., Ramos, S., Miura, Y., Furukawa, M., Aspenström, P., and Rivero, F. (2008). Characterization of RhoBTB-dependent Cul3 ubiquitin ligase complexes —

Evidence for an autoregulatory mechanism. *Experimental Cell Research*, *314*(19), 3453–3465. https://doi.org/https://doi.org/10.1016/j.yexcr.2008.09.005

Berzat, A. C., Buss, J. E., Chenette, E. J., Weinbaum, C. A., Shutes, A., Der, C. J., Minden, A., and Cox, A. D. (2005). Transforming activity of the Rho-family GTPase, Wrch-1, a Wnt-regulated Cdc42 Homolog, is dependent on a novel carboxyl-terminal palmitoylation motif. *Journal of Biological Chemistry* , *280*(38), 33055–33065. https://doi.org/10.1074/jbc.M507362200

Besray Unal, E., Kiel, C., Benisty, H., Campbell, A., Pickering, K., Blüthgen, N., Sansom, O. J., and Serrano, L. (2018). Systems level expression correlation of Ras GTPase regulators. *Cell Communication and Signaling*, *16*(1), 46. https://doi.org/10.1186/s12964-018-0256-8

Bhavsar, P. J., Infante, E., Khwaja, A., & Ridley, A. J. (2013). Analysis of Rho GTPase expression in T-ALL identifies RhoU as a target for Notch involved in T-ALL cell migration. *Oncogene*, *32*(2), 198–208. https://doi.org/10.1038/onc.2012.42

Bidaud-Meynard, A., Binamé, F., Lagrée, V., and Moreau, V. (2019). Regulation of Rho GTPase activity at the leading edge of migrating cells by p190RhoGAP. *Small GTPases*, *10*(2), 99–110. https://doi.org/10.1080/21541248.2017.1280584

Bischoff, F. R., Klebe, C., Kretschmer, J., Wittinghofer, A., and Ponstingl, H. (1994). RanGAP1 induces GTPase activity of nuclear Ras-related Ran. *Proceedings of the National Academy of Sciences*, *91*(7), 2587 LP-2591. https://doi.org/10.1073/pnas.91.7.2587

Bischoff, F. R., and Ponstingl, H. (1991). Catalysis of guanine nucleotide exchange on Ran by the mitotic regulator RCC1. *Nature*, *354*(6348), 80–82. https://doi.org/10.1038/354080a0

Bivona, T. G., Quatela, S. E., Bodemann, B. O., Ahearn, I. M., Soskis, M. J., Mor, A., Miura, J., Wiener, H. H., Wright, L., Saba, S. G., Yim, D., Fein, A., Pérez de Castro, I., Li, C., Thompson, C. B., Cox, A. D., and Philips, M. R. (2006). PKC regulates a farnesyl-electrostatic switch on K-Ras that promotes its association with Bcl-Xl on mitochondria and induces apoptosis. *Molecular Cell*, *21*(4), 481–493. https://doi.org/https://doi.org/10.1016/j.molcel.2006.01.012

Blom, M., Reis, K., and Aspenström, P. (2018). RhoD localization and function is dependent on its GTP/GDP-bound state and unique N-terminal motif. *European Journal of Cell Biology*, *97*(6), 393–401. https://doi.org/https://doi.org/10.1016/j.ejcb.2018.05.003

Blom, M., Reis, K., Heldin, J., Kreuger, J., and Aspenström, P. (2017). The atypical Rho GTPase RhoD is a regulator of actin cytoskeleton dynamics and directed cell migration. *Experimental Cell Research*, *352*(2), 255–264.

https://doi.org/https://doi.org/10.1016/j.yexcr.2017.02.013

Blom, M., Reis, K., Nehru, V., Blom, H., Gad, A. K. B., and Aspenström, P. (2015). RhoD is a Golgi component with a role in anterograde protein transport from the ER to the plasma membrane. *Experimental Cell Research*, *333*(2), 208–219. https://doi.org/https://doi.org/10.1016/j.yexcr.2015.02.023

Blondel, M., Galan, J. M., Chi, Y., Lafourcade, C., Longaretti, C., Deshaies, R. J., and Peter, M. (2000). Nuclear-specific degradation of Far1 is controlled by the localization of the F-box protein Cdc4. *The EMBO Journal*, *19*(22), 6085–6097. https://doi.org/10.1093/emboj/19.22.6085

Bloom, J., Amador, V., Bartolini, F., DeMartino, G., and Pagano, M. (2003). Proteasome-mediated degradation of p21 via N-terminal ubiquitinylation. *Cell*, *115*(1), 71–82. https://doi.org/10.1016/s0092-8674(03)00755-4

Blume-Jensen, P., and Hunter, T. (2001). Oncogenic kinase signalling. *Nature*, *411*(6835), 355–365. https://doi.org/10.1038/35077225

Boriack-Sjodin, P. A., Margarit, S. M., Bar-Sagi, D., and Kuriyan, J. (1998). The structural basis of the activation of Ras by Sos. *Nature*, *394*(6691), 337–343. https://doi.org/10.1038/28548

Bos, J. L. J., Rehmann, H., and Wittinghofer, A. (2007). GEFs and GAPs: Critical elements in the control of small G proteins. *Cell*, *129*(5), 865–877. https://doi.org/https://doi.org/10.1016/j.cell.2007.05.018

Boswell, S. A., Ongusaha, P. P., Nghiem, P., and Lee, S. W. (2007). The protective role of a small GTPase RhoE against UVB-induced DNA damage in keratinocytes. *Journal of Biological Chemistry* , *282*(7), 4850–4858. https://doi.org/10.1074/jbc.M610532200

Boulter, E., Garcia-Mata, R., Guilluy, C., Dubash, A., Rossi, G., Brennwald, P. J., and Burridge, K. (2010). Regulation of Rho GTPase crosstalk, degradation and activity by RhoGDI1. *Nature Cell Biology*, *12*(5), 477–483. https://doi.org/10.1038/ncb2049

Bourdoulous, S., Orend, G., MacKenna, D. A., Pasqualini, R., and Ruoslahti, E. (1998). Fibronectin matrix regulates activation of RHO and CDC42 GTPases and cell cycle progression. *Journal of Cell Biology*, *143*(1), 267–276. https://doi.org/10.1083/jcb.143.1.267

Boureux, A., Vignal, E., Faure, S., and Fort, P. (2006). Evolution of the Rho-family of Ras-like GTPases in eukaryotes. *Molecular Biology and Evolution*, *24*(1), 203–216. https://doi.org/10.1093/molbev/msl145

Bourne, H. R., Sanders, D. A., and McCormick, F. (1991). The GTPase superfamily: conserved structure and molecular mechanism. *Nature*, *349*(6305), 117–127. https://doi.org/10.1038/349117a0

Boyrie, S., Delmas, C., Lemarié, A., Lubrano, V., Dahan, P., Malric, L., Luis, J., Gilhodes, J., Tosolini, M., Mouly, L., Lehmann, M., Toulas, C., Cohen-Jonathan Moyal, E., and Monferran, S. (2018). RND1 regulates migration of human glioblastoma stem-like cells according to their anatomical localization and defines a prognostic signature in glioblastoma. *Oncotarget*, *9*(73), 33788–33803. https://doi.org/10.18632/oncotarget.26082

Bozza, W. P., Zhang, Y., Hallett, K., Rosado, L. A. R., Rivera Rosado, L. A., and Zhang, B. (2015). RhoGDI deficiency induces constitutive activation of Rho GTPases and COX-2 pathways in association with breast cancer progression. *Oncotarget; Vol 6, No 32*, *6*(32). http://www.oncotarget.com/index.php?journal=oncotargetandamp

Breitschopf, K., Bengal, E., Ziv, T., Admon, A., and Ciechanover, A. (1998). A novel site for ubiquitination: the N-terminal residue, and not internal lysines of MyoD, is essential for conjugation and degradation of the protein. *The EMBO Journal*, *17*(20), 5964–5973. https://doi.org/10.1093/emboj/17.20.5964

Brückner, A., Polge, C., Lentze, N., Auerbach, D., and Schlattner, U. (2009). Yeast Two-Hybrid, a powerful tool for systems biology. *International Journal of Molecular Sciences*, *10*(6), 2763–2788. https://doi.org/10.3390/ijms10062763

Brunet, N., Morin, A., and Olofsson, B. (2002). RhoGDI-3 regulates RhoG and targets this protein to the Golgi complex through its unique N-terminal domain. *Traffic (Copenhagen, Denmark)*, *3*(5), 342–357. http://www.ncbi.nlm.nih.gov/pubmed/11967128

Buchwald, M., Pietschmann, K., Brand, P., Günther, A., Mahajan, N. P., Heinzel, T., and Krämer, O. H. (2013). SIAH ubiquitin ligases target the nonreceptor tyrosine kinase ACK1 for ubiquitinylation and proteasomal degradation. *Oncogene*, *32*(41), 4913–4920. https://doi.org/10.1038/onc.2012.515

Buday, L., and Downward, J. (2008). Many faces of Ras activation. *Biochimica et Biophysica Acta (BBA) - Reviews on Cancer*, *1786*(2), 178–187. https://doi.org/https://doi.org/10.1016/j.bbcan.2008.05.001

Bustelo, X. R. (2014). Vav family exchange factors: an integrated regulatory and functional view. *Small GTPases*, *5*(2), 9. https://doi.org/10.4161/21541248.2014.973757

Bustos, R. I., Forget, M.-A., Settleman, J. E., and Hansen, S. H. (2008). Coordination of Rho and Rac GTPase function via p190B RhoGAP. *Current Biology*, *18*(20), 1606–1611.

https://doi.org/https://doi.org/10.1016/j.cub.2008.09.019

Caino, M. C., and Altieri, D. C. (2017). Syntaphilin regulates mitochondrial dynamics and tumor cell invasion. *The FASEB Journal*, *31*(1_supplement), 631.3-631.3. https://doi.org/10.1096/fasebj.31.1_supplement.631.3

Cao, Z., Li, X., Li, J., Kang, B., Chen, J., Luo, W., and Huang, C. (2014). SUMOylation of RhoGDIα is required for its repression of cyclin D1 expression and anchorage-independent growth of cancer cells. *Molecular Oncology*, *8*(2), 285–296. https://doi.org/https://doi.org/10.1016/j.molonc.2013.11.006

Carney, D. S., Davies, B. A., and Horazdovsky, B. F. (2006). Vps9 domain-containing proteins: activators of Rab5 GTPases from yeast to neurons. *Trends in Cell Biology*, *16*(1), 27–35. https://doi.org/https://doi.org/10.1016/j.tcb.2005.11.001

Caron, E. (2003). Cellular functions of the Rap1 GTP-binding protein: a pattern emerges. *Journal of Cell Science*, *116*(3), 435 LP-440. https://doi.org/10.1242/jcs.00238

Chan, A. Y., Coniglio, S. J., Chuang, Y. Y., Michaelson, D., Knaus, U. G., Philips, M. R., and Symons, M. (2005). Roles of the Rac1 and Rac3 GTPases in human tumor cell invasion. *Oncogene*, *24*(53), 7821–7829. https://doi.org/10.1038/sj.onc.1208909

Chan, W., Sit, S.-T., and Manser, E. (2011). The Cdc42-associated kinase ACK1 is not autoinhibited but requires Src for activation. *Biochemical Journal*, *435*(2), 355–364. https://doi.org/10.1042/BJ20102156

Chan, W., Tian, R., Lee, Y.-F., Sit, S. T., Lim, L., and Manser, E. (2009). Down-regulation of active ACK1 is mediated by association with the E3 ubiquitin ligase Nedd4-2. *Journal of Biological Chemistry* , *284*(12), 8185–8194. https://doi.org/10.1074/jbc.M806877200

Chandra, A., Grecco, H. E., Pisupati, V., Perera, D., Cassidy, L., Skoulidis, F., Ismail, S. A., Hedberg, C., Hanzal-Bayer, M., Venkitaraman, A. R., Wittinghofer, A., and Bastiaens, P. I. H. (2012). The GDI-like solubilizing factor PDEδ sustains the spatial organization and signalling of Ras family proteins. *Nature Cell Biology*, *14*(2), 148–158. https://doi.org/10.1038/ncb2394

Chang, F., Lemmon, C., Lietha, D., Eck, M., and Romer, L. (2011). Tyrosine phosphorylation of Rac1: a role in regulation of cell spreading. *PloS One*, *6*(12), e28587–e28587. https://doi.org/10.1371/journal.pone.0028587

Chardin, P., Paris, S., Antonny, B., Robineau, S., Béraud-Dufour, S., Jackson, C. L., and Chabre, M. (1996). A human exchange factor for ARF contains Sec7- and pleckstrin-homology domains. *Nature*, *384*(6608), 481–484. https://doi.org/10.1038/384481a0

Chauhan, B. K., Lou, M., Zheng, Y., and Lang, R. A. (2011). Balanced Rac1 and RhoA activities regulate cell shape and drive invagination morphogenesis in epithelia. *Proceedings of the National Academy of Sciences*, *108*(45), 18289 LP-18294. https://doi.org/10.1073/pnas.1108993108

Chen, Z., Sun, J., Pradines, A., Favre, G., Adnane, J., and Sebti, S. M. (2000). Both farnesylated and geranylgeranylated RhoB inhibit malignant transformation and suppress human tumor growth in nude mice. *Journal of Biological Chemistry*, *275*(24), 17974–17978. https://doi.org/10.1074/jbc.C000145200

Chenette, E. J., Abo, A., and Der, C. J. (2005). Critical and distinct roles of amino- and carboxyl-terminal sequences in regulation of the biological activity of the Chp atypical Rho GTPase. *Journal of Biological Chemistry* , *280*(14), 13784–13792. https://doi.org/10.1074/jbc.M411300200

Chenette, E. J., Mitin, N. Y., and Der, C. J. (2006). Multiple sequence elements facilitate Chp Rho GTPase subcellular location, membrane association, and transforming activity. *Molecular Biology of the Cell*, *17*(7), 3108–3121. https://doi.org/10.1091/mbc.e05-09-0896

Cheng, J., Wang, H., and Guggino, W. B. (2005). Regulation of Cystic Fibrosis transmembrane regulator trafficking and protein expression by a Rho-family small GTPase TC10. *Journal of Biological Chemistry* , *280*(5), 3731–3739. https://doi.org/10.1074/jbc.M410026200

Cheng, L., Mahon, G. M., Kostenko, E. V, and Whitehead, I. P. (2004). Pleckstrin Homology domain-mediated activation of the Rho-specific Guanine Nucleotide Exchange Factor Dbs by Rac1. *Journal of Biological Chemistry* , *279*(13), 12786–12793. https://doi.org/10.1074/jbc.M313099200

Cherfils, J., and Zeghouf, M. (2013). Regulation of Small GTPases by GEFs, GAPs, and GDIs. *Physiological Reviews*, *93*(1).

Chianale, F., Rainero, E., Cianflone, C., Bettio, V., Pighini, A., Porporato, P. E., Filigheddu, N., Serini, G., Sinigaglia, F., Baldanzi, G., and Graziani, A. (2010). Diacylglycerol kinase α mediates HGF-induced Rac activation and membrane ruffling by regulating atypical PKC and RhoGDI. *Proceedings of the National Academy of Sciences*, *107*(9), 4182 LP-4187. https://doi.org/10.1073/pnas.0908326107

Chiang, S.-H., Baumann, C. A., Kanzaki, M., Thurmond, D. C., Watson, R. T., Neudauer, C. L., Macara, I. G., Pessin, J. E., and Saltiel, A. R. (2001). Insulin-stimulated GLUT4 translocation requires the CAP-dependent activation of TC10. *Nature*, *410*(6831), 944–948. https://doi.org/10.1038/35073608

Cho, H. J., Baek, K. E., Park, S.-M., Kim, I.-K., Choi, Y.-L., Cho, H.-J., Nam, I.-K., Hwang, E. M., Park, J.-Y., Han, J. Y., Kang, S. S., Kim, D. C., Lee, W. S., Lee, M.-N., Oh, G. T., Kim, J. W., Lee, C. W., and Yoo, J. (2009). RhoGDI2 expression is associated with tumor growth and malignant progression of gastric cancer. *Clinical Cancer Research*, *15*(8), 2612 LP-2619. https://doi.org/10.1158/1078-0432.CCR-08-2192

Cho, H. J., Baek, K. E., and Yoo, J. (2010). RhoGDI2 as a therapeutic target in cancer. *Expert Opinion on Therapeutic Targets*, *14*(1), 67–75. https://doi.org/10.1517/14728220903449251

Cho, H. J., Hwang, Y.-S., Yoon, J., Lee, M., Lee, H. G., and Daar, I. O. (2018). EphrinB1 promotes cancer cell migration and invasion through the interaction with RhoGDI1. *Oncogene*, *37*(7), 861–872. https://doi.org/10.1038/onc.2017.386

Cho, H. J., Kim, J.-T., Baek, K. E., Kim, B.-Y., and Lee, H. G. (2019). Regulation of Rho GTPases by RhoGDIs in human cancers. *Cells*, *8*(9), 1037. https://doi.org/10.3390/cells8091037

Choi, Y. M., Kim, K. B., Lee, J. H., Chun, Y. K., An, I. S., An, S., and Bae, S. (2017). DBC2/RhoBTB2 functions as a tumor suppressor protein via Musashi-2 ubiquitination in breast cancer. *Oncogene*, *36*(20), 2802–2812. https://doi.org/10.1038/onc.2016.441

Choy, E., Chiu, V. K., Silletti, J., Feoktistov, M., Morimoto, T., Michaelson, D., Ivanov, I. E., and Philips, M. R. (1999). Endomembrane trafficking of Ras: The CAAX motif targets proteins to the ER and Golgi. *Cell*, *98*(1), 69–80. https://doi.org/https://doi.org/10.1016/S0092-8674(00)80607-8

Chuang, T. H., Bohl, P., Bokochs, G. M., Bohl, B. P., and Bokoch, G. M. (1993). Biologically active lipids are regulators of Rac.GDI complexation. *Journal of Biological Chemistry* , *268*(35), 26206–26211. http://www.jbc.org/content/268/35/26206.abstract

Chuang, Y., Valster, A., Coniglio, S. J., Backer, J. M., and Symons, M. (2007). The atypical Rho-family GTPase Wrch-1 regulates focal adhesion formation and cell migration. *Journal of Cell Science*, *120*(11), 1927 LP-1934. https://doi.org/10.1242/jcs.03456

Chunqiu Hou, J., and Pessin, J. E. (2003). Lipid raft targeting of the TC10 amino terminal domain is responsible for disruption of adipocyte cortical actin. *Molecular Biology of the Cell*, *14*(9), 3578–3591. https://doi.org/10.1091/mbc.e03-01-0012

Ciechanover, A., DiGiuseppe, J. A., Bercovich, B., Orian, A., Richter, J. D., Schwartz, A. L., and Brodeur, G. M. (1991). Degradation of nuclear oncoproteins by the ubiquitin system in vitro. *Proceedings of the National Academy of Sciences of the United States of America*, *88*(1), 139–143. https://doi.org/10.1073/pnas.88.1.139

Ciechanover, A., and Ben-Saadon, R. (2004). N-terminal ubiquitination: more protein substrates join in. *Trends in Cell Biology*, *14*(3), 103–106. https://doi.org/10.1016/j.tcb.2004.01.004

Citalán-Madrid, A. F., García-Ponce, A., Vargas-Robles, H., Betanzos, A., and Schnoor, M. (2013). Small GTPases of the Ras superfamily regulate intestinal epithelial homeostasis and barrier function via common and unique mechanisms. *Tissue Barriers*, *1*(5), e26938. https://doi.org/10.4161/tisb.26938

Clark, E. A., Golub, T. R., Lander, E. S., and Hynes, R. O. (2000). Genomic analysis of metastasis reveals an essential role for RhoC. *Nature*, *406*(6795), 532–535. https://doi.org/10.1038/35020106

Clayton, N. S., Fox, M., Vicenté-Garcia, J. J., Schroeder, C. M., Littlewood, T. D., Wilde, J. I., Corry, J., Krishnan, K., Zhang, Q., Wakelam, M. J. O., Brown, M. J. B., Crafter, C., Mott, H. R., and Owen, D. (2019). Assembly of novel, nuclear dimers of the PI3-Kinase regulatory subunits underpins the pro-proliferative activity of the Cdc42-activated tyrosine kinase, ACK. *BioRxiv*, 791277. https://doi.org/10.1101/791277

Colicelli, J. (2004). Human RAS superfamily proteins and related GTPases. *Science's STKE : Signal Transduction Knowledge Environment*, *2004*(250), RE13-RE13. https://doi.org/10.1126/stke.2502004re13

Color-Aparicio, V. M., Cervantes-Villagrana, R. D., García-Jiménez, I., Beltrán-Navarro, Y. M., Castillo-Kauil, A., Escobar-Islas, E., Reyes-Cruz, G., and Vázquez-Prado, J. (2020). Endothelial cell sprouting driven by RhoJ directly activated by a membrane-anchored Intersectin 1 (ITSN1) RhoGEF module. *Biochemical and Biophysical Research Communications*. https://doi.org/https://doi.org/10.1016/j.bbrc.2020.01.068

Cotteret, S., Jaffer, Z. M., Beeser, A., and Chernoff, J. (2003). p21-Activated Kinase 5 (Pak5) localizes to mitochondria and inhibits apoptosis by phosphorylating BAD. *Molecular and Cellular Biology*, *23*(16), 5526 LP-5539. https://doi.org/10.1128/MCB.23.16.5526-5539.2003

Coulombe, P., Rodier, G., Bonneil, E., Thibault, P., and Meloche, S. (2004). N-Terminal ubiquitination of extracellular signal-regulated kinase 3 and p21 directs their degradation by the proteasome. *Molecular and Cellular Biology*, *24*(14), 6140–6150. https://doi.org/10.1128/MCB.24.14.6140-6150.2004

Covill-Cooke, C., Toncheva, V. S., Drew, J., Birsa, N., López-Doménech, G., and Kittler, J. T. (2020). Peroxisomal fission is modulated by the mitochondrial Rho-GTPases, Miro1 and Miro2. *EMBO Reports*, *21*(2), e49865. https://doi.org/10.15252/embr.201949865

Crespo, P., Schuebel, K. E., Ostrom, A. A., Gutkind, J. S., and Bustelo, X. R. (1997). Phosphotyrosine-dependent activation of Rac-1 GDP/GTP exchange by the vav proto-oncogene product. *Nature*, *385*(6612), 169–172. https://doi.org/10.1038/385169a0

D'Souza-Schorey, C., and Stahl, P. D. (1995). Myristoylation is required for the intracellular localization and endocytic function of ARF6. *Experimental Cell Research*, *221*(1), 153–159. https://doi.org/https://doi.org/10.1006/excr.1995.1362

Dart, A. E., Box, G. M., Court, W., Gale, M. E., Brown, J. P., Pinder, S. E., Eccles, S. A., and Wells, C. M. (2015). PAK4 promotes kinase-independent stabilization of RhoU to modulate cell adhesion. *Journal of Cell Biology*, *211*(4), 863–879. https://doi.org/10.1083/jcb.201501072

de León-Bautista, M. P., Cardenas-Aguayo, M. D. C., Casique-Aguirre, D., Almaraz-Salinas, M., Parraguirre-Martinez, S., Olivo-Diaz, A., Thompson-Bonilla, M. D. R., and Vargas, M. (2016). Immunological and functional characterization of RhoGDI3 and its molecular targets RhoG and RhoB in human pancreatic cancerous and normal cells. *PloS One*, *11*(11), e0166370–e0166370. https://doi.org/10.1371/journal.pone.0166370

De, P., Peng, Q., Traktuevc, D. O., Li, W., Yoder, M. C., March, K. L., and Durden, D. L. (2009). Expression of RAC2 in endothelial cells is required for the postnatal neovascular response. *Experimental Cell Research*, *315*(2), 248–263. https://doi.org/https://doi.org/10.1016/j.yexcr.2008.10.003

de Toledo, M., Senic-Matuglia, F., Salamero, J., Uze, G., Comunale, F., Fort, P., and Blangy, A. (2003). The GTP/GDP cycling of Rho GTPase TCL is an essential regulator of the early endocytic pathway. *Molecular Biology of the Cell*, *14*(12), 4846–4856. https://doi.org/10.1091/mbc.e03-04-0254

Deng, L., Wang, C., Spencer, E., Yang, L., Braun, A., You, J., Slaughter, C., Pickart, C., and Chen, Z. J. (2000). Activation of the IκB kinase complex by TRAF6 requires a dimeric ubiquitin-conjugating enzyme complex and a unique polyubiquitin chain. *Cell*, *103*(2), 351–361. https://doi.org/https://doi.org/10.1016/S0092-8674(00)00126-4

DerMardirossian, C., and Bokoch, G. M. (2005). GDIs: central regulatory molecules in Rho GTPase activation. *Trends in Cell Biology*, *15*(7), 356–363. https://doi.org/https://doi.org/10.1016/j.tcb.2005.05.001

DerMardirossian, C., Rocklin, G., Seo, J.-Y., and Bokoch, G. M. (2006). Phosphorylation of RhoGDI by Src regulates Rho GTPase binding and cytosol-membrane cycling. *Molecular Biology of the Cell*, *17*(11), 4760–4768. https://doi.org/10.1091/mbc.E06-06-0533

Desai, S. P., Bhatia, S. N., Toner, M., and Irimia, D. (2013). Mitochondrial localization and the persistent migration of epithelial cancer cells. *Biophysical Journal*, *104*(9), 2077–2088. https://doi.org/https://doi.org/10.1016/j.bpj.2013.03.025

Donaldson, J. G., and Jackson, C. L. (2011). ARF family G proteins and their regulators: roles in membrane transport, development and disease. *Nature Reviews. Molecular Cell Biology*, *12*(6), 362–375. https://doi.org/10.1038/nrm3117

Dong, Z., Liu, Y., Lu, S., Wang, A., Lee, K., Wang, L.-H., Revelo, M., and Lu, S. (2006). Vav3 oncogene is overexpressed and regulates cell growth and androgen receptor activity in human prostate cancer. *Molecular Endocrinology*, *20*(10), 2315–2325. https://doi.org/10.1210/me.2006-0048

Dou, Z., Xu, C., Donahue, G., Shimi, T., Pan, J.-A., Zhu, J., Ivanov, A., Capell, B. C., Drake, A. M., Shah, P. P., Catanzaro, J. M., Ricketts, M. D., Lamark, T., Adam, S. A., Marmorstein, R., Zong, W.-X., Johansen, T., Goldman, R. D., Adams, P. D., and Berger, S. L. (2015). Autophagy mediates degradation of nuclear lamina. *Nature*, *527*(7576), 105–109. https://doi.org/10.1038/nature15548

Dovas, A., and Couchman, J. R. (2005). RhoGDI: multiple functions in the regulation of Rho-family GTPase activities. *Biochemical Journal*, *390*(1), 1–9. https://doi.org/10.1042/BJ20050104

Dransart, E., Olofsson, B., and Cherfils, J. (2005). RhoGDIs Revisited: Novel roles in Rho regulation. *Traffic*, *6*(11), 957–966. https://doi.org/10.1111/j.1600-0854.2005.00335.x

Dubash, A. D., Guilluy, C., Srougi, M. C., Boulter, E., Burridge, K., and García-Mata, R. (2011). The small GTPase RhoA localizes to the nucleus and is activated by Net1 and DNA damage signals. *PLoS ONE*, *6*(2). https://doi.org/10.1371/journal.pone.0017380

Eden, S., Rohatgi, R., Podtelejnikov, A. V, Mann, M., and Kirschner, M. W. (2002). Mechanism of regulation of WAVE1-induced actin nucleation by Rac1 and Nck. *Nature*, *418*(6899), 790–793. https://doi.org/10.1038/nature00859

Elfenbein, A., Rhodes, J. M., Meller, J., Schwartz, M. A., Matsuda, M., and Simons, M. (2009). Suppression of RhoG activity is mediated by a syndecan 4-synectin-RhoGDI1 complex and is reversed by PKCalpha in a Rac1 activation pathway. *The Journal of Cell Biology*, *186*(1), 75–83. https://doi.org/10.1083/jcb.200810179

Ellerbroek, S. M., Wennerberg, K., Arthur, W. T., Dunty, J. M., Bowman, D. R., DeMali, K. A., Der, C., and Burridge, K. (2004). SGEF, a RhoG guanine nucleotide exchange factor that stimulates macropinocytosis. *Molecular Biology of the Cell*, *15*(7), 3309–3319. https://doi.org/10.1091/mbc.e04-02-0146

Ellis, S., and Mellor, H. (2000). The novel Rho-family GTPase Rif regulates coordinated actin-based membrane rearrangements. *Current Biology*, *10*(21), 1387–1390. https://doi.org/https://doi.org/10.1016/S0960-9822(00)00777-6

Espinosa, E. J., Calero, M., Sridevi, K., and Pfeffer, S. R. (2009). RhoBTB3: a Rho GTPase-family ATPase required for endosome to Golgi transport. *Cell*, *137*(5), 938–948. https://doi.org/10.1016/j.cell.2009.03.043

Farrugia, A. J., and Calvo, F. (2016). The Borg family of Cdc42 effector proteins Cdc42EP1–5. *Biochemical Society Transactions*, *44*(6), 1709–1716. https://doi.org/10.1042/BST20160219

Fauré, J., Vignais, P. V, and Dagher, M.-C. (1999). Phosphoinositide-dependent activation of Rho A involves partial opening of the RhoA/Rho-GDI complex. *European Journal of Biochemistry*, *262*(3), 879–889. https://doi.org/10.1046/j.1432-1327.1999.00458.x

Fei, F., Kweon, S. S.-M., Haataja, L., De Sepulveda, P., Groffen, J., Heisterkamp, N., Ridley, A., Boulter, E., Garcia-Mata, R., Guilluy, C., Dubash, A., Rossi, G., Brennwald, P., Burridge, K., Dovas, A., Couchman, J., Dransart, E., Olofsson, B., Cherfils, J., … Groffen, J. (2010). The Fer tyrosine kinase regulates interactions of Rho GDP-Dissociation Inhibitor a with the small GTPase Rac. *BMC Biochemistry*, *11*(1), 48. https://doi.org/10.1186/1471-2091-11-48

Fernandez-Borja, M., Janssen, L., Verwoerd, D., Hordijk, P., and Neefjes, J. (2005). RhoB regulates endosome transport by promoting actin assembly on endosomal membranes through Dia1. *Journal of Cell Science*, *118*(12), 2661 LP-2670. https://doi.org/10.1242/jcs.02384

Fernandez-Zapico, M. E., Gonzalez-Paz, N. C., Weiss, E., Savoy, D. N., Molina, J. R., Fonseca, R., Smyrk, T. C., Chari, S. T., Urrutia, R., and Billadeau, D. D. (2005). Ectopic expression of VAV1 reveals an unexpected role in pancreatic cancer tumorigenesis. *Cancer Cell*, *7*(1), 39–49. https://doi.org/10.1016/j.ccr.2004.11.024

Finlin, B. S., Crump, S. M., Satin, J., and Andres, D. A. (2003). Regulation of voltage-gated calcium channel activity by the Rem and Rad GTPases. *Proceedings of the National Academy of Sciences*, *100*(24), 14469 LP-14474. https://doi.org/10.1073/pnas.2437756100

Florke, R. R., Young, G. T., and Hamann, M. J. (2017). Unraveling a model of TCL/RhoJ allosterism using TC10 reverse chimeras. *Small GTPases*, 1–8. https://doi.org/10.1080/21541248.2017.1347599

Floyd, Z. E., Trausch-Azar, J. S., Reinstein, E., Ciechanover, A., and Schwartz, A. L. (2001). The nuclear ubiquitin-proteasome system degrades MyoD. *Journal of Biological Chemistry*, *276*(25), 22468–22475. https://doi.org/10.1074/jbc.M009388200

Fox, M., Crafter, C., and Owen, D. (2019). The non-receptor tyrosine kinase ACK: regulatory mechanisms, signalling pathways and opportunities for attACKing cancer. *Biochemical Society Transactions*, *47*(6), 1715–1731. https://doi.org/10.1042/BST20190176

Fransson, Å., Ruusala, A., and Aspenström, P. (2003). Atypical Rho GTPases have roles in mitochondrial homeostasis and apoptosis. *Journal of Biological Chemistry* , *278*(8), 6495–6502. https://doi.org/10.1074/jbc.M208609200

Fransson, Å., Ruusala, A., Aspenström, P., and Aspenstro, P. (2006). The atypical Rho GTPases Miro-1 and Miro-2 have essential roles in mitochondrial trafficking. *Biochemical and Biophysical Research Communications*, *344*(2), 500–510. https://doi.org/https://doi.org/10.1016/j.bbrc.2006.03.163

Frederick, R. L., McCaffery, J. M., Cunningham, K. W., Okamoto, K., and Shaw, J. M. (2004). Yeast Miro GTPase, Gem1p, regulates mitochondrial morphology via a novel pathway . *Journal of Cell Biology*, *167*(1), 87–98. https://doi.org/10.1083/jcb.200405100

Freeman, J. L., Abo, A., and Lambeth, J. D. (1996). Rac "insert region" is a novel effector region that is implicated in the activation of NADPH oxidase, but not PAK65. *The Journal of Biological Chemistry*, *271*(33), 19794–19801. https://doi.org/10.1074/jbc.271.33.19794

Freeman, S. N., Ma, Y., and Cress, W. D. (2008). RhoBTB2 (DBC2) is a mitotic E2F1 target gene with a novel role in apoptosis. *Journal of Biological Chemistry* , *283*(4), 2353–2362. https://doi.org/10.1074/jbc.M705986200

Fritz, G., Just, I., and Kaina, B. (1999). Rho GTPases are over-expressed in human tumors. *International Journal of Cancer*, *81*(5), 682–687. https://doi.org/10.1002/(SICI)1097-0215(19990531)81:5<682::AID-IJC2>3.0.CO;2-B

Fueller, F., and Kubatzky, K. F. (2008). The small GTPase RhoH is an atypical regulator of haematopoietic cells. *Cell Communication and Signaling*, *6*(1), 6. https://doi.org/10.1186/1478-811X-6-6

Fujita, A., Koinuma, S., Yasuda, S., Nagai, H., Kamiguchi, H., Wada, N., and Nakamura, T. (2013). GTP hydrolysis of TC10 promotes neurite outgrowth through exocytic fusion of Rab11- and L1-containing vesicles by releasing exocyst component Exo70. *PloS One*, *8*(11), e79689–e79689. https://doi.org/10.1371/journal.pone.0079689

Furuhjelm, J., and Peränen, J. (2003). The C-terminal end of R-Ras contains a focal adhesion targeting signal. *Journal of Cell Science*, *116*(18), 3729 LP-3738. https://doi.org/10.1242/jcs.00689

Gajiwala, K. S., Maegley, K., Ferre, R., He, Y.-A., and Yu, X. (2013). Ack1: Activation and regulation by allostery. *PLOS ONE*, *8*(1), e53994. https://doi.org/10.1371/journal.pone.0053994

Galisteo, M. L., Yang, Y., Ureña, J., Schlessinger, J., Galisteo, M. L., Yang, Y., and Uren, J. (2006). Activation of the nonreceptor protein tyrosine kinase Ack by multiple extracellular stimuli. *Proceedings of the National Academy of Sciences*, *103*(26), 9796 LP-9801. https://doi.org/10.1073/pnas.0603714103

Garnett, M. J., Mansfeld, J., Godwin, C., Matsusaka, T., Wu, J., Russell, P., Pines, J., and Venkitaraman, A. R. (2009). UBE2S elongates ubiquitin chains on APC/C substrates to promote mitotic exit. *Nature Cell Biology*, *11*(11), 1363–1369. https://doi.org/10.1038/ncb1983

Gasman, S., Kalaidzidis, Y., and Zerial, M. (2003). RhoD regulates endosome dynamics through Diaphanous-related Formin and Src tyrosine kinase. *Nature Cell Biology*, *5*(3), 195–204. https://doi.org/10.1038/ncb935

Gauthier-Rouvière, C., Vignal, E., Mériane, M., Roux, P., Montcourier, P., and Fort, P. (1998). RhoG GTPase controls a pathway that independently activates Rac1 and Cdc42Hs. *Molecular Biology of the Cell*, *9*(6), 1379–1394. https://doi.org/10.1091/mbc.9.6.1379

Gerlach, B., Cordier, S. M., Schmukle, A. C., Emmerich, C. H., Rieser, E., Haas, T. L., Webb, A. I., Rickard, J. A., Anderton, H., Wong, W. W.-L., Nachbur, U., Gangoda, L., Warnken, U., Purcell, A. W., Silke, J., and Walczak, H. (2011). Linear ubiquitination prevents inflammation and regulates immune signalling. *Nature*, *471*(7340), 591–596. https://doi.org/10.1038/nature09816

Giang Ho, T. T., Stultiens, A., Dubail, J., Lapière, C. M., Nusgens, B. V., Colige, A. C., Deroanne, C. F., Lapiere, C. M., Nusgens, B. V., Colige, A. C., and Deroanne, C. F. (2011). RhoGDIα-dependent balance between RhoA and RhoC is a key regulator of cancer cell tumorigenesis. *Molecular Biology of the Cell*, *22*(17), 3263–3275. https://doi.org/10.1091/mbc.E11-01-0020

Gildea, J. J., Seraj, M. J., Oxford, G., Harding, M. A., Hampton, G. M., Moskaluk, C. A., Frierson, H. F., Conaway, M. R., and Theodorescu, D. (2002). RhoGDI2 is an invasion and metastasis suppressor gene in human cancer. *Cancer Research*, *62*(22), 6418–6423. http://www.ncbi.nlm.nih.gov/pubmed/12438227

Glickman, M. H., and Ciechanover, A. (2002). The ubiquitin-proteasome proteolytic pathway: destruction for the sake of construction. *Physiological Reviews*, *82*(2), 373–428. https://doi.org/10.1152/physrev.00027.2001

Goh, L. K., Huang, F., Kim, W., Gygi, S., and Sorkin, A. (2010). Multiple mechanisms collectively regulate clathrin-mediated endocytosis of the epidermal growth factor receptor. *Journal of Cell Biology*, *189*(5), 871–883. https://doi.org/10.1083/jcb.201001008

Goh, L. L., and Manser, E. (2010). The RhoA GEF Syx is a target of Rnd3 and regulated via a Raf1-like ubiquitin-related domain. *PLOS ONE*, *5*(8), e12409. https://doi.org/10.1371/journal.pone.0012409

Goicoechea, S. M., Zinn, A., Awadia, S. S., Snyder, K., and Garcia-Mata, R. (2017). A RhoG-mediated signaling pathway that modulates invadopodia dynamics in breast cancer cells. *Journal of Cell Science*, *130*(6), 1064 LP-1077. https://doi.org/10.1242/jcs.195552

Goitre, L., Trapani, E., Trabalzini, L., and Retta, S. F. (2014). The Ras superfamily of small GTPases: the unlocked secrets. *Methods in Molecular Biology (Clifton, N.J.)*, *1120*, 1–18. https://doi.org/10.1007/978-1-62703-791-4_1

Goldberg, J. (1998). Structural basis for activation of ARF GTPase: Mechanisms of guanine nucleotide exchange and GTP–myristoyl switching. *Cell*, *95*(2), 237–248. https://doi.org/https://doi.org/10.1016/S0092-8674(00)81754-7

Golding, A. E., Visco, I., Bieling, P., and Bement, W. M. (2019). Extraction of active Rho GTPases by RhoGDI regulates spatiotemporal patterning of Rho GTPases. *ELife*, *8*, e50471. https://doi.org/10.7554/eLife.50471

Golovanov, A. P., Chuang, T.-H., DerMardirossian, C., Barsukov, I., Hawkins, D., Badii, R., Bokoch, G. M., Lian, L.-Y., & Roberts, G. C. K. (2001). Structure-activity relationships in flexible protein domains: regulation of rho GTPases by RhoGDI and D4 GDI1 1Edited by P. E. Wright. *Journal of Molecular Biology*, *305*(1), 121–135. https://doi.org/https://doi.org/10.1006/jmbi.2000.4262

Gómez Del Pulgar, T., Valdés-Mora, F., Bandrés, E., Pérez-Palacios, R., Espina, C., Cejas, P., García-Cabezas, M. A., Nistal, M., Casado, E., González-Barón, M., García-Foncillas, J., and Lacal, J. C. (2008). Cdc42 is highly expressed in colorectal adenocarcinoma and downregulates ID4 through an epigenetic mechanism. *International Journal of Oncology*, *33*(1), 185–193. http://www.ncbi.nlm.nih.gov/pubmed/18575765

Gorelik, R., Yang, C., Kameswaran, V., Dominguez, R., and Svitkina, T. (2010). Mechanisms of plasma membrane targeting of formin mDia2 through its amino terminal domains. *Molecular Biology of the Cell*, *22*(2), 189–201. https://doi.org/10.1091/mbc.e10-03-0256

Greenman, C., Stephens, P., Smith, R., Dalgliesh, G. L., Hunter, C., Bignell, G., Davies, H., Teague, J., Butler, A., Stevens, C., Edkins, S., O'Meara, S., Vastrik, I., Schmidt, E. E.,

Avis, T., Barthorpe, S., Bhamra, G., Buck, G., Choudhury, B.,Stratton, M. R. (2007). Patterns of somatic mutation in human cancer genomes. *Nature*, *446*(7132), 153–158. https://doi.org/10.1038/nature05610

Griner, E. M., Churchill, M. E. A., Brautigan, D. L., and Theodorescu, D. (2013). PKCα phosphorylation of RhoGDI2 at Ser31 disrupts interactions with Rac1 and decreases GDI activity. *Oncogene*, *32*(8), 1010–1017. https://doi.org/10.1038/onc.2012.124

Griner, E. M., Dancik, G. M., Costello, J. C., Owens, C., Guin, S., Edwards, M. G., Brautigan, D. L., and Theodorescu, D. (2015). RhoC is an unexpected target of RhoGDI2 in prevention of lung colonization of bladder cancer. *Molecular Cancer Research : MCR*, *13*(3), 483–492. https://doi.org/10.1158/1541-7786.MCR-14-0420

Grøvdal, L. M., Johannessen, L. E., Rødland, M. S., Madshus, I. H., and Stang, E. (2008). Dysregulation of Ack1 inhibits down-regulation of the EGF receptor. *Experimental Cell Research*, *314*(6), 1292–1300. https://doi.org/https://doi.org/10.1016/j.yexcr.2007.12.017

Gu Cho, Y., Joon Choi, B., Jae Kim, C., Hwi Song, J., Zhang, C., Woo Nam, S., Young Lee, J., and Sang Park, W. (2008). Genetic analysis of the DBC2 gene in gastric cancer. *Acta Oncologica*, *47*(3), 366–371. https://doi.org/10.1080/02841860701644094

Gu, Y., Jasti, A. C., Jansen, M., and Siefring, J. E. (2005). RhoH, a hematopoietic-specific Rho GTPase, regulates proliferation, survival, migration, and engraftment of hematopoietic progenitor cells. *Blood*, *105*(4), 1467–1475. https://doi.org/10.1182/blood-2004-04-1604

Guilluy, C., Garcia-Mata, R., and Burridge, K. (2011). Rho protein crosstalk: another social network? *Trends in Cell Biology*, *21*(12), 718–726. https://doi.org/https://doi.org/10.1016/j.tcb.2011.08.002

Gururaj, A. E., Rayala, S. K., & Kumar, R. (2005). p21-activated kinase signaling in breast cancer. Breast Cancer Research : BCR, 7(1), 5–12. https://doi.org/10.1186/bcr961

Gustavsson, A., Yuan, M., & Fällman, M. (2004). Temporal Dissection of β1-Integrin Signaling Indicates a Role for p130Cas-Crk in Filopodia Formation. *Journal of Biological Chemistry* , *279*(22), 22893–22901. http://www.jbc.org/content/279/22/22893.abstract

Haataja, L., Groffen, J., and Heisterkamp, N. (1997). Characterization of RAC3, a novel member of the Rho-family . *Journal of Biological Chemistry* , *272*(33), 20384–20388. https://doi.org/10.1074/jbc.272.33.20384

Hajdo-Milašinović, A., Ellenbroek, S. I. J., van Es, S., van der Vaart, B., and Collard, J. G. (2007). Rac1 and Rac3 have opposing functions in cell adhesion and differentiation of neuronal cells. *Journal of Cell Science*, *120*(4), 555 LP-566.

https://doi.org/10.1242/jcs.03364

Hamaguchi, M., Meth, J. L., von Klitzing, C., Wei, W., Esposito, D., Rodgers, L., Walsh, T., Welcsh, P., King, M.-C., and Wigler, M. H. (2002). DBC2, a candidate for a tumor suppressor gene involved in breast cancer. *Proceedings of the National Academy of Sciences*, *99*(21), 13647–13652. https://doi.org/10.1073/pnas.212516099

Han, S.-W., Kim, H.-P., Shin, J.-Y., Jeong, E.-G., Lee, W.-C., Kim, K. Y., Park, S. Y., Lee, D.-W., Won, J.-K., Jeong, S.-Y., Park, K. J., Park, J.-G., Kang, G. H., Seo, J.-S., Kim, J.-I., and Kim, T.-Y. (2014). RNA editing in RHOQ promotes invasion potential in colorectal cancer. *The Journal of Experimental Medicine*, *211*(4), 613–621. https://doi.org/10.1084/jem.20132209

Hancock, J. F., and Hall, A. (1993). A novel role for RhoGDI as an inhibitor of GAP proteins. *The EMBO Journal*, *12*(5), 1915–1921.

Hancock, J. F., Paterson, H., and Marshall, C. J. (1990). A polybasic domain or palmitoylation is required in addition to the CAAX motif to localize p21ras to the plasma membrane. *Cell*, *63*(1), 133–139. https://doi.org/10.1016/0092-8674(90)90294-o

Hart, M. J., Eva, A., Evans, T., Aaronson, S. A., and Cerione, R. A. (1991). Catalysis of guanine nucleotide exchange on the CDC42Hs protein by the dbloncogene product. *Nature*, *354*(6351), 311–314. https://doi.org/10.1038/354311a0

Hart, M. J. M., Maru, Y., Leonard, D., Witte, O. N. O., Evans, T., and Cerione, R. R. A. (1992). A GDP dissociation inhibitor that serves as a GTPase inhibitor for the Ras-like protein CDC42Hs. *Science*, *258*(5083), 812–816.

Harvey, J. J. (1964). An unidentified virus which causes the rapid production of tumours in mice. *Nature*, *204*(4963), 1104–1105. https://doi.org/10.1038/2041104b0

Héraud, C., Pinault, M., Lagrée, V., and Moreau, V. (2019). p190RhoGAPs, the ARHGAP35- and ARHGAP5-encoded proteins, in health and disease. *Cells*, *8*(4), 351. https://doi.org/10.3390/cells8040351

Hershko, A., and Ciechanover, A. (1998). The ubiquitin system. *Annual Review of Biochemistry*, *67*, 425–479. https://doi.org/10.1146/annurev.biochem.67.1.425

Hidalgo-Carcedo, C., Hooper, S., Chaudhry, S. I., Williamson, P., Harrington, K., Leitinger, B., and Sahai, E. (2011). Collective cell migration requires suppression of actomyosin at cell–cell contacts mediated by DDR1 and the cell polarity regulators Par3 and Par6. *Nature Cell Biology*, *13*(1), 49–59. https://doi.org/10.1038/ncb2133

Hirsch, D. S., Shen, Y., and Wu, W. J. (2006). Growth and motility inhibition of breast cancer cells by Epidermal Growth Factor Receptor degradation is correlated with inactivation of Cdc42. *Cancer Research*, *66*(7), 3523 LP-3530. https://doi.org/10.1158/0008-5472.CAN-05-1547

Ho, H., Soto Hopkin, A., Kapadia, R., Vasudeva, P., Schilling, J., and Ganesan, A. K. (2013). RhoJ modulates melanoma invasion by altering actin cytoskeletal dynamics. *Pigment Cell and Melanoma Research*, *26*(2), 218–225. https://doi.org/10.1111/pcmr.12058

Ho, T. T. G., Merajver, S. D., Lapière, C. M., Nusgens, B. V, and Deroanne, C. F. (2008). RhoA-GDP Regulates RhoB Protein Stability: Potential involvement of RhoGDIα. *Journal of Biological Chemistry*, *283*(31), 21588–21598. https://doi.org/10.1074/jbc.M710033200

Hodge, R. G., and Ridley, A. J. (2016). Regulating Rho GTPases and their regulators. *Nature Reviews Molecular Cell Biology*, *17*(8), 496–510. https://doi.org/10.1038/nrm.2016.67

Hodge, R. G., and Ridley, A. J. (2017). Regulation and functions of RhoU and RhoV. *Small GTPases*, *11*(1), 8–15. https://doi.org/10.1080/21541248.2017.1362495

Horii, Y., Beeler, J. F., Sakaguchi, K., Tachibana, M., and Miki, T. (1994). A novel oncogene, ost, encodes a guanine nucleotide exchange factor that potentially links Rho and Rac signaling pathways. *The EMBO Journal*, *13*(20), 4776–4786. https://pubmed.ncbi.nlm.nih.gov/7957046

Horiuchi, A., Imai, T., Wang, C., Ohira, S., Feng, Y., Nikaido, T., & Konishi, I. (2003). Up-Regulation of Small GTPases, RhoA and RhoC, Is Associated with Tumor Progression in Ovarian Carcinoma. *Laboratory Investigation*, *83*(6), 861–870. https://doi.org/10.1097/01.LAB.0000073128.16098.31

Hu, L., Zou, H., Zhan, S., and Cao, K. (2007). Biphasic expression of RhoGDI2 in the progression of breast cancer and its negative relation with lymph node metastasis. *Oncology Reports*. https://doi.org/10.3892/or.17.6.1383

Huang, D., Lu, W., Zou, S., Wang, H., Jiang, Y., Zhang, X., Li, P., Songyang, Z., Wang, L., Wang, J., Huang, J., and Fang, L. (2017). Rho GDP-dissociation inhibitor α is a potential prognostic biomarker and controls telomere regulation in colorectal cancer. *Cancer Science*, *108*(7), 1293–1302. https://doi.org/10.1111/cas.13259

Huang, M., & Prendergast, G. C. (2006). RhoB in cancer suppression. *Histology and Histopathology*, *21*(2), 213–218. https://doi.org/10.14670/HH-21.213

Inoki, K., Li, Y., Xu, T., and Guan, K.-L. (2003). Rheb GTPase is a direct target of TSC2 GAP

activity and regulates mTOR signaling. *Genes and Development*, *17*(15), 1829–1834. https://doi.org/10.1101/gad.1110003

Isasa, M., Katz, E. J., Kim, W., Yugo, V., González, S., Kirkpatrick, D. S., Thomson, T. M., Finley, D., Gygi, S. P., and Crosas, B. (2010). Monoubiquitination of RPN10 regulates substrate recruitment to the proteasome. *Molecular Cell*, *38*(5), 733–745. https://doi.org/10.1016/j.molcel.2010.05.001

Jaffe, A. B., and Hall, A. (2005). RHO GTPASES: Biochemistry and biology. *Annual Review of Cell and Developmental Biology*, *21*(1), 247–269. https://doi.org/10.1146/annurev.cellbio.21.020604.150721

Jaiswal, M., Fansa, E. K., Dvorský, R., Ahmadian, M. R., Communication, S., Jaiswal, M., Fansa, E. K., Dvorsky, R., and Ahmadian, M. R. (2012). New insight into the molecular switch mechanism of human Rho-family proteins: Shifting a paradigm. *Biological Chemistry*, *394*(1), 89–95. https://doi.org/10.1515/hsz-2012-0207

Jeong, H.-W., Li, Z., Brown, M. D., and Sacks, D. B. (2007). IQGAP1 binds Rap1 and modulates its activity. *Journal of Biological Chemistry*, *282*(28), 20752–20762. http://www.jbc.org/content/282/28/20752.abstract

Ji, J., Feng, X., Shi, M., Cai, Q., Yu, Y., Zhu, Z., and Zhang, J. (2015). Rac1 is correlated with aggressiveness and a potential therapeutic target for gastric cancer. *International Journal of Oncology*, *46*(3), 1343–1353. https://doi.org/10.3892/ijo.2015.2836

Ji, W., and Rivero, F. (2016). Atypical Rho GTPases of the RhoBTB subfamily: roles in vesicle trafficking and tumorigenesis. *Cells*, *5*(2), 28. https://doi.org/10.3390/cells5020028

Jiang, K., Sun, J., Cheng, J., Djeu, J. Y., Wei, S., and Sebti, S. (2004). Akt mediates Ras downregulation of RhoB, a suppressor of transformation, invasion, and metastasis. *Molecular and Cellular Biology*, *24*(12), 5565 LP-5576. https://doi.org/10.1128/MCB.24.12.5565-5576.2004

Jiang, W. G., Watkins, G., Lane, J., Cunnick, G. H., Douglas-Jones, A., Mokbel, K., and Mansel, R. E. (2003). Prognostic value of Rho GTPases and Rho Guanine Nucleotide Dissociation Inhibitors in human breast cancers. *Clinical Cancer Research*, *9*(17), 6432 LP-6440. http://clincancerres.aacrjournals.org/content/9/17/6432.abstract

Jiang, W., Sordella, R., Chen, G.-C., Hakre, S., Roy, A. L., and Settleman, J. (2005). An FF domain-dependent protein interaction mediates a signaling pathway for growth factor-induced gene expression. *Molecular Cell*, *17*(1), 23–35. https://doi.org/https://doi.org/10.1016/j.molcel.2004.11.024

Jin, X., Jin, H. R., Jung, H. S., Lee, S. J., Lee, J.-H., and Lee, J. J. (2010). An atypical E3 ligase zinc finger protein 91 stabilizes and activates NF-kappaB-inducing kinase via Lys63-linked ubiquitination. *The Journal of Biological Chemistry*, *285*(40), 30539–30547. https://doi.org/10.1074/jbc.M110.129551

Jin, Z., Han, Y.-X., and Han, X.-R. (2013). Downregulated RhoBTB2 expression contributes to poor outcome in osteosarcoma patients. *Cancer Biotherapy and Radiopharmaceuticals*, *28*(10), 709–716. https://doi.org/10.1089/cbr.2012.1386

Joberty, G., Perlungher, R. R., and Macara, I. G. (1999). The Borgs, a new family of Cdc42 and TC10 GTPase-interacting proteins. *Molecular and Cellular Biology*, *19*(10), 6585–6597. http://www.ncbi.nlm.nih.gov/pubmed/10490598

Jun Cho, H., Kim, I.-K., Park, S.-M., Eun Baek, K., Nam, I.-K., Park, S.-H., Ryu, K.-J., Choi, J., Ryu, J., Hong, S.-C., Jeong, S.-H., Lee, Y.-J., Ko, G.-H., Won Kim, J., Won Lee, C., Soo Kang, S., and Yoo, J. (2014). VEGF-C mediates RhoGDI2-induced gastric cancer cell metastasis and cisplatin resistance. *International Journal of Cancer*, *135*(7), 1553–1563. https://doi.org/10.1002/ijc.28801

Kalpana, G., Figy, C., Yeung, M., and Yeung, K. C. (2019). Reduced RhoA expression enhances breast cancer metastasis with a concomitant increase in CCR5 and CXCR4 chemokines signaling. *Scientific Reports*, *9*(1), 16351. https://doi.org/10.1038/s41598-019-52746-w

Kaminuma, O., Deckert, M., Elly, C., Liu, Y. C., and Altman, A. (2001). Vav-Rac1-mediated activation of the c-Jun N-terminal kinase/c-Jun/AP-1 pathway plays a major role in stimulation of the distal NFAT site in the interleukin-2 gene promoter. *Molecular and Cellular Biology*, *21*(9), 3126–3136. https://doi.org/10.1128/MCB.21.9.3126-3136.2001

Kato-Stankiewicz, J., Ueda, S., Kataoka, T., Kaziro, Y., and Satoh, T. (2001). Epidermal Growth Factor stimulation of the ACK1/Dbl pathway in a Cdc42 and Grb2-dependent manner. *Biochemical and Biophysical Research Communications*, *284*(2), 470–477. https://doi.org/https://doi.org/10.1006/bbrc.2001.5004

Kato, J., Kaziro, Y., and Satoh, T. (2000). Activation of the guanine nucleotide exchange factor Dbl following ACK1-dependent tyrosine phosphorylation. *Biochemical and Biophysical Research Communications*, *268*(1), 141–147. https://doi.org/10.1006/bbrc.2000.2106

Katoh, H., Hiramoto, K., and Negishi, M. (2006). Activation of Rac1 by RhoG regulates cell migration. *Journal of Cell Science*, *119*(1), 56 LP-65. https://doi.org/10.1242/jcs.02720

Katoh, M. (2002). Molecular cloning and characterization of WRCH2 on human chromosome 15q15. *International Journal of Oncology*, *20*(5), 977–982.

Katzav, S., Martin-Zanca, D., and Barbacid, M. (1989). vav, a novel human oncogene derived from a locus ubiquitously expressed in hematopoietic cells. *The EMBO Journal*, *8*(8), 2283–2290. http://www.ncbi.nlm.nih.gov/pubmed/2477241

Kay, L., Pienaar, I. S., Cooray, R., Black, G., and Soundararajan, M. (2018). Understanding Miro GTPases: Implications in the treatment of neurodegenerative disorders. *Molecular Neurobiology*, *55*(9), 7352–7365. https://doi.org/10.1007/s12035-018-0927-x

Kelley, L. C., and Weed, S. A. (2012). Cortactin is a substrate of activated Cdc42-associated kinase 1 (ACK1) during ligand-induced epidermal growth factor receptor downregulation. *PloS One*, *7*(8), e44363–e44363. https://doi.org/10.1371/journal.pone.0044363

Kim, C. A., and Bowie, J. U. (2003). SAM domains: uniform structure, diversity of function. *Trends in Biochemical Sciences*, *28*(12), 625–628. https://doi.org/https://doi.org/10.1016/j.tibs.2003.11.001

Kim, C., Yang, H., Fukushima, Y., Saw, P. E., Lee, J., Park, J.-S., Park, I., Jung, J., Kataoka, H., Lee, D., Do Heo, W., Kim, I., Jon, S., Adams, R. H., Nishikawa, S.-I., Uemura, A., and Koh, G. Y. (2014). Vascular RhoJ is an effective and selective target for tumor angiogenesis and vascular disruption. *Cancer Cell*, *25*(1), 102–117. https://doi.org/https://doi.org/10.1016/j.ccr.2013.12.010

Kim, J.-H., Yu, S., Chen, J. D., and Kong, A. N. (2013). The nuclear cofactor RAC3/AIB1/SRC-3 enhances Nrf2 signaling by interacting with transactivation domains. *Oncogene*, *32*(4), 514–527. https://doi.org/10.1038/onc.2012.59

Kim, K., and Kim, Y.-J. (2019). The BTB domain protein-Cul3 complex is a novel regulator of collagen expression in breast cancer. *The FASEB Journal*, *33*(1_supplement), 802.38-802.38. https://doi.org/10.1096/fasebj.2019.33.1_supplement.802.38

Kim, O., Yang, J., and Qiu, Y. (2002). Selective activation of small GTPase RhoA by tyrosine kinase Etk through its Pleckstrin Homology domain. *Journal of Biological Chemistry* , *277*(33), 30066–30071. https://doi.org/10.1074/jbc.M201713200

Kim, T. K., and Maniatis, T. (1996). Regulation of interferon-gamma-activated STAT1 by the ubiquitin-proteasome pathway. *Science (New York, N.Y.)*, *273*(5282), 1717–1719. https://doi.org/10.1126/science.273.5282.1717

Kirisako, T., Kamei, K., Murata, S., Kato, M., Fukumoto, H., Kanie, M., Sano, S., Tokunaga, F., Tanaka, K., and Iwai, K. (2006). A ubiquitin ligase complex assembles linear polyubiquitin chains. *The EMBO Journal*, *25*(20), 4877–4887. https://doi.org/10.1038/sj.emboj.7601360

Kirkpatrick, D. S., Hathaway, N. A., Hanna, J., Elsasser, S., Rush, J., Finley, D., King, R. W.,

and Gygi, S. P. (2006). Quantitative analysis of in vitro ubiquitinated cyclin B1 reveals complex chain topology. *Nature Cell Biology*, *8*(7), 700–710. https://doi.org/10.1038/ncb1436

Kissil, J. L., Walmsley, M. J., Hanlon, L., Haigis, K. M., Bender Kim, C. F., Sweet-Cordero, A., Eckman, M. S., Tuveson, D. A., Capobianco, A. J., Tybulewicz, V. L. J., and Jacks, T. (2007). Requirement for Rac1 in a K-ras–induced lung cancer in the mouse. *Cancer Research*, *67*(17), 8089 LP-8094. https://doi.org/10.1158/0008-5472.CAN-07-2300

Kleer, C. G., van Golen, K. L., Zhang, Y., Wu, Z.-F., Rubin, M. A., and Merajver, S. D. (2002). Characterization of RhoC Expression in Benign and Malignant Breast Disease: A potential new marker for small breast carcinomas with metastatic ability. *The American Journal of Pathology*, *160*(2), 579–584. https://doi.org/https://doi.org/10.1016/S0002-9440(10)64877-8

Klosowiak, J. L., Focia, P. J., Chakravarthy, S., Landahl, E. C., Freymann, D. M., and Rice, S. E. (2013). Structural coupling of the EF hand and C-terminal GTPase domains in the mitochondrial protein Miro. *EMBO Reports*, *14*(11), 968–974. https://doi.org/10.1038/embor.2013.151

Koh, W., Mahan, R. D., and Davis, G. E. (2008). Cdc42- and Rac1-mediated endothelial lumen formation requires Pak2, Pak4 and Par3, and PKC-dependent signaling. *Journal of Cell Science*, *121*(7), 989 LP-1001. https://doi.org/10.1242/jcs.020693

Koizumi, K., Takano, K., Kaneyasu, A., Watanabe-Takano, H., Tokuda, E., Abe, T., Watanabe, N., Takenawa, T., and Endo, T. (2012). RhoD activated by fibroblast growth factor induces cytoneme-like cellular protrusions through mDia3C. *Molecular Biology of the Cell*, *23*(23), 4647–4661. https://doi.org/10.1091/mbc.e12-04-0315

Kondo, T., Sentani, K., Oue, N., Yoshida, K., Nakayama, H., and Yasui, W. (2004). Expression of *Rho*C is associated with metastasis of gastric carcinomas. *Pathobiology*, *71*(1), 19–25. https://doi.org/10.1159/000072958

Korkina, O., Dong, Z., Marullo, A., Warshaw, G., Symons, M., and Ruggieri, R. (2013). The MLK-related Kinase (MRK) is a novel RhoC effector that mediates Lysophosphatidic Acid (LPA)-stimulated tumor cell invasion. *Journal of Biological Chemistry* , *288*(8), 5364–5373. https://doi.org/10.1074/jbc.M112.414060

Kozma, R., Ahmed, S., Best, A., and Lim, L. (1995). The Ras-related protein Cdc42Hs and bradykinin promote formation of peripheral actin microspikes and filopodia in Swiss 3T3 fibroblasts. *Molecular and Cellular Biology*, *15*(4), 1942–1952. https://doi.org/10.1128/mcb.15.4.1942

Krieser, R. J., and Eastman, A. (1999). Cleavage and nuclear translocation of the caspase 3 substrate Rho GDP-dissociation inhibitor, D4-GDI, during apoptosis. *Cell Death and Differentiation*, *6*(5), 412–419. https://doi.org/10.1038/sj.cdd.4400515

Kühn, S., and Geyer, M. (2014). Formins as effector proteins of Rho GTPases. *Small GTPases*, *5*, e29513–e29513. https://doi.org/10.4161/sgtp.29513

Kumar, R., Gururaj, A. E., and Barnes, C. J. (2006). p21-activated kinases in cancer. *Nature Reviews Cancer*, *6*(6), 459–471. https://doi.org/10.1038/nrc1892

Kuroda, S., Kikuchi, A., Hirata, K., Masuda, T., Kishi, K., Sasaki, T., and Takai, Y. (1992). Cooperative function of rho GDS and rho GDI to regulate rho p21 activation in smooth muscle. *Biochemical and Biophysical Research Communications*, *185*(1), 473–480. https://doi.org/10.1016/s0006-291X(05)81009-5

Kuželová, K., Grebeňová, D., Holoubek, A., Röselová, P., and Obr, A. (2014). Group I PAK Inhibitor IPA-3 induces cell death and affects cell adhesivity to fibronectin in human hematopoietic cells. *PLOS ONE*, *9*(3), e92560. https://doi.org/10.1371/journal.pone.0092560

Kyrkou, A., Soufi, M., Bahtz, R., Ferguson, C., Bai, M., Parton, R. G., Hoffmann, I., Zerial, M., Fotsis, T., and Murphy, C. (2013). RhoD participates in the regulation of cell-cycle progression and centrosome duplication. *Oncogene*, *32*(14), 1831–1842. https://doi.org/10.1038/onc.2012.195

la Cour, T., Kiemer, L., Molgaard, A., Gupta, R., Skriver, K., and Brunak, S. (2004). Analysis and prediction of leucine-rich nuclear export signals. *Protein Engineering, Design and Selection : PEDS*, *17*(6), 527–536. https://doi.org/10.1093/protein/gzh062

Lai, C. C., Boguski, M., Broek, D., and Powers, S. (1993). Influence of guanine nucleotides on complex formation between Ras and CDC25 proteins. *Molecular and Cellular Biology*, *13*(3), 1345–1352. https://doi.org/10.1128/mcb.13.3.1345

Lam, B. D., and Hordijk, P. L. (2013). The Rac1 hypervariable region in targeting and signaling. *Small GTPases*, *4*(2), 78–89. https://doi.org/10.4161/sgtp.23310

Laminet, A. A., Ziegelhoffer, T., Georgopoulos, C., and Plückthun, A. (1990). The Escherichia coli heat shock proteins GroEL and GroES modulate the folding of the beta-lactamase precursor. *The EMBO Journal*, *9*(7), 2315–2319. https://pubmed.ncbi.nlm.nih.gov/2192863

Lammers, M., Meyer, S., Kühlmann, D., and Wittinghofer, A. (2008). Specificity of interactions between mDia isoforms and Rho proteins. *The Journal of Biological Chemistry*, *283*(50),

35236–35246. https://doi.org/10.1074/jbc.M805634200

Lanning, C. C., Daddona, J. L., Ruiz-Velasco, R., Shafer, S. H., and Williams, C. L. (2004). The Rac1 C-terminal polybasic region regulates the nuclear localization and protein degradation of Rac1. *Journal of Biological Chemistry*, *279*(42), 44197–44210. https://doi.org/10.1074/jbc.M404977200

Lassus, P., Roux, P., Zugasti, O., Philips, A., Fort, P., and Hibner, U. (2000). Extinction of Rac1 and Cdc42Hs signalling defines a novel p53-dependent apoptotic pathway. *Oncogene*, *19*(20), 2377–2385. https://doi.org/10.1038/sj.onc.1203553

LaVallie, E. R., Lu, Z., Diblasio-Smith, E. A., Collins-Racie, L. A., and McCoy, J. M. (2000). [21] Thioredoxin as a fusion partner for production of soluble recombinant proteins in Escherichia coli. *Methods in Enzymology*, *326*, 322–340. https://doi.org/10.1016/S0076-6879(00)26063-1

Lazer, G., Idelchuk, Y., Schapira, V., Pikarsky, E., and Katzav, S. (2009). The haematopoietic specific signal transducer Vav1 is aberrantly expressed in lung cancer and plays a role in tumourigenesis. *The Journal of Pathology*, *219*(1), 25–34. https://doi.org/10.1002/path.2579

Lee, H. S., Cheerathodi, M., Chaki, S. P., Reyes, S. B., Zheng, Y., Lu, Z., Paidassi, H., DerMardirossian, C., Lacy-Hulbert, A., Rivera, G. M., and McCarty, J. H. (2015). Protein Tyrosine Phosphatase-PEST and β8 Integrin regulate spatiotemporal patterns of RhoGDI1 activation in migrating cells. *Molecular and Cellular Biology*, *35*(8), 1401 LP-1413. https://doi.org/10.1128/MCB.00112-15

Lee, K., Liu, Y., Mo, J. Q., Zhang, J., Dong, Z., Lu, S., Bustelo, X., Bustelo, X., Katzav, S., Martin-Zanca, D., Barbacid, M., Zugaza, J., Lopez-Lago, M., Caloca, M., Dosil, M., Movilla, N., Bustelo, X., Moores, S., Selfors, L., Pietras, R. (2008). Vav3 oncogene activates estrogen receptor and its overexpression may be involved in human breast cancer. *BMC Cancer*, *8*(1), 158. https://doi.org/10.1186/1471-2407-8-158

Lei, X., Li, Y.-F., Chen, G.-D., Ou, D.-P., Qiu, X.-X., Zuo, C.-H., and Yang, L.-Y. (2015). Ack1 overexpression promotes metastasis and indicates poor prognosis of hepatocellular carcinoma. *Oncotarget*, *6*(38), 40622–40641. https://doi.org/10.18632/oncotarget.5872

Lelias, J. M., Adra, C. N., Wulf, G. M., Guillemot, J. C., Khagad, M., Caput, D., and Lim, B. (1993). cDNA cloning of a human mRNA preferentially expressed in hematopoietic cells and with homology to a GDP-dissociation inhibitor for the rho GTP-binding proteins. *Proceedings of the National Academy of Sciences*, *90*(4), 1479 LP-1483. https://doi.org/10.1073/pnas.90.4.1479

Leung, T., Chen, X. Q., Manser, E., and Lim, L. (1996). The p160 RhoA-binding kinase ROK alpha is a member of a kinase family and is involved in the reorganization of the cytoskeleton. *Molecular and Cellular Biology*, *16*(10), 5313–5327. https://doi.org/10.1128/mcb.16.10.5313

Lévay, M., Bartos, B., and Ligeti, E. (2013). p190RhoGAP has cellular RacGAP activity regulated by a polybasic region. *Cellular Signalling*, *25*(6), 1388–1394. https://doi.org/https://doi.org/10.1016/j.cellsig.2013.03.004

Li, F., Yi, L., Zhao, L., Itzen, A., Goody, R. S., and Wu, Y.-W. (2014). The role of the hypervariable C-terminal domain in Rab GTPases membrane targeting. *Proceedings of the National Academy of Sciences of the United States of America*, *111*(7), 2572–2577. https://doi.org/10.1073/pnas.1313655111

Li, Q., Yao, L., Wei, Y., Geng, S., He, C., and Jiang, H. (2015). Role of RHOT1 on migration and proliferation of pancreatic cancer. *American Journal of Cancer Research*, *5*(4), 1460–1470. https://www.ncbi.nlm.nih.gov/pubmed/26101710

Li, X., Bu, X., Lu, B., Avraham, H., Flavell, R. A., and Lim, B. (2002). The hematopoiesis-specific GTP-binding protein RhoH is GTPase deficient and modulates activities of other Rho GTPases by an inhibitory function. *Molecular and Cellular Biology*, *22*(4), 1158 LP-1171. http://mcb.asm.org/content/22/4/1158.abstract

Li, X. R., Ji, F., Ouyang, J., Wu, W., Qian, L. Y., and Yang, K. Y. (2006). Overexpression of RhoA is associated with poor prognosis in hepatocellular carcinoma. *European Journal of Surgical Oncology (EJSO)*, *32*(10), 1130–1134. https://doi.org/https://doi.org/10.1016/j.ejso.2006.05.012

Lin, Q., Fuji, R. N., Yang, W., and Cerione, R. A. (2003). RhoGDI is required for Cdc42-mediated cellular transformation. *Current Biology*, *13*(17), 1469–1479. https://doi.org/https://doi.org/10.1016/S0960-9822(03)00613-4

Lin, Q., Lo, C. G., Cerione, R. A., and Yang, W. (2002). The Cdc42 target ACK2 interacts with Sorting Nexin 9 (SH3PX1) to regulate Epidermal Growth Factor Receptor degradation. *Journal of Biological Chemistry* , *277*(12), 10134–10138. https://doi.org/10.1074/jbc.M110329200

Lin, Q., Wang, J., Childress, C., Sudol, M., Carey, D. J., Yang, W., Al, L. I. N. E. T., and Iol, M. O. L. C. E. L. L. B. (2010). HECT E3 ubiquitin ligase Nedd4-1 ubiquitinates ACK and regulates Epidermal Growth Factor (EGF)-induced degradation of EGF receptor and ACK. *Molecular and Cellular Biology*, *30*(6), 1541 LP-1554. https://doi.org/10.1128/MCB.00013-10

Lin, Q., Wang, J., Childress, C., and Yang, W. (2012). The activation mechanism of ACK1 (activated Cdc42-associated tyrosine kinase 1). *Biochemical Journal*, *445*(2), 255–264. https://doi.org/10.1042/BJ20111575

Lin, R., Bagrodia, S., Cerione, R., and Manor, D. (1997). A novel Cdc42Hs mutant induces cellular transformation. *Current Biology*, *7*(10), 794–797. https://doi.org/https://doi.org/10.1016/S0960-9822(06)00338-1

Linderoth, E., Pilia, G., Mahajan, N. P., and Ferby, I. (2013). Activated Cdc42-associated Kinase 1 (Ack1) is required for Tumor Necrosis Factor-related Apoptosis-inducing Ligand (TRAIL) receptor recruitment to lipid rafts and induction of cell death. *Journal of Biological Chemistry* , *288*(46), 32922–32931. http://www.jbc.org/content/288/46/32922.abstract

Linseman, D. A., Heidenreich, K. A., and Fisher, S. K. (2001). Stimulation of M3 muscarinic receptors induces phosphorylation of the Cdc42 effector activated Cdc42Hs-associated kinase-1 via a Fyn tyrosine kinase signaling pathway. *The Journal of Biological Chemistry*, *276*(8), 5622–5628. https://doi.org/10.1074/jbc.M006812200

Liu, B., Lin, X., Yang, X., Dong, H., Yue, X., Andrade, K. C., Guo, Z., Yang, J., Wu, L., Zhu, X., Zhang, S., Tian, D., Wang, J., Cai, Q., Chen, Q., Mao, S., Chen, Q., and Chang, J. (2015). Downregulation of RND3/RhoE in glioblastoma patients promotes tumorigenesis through augmentation of notch transcriptional complex activity. *Cancer Medicine*, *4*(9), 1404–1416. https://doi.org/10.1002/cam4.484

Liu, M., Tang, Q., Qiu, M., Lang, N., Li, M., Zheng, Y., and Bi, F. (2011). miR-21 targets the tumor suppressor RhoB and regulates proliferation, invasion and apoptosis in colorectal cancer cells. *FEBS Letters*, *585*(19), 2998–3005. https://doi.org/10.1016/j.febslet.2011.08.014

Liu, N., Zhang, G., Bi, F., Pan, Y., Xue, Y., Shi, Y., Yao, L., Zhao, L., Zheng, Y., and Fan, D. (2007). RhoC is essential for the metastasis of gastric cancer. *Journal of Molecular Medicine*, *85*(10), 1149–1156. https://doi.org/10.1007/s00109-007-0217-y

Liu, S., Sawada, T., Lee, S., Yu, W., Silverio, G., Alapatt, P., Millan, I., Shen, A., Saxton, W., Kanao, T., Takahashi, R., Hattori, N., Imai, Y., and Lu, B. (2012). Parkinson's disease-associated kinase PINK1 regulates Miro protein level and axonal transport of mitochondria. *PLoS Genetics*, *8*(3), e1002537–e1002537. https://doi.org/10.1371/journal.pgen.1002537

Liu, X., Chen, D., and Liu, G. (2014). Overexpression of RhoA promotes the proliferation and migration of cervical cancer cells. *Bioscience, Biotechnology, and Biochemistry*, *78*(11), 1895–1901. https://doi.org/10.1080/09168451.2014.943650

Liu, Y., Cheng, G., Song, Z., Xu, T., Ruan, H., Cao, Q., Wang, K., Bao, L., Liu, J., Zhou, L., Liu, D., Yang, H., Chen, K., and Zhang, X. (2019). RAC2 acts as a prognostic biomarker and promotes the progression of clear cell renal cell carcinoma. *International Journal of Oncology*, 645–656. https://doi.org/10.3892/ijo.2019.4849

Lougheed, J. C., Chen, R.-H., Mak, P., and Stout, T. J. (2004). Crystal structures of the phosphorylated and unphosphorylated kinase domains of the Cdc42-associated tyrosine kinase ACK1. *Journal of Biological Chemistry* , *279*(42), 44039–44045. https://doi.org/10.1074/jbc.M406703200

Lowy, D. R., and Willumsen, B. M. (1993). Function and regulation of ras. *Annual Review of Biochemistry*, *62*, 851–891. https://doi.org/10.1146/annurev.bi.62.070193.004223

Lu, A., and Pfeffer, S. R. (2013). Golgi-associated RhoBTB3 targets Cyclin E for ubiquitylation and promotes cell cycle progression. *Journal of Cell Biology*, *203*(2), 233–250. https://doi.org/10.1083/jcb.201305158

Ludwig, K., and Parsons, S. J. (2011). The tumor suppressor, p190RhoGAP, differentially initiates apoptosis and confers Docetaxel sensitivity to breast cancer cells. *Genes and Cancer*, *2*(1), 20–30. https://doi.org/10.1177/1947601911402680

Luo, J., Xu, T., Li, C., Ba, X., Wang, X., Jiang, Y., and Zeng, X. (2013). p85-RhoGDI2, a novel complex, is required for PSGL-1-induced B1 integrin-mediated lymphocyte adhesion to VCAM-1. *International Journal of Biochemistry and Cell Biology*, *45*(12), 2764–2773. https://doi.org/10.1016/j.biocel.2013.09.005

Ma, Y., McCarty, S. K., Kapuriya, N. P., Brendel, V. J., Wang, C., Zhang, X., Jarjoura, D., Saji, M., Chen, C.-S., & Ringel, M. D. (2013). Development of p21 activated kinase-targeted multikinase inhibitors that inhibit thyroid cancer cell migration. *The Journal of Clinical Endocrinology and Metabolism*, *98*(8), E1314–E1322. https://doi.org/10.1210/jc.2012-3937

MacAskill, A. F., Rinholm, J. E., Twelvetrees, A. E., Arancibia-Carcamo, I. L., Muir, J., Fransson, A., Aspenstrom, P., Attwell, D., and Kittler, J. T. (2009). Miro1 is a calcium Sensor for glutamate receptor-dependent localization of mitochondria at synapses. *Neuron*, *61*(4), 541–555. https://doi.org/https://doi.org/10.1016/j.neuron.2009.01.030

Machacek, M., Hodgson, L., Welch, C., Elliott, H., Pertz, O., Nalbant, P., Abell, A., Johnson, G. L., Hahn, K. M., and Danuser, G. (2009). Coordination of Rho GTPase activities during cell protrusion. *Nature*, *461*(7260), 99–103. https://doi.org/10.1038/nature08242

Machesky, L. M., and Insall, R. H. (1998). Scar1 and the related Wiskott–Aldrich syndrome protein, WASP, regulate the actin cytoskeleton through the Arp2/3 complex. *Current*

Biology, *8*(25), 1347–1356. https://doi.org/https://doi.org/10.1016/S0960-9822(98)00015-3

Madigan, J. P., Bodemann, B. O., Brady, D. C., Dewar, B. J., Keller, P. J., Leitges, M., Philips, M. R., Ridley, A. J., Der, C. J., and Cox, A. D. (2009). Regulation of Rnd3 localization and function by protein kinase Cα-mediated phosphorylation. *Biochemical Journal*, *424*(1), 153–161. https://doi.org/10.1042/BJ20082377

Mahajan, K., Coppola, D., Challa, S., Fang, B., Chen, Y. A., Zhu, W., Lopez, A. S., Koomen, J., Engelman, R. W., Rivera, C., Muraoka-Cook, R. S., Cheng, J. Q., Schönbrunn, E., Sebti, S. M., Earp, H. S., and Mahajan, N. P. (2010). Ack1 mediated AKT/PKB tyrosine 176 phosphorylation regulates its activation. *PLoS ONE*, *5*(3), e9646. https://doi.org/10.1371/journal.pone.0009646

Mahajan, K., Coppola, D., Chen, Y. A., Zhu, W., Lawrence, H. R., Lawrence, N. J., and Mahajan, N. P. (2012). Ack1 tyrosine kinase activation correlates with pancreatic cancer progression. *The American Journal of Pathology*, *180*(4), 1386–1393. https://doi.org/10.1016/j.ajpath.2011.12.028

Mahajan, K., Coppola, D., Rawal, B., Chen, Y. A., Lawrence, H. R., Engelman, R. W., Lawrence, N. J., and Mahajan, N. P. (2012). Ack1-mediated androgen receptor phosphorylation modulates radiation resistance in castration-resistant prostate cancer. *Journal of Biological Chemistry*, *287*(26), 22112–22122. https://doi.org/10.1074/jbc.M112.357384

Mahajan, K., Lawrence, H. R., Lawrence, N. J., and Mahajan, N. P. (2014). ACK1 tyrosine kinase interacts with histone demethylase KDM3A to regulate the mammary tumor oncogene HOXA1. *The Journal of Biological Chemistry*, *289*(41), 28179–28191. https://doi.org/10.1074/jbc.M114.584425

Mahajan, K., and Mahajan, N. P. (2013). ACK1 tyrosine kinase: targeted inhibition to block cancer cell proliferation. *Cancer Letters*, *338*(2), 185–192. https://doi.org/10.1016/j.canlet.2013.04.004

Mahajan, K., and Mahajan, N. P. (2014). ACK1/TNK2 tyrosine kinase: An emerging target for cancer therapeutics. *AACR Education Book*, *2014*(1), 97–102. https://doi.org/10.1158/AACR.EDB-14-6109

Mahajan, K., and Mahajan, N. P. (2015). ACK1/TNK2 tyrosine kinase: molecular signaling and evolving role in cancers. *Oncogene*, *34*(32), 4162–4167. https://doi.org/10.1038/onc.2014.350

Mahajan, N. P., Liu, Y., Majumder, S., Warren, M. R., Parker, C. E., Mohler, J. L., Earp, H. S., and Whang, Y. E. (2007). Activated Cdc42-associated kinase Ack1 promotes prostate

cancer progression via androgen receptor tyrosine phosphorylation. *Proceedings of the National Academy of Sciences*, *104*(20), 8438–8443. https://doi.org/10.1073/pnas.0700420104

Mahajan, N. P., Whang, Y. E., Mohler, J. L., and Earp, H. S. (2005). Activated Tyrosine Kinase Ack1 Promotes Prostate Tumorigenesis: Role of Ack1 in polyubiquitination of tumor suppressor Wwox. *Cancer Research*, *65*(22), 10514–10523. https://doi.org/10.1158/0008-5472.CAN-05-1127

Mahendrarajah, N., Borisova, M. E., Reichardt, S., Godmann, M., Sellmer, A., Mahboobi, S., Haitel, A., Schmid, K., Kenner, L., Heinzel, T., Beli, P., and Krämer, O. H. (2017). HSP90 is necessary for the ACK1-dependent phosphorylation of STAT1 and STAT3. *Cellular Signalling*, *39*, 9–17. https://doi.org/https://doi.org/10.1016/j.cellsig.2017.07.014

Manser, E., Leung, T., Salihuddin, H., Tan, L., and Lim, L. (1993). A non-receptor tyrosine kinase that inhibits the GTPase activity of p21cdc42. *Nature*, *363*(6427), 364–367. https://doi.org/10.1038/363364a0

Manser, E., Leung, T., Salihuddin, H., Zhao, Z., and Lim, L. (1994). A brain serine/threonine protein kinase activated by Cdc42 and Rac1. *Nature*, *367*(6458), 40–46. https://doi.org/10.1038/367040a0

Mao, H., Zhang, L., Yang, Y., Sun, J., Deng, B., Feng, J., Shao, Q., Feng, A., Song, B., and Qu, X. (2011). RhoBTB2 (DBC2) functions as tumor suppressor via inhibiting proliferation, preventing colony formation and inducing apoptosis in breast cancer cells. *Gene*, *486*(1), 74–80. https://doi.org/https://doi.org/10.1016/j.gene.2011.07.018

Marzouk, S. El, Schultz-Norton, J. R., Likhite, V. S., McLeod, I. X., Yates, J. R., and Nardulli, A. M. (2007). Rho GDP dissociation inhibitor α interacts with estrogen receptor α and influences estrogen responsiveness. *Journal of Molecular Endocrinology*, *39*(4), 249–259. https://doi.org/10.1677/JME-07-0055

Mazières, J., Tillement, V., Allal, C., Clanet, C., Bobin, L., Chen, Z., Sebti, S. M., Favre, G., and Pradines, A. (2005). Geranylgeranylated, but not farnesylated, RhoB suppresses Ras transformation of NIH-3T3 cells. *Experimental Cell Research*, *304*(2), 354–364. https://doi.org/https://doi.org/10.1016/j.yexcr.2004.10.019

McKinnon, C. M., Lygoe, K. A., Skelton, L., Mitter, R., and Mellor, H. (2008). The atypical Rho GTPase RhoBTB2 is required for expression of the chemokine CXCL14 in normal and cancerous epithelial cells. *Oncogene*, *27*(54), 6856–6865. https://doi.org/10.1038/onc.2008.317

McKinnon, C. M., and Mellor, H. (2017). The tumor suppressor RhoBTB1 controls Golgi

integrity and breast cancer cell invasion through METTL7B. *BMC Cancer*, *17*(1), 145. https://doi.org/10.1186/s12885-017-3138-3

Meinohl, C., Barnard, J. S., Fritz-Wolf, K., Unger, M., Porr, A., Heipel, M., Wirth, S., Madlung, J., Nordheim, A., Menke, A., Becker, K., and Giehl, K. (2019). Galectin-8 binds to the farnesylated C-terminus of K-Ras4B and modifies Ras/ERK signaling and migration in pancreatic and lung carcinoma cells. *Cancers* (Vol. 12, Issue 1). https://doi.org/10.3390/cancers12010030

Mellor, H., Flynn, P., Nobes, C. D., Hall, A., and Parker, P. J. (1998). PRK1 is targeted to endosomes by the small GTPase, RhoB. *Journal of Biological Chemistry* , *273*(9), 4811–4814. https://doi.org/10.1074/jbc.273.9.4811

Michaelson, D., Silletti, J., Murphy, G., D'Eustachio, P., Rush, M., and Philips, M. R. (2001). Differential localization of Rho GTPases in live cells: regulation by hypervariable regions and RhoGDI binding. *The Journal of Cell Biology*, *152*(1), 111–126. https://doi.org/10.1083/jcb.152.1.111

Michaelson, D., Abidi, W., Guardavaccaro, D., Zhou, M., Ahearn, I., Pagano, M., and Philips, M. R. (2008). Rac1 accumulates in the nucleus during the G2 phase of the cell cycle and promotes cell division. *Journal of Cell Biology*, *181*(3), 485–496. https://doi.org/10.1083/jcb.200801047

Milburn, M. V, Tong, L., deVos, A. M., Brunger, A., Yamaizumi, Z., Nishimura, S., and Kim, S. H. (1990). Molecular switch for signal transduction: structural differences between active and inactive forms of protooncogenic ras proteins. *Science (New York, N.Y.)*, *247*(4945), 939–945. https://doi.org/10.1126/science.2406906

Milia, J., Teyssier, F., Dalenc, F., Ader, I., Delmas, C., Pradines, A., Lajoie-Mazenc, I., Baron, R., Bonnet, J., Cohen-Jonathan, E., Favre, G., and Toulas, C. (2005). Farnesylated RhoB inhibits radiation-induced mitotic cell death and controls radiation-induced centrosome overduplication. *Cell Death and Differentiation*, *12*(5), 492–501. https://doi.org/10.1038/sj.cdd.4401586

Mino, A., Troeger, A., Brendel, C., Cantor, A., Harris, C., Ciuculescu, M. F., and Williams, D. A. (2018). RhoH participates in a multi-protein complex with the zinc finger protein kaiso that regulates both cytoskeletal structures and chemokine-induced T cells. *Small GTPases*, *9*(3), 260–273. https://doi.org/10.1080/21541248.2016.1220780

Minzhou, H., B., D. J., C., P. G., and D., L.-K. L. (2007). RhoB regulates PDGFR-β trafficking and signaling in vascular smooth muscle cells. *Arteriosclerosis, Thrombosis, and Vascular Biology*, *27*(12), 2597–2605. https://doi.org/10.1161/ATVBAHA.107.154211

Mira, J.-P., Benard, V., Groffen, J., Sanders, L. C., and Knaus, U. G. (2000). Endogenous, hyperactive Rac3 controls proliferation of breast cancer cells by a p21-activated kinase-dependent pathway. *Proceedings of the National Academy of Sciences*, *97*(1), 185 LP-189. https://doi.org/10.1073/pnas.97.1.185

Miyazaki, K., Ozaki, T., Kato, C., Hanamoto, T., Fujita, T., Irino, S., Watanabe, K., Nakagawa, T., and Nakagawara, A. (2003). A novel HECT-type E3 ubiquitin ligase, NEDL2, stabilizes p73 and enhances its transcriptional activity. *Biochemical and Biophysical Research Communications*, *308*(1), 106–113. https://doi.org/10.1016/S0006-291X(03)01347-0

Mizushima, N., Levine, B., Cuervo, A. M., and Klionsky, D. J. (2008). Autophagy fights disease through cellular self-digestion. *Nature*, *451*(7182), 1069–1075. https://doi.org/10.1038/nature06639

Modzelewska, K., Newman, L. P., Desai, R., and Keely, P. J. (2006). Ack1 mediates Cdc42-dependent cell migration and signaling to p130Cas. *Journal of Biological Chemistry* , *281*(49), 37527–37535. http://www.jbc.org/content/281/49/37527.abstract

Moissoglu, K., McRoberts, K. S., Meier, J. A., Theodorescu, D., and Schwartz, M. A. (2009). Rho GDP dissociation inhibitor 2 suppresses metastasis via unconventional regulation of Rho GTPases. *Cancer Research*, *69*(7), 2838–2844. https://doi.org/10.1158/0008-5472.CAN-08-1397

Moon, H., Jeong, S.-H., Ju, Y., Jeong, C., Lee, J. S., Lee, Y., Hong, S., Choi, S., Ha, W.-S., Park, S.-T., and Jung, E. (2010). Up-regulation of RhoGDI2 in human breast cancer and its prognostic implications. *Cancer Research and Treatment*, *42*(3), 151. https://doi.org/10.4143/crt.2010.42.3.151

Moore, K. A., Sethi, R., Doanes, A. M., Johnson, T. M., Pracyk, J. B., Kirby, M., Irani, K., Goldschmidt-Clermont, P. J., and Finkel, T. (1997). Rac1 is required for cell proliferation and G2/M progression. *The Biochemical Journal*, *326 (Pt 1*(Pt 1), 17–20. https://doi.org/10.1042/bj3260017

Morin, A., Cordelières, F. P., Cherfils, J., and Olofsson, B. (2010). RhoGDI3 and RhoG: Vesicular trafficking and interactions with the Sec3 Exocyst subunit. *Small GTPases*, *1*(3), 142–156. https://doi.org/10.4161/sgtp.1.3.15112

Morris, C. M., Haataja, L., McDonald, M., Gough, S., Markie, D., Groffen, J., and Heisterkamp, N. (2000). The small GTPase RAC3 gene is located within chromosome band 17q25.3 outside and telomeric of a region commonly deleted in breast and ovarian tumours. *Cytogenetic and Genome Research*, *89*(1–2), 18–23. https://doi.org/10.1159/000015583

Mouly, L., Gilhodes, J., Lemarié, A., Cohen-Jonathan Moyal, E., Toulas, C., Favre, G., Sordet, O., Monferran, S., Moyal, E. C.-J., Toulas, C., Favre, G., Sordet, O., and Monferran, S. (2019). The RND1 small GTPase: Main functions and emerging role in oncogenesis. *International Journal of Molecular Sciences*, *20*(15), 3612. https://doi.org/10.3390/ijms20153612

Movilla, N., and Bustelo, X. R. (1999). Biological and regulatory properties of Vav-3, a new member of the Vav family of oncoproteins. *Molecular and Cellular Biology*, *19*(11), 7870–7885. http://www.ncbi.nlm.nih.gov/pubmed/10523675

Moyers, J. S., Bilan, P. J., Reynet, C., and Kahn, C. R. (1996). Overexpression of Rad inhibits glucose uptake in cultured muscle and fat cells. *The Journal of Biological Chemistry*, *271*(38), 23111–23116. https://doi.org/10.1074/jbc.271.38.23111

Müller, M. P., and Goody, R. S. (2018). Molecular control of Rab activity by GEFs, GAPs and GDI. *Small GTPases*, *9*(1–2), 5–21. https://doi.org/10.1080/21541248.2016.1276999

Muñoz-Maldonado, C., Zimmer, Y., and Medová, M. (2019). A comparative analysis of individual RAS mutations in cancer biology. *Frontiers in Oncology*, *9*, 1088. https://doi.org/10.3389/fonc.2019.01088

Murali, A., and Rajalingam, K. (2014). Small Rho GTPases in the control of cell shape and mobility. *Cellular and Molecular Life Sciences*, *71*(9), 1703–1721. https://doi.org/10.1007/s00018-013-1519-6

Murphy, C., Saffrich, R., Grummt, M., Gournier, H., Rybin, V., Rubino, M., Auvinen, P., Lütcke, A., Parton, R. G., and Zerial, M. (1996). Endosome dynamics regulated by a Rho protein. *Nature*, *384*(6608), 427–432. https://doi.org/10.1038/384427a0

Murphy, C., Saffrich, R., Olivo-Marin, J.-C., Giner, A., Ansorge, W., Fotsis, T., and Zerial, M. (2001). Dual function of rhoD in vesicular movement and cell motility. *European Journal of Cell Biology*, *80*(6), 391–398. https://doi.org/https://doi.org/10.1078/0171-9335-00173

Nakata, Y., Kondoh, K., Fukushima, S., Hashiguchi, A., Du, W., Hayashi, M., Fujimoto, J., Hata, J., and Yamada, T. (2008). Mutated D4-guanine diphosphate–dissociation inhibitor is found in human leukemic cells and promotes leukemic cell invasion. *Experimental Hematology*, *36*(1), 37–50. https://doi.org/10.1016/j.exphem.2007.08.023

Navarro-Lérida, I., Pellinen, T., Sanchez, S. A., Guadamillas, M. C., Wang, Y., Mirtti, T., Calvo, E., and Del Pozo, M. A. (2015). Rac1 nucleocytoplasmic shuttling drives nuclear shape changes and tumor invasion. *Developmental Cell*, *32*(3), 318–334. https://doi.org/10.1016/j.devcel.2014.12.019

Nehru, V., Almeida, F. N., and Aspenström, P. (2013). Interaction of RhoD and ZIP kinase modulates actin filament assembly and focal adhesion dynamics. *Biochemical and Biophysical Research Communications*, *433*(2), 163–169. https://doi.org/https://doi.org/10.1016/j.bbrc.2013.02.046

Nguyen, L. K., Kholodenko, B. N., and von Kriegsheim, A. (2018). Rac1 and RhoA: Networks, loops and bistability. *Small GTPases*, *9*(4), 316–321. https://doi.org/10.1080/21541248.2016.1224399

Nikolova, E., Mitev, V., Zhelev, N., Deroanne, C. F., and Poumay, Y. (2007). The small Rho GTPase Rac1 controls normal human dermal fibroblasts proliferation with phosphorylation of the oncoprotein c-myc. *Biochemical and Biophysical Research Communications*, *359*(3), 834–839. https://doi.org/https://doi.org/10.1016/j.bbrc.2007.05.214

Nishiya, N., Kiosses, W. B., Han, J., and Ginsberg, M. H. (2005). An α4 integrin–paxillin–Arf-GAP complex restricts Rac activation to the leading edge of migrating cells. *Nature Cell Biology*, *7*(4), 343–352. https://doi.org/10.1038/ncb1234

Niu, H., Wu, B., Jiang, H., Li, H., Zhang, Y., Peng, Y., and He, P. (2014). Mechanisms of RhoGDI2 mediated lung cancer epithelial-mesenchymal transition suppression. *Cellular Physiology and Biochemistry*, *34*(6), 2007–2016. https://doi.org/10.1159/000366396

Niu, J., Shi, Y., Iwai, K., and Wu, Z.-H. (2011). LUBAC regulates NF-kappaB activation upon genotoxic stress by promoting linear ubiquitination of NEMO. *The EMBO Journal*, *30*(18), 3741–3753. https://doi.org/10.1038/emboj.2011.264

Nobes, C. D., and Hall, A. (1995). Rho, rac, and cdc42 GTPases regulate the assembly of multimolecular focal complexes associated with actin stress fibres, lamellipodia, and filopodia. *Cell*, *81*(1), 53–62. https://doi.org/10.1016/0092-8674(95)90370-4

Nobes, C. D., and Hall, A. (1999). Rho GTPases control polarity, protrusion, and adhesion during cell movement . *The Journal of Cell Biology*, *144*(6), 1235–1244. https://doi.org/10.1083/jcb.144.6.1235

Nobes, C. D., Lauritzen, I., Mattei, M.-G., Paris, S., Hall, A., and Chardin, P. (1998). A new member of the Rho-family, Rnd1, promotes disassembly of actin filament structures and loss of cell adhesion . *The Journal of Cell Biology*, *141*(1), 187–197. https://doi.org/10.1083/jcb.141.1.187

Nomanbhoy, T. K., and Cerione, R. (1996). Characterization of the interaction between RhoGDI and Cdc42Hs using fluorescence spectroscopy. *The Journal of Biological Chemistry*, *271*(17), 10004–10009. https://doi.org/10.1074/jbc.271.17.10004

O'Mealey, G. B., Plafker, K. S., Berry, W. L., Janknecht, R., Chan, J. Y., and Plafker, S. M. (2017). A PGAM5–KEAP1–Nrf2 complex is required for stress-induced mitochondrial retrograde trafficking. *Journal of Cell Science*, *130*(20), 3467 LP-3480. https://doi.org/10.1242/jcs.203216

Oda, T., Muramatsu, M., Isogai, T., Masuho, Y., Asano, S., and Yamashita, T. (2001). HSH2: A novel SH2 domain-containing adapter protein involved in tyrosine kinase signaling in hematopoietic cells. *Biochemical and Biophysical Research Communications*, *288*(5), 1078–1086. https://doi.org/https://doi.org/10.1006/bbrc.2001.5890

Oeding, S. J., Majstrowicz, K., Hu, X.-P., Schwarz, V., Freitag, A., Honnert, U., Nikolaus, P., and Bähler, M. (2018). Identification of Miro1 and Miro2 as mitochondrial receptors for myosin XIX. *Journal of Cell Science*, *131*(17), jcs219469. https://doi.org/10.1242/jcs.219469

Ohta, Y., Hartwig, J. H., and Stossel, T. P. (2006). FilGAP, a Rho- and ROCK-regulated GAP for Rac binds filamin A to control actin remodelling. *Nature Cell Biology*, *8*(8), 803–814. https://doi.org/10.1038/ncb1437

Ohtake, F., Saeki, Y., Ishido, S., Kanno, J., and Tanaka, K. (2016). The K48-K63 branched ubiquitin chain regulates NF-κB signaling. *Molecular Cell*, *64*(2), 251–266. https://doi.org/10.1016/j.molcel.2016.09.014

Oinuma, I., Kawada, K., Tsukagoshi, K., and Negishi, M. (2012). Rnd1 and Rnd3 targeting to lipid raft is required for p190 RhoGAP activation. *Molecular Biology of the Cell*, *23*(8), 1593–1604. https://doi.org/10.1091/mbc.e11-11-0900

Oishi, A., Makita, N., Sato, J., and Iiri, T. (2012). Regulation of RhoA signaling by the cAMP-dependent phosphorylation of RhoGDIα. *Journal of Biological Chemistry* , *287*(46), 38705–38715. https://doi.org/10.1074/jbc.M112.401547

Okada, T., Sinha, S., Esposito, I., Schiavon, G., López-Lago, M. A., Su, W., Pratilas, C. A., Abele, C., Hernandez, J. M., Ohara, M., Okada, M., Viale, A., Heguy, A., Socci, N. D., Sapino, A., Seshan, V. E., Long, S., Inghirami, G., Rosen, N., and Giancotti, F. G. (2015). The Rho GTPase Rnd1 suppresses mammary tumorigenesis and EMT by restraining Ras-MAPK signalling. *Nature Cell Biology*, *17*(1), 81–94. https://doi.org/10.1038/ncb3082

Olofsson, B. (1999). Rho guanine dissociation inhibitors: pivotal molecules in cellular signalling. *Cellular Signalling*, *11*(8), 545–554. http://www.ncbi.nlm.nih.gov/pubmed/10433515

Olson, M. F., Ashworth, A., and Hall, A. (1995). An essential role for Rho, Rac, and Cdc42 GTPases in cell cycle progression through G1. *Science*, *269*(5228), 1270 LP-1272.

https://doi.org/10.1126/science.7652575

Orgaz, J. L., Herraiz, C., and Sanz-Moreno, V. (2014). Rho GTPases modulate malignant transformation of tumor cells. *Small GTPases*, *5*, e29019–e29019. https://doi.org/10.4161/sgtp.29019

Owen, D., & Mott, H. R. (2005). Structural Analysis of Rho Protein Complexes. In E. Manser (Ed.), *RHO Family GTPases* (pp. 31–72). Springer-Verlag. https://doi.org/10.1007/1-4020-3462-8_3

Pacary, E., Heng, J., Azzarelli, R., Riou, P., Castro, D., Lebel-Potter, M., Parras, C., Bell, D. M., Ridley, A. J., Parsons, M., and Guillemot, F. (2011). Proneural transcription factors regulate different steps of cortical neuron migration through Rnd-mediated inhibition of RhoA signaling. *Neuron*, *69*(6), 1069–1084. https://doi.org/https://doi.org/10.1016/j.neuron.2011.02.018

Pan, X., Eathiraj, S., Munson, M., and Lambright, D. G. (2006). TBC-domain GAPs for Rab GTPases accelerate GTP hydrolysis by a dual-finger mechanism. *Nature*, *442*(7100), 303–306. https://doi.org/10.1038/nature04847

Pan, Y., Bi, F., Liu, N., Xue, Y., Yao, X., Zheng, Y., and Fan, D. (2004). Expression of seven main Rho-family members in gastric carcinoma. *Biochemical and Biophysical Research Communications*, *315*(3), 686–691. https://doi.org/https://doi.org/10.1016/j.bbrc.2004.01.108

Pandey, A., Dan, I., Kristiansen, T. Z., Watanabe, N. M., Voldby, J., Kajikawa, E., Khosravi-Far, R., Blagoev, B., and Mann, M. (2002). Cloning and characterization of PAK5, a novel member of mammalian p21-activated kinase-II subfamily that is predominantly expressed in brain. *Oncogene*, *21*(24), 3939–3948. https://doi.org/10.1038/sj.onc.1205478

Pao-Chun, L., Chan, P. M., Chan, W., and Manser, E. (2009). Cytoplasmic ACK1 interaction with multiple receptor tyrosine kinases is mediated by Grb2: An analysis of ACK1 effects on Axl signaling . *Journal of Biological Chemistry* , *284*(50), 34954–34963. https://doi.org/10.1074/jbc.M109.072660

Patel, P. H., Thapar, N., Guo, L., Martinez, M., Maris, J., Gau, C.-L., Lengyel, J. A., and Tamanoi, F. (2003). Drosophila Rheb GTPase is required for cell cycle progression and cell growth. *Journal of Cell Science*, *116*(17), 3601 LP-3610. https://doi.org/10.1242/jcs.00661

Patel, V., Rosenfeldt, H. M., Lyons, R., Servitja, J.-M., Bustelo, X. R., Siroff, M., and Gutkind, J. S. (2007). Persistent activation of Rac1 in squamous carcinomas of the head and neck: evidence for an EGFR/Vav2 signaling axis involved in cell invasion. *Carcinogenesis*, *28*(6),

1145–1152. https://doi.org/10.1093/carcin/bgm008

Pei, H., Guo, Z., Wang, Z., Dai, Y., Zheng, L., Zhu, L., Zhang, J., Hu, W., Nie, J., Mao, W., Jia, X., Li, B., Hei, T. K., and Zhou, G. (2018). RAC2 promotes abnormal proliferation of quiescent cells by enhanced JUNB expression via the MAL-SRF pathway. *Cell Cycle*, *17*(9), 1115–1123. https://doi.org/10.1080/15384101.2018.1480217

Pellegrin, S., and Mellor, H. (2005). The Rho-family GTPase Rif induces filopodia through mDia2. *Current Biology*, *15*(2), 129–133. https://doi.org/https://doi.org/10.1016/j.cub.2005.01.011

Pérez-Sala, D., Boya, P., Ramos, I., Herrera, M., and Stamatakis, K. (2009). The C-Terminal sequence of RhoB directs protein degradation through an endo-lysosomal pathway. *PLOS ONE*, *4*(12), e8117. https://doi.org/10.1371/journal.pone.0008117

Peters, D. T., Kay, L., Eswaran, J., Lakey, J. H., and Soundararajan, M. (2018). Human Miro proteins act as NTP Hydrolases through a novel, non-canonical catalytic mechanism. *International Journal of Molecular Sciences*, *19*(12), 3839. https://doi.org/10.3390/ijms19123839

Pfeffer, S., and Aivazian, D. (2004). Targeting Rab GTPases to distinct membrane compartments. *Nature Reviews Molecular Cell Biology*, *5*(11), 886–896. https://doi.org/10.1038/nrm1500

Phillips, M. J., Calero, G., Chan, B., Ramachandran, S., and Cerione, R. A. (2008). Effector proteins exert an important influence on the signaling-active state of the small GTPase Cdc42. *Journal of Biological Chemistry*, *283*(20), 14153–14164. https://doi.org/10.1074/jbc.M706271200

Pintard, L., Willems, A., and Peter, M. (2004). Cullin-based ubiquitin ligases: Cul3–BTB complexes join the family. *The EMBO Journal*, *23*(8), 1681–1687. https://doi.org/10.1038/sj.emboj.7600186

Pirone, D. M., Fukuhara, S., Gutkind, J. S., and Burbelo, P. D. (2000). SPECs, Small Binding Proteins for Cdc42. *Journal of Biological Chemistry*, *275*(30), 22650–22656. https://doi.org/10.1074/jbc.M002832200

Platko, J. V, Leonard, D. A., Adra, C. N., Shaw, R. J., Cerione, R. A., and Lim, B. (1995). A single residue can modify target-binding affinity and activity of the functional domain of the Rho subfamily GDP dissociation inhibitors. *Proceedings of the National Academy of Sciences of the United States of America*, *92*(7), 2974–2978. http://www.ncbi.nlm.nih.gov/pubmed/7708758

Potapova, T. A., Daum, J. R., Byrd, K. S., and Gorbsky, G. J. (2009). Fine tuning the cell cycle: activation of the Cdk1 inhibitory phosphorylation pathway during mitotic exit. *Molecular Biology of the Cell*, *20*(6), 1737–1748. https://doi.org/10.1091/mbc.e08-07-0771

Pradip, D., Peng, X., and Durden, D. L. (2003). Rac2 specificity in macrophage integrin signaling: Potential role for Syk kinase . *Journal of Biological Chemistry* , *278*(43), 41661–41669. https://doi.org/10.1074/jbc.M306491200

Pratt, E. P. S., Owens, J. L., Hockerman, G. H., and Hu, C.-D. (2016). Bimolecular Fluorescence Complementation (BiFC) Analysis of protein-protein Interactions and assessment of subcellular localization in live cells. *Methods in Molecular Biology (Clifton, N.J.)*, *1474*, 153–170. https://doi.org/10.1007/978-1-4939-6352-2_9

Prieto-Echagüe, V., Gucwa, A., Brown, D. A., and Miller, W. T. (2010). Regulation of Ack1 localization and activity by the amino-terminal SAM domain. *BMC Biochemistry*, *11*(1), 42. https://doi.org/10.1186/1471-2091-11-42

Prieto-Echagüe, V., Miller, W. T., Prieto-Echagüe, V., and Miller, W. T. (2011). Regulation of ack-family nonreceptor tyrosine kinases. *Journal of Signal Transduction*, *2011*, 742372. https://doi.org/10.1155/2011/742372

Prive, G. G., Milburn, M. V, Tong, L., de Vos, A. M., Yamaizumi, Z., Nishimura, S., and Kim, S. H. (1992). X-ray crystal structures of transforming p21 ras mutants suggest a transition-state stabilization mechanism for GTP hydrolysis. *Proceedings of the National Academy of Sciences of the United States of America*, *89*(8), 3649–3653. https://doi.org/10.1073/pnas.89.8.3649

Prudnikova, T. Y., Rawat, S. J., and Chernoff, J. (2015). Molecular Pathways: Targeting the kinase effectors of Rho-family GTPases. *Clinical Cancer Research*, *21*(1), 24 LP-29. https://doi.org/10.1158/1078-0432.CCR-14-0827

Pylypenko, O., Rak, A., Durek, T., Kushnir, S., Dursina, B. E., Thomae, N. H., Constantinescu, A. T., Brunsveld, L., Watzke, A., Waldmann, H., Goody, R. S., and Alexandrov, K. (2006). Structure of doubly prenylated Ypt1:GDI complex and the mechanism of GDI-mediated Rab recycling. *The EMBO Journal*, *25*(1), 13–23. https://doi.org/10.1038/sj.emboj.7600921

Qin, C.-D., Ma, D.-N., Zhang, S.-Z., Zhang, N., Ren, Z.-G., Zhu, X.-D., Jia, Q.-A., Chai, Z.-T., Wang, C.-H., Sun, H.-C., and Tang, Z.-Y. (2018). The Rho GTPase Rnd1 inhibits epithelial–mesenchymal transition in hepatocellular carcinoma and is a favorable anti-metastasis target. *Cell Death and Disease*, *9*(5), 486. https://doi.org/10.1038/s41419-018-0517-x

Qiu, R. G., Abo, A., McCormick, F., and Symons, M. (1997). Cdc42 regulates anchorage-independent growth and is necessary for Ras transformation. *Molecular and Cellular Biology*, *17*(6), 3449 LP-3458. https://doi.org/10.1128/MCB.17.6.3449

Raftopoulou, M., and Hall, A. (2004). Cell migration: Rho GTPases lead the way. *Developmental Biology*, *265*(1), 23–32. https://doi.org/https://doi.org/10.1016/j.ydbio.2003.06.003

Rak, A., Pylypenko, O., Durek, T., Watzke, A., Kushnir, S., Brunsveld, L., Waldmann, H., Goody, R. S., and Alexandrov, K. (2003). Structure of Rab GDP-Dissociation Inhibitor in complex with prenylated YPT1 GTPase. *Science*, *302*(5645), 646 LP-650. https://doi.org/10.1126/science.1087761

Rane, C. K., & Minden, A. (2019). P21 activated kinase signaling in cancer. *Seminars in Cancer Biology*, *54*, 40–49. https://doi.org/https://doi.org/10.1016/j.semcancer.2018.01.006

Rapley, J., Tybulewicz, V. L. J., and Rittinger, K. (2008). Crucial structural role for the PH and C1 domains of the Vav1 exchange factor. *EMBO Reports*, *9*(7), 655–661. https://doi.org/10.1038/embor.2008.80

Razidlo, G. L., Magnine, C., Sletten, A. C., Hurley, R. M., Almada, L. L., Fernandez-Zapico, M. E., Ji, B., and McNiven, M. A. (2015). Targeting pancreatic cancer metastasis by inhibition of Vav1, a driver of tumor cell invasion. *Cancer Research*, *75*(14), 2907–2915. https://doi.org/10.1158/0008-5472.CAN-14-3103

Reid, T., Furuyashiki, T., Ishizaki, T., Watanabe, G., Watanabe, N., Fujisawa, K., Morii, N., Madaule, P., and Narumiya, S. (1996). Rhotekin, a new putative target for Rho bearing homology to a serine/threonine kinase, PKN, and Rhophilin in the Rho-binding domain. *Journal of Biological Chemistry* , *271*(23), 13556–13560. https://doi.org/10.1074/jbc.271.23.13556

Reinstein, E., Scheffner, M., Oren, M., Ciechanover, A., and Schwartz, A. (2000). Degradation of the E7 human papillomavirus oncoprotein by the ubiquitin-proteasome system: targeting via ubiquitination of the N-terminal residue. *Oncogene*, *19*(51), 5944–5950. https://doi.org/10.1038/sj.onc.1203989

Renault, L., Kuhlmann, J., Henkel, A., and Wittinghofer, A. (2001). Structural basis for guanine nucleotide exchange on Ran by the Regulator of Chromosome Condensation (RCC1). *Cell*, *105*(2), 245–255. https://doi.org/https://doi.org/10.1016/S0092-8674(01)00315-4

Ridley, A. J. (2006). Rho GTPases and actin dynamics in membrane protrusions and vesicle trafficking. *Trends in Cell Biology*, *16*(10), 522–529.

https://doi.org/https://doi.org/10.1016/j.tcb.2006.08.006

Ridley, A. J., and Hall, A. (1992). The small GTP-binding protein rho regulates the assembly of focal adhesions and actin stress fibres in response to growth factors. *Cell*, *70*(3), 389–399. https://doi.org/https://doi.org/10.1016/0092-8674(92)90163-7

Riento, K., Guasch, R. M., Garg, R., Jin, B., and Ridley, A. J. (2003). RhoE binds to ROCK I and inhibits downstream signaling. *Molecular and Cellular Biology*, *23*(12), 4219 LP-4229. https://doi.org/10.1128/MCB.23.12.4219-4229.2003

Riento, K., Totty, N., Villalonga, P., Garg, R., Guasch, R., and Ridley, A. J. (2005). RhoE function is regulated by ROCK I-mediated phosphorylation. *The EMBO Journal*, *24*(6), 1170–1180. https://doi.org/10.1038/sj.emboj.7600612

Riou, P., Kjær, S., Garg, R., Purkiss, A., George, R., Cain, R. J., Bineva, G., Reymond, N., McColl, B., Thompson, A. J., O'Reilly, N., McDonald, N. Q., Parker, P. J., and Ridley, A. J. (2013). 14-3-3 proteins interact with a hybrid prenyl-phosphorylation motif to inhibit G proteins. *Cell*, *153*(3), 640–653. https://doi.org/10.1016/j.cell.2013.03.044

Risse Sarah L, Belen, V., F, B. M., Pontus, A., P, P. R., Luc, B., and R, A. M. (2013). SH3-mediated targeting of Wrch1/RhoU by multiple adaptor proteins. In *Biological Chemistry* (Vol. 394, p. 421). https://doi.org/10.1515/hsz-2012-0246

Rittinger, K., Walker, P. A., Eccleston, J. F., Smerdon, S. J., and Gamblin, S. J. (1997). Structure at 1.65 Å of RhoA and its GTPase-activating protein in complex with a transition-state analogue. *Nature*, *389*(6652), 758–762. https://doi.org/10.1038/39651

Roberts, P. J., Mitin, N., Keller, P. J., Chenette, E. J., Madigan, J. P., Currin, R. O., Cox, A. D., Wilson, O., Kirschmeier, P., and Der, C. J. (2008). Rho-family GTPase modification and dependence on CAAX motif-signaled posttranslational modification. *The Journal of Biological Chemistry*, *283*(37), 25150–25163. https://doi.org/10.1074/jbc.M800882200

Rocks, O., Mueller, P. M., Rademacher, J., Bagshaw, R. D., Alp, K. M., Giudice, G., Heinrich, L. E., Barth, C., Eccles, R. L., Sanchez-Castro, M., Mbamalu, G., Tucholska, M., Spatt, L., Wortmann, C., Czajkowski, M. T., Welke, R. W., Zhang, S., Nguyen, V., Brandeburg, L., Petsalaki, E. (2018). Systematic characterization of RhoGEF/RhoGAP regulatory proteins reveals organization principles of Rho GTPase signaling. *BioRxiv*, 354316. https://doi.org/10.1101/354316

Rodrigo-Brenni, M. C., and Morgan, D. O. (2007). Sequential E2s drive polyubiquitin chain assembly on APC targets. *Cell*, *130*(1), 127–139. https://doi.org/https://doi.org/10.1016/j.cell.2007.05.027

Rolli-Derkinderen, M., Toumaniantz, G., Pacaud, P., and Loirand, G. (2010). RhoA phosphorylation induces Rac1 release from Guanine Dissociation Inhibitor α and stimulation of vascular smooth muscle cell migration. *Molecular and Cellular Biology*, *30*(20), 4786 LP-4796. https://doi.org/10.1128/MCB.00381-10

Rusyn, E. V, Reynolds, E. R., Shao, H., Grana, T. M., Chan, T. O., Andres, D. A., and Cox, A. D. (2000). Rit, a non-lipid-modified Ras-related protein, transforms NIH3T3 cells without activating the ERK, JNK, p38 MAPK or PI3K/Akt pathways. *Oncogene*, *19*(41), 4685–4694. https://doi.org/10.1038/sj.onc.1203836

Sadowski, M., and Sarcevic, B. (2010). Mechanisms of mono- and poly-ubiquitination: Ubiquitination specificity depends on compatibility between the E2 catalytic core and amino acid residues proximal to the lysine. *Cell Division*, *5*, 19. https://doi.org/10.1186/1747-1028-5-19

Salaun, C., Greaves, J., and Chamberlain, L. H. (2010). The intracellular dynamic of protein palmitoylation. *The Journal of Cell Biology*, *191*(7), 1229–1238. https://doi.org/10.1083/jcb.201008160

Sandrock, K., Bielek, H., Schradi, K., Schmidt, G., and Klugbauer, N. (2010). The nuclear import of the small GTPase Rac1 is mediated by the direct interaction with Karyopherin α2. *Traffic*, *11*(2), 198–209. https://doi.org/10.1111/j.1600-0854.2009.01015.x

Saras, J., Wollberg, P., and Aspenström, P. (2004). Wrch1 is a GTPase-deficient Cdc42-like protein with unusual binding characteristics and cellular effects. *Experimental Cell Research*, *299*(2), 356–369. https://doi.org/https://doi.org/10.1016/j.yexcr.2004.05.029

Satoh, T., Kato, J., Nishida, K., and Kaziro, Y. (1996). Tyrosine phosphorylation of ACK in response to temperature shift-down, hyperosmotic shock, and epidermal growth factor stimulation. *FEBS Letters*, *386*(2–3), 230–234. https://doi.org/10.1016/0014-5793(96)00449-8

Schaefer, A., Reinhard, N. R., & Hordijk, P. L. (2014). Toward understanding RhoGTPase specificity: structure, function and local activation. *Small GTPases*, *5*(2), e968004. https://doi.org/10.4161/21541248.2014.968004

Scheffzek, K., Ahmadian, M. R., Kabsch, W., Wiesmüller, L., Lautwein, A., Schmitz, F., and Wittinghofer, A. (1997). The Ras-RasGAP complex: Structural basis for GTPase activation and its loss in oncogenic Ras mutants. *Science*, *277*(5324), 333 LP-339. https://doi.org/10.1126/science.277.5324.333

Scheffzek, K., Stephan, I., Jensen, O. N., Illenberger, D., and Gierschik, P. (2000). The Rac-RhoGDI complex and the structural basis for the regulation of Rho proteins by RhoGDI. *Nature Structural Biology*, *7*(2), 122–126. https://doi.org/10.1038/72392

Scherle, P., Behrens, T., Staudt, L. M., Staudtt, L. M., and Staudt, L. M. (1993). Ly-GDI, a GDP-dissociation inhibitor of the RhoA GTP-binding protein, is expressed preferentially in lymphocytes. *Proceedings of the National Academy of Sciences*, *90*(16), 7568 LP-7572. https://doi.org/10.1073/pnas.90.16.7568

Schröter, C. J., Braun, M., Englert, J., Beck, H., Schmid, H., and Kalbacher, H. (1999). A rapid method to separate endosomes from lysosomal contents using differential centrifugation and hypotonic lysis of lysosomes. *Journal of Immunological Methods*, *227*(1), 161–168. https://doi.org/https://doi.org/10.1016/S0022-1759(99)00079-4

Schuebel, K. E. (1998). Phosphorylation-dependent and constitutive activation of Rho proteins by wild-type and oncogenic Vav-2. *The EMBO Journal*, *17*(22), 6608–6621. https://doi.org/10.1093/emboj/17.22.6608

Schuler, M.-H., Lewandowska, A., Caprio, G. Di, Skillern, W., Upadhyayula, S., Kirchhausen, T., Shaw, J. M., and Cunniff, B. (2017). Miro1-mediated mitochondrial positioning shapes intracellular energy gradients required for cell migration. *Molecular Biology of the Cell*, *28*(16), 2159–2169. https://doi.org/10.1091/mbc.e16-10-0741

Schwartz, M. (2004). Rho signalling at a glance. *Journal of Cell Science*, *117*(23), 5457 LP-5458. https://doi.org/10.1242/jcs.01582

Shalom-Feuerstein, R., Plowman, S. J., Rotblat, B., Ariotti, N., Tian, T., Hancock, J. F., and Kloog, Y. (2008). K-Ras nanoclustering is subverted by overexpression of the scaffold protein Galectin-3. *Cancer Research*, *68*(16), 6608 LP-6616. https://doi.org/10.1158/0008-5472.CAN-08-1117

Shapiro, A. D., and Pfeffer, S. R. (1995). Quantitative analysis of the interactions between prenyl Rab9, GDP dissociation inhibitor-alpha, and guanine nucleotides. *Journal of Biological Chemistry* , *270*(19), 11085–11090. https://doi.org/10.1074/jbc.270.19.11085

Shen, C.-H., Chen, H.-Y., Lin, M.-S., Li, F.-Y., Chang, C.-C., Kuo, M.-L., Settleman, J., and Chen, R.-H. (2008). Breast tumor kinase phosphorylates p190RhoGAP to regulate Rho and Ras and promote breast carcinoma growth, migration, and invasion. *Cancer Research*, *68*(19), 7779 LP-7787. https://doi.org/10.1158/0008-5472.CAN-08-0997

Shen, F., Lin, Q., Gu, Y., Childress, C., and Yang, W. (2007). Activated Cdc42-associated kinase 1 is a component of EGF receptor signaling complex and regulates EGF receptor degradation. *Molecular Biology of the Cell*, *18*(3), 732—742.

https://doi.org/10.1091/mbc.e06-02-0142

Shen, H., Ferguson, S. M., Dephoure, N., Park, R., Yang, Y., Volpicelli-Daley, L., Gygi, S., Schlessinger, J., and De Camilli, P. (2011). Constitutive activated Cdc42-associated kinase (Ack) phosphorylation at arrested endocytic clathrin-coated pits of cells that lack dynamin. *Molecular Biology of the Cell*, *22*(4), 493–502. https://doi.org/10.1091/mbc.E10-07-0637

Shepelev, M. V, Chernoff, J., and Korobko, I. V. (2011). Rho-family GTPase Chp/RhoV induces PC12 apoptotic cell death via JNK activation. *Small GTPases*, *2*(1), 17–26. https://doi.org/10.4161/sgtp.2.1.15229

Shepelev, M. V, & Korobko, I. V. (2013). The RHOV gene is overexpressed in human non–small cell lung cancer. *Cancer Genetics*, *206*(11), 393–397. https://doi.org/https://doi.org/10.1016/j.cancergen.2013.10.006

Shimomura, A., Ohama, T., Hori, M., and Ozaki, H. (2009). 17Beta-estradiol induces gastrointestinal motility disorder by decreasing CPI-17 phosphorylation via changes in Rho-family G-protein Rnd expression in small intestine. *The Journal of Veterinary Medical Science*, *71*(12), 1591–1597. https://doi.org/10.1292/jvms.001591

Shirakawa, R., and Horiuchi, H. (2015). Ral GTPases: crucial mediators of exocytosis and tumourigenesis. *The Journal of Biochemistry*, *157*(5), 285–299. https://doi.org/10.1093/jb/mvv029

Shisheva, A., Chinni, S. R., and DeMarco, C. (1999). General role of GDP Dissociation Inhibitor 2 in membrane release of Rab proteins: Modulations of its functional interactions by in vitro and in vivo structural modifications. *Biochemistry*, *38*(36), 11711–11721. https://doi.org/10.1021/bi990200r

Shurin, G. V, Tourkova, I. L., and Shurin, M. R. (2008). Low-dose chemotherapeutic agents regulate small Rho GTPase activity in dendritic cells. *Journal of Immunotherapy (Hagerstown, Md. : 1997)*, *31*(5), 491–499. https://doi.org/10.1097/CJI.0b013e318176fae4

Shutes, A., Berzat, A. C., Chenette, E. J., Cox, A. D., and Der, C. J. B. T.-M. in E. (2006). Biochemical analyses of the Wrch atypical Rho-family GTPases. In *Regulators and Effectors of Small GTPases: Rho-family* (Vol. 406, pp. 11–26). Academic Press. https://doi.org/https://doi.org/10.1016/S0076-6879(06)06002-2

Shutes, A., Berzat, A. C., Cox, A. D., and Der, C. J. (2004). Atypical mechanism of regulation of the Wrch-1 Rho-family small GTPase. *Current Biology*, *14*(22), 2052–2056. https://doi.org/https://doi.org/10.1016/j.cub.2004.11.011

Siddique, S. M., Kubouchi, K., Shinmichi, Y., Sawada, N., Sugiura, R., Itoh, Y., Uehara, S., Nishimura, K., Okamura, S., Ohsaki, H., Kamoshida, S., Yamashita, Y., Tamura, S., Sonoki, T., Matsuoka, H., Itoh, T., and Mukai, H. (2019). PKN1 kinase-negative knock-in mice develop splenomegaly and leukopenia at advanced age without obvious autoimmune-like phenotypes. *Scientific Reports*, *9*(1), 13977. https://doi.org/10.1038/s41598-019-50419-2

Sidhu, R. S., and Bhullar, R. P. (2001). Rab3B in human platelet is membrane bound and interacts with Ca^{2+}/Calmodulin. *Biochemical and Biophysical Research Communications*, *289*(5), 1039–1043. https://doi.org/https://doi.org/10.1006/bbrc.2001.6113

Slaymi, C., Vignal, E., Crès, G., Roux, P., Blangy, A., Raynaud, P., and Fort, P. (2019). The atypical RhoU/Wrch1 Rho GTPase controls cell proliferation and apoptosis in the gut epithelium. *Biology of the Cell*, *111*(5), 121–141. https://doi.org/10.1111/boc.201800062

Smotrys, J. E., and Linder, M. E. (2004). Palmitoylation of intracellular signaling proteins: regulation and function. *Annual Review of Biochemistry*, *73*(1), 559–587. https://doi.org/10.1146/annurev.biochem.73.011303.073954

Song, Q., Xu, Y., Yang, C., Chen, Z., Jia, C., Chen, J., Zhang, Y., Lai, P., Fan, X., Zhou, X., Lin, J., Li, M., Ma, W., Luo, S., and Bai, X. (2014). miR-483-5p promotes invasion and metastasis of lung adenocarcinoma by targeting RhoGDI1 and ALCAM. *Cancer Research*, *74*(11), 3031 LP-3042. https://doi.org/10.1158/0008-5472.CAN-13-2193

Soriano-Castell, D., Chavero, A., Rentero, C., Bosch, M., Vidal-Quadras, M., Pol, A., Enrich, C., and Tebar, F. (2017). ROCK1 is a novel Rac1 effector to regulate tubular endocytic membrane formation during clathrin-independent endocytosis. *Scientific Reports*, *7*(1), 6866. https://doi.org/10.1038/s41598-017-07130-x

Spencer, M. L., Shao, H., and Andres, D. A. (2002). Induction of neurite extension and survival in pheochromocytoma cells by the Rit GTPase. *The Journal of Biological Chemistry*, *277*(23), 20160–20168. https://doi.org/10.1074/jbc.M201092200

Spiering, D., & Hodgson, L. (2011). Dynamics of the Rho-family small GTPases in actin regulation and motility. *Cell Adhesion & Migration*, *5*(2), 170–180. https://doi.org/10.4161/cam.5.2.14403

Stiegler, A. L., and Boggon, T. J. (2018). The N-terminal GTPase domain of p190RhoGAP proteins is a pseudoGTPase. *Structure (London, England : 1993)*, *26*(11), 1451–1461.e4. https://doi.org/10.1016/j.str.2018.07.015

Stogios, P. J., and Privé, G. G. (2004). The BACK domain in BTB-kelch proteins. *Trends in*

Biochemical Sciences, *29*(12), 634–637. https://doi.org/https://doi.org/10.1016/j.tibs.2004.10.003

Straub, J., Konrad, E. D. H., Grüner, J., Toutain, A., Bok, L. A., Cho, M. T., Crawford, H. P., Dubbs, H., Douglas, G., Jobling, R., Johnson, D., Krock, B., Mikati, M. A., Nesbitt, A., Nicolai, J., Phillips, M., Poduri, A., Ortiz-Gonzalez, X. R., Powis, Z., … Zweier, C. (2018). Missense variants in RHOBTB2 cause a developmental and Epileptic Encephalopathy in humans, and altered levels cause neurological defects in Drosophila. *American Journal of Human Genetics*, *102*(1), 44–57. https://doi.org/10.1016/j.ajhg.2017.11.008

Su, L., Lineberry, N., Huh, Y., Soares, L., and Fathman, C. G. (2006). A novel E3 ubiquitin ligase substrate screen identifies Rho Guanine Dissociation Inhibitor as a substrate of Gene Related to Anergy in Lymphocytes. *The Journal of Immunology*, *177*(11), 7559 LP-7566. https://doi.org/10.4049/jimmunol.177.11.7559

Suehiro, J., Kanki, Y., Makihara, C., Schadler, K., Miura, M., Manabe, Y., Aburatani, H., Kodama, T., and Minami, T. (2014). Genome-wide approaches reveal functional Vascular Endothelial Growth Factor (VEGF)-inducible Nuclear Factor of Activated T Cells (NFAT) c1 binding to angiogenesis-related genes in the endothelium. *Journal of Biological Chemistry* , *289*(42), 29044–29059. https://doi.org/10.1074/jbc.M114.555235

Sulciner, D. J., Irani, K., Yu, Z. X., Ferrans, V. J., Goldschmidt-Clermont, P., and Finkel, T. (1996). Rac1 regulates a cytokine-stimulated, redox-dependent pathway necessary for NF-kappaB activation. *Molecular and Cellular Biology*, *16*(12), 7115 LP-7121. https://doi.org/10.1128/MCB.16.12.7115

Suwa, H., Ohshio, G., Imamura, T., Watanabe, G., Arii, S., Imamura, M., Narumiya, S., Hiai, H., and Fukumoto, M. (1998). Overexpression of the RhoC gene correlates with progression of ductal adenocarcinoma of the pancreas. *British Journal of Cancer*, *77*(1), 147–152. https://doi.org/10.1038/bjc.1998.23

Sztul, E., Chen, P.-W., Casanova, J. E., Cherfils, J., Dacks, J. B., Lambright, D. G., Lee, F.-J. S., Randazzo, P. A., Santy, L. C., Schürmann, A., Wilhelmi, I., Yohe, M. E., and Kahn, R. A. (2019). ARF GTPases and their GEFs and GAPs: concepts and challenges. *Molecular Biology of the Cell*, *30*(11), 1249–1271. https://doi.org/10.1091/mbc.E18-12-0820

Tajadura-Ortega, V., Garg, R., Allen, R., Owczarek, C., Bright, M. D., Kean, S., Mohd-Noor, A., Grigoriadis, A., Elston, T. C., Hahn, K. M., and Ridley, A. J. (2018). An RNAi screen of Rho signalling networks identifies RhoH as a regulator of Rac1 in prostate cancer cell migration. *BMC Biology*, *16*(1). https://doi.org/10.1186/s12915-018-0489-4

Tanaka, H., Fujita, H., Katoh, H., Mori, K., and Negishi, M. (2002). Vps4-A (vacuolar protein

sorting 4-A) is a binding partner for a novel Rho-family GTPase, Rnd2. *The Biochemical Journal*, *365*(Pt 2), 349–353. https://doi.org/10.1042/BJ20020062

Tanaka, H., Katoh, H., and Negishi, M. (2006). Pragmin, a novel effector of Rnd2 GTPase, stimulates RhoA Activity. *Journal of Biological Chemistry* , *281*(15), 10355–10364. https://doi.org/10.1074/jbc.M511314200

Tang, B. L. (2015). Miro GTPases in mitochondrial transport, homeostasis and pathology. *Cells*, *5*(1), 1. https://doi.org/10.3390/cells5010001

Tapper, J., Kettunen, E., El-Rifai, W., Seppälä, M., Andersson, L. C., and Knuutila, S. (2001). Changes in gene expression during progression of ovarian carcinoma. *Cancer Genetics and Cytogenetics*, *128*(1), 1–6. https://doi.org/https://doi.org/10.1016/S0165-4608(01)00386-7

Tcherkezian, J., and Lamarche-Vane, N. (2007). Current knowledge of the large RhoGAP family of proteins. *Biology of the Cell*, *99*(2), 67–86. https://doi.org/10.1042/BC20060086

ten Klooster, J. P., Jaffer, Z. M., Chernoff, J., and Hordijk, P. L. (2006). Targeting and activation of Rac1 are mediated by the exchange factor β-Pix . *Journal of Cell Biology*, *172*(5), 759–769. https://doi.org/10.1083/jcb.200509096

Teo, M., Tan, L., Lim, L., and Manser, E. (2001). The tyrosine kinase ACK1 associates with clathrin-coated vesicles through a binding motif shared by Arrestin and other adaptors. *Journal of Biological Chemistry* , *276*(21), 18392–18398. https://doi.org/10.1074/jbc.M008795200

Thaker, Y. R., Recino, A., Raab, M., Jabeen, A., Wallberg, M., Fernandez, N., and Rudd, C. E. (2017). Activated Cdc42-associated kinase 1 (ACK1) binds the sterile α motif (SAM) domain of the adaptor SLP-76 and phosphorylates proximal tyrosines. *Journal of Biological Chemistry* , *292*(15), 6281–6290. https://doi.org/10.1074/jbc.M116.759555

Theodorescu, D. (2004). Reduced expression of metastasis suppressor RhoGDI2 is associated with decreased survival for patients with bladder cancer. *Clinical Cancer Research*, *10*(11), 3800–3806. https://doi.org/10.1158/1078-0432.CCR-03-0653

Tin, B., Jing, S., Chin, S., Jie, W., and Ullrich, A. (2010). Somatic mutation in the ACK1 ubiquitin association domain enhances oncogenic signaling through EGFR regulation in renal cancer derived cells. *Molecular Oncology*, *4*(4), 323–334. https://doi.org/10.1016/j.molonc.2010.03.001

Tkachenko, E., Sabouri-Ghomi, M., Pertz, O., Kim, C., Gutierrez, E., Machacek, M., Groisman, A., Danuser, G., and Ginsberg, M. H. (2011). Protein kinase A governs a RhoA–RhoGDI protrusion–retraction pacemaker in migrating cells. *Nature Cell Biology*, *13*(6), 660–667.

https://doi.org/10.1038/ncb2231

Tokunaga, F., Nakagawa, T., Nakahara, M., Saeki, Y., Taniguchi, M., Sakata, S., Tanaka, K., Nakano, H., and Iwai, K. (2011). SHARPIN is a component of the NF-κB-activating linear ubiquitin chain assembly complex. *Nature*, *471*(7340), 633–636. https://doi.org/10.1038/nature09815

Toma-Fukai, S., Shimizu, T., and Gtpases, S. (2019). Structural insights into the regulation mechanism of small GTPases by GEFs. *Molecules (Basel, Switzerland)*, *24*(18), 3308. https://doi.org/10.3390/molecules24183308

Tong, J., Li, L., Ballermann, B., and Wang, Z. (2016). Phosphorylation and activation of RhoA by ERK in response to Epidermal Growth Factor stimulation. *PLOS ONE*, *11*(1), e0147103. https://doi.org/10.1371/journal.pone.0147103

Troeger, A., Chae, H.-D., Senturk, M., Wood, J., and Williams, D. A. (2013). A unique carboxyl-terminal insert domain in the hematopoietic-specific, GTPase-deficient Rho GTPase RhoH regulates post-translational processing. *Journal of Biological Chemistry* , *288*(51), 36451–36462. https://doi.org/10.1074/jbc.M113.505727

Trotman, L. C., Wang, X., Alimonti, A., Chen, Z., Teruya-Feldstein, J., Yang, H., Pavletich, N. P., Carver, B. S., Cordon-Cardo, C., Erdjument-Bromage, H., Tempst, P., Chi, S., Kim, H., Misteli, T., Jiang, X., and Pandolfi, P. P. (2007). Ubiquitination regulates PTEN nuclear import and tumor suppression. *Cell*, *128*(1), 141–156. https://doi.org/10.1016/j.cell.2006.11.040

Tsuji, T., Ishizaki, T., Okamoto, M., Higashida, C., Kimura, K., Furuyashiki, T., Arakawa, Y., Birge, R. B., Nakamoto, T., Hirai, H., and Narumiya, S. (2002). ROCK and mDia1 antagonize in Rho-dependent Rac activation in Swiss 3T3 fibroblasts . *Journal of Cell Biology*, *157*(5), 819–830. https://doi.org/10.1083/jcb.200112107

Tucci, M. G., Lucarini, G., Brancorsini, D., Zizzi, A., Pugnaloni, A., Giacchetti, A., Ricotti, G., and Biagini, G. (2007). Involvement of E-cadherin, β-catenin, Cdc42 and CXCR4 in the progression and prognosis of cutaneous melanoma. *British Journal of Dermatology*, *157*(6), 1212–1216. https://doi.org/10.1111/j.1365-2133.2007.08246.x

Turner, M., and Billadeau, D. D. (2002). VAV proteins as signal integrators for multi-subunit immune-recognition receptors. *Nature Reviews Immunology*, *2*(7), 476–486. https://doi.org/10.1038/nri840

Uen, Y.-H., Fang, C.-L., Hseu, Y.-C., Shen, P.-C., Yang, H.-L., Wen, K.-S., Hung, S.-T., Wang, L.-H., and Lin, K.-Y. (2015). VAV3 Oncogene expression in colorectal cancer: Clinical

aspects and functional characterization. *Scientific Reports*, *5*, 9360. https://doi.org/10.1038/srep09360

Ueyama, T., Son, J., Kobayashi, T., Hamada, T., Nakamura, T., Sakaguchi, H., Shirafuji, T., and Saito, N. (2013). Negative charges in the flexible N-terminal domain of Rho GDP-Dissociation Inhibitors (RhoGDIs) regulate the targeting of the RhoGDI–Rac1 complex to membranes. *The Journal of Immunology*, *191*(5), 2560 LP-2569. https://doi.org/10.4049/jimmunol.1300209

Ugolev, Y., Molshanski-Mor, S., Weinbaum, C., and Pick, E. (2006). Liposomes comprising anionic but not neutral phospholipids cause dissociation of Rac (1 or 2)·RhoGDI complexes and support amphiphile-independent NADPH oxidase activation by such complexes. *Journal of Biological Chemistry* , *281*(28), 19204–19219. https://doi.org/10.1074/jbc.M600042200

Unsal-kacmaz, K., Ragunathan, S., Rosfjord, E., Dann, S., Grillo, M., Hernandez, R., Mack, F., and Klippel, A. (2011). The interaction of PKN3 with RhoC promotes malignant growth. *Molecular Oncology*, *6*(3), 284–298. https://doi.org/10.1016/j.molonc.2011.12.001

Valencia, A., Chardin, P., Wittinghofer, A., and Sander, C. (1991). The ras protein family: evolutionary tree and role of conserved amino acids. *Biochemistry*, *30*(19), 4637–4648. http://www.ncbi.nlm.nih.gov/pubmed/2029511

van der Horst, E. H., Degenhardt, Y. Y., Strelow, A., Slavin, A., Chinn, L., Orf, J., Rong, M., Li, S., See, L.-H., Nguyen, K. Q. C., Hoey, T., Wesche, H., and Powers, S. (2005). Metastatic properties and genomic amplification of the tyrosine kinase gene ACK1. *Proceedings of the National Academy of Sciences of the United States of America*, *102*(44), 15901–15906. https://doi.org/10.1073/pnas.0508014102

van Hennik, P. B., Klooster, J. P. ten, Halstead, J. R., Voermans, C., Anthony, E. C., Divecha, N., and Hordijk, P. L. (2003). The C-terminal domain of Rac1 contains two motifs that control targeting and signaling specificity. *Journal of Biological Chemistry*, *278*(40), 39166–39175. https://doi.org/10.1074/jbc.M307001200

Vega, F. M., Fruhwirth, G., Ng, T., and Ridley, A. J. (2011). RhoA and RhoC have distinct roles in migration and invasion by acting through different targets. *The Journal of Cell Biology*, *193*(4), 655–665. https://doi.org/10.1083/jcb.201011038

Vetter, I. R., Nowak, C., Nishimoto, T., Kuhlmann, J., and Wittinghofer, A. (1999). Structure of a Ran-binding domain complexed with Ran bound to a GTP analogue: implications for nuclear transport. *Nature*, *398*(6722), 39–46. https://doi.org/10.1038/17969

Vetter, I. R., and Wittinghofer, A. (2001). The guanine nucleotide-binding switch in three dimensions. *Science*, *294*(5545), 1299 LP-1304. https://doi.org/10.1126/science.1062023

Vicente-García, J. J. (2009). Identification of new activated Cdc42 kinase (ACK1) binding proteins and characterisation of the ACK1-STAT3 interaction / José Julio Vicente-García. (U. of C. D. of Biochemistry (ed.)). 2009.

Vigil, D., Cherfils, J., Rossman, K. L., and Der, C. J. (2010). Ras superfamily GEFs and GAPs: validated and tractable targets for cancer therapy? *Nature Reviews. Cancer*, *10*(12), 842–857. https://doi.org/10.1038/nrc2960

Vignal, E., Blangy, A., Martin, M., Gauthier-Rouvière, C., and Fort, P. (2001). Kinectin is a key effector of RhoG microtubule-dependent cellular activity. *Molecular and Cellular Biology*, *21*(23), 8022–8034. https://doi.org/10.1128/MCB.21.23.8022-8034.2001

Vigorito, E., Billadeu, D. D., Savoy, D., McAdam, S., Doody, G., Fort, P., and Turner, M. (2003). RhoG regulates gene expression and the actin cytoskeleton in lymphocytes. *Oncogene*, *22*(3), 330–342. https://doi.org/10.1038/sj.onc.1206116

Villalonga, P., Guasch, R. M., Riento, K., and Ridley, A. J. (2004). RhoE inhibits cell cycle progression and Ras-induced transformation. *Molecular and Cellular Biology*, *24*(18), 7829 LP-7840. https://doi.org/10.1128/MCB.24.18.7829-7840.2004

Vincent, S., Jeanteur, P., and Fort, P. (1992). Growth-regulated expression of RhoG, a new member of the ras homolog gene family. *Molecular and Cellular Biology*, *12*(7), 3138 LP-3148. https://doi.org/10.1128/MCB.12.7.3138

Volpicelli-Daley, L. A., Li, Y., Zhang, C.-J., and Kahn, R. A. (2005). Isoform-selective effects of the depletion of ADP-ribosylation factors 1-5 on membrane traffic. *Molecular Biology of the Cell*, *16*(10), 4495–4508. https://doi.org/10.1091/mbc.e04-12-1042

von Mikecz, A. (2006). The nuclear ubiquitin-proteasome system. *Journal of Cell Science*, *119*(10), 1977–1984. https://doi.org/10.1242/jcs.03008

Wang, D.-A., and Sebti, S. M. (2005). Palmitoylated cysteine 192 is required for RhoB tumor-suppressive and apoptotic activities. *Journal of Biological Chemistry* , *280*(19), 19243–19249. https://doi.org/10.1074/jbc.M411472200

Wang, D. Z. M., Nur-E-Kamal, M. S. A., Tikoo, A., Montague, W., and Maruta, H. (1997). The GTPase and Rho GAP domains of p190, a tumor suppressor protein that binds the M(r) 120,000 Ras GAP, independently function as Anti-Ras tumor suppressors. *Cancer Research*, *57*(12), 2478–2484.

Wang, H., Wang, B., Liao, Q., An, H., Li, W., Jin, X., Cui, S., and Zhao, L. (2014). Overexpression of RhoGDI, a novel predictor of distant metastasis, promotes cell proliferation and migration in hepatocellular carcinoma. *FEBS Letters*, *588*(3), 503–508. https://doi.org/https://doi.org/10.1016/j.febslet.2013.12.016

Wang, H., Zeng, X., Fan, Z., and Lim, B. (2010). RhoH plays distinct roles in T-cell migrations induced by different doses of SDF1 alpha. *Cellular Signalling*, *22*(7), 1022–1032. https://doi.org/10.1016/j.cellsig.2010.02.005

Wang, J.-Q., Zhu, S., Wang, Y., Wang, F., An, C., Jiang, D., Gao, L., Tu, Y., Zhu, X., Wang, Y., Liu, H., Gong, J., Sun, Z., Wang, X., Liu, L., Yang, K., Guo, C., and Tang, T.-S. (2019). Miro2 supplies a platform for Parkin translocation to damaged mitochondria. *Science Bulletin*, *64*(11), 730–747. https://doi.org/https://doi.org/10.1016/j.scib.2019.04.033

Wang, P.-Y., Chang, K.-T., Lin, Y.-M., Kuo, T.-Y., and Wang, G.-S. (2018). Ubiquitination of MBNL1 is required for its cytoplasmic localization and function in promoting neurite outgrowth. *Cell Reports*, *22*(9), 2294–2306. https://doi.org/10.1016/j.celrep.2018.02.025

Wang, S., Watanabe, T., Noritake, J., Fukata, M., Yoshimura, T., Itoh, N., Harada, T., Nakagawa, M., Matsuura, Y., Arimura, N., and Kaibuchi, K. (2007). IQGAP3, a novel effector of Rac1 and Cdc42, regulates neurite outgrowth. *Journal of Cell Science*, *120*(4), 567 LP-577. https://doi.org/10.1242/jcs.03356

Ward, Y., Yap, S.-F., Ravichandran, V., Matsumura, F., Ito, M., Spinelli, B., and Kelly, K. (2002). The GTP binding proteins Gem and Rad are negative regulators of the Rho–Rho kinase pathway . *The Journal of Cell Biology*, *157*(2), 291–302. https://doi.org/10.1083/jcb.200111026

Watanabe, G., Saito, Y., Madaule, P., Ishizaki, T., Fujisawa, K., Morii, N., Mukai, H., Ono, Y., Kakizuka, A., and Narumiya, S. (1996). Protein Kinase N (PKN) and PKN-related protein Rhophilin as targets of small GTPase Rho. *Science*, *271*(5249), 645 LP-648. https://doi.org/10.1126/science.271.5249.645

Watson, R. T., Furukawa, M., Chiang, S.-H., Boeglin, D., Kanzaki, M., Saltiel, A. R., and Pessin, J. E. (2003). The exocytotic trafficking of TC10 occurs through both classical and nonclassical secretory transport pathways in 3T3L1 adipocytes. *Molecular and Cellular Biology*, *23*(3), 961 LP-974. https://doi.org/10.1128/MCB.23.3.961-974.2003

Weihofen, A., Thomas, K. J., Ostaszewski, B. L., Cookson, M. R., and Selkoe, D. J. (2009). Pink1 forms a multiprotein complex with Miro and Milton, linking Pink1 function to mitochondrial trafficking. *Biochemistry*, *48*(9), 2045–2052. https://doi.org/10.1021/bi8019178

Welman, A., Burger, M. M., and Hagmann, J. (2000). Structure and function of the C-terminal hypervariable region of K-Ras4B in plasma membrane targetting and transformation. *Oncogene*, *19*(40), 4582–4591. https://doi.org/10.1038/sj.onc.1203818

Wennerberg, K., and Der, C. J. (2004). Rho-family GTPases: it's not only Rac and Rho (and I like it). *Journal of Cell Science*, *117*(8), 1301–1312. https://doi.org/10.1242/jcs.01118

Wennerberg, K., Forget, M.-A., Ellerbroek, S. M., Arthur, W. T., Burridge, K., Settleman, J., Der, C. J., and Hansen, S. H. (2003). Rnd proteins function as RhoA antagonists by activating p190 RhoGAP. *Current Biology*, *13*(13), 1106–1115. https://doi.org/https://doi.org/10.1016/S0960-9822(03)00418-4

Wheeler, A. P., and Ridley, A. J. (2004). Why three Rho proteins? RhoA, RhoB, RhoC, and cell motility. *Experimental Cell Research*, *301*(1), 43–49. https://doi.org/https://doi.org/10.1016/j.yexcr.2004.08.012

Wherlock, M., Gampel, A., Futter, C., and Mellor, H. (2004). Farnesyltransferase inhibitors disrupt EGF receptor traffic through modulation of the RhoB GTPase. *Journal of Cell Science*, *117*(15), 3221 LP-3231. https://doi.org/10.1242/jcs.01193

Withers, C. N., Brown, D. M., Byiringiro, I., Allen, M. R., Condon, K. W., Satin, J., and Andres, D. A. (2017). Rad GTPase is essential for the regulation of bone density and bone marrow adipose tissue in mice. *Bone*, *103*, 270–280. https://doi.org/https://doi.org/10.1016/j.bone.2017.07.018

Wu, S.-K., Zeng, K., Wilson, I. A., and Balch, W. E. (1996). Structural insights into the function of the Rab GDI superfamily. *Trends in Biochemical Sciences*, *21*(12), 472–476. https://doi.org/https://doi.org/10.1016/S0968-0004(96)10062-1

Wu, T., Merbl, Y., Huo, Y., Gallop, J. L., Tzur, A., and Kirschner, M. W. (2010). UBE2S drives elongation of K11-linked ubiquitin chains by the Anaphase-Promoting Complex. *Proceedings of the National Academy of Sciences*, *107*(4), 1355 LP-1360. https://doi.org/10.1073/pnas.0912802107

Wu, W. J., Tu, S., and Cerione, R. A. (2003). Activated Cdc42 sequesters c-Cbl and prevents EGF receptor degradation. *Cell*, *114*(6), 715–725. https://doi.org/10.1016/s0092-8674(03)00688-3

Wu, Y., Moissoglu, K., Wang, H., Wang, X., Frierson, H. F., Schwartz, M. A., and Theodorescu, D. (2009). Src phosphorylation of RhoGDI2 regulates its metastasis suppressor function. *Proceedings of the National Academy of Sciences*, *106*(14), 5807 LP-5812. https://doi.org/10.1073/pnas.0810094106

Xiao, Y., Lin, V. Y., Ke, S., Lin, G. E., Lin, F.-T., and Lin, W.-C. (2014). 14-3-3τ promotes breast cancer invasion and metastasis by inhibiting RhoGDIα. *Molecular and Cellular Biology*, *34*(14), 2635 LP-2649. https://doi.org/10.1128/MCB.00076-14

Xu, R., Wu, X., Zhang, S., Li, C., Yang, L., Li, D., Zhang, B., Zhang, Y., Jin, J., Zhang, B. (2013). The tumor suppressor gene RhoBTB1 is a novel target of miR-31 in human colon cancer. *International Journal of Oncology*, *42*(2), 676–682.

Xu, G., and Jaffrey, S. R. (2011). The new landscape of protein ubiquitination. *Nature Biotechnology*, *29*(12), 1098–1100. https://doi.org/10.1038/nbt.2061

Xu, S.-H., Huang, J.-Z., Xu, M.-L., Yu, G., Yin, X.-F., Chen, D., and Yan, G.-R. (2015). ACK1 promotes gastric cancer epithelial-mesenchymal transition and metastasis through AKT-POU2F1-ECD signalling. *The Journal of Pathology*, *236*(2), 175–185. https://doi.org/10.1002/path.4515

Yamaguchi, R., and Newport, J. (2003). A Role for Ran-GTP and Crm1 in blocking re-replication. *Cell*, *113*(1), 115–125. https://doi.org/https://doi.org/10.1016/S0092-8674(03)00200-9

Yamaoka, S., and Hara-Nishimura, I. (2014). The mitochondrial Ras-related GTPase Miro: views from inside and outside the metazoan kingdom. In *Frontiers in Plant Science* (Vol. 5, p. 350). https://www.frontiersin.org/article/10.3389/fpls.2014.00350

Yamaoka, S., Nakajima, M., Fujimoto, M., and Tsutsumi, N. (2011). MIRO1 influences the morphology and intracellular distribution of mitochondria during embryonic cell division in Arabidopsis. *Plant Cell Reports*, *30*(2), 239–244. https://doi.org/10.1007/s00299-010-0926-5

Yamazaki, T., Zaal, K., Hailey, D., Presley, J., Lippincott-Schwartz, J., and Samelson, L. E. (2002). Role of Grb2 in EGF-stimulated EGFR internalization. *Journal of Cell Science*, *115*(9), 1791 LP-1802. http://jcs.biologists.org/content/115/9/1791.abstract

Yang, N., Higuchi, O., Ohashi, K., Nagata, K., Wada, A., Kangawa, K., Nishida, E., and Mizuno, K. (1998). Cofilin phosphorylation by LIM-kinase 1 and its role in Rac-mediated actin reorganization. *Nature*, *393*(6687), 809–812. https://doi.org/10.1038/31735

Yang, R.-M., Zhan, M., Xu, S.-W., Long, M.-M., Yang, L.-H., Chen, W., Huang, S., Liu, Q., Zhou, J., Zhu, J., and Wang, J. (2017). miR-3656 expression enhances the chemosensitivity of pancreatic cancer to gemcitabine through modulation of the RHOF/EMT axis. *Cell Death and Disease*, *8*(10), e3129–e3129. https://doi.org/10.1038/cddis.2017.530

Yang, W., Lin, Q., Guan, J.-L., and Cerione, R. A. (1999). Activation of the Cdc42-associated

Tyrosine Kinase-2 (ACK-2) by Cell adhesion via Integrin β1. *Journal of Biological Chemistry*, *274*(13), 8524–8530. http://www.jbc.org/content/274/13/8524.abstract

Yang, W., Lo, C. G., Dispenza, T., and Cerione, R. A. (2001). The Cdc42 target ACK2 directly interacts with clathrin and influences clathrin assembly. *Journal of Biological Chemistry* , *276*(20), 17468–17473. https://doi.org/10.1074/jbc.M010893200

Yang, Z., Rayala, S., Nguyen, D., Vadlamudi, R. K., Chen, S., and Kumar, R. (2005). Pak1 Phosphorylation of Snail, a master regulator of epithelial-to-mesenchyme transition, modulates Snail's subcellular localization and functions. *Cancer Research*, *65*(8), 3179 LP-3184. https://doi.org/10.1158/0008-5472.CAN-04-3480

Yasuda, S., Oceguera-Yanez, F., Kato, T., Okamoto, M., Yonemura, S., Terada, Y., Ishizaki, T., and Narumiya, S. (2004). Cdc42 and mDia3 regulate microtubule attachment to kinetochores. *Nature*, *428*(6984), 767–771. https://doi.org/10.1038/nature02452

Ye, H., Zhang, Y., Geng, L., and Li, Z. (2014). Cdc42 expression in cervical cancer and its effects on cervical tumor invasion and migration. *International Journal of Oncology*. https://doi.org/10.3892/ijo.2014.2748

Yi, B., Zhang, Y., Zhu, D., Zhang, L., Song, S., He, S., Zhang, B., Li, D., Z. (2015). Overexpression of RhoGDI2 correlates with the progression and prognosis of pancreatic carcinoma. *Oncology Reports*, *33*(3), 1201–1206.

Yokoyama, N., Lougheed, J., and Miller, W. T. (2005). Phosphorylation of WASP by the Cdc42-associated Kinase ACK1: Dual hydroxyamino acid specificity in a tyrosine kinase . *Journal of Biological Chemistry* , *280*(51), 42219–42226. http://www.jbc.org/content/280/51/42219.abstract

Yokoyama, N., and Miller, W. T. (2003). Biochemical properties of the Cdc42-associated tyrosine kinase ACK1. Substrate specificity, autophosphorylation, and interaction with Hck. *The Journal of Biological Chemistry*, *278*(48), 47713–47723. https://doi.org/10.1074/jbc.M306716200

Yu, J., Zhang, D., Liu, J., Li, J., Yu, Y., Wu, X.-R. R., and Huang, C. (2012). RhoGDI SUMOylation at Lys-138 Increases Its Binding Activity to Rho GTPase and Its Inhibiting Cancer Cell Motility. *Journal of Biological Chemistry* , *287*(17), 13752–13760. https://doi.org/10.1074/jbc.M111.337469

Zalcman, G., Closson, V., Camonis, J., Honoré, N., Rousseau-Merck, M. F., Tavitian, A., and Olofsson, B. (1996). RhoGDI-3 is a new GDP dissociation inhibitor (GDI). Identification of a non-cytosolic GDI protein interacting with the small GTP-binding proteins RhoB and RhoG. *The Journal of Biological Chemistry*, *271*(48), 30366–30374.

http://www.ncbi.nlm.nih.gov/pubmed/8939998

Zerial, M., and McBride, H. (2001). Rab proteins as membrane organizers. *Nature Reviews Molecular Cell Biology*, *2*(2), 107–117. https://doi.org/10.1038/35052055

Zhang, B., Zhang, Y., Dagher, M.-C., & Shacter, E. (2005). Rho GDP dissociation inhibitor protects cancer cells against drug-induced apoptosis. *Cancer Research*, *65*(14), 6054–6062. https://doi.org/10.1158/0008-5472.CAN-05-0175

Zhang, C.-S., Liu, Q., Li, M., Lin, S.-Y., Peng, Y., Wu, D., Li, T. Y., Fu, Q., Jia, W., Wang, X., Ma, T., Zong, Y., Cui, J., Pu, C., Lian, G., Guo, H., Ye, Z., and Lin, S.-C. (2015). RHOBTB3 promotes proteasomal degradation of HIFα through facilitating hydroxylation and suppresses the Warburg effect. *Cell Research*, *25*(9), 1025–1042. https://doi.org/10.1038/cr.2015.90

Zhang, Y., Rosado, L. A. R., Moon, S. Y., Zhang, B., Rivera Rosado, L. A., Moon, S. Y., and Zhang, B. (2009). Silencing of D4-GDI inhibits growth and invasive behavior in MDA-MB-231 cells by activation of Rac-dependent p38 and JNK signaling. *The Journal of Biological Chemistry*, *284*(19), 12956–12965. https://doi.org/10.1074/jbc.M807845200

Zheng, Z., Liu, B., and Wu, X. (2015). RhoGDI2 up-regulates P-glycoprotein expression via Rac1 in gastric cancer cells. *Cancer Cell International*, *15*(1), 41. https://doi.org/10.1186/s12935-015-0190-4

Zhu, G., Wang, Y., Huang, B., Liang, J., Ding, Y., Xu, A., & Wu, W. (2012). A Rac1/PAK1 cascade controls β-catenin activation in colon cancer cells. *Oncogene*, *31*(8), 1001–1012. https://doi.org/10.1038/onc.2011.294

Zhu, Y., Liu, C., Tummala, R., Nadiminty, N., Lou, W., and Gao, A. C. (2013). RhoGDIα downregulates androgen receptor signaling in prostate cancer cells. *The Prostate*, *73*(15), 1614–1622. https://doi.org/10.1002/pros.22615

Zohn, I. M., Campbell, S. L., Khosravi-Far, R., Rossman, K. L., and Der, C. J. (1998). Rho-family proteins and Ras transformation: the RHOad less traveled gets congested. *Oncogene*, *17*(11), 1415–1438. https://doi.org/10.1038/sj.onc.1202181

Zong, H., Kaibuchi, K., and Quilliam, L. A. (2001). The insert region of RhoA is essential for Rho kinase activation and cellular transformation. *Molecular and Cellular Biology*, *21*(16), 5287–5298. https://doi.org/10.1128/MCB.21.16.5287-5298.2001

Appendix

Appendix 1.1: The percentage sequence similarity shared between Rho-family GTPases

	RhoBTB3	Miro1	Miro2	RhoBTB1	RhoBTB2	RhoH	Rnd1	Rnd2	Rnd3	RhoD	RhoF	RhoA	RhoC	RhoB	Wrch2	Wrch1	TC10	TCL	Cdc42	RhoG	Rac2	Rac1	Rac3
RhoBTB3		15	14	25	25	26	16	16	17	19	17	19	17	19	15	17	22	19	17	19	19	20	18
Miro1	15		60	17	18	21	19	17	21	28	26	22	22	23	25	27	25	24	24	24	24	25	25
Miro2	14	60		16	19	20	23	20	22	27	24	25	25	27	26	26	22	22	24	27	27	26	28
RhoBTB1	25	17	16		70	34	33	31	30	34	28	38	37	38	34	32	38	35	40	40	41	42	41
RhoBTB2	25	18	19	70		32	32	31	29	34	28	39	37	38	33	32	39	37	40	40	42	42	41
RhoH	26	21	20	34	32		29	32	36	38	33	40	40	41	41	38	40	39	42	40	40	41	40
Rnd1	16	19	23	32	32	29		53	61	37	39	41	42	41	31	32	36	34	37	37	39	39	38
Rnd2	16	17	20	31	31	32	53		63	39	41	46	47	43	28	31	36	35	37	41	40	41	39
Rnd3	17	21	22	29	29	36	61	63		37	40	48	48	47	31	32	39	35	38	41	39	42	40
RhoD	19	28	27	34	35	38	37	39	37		49	49	49	49	39	36	42	38	43	44	46	49	49
RhoF	17	26	24	28	28	33	39	41	40	49		47	48	47	36	37	46	43	43	46	50	59	47
RhoA	19	22	25	38	39	40	41	46	48	49	47		92	85	40	44	51	48	53	55	53	57	55
RhoC	17	22	25	37	37	40	42	47	48	49	48	92		85	40	44	50	49	51	55	53	57	54
RhoB	19	23	27	38	38	41	41	43	47	49	47	85	85		42	45	51	48	50	53	54	55	54
Wrch2	15	25	26	34	33	41	31	28	31	39	36	40	40	42		59	51	48	53	46	51	52	53
Wrch1	17	27	26	32	32	37	32	31	32	36	37	44	44	45	59		50	46	56	48	54	54	54
TC10	22	25	22	38	39	40	36	36	39	42	46	51	50	51	51	50		76	66	54	60	62	61
TCL	19	24	22	35	37	39	34	35	35	38	44	48	49	48	48	46	76		63	53	58	60	59
Cdc42	17	24	24	40	40	42	37	37	38	43	43	53	51	50	53	56	66	63		61	69	71	70
RhoG	19	24	27	39	40	40	37	41	41	44	46	55	55	53	46	48	54	53	60		72	72	70
Rac2	19	24	27	41	42	40	39	40	39	46	50	53	53	54	50	54	60	58	69	72		92	89
Rac1	20	25	26	42	42	41	39	41	42	49	49	57	57	55	52	54	62	60	71	72	92		93
Rac3	18	25	28	41	41	40	38	39	40	49	47	55	54	54	53	54	61	59	70	70	89	93	